

Methods in
Molecular Biology 2166

Springer Protocols

Manfred Heinlein *Editor*

RNA Tagging

Methods and Protocols



 Humana Press

METHODS IN MOLECULAR BIOLOGY

Series Editor

John M. Walker

School of Life and Medical Sciences

University of Hertfordshire

Hatfield, Hertfordshire, UK

For further volumes:

<http://www.springer.com/series/7651>

For over 35 years, biological scientists have come to rely on the research protocols and methodologies in the critically acclaimed *Methods in Molecular Biology* series. The series was the first to introduce the step-by-step protocols approach that has become the standard in all biomedical protocol publishing. Each protocol is provided in readily-reproducible step-by-step fashion, opening with an introductory overview, a list of the materials and reagents needed to complete the experiment, and followed by a detailed procedure that is supported with a helpful notes section offering tips and tricks of the trade as well as troubleshooting advice. These hallmark features were introduced by series editor Dr. John Walker and constitute the key ingredient in each and every volume of the *Methods in Molecular Biology* series. Tested and trusted, comprehensive and reliable, all protocols from the series are indexed in PubMed.

RNA Tagging

Methods and Protocols

Edited by

Manfred Heinlein

Institut de Biologie Moléculaire des Plantes (IBMP-CNRS), Université de Strasbourg, Strasbourg, France

 **Humana Press**

Editor

Manfred Heinlein
Institut de Biologie Moléculaire des
Plantes (IBMP-CNRS)
Université de Strasbourg
Strasbourg, France

ISSN 1064-3745 ISSN 1940-6029 (electronic)
Methods in Molecular Biology
ISBN 978-1-0716-0711-4 ISBN 978-1-0716-0712-1 (eBook)
<https://doi.org/10.1007/978-1-0716-0712-1>

© Springer Science+Business Media, LLC, part of Springer Nature 2020

This work is subject to copyright. All rights are reserved by the Publisher, whether the whole or part of the material is concerned, specifically the rights of translation, reprinting, reuse of illustrations, recitation, broadcasting, reproduction on microfilms or in any other physical way, and transmission or information storage and retrieval, electronic adaptation, computer software, or by similar or dissimilar methodology now known or hereafter developed.

The use of general descriptive names, registered names, trademarks, service marks, etc. in this publication does not imply, even in the absence of a specific statement, that such names are exempt from the relevant protective laws and regulations and therefore free for general use.

The publisher, the authors, and the editors are safe to assume that the advice and information in this book are believed to be true and accurate at the date of publication. Neither the publisher nor the authors or the editors give a warranty, expressed or implied, with respect to the material contained herein or for any errors or omissions that may have been made. The publisher remains neutral with regard to jurisdictional claims in published maps and institutional affiliations.

This Humana imprint is published by the registered company Springer Science+Business Media, LLC, part of Springer Nature.

The registered company address is: 1 New York Plaza, New York, NY 10004, U.S.A.

Preface

RNA molecules play diverse roles in the cell owing to their secondary structure and interaction with various proteins and nucleic acids. To study the composition, localization, dynamics, and function of these functional RNA complexes in vitro or in live cells and tissues of animals and plants requires the specific tagging of the RNA or of RNA-binding proteins with suitable reporter molecules. This book provides a compendium of state-of-the-art methods for the labeling, detection, and purification of RNA and RNA–protein complexes and thereby constitutes an important toolbox for researchers interested in understanding the complex roles of RNA molecules in development, signaling, and disease. In addition to studying the natural function of RNA molecules within cells, numerous labs have developed methods to actually apply RNA molecules as guides for the sequence-specific cleavage, modification, or imaging of RNA and DNA. Therefore, this book also includes protocols that apply RNA molecules as sequence-specific guide molecules.

The protocol chapters of this book are organized in six parts. Part I provides protocols for the in situ detection of RNA molecules using fluorescent in situ hybridization (FISH) techniques, whereas Part II provides protocols for the tagging of RNA molecules for specific detection in live cells by fluorescent RNA-binding proteins. A dedicated review article describes the imaging of RNA molecules with fluorogens that bind to RNA targets tagged with specific light-up RNA aptamers. Part III contains protocols for monitoring RNA uptake by cells or for addressing RNA transport between cells. Important protocols useful for the characterization of RNA-binding proteins and protein complexes are presented in Part IV. Part V is dedicated to protocols for the application of RNA molecules as guides in RNA-mediated editing and imaging of chromosome loci. Starting with an overview article about CRISPR guide RNA design for genome editing, this part continues by presenting protocols in which RNA molecules are applied to guide nuclease-deactivated CRISPR-associated protein 9 (dCas9) for the imaging of specific genome loci. Another interesting protocol in this part of the book allows the in vivo monitoring of transcribed loci by imaging tagged nascent messenger RNA molecules emerging during gene transcription. The final Part VI provides advanced protocols for the functional analysis of RNA molecules. These include the detection of small RNAs involved in RNA silencing by Northern blot hybridization, the monitoring of miRNA-mediated RNA silencing events with an in vivo reporter system, the isolation and characterization of RNA molecules associated with polyribosomes, a protocol for transfection of RNA molecules into plant protoplasts, and also the biochemical in vitro modification and tagging of RNA molecules for imaging and structural analysis.

The experimental protocols are provided by leading experts with hands-on experience in the respective method. I hope that the provision of these protocols will further stimulate research in RNA biology and that the research community interested in this field will accept this book as an important reference.

I am very grateful to all the authors who contributed to this book. I also thank the series editor, John M. Walker, for his continuous support in developing this volume.

Strasbourg, France

Manfred Heinlein

Contents

<i>Preface</i>	<i>v</i>
<i>Contributors</i>	<i>xi</i>
PART I IN SITU DETECTION OF RNA MOLECULES USING FISH TECHNIQUES	
1 Tagging and Application of RNA Probes for Sequence-Specific Visualization of RNAs by Fluorescent In Situ Hybridization	3
<i>Thomas Dresselhaus and Andrea Bleckmann</i>	
2 Quantitative Fluorescence In Situ Hybridization Detection of Plant mRNAs with Single-Molecule Resolution	23
<i>Kun Huang, Mona Batish, Chong Teng, Alex Harkess, Blake C. Meyers, and Jeffrey L. Caplan</i>	
3 Visualization of Endoplasmic Reticulum-Associated mRNA in Mammalian Cells	35
<i>Jingze J. Wu and Alexander F. Palazzo</i>	
4 Simultaneous Detection of mRNA and Protein in <i>S. cerevisiae</i> by Single-Molecule FISH and Immunofluorescence	51
<i>Evelina Tutucci and Robert H. Singer</i>	
PART II IN VIVO IMAGING OF RNA TRANSPORT AND LOCALIZATION	
5 Development and Applications of Fluorogen/Light-Up RNA Aptamer Pairs for RNA Detection and More	73
<i>Michael Ryckelynck</i>	
6 Visualization of Transiently Expressed mRNA in Plants Using MS2	103
<i>Eduardo José Peña and Manfred Heinlein</i>	
7 New Generations of MS2 Variants and MCP Fusions to Detect Single mRNAs in Living Eukaryotic Cells	121
<i>Xavier Pichon, Marie-Cécile Robert, Edouard Bertrand, Robert H. Singer, and Evelina Tutucci</i>	
8 In Vivo Imaging of Mobile mRNAs in Plants Using MS2	145
<i>Kai-Ren Luo, Nien-Chen Huang, and Tien-Shin Yu</i>	
9 RNA Imaging with RNase-Inactivated Csy4 in Plants and Filamentous Fungi	157
<i>David Burnett, Alexander Lichius, and Jens Tilsner</i>	
PART III IMAGING AND ANALYSIS OF RNA UPTAKE AND TRANSPORT BETWEEN CELLS	
10 Utilizing Potato Virus X to Monitor RNA Movement	181
<i>Zhiming Yu, Sung Ki Cho, Pengcheng Zhang, Yiguo Hong, and David J. Hannapel</i>	

11	A Protocol for Non-biased Identification of RNAs Transferred Between Heterologous Mammalian Cell Types Using RNA Tagging, Cell Sorting, and Sequencing.	195
	<i>Sandipan Dasgupta and Jeffrey E. Gerst</i>	
12	Synthesizing Fluorescently Labeled dsRNAs and sRNAs to Visualize Fungal RNA Uptake	215
	<i>Rachael Hamby, Ming Wang, Lulu Qiao, and Hailing Jin</i>	
13	Labeling of dsRNA for Fungal Uptake Detection Analysis	227
	<i>Matteo Galli, Jafargholi Imani, and Karl-Heinz Kogel</i>	
PART IV IDENTIFICATION AND ANALYSIS OF RNA-BINDING PROTEINS		
14	Using RNA Affinity Purification Followed by Mass Spectrometry to Identify RNA-Binding Proteins (RBPs)	241
	<i>Mengge Shan and Brian D. Gregory</i>	
15	Plant Individual Nucleotide Resolution Cross-Linking and Immunoprecipitation to Characterize RNA-Protein Complexes	255
	<i>Tino Köster and Dorothee Staiger</i>	
16	A Single-Molecule RNA Mobility Assay to Identify Proteins that Link RNAs to Molecular Motors	269
	<i>Varun Bhaskar, Min Jia, and Jeffrey A. Chao</i>	
17	<i>Proximity-CLIP</i> Provides a Snapshot of Protein-Occupied RNA Elements at Subcellular Resolution and Transcriptome-Wide Scale.	283
	<i>Daniel Benhalevy and Markus Hafner</i>	
18	Double-Stranded RNA Pull-Down to Characterize Viral Replication Complexes in Plants.	307
	<i>Marco Incarbone and Christophe Ritzenthaler</i>	
PART V RNAs AS GUIDES FOR GENOME EDITING AND IMAGING OF CHROMOSOME LOCI		
19	CRISPR Guide RNA Design Guidelines for Efficient Genome Editing	331
	<i>Patrick Schindele, Felix Wolter, and Holger Puchta</i>	
20	Live-Cell CRISPR Imaging in Plant Cells with a Telomere-Specific Guide RNA	343
	<i>Solmaz Khosravi, Steven Dreissig, Patrick Schindele, Felix Wolter, Twan Ruten, Holger Puchta, and Andreas Houben</i>	
21	Live-Cell Imaging of Genomic Loci Using CRISPR/Molecular Beacon Hybrid Systems.	357
	<i>Xiaotian Wu, Yachen Ying, Shiqi Mao, Christopher J. Krueger, and Antony K. Chen</i>	
22	Using RNA Tags for Multicolor Live Imaging of Chromatin Loci and Transcription in <i>Drosophila</i> Embryos	373
	<i>Hongtao Chen and Thomas Gregor</i>	

PART VI SPECIFIC TECHNIQUES FOR THE ANALYSIS OF RNA FUNCTIONS

23	Integrated Genome-Scale Analysis and Northern Blot Detection of Retrotransposon siRNAs Across Plant Species	387
	<i>Marcel Böhrer, Bart Rymen, Christophe Himber, Aude Gerbaud, David Pflieger, Debbie Laudencia-Chingcuanco, Amy Cartwright, John Vogel, Richard Sibout, and Todd Blevins</i>	
24	Transfection of Small Noncoding RNAs into <i>Arabidopsis thaliana</i> Protoplasts	413
	<i>Stéphanie Lalande, Marjorie Chery, Elodie Ubrig, Guillaume Hummel, Julie Kubina, Angèle Geldreich, and Laurence Drouard</i>	
25	In Vivo Reporter System for miRNA-Mediated RNA Silencing	431
	<i>Károly Fátýol</i>	
26	TRAP-SEQ of Eukaryotic Translatomes Applied to the Detection of Polysome-Associated Long Noncoding RNAs	451
	<i>Soledad Traubenik, Flavio Blanco, María Eugenia Zanetti, and Mauricio A. Reynoso</i>	
27	Posttranscriptional Suzuki-Miyaura Cross-Coupling Yields Labeled RNA for Conformational Analysis and Imaging	473
	<i>Manisha B. Walunj and Seergazhi G. Srivatsan</i>	
	<i>Index</i>	487

Contributors

- MONA BATISH • *Departments of Biological Sciences and Medical & Molecular Sciences, University of Delaware, Newark, DE, USA*
- DANIEL BENHALEVY • *Laboratory of Muscle Stem Cells and Gene Regulation, National Institute of Arthritis and Musculoskeletal and Skin Diseases, National Institutes of Health, Bethesda, MD, USA*
- EDOUARD BERTRAND • *Institut de Génétique Moléculaire de Montpellier, Université de Montpellier, CNRS, Montpellier, France; Department of Anatomy and Structural Biology, Albert Einstein College of Medicine, Bronx, NY, USA*
- VARUN BHASKAR • *Friedrich Miescher Institute for Biomedical Research, Basel, Switzerland*
- FLAVIO BLANCO • *Instituto de Biotecnología y Biología Molecular, Facultad de Ciencias Exactas, Universidad Nacional de La Plata, Centro Científico y Tecnológico-La Plata, Consejo Nacional de Investigaciones Científicas y Técnicas, La Plata, Argentina*
- ANDREA BLECKMANN • *Cell Biology and Plant Biochemistry, Regensburg Center for Biochemistry, University of Regensburg, Regensburg, Germany*
- TODD BLEVINS • *Institut de Biologie Moléculaire des Plantes, CNRS UPR2357, Université de Strasbourg, Strasbourg, France*
- MARCEL BÖHRER • *Institut de Biologie Moléculaire des Plantes, CNRS UPR2357, Université de Strasbourg, Strasbourg, France*
- DAVID BURNETT • *Cell and Molecular Sciences, The James Hutton Institute, Dundee, UK; Biomedical Sciences Research Complex, The University of St Andrews, St. Andrews, UK*
- JEFFREY L. CAPLAN • *Department of Plant and Soil Sciences, University of Delaware, Newark, DE, USA; Delaware Biotechnology Institute, University of Delaware, Newark, DE, USA*
- AMY CARTWRIGHT • *DOE Joint Genome Institute, Lawrence Berkeley National Laboratory, Berkeley, CA, USA*
- JEFFREY A. CHAO • *Friedrich Miescher Institute for Biomedical Research, Basel, Switzerland*
- ANTONY K. CHEN • *Department of Biomedical Engineering, College of Engineering, Peking University, Beijing, China*
- HONGTAO CHEN • *Lewis-Sigler Institute for Integrative Genomics, Princeton University, Princeton, NJ, USA*
- MARJORIE CHERY • *Institut de Biologie Moléculaire des Plantes—CNRS, Université de Strasbourg, Strasbourg, France*
- SUNG KI CHO • *Dura-Line Corporation, Clinton, TN, USA*
- SANDIPAN DASGUPTA • *Department of Molecular Genetics, Weizmann Institute of Science, Rehovot, Israel*
- STEVEN DREISSIG • *Leibniz Institute of Plant Genetics and Crop Plant Research (IPK), Gatersleben, Germany*
- THOMAS DRESSSELHAUS • *Cell Biology and Plant Biochemistry, Regensburg Center for Biochemistry, University of Regensburg, Regensburg, Germany*
- LAURENCE DROUARD • *Institut de Biologie Moléculaire des Plantes—CNRS, Université de Strasbourg, Strasbourg, France*
- KÁROLY FÁTYOL • *Agricultural Biotechnology Institute, National Agricultural Research and Innovation Centre, Gödöllő, Hungary*

- MATTEO GALLI • *Research Centre for BioSystems, Land Use and Nutrition, Institute of Phytopathology, Justus Liebig University Giessen, Giessen, Germany*
- ANGÈLE GELDREICH • *Institut de Biologie Moléculaire des Plantes—CNRS, Université de Strasbourg, Strasbourg, France*
- AUDE GERBAUD • *Institut de Biologie Moléculaire des Plantes, CNRS UPR2357, Université de Strasbourg, Strasbourg, France*
- JEFFREY E. GERST • *Department of Molecular Genetics, Weizmann Institute of Science, Rehovot, Israel*
- THOMAS GREGOR • *Lewis-Sigler Institute for Integrative Genomics, Princeton University, Princeton, NJ, USA; Joseph Henry Laboratories of Physics, Princeton University, Princeton, NJ, USA; Department of Developmental and Stem Cell Biology, UMR3738, Institut Pasteur, Paris, France*
- BRIAN D. GREGORY • *Department of Biology, University of Pennsylvania, Philadelphia, PA, USA; Genomics and Computational Biology Graduate Group, University of Pennsylvania, Philadelphia, PA, USA*
- MARKUS HAFNER • *Laboratory of Muscle Stem Cells and Gene Regulation, National Institute of Arthritis and Musculoskeletal and Skin Diseases, National Institutes of Health, Bethesda, MD, USA*
- RACHAEL HAMBY • *Department of Microbiology and Plant Pathology, Center for Plant Cell Biology, Institute for Integrative Genome Biology, University of California, Riverside, CA, USA*
- DAVID J. HANNAPEL • *Plant Biology Major, Iowa State University, Ames, IA, USA*
- ALEX HARKESS • *Donald Danforth Plant Science Center, St. Louis, MO, USA*
- MANFRED HEINLEIN • *Institut de Biologie Moléculaire des Plantes du CNRS, Université de Strasbourg, Strasbourg, France*
- CHRISTOPHE HIMBER • *Institut de Biologie Moléculaire des Plantes, CNRS UPR2357, Université de Strasbourg, Strasbourg, France*
- YIGUO HONG • *Research Centre for Plant RNA Signaling, College of Life and Environmental Sciences, Hangzhou Normal University, Hangzhou, China; Warwick-Hangzhou RNA Signaling Joint Laboratory, School of Life Sciences, University of Warwick, Warwick, UK; Worcester-Hangzhou Joint Molecular Plant Health Laboratory, Institute of Science and the Environment, University of Worcester, Worcester, UK*
- ANDREAS HOUBEN • *Leibniz Institute of Plant Genetics and Crop Plant Research (IPK), Gatersleben, Germany*
- KUN HUANG • *Department of Plant and Soil Sciences, University of Delaware, Newark, DE, USA; Delaware Biotechnology Institute, University of Delaware, Newark, DE, USA*
- NIEN-CHEN HUANG • *Institute of Plant and Microbial Biology, Academia Sinica, Taipei, Taiwan*
- GUILLAUME HUMMEL • *Institut de Biologie Moléculaire des Plantes—CNRS, Université de Strasbourg, Strasbourg, France*
- JAFARGHOLI IMANI • *Research Centre for BioSystems, Land Use and Nutrition, Institute of Phytopathology, Justus Liebig University Giessen, Giessen, Germany*
- MARCO INCARBONE • *Gregor Mendel Institute of Molecular Plant Biology, Vienna, Austria*
- MIN JIA • *Friedrich Miescher Institute for Biomedical Research, Basel, Switzerland; University of Basel, Basel, Switzerland*
- HAILING JIN • *Department of Microbiology and Plant Pathology, Center for Plant Cell Biology, Institute for Integrative Genome Biology, University of California, Riverside, CA, USA*
- SOLMAZ KHOSRAVI • *Leibniz Institute of Plant Genetics and Crop Plant Research (IPK), Gatersleben, Germany*

- KARL-HEINZ KOGEL • *Research Centre for BioSystems, Land Use and Nutrition, Institute of Phytopathology, Justus Liebig University Giessen, Giessen, Germany*
- TINO KÖSTER • *RNA Biology and Molecular Physiology, Faculty of Biology, Bielefeld University, Bielefeld, Germany*
- CHRISTOPHER J. KRUEGER • *Department of Biomedical Engineering, College of Engineering, Peking University, Beijing, China; Wallace H. Coulter Department of Biomedical Engineering, Georgia Institute of Technology, Atlanta, GA, USA*
- JULIE KUBINA • *Institut de Biologie Moléculaire des Plantes—CNRS, Université de Strasbourg, Strasbourg, France*
- STÉPHANIE LALANDE • *Institut de Biologie Moléculaire des Plantes—CNRS, Université de Strasbourg, Strasbourg, France*
- DEBBIE LAUDENCIA-CHINGCUANCO • *USDA ARS Western Regional Research Center, Albany, CA, USA*
- ALEXANDER LICHIOUS • *Department of Microbiology, The University of Innsbruck, Innsbruck, Austria*
- KAI-REN LUO • *Institute of Plant and Microbial Biology, Academia Sinica, Taipei, Taiwan*
- SHIQI MAO • *Department of Biomedical Engineering, College of Engineering, Peking University, Beijing, China*
- BLAKE C. MEYERS • *Donald Danforth Plant Science Center, St. Louis, MO, USA*
- ALEXANDER F. PALAZZO • *Department of Biochemistry, University of Toronto, Toronto, ON, Canada*
- EDUARDO JOSÉ PEÑA • *Instituto de Biotecnología y Biología Molecular, CCT—La Plata CONICET, Fac. Cs. Exactas, U.N.L.P., La Plata, Argentina*
- DAVID PELIEGER • *Institut de Biologie Moléculaire des Plantes, CNRS UPR2357, Université de Strasbourg, Strasbourg, France*
- XAVIER PICHON • *Institut de Génétique Moléculaire de Montpellier, Université de Montpellier, CNRS, Montpellier, France; Equipe labélisée Ligue Nationale Contre le Cancer, Montpellier, France*
- HOLGER PUCHTA • *Botanical Institute, Karlsruhe Institute of Technology, Karlsruhe, Germany*
- LULU QIAO • *Department of Microbiology and Plant Pathology, Center for Plant Cell Biology, Institute for Integrative Genome Biology, University of California, Riverside, CA, USA*
- MAURICIO A. REYNOSO • *Instituto de Biotecnología y Biología Molecular, Facultad de Ciencias Exactas, Universidad Nacional de La Plata, Centro Científico y Tecnológico-La Plata, Consejo Nacional de Investigaciones Científicas y Técnicas, La Plata, Argentina*
- CHRISTOPHE RITZENTHALER • *Institut de Biologie Moléculaire des Plantes du CNRS, UPR 2357, Université de Strasbourg, Strasbourg, France*
- MARIE-CÉCILE ROBERT • *Institut de Génétique Moléculaire de Montpellier, Université de Montpellier, CNRS, Montpellier, France*
- TWAN RUTTEN • *Leibniz Institute of Plant Genetics and Crop Plant Research (IPK), Gatersleben, Germany*
- MICHAEL RYCKELYNCK • *Université de Strasbourg, CNRS, Architecture et Réactivité de l'ARN, UPR 9002, Strasbourg, France*
- BART RYMEN • *Institut de Biologie Moléculaire des Plantes, CNRS UPR2357, Université de Strasbourg, Strasbourg, France*
- PATRICK SCHINDELE • *Botanical Institute, Karlsruhe Institute of Technology, Karlsruhe, Germany*

- MENGGE SHAN • *Department of Biology, University of Pennsylvania, Philadelphia, PA, USA; Genomics and Computational Biology Graduate Group, University of Pennsylvania, Philadelphia, PA, USA*
- RICHARD SIBOUT • *INRAE, UR BIA, Nantes, France; Institut Jean-Pierre Bourgin, UMR 1318, INRAE, AgroParisTech, CNRS, Université Paris-Saclay, Versailles, France*
- ROBERT H. SINGER • *Department of Anatomy and Structural Biology, Albert Einstein College of Medicine, Bronx, NY, USA; Gruss-Lipper Biophotonics Center, Albert Einstein College of Medicine, Bronx, NY, USA; Janelia Research Campus of the HHMI, Ashburn, VA, USA*
- SEERGAZHI G. SRIVATSAN • *Department of Chemistry, Indian Institute of Science Education and Research (IISER), Pune, India*
- DOROTHEE STAIGER • *RNA Biology and Molecular Physiology, Faculty of Biology, Bielefeld University, Bielefeld, Germany*
- CHONG TENG • *Donald Danforth Plant Science Center, St. Louis, MO, USA*
- JENS TILSNER • *Cell and Molecular Sciences, The James Hutton Institute, Dundee, UK; Biomedical Sciences Research Complex, The University of St Andrews, St. Andrews, UK*
- SOLEDAD TRAUBENIK • *Instituto de Biotecnología y Biología Molecular, Facultad de Ciencias Exactas, Universidad Nacional de La Plata, Centro Científico y Tecnológico-La Plata, Consejo Nacional de Investigaciones Científicas y Técnicas, La Plata, Argentina*
- EVELINA TUTUCCI • *Department of Anatomy and Structural Biology, Albert Einstein College of Medicine, Bronx, NY, USA; Systems Biology Lab, Amsterdam Institute of Molecular and Life Sciences (AIMMS), Vrije Universiteit Amsterdam, Amsterdam, The Netherlands*
- ELODIE UBRIG • *Institut de Biologie Moléculaire des Plantes—CNRS, Université de Strasbourg, Strasbourg, France*
- JOHN VOGEL • *DOE Joint Genome Institute, Lawrence Berkeley National Laboratory, Berkeley, CA, USA*
- MANISHA B. WALUNJ • *Department of Chemistry, Indian Institute of Science Education and Research (IISER), Pune, India*
- MING WANG • *Department of Microbiology and Plant Pathology, Center for Plant Cell Biology, Institute for Integrative Genome Biology, University of California, Riverside, CA, USA*
- FELIX WOLTER • *Botanical Institute, Karlsruhe Institute of Technology, Karlsruhe, Germany*
- JINGZE J. WU • *Department of Biochemistry, University of Toronto, Toronto, ON, Canada*
- XIAOTIAN WU • *Department of Biomedical Engineering, College of Engineering, Peking University, Beijing, China*
- YACHEN YING • *Department of Biomedical Engineering, College of Engineering, Peking University, Beijing, China*
- TIEN-SHIN YU • *Institute of Plant and Microbial Biology, Academia Sinica, Taipei, Taiwan*
- ZHIMING YU • *Research Centre for Plant RNA Signaling, College of Life and Environmental Sciences, Hangzhou Normal University, Hangzhou, China*
- MARÍA EUGENIA ZANETTI • *Instituto de Biotecnología y Biología Molecular, Facultad de Ciencias Exactas, Universidad Nacional de La Plata, Centro Científico y Tecnológico-La Plata, Consejo Nacional de Investigaciones Científicas y Técnicas, La Plata, Argentina*
- PENGCHENG ZHANG • *Research Centre for Plant RNA Signaling, College of Life and Environmental Sciences, Hangzhou Normal University, Hangzhou, China*

Part I

In Situ Detection of RNA Molecules Using FISH Techniques



Chapter 1

Tagging and Application of RNA Probes for Sequence-Specific Visualization of RNAs by Fluorescent In Situ Hybridization

Thomas Dresselhaus and Andrea Bleckmann

Abstract

To understand the development and differentiation processes within a tissue and a cell, analysis of the cell type-specific gene expression pattern as well as the subcellular localization of the produced RNAs is essential. The simplest and fastest method to visualize RNA molecules is in situ hybridization (ISH) on whole-tissue samples. Over the past 40 years, various labeling and visualization techniques have been established to analyze either the expression domain of genes in tissues (using the classical chromogenic detection system) or the specific subcellular localization of mRNAs (using fluorescently labeled probes). By using the Arabidopsis root tip as an example tissue, we describe and compare classic in situ hybridization techniques. The protocols described can be easily transferred to almost all other tissues or model organism with slight modifications.

Key words Fluorescent RNA in situ hybridization, Whole mount, FISH, TSA, Subcellular RNA detection, Root, Arabidopsis

1 Introduction

RNA in situ hybridization is the most accurate method to study gene expression patterns and is superior to approaches such as RNA detection by Northern blots lacking cellular resolution or promoter-marker studies that are often misleading due to stability differences of markers, their products, and the RNA of interest. RNA in situ hybridization is especially applied to study spatial and temporal gene expression patterns during development, but also in differentiated tissues [1, 2]. Classical RNA in situ hybridization is a rather cheap and fast method to analyze specific gene expression in tissues or at the subcellular level in a 2–3-day experiment. In this chapter, we describe and compare three different detection systems for whole-mount RNA in situ hybridization (ISH) to visualize specific RNAs in the root tip of *Arabidopsis thaliana* (Fig. 1). In an ISH experiment the cells are fixed, and the in vivo-produced

RNA ISH using NBT/BCIP	RNA ISH using Fast Red	RNA ISH using TSA
<p>Pros: highly sensitive, low background, robust reaction, good DIC images</p> <p>Cons: No subcellular resolution, middle cellular resolution, no counterstaining</p>	<p>Pros: can be visualised at a confocal, nuclei counterstaining possible, high cellular resolution</p> <p>Cons: Less sensitive, no subcellular resolution, no tissue clearing</p>	<p>Pros: Highly sensitive, high cellular and subcellular resolution, nuclei counterstaining possible</p> <p>Cons: Susceptible to high background, expensive</p>

Fig. 1 Comparison of the different staining methods. See text for details

mRNA is marked by the hybridization of a labeled antisense RNA probe, which is used for detection. The labeled antisense probes can be easily generated by transcription from a PCR product of a gene of interest in the presence of a small fraction of labeled uracil. Commonly used labels are digoxigenin, biotin, and fluorescein, which do not interfere with the RNA polymerase during RNA synthesis and which do not hinder nucleic acid hybridization. Afterwards, the bound probe can be visualized by enzyme-coupled antibodies in the investigated tissues and cells, respectively. The alkaline phosphatase (AP)-coupled antibody detecting the labeled probe facilitates the production of a precipitating dye, which indicates the tissue region/cell containing the target RNA. Using (1) BCIP/NBT as substrates, the specific RNA-containing tissues become blue in color and can be documented using light microscopy techniques such as differential interference contrast (DIC) microscopy. Alternatively, if (2) Fast Red is used as substrate, it is converted to a purple fluorescent stain, which can be visualized either by light microscopy or by a confocal microscope for higher

cellular resolution. To analyze mRNA distribution with a subcellular resolution, (3) a sensitive fluorescence detection system based on the enzymatic activity of a horseradish peroxidase (HRP) can be used. In combination with a tyramide signal amplification (TSA) system, the enzyme catalyzes multiple fluorescent labeling of the antibody. This enables to detect specific RNAs including mRNAs and small noncoding RNAs with high sensitivity and to determine their location with resolution at the subcellular level [3].

The enzymatic signal amplification achieved by the alkaline phosphatase or the peroxidase is essential for mRNA visualization in whole tissues, especially if cells will be analyzed deeper in the tissue. The fluorescent signal emitted by directly fluorescent-labeled RNA probes or fluorescent-labeled antibodies is often too weak and can commonly only be visualized in close proximity to the cover slide.

In conclusion, we recommend to use AP with NBT/BCIP for general expression studies and the HRP with TSA for the analysis of subcellular RNA distribution. The presented protocols are based on [4, 5] with modifications. A workflow overview can be found in Fig. 2. Variations of the protocols optimized for germline cells, oviducts, and developing seeds have been published elsewhere [6].

2 Materials

2.1 Labware

1. Pipettes.
2. PCR machine.
3. Agarose gel electrophoresis equipment.
4. Thermoshaker.
5. Benchtop centrifuge.
6. Plant growth chamber.
7. Sterilization oven.
8. Bottles with thermostable (≥ 200 °C) screw cap and pouring rings.
9. Razor blade.
10. Tweezers.
11. Syringe cannulas.
12. Vacuum concentrator.
13. Sieves to carry tissue samples for liquid exchange (*see Note 1*).
14. Glass petri dishes.
15. Glass Pasteur pipettes.
16. Shaker.
17. Sterile multi-well plates (fitting to the sieve size).

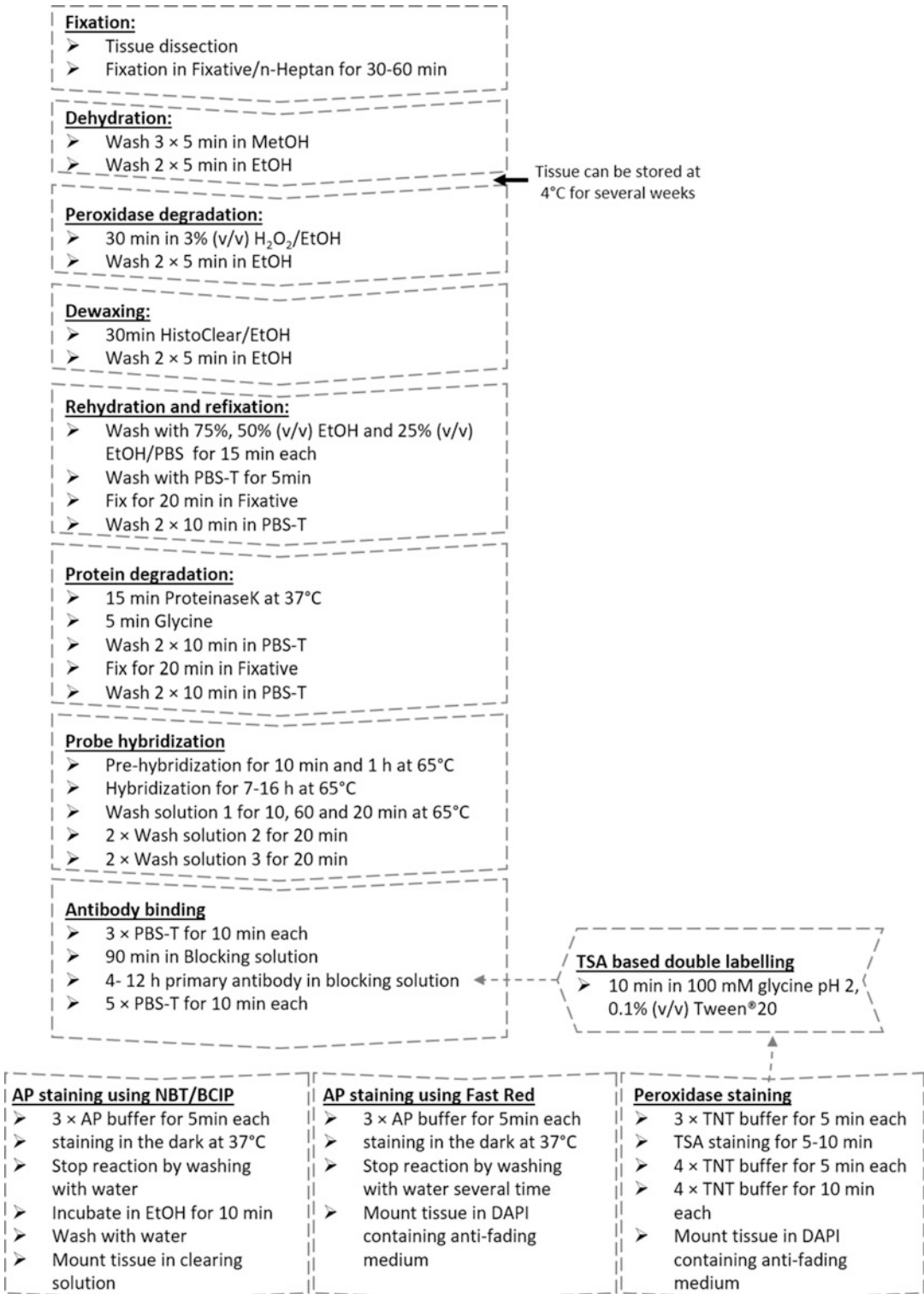


Fig. 2 Workflow diagram summarizing the ISH procedure

18. Hybridization oven.
19. Glass slides for microscopy.
20. Glass coverslips.
21. Clear nail polish.

2.2 Plant Growth Material

1. *Arabidopsis thaliana* Col-0 seeds.
2. 6% (v/v) Sodium hypochlorite solution.
3. 0.1% (w/v) Agarose in water, freshly autoclaved.
4. Squared petri dishes.
5. ½ Murashige and Skoog (MS) plates: ½ MS medium including vitamins and MES buffer pH 5.8 adjusted by potassium hydroxide and 0.8% (w/v) plant agar, autoclaved and poured into squared plates.

2.3 Synthesis of Labeled RNA Probes

1. PCR kit.
2. RNase-free double-distilled water.
3. T7 RNA polymerase (store at -20°C).
4. SP6 RNA polymerase (store at -20°C).
5. 10× Transcription buffer (supplied with the RNA polymerase).
6. 10× DIG RNA-labeling mix: 10 mM ATP, 10 mM CTP, 10 mM GTP, 6.5 mM UTP, 3.5 mM digoxigenin-11-UTP (store at -20°C).
7. 10× Fluorescein RNA-labeling mix: 10 mM ATP, 10 mM CTP, 10 mM GTP, 6.5 mM UTP, 3.5 mM fluorescein-12-UTP, pH 7.5 (store at -20°C).
8. RNase inhibitor (store at -20°C).
9. 20 mg/mL tRNA from *E. coli* (in RNase-free water; store in aliquots at -20°C).
10. DNase I (RNase-free; store at -20°C).
11. 0.5 M Ethylene-diamine-tetra-acetic acid (EDTA), pH 8.0 (RNase free).
12. 10 M Lithium chloride (LiCl), diethyl pyrocarbonate (DEPC) treated (*see* Subheading 3.1, step 4).
13. 2× Alkaline hydrolysis buffer: Mix freshly 600 μL of RNase-free double-distilled water, 240 μL of 0.5 M Na_2CO_3 , and 160 μL of 0.5 M NaHCO_3 .
14. Acetic acid.
15. 3 M Sodium acetate.
16. 10× 3-Morpholinopropane-1-sulfonic acid (MOPS) buffer: 0.4 M MOPS, 0.1 M sodium acetate, 0.01 M EDTA, pH 7.0. Prepare in RNase-free double-distilled water and

store in the dark. The buffer should be discarded when it turns yellow.

17. 2× RNA-loading dye: 95% Formamide, 0.025% SDS, 0.025% bromophenol blue, 0.025% xylene cyanol FF, 0.025% ethidium bromide, 0.5 mM EDTA.
18. Agarose.
19. 37% Formaldehyde.
20. 10× 3-(N-morpholino)propanesulfonic acid (MOPS): 0.4 M MOPS (pH 7.0), 0.1 M sodium acetate, 0.01 M EDTA (pH 8.0). All dilutions should be prepared with RNase-free double-distilled water.

2.4 Whole-Mount In Situ Hybridization (WISH)

1. 3% (v/v) H₂O₂ in double-distilled water.
2. 10% (w/v) Formaldehyde stock solution: Prepare a 10% (w/v) solution of paraformaldehyde in RNase-free double-distilled water. Heat solution (≥ 60 °C) carefully and add a few drops of 1 N NaOH until the solution becomes clear (pH ~8); check the pH using a pH paper indicator and store the solution in single-use aliquots at -20 °C. (Cautions: Vapors are toxic; work under a fume hood).
3. 10× Phosphate-buffered saline (PBS): 1.3 M NaCl, 70 mM Na₂HPO₄, 30 mM NaH₂PO₄, pH 7.4, treated with DEPC. Prepare all dilutions with RNase-free double-distilled water.
4. Fixative: 4% (w/v) Formaldehyde (from 10% stock solution), 15% (v/v) dimethyl sulfoxide (DMSO), 0.1% (v/v) Tween[®]20, in 1× PBS.
5. n-Heptan.
6. PBS-T: 1× PBS, 0.1% (v/v) Tween[®]20.
7. HistoClear/ethanol (1/1).
8. Freshly prepared 3% (v/v) H₂O₂ in ethanol.
9. 20× Saline sodium citrate buffer (SSC): 3 M NaCl, 0.3 M sodium citrate; adjust the pH to 7.0 with HCl and treat with DEPC. All dilutions should be prepared with RNase-free double-distilled water.
10. 75% (v/v) Ethanol in RNase-free double-distilled water.
11. 80% (v/v) Ethanol in RNase-free double distilled water.
12. 50% (v/v) Ethanol in PBS.
13. 25% (v/v) Ethanol in PBS.
14. Proteinase K stock solution: 25 mg/mL Proteinase K in RNase-free double-distilled water (store in single-use aliquots at -20 °C).

15. 10× Glycine solution: 200 mg/mL Glycine in RNase-free 10× PBS. Store aliquots at -20°C . Dilutions should be prepared with RNase-free double-distilled water.
16. 50 mg/mL Heparin stock solution (store at -20°C).
17. RNase-free fragmentized sperm DNA: Purify a fragmentized DNA (~500 bp) solution by phenol-chloroform-isoamyl alcohol extraction followed by a chloroform extraction and an ethanol precipitation. Resuspend in RNase-free double-distilled water. Adjust DNA concentration to 10–12 mg/mL using RNase-free double-distilled water.
18. Pre-hybridization solution: 50% (v/v) Formamide, 5× SSC, 0.1% (v/v) Tween[®]20, and 0.1 mg/mL heparin in RNase-free double-distilled water.
19. Washing solution 1: 50% (v/v) formamide, 2× SSC, 0.1% (v/v) Tween[®]20 in RNase-free double-distilled water.
20. Washing solution 2: 2× SSC, 0.1% (v/v) Tween[®]20 in RNase-free double-distilled water.
21. Washing solution 3: 0.2× SSC, 0.1% (v/v) Tween[®]20 in RNase-free double-distilled water.
22. Blocking solution: 3% (w/v) Bovine serum albumin (BSA) in PBS-T. Prepare freshly before use.
23. Anti-digoxigenin-AP-conjugated antibody (e.g., 1:2000 of the antibody 11093274910 from Roche in blocking solution).
24. Anti-digoxigenin-HRP-conjugated antibody (e.g., 1:1000 of the antibody NEF832001EA from Perkin Elmer in blocking solution).
25. Anti-fluorescein-HRP-conjugated antibody (e.g., 1:1000 of the antibody NEF710001EA from Perkin Elmer in blocking solution).
26. 1 M MgCl₂ (DEPC treated; *see* Subheading 3.1, step 4).
27. 2 M Levamisole in RNase-free double-distilled water (store aliquots at -20°C).
28. Alkaline phosphatase (AP) buffer: 0.1 M Tris-HCl (pH 9.5), 0.1 M NaCl, 50 mM MgCl₂ (freshly added), 0.1% (v/v) Tween[®]20.
29. 50 mg/mL Nitroblue tetrazolium chloride (NBT) stock solution (store at -20°C).
30. 50 mg/mL 5-Bromo-4-chloro-3-indoxyl phosphate (BCIP) stock solution (store at -20°C).
31. AP staining solution: AP buffer containing 2 mM levamisole, 220 μg/mL NBT, and 180 μg/mL BCIP.
32. TNT buffer: 0.1 M Tris-HCl (pH 7.5), 0.15 M NaCl, 0.05% (v/v) Tween[®]20.

33. TSA staining solution: Always prepare fresh following the manufacturer's instructions (e.g., TSA-Plus-Cyanine3-Kit; PerkinElmer).
34. Fast Red staining solution: Always prepare fresh following the manufacturer's instructions (e.g., SIGMAFAST™ Fast Red TR/Naphthol AS-MX tablets).
35. 100 mM Glycine pH 2, 0.1% (v/v) Tween®20.
36. Clearing solution: 70% (w/v) Chloral hydrate in 10% (v/v) glycerol.
37. DAPI-containing anti-fading mounting media.
38. 77% (v/v) Glycerol in PBS.

3 Methods

3.1 RNase Decontamination of Solutions, Glass- and Plasticware

1. Use sterile, disposable plasticware whenever possible—these should be RNase free.
2. Decontaminate other plasticware from RNases by soaking in 3% (v/v) hydrogen peroxide for 10 min followed by extensively rinsing with RNase-free double-distilled water.
3. Decontaminate glassware by baking at ≥ 180 °C for several hours (caution: use bottles with heat-resistant lids and pour ring).
4. Treat all solutions that are not containing compounds with primary amine groups with DEPC. Add 1 mL DEPC to 1 L solution, stir for ≥ 2 h, and autoclave to inactivate DEPC.

3.2 In Vitro Transcription of Labeled Probes

1. Select a 300–500-nucleotide (nt)-long region on the mRNA, which shows only low identity to related sequences (*see* Notes 2 and 3).
2. Design forward and reverse primers to amplify the DNA of the selected region by PCR from reverse-transcribed mRNA. To generate an antisense probe (complementary to the in vivo-transcribed RNA), the reverse primer starts with the T7 RNA polymerase promoter sequence (5'-TAATACGACTCACTATAG-3') (*see* Notes 4–6).
3. Perform PCR reaction according to the manufacturer's instructions.
4. Clean up the PCR product by a DNA purification kit according to the manufacturer's instructions and elute in RNase-free double-distilled water.
5. Set up a DIG RNA-labeling reaction according to the manufacturer's instructions (e.g.: DIG RNA Labeling Kit (SP6/T7), MERCK) (*see* Note 7).

6. Afterwards, add 1 U DNase I and incubate for 15 min at 37 °C to degrade the DNA template.
7. Transfer to ice and add 0.8 μL 0.5 M EDTA.
8. Add 1 μL 10 M LiCl.
9. Add 75 μL 100% (v/v) ethanol.
10. Precipitate RNA for ≥30 min at –80 °C.
11. Centrifuge for 30 min at ≥16,000 rcf and 4 °C.
12. Wash pellet with 80% (v/v) ethanol.
13. Centrifuge for 10 min at ≥16,000 rcf and 4 °C.
14. Let the pellet dry.
15. Dissolve the pellet in 100 μL RNase-free double-distilled water (*see* **Notes 8** and **9**).
16. Verify probe quality by separation in a denaturing agarose gel electrophoresis (*see* **Note 10**).

3.3 Growth of the Plant Material

1. Sterilize Col-0 seeds by washing them in 6% (v/v) sodium hypochlorite solution for 10 min.
2. Wash the seeds three times with ethanol.
3. Wash the seeds two times with sterile water.
4. Resuspend the seeds in 0.1% sterile agarose and stratify for 24 h at 4 °C.
5. Spread the seeds in lines on ½ MS plates using sterile Pasteur pipettes.
6. Incubate the plates vertically in a plant growth chamber for 7–10 days.

3.4 Tissue Fixation

All steps should be performed on a slowly rotating shaker. Liquid exchange from the glass petri dish or the multi-well plate should be performed using a 1 mL pipette with filter tips or baked glass Pasteur pipettes.

1. Prepare fresh fixative:n-heptane (1:1) emulsion by strong vortexing and shaking.
2. Add 1 mL of the emulsion to a 1.5 mL reaction tube for each sample.
3. Cut ~0.5 cm of the root tip using a razor blade, collect the tip, and transfer it as fast as possible into the fixative:n-heptane (1:1) emulsion using a tweezer. Only use roots growing on the medium surface. Collect ~20–30 root tips per tube.
4. Apply vacuum infiltration for 10–30 min (*see* **Note 11**).
5. Incubate the tissue for additional 30–60 min at room temperature (*see* **Note 12**).

6. Wash the tissue at least three times for 5 min with methanol by removing and applying the solution to the tube using a pipette, without touching the tissue.
7. Transfer the tissue using a tweezer to a sieve, which is standing in a glass petri dish half filled with ethanol (*see Note 13*).
8. Wash the tissue containing sieves two times for 5 min with ethanol by exchanging the liquid in the glass petri dish (*see Note 14*).

For the following steps, exchange the liquid in the glass petri dish containing the sieve. Take care that the entire liquid is removed from the petri dish before applying the next solution, but do not apply the solution into the sieve, as this may lead to damage or loss of the tissue sample.

3.5 Degradation of Endogenous Peroxidase

This step is only required if the HRP/TSA detection system shall be applied:

1. Incubate the sieves for 1 h in freshly prepared 3% (v/v) H₂O₂/ethanol.
2. Wash the sieves twice for 5 min with ethanol.

3.6 Permeabilization of the Tissue

1. Incubate the sieves in HistoClear/ethanol (1/1) solution for 30 min.
2. Wash the sieves three times each for 5 min with ethanol (*see Notes 15 and 16*).
3. Incubate the sieves in 75% and 50% (v/v) ethanol followed by incubation in 25% (v/v) ethanol/PBS for 15 min each.
4. Wash the sieves with PBS-T for 5 min.
5. Cross-link the tissue for 20 min by changing the liquid in the glass petri dish to fixative.
6. Wash the sieves twice with PBS-T for 10 min each.
7. Incubate the sieves in freshly prepared pre-warmed 150–400 µg/mL proteinase K solution for 15 min at 37 °C to degrade proteins bound to RNA (*see Note 17*).
8. Stop reaction by exchanging the liquid against glycine solution and incubate for 5 min.
9. Wash the sieves twice in PBS-T for 10 min each.
10. Cross-link the tissue for 20 min by sieve incubation in fixative.
11. Wash the sieves twice in PBS-T for 10 min each.

3.7 Hybridization of Probes

1. Incubate the sieves in pre-hybridization mix for 10 min and 60 min at the desired hybridization temperature (*see Note 18*).
2. Prepare the hybridization mix: Add freshly denatured fragmented salmon sperm DNA (denatured for 10 min at 95 °C) to a

final concentration of 1 mg/mL to pre-hybridization mix. Add labeled probe (*see Note 19*) and denature the solution for 10 min at 65 °C followed by incubation for 2 min on ice.

3. Distribute the sieves into multi-well plates.
4. Incubate the independent sieves 7–16 h with hybridization mix containing the individual probes at the selected hybridization temperature.
5. Wash three times with pre-warmed washing solution 1, first for 10 min, then for 60 min, and finally for 20 min at hybridization temperature.
6. Wash the sieves twice with washing solution 2 and twice with washing solution 3 for 20 min each at room temperature, to remove nonspecific and/or repetitive DNA/RNA hybridization.

3.8 Antibody Binding

1. Wash the sieves three times in PBS-T for 10 min each.
2. Incubate the sieves in blocking solution for 60 min.
3. Add the selected antibody diluted in blocking solution to the well and incubate the sieves in the well for 4–15 h at 21 °C (*see Note 20*).
4. Wash the sieves eight times with PBS-T for 10 min each.

3.9 Staining and Visualization of RNA

For RNA visualization choose between the three staining methods Subheadings 3.9.1–3.9.3 (*see Note 20*).

3.9.1 Chromogenic AP-Based Staining Using NBT/BCIP as Substrate

1. Wash the sieves twice with AP buffer.
2. Incubate the sieves in pre-warmed (37 °C) AP staining solution in the dark at 37 °C until a dark blue indigo staining is visible (initially check every 5 min; afterwards the periods can be extended).
3. Stop the reaction with 100% (v/v) ethanol for 10 min.
4. Rehydrate tissues with 50% (v/v) ethanol for 10 min.
5. Rehydrate tissues two times with PBS-T for 10 min.
6. For DIC microscopy, the roots are transferred and separated in a drop of clearing solution on a glass slide using a tweezer and cannulas (*see Note 21*).

A staining example is shown in Fig. 3a, c using *PLETHORAI (PLT1)* DIG- and *PLETOHORA3 (PLT3)* FITC-labeled probes.

3.9.2 Fluorescent AP-Based Staining Using Fast Red as a Substrate

1. Wash samples twice with AP buffer.
2. Incubate samples in pre-warmed (37 °C) Fast Red staining solution.

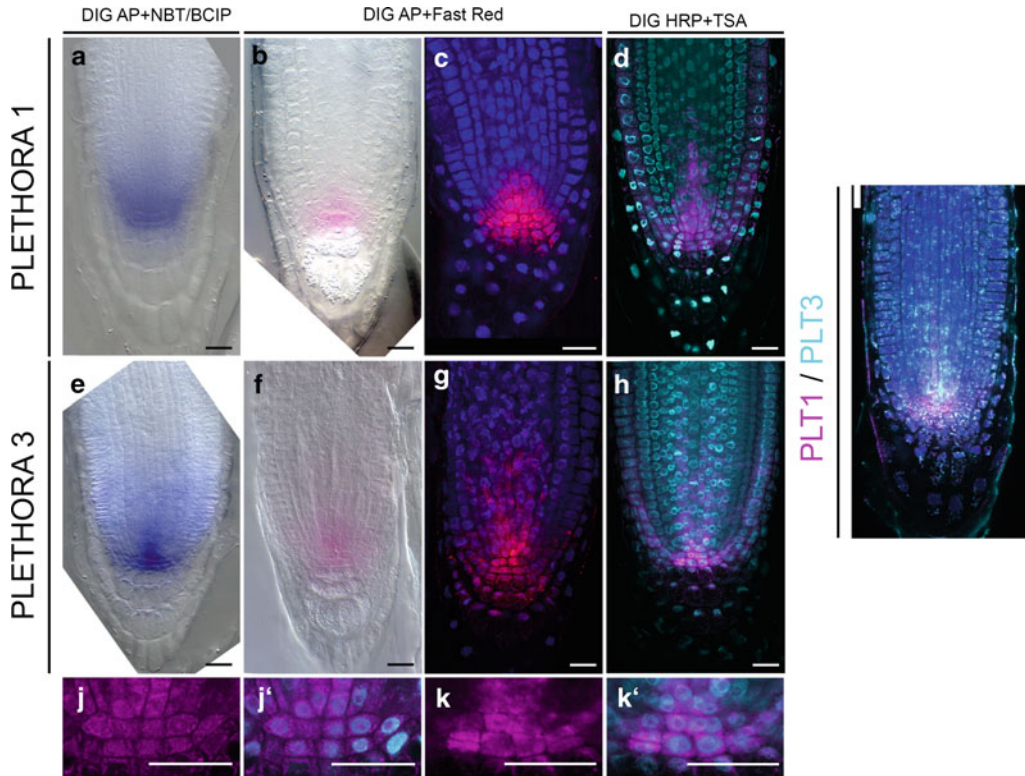


Fig. 3 Expression of the *PLETHORA* transcription factor genes in the root tip of *Arabidopsis*. Visualization of *PLT1* and *PLT3* mRNA by (fluorescent) whole-mount RNA ISH. (**a–d**) ISH using *PLT1*-specific DIG-labeled probes and (**e–h**) *PLT3*-specific FITC-labeled probes (**i**). (**a, e**) An alkaline phosphatase-linked antibody was used in combination with NBT/BCIP substrate for *PLT1*-specific DIG probe detection. (**b, f**) and (**c, g**) An alkaline phosphatase-linked antibody was used in combination with Fast Red substrate for *PLT1*-specific DIG probe detection. Nuclei are counterstained with DAPI (in **c, d, g, h, j',** and **k'**). (**d, h, j–k'**) *PLT1*-specific DIG probe detected with peroxidase-labeled antibody in combination with the TSA system TSATM Plus CY3 (magenta). (**i**) Co-stained *PLT1* (magenta) and *PLT3* (cyan) mRNA after two rounds of TSA staining (*PLT1* DIG-labeled mRNA stained with TSATM Plus Cyanine 3-Kit and *PLT3* FITC-labeled mRNA stained with TSATM Plus FITC-Kit (PerkinElmer). Subcellular mRNA distribution of *PLT1* (**j–j'**) and *PLT3* (**k–k'**). Scale bars are 20 μm

3. Incubate samples in the dark at 37 °C until a red staining is visible (initially check every 10 min; afterwards the periods can be extended).
4. Stop the reaction by washing the samples four times with PBS-T (*see* **Note 22**).
5. For light microscopy, the roots are transferred and separated in a drop of 77% (v/v) glycerol/PBS on a glass slide using a tweezer and cannulas.
6. For fluorescent microscopy the roots are transferred and separated in a drop of DAPI-containing anti-fading mounting

medium on a glass slide using a tweezer and cannulas (*see Note 21*).

- Analyze samples by fluorescence microscopy using either a bright-field microscope or a confocal laser scanning microscope (CLSM) using appropriate setting (*see Note 23*).

A staining example is shown in Fig. 3b, c, f, g using *PLT1* DIG- and *PLT3* FITC-labeled probes, respectively. Whereas Fig. 3b, f shows light microscopy images, Fig. 3c, g is acquired at a CLSM.

3.9.3 HRP-Based TSA Staining

- Wash the Sieves Twice with TNT Buffer.
- Incubate the sieves for 5–15 min in fresh TSA staining solution (*see Note 24*).
- Wash the sieves four times with TNT buffer for 5 min each.
- Wash the sieves four times with TNT buffer for 10 min each.
- Transfer and separate the roots in a drop of DAPI-containing anti-fading mounting medium on a glass slide using a tweezer and cannulas (*see Note 21*).
- Analyze samples using a CLSM. Microscope settings depend on the fluorescent dye used (*see Note 25*).

A staining example is shown in Fig. 3d, h using *PLT1* DIG- and *PLT3* FITC-labeled probes, respectively, each in combination with a TSA-CY3 substrate.

3.10 Double-TSA Labeling

- Follow the experimental procedure described in Subheading 3.4 up to **step 2** of Subheading 3.7.
- At **step 3** of Subheading 3.7, apply two different labeled probes in hybridization mix to the tissue (e.g., one labeled with DIG, the other labeled with FITC (*see Note 26*)) and incubate the independent sieves 7–16 h at the selected hybridization temperature.
- Wash three times with pre-warmed washing solution 1, first for 10 min, then for 60 min, and finally for 20 min at hybridization temperature.
- Wash the sieves twice with washing solution 2 and twice with washing solution 3 for 20 min each at room temperature, to remove nonspecific and/or repetitive DNA/RNA hybridization.
- Wash the sieves three times in PBS-T for 10 min each.
- Incubate the sieves in blocking solution for 60 min.
- Add one antibody directed against one labeled probe diluted in blocking solution to the well and incubate the sieves in the well for 4–15 h at 21 °C (*see Note 27*).
- Wash the sieves eight times with PBS-T for 10 min each.

9. Wash the sieves twice with TNT buffer.
10. Incubate the sieves for 5–15 min in fresh TSA staining solution.
11. Wash the sieves four times with TNT buffer for 5 min each.
12. Deactivate the HRP by sieve incubation in 100 mM glycine pH 2.0 and 0.1% (v/v) Tween[®]20 for 10 min.
13. Wash the sieves with PBS-T buffer.
14. Add the other antibody directed against the other labeled probe diluted in blocking solution to the well and incubate the sieves in the well for 4–15 h at 21 °C.
15. Wash the sieves eight times with PBS-T for 10 min each.
16. Wash the sieves twice with TNT buffer.
17. Incubate the sieves for 5–15 min in fresh TSA staining solution (use another fluorescent dye as in the first round) (*see Note 25*).
18. Wash the sieves four times with TNT buffer for 5 min each.
19. Wash the sieves four times with TNT buffer for 10 min each.
20. Transfer and separate the roots in a drop of DAPI-containing anti-fading mounting medium on a glass slide using a tweezer and cannulas (*see Note 21*).
21. Analyze samples using a CLSM. Microscope settings depend on the fluorescent dye used (*see Note 25*).

A double-TSA staining example is shown in Fig. 3i, using *PLT1* DIG probes visualized by HRP and TSA CY3 as well as *PLT3* FITC probes stained by HRP and TSA FITC.

The combination of HRP- and AP-based staining is straightforward as both antibodies can be applied at the same time. The TSA staining reaction should be performed (*see* Subheading 3.9.3, steps 1–4) before the AP staining reaction (*see* Subheading 3.9.2, steps 1–7).

3.11 Examples for the Different Staining Methods

Figure 3 shows the results of different staining methods using DIG- or FITC-labeled probes for the detection of *PLT* mRNAs (Fig. 3). The overlapping expression pattern of *PLT1* and *PLT3* genes is demonstrated. Both genes are highly expressed in the region of the quiescent center (QC) of the root and the surrounding stem cells, which can be visualized with all three methods. Using light microscopy, NBT/BCIP staining shows a significant better contrast compared to Fast Red staining. However, Fast Red-stained tissue provides a much higher cellular resolution than NBT/BCIP staining when observed by confocal microscopy, particularly when combined with DAPI counterstaining of the DNA. However, although this method allows to identify and demonstrate a cell-specific mRNA expression pattern, only the TSA system permits to

determine mRNA distribution at the subcellular level. Using the TSA system, it could be demonstrated that the *PLT1* and *PLT3* mRNAs are equally distributed throughout the cell (Fig. 3d, h). The main pros and cons of the different staining methods are summarized in Fig. 1.

4 Notes

1. For manual RNA (F)ISH experiments, self-made sieves prepared from stainless-steel mesh (mesh width of 25–100 μm) glued to reaction tube slices by heat can be used. Cut a 1.5 or 15 mL tube in ~ 0.8 cm rings. Heat one ring side until the plastic starts to melt and push it on the mesh. Control that the plastic completely seal the ring to the mesh. Remove the surrounding mesh. The resulting sieve can be used in the ISH experiment after sterilization with hydrogen peroxide. The sieves are placed in a glass petri dish or multi-well plates and the solution is exchanged outside of the sieve(s). During liquid exchange take care that the liquid is removed completely before adding the new liquid.
2. Coding sequence, 5' and 3' untranslated regions can be used. If possible select several nonoverlapping regions of the mRNA-encoding DNA for probe synthesis. Hybridization with either probe should lead to the same staining pattern. If hybridization leads to low signal strength, the application of a combination of different probes allows to increase antigen concentration at the target mRNA and thereby to increase staining intensity. An entire transcript can also be used for probe synthesis but needs to be fragmented to ~ 500 nucleotides, as long probes may have negative effects on hybridization efficiencies due to tissue penetration problems.
3. To establish RNA ISH experiments in your lab, start with probes that have been published and are known to detect an already described target mRNA expression pattern in your tissue of interest. Do not use a ubiquitously expressed gene for a start, as its stained RNA is difficult to be distinguished from background signals. The optimal negative control for RNA ISH experiments is the same antisense probe applied to mutant tissues that have no or at least a reduced specific transcript level. Potential cross hybridization of probes to related sequences leading to distorted staining pattern can only be identified using this control. The classic negative control—a sense probe—can generate strong staining if part of your gene of interest is also transcribed in antisense direction. Sense control probes are therefore not always applicable. Alternatively, a probe of comparable length and uracil content can be used as

negative control either if the corresponding gene is not expressed in the analyzed tissue or if the probe is transcribed from a scrambled sequence.

4. Alternatively, the SP6 RNA polymerase can be used for probe synthesis. In this case the SP6 promoter sequence (5'-ATTTAGGTGACACTATAG-3') must be added to the reverse primer. Sometimes, the transcription efficiency by SP6 polymerase is higher than by T7 polymerase.
5. To generate a sense probe, based on gene orientation, the promoter sequence is added to the forward primer.
6. Alternatively, to the template generation by PCR, the amplified mRNA region can be cloned into a plasmid, which contains T7 and SP6 RNA polymerase promoter sequences in the flanking regions. To use the plasmid DNA as template for the following *in vitro* transcription, it needs to be linearized at unique recognition sites for restriction enzymes creating blunt end or 5'-overhangs. Those restriction sites should be flanking the insert and located as close to the inserted sequence as possible. No terminator region flanks the insert, so the *in vitro* transcription stops when the template end is reached. The sequence between insert and cutting site will therefore be transcribed as well.
7. For double-labeling experiments a fluorescein- or biotin-labeled probe is needed.
8. Store probe in aliquots at $-80\text{ }^{\circ}\text{C}$ and avoid repeated freeze/thaw cycles.
9. Longer probes (>500 nts) can have negative effects on hybridization efficiencies or tissue penetration depth. The size can be reduced by hydrolysis to generate an optimal probe length of $\sim 300\text{--}500$ nts. For that propose, add 1 volume of freshly prepared alkaline hydrolysis buffer and incubate at $60\text{ }^{\circ}\text{C}$ for a calculated time (t) (t [min] = (probe length [kb]–desired probe length [kb])/($0.11 \times$ probe length [kb] \times desired probe length [kb])) [5]. Add acetic acid to a final concentration of 0.5% (v/v) and sodium acetate to a final concentration of 0.1 M to stop hydrolysis. Add 1 volume of isopropanol and incubate for ≥ 30 min at $-80\text{ }^{\circ}\text{C}$. Centrifuge ($\geq 16,000$ rcf) for 30 min at $4\text{ }^{\circ}\text{C}$. Wash pellet with 80% (v/v) ethanol. Centrifuge ($\geq 16,000$ rcf) for 10 min at $4\text{ }^{\circ}\text{C}$. Dissolve pellet after drying in 100 μL RNase-free double-distilled water.
10. To make a denaturing formaldehyde gel in MOPS buffer, melt 1 g of agarose in 72 mL of deionized water, add 10 mL of $10\times$ MOPS buffer and mix, add 18 mL of 37% formaldehyde in a fume hood and mix thoroughly, and pour the gel. Mix RNA samples and RNA ladder with RNA-loading dye, denature the samples at $70\text{ }^{\circ}\text{C}$ for 10 min, and chill on ice for 3 min

before loading them onto the gel. Use 1× MOPS buffer as running buffer. There is no need to stain the gel as ethidium bromide is present in the 2× RNA-loading dye.

11. We recommend to vacuum-infiltrate tissues using a vacuum concentrator, but a general vacuum pump is also fine. In that case apply the vacuum slowly to avoid tissue loss due to air bubbles.
12. We have extended this step up to 5 h and never observed an obvious difference in experimental result.
13. The tissue can be handled in the reaction tube as well, but the transfer to a sieve makes the liquid exchange much easier and faster. Also, any tissue sample losses during liquid exchange are minimized.
14. The fixed/dehydrated tissues can be stored in ethanol at 4 °C for several weeks.
15. From this step onwards, the sieves can be separated and further treated in wells of a multi-well plate, if different tissue samples are treated.
16. From this step onwards, the sieves with samples can also be mounted onto a liquid-handling robot system.
17. Critical Step! Proteinase K treatment can have negative effect on tissue integrity. However, if the proteinase K concentration is too low or if the time of proteinase K treatment is too short, the probe may not be able to hybridize with the protein-covered mRNA, thus resulting in a bad outcome of the experiment. We recommend testing different proteinase K concentrations to optimize the conditions.
18. We usually use a hybridization temperature of 65 °C, which works in most cases.
19. High probe concentration will lead to elevated background due to unspecific binding. We usually use a series of 0.1–2% of the original probe reaction mix in a 1 mL hybridization mixture to identify the perfect probe concentration.
20. Which antibody you should use depends on the probe label and the staining reaction you would like to perform. For a DIG-labeled probe and the NBT/BCIP or Fast Red labeling reaction, use a dilution of an anti-digoxigenin-AP-conjugate antibody. We used a 1:2000 dilution of the listed antibody. If you would like to perform a TSA staining reaction using the same probe, use an anti-digoxigenin-HRP-conjugated antibody. We used a 1:1000 dilution of the listed antibody. If you apply a fluorescein-labeled probe and a TSA staining reaction you need an anti-fluorescein-HRP-conjugated antibody. We used a 1:1000 dilution of the listed antibody.

21. Tissue is transferred into a drop of the desired mounting solution and the root tips are separated under a stereomicroscope. To prevent tissue crushing when covering the tissue sample with a coverslip, we use a drop of clear nail polish on the glass slide at the edges of the cover glass as spacer.
22. Do not use ethanol to stop the reaction or clearing solution like for NBT/BCIP staining procedure. The precipitated Fast Red is washed out by ethanol and bleached by clearing solution. Thus, it is not possible to clear the tissue for optimizing DIC microscopy images.
23. For the Fast Red dye, we used a 561 nm laser for excitation and the emission was detected between 570 and 640 nm. The DNA was counterstained with DAPI, which was excited at 405 nm and the emitted fluorescence was detected in the range of 420–470 nm.
24. The TSA staining reaction leads to the multi-labeling of the antibody and the enzyme itself, leading to its inactivation. Prolonged staining reactions are useless and will only increase the background.
25. For the TSA-CY3 staining, we used a 561 nm laser for excitation and the emission was detected between 570 and 640 nm. For the TSA-FITC staining, we used a 488 nm laser for excitation and the emission was detected between 500 and 550 nm. The DNA was counterstained with DAPI, which was excited at 405 nm and the emitted fluorescence was detected between 420 and 470 nm.
26. Try both labeling orientations: probe 1 labeled with DIG and probe 2 with FITC and vice versa, as the probes might have different efficiencies.
27. You may first apply the anti-digoxigenin-HRP-conjugated antibody and perform the staining reaction before applying the anti-fluorescein-HRP-conjugated antibody and the second staining reaction. However, to optimize the labeling, also try to do it the other way around.

Acknowledgments

This study was supported by the Collaborate Research Center SFB960 of the German Research Foundation (DFG—Germany) with funding to T.D.

References

1. Lécuyer E, Yoshida H, Parthasarathy N et al (2007) Global analysis of mRNA localization reveals a prominent role in organizing cellular architecture and function. *Cell* 131:174–187. <https://doi.org/10.1016/j.cell.2007.08.003>
2. Lawrence JB, Singer RH (1986) Intracellular localization of messenger RNAs for cytoskeletal proteins. *Cell* 45:407–415. [https://doi.org/10.1016/0092-8674\(86\)90326-0](https://doi.org/10.1016/0092-8674(86)90326-0)
3. Ghosh Dastidar M, Mosiolek M, Bleckmann A et al (2016) Sensitive whole mount in situ localization of small RNAs in plants. *Plant J* 88:694–702. <https://doi.org/10.1111/tpj.13270>
4. Jackson DP (1992) In situ hybridization in plants. In: Bowles DJ, Gurr SJ, McPherson M (eds) *Molecular plant pathology: a practical approach series 1*. Oxford University Press, Oxford, pp 163–174
5. Hejátko J, Blilou I, Brewer PB et al (2006) In situ hybridization technique for mRNA detection in whole mount Arabidopsis samples. *Nat Protoc* 1:1939–1946. <https://doi.org/10.1038/nprot.2006.333>
6. Bleckmann A, Dresselhaus T (2016) Fluorescent whole-mount RNA in situ hybridization (F-WISH) in plant germ cells and the fertilized ovule. *Methods* 98:66–73. <https://doi.org/10.1016/j.ymeth.2015.10.019>



Quantitative Fluorescence In Situ Hybridization Detection of Plant mRNAs with Single-Molecule Resolution

Kun Huang, Mona Batish, Chong Teng, Alex Harkess, Blake C. Meyers, and Jeffrey L. Caplan

Abstract

Single-molecule FISH (smFISH) has been widely used in animal tissue to localize and quantify RNAs with high specificity. This protocol describes an smFISH method optimized for highly autofluorescent plant tissue. It provides details on fixation buffers and protocols to protect the integrity of plant samples. We also provide smFISH hybridization conditions to detect plant RNA with ~50 fluorescently labeled DNA oligonucleotides. In addition, this protocol provides instructions on linear spectral unmixing of smFISH signal from background autofluorescence by confocal microscopy and a method to quantify the smFISH spots that reflect the copy number of target RNA.

Key words FISH, Single-molecule, In situ hybridization, Quantification, RNAs, Plant, Autofluorescence, Confocal, Linear spectral unmixing, Spectra

1 Introduction

The method of in situ hybridization is a powerful tool to add molecular context and localization at a tissue and cellular level to DNA [1], RNA [2], and chromosomes [3], using microscopic tools [4]. First-generation methods for in situ hybridization in plants detect messenger RNA (mRNA) used in vitro-transcribed digoxigenin (DIG)-labeled RNA probes. The enzymatic activity of DIG hydrolyzes its substrates and precipitates a purple/red color at its localization [5]. This result can be detected using bright-field light microscopes. Fluorescent in situ hybridization (FISH) in plants was achieved next, either by introduction of the fluorescent DIG substrates or by amplification of the DIG-labeled probes with fluorophore-coupled antibodies. The fluorescence generated using this method could be detected using a fluorescence wide-field microscope or a laser scanning confocal microscope. However, none of these methods provided single-molecule resolution, which is important to study the changes in RNA transcriptional levels

among individual cells as an important regulatory step controlling cellular processes [6]. Even subtle changes in RNA location and copy number at a particular time are critical for deciding the fate of a single cell [7]. To address this need, many in situ technologies have been developed that allow imaging of mRNAs at a single-molecule level, termed as single-molecule fluorescence in situ hybridization (smFISH) [8]. smFISH detects single mRNAs using an array of fluorescently labeled short oligonucleotide (17–22 nt) probes that hybridize to the target [9]. This method has been demonstrated to detect mRNA with high specificity in bacteria, yeast [8], mammalian cells [10], *C. elegans* [8], neuron cells [9], and single plant cells [11].

In this chapter, we describe an smFISH protocol that could be used in highly autofluorescent plant tissues. This protocol introduces PHEM (PIPES, HEPES, EGTA, MgSO_4) buffer to the fixation step to ensure the integrity of the treated plant cells. We also introduce linear spectral unmixing and an emission fingerprinting imaging mode to eliminate the interference by plant autofluorescence [12]. Finally, the protocol includes an approach for quantification of the smFISH signal in each sample.

2 Materials

Prepare all the solutions using Nanopure water. Do not use DEPC-treated water. All solutions should be stored at room temperature (25 °C) unless specified. Do not add Tween or other detergents to the solutions.

2.1 Sample Fixation, Embedding, and Sectioning

1. PHEM buffer (2×): 60 mM PIPES, 5 mM HEPES, 10 mM EGTA, 2 mM MgSO_4 , pH 8. Weigh 18.14 g of PIPES, 6.5 g of HEPES, 3.8 g EGTA, and 0.99 g MgSO_4 and add water to a volume of 500 mL. Store at 4 °C.
2. Fixation buffer: 4% Paraformaldehyde in PHEM buffer (1×). Add 1 ampoule (10 mL) of 16% paraformaldehyde to 30 mL PHEM buffer (1×). Fixation buffer should be prepared in a chemical fume hood.
3. Water bath at 50 °C.
4. Dissecting microscope.
5. Slide warmer.
6. Razor blades.
7. 20 mL Glass scintillation vials.
8. PBS buffer (10×): Dissolve 80 g of NaCl, 2 g of KCl, 14.4 g of Na_2HPO_4 , and 2.4 g of KH_2PO_4 . Adjust the pH to 7.1 and bring volume to 1 L with water. Autoclave sterilize and store at room temperature.

9. Ethanol.
10. HistoClear.
11. Wax.
12. 58 °C Oven.
13. Tissue embedding and processing cassettes.
14. Glass slides: Fisherbrand™ Tissue Path Superfrost™ Plus Gold Slides.
15. Paintbrushes: #0 Watercolor paintbrushes.
16. Paraffin microtome.
17. Vacuum bell jar and vacuum pump.

2.2 Pre-hybridization Slide Preparation

1. Ethanol series: Prepare a dilution series by adding water to 200 proof ethanol: 100%, 100%, 95%, 80%, 70%, 50%, 30%, and 10%. Put at least 250 mL of each dilution into a glass container.
2. Histo-Clear solution: Use 100% solution.
3. Protease stock solution: 50 mg/mL Protease. Dissolve 0.5 g protease in 10 mL water. Predigest the solution by incubating at 37 °C for 4 h. Store 650 µL aliquots at -20 °C.
4. TE solution: 10 mM Tris-HCl, 1 mM disodium EDTA, pH 8.0.
5. TE-protease solution: Prepare right before use. Pre-warm TE solution to 37 °C. Mix 1 aliquot (650 µL) of 50 mg/mL protease in 250 mL of TE solution.
6. 37 °C Incubator.
7. Phosphate-buffered saline (PBS; 1×): Dilute from PBS buffer (10×) with water.
8. 10% Glycine solution: Dissolve 5 g glycine in 50 mL water, filter sterilize, and then store at 4 °C.
9. 0.2% Glycine solution: Add 5 mL 10% glycine solution to 250 mL of PBS (1×).
10. TAE buffer: To 393 mL of nuclease-free water, add 5.2 mL of triethanolamine and 1.6 mL of HCl. Add 2 mL of acetic anhydride right before use. TAE buffer should be prepared in the chemical fume hood.
11. Glass staining dishes.
12. Slide holder (25 slide unit).

2.3 Hybridization

1. 100 mg/mL tRNA: Dilute 1 g tRNA in 1 mL RNase-free water. Store at -20 °C.
2. 50% Dextran sulfate solution: Add about 7 mL water to 5 g dextran sulfate powder. Heat the solution at 80 °C for about

1 h until it completely dissolves. Bring the volume to 10 mL. Mix well and store at -20°C .

3. Deionized formamide: Formamide is a teratogen and should be used in a chemical fume hood.
4. $20\times$ Saline sodium citrate buffer ($20\times$ SSC): Add 3 M NaCl to 0.3 M sodium citrate, pH 7.0.
5. Hybridization buffer: 10% Dextran sulfate (wt/vol), 1 $\mu\text{g}/\mu\text{L}$ tRNA, 2 mM vanadyl ribonucleoside complex, 0.02% RNase-free BSA, 10% formamide, SSC buffer ($2\times$). Filter sterilize and store at -20°C as 1 mL aliquots.
6. Hybridization oven.
7. Flat-bottom dishes (for humidity chamber).
8. Parafilm.
9. HybriSlip™ membrane hybridization covers.
10. Plastic wrap.

2.4

Post-hybridization Washing and Mounting

1. Washing buffer: 10% Formamide, SSC ($2\times$). Add 10 mL formamide and 10 mL SSC ($20\times$) to 80 mL water.
2. Glass dishes.
3. Rocking platform.
4. Mounting medium: SlowFade™ Diamond Antifade mounting medium with DAPI.
5. Clear nail polish.
6. #1.5 Cover glasses.

2.5

Imaging Acquisition and Analysis

1. Confocal microscope that has spectral unmixing capability.
2. Alpha Plan-Apochromat $100\times/1.46$ Oil DIC lens.
3. ImageJ or Volocity software (Quorum Technologies; *see Note 1*).

3 Methods

3.1 Probe Design

The target RNA sequence should be longer than 850 nt to ensure successful detection. Ideally, around 50 probes (minimum 25) are designed, distributed along the mRNA sequence. Each probe is 17–22 nt in length. The probes are designed using a Web program: Stellaris Probe Designer (<https://www.biosearchtech.com/support/tools/design-software/stellaris-probe-designer>). The designed probes could be directly ordered from the oligonucleotide synthesis companies with a coupled fluorophore for detection. The probes could also be ordered with a 3' end amino group and coupled with fluorophores manually [9]. In this protocol, the probes are coupled with the Alexa Fluor® 594 dye (“AF594”).

3.2 Sample Fixation

1. Dissect the samples (maize anthers as an example in this protocol) using a dissecting microscope with a fine knife and forceps.
2. Place samples in 20 mL glass scintillation vials. Immediately immerse the sample in fixation buffer. The volume of fixation buffer should be at least 15 times the relative volume of the sample.
3. Apply 0.08 MPa vacuum to the sample in a bell jar for 15 min and then release the pressure. Repeat this step three times or until the samples sink (*see Note 2*).
4. Store the samples at 4 °C. Samples can be stored for up to 7 days.

3.3 Paraffin Embedding and Sectioning

1. Fixed samples are then rinsed with PBS (1×) buffer for 30 min. And then dehydrate by going through an ethanol series (0%, 10%, 30%, 50%, 70%, 90%, 100%), 30 min each step.
2. Dehydrate the sample an additional two times, 30 min each time with 100% ethanol. Then leave the sample in 100% ethanol at 4 °C overnight.
3. Warm up the sample to room temperature.
4. Treat the sample with ethanol/Histo-Clear series (75% ethanol/25% Histo-Clear, 50% ethanol/50% Histo-Clear, 25% ethanol/75% Histo-Clear) for 1 h each step.
5. Immerse the sample in pure Histo-Clear three times, 1 h each time.
6. Leave about 5 mL Histo-Clear in the glass scintillation vial, add wax to fill the vial, and leave it in a 58 °C oven overnight.
7. Add wax to the vial every hour till the vial is completely filled with melted wax. Pour out the solution, and add in pure melted wax.
8. Replace the wax every 3 h four times.
9. Cast the processed samples onto the tissue-embedding and -processing cassettes and wait till the wax is solidified and completely cool.
10. Paraffin-embedded samples can be stored at 4 °C for up to 6 months.
11. Start a 50 °C water bath and 37 °C slide warmer.
12. Trim paraffin blocks into a trapezoid shape with a thin layer (about 2–3 mm) of paraffin on each side of the sample.
13. Collect sections with about 10 µm thickness. Examine the sections using a dissecting microscope to make sure that the collected sections have the desired morphology. Transfer 2–4 sections to the water bath with a paintbrush. Collect the sections onto a glass slide.
14. Leave the slides on the slide warmer to dry for at least 24 h. Dried slides can be stored at 4 °C for up to 1 week.

3.4 Pre-hybridization

Sample Preparation

1. Set up an incubator at 37 °C. Pre-warm the TE-protease solution to 37 °C.
2. Lay slides in a slide holder. Immerse the slides twice in Histo-Clear solution, 10 min each time.
3. Wash off the Histo-Clear solution by immersing the slides two times in 100% ethanol for 1 min each time.
4. Rehydrate the slides by immersing them successively for 30 s in each solution of 95%, 80%, 70%, 30%, and 10% ethanol (vol/vol).
5. Rinse the slides with water for 1 min.
6. Wash the slides two times for 2 min with PBS.
7. Transfer the slides to the TE-protease buffer prewarmed to 37 °C and incubate for 20 min (*see Note 3*).
8. Neutralize any formaldehyde autofluorescence by incubating the slides in glycine solution for at least 2 min. This step can be extended to 30 min.
9. Rinse the slides two times for 2 min with PBS (1×).
10. Prepare fresh TAE solution during the previous step. Incubate the slides in TAE solution for 10 min with gentle agitation (*see Note 4*).
11. Wash the slides two times for 2 min in PBS (1×).
12. Wash the slides in water for 1 min.
13. Dehydrate the slides by immersing them successively for 1 min in each solution of 10%, 30%, 50%, 70%, 80%, and 95% ethanol.
14. Incubate the slides two times for 1 min in 100% ethanol.
15. Store the slides in 100% ethanol for at least 2 h for sample permeabilization. Slides may be stored at 4 °C for up to 4 weeks.

3.5 Hybridization

1. Dilute the hybridization probe (*see Note 5*) to a stock concentration of 100 ng/μL using nuclease-free water. The starting probe concentration should be 1 ng/μL for most plant tissues (*see Note 6*). To prepare a hybridization mix, add 1 μL probe stock to 99 μL hybridization buffer to make a working stock. Mix the solution well by pipetting up and down several times, without causing bubbles.
2. Take out the slides from the 4 °C storage and warm up to room temperature.
3. Wash the slides in washing buffer for 2 min.
4. Apply 100 μL hybridization mix to each slide.
5. Apply the membrane hybridization cover, and tap on the membrane as it is lowered down to completely wet the tissue. Try to avoid bubbles.

6. Prepare a humidity chamber by laying parafilm on top of flat, wet tissue paper. Cut two diagonal corners of the parafilm to allow water to evaporate.
7. Lay the slides flat in the humidity chamber.
8. Incubate the slides in a 37 °C hybridization oven overnight.

3.6 Post-hybridization Washing

1. After hybridization, transfer the slides to a flat dish.
2. Float the hybridization membranes by adding 100 mL washing buffer to the dish.
3. Wash the slides three times for 20 min with 100 mL washing buffer.
4. Replace the washing buffer with 2× SSC, and allow the slides to equilibrate for 2 min.

3.7 Slide Mounting

1. Take the slides out from the washing buffer, and drain the buffer on a paper towel.
2. Add three drops of mounting medium to each slide.
3. Place a clean cover glass over the samples. Lower carefully to avoid bubbles.
4. Seal the sides of the cover glasses with clear nail polish.
5. Store the slides at 4 °C until they are imaged.

3.8 Imaging and Image Processing

Images should be captured using a confocal microscope with the capability of spectral imaging and linear unmixing. We used a Zeiss LSM 880 laser scanning confocal microscope with an Alpha Plan-Apochromat 100x/1.46 Oil DIC lens to acquire in situ images using emission online fingerprinting mode (*see Note 7*).

1. Acquire a positive control emission spectrum using pure dye with Lambda mode, in this case, AF594. Save this spectrum as the positive control.
2. Acquire autofluorescence spectra using unlabeled sample with Lambda mode. Save this spectrum as the autofluorescence.
3. At emission fingerprinting mode, assign detector RS1 and RS2 with positive control and autofluorescence, respectively. Then perform a slow scan at laser speed 4.
4. Tile imaging can be applied for large samples. In this case, we used a 2×2 tile with 10% overlap.
5. After imaging, stitch the tiles with a 0.90 correlation threshold using Zen software.
6. Filter the image using the 3, 3, 1 Median filter using Zen software.
7. Adjust brightness and contrast equally for all images.

3.9 Image Quantification

The number of localization events for each transcript can be calculated using Volocity or any other spot detection software, for example SpotCounter plug-in of ImageJ [13], or FISH-quant [14]. We used Volocity for generating the figure. However, directions for using the more readily available ImageJ FIJI software are provided below (For Volocity software parameters, *see* **Note 1**).

1. Remove noise using a noise filter. For ImageJ users, this step is done using Plugin → Analysis → SpotCounter. Set the prefilter to Gaussian1_5.
2. Set the intensity threshold and size limit to capture only the smFISH signal dots but not the background noise. The smFISH signal looks like punctate dots, while the background usually has undefined shapes and mixed intensity values. In Image J, set BoxSize to 6. Choose the Noise tolerance level so that only the smFISH dots were detected (with the check box for Check Settings selected).
3. Count the number of RNA spots detected.
4. At least three replicates should be used for statistical analysis.

4 Notes

1. We used Volocity for detecting smFISH signal. Any other dot detection software and smFISH image processing software can also be used, for example FISH-quant [14]. For Volocity users, the pathway we created was as follows: Remove noise using Volocity default noise filter. Create a Find Object pipeline for the R1 channel. We set a lower intensity threshold at 2, with a minimum object size of $0.01 \mu\text{m}^2$. The parameters we used are Clip to ROIs (draw a circle at the region of interest), Separate Touching Objects ($0.05 \mu\text{m}^3$), Exclude Object ($<0.05 \mu\text{m}^3$), and Exclude Object ($>0.8 \mu\text{m}^3$).
2. A good chemical fixation is critical for preserving the RNAs and shapes of the plant cells. Some plant samples are very difficult to fix. The ultimate standard is to have the sample sink to the bottom of the fixative. An extended vacuum time can be applied for hard-to-fix samples. A lightweight object could also be used to hold the sample below the fixation solution level to help penetration of the fixative.
3. Protease concentration and incubation times could affect the signal/background ratio. Generally, an incubation with 50 mg/mL protease for 20 min works for most plant tissues. If the obtained smFISH signal is weak, a higher protease concentration and longer incubation time can be used to increase probe penetration.
4. Treatment with triethanolamine-acetic anhydride (TAE) acetylates the positively charged amino groups. We use this step to

eliminate nonspecific binding of the probes. This step could be omitted when the target mRNAs are highly expressed.

5. We usually include hybridizations with a positive control probe and a negative control probe in each experiment. Any highly expressed gene or housekeeping gene can be used as a positive control. A scrambled sequence or a sequence from a gene of a different species could be used as a negative control. In the smFISH experiment shown in Fig. 1, we used a mouse

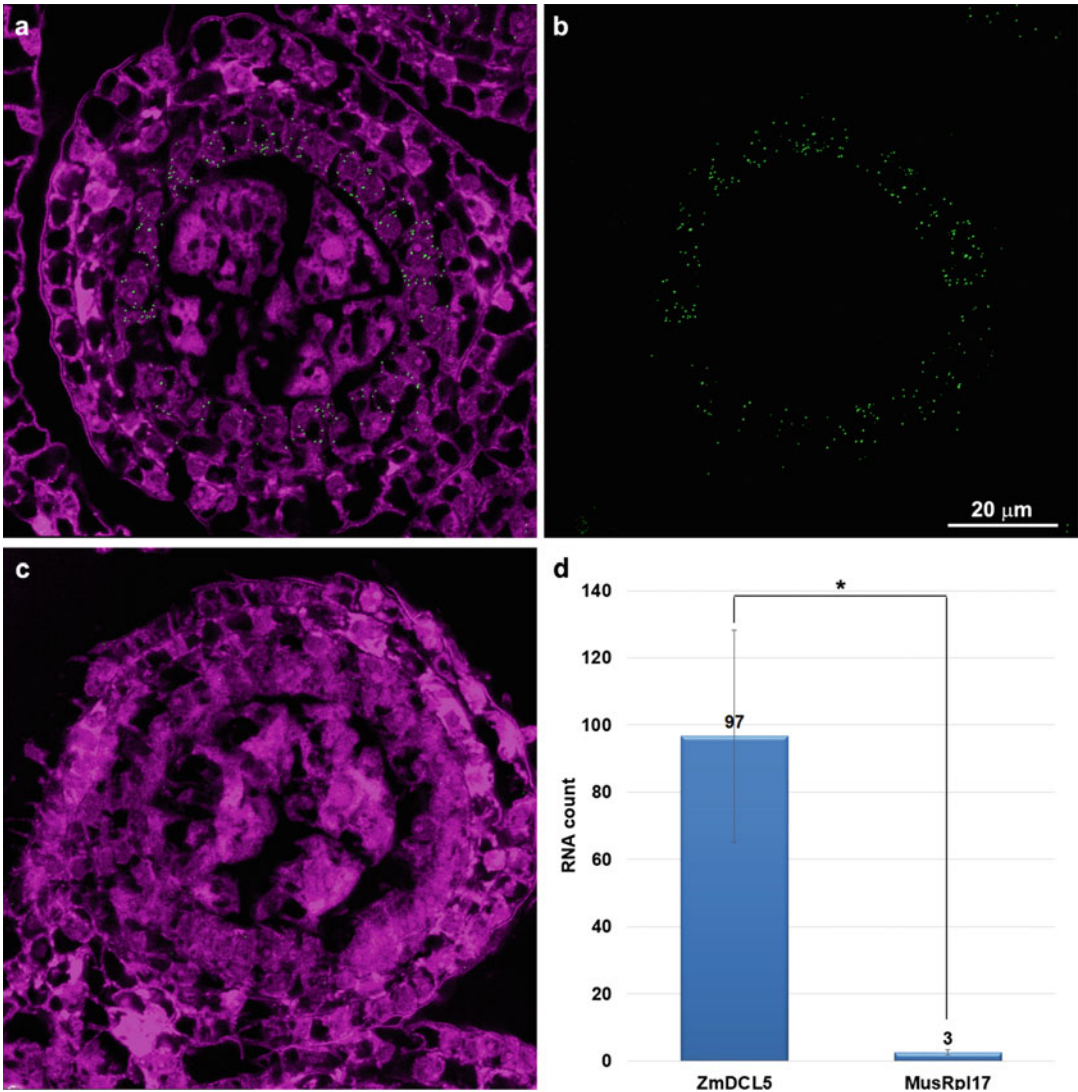


Fig. 1 An example of smFISH imaging in plant tissue. **(a)** Early-stage maize anthers were hybridized with probes against the maize gene encoding Dicer-like 5 (DCL5). Green smFISH spots correspond to DCL5 specifically localized to tapetal cell layer. Magenta shows autofluorescence of anther tissue layers. **(b)** The green smFISH signal spots of the image in panel **(a)**. **(c)** Mouse ribosomal protein 17 (MusRpl17) was used as a negative control. **(d)** After quantification with Volocity, we detected 97 localization events for DCL5 and 3 for the negative control. Error bars show standard error. Significance level: <0.05 , *; <0.01 , **

ribosomal protein 17mRNA (MusRpl17) as a negative control for maize tissue.

6. The concentration of the probe that should be applied varies from sample to sample. The starting concentration should be 1 ng/ μ L. Increase the concentration if the obtained smFISH signal is too weak. If high background is observed, decrease the probe concentration first to 0.3 ng/ μ L, and then to 0.1 ng/ μ L.
7. For confocal microscopes that do not have an emission online fingerprinting mode, a spectral image could be acquired and then linear unmixed using the positive and autofluorescence spectra.

Acknowledgments

This project was supported by the US NSF Plant Genome Research Program, awards 1649424, 1611853, and 1754097. We would like to thank members of the Batish lab for input on single-molecule in situ hybridization, and members of the Meyers and Caplan labs for help and support. Microscopy equipment was acquired with a shared instrumentation grant (S10 OD016361) and access was supported by the NIH-NIGMS (P20 GM103446), the NSF (IIA-1301765), and the State of Delaware.

References

1. Anamthawatjonsson K, Reader SM (1995) Pre-annealing of total genomic DNA probes for simultaneous genomic in-situ hybridization. *Genome* 38(4):814–816
2. Maluszynska J, Schweizer D (1989) Ribosomal RNA genes in B chromosomes of *Crepis capillaris* detected by non-radioactive in situ hybridization. *Heredity* 62(Pt 1):59–65
3. Fransz PF, Stam M, Montijn B, TenHooen R, Wiegant J, Kooter JM, Oud O, Nanninga N (1996) Detection of single-copy genes and chromosome rearrangements in *Petunia hybrida* by fluorescence in situ hybridization. *Plant J* 9(5):767–774
4. Weiss H, Pasierbek P, Maluszynska J (2000) An improved nonfluorescent detection system for in situ hybridization in plants. *Biotech Histochem* 75(2):49–53
5. Trinh le A, McCutchen MD, Bonner-Fraser M, Fraser SE, Bumm LA, McCauley DW (2007) Fluorescent in situ hybridization employing the conventional NBT/BCIP chromogenic stain. *BioTechniques* 42(6):756–759. <https://doi.org/10.2144/000112476>
6. Taniguchi Y, Choi PJ, Li GW, Chen H, Babu M, Hearn J, Emili A, Xie XS (2010) Quantifying *E. coli* proteome and transcriptome with single-molecule sensitivity in single cells. *Science* 329(5991):533–538. <https://doi.org/10.1126/science.1188308>
7. Tutucci E, Livingston NM, Singer RH, Wu B (2018) Imaging mRNA in vivo, from birth to death. *Annu Rev Biophys* 47:85–106. <https://doi.org/10.1146/annurev-biophys-070317-033037>
8. Raj A, van den Bogaard P, Rifkin SA, van Oudenaarden A, Tyagi S (2008) Imaging individual mRNA molecules using multiple singly labeled probes. *Nat Methods* 5(10):877–879
9. Batish M, Raj A, Tyagi S (2011) Single molecule imaging of RNA in situ. *Methods Mol Biol* 714:3–13. https://doi.org/10.1007/978-1-61779-005-8_1
10. Vargas DY, Shah K, Batish M, Levandoski M, Sinha S, Marras SA, Schedl P, Tyagi S (2011) Single-molecule imaging of transcriptionally coupled and uncoupled splicing. *Cell* 147(5):1054–1065. <https://doi.org/10.1016/j.cell.2011.10.024>
11. Rosa S, Duncan S, Dean C (2016) Mutually exclusive sense-antisense transcription at FLC

- facilitates environmentally induced gene repression. *Nat Commun* 7:13031
12. Huang K, Baldrich P, Meyers BC, Caplan JL (2019) sRNA-FISH: versatile fluorescent in situ detection of small RNAs in plants. *Plant J* 98:359–369. <https://doi.org/10.1111/tpj.14210>
 13. Schindelin J, Arganda-Carreras I, Frise E, Kaynig V, Longair M, Pietzsch T, Preibisch S, Rueden C, Saalfeld S, Schmid B, Tinevez JY, White DJ, Hartenstein V, Eliceiri K, Tomancak P, Cardona A (2012) Fiji: an open-source platform for biological-image analysis. *Nat Methods* 9(7):676–682. <https://doi.org/10.1038/Nmeth.2019>
 14. Mueller F, Senecal A, Tantale K, Marie-Nelly-H, Ly N, Collin O, Basyuk E, Bertrand E, Darzacq X, Zimmer C (2013) FISH-quant: automatic counting of transcripts in 3D FISH images. *Nat Methods* 10(4):277–278



Visualization of Endoplasmic Reticulum-Associated mRNA in Mammalian Cells

Jingze J. Wu and Alexander F. Palazzo

Abstract

In eukaryotes, most mRNAs that encode secretory or membrane-bound proteins are translated by ribosomes associated with the surface of the endoplasmic reticulum (ER). Other such mRNAs are tethered to the ER by mRNA receptors. However, there has been much debate as to whether all mRNAs, regardless of their encoded polypeptide, are anchored to the ER at some low level. Here we describe a protocol to visualize ER-associated mRNAs in tissue culture cells by single-molecule fluorescence in situ hybridization (smFISH). Using this protocol, we have established that a subset of all mRNAs, regardless of whether they encode secretory or cytosolic proteins, are ER associated in a ribosome-dependent manner.

Key words mRNA, Single-molecule localization, Cell extraction, Endoplasmic reticulum, Ribosomes

1 Introduction

In eukaryotes translation can occur in one of the two general compartments: free floating in the cytosol and attached to the surface of the endoplasmic reticulum (ER) [1]. Generally, it was believed that mRNAs encoding either cytosolic or nuclear proteins were translated exclusively in the former while mRNAs that encoded secretory, organellar, or membrane-bound proteins were mostly translated in the latter. The major difference between the two is that on the ER, ribosomes bind to the Sec61 translocon, which enables the newly synthesized polypeptide chain to traverse the membrane as it is translated, allowing for transmembrane domains to partition into the membrane, or luminal proteins to partition into the ER [2]. As a result, the newly synthesized protein adopts the right topology.

Generally, it is believed that the partitioning of an mRNA to one of these two compartments is dictated by the properties of the nascent polypeptide chain. In particular, any mRNA-ribosome-nascent polypeptide chain complex that contains a hydrophobic stretch of amino acids will recruit the signal recognition particle

(SRP) [3]. The SRP in turn mediates the recruitment of the mRNA-ribosome-nascent polypeptide chain complex to the SRP receptor which is present on the surface of the ER [4]. Once it has reached the ER, the ribosome directly binds to the surface of the translocon [5, 6]. The nascent chain is then transferred from the SRP to the translocon which allows it either to translocate across the membrane into the lumen of the ER or to diffuse through a lateral gate and incorporate into the membrane [2]. The idea that the SRP drives much of the membrane association of mRNAs has been validated through the examination of ER-derived ribosome-protected mRNA footprints [7].

Despite all this, the strict division between the cytosol and ER is not absolute. Many mRNAs that encode secretory proteins are translated by free ribosomes in the cytosol and their translational products are post-translationally targeted to the secretory pathway [8]. It is likely that these mRNAs encode nascent polypeptides that inefficiently recruit the SRP because they have short and/or mildly hydrophobic polypeptides. In addition, we and others have documented that a small fraction of all mRNAs that encode cytosolic or nuclear proteins are anchored to the ER by ribosomes [9–11]. This ER association is due to the initiation of translation by translocon-bound ribosomes. It turns out that non-translating ribosomes can associate with translocons and are capable of initiating translation [12–14]. In this case anchoring of mRNAs to translocon-bound ribosomes would occur before the emergence of any nascent polypeptide. These ribosomes would then translate the mRNAs on the surface of the ER. Due to the absence of any hydrophobic stretch, the nascent polypeptide would not be able to access the translocon. Instead the polypeptide would stay in the cytosol, despite the fact that it is synthesized from a translocon-bound ribosome. Indeed, since ribosomes that synthesize cytosolic loops of polytopic membrane-bound proteins remain associated to the translocon [15], it is clear that translocon-bound ribosomes can synthesize long polypeptide stretches that remain in the cytosol.

In addition to this, we and others have documented that mRNAs can associate with RNA-binding proteins that are present on the surface of the ER [16–19]. This allows for alternative ways of associating with the ER that are independent of the encoded polypeptide.

Here, we present a protocol to interrogate whether given mRNAs are anchored to the ER by single-molecule fluorescent in situ hybridization (smFISH), a powerful technique that allows the detection of mRNAs using a pool of probes (Fig. 1). Using appropriate controls (Fig. 2), we have shown that smFISH can be used to readily detect target mRNAs with high confidence. The resulting smFISH foci can be easily analyzed by most imaging software (for example, *see* Fig. 3) allowing the researcher to assess the number of a particular mRNA per cell. We have coupled this imaging

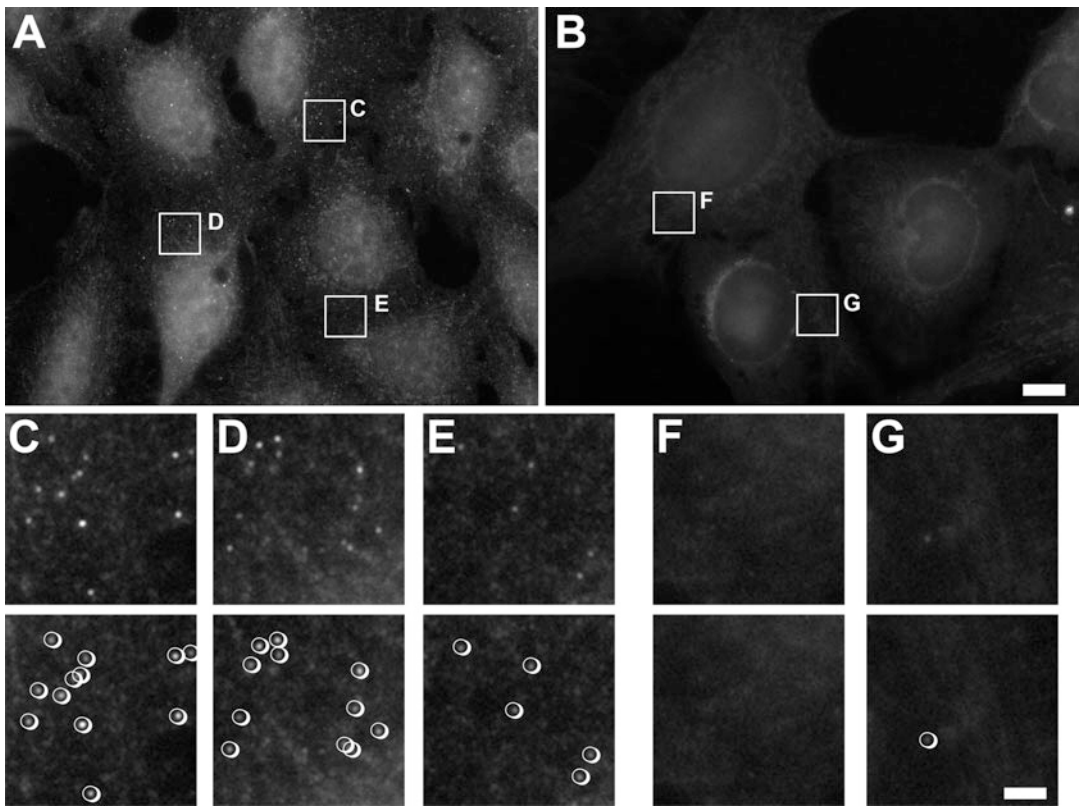


Fig. 1 Single-molecule FISH with control staining for autofluorescence. (a–g) Images of U2OS cells stained with (a, c–e) or without (b, f, g) Stellaris smFISH for *Gspt1* mRNA. Magnifications of the indicated inset are shown in (c–g). mRNA foci that are positively scored are circled. Note the presence of weaker foci in the stained cells (C–E) that are not true signals. Also note the presence of false-positive foci that appear due to autofluorescence (an example is circled in g). Scale bars = 10 μm (b); 50 μm (g)

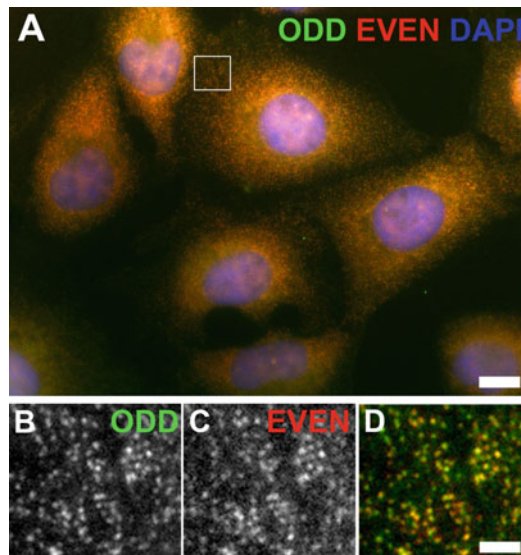


Fig. 2 Validation of single-molecule FISH by co-localizing complementary probes. (a–d) Image of U2OS cells stained for DNA (DAPI) and *GAPDH* mRNA using Stellaris smFISH probes, where the odd-numbered probes are conjugated to Quazar570, while the even-numbered probes are conjugated to Quazar670. A magnification of the white box in (a) is shown in (b–d). Scale bars = 10 μm (a); 50 μm (b)

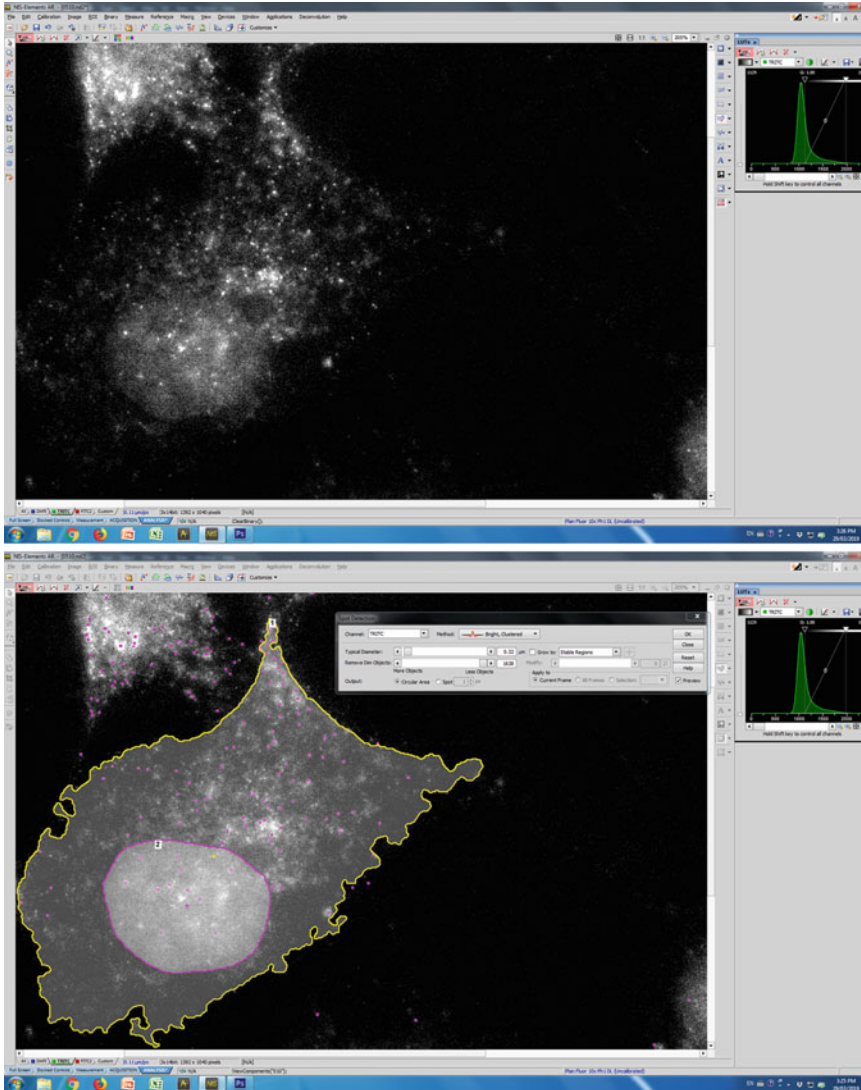


Fig. 3 Single-molecule FISH analysis. The analysis of smFISH using the Spot Detection module in NIS-Elements software. The top panel is an example of a raw image of smFISH of *GAPDH* mRNA in digitonin-extracted U2OS cells using Stellaris smFISH probes conjugated to Quazar570. The bottom panel is the same image where ROIs for the nucleus (magenta, ROI #1) and cell body (yellow, ROI #2) have been selected to be analyzed using the Spot Detection Module, with each selected foci colored in magenta

technique with a method to remove all the non-ER cytoplasmic content of cells. This involves the selective permeabilization of the plasma membrane using low levels of digitonin, which selectively removes cytosolic contents from mammalian cells, including proteins, mRNA, and ribosomes that are not tethered to the ER [14, 16, 20, 21]. Furthermore, when digitonin extraction is performed in a sucrose-containing buffer that preserves the integrity of the ER [22], mRNA-ER interactions are maintained

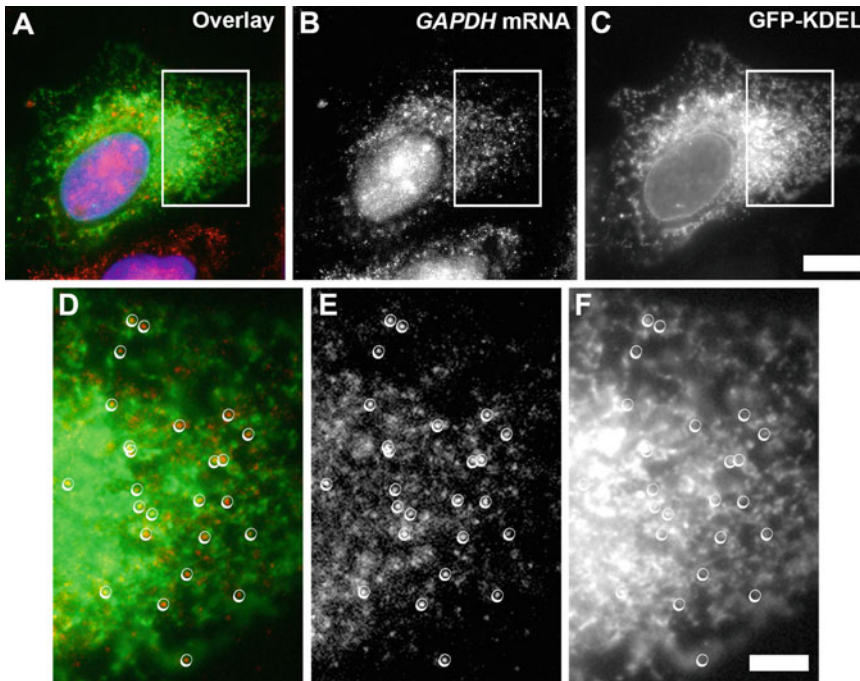


Fig. 4 Co-localization of GAPDH mRNA with the ER marker GFP-KDEL. (a–f) Image of a U2OS cell expressing GFP-KDEL (b), which was digitonin extracted and probed for *GAPDH* mRNA (c). Overlay of GFP-KDEL (green), *GAPDH* mRNA (red), and DAPI (blue) is shown in (a). Magnifications of the indicated inset are shown in (d–f). mRNA foci that are positively scored are circled. Scale bars = 10 μm (C); 30 μm (f)

[16, 21]. Combining this technique with smFISH can allow one to quantitatively assess how various mRNA species associate with the ER. We have used this protocol to determine that a small fraction of all mRNAs are anchored to the ER despite the fact that they encode proteins that do not engage the SRP-targeting system [11, 18] (Fig. 4).

2 Materials

2.1 Cell Culture Preparation

1. Dulbecco's modified Eagle medium (DMEM) supplemented with 10% fetal bovine serum and 1% penicillin/streptomycin (*see Note 1*).
2. Human osteosarcoma cells (U2OS): Maintain in DMEM medium supplemented with 10% fetal bovine serum and 1% penicillin/streptomycin in a 5% CO₂ incubator at 37 °C (*see Note 2*).
3. Porcelain coverslip staining racks.
4. Jeweler's forceps (*see Note 3*).

5. Circular glass coverslips (#1.5, 12 mm): Treat with 2 M HCl for 5 min, wash under a continuous stream of deionized water for at least 15 min, immerse in 75% ethanol for 15 min, dry in a biosafety cabinet to maintain sterility, and place it under UV for 1 h. Finally, store the dried coverslips in a sterile 10 mm petri dish at room temperature. Seal with parafilm to prevent contamination (*see Note 4*).
6. 12-Well cell culture plates.

2.2 Digitonin Extraction

1. 5% (w/v) Digitonin extraction buffer: Dissolve powdered digitonin in RNase-free Milli-Q water and store small aliquots at -20°C until needed.
2. 0.025% Digitonin extraction buffer: Dilute 5% digitonin extraction buffer 1:200 with warm CHO buffer immediately prior to use.
3. CHO buffer: 115 mM KAc, 25 mM HEPES pH 7.4, 2.5 mM MgCl_2 , 2 mM EGTA, and 150 mM sucrose in RNase-free water. Store at 4°C (*see Note 5*).
4. Heat block set to 40°C : To ensure that the heat block is sterile and RNase free, apply a few drops of deionized water to the surface of the heat block and cover this with a layer of parafilm. Remove any bubbles using RNase-free gloves by pressing firmly onto the parafilm to ensure a flat working surface.
5. RNase-free filter tips.
6. PBS: 0.14 M NaCl, 0.003 M KCl, 0.01 M Na_2HPO_4 , 0.002 M KH_2PO_4 , pH 7.4. Combine deionized H_2O to a final volume of 1 L.
7. 4% Paraformaldehyde fixing solution: Dilute 37% paraformaldehyde in PBS immediately prior to extraction.
8. 250 mL Beakers.
9. Methanol: Pour about 200 mL of methanol into a 250 mL beaker and store at -20°C for at least 30 min prior to experiment (*see Note 6*).
10. 35 mm Cell culture dishes.
11. Kimwipes.
12. RNase-free gloves.

2.3 smFISH Staining

1. $10\times$ Saline sodium citrate (SSC) buffer: 1.5 M NaCl, 150 mM sodium citrate, pH 8.0.
2. FISH hybridization buffer: $2\times$ SSC, 100 mg/mL dextran sulfate, 1 mg/mL yeast tRNA, 5 mM vanadyl riboside complex, 10% formaldehyde. Make up to 1 L, and store aliquots of 1 mL at -20°C (*see Note 7*).

3. 10% Formamide wash buffer: $2 \times$ SSC, 10% formamide. Make up to 1 L. Store at room temperature.
4. Stellaris mRNA probes (LGC Biosearch Technologies): Dissolve Stellaris mRNA lyophilized probes in RNase-free water to a final concentration of $12.5 \mu\text{M}$ and store at -20°C (*see* **Notes 8** and **9**) in a dark tube (*see* **Note 10**).
5. smFISH staining dish: Moisten the base of a 150 mm petri dish with deionized water, and then place a piece of parafilm cut to the size of the dish on top of the wet surface. Smooth out any excess water and bubbles underneath the parafilm using RNase-free gloves, so that the surface is flat (similar to the heat block parafilm preparation, refer to Subheading **2.2**, **item 4**).
6. Mounting solution with DAPI (*see* **Note 11**).

3 Methods

3.1 Digitonin Extraction

1. Seed cells on 12 mm acid-treated coverslips in 12-well cell culture plates at least 1 day prior to the experiment (*see* **Note 12**).
2. Pipette 100 μL of 0.025% digitonin extraction solution onto the parafilm on top of the 40°C heat block. It should form a firm liquid droplet. Repeat this process until the number of drops equals the number of coverslips to be extracted. This should be done immediately before you plan to extract and fix the cells.
3. To two 35 mm dishes, add 3 mL of warm (37°C) CHO buffer each.
4. To a 12-well plate, add 1 mL of 4% paraformaldehyde fixing solution per well per coverslip (adjust as needed). Place these near the heat block. For example, if there are eight coverslips in the experiment, add 1 mL of 4% paraformaldehyde fixing solution to 8 wells of a 12-well plate, and place aside to facilitate quick fixation later.
5. Remove the cells from the 37°C incubator and place them near the heat block.
6. Using a pair of jeweler's forceps, remove a coverslip from the 12-well and dip it into the two 35 mm dishes with CHO buffer (*see* **step 3**) consecutively to wash off excess media.
7. Quickly blot off excess liquid from the coverslip by touching the edge of the coverslip to a Kimwipe sheet (*see* **Note 13**), and then place the coverslip on a droplet of digitonin extraction buffer (*see* **step 2**) on the heat block, cell side down. When

blotting off the excess wash buffer, do not let the cells dry out as this will damage them.

8. After 20 s, remove the coverslip and place it cell side up into one of the free wells of the 12-well plate with 4% paraformaldehyde (*see* **step 4**). At this stage the cells are fixed and can be left aside until all the other coverslips are processed.
9. Repeat **steps 6–8** for the remaining coverslips. In addition to the main experiment, a series of control experiments should ideally be performed in tandem to validate the smFISH data (*see* **Notes 9, 14–17**). Other experiments can be conducted to ensure that the cytosol has been completely extracted (*see* **Note 18**).
10. Let coverslips sit in fixing solution for at least 15 min at room temperature.
11. Wash coverslips in PBS three times to remove the paraformaldehyde.
12. After the washes, transfer the coverslips onto a porcelain coverslip staining rack, ensuring that they are fully immersed in ice-cold methanol ($-20\text{ }^{\circ}\text{C}$) in a 250 mL beaker (*see* **Note 6**), for 30 min. Typically, we keep the beaker in a $-20\text{ }^{\circ}\text{C}$ freezer during the course of the experiment.
13. Transfer the rack from the methanol to a new 250 mL beaker containing room-temperature PBS (about 200 mL) to rehydrate the cells for 15 min.
14. Transfer the rack to a new 250 mL beaker with room-temperature PBS (about 200 mL) a second time to remove any remaining methanol and allow to sit for 15 min.

3.2 smFISH Staining and Mounting onto Slides

1. To prepare for the next washing steps, lay down a strip of parafilm on a wet flat surface, and remove any excess water, bubbles, or creases using RNase-free gloves.
2. For each coverslip, pipette 500 μL of 10% formamide wash buffer (*see* Subheading 2.3, **item 3**, **Note 19**) onto the parafilm, such that it forms a firm liquid droplet.
3. Pick up each coverslip with forceps and quickly wipe the non-cell side with a Kimwipe until it is dry (*see* **Note 20**). Carefully transfer each coverslip cell side down onto the droplet of 10% formamide wash buffer and incubate for 5 min.
4. Repeat Subheadings 3.1, **steps 1–3**, to wash a second time.
5. Pipette 100 μL of FISH hybridization buffer with diluted Stellaris probes (*see* Subheading 2.3, **item 4**), or scrambled probes as control (*see* **Note 21**), onto the parafilm in the smFISH staining dish (*see* Subheading 2.3, **item 5**), so that it

forms a firm liquid droplet. Pipette as many droplets as there are coverslips to be stained.

6. Pick up each coverslip with forceps and quickly wipe the non-cell side with a Kimwipe until it is dry and free of salt crystals (*see Note 20*). Carefully transfer each coverslip cell side down onto the droplet of FISH hybridization buffer with diluted Stellaris probes, so that the coverslip floats on top of the liquid, leaving its cell side fully immersed while leaving the opposite side dry.
7. After transferring all the coverslips onto the parafilm, place the lid onto the petri dish and seal edges with parafilm. Place the petri dish into a 37 °C cell incubator for 24–48 h.
8. Again, lay down a fresh strip of parafilm on a wet flat surface, and remove any excess water, bubbles, or creases using RNase-free gloves.
9. For each coverslip pipette three droplets of 500 µL of 10% formamide wash buffer onto the parafilm.
10. Remove the petri dish from the 37 °C cell incubator. Slowly pipette 200 µL of 10% formamide wash buffer directly beside each coverslip and allow for the wash buffer to seep beneath each coverslip, floating it above the parafilm (*see Note 22*).
11. Carefully pick up the coverslip with forceps, transfer it onto one of the wash droplets on the strip of parafilm (*see Subheading 3.2, step 9*), and let sit for 5 min at room temperature. Repeat this process twice more by transferring each coverslip onto a fresh droplet of wash buffer after 5 min.
12. The smFISH-stained cells can at this stage be immunostained to co-localize smFISH foci with ER markers (*see Note 23*).
13. In between washes, prepare sterile glass slides by pipetting ~15 µL of DAPI mounting solution onto each glass slide (*see Note 11*).
14. After three washes, carefully remove each coverslip from the droplets of wash buffer and dry any excess liquid with Kim-wipes. Each coverslip is then placed, cell side down, onto a droplet of DAPI mounting solution on the glass slides.
15. Slides are then labeled and can be stored at 4 °C. Note that slides should be allowed to dry for at least 24 h prior to imaging.

3.3 Imaging and Quantification

1. smFISH-stained cells are imaged with an epifluorescence or a confocal microscope using a 60× PlanApo objective (*see Note 24*).
2. Acquire images of the smFISH and DAPI channel for each field (*see Note 25*).

3. Process the imaging data with imaging software (*see Note 24*).
4. Select regions of interest (ROI) for the whole cell and nucleus, and then identify and count the fluorescent spots. The quantification of foci can then be used to determine the relative association of any given Stellaris probe marked mRNA to the ER (*see Note 26*).

4 Notes

1. To ensure sterility, add the fetal bovine serum and penicillin/streptomycin to the DMEM in a biosafety cabinet. Since we found that using cold DMEM can cause some U2OS cells to detach during cell maintenance, we warm the DMEM in a 37 °C water bath for at least 15 min prior to usage.
2. It is very helpful to use cell culture lines that have a very well-defined ER morphology. To that extent, we primarily use human osteosarcoma cells (U2OS) and green African monkey kidney fibroblast-like cells (COS7) in our experiments.
3. Sterilize by flaming the tips of the forceps for 2–5 s prior to use. Ensure that the tips are not too hot when interacting with coverslips, so as not to damage coverslips/cells.
4. Treating coverslips with acid helps to etch and clean the surface, which in turn helps promote cell spreading. Well-spread cells permeabilize much more efficiently than rounded cells for reasons that are still not entirely clear. Post-acid treatment, ample washes with deionized H₂O are necessary to remove the acid completely and thus prevent unwanted acid contamination in later steps. UV treatment prior to storage helps to sterilize the coverslips.
5. Warm up 1× CHO buffer in 37 °C water bath prior to use. Typically, about 10–25 mL of 1× CHO buffer is used per experiment which could consist of two to a dozen 12 mm coverslips. CHO buffer was formulated to maintain the integrity of ER preparations isolated from cell lysates [22].
6. We found that using ice-cold methanol extraction prior to coverslip mounting helps reduce autofluorescent signals during imaging.
7. Since we typically dilute the Stellaris probes 1:50 in deionized H₂O, and about 100 µL of the final diluted probe solution is used per 12 mm coverslip, 1 mL of FISH hybridization buffer is generally used in an experiment consisting of ten 12 mm coverslips. Use this as a general rule of thumb as to how many 1 mL aliquots of FISH buffer to thaw out, so as to avoid refreezing and rethawing.

8. These probes consist of a pool of oligonucleotides that are end-labeled with fluorophores. The sequences of these oligonucleotides can be designed on the company website (<https://www.biosearchtech.com/stellaris-designer>). Aim to have >20 probes per mRNA transcript. When visualizing short mRNAs, the limited amount of sequence can limit how many probes are made. For example with the *Sec61β* mRNA, which is only 564 nucleotides long, we have worked with as little as 12 probes [18].
9. To ensure that smFISH probes are specific for any given mRNA target, one can split the pool of Stellaris probes in two, with the odd and even probes conjugated to different fluorophores, as we have done previously [11]. This is only possible for transcripts that are stained with a high number of probes (>30). When the samples are stained with these two pools, all the foci should be visible in both fluorescent channels. An example is shown in Fig. 2 where GAPDH is stained with two sets of probes (odd probes are conjugated to Quazar570, while even probes are conjugated to Quazar670). In this particular experiment >90% of the foci co-localize. This control can be critical as many dim foci that are due to either background staining or autofluorescence may be mistaken for true mRNA-derived signals. Once this procedure is performed one can estimate how many foci are expected for that particular mRNA in a given cell type under a particular condition. We suspect that many studies involving Stellaris probes overestimate the number of mRNA foci by counting some of these background/autofluorescent foci signals.
10. Due to the light-sensitive nature of the probes, storing them in a dark tube or wrapping it in aluminum foil ensures that they do not lose their fluorescence in storage.
11. We use about 15 μL of mounting solution per 12 mm coverslip. Note that, since the solution is very viscous, it may be difficult to pipette accurately. Cutting the pipette tip to create a wider opening (>2 mm in diameter) helps in transferring the full amount of mounting solution.
12. For optimal digitonin extraction efficiency, as well as visualization by microscopy, one should aim for ~70% confluency prior to extraction. This typically entails seeding coverslips at ~30% confluency the day prior to the experiment. Ensure that coverslips are not overgrown, as it makes visualization of individual cells by microscopy extremely difficult.
13. When blotting excess liquid off with the Kimwipe, we found it most efficient to tilt the coverslip so that all of the liquid collects into a droplet—then blotting this droplet with the Kimwipe by pressing the tissue against the coverslip edge.

Immediately following, it is often best to wipe the non-cell side of the coverslip dry, to prevent bubbles and ensure clarity during imaging.

14. To determine the degree of ER association, one should stain cells where the digitonin extraction step is skipped (Subheading 3.1, steps 7 and 8). This can serve as a baseline control for any given experimental set. The membrane of these cells will be extracted during the incubation with ice-cold methanol (*see* Subheading 3.1, step 13).
15. To ensure that the observed smFISH mRNAs are truly anchored to the ER, it is also worthwhile to extend the length of extraction to ensure that all cells are permeabilized and all free mRNAs have diffused away, as we have done previously [11]. This can be tricky as the general integrity of the ER begins to deteriorate after very long extraction times. The degree of extraction can be assessed by phase or DIC microscopy. Extracted cells have a less dense cytoplasm, a more defined nuclear rim, and an increase in the number of round organelles—we believe this is due to mitochondria losing their extended shape during extraction.
16. To further validate that observed smFISH mRNA foci are anchored to the ER, smFISH signals can be co-imaged with an ER marker, such as GFP-KDEL (Fig. 4), or with an ER protein that is stained by immunofluorescence (*see* Note 23). One should be aware that certain overexpressed markers can disrupt mRNA-ER association. For example, we have observed that overexpression of GFP-Sec61 β disrupts the ER association of all other mRNAs [11, 18]. This is likely due to the *GFP-Sec61 β* mRNA effectively outcompeting all other mRNAs from ER-binding sites. Indeed, to further validate that observed smFISH mRNA foci are truly anchored to the ER, one can overexpress GFP-Sec61 β , and assess whether these foci disappear after digitonin extraction [11, 18].
17. To test for if smFISH RNA foci are associating with the ER in a translation-dependent manner, cells can be treated with compounds that dissociate ribosomes from the mRNA, such as puromycin [16].
18. To ensure that the cytosol has been extracted, one can stain the unextracted and extracted cells for various components. For cytosolic proteins, it is best to immunostain those that are present in the cytosol and nucleus, such as adenosine kinase [16], so that in the extracted cells the immunofluorescence signal is present only in the nuclear compartment. For mRNAs, those that encode cytosolic or nuclear proteins can be stained by smFISH; however digitonin extraction only removes about 90% of these from the cytosol, with the

remaining foci co-localizing with the ER [11]. Finally, one can immunostain ribosomes, which are partially removed by digitonin extraction, with the extraction-resistant signal co-localizing with the ER [16].

19. This buffer is optimized for Stellaris mRNA probes, and the concentration of formamide may vary with different FISH probes used. These washes should be performed with 500 μL droplets (*see* Subheading 3.2, **steps 2** and **9**) to conserve on formamide and reduce waste.
20. If the back surface of the coverslip is wet, it may draw the wash or the FISH hybridization buffer up over the top of the coverslip and away from the cell-facing side. This will lead to ineffective washing and staining. Dried salt crystals on the back surface will also cause problems. These salt crystals can be removed using a Kimwipe that has been moistened with some water.
21. All experiments should include a coverslip where the Stellaris probes are omitted (an example is shown in Fig. 1), or even better, with a set of probes with scrambled sequences. Ideally, cells that do not express the mRNA of interest (e.g., due to CRISPR/Cas9 deletion of its gene) make the best controls. Images taken of these cells will give a baseline of the type of fluorescence one should expect due to autofluorescence and binding of probes to nonoptimal target sequences. This will give some degree of certainty that the foci observed in a stained sample are brighter than either autofluorescence or probes hybridizing to off-target mRNAs. Despite this, unstained cells can have foci-resembling smFISH signals (*see* example in Fig. 1g). These controls are especially important when one is analyzing mRNAs stained with few probes, such as the *Sec61 β* mRNA.
22. Provided that the back side of the coverslip is dry and does not have any residual salt crystals, the liquid should seep underneath it by capillary action. If too much of the FISH hybridization buffer has evaporated, the wash buffer may not effectively seep underneath the coverslip. In this case, use a pair of forceps to slowly pry the coverslip from the parafilm until the liquid is drawn under. If this procedure is done too quickly, the added shear force may disrupt the integrity of the cells. Also, do not use excessive force, as this may break the coverslip. If this is a constant problem, consider using more probe solution so that it does not dry over the course of incubation. Alternatively, you can place a stack of Kimwipes drenched in deionized water in the incubation chamber to increase the humidity.
23. Co-staining of mRNA by smFISH with an ER marker by immunofluorescence can help to assess the degree of ER

association [16]. Before the smFISH-stained coverslips are processed for immunofluorescence, we recommend that they be extensively washed with PBS to fully remove any formamide, which can reduce the efficiency of immunolabeling. For the immunostaining, it is best to use purified antibodies and to avoid whole-serum preparations as these tend to contain RNase which will reduce the smFISH signal. Many protocols use whole serum to reduce background staining; however we have found that this can be done by including 1% bovine serum albumin and 0.1% Triton-X100 to the primary and secondary antibody solutions.

24. We use Nikon Imaging Software (NIS-Elements) to collect and process the micrographs.
25. To ensure that the fluorescence intensities between fields are comparable, the exposure time should remain constant between different fields of view and different coverslips. Furthermore, all of the imaging of one experimental set should be done in one sitting to minimize any day-to-day fluctuations in the intensity of the excitation light source.
26. To identify spots, use the Spot Detection Module on NIS-Elements (Fig. 3) using the Bright, Clustered Method option. For settings, for the “Typical Diameter” we use 0.32 μm , and for the “Remove Dim Objects” we set the level so that few to no spots are selected in images taken in parallel of cells where we either omit the smFISH probes or stain with scrambled probes (*see Note 19*). This is essential as there is always a low level of staining caused by autofluorescence or probes binding to suboptimal targets. The total number of spots in whole cell and nuclear ROIs are counted automatically using the “Automated Measurement Results” and the number of spots in the cytoplasm is calculated by subtracting the nuclear spots from the total cell spots. The number of nuclear foci can be used as a control to ensure that the unextracted and digitonin-extracted cells have been stained equally well. Nuclei should be impervious to digitonin extraction [20].

References

1. Cui XA, Palazzo AF (2014) Localization of mRNAs to the endoplasmic reticulum. *Wiley Interdiscip Rev RNA* 5:481–492
2. Rapoport TA (2007) Protein translocation across the eukaryotic endoplasmic reticulum and bacterial plasma membranes. *Nature* 450:663–669
3. Walter P, Ibrahimi I, Blobel G (1981) Translocation of proteins across the endoplasmic reticulum. I. Signal recognition protein (SRP) binds to in-vitro-assembled polysomes synthesizing secretory protein. *J Cell Biol* 91:545–550
4. Gilmore R, Blobel G, Walter P (1982) Protein translocation across the endoplasmic reticulum. I. Detection in the microsomal membrane of a receptor for the signal recognition particle. *J Cell Biol* 95:463–469
5. Görlich D, Prehn S, Hartmann E et al (1992) A mammalian homolog of SEC61p and SECYp is

- associated with ribosomes and nascent polypeptides during translocation. *Cell* 71:489–503
6. Görlich D, Rapoport TA (1993) Protein translocation into proteoliposomes reconstituted from purified components of the endoplasmic reticulum membrane. *Cell* 75:615–630
 7. Jan CH, Williams CC, Weissman JS (2014) Principles of ER cotranslational translocation revealed by proximity-specific ribosome profiling. *Science* 346:1257521
 8. Ng DT, Brown JD, Walter P (1996) Signal sequences specify the targeting route to the endoplasmic reticulum membrane. *J Cell Biol* 134:269–278
 9. Pyhtila B, Zheng T, Lager PJ et al (2008) Signal sequence- and translation-independent mRNA localization to the endoplasmic reticulum. *RNA* 14:445–453
 10. Jagannathan S, Reid DW, Cox AH et al (2014) De novo translation initiation on membrane-bound ribosomes as a mechanism for localization of cytosolic protein mRNAs to the endoplasmic reticulum. *RNA* 20:1489–1498
 11. Voigt F, Zhang H, Cui XA et al (2017) Single-molecule quantification of translation-dependent association of mRNAs with the endoplasmic reticulum. *Cell Rep* 21:3740–3753
 12. Seiser RM, Nicchitta CV (2000) The fate of membrane-bound ribosomes following the termination of protein synthesis. *J Biol Chem* 275:33820–33827
 13. Potter MD, Nicchitta CV (2002) Endoplasmic reticulum-bound ribosomes reside in stable association with the translocon following termination of protein synthesis. *J Biol Chem* 277:23314–23320
 14. Lerner RS, Seiser RM, Zheng T et al (2003) Partitioning and translation of mRNAs encoding soluble proteins on membrane-bound ribosomes. *RNA* 9:1123–1137
 15. Mothes W, Heinrich SU, Graf R et al (1997) Molecular mechanism of membrane protein integration into the endoplasmic reticulum. *Cell* 89:523–533
 16. Cui XA, Zhang H, Palazzo AF (2012) p180 Promotes the Ribosome-Independent Localization of a Subset of mRNA to the Endoplasmic Reticulum. *PLoS Biol* 10:e1001336
 17. Cui XA, Zhang Y, Hong SJ et al (2013) Identification of a region within the placental alkaline phosphatase mRNA that mediates p180-dependent targeting to the endoplasmic reticulum. *J Biol Chem* 288:29633–29641
 18. Cui XA, Zhang H, Ilan L et al (2015) mRNA encoding Sec61 β , a tail-anchored protein, is localized on the endoplasmic reticulum. *J Cell Sci* 128:3398–3410
 19. Hsu JC-C, Reid DW, Hoffman AM et al (2018) Oncoprotein AEG-1 is an endoplasmic reticulum RNA-binding protein whose interactome is enriched in organelle resident protein-encoding mRNAs. *RNA* 24:688–703
 20. Adam SA, Marr RS, Gerace L (1990) Nuclear protein import in permeabilized mammalian cells requires soluble cytoplasmic factors. *J Cell Biol* 111:807–816
 21. Cui XA, Palazzo AF (2012) Visualization of endoplasmic reticulum localized mRNAs in mammalian cells. *J Vis Exp* 70:e50066
 22. Allan V (1995) Protein phosphatase I regulates the cytoplasmic dynein-driven formation of endoplasmic reticulum networks in vitro. *J Cell Biol* 128:879–891



Simultaneous Detection of mRNA and Protein in *S. cerevisiae* by Single-Molecule FISH and Immunofluorescence

Evelina Tutucci and Robert H. Singer

Abstract

Single-molecule fluorescent in situ hybridization (smFISH) enables the detection and quantification of endogenous mRNAs within intact fixed cells. This method utilizes tens of singly labeled fluorescent DNA probes hybridized against the mRNA of interest, which can be detected by using standard wide-field fluorescence microscopy. This approach provides the means to generate absolute quantifications of gene expression within single cells, which can be used to link molecular fluctuations to phenotypes. To be able to correlate the expression of an mRNA and a protein of interest in individual cells, we combined smFISH with immunofluorescence (IF) in yeast cells. Here, we present our smFISH-IF protocol to visualize and quantify two cell cycle-controlled mRNAs (*CLN2* and *ASH1*) and the cell cycle marker alpha-tubulin in *S. cerevisiae*. This protocol, which is performed over 2 days, can be used to visualize up to three colors at the time (i.e., two mRNAs, one protein). Even if the described protocol is designed for *S. cerevisiae*, we think that the considerations discussed here can be useful to develop and troubleshoot smFISH-IF protocols for other model organisms.

Key words smFISH, Immunofluorescence, smFISH-IF, Single molecule, RNA FISH, RNA localization, Single-cell imaging, Cell cycle, *S. cerevisiae*

1 Introduction

Within single cells, molecules fluctuate in a stochastic fashion depending on their rate of synthesis and degradation. These fluctuations impact on the single-cell physiology, growth, fitness, and phenotypic heterogeneity [1]. Part of this variability is generated during the process of gene expression. Thus, tools yielding quantitative information on this process are of key importance to examine the biological consequences of molecular fluctuations. To this end the Singer lab developed single-molecule RNA fluorescent in situ hybridization to visualize and count absolute mRNA numbers in fixed cells [2]. This noninvasive approach allows a snapshot of intact cells where mRNAs can be localized and quantified without losing

the information coming from a single cell, as it happens with global mRNA measurements (i.e., qPCR, northern blot, RNA sequencing). By hybridizing tens of DNA probes conjugated to one or multiple fluorophores to the mRNA of interest, enough fluorescence is concentrated to detect an mRNA as a diffraction-limited spot. This method is not only useful to detect single mRNAs in the cytoplasm, but it can also be used to infer the number of nascent RNAs at a transcription site based on its fluorescence intensity [3, 4]. Recent advancements in probe design, fluorophores, detectors, and imaging analysis improved the robustness of this technique, which is now the method of choice to precisely quantify low-abundance mRNAs in all organisms, cell types, as well as tissues [5–11]. Many smFISH studies revealed significant cell-to-cell variability in mRNA concentrations, which influences many cellular processes, such as cell differentiation, development, and population fitness [5, 12]. Also, the possibility to localize mRNAs with subcellular resolution (i.e., nucleus vs. cytoplasm [13], yeast bud [14], polarized intestinal epithelial cells [15], or neuronal dendrites [16]) was important to understand how different stages of gene expression from transcription to degradation are coordinated [12, 14, 16].

Nonetheless, to extend the use of smFISH to report on complex cellular states, it is important to be able to look at more than one mRNA at the time or simultaneously look at mRNAs and proteins within single cells. Multicolor smFISH can be easily implemented to visualize up to four distinct mRNA species labeled, i.e., with Cy5, Cy3.5, Cy3, or FITC fluorophores [17]. More recently, several multiplexing single-mRNA imaging approaches have been developed based on different barcoding schemes and repeated rounds of hybridization, which allowed one to visualize potentially up to thousands of different mRNAs in single yeast or mammalian cells [18–20]. Although computationally demanding, this multiplexed imaging-based approach represents a powerful tool to perform in situ transcriptomics, complementing single-cell sequencing methods, especially for low-abundance mRNAs. Extended discussion on these approaches can be found elsewhere [11, 21].

Alternatively, to characterize a cellular state, an mRNA and a protein can be simultaneously visualized in single cells to gain further information about their function. For instance, to correlate the mRNA expression with the stage of the cell cycle, smFISH for a cell cycle-regulated mRNA can be combined with immunofluorescence (IF) for a cell cycle marker. Here, we describe a protocol to visualize two cell cycle-controlled mRNAs. The first is *CLN2*, a cyclin expressed in late G1 phase when it associates with the cyclin-dependent kinase Cdc28p to activate its kinase activity [22]. The second mRNA is *ASH1*, the best characterized yeast-localized mRNA [23–26]. *ASH1* mRNA is precisely expressed during anaphase, when it localizes to the bud tip to be locally translated and to control the mating-type selection in the daughter cell of wild-type

S. cerevisiae [27]. To distinguish the different phases of the cell cycle we performed IF against the microtubule component α -tubulin, encoded by the gene *TUB1*. Because during mitosis the microtubules extend from the spindle pole bodies between the mother and daughter cell [28], monitoring tubulin expression can provide precise information about the cell cycle phase that can be correlated with mRNA expression.

Few smFISH-IF protocols have been recently published for mammalian or insect cells [29, 30]. Here, we present our current smFISH-IF protocol for the model organism *S. cerevisiae*, which can be used to visualize up to three colors at the time (i.e., two mRNAs and one protein). The protocol is performed over 2 days, followed by imaging and analysis. The major steps are DAY 1, (1) coverslip coating (1 h); (2) growth, fixation, and permeabilization of the cells (overnight growth + ~4-h processing time); DAY 2, (3) smFISH hybridization and washes (4 h); (4) immunofluorescence and mounting (3 h); DAY 3, (5) image acquisition; and (6) imaging analysis (time depends on the aim of the experiment).

This approach can be applied to many different biological questions and model organisms; the limitation is the restricted number and the specificity of primary antibodies available, which can be circumvented by using tagged proteins. Subheading 4 describes alternative approaches to simultaneously visualize more than one mRNA and protein. These considerations may be useful as a primer to develop or troubleshoot smFISH-IF protocols for other yeast species or other model organisms.

2 Materials

Prepare all solutions using double-distilled ultrapure RNase-free water (DDW). Paraformaldehyde and deionized formamide are hazardous solutions. Wear protective gloves and handle them under a fume hood.

1. 0.1 N HCl.
2. 70% Ethanol.
3. Noncoated coverslips: 0.13–0.17 mm thick; diameter 18 mm.
4. Twelve-well culture dish.
5. 0.01% Poly-L-lysine.
6. 15 and 50 mL plastic tubes.
7. 1.5 mL Tubes.
8. Refrigerated centrifuges for 1.5 mL or 50 mL tubes.
9. Parafilm.

10. Incubators: For yeast cultures (25–30 °C); for smFISH hybridization ad washes (37 °C).
11. Yeast strain: *S. cerevisiae* BY4741 (MATa; his3Δ1; leu2Δ0; met15Δ0; ura3Δ0).
12. Synthetic complete medium (SC medium): 6.7 g/L Yeast nitrogen base (YNB) with ammonium sulfate, 2 g/L SC complete mix (e.g., Sunrise Science Products), 20 g/L D-(+) glucose >99.5%. Sterilize in the autoclave.
13. 32% (w/v) Paraformaldehyde. Store at room temperature (RT) and protect from light.
14. 3 M D-sorbitol: Filter sterilize and store at 4 °C.
15. Buffer B: 1.2 M Sorbitol, 100 mM potassium phosphate buffer [pH 7.5]. Store at 4 °C.
16. 200 mM Vanadyl ribonucleoside complex (VRC) stock solution: Dissolve the powder in the vial at 65 °C for 10 min and store aliquots at –20 °C.
17. Lyticase solution: Resuspend 25 K units in 1 mL 50% glycerol and 1× PBS. Store aliquots at –20 °C.
18. Spheroplast buffer: 1.2 M Sorbitol, 100 mM KHPO₄ [pH 7.5], 20 mM VRC, 20 mM β-mercaptoethanol, Lyticase (25 U per OD of cells).
19. TE buffer: 10 mM Tris-Cl [pH 8], 1 mM ethylenediaminetetraacetic acid (EDTA) [pH 8].
20. smFISH probe mix:
21. *ASH1*-Q670 probe set: smFISH probes mixed in an equimolar ratio and hybridizing to different positions along the *ASH1* mRNA (*see Note 1*) (cagcagataatgcatgcagt, gctattgcatggaatccg, atcggttgtgatattgtcc, aatacttctaggactgtct, aattggcgacacattgagcg, ccaagtatttcgtagccaa, gctggtgcagtatttgatt, gtaatccatatgatgtggcg, aattctggtgaattgcctgg, atctgagataagcttgccct, gaccatagttcaatggatt, acaatggtagtcgaggtgt, aagagacggacgatagcctg, agtgatggtaggctttgtg, gggtaataattgcagatgcc, gtgctgcgttttctgtaaa, acgttttgatgtatcaggga, tgggtaagatcagtttcca, gtcttgatagttgtatcct, ccacttctcgcgtatttta, gttgggtatacttaatggct, caattccttgccgtaattga, aacttgacgacctagtcga, atgattccttagacggg-gaa, gaggagtaatactccatgca, tattggttggtggactcatc, aaaagaggcctcactcct, atcgttattgctggattcc, ttccacgtaattgtctttga, gcatttggcatgggaaatga, actgttcgctttttgtgac, gtctctattcgcaagcaatt, tgtctttagatggttccct, gtcttgacagtgtaccgaaa, ggtgaggatgatcttgatct, gataattgggtgaccttggg, gggagagtcgagagcaaatc, atttgatgatcttcgagggc, tacttcccttttctgattatg, tgtgacgagtggtgatgag, gggcgaaactactcgaatgac, gttacatagctgatcttgct, aataagcaacggtacccctc, ctctactgtctcagttatgt, cgcggcgtgtcgatgaaaa). Resuspend the

probe set in TE buffer to a final concentration of 25 μ M and store in aliquots protected from light at -20°C .

22. *CLN2*-Q570 probe set: smFISH probes mixed in an equimolar ratio and hybridizing to different positions along the *CLN2* mRNA (*see Note 1*) (ttgatgacgagtccatacg, cggatagtagtccggtttag, attctgcattagatagctca, ttcttgacgacatttcgaagt, aacattgggtggagatttctt, gctggtctattagtttggga, taatgttgacattgtttcc, ccacagacagctcgaacaaa, ataccatttgctactcgagt, ctcttggacaataagcggtc, acaaccaatttggcttggtc, agccaaccagagacaagtag, atgatgtgattacaaccgcc, ccagtagggatgactacatt, gggttgggaccataaaatct, cagagagtgcaggtatacgt, gaccatcaccacagtaatga, gtctagtatatgtctttcca, gactgacgtttttcagagca, tctacagtgcatcactatc, ttaagtctctctctctctc, ctaagtaagtcgtactgcca, gagaatatgccgtgcatgatac, aaaggaccgtggtcttgatt, gctttctgatgtcattggag, atgccgttcattaaggact, cttccatcaaggagtagga, agaacaccattgaccgtttt, caagtgatattctttcact, gttgga-tgcaatttgcagtt, gatatggtaagctttctcga, ttcgaagagcatgatgggg, gcgaaggaatggatgtgcta, gagtgtggctttgagatgag, atcagagagt-gagctcatgt, catattccggctgaaaacgc, cttggagtgattgggtgatga, ctgct-gaccaaattggtaca, gtgctaccacatatactgtt, ttcaccagactattcacact, tttgttcgtagatcctttgt, atcattggttgcgttattgc, ttggtttctctgttagact, attgaggaatgcgccgttg, ggggaacattccatggtaa, ctatttatggctccagttgg, gatgaggcactgctagattt, ggtattgcccataccaaaag). Resuspend the probe mix in TE buffer to a final concentration of 25 μ M and store in aliquots protected from light at -20°C .
23. Competitor DNA/RNA: 10 mg/mL Sheared salmon sperm DNA, 10 mg/mL *E. coli* tRNA. Store at -20°C .
24. Vacufuge: To lyophilize smFISH probes.
25. 100 mm and 150 mm petri dishes.
26. Kimtech tissues.
27. $20\times$ Saline sodium citrate (SSC) buffer: 3 M NaCl, 0.3 M sodium citrate-HCl, pH 7.0.
28. smFISH pre-hybridization solution: 10% Formamide, $2\times$ SSC.
29. Solution F: 20% Formamide, 10 mM NaHPO_4 , pH 7.5. Prepare fresh.
30. Solution H: $4\times$ SSC, 2 mg/ml BSA, 10 mM VRC. Prepare fresh.
31. $2\times$ SSC: Dilute $20\times$ SSC 1:10 with DDW. Store at room temperature.
32. $1\times$ SSC: Dilute $20\times$ SSC 1:20 with DDW. Store at room temperature.
33. 10% Formamide/ $2\times$ SSC solution: Prepare fresh.
34. $2\times$ SSC/0.1% Triton X-100 solution.

35. 1 × Phosphate-buffered saline (PBS): 137 mM NaCl, 2.7 mM KCl, 8 mM Na₂HPO₄, and 2 mM KH₂PO₄.
36. 4% PFA-PBS solution.
37. Immunofluorescence solution (IF solution): 0.1% RNase-free bovine serum albumin (BSA) in PBS.
38. Primary antibody: Resuspend the alpha-tubulin monoclonal antibody in 2 mM Na azide, 1% BSA, and PBS.
39. Secondary antibody: Goat anti-mouse IgG (H + L) cross-adsorbed secondary antibody conjugated to Alexa Fluor 647 or other fluorophores.
40. Mounting solution with the blue fluorescent DNA staining agent 4',6-diamidino-2-phenylindole (DAPI).
41. Transparent nail polish.
42. Wide-field epifluorescence microscope (*see Note 2*).
43. smFISH analysis software (*see Note 3*).
44. Imaging processing software (*see Note 4*).

3 Methods

3.1 Coverslip Washing and Coating

1. Use a 1 L beaker to boil two packages (~200 pieces) of microscope coverslips in 500 mL of 0.1 N HCl for 20–30 min. Gently stir to separate the covers.
2. Rinse the coverslips ten times with water, autoclave, and keep them at 4 °C in 70% ethanol for up to a year.
3. On the day of the smFISH-IF, place the coverslips on a clean chromatography paper, air-dry the ethanol and rinse with water, aspirate the excess water, and air-dry. Treat the coverslips for 20 min at room temperature (RT) with 200 μL of 0.01% (w/v) poly-L-lysine. Aspirate the poly-L-lysine solution and let the covers air-dry. Wash three times with DDW and allow to air-dry.
4. Use forceps to place each coverslip, with the poly-L-lysine-coated side up, into a single well of a 6-well culture dish and store the dish at RT. Coverslips need to be completely dried.

3.2 Growth, Fixation, and Permeabilization of Yeast Cells

1. At the appropriate temperature (25–30 °C), grow overnight a low-density yeast culture in SC complete and then dilute it again in 25 ml of fresh medium to an OD₆₀₀ ~0.1; allow to grow until OD₆₀₀ 0.3–0.4. At this point, fix the cells (*see Note 5*).

2. Harvest the culture at OD_{600} 0.3–0.4 by pouring 21.85 mL of the yeast culture in a 50 ml plastic tube and adding 3.15 mL of 32% (w/v) paraformaldehyde. Mix gently and incubate at RT for 45 min with constant shaking (*see Note 6*).
3. Centrifuge the cells at $2400 \times g$ for 3 min at 4 °C and wash three times with 10 mL of ice-cold buffer B.
4. Resuspend cells in 1 mL of ice-cold buffer B and transfer them to a 1.5 mL tube.
5. Centrifuge cells at $2400 \times g$ for 3 min at 4 °C, remove all buffer B, and resuspend cells in 500 μ L of spheroplasting buffer containing the Lyticase (use 25 U of enzyme per mL \times OD_{600} of cells, i.e., 21.85 mL of cultures at OD_{600} ~0.4 = $21.85 \times 0.4 = 8.74$; thus, add 8.74 μ L of Lyticase per sample).
6. Incubate the cells in a water bath at 30 °C for 7–8 min, inverting gently and frequently (*see Note 7*).
7. After 5 min of Lyticase treatment take 5 μ L sample on a slide, cover it with a coverslip, and observe the cells with phase-contrast illumination. After Lyticase treatment, cells should appear opaque.
8. Take samples every 2 min and stop the Lyticase treatment when 50% of the cells in the sample are opaque (Fig. 1).

~50% digested spheroplasts

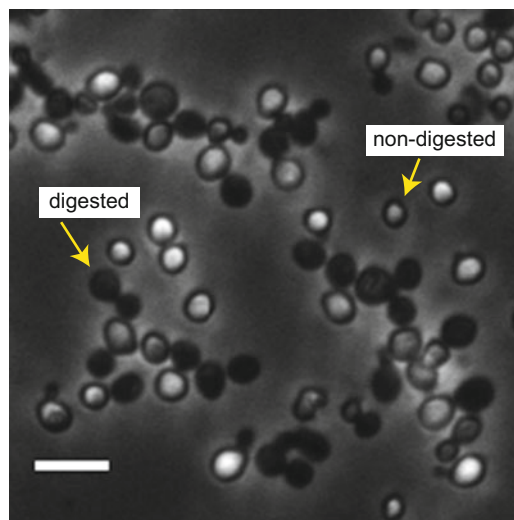


Fig. 1 Yeast cells treated for 7–8 min with Lyticase. Digested cells are imaged using phase-contrast illumination. Upon cell wall digestion, cells appear opaque. The treatment is stopped when 50–60% of the cells in the sample are opaque. Scale bar = 20 μ m

9. Centrifuge the cells for 4 min at $1300 \times g$ at $4\text{ }^{\circ}\text{C}$ and wash them once with $500\text{ }\mu\text{L}$ of ice-cold buffer B. Do not vortex but resuspend the cells with the pipet. Cells are fragile after the Lyticase treatment.
10. Resuspend the cells in $900\text{ }\mu\text{L}$ of ice-cold buffer B. Drop $200\text{ }\mu\text{L}$ on each poly-L-lysine-treated coverslip. With this amount of cultures 5–6 coverslips can be prepared for each sample that can be then hybridized with different probes or antibodies.
11. Incubate for 30–90 min at $4\text{ }^{\circ}\text{C}$ to allow the cells to adhere to the coverslips.
12. Wash once each well with 2 mL ice-cold buffer B. Gently aspirate the buffer and add 2 mL of cold 70% ethanol. Seal the plate with parafilm and store at $-20\text{ }^{\circ}\text{C}$ (*see Note 8*).

3.3 Hybridization

1. Move the coverslips for hybridization into a new 12-well plate. Rehydrate the cells by two washes with 2 mL of $2\times\text{ SSC}$, each for 5 min at RT (*see Note 9*).
2. Incubate the coverslips in 2 mL of pre-hybridization solution for 30 min at RT (*see Note 10*).
3. For each coverslip, combine $0.125\text{ }\mu\text{L}$ of the original stock of probes for the mRNA of interest (stock concentration = $25\text{ }\mu\text{M}$) with $5\text{ }\mu\text{L}$ of the DNA/RNA competitor. Lyophilize in a Vacufuge at $45\text{ }^{\circ}\text{C}$ (*see Note 11*).
4. $12.5\text{ }\mu\text{L}$ of solution F coverslips: Heat at $95\text{ }^{\circ}\text{C}$ for 2 min. Let the solution cool at RT for about 5 min. Keep probes in the dark to prevent photobleaching.
5. Add $12.5\text{ }\mu\text{L}$ of solution H per each coverslip. The resulting hybridization solution in the well ($25\text{ }\mu\text{L}$) now contains 125 nM probe mixture and 10% formamide.
6. Cover the bottom of a 150 mm petri dish with parafilm and tape it to the bottom to keep the surface flat (Fig. 2a).
7. Transfer $23\text{ }\mu\text{L}$ of the hybridization solution from step 5 onto the parafilm, one drop for each coverslip. By using the forceps, take the coverslip from each well, remove from each coverslip the leftover pre-hybridization solution using a Kimtech tissue, and place each coverslip face down onto the prepared hybridization drop. Place a small container (e.g., the cap of a 15 mL plastic tube) toward the edge of the Petri dish and fill it with DDW. Cover and seal the petri dish with parafilm to create a hybridization chamber. Incubate in the dark at $37\text{ }^{\circ}\text{C}$ for 3 h. Incubate at $37\text{ }^{\circ}\text{C}$ the pre-hybridization solution that you will use for the following washes (**step 8**).

8. Use forceps to place the coverslips, facing up, back into a 12-well plate containing 2 mL of pre-warmed pre-hybridization solution. Cover the 12-well plate with aluminum foil. Incubate for 15 min at 37 °C.
9. Aspirate the solution carefully, replace with 2 mL of pre-warmed pre-hybridization buffer, and incubate again for 15 min at 37 °C.
10. Wash once with 2 mL 2× SSC/0.1% Triton X-100 solution for 5 min at RT (*see Note 12*).
11. Wash once with 2 mL of 2× SSC for 5 min at RT.
12. Wash once with 2 mL of 1× SSC for 5 min at RT.

3.4 Immuno-fluorescence (IF)

1. Fix the coverslips with 2 mL of 4% PFA in PBS for 10 min at RT.
2. Wash once with 2 mL of PBS for 5 min at RT.
3. Prepare an IF chamber using a 150 mm petri dish (Fig. 2b). Glue to the bottom of the dish the inverted cap of 1.5 mL tubes. Use the caps to place the coverslips face up.
4. Incubate the coverslips in 190 µL of IF solution for 30 min at RT (prepare 200 µL IF solution per coverslip).
5. Fill a 50 mL beaker with PBS till the top.

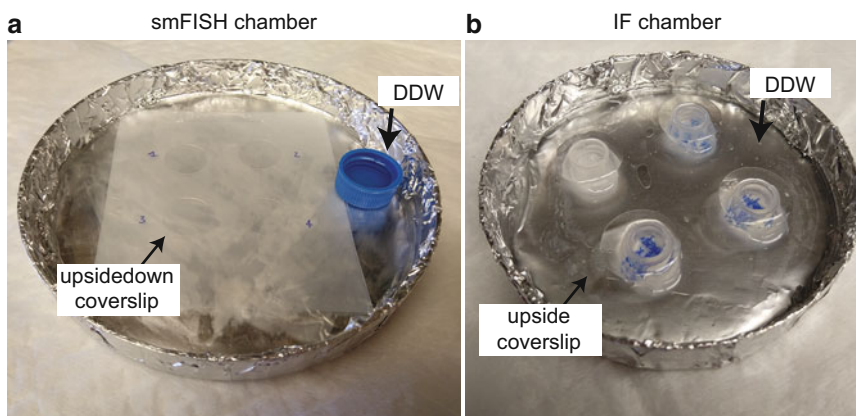


Fig. 2 Example of smFISH or IF chambers. **(a)** A humidified chamber for smFISH is created by wrapping a 15 cm petri dish with aluminum foil and by covering the bottom of the dish with parafilm. A 15 mL plastic cap filled with DDW is placed toward the edge of the dish. The dish is closed and sealed with parafilm to make a hybridization chamber and to avoid evaporation of the hybridization mix. **(b)** A humidified chamber for IF is prepared by covering a 10 cm petri dish with aluminum foil. The coverslips are placed upside on an inverted 1.5 mL tube cap glued to the bottom of the dish to act as a stand. DDW is added at the bottom of the dish (~5 mL). The dish is closed and incubated at RT

Table 1
Fluorophore combinations recommended for multicolor smFISH-IF

	smFISH 1st	smFISH 2nd	IF	Example	Notes
One-color smFISH + one-color IF (option 1)	Quasar 570/Cy3	XXX	Alexa 647	Figure 3	
One-color smFISH + one-color IF (option 2)	Quasar 670/Cy5	XXX	Alexa 555	Figure 4	If the signal from the IF is very strong and it bleeds through in the CY5 channel, you can use a secondary conjugated with Alexa 488
Two-color smFISH + one-color IF	Quasar 570/Cy3	Quasar 670/Cy5	Alexa 488	Figure 5	

6. Take the coverslip with the forceps and rinse it in the beaker. Place the coverslip back in the IF chamber and incubate with the coverslip with 190 μ L of primary antibody (mouse anti-alpha-tubulin, 1:1000) in IF solution for 45 min at RT (*see Note 13*).
7. Wash the coverslips three times with 190 μ L PBS for 5 min at RT.
8. Incubate with 190 μ L of secondary antibody (goat anti-mouse Alexa 647, 1:1500) in PBS 1 \times and BSA 0.1% for 45 min at RT (prepare 200 μ L per coverslip) (*see Note 14* and Table 1).
9. Wash three times with 190 μ L PBS for 5 min at RT.
10. Before mounting, dip coverslip in 100% EtOH, and let them dry completely at RT and protected from the light.
11. Invert coverslips and place cells facing down onto a drop (~20 μ L) of mounting solution with DAPI placed on a glass slide. Allow the mounting solution to polymerize at RT, overnight and in the dark.
12. Seal coverslips with transparent nail polish and let them dry (*see Note 15*).
13. Image the slides by fluorescence microscopy (*see Note 16*).

3.5 Image Acquisition

1. Use of a wide-field epifluorescence microscope with a motorized scanning stage, a high numerical aperture objective ~1.4NA, and narrow-band-pass filters (*see Note 17*).
2. Optically section the cells with a 200 nm Z step, spanning 8 μ m Z depth to encompass the entire cell thickness.

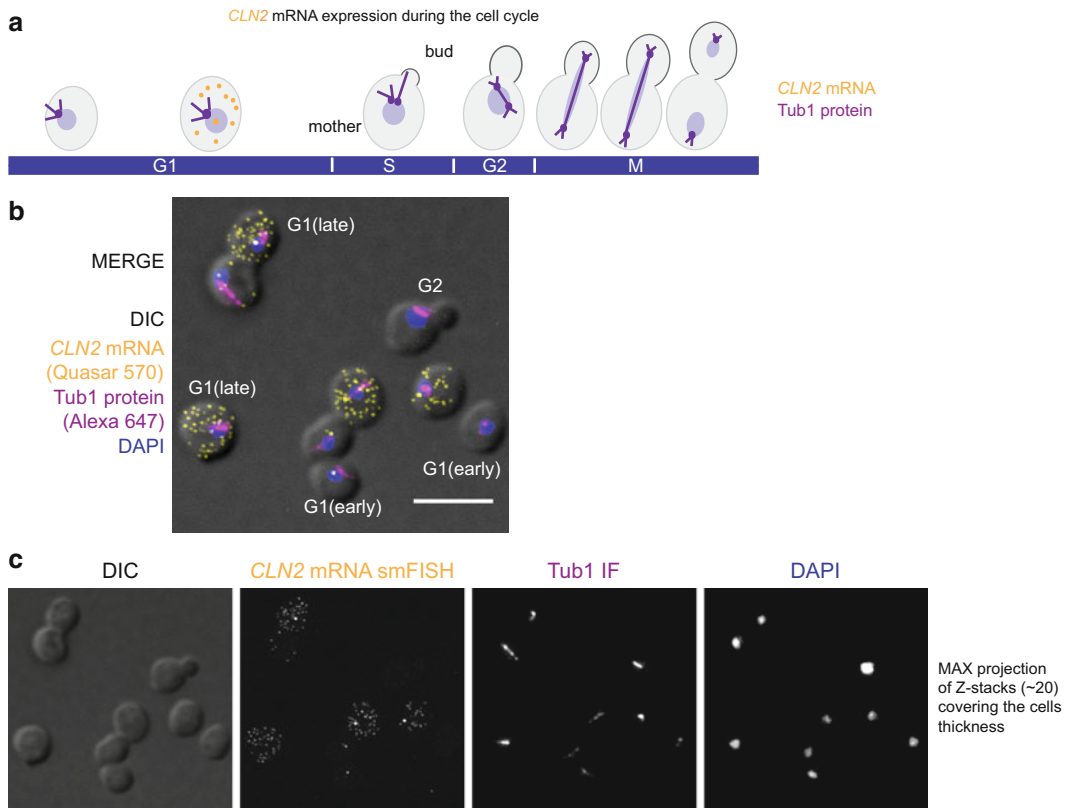


Fig. 3 smFISH-IF for the cyclin *CLN2* mRNA and the tubulin protein. **(a)** Schematic representation of *CLN2* mRNA expression during the cell cycle. Yellow dots represent *CLN2* mRNA in the cytoplasm and transcription sites in the nucleus, which are brighter than the cytoplasmic mRNAs. Tubulin co-localizes with the spindle pole body, which is duplicated during S phase. The bud emergence starts during S phase and ends with the formation of the daughter cell. During anaphase, the microtubules stretch between the mother and the daughter cell. The *CLN2* mRNA is transcribed during late G1 and it diffusely localizes in the cytoplasm. **(b)** MERGE maximally projected image: *CLN2* mRNA smFISH Quasar 570 (yellow), tubulin IF Alexa 647 (magenta), and DAPI (blue) merged to a single-plane DIC image (gray). The cell cycle phase of few representative cells is indicated in the image. Scale bar 10 μ m. **(c)** Maximally projected channels from image shown in **(b)** are individually displayed

3. For smFISH performed using Quasar 670 (CY5 filter) or Quasar 570 (CY3 filter), use an exposure time between 750 and 1000 ms to acquire each Z plane and 100% light power (120 W Mercury Arc lamp).
4. For IF performed using Alexa 647 (CY5 filter), Alexa 555 (CY3 filter), or Alexa 488 (FITC filter) dyes, expose each Z plane 300–500 ms, and 100% light power.
5. For the DAPI channel use 25–50 ms exposure and 12.5% light source power.
6. Acquire the differential interference contrast (DIC) image for 50–100 ms on a single plane (*see Note 2*).

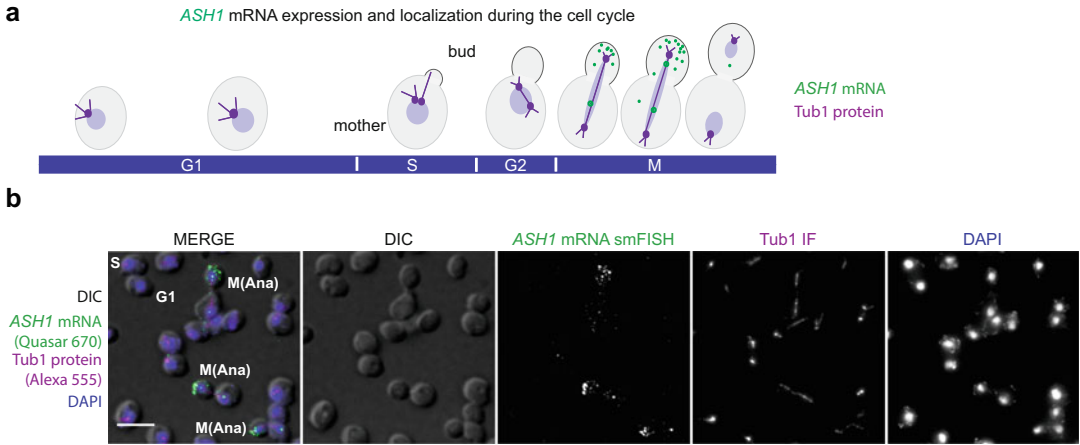


Fig. 4 smFISH-IF for the cyclin *ASH1* mRNA and the tubulin protein. **(a)** Schematic representation of *ASH1* mRNA expression and localization during the cell cycle. Green dots represent *ASH1* mRNA in the cytoplasm and transcription sites in the nucleus, which are brighter than the cytoplasmic mRNAs. Tubulin 1 co-localizes with the spindle pole body, which is duplicated during S phase. The bud emergence starts during S phase and ends with the formation of the daughter cell. During anaphase, the microtubules stretch between the mother and the daughter cell. At this time, the *ASH1* mRNA is rapidly transcribed and it localizes at the bud tip. **(b)** MERGE maximally projected image: *ASH1* mRNA smFISH Quasar 670 (green), tubulin IF Alexa 555 (magenta), and DAPI (blue) merged to a single-plane DIC image (gray). The cell cycle phase of few representative cells is indicated on the image. Scale bar 10 μm **(c)**; maximally projected channels from image shown in **(b)** are individually displayed

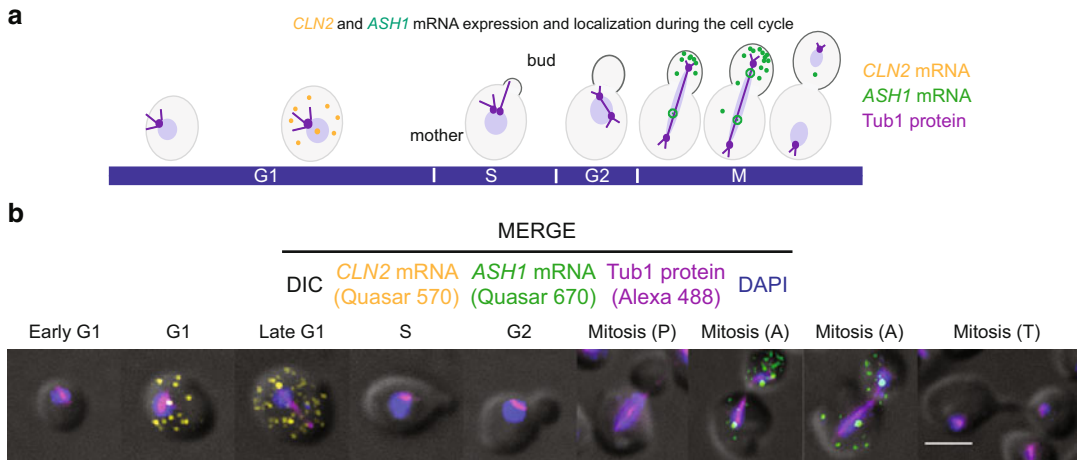


Fig. 5 smFISH-IF for the cyclin *CLN2* and *ASH1* mRNAs and the tubulin protein. **(a)** Schematic representation of *CLN2* and *ASH1* mRNA expression and localization during the cell cycle. **(b)** MERGE maximally projected image: *ASH1* mRNA smFISH Quasar 670 (green), *CLN2* mRNA smFISH Quasar 570 (yellow), tubulin IF Alexa 488 (magenta), and DAPI (blue) merged to a single-plane DIC image (gray). The cell cycle phase of few representative is indicated on the top of the image (*P* prophase; *A* anaphase; *T* telophase). Scale bar 3 μm

3.6 Single-Molecule Detection

To detect single mRNAs, we recommend the use of the freely available software FISH-quant [31]. Here we summarize the standard procedure using FISH-quant to measure the number of mRNAs in the cytoplasm and nascent transcripts at transcription sites. smFISH-IF was performed for the *CLN2* mRNA and for tubulin proteins (Fig. 3). The details for the mRNA quantification steps are exemplified in Fig. 6.

1. Define the outline of all the cells included in the analysis using either the Cy3 or the Cy5 channel. At this stage also select the transcription sites.
2. Subtract the background using the 3D_LoG option (Size 5; Standard deviation 1).
3. Pre-detect the mRNAs for one specific cell for which you defined the outline before (*see step 1*), and where you can easily count the mRNAs. Adjust the parameters to make sure that the program detects the number of mRNAs that you expect. Apply the settings to the entire image.
4. Fit the spots in the cytoplasm to a three-dimensional (3D) Gaussian to determine the coordinates of the mRNAs.
5. Check if the selected setting recognized most mRNAs (>95%). The intensity and width of the 3D Gaussian curve can be adjusted to exclude nonspecific signal. If the selected settings are satisfactory, you can save the detection settings and detected spots (Fig. 6b).
6. If many images are analyzed, create the outlines for all your images first. Then open in Tools> Batch processing. Load your previously saved settings for all your outlines. Process all your images in batch.
7. Use the option “average of thresholded spots” to obtain the average intensity of all the mRNAs and use it to determine the intensity of each transcription site.
8. To generate the settings for the transcription site selection open Tools> TxSite quantification. Load the image of the “average of thresholded spots” and quantify the TxSite for all sites. Save the setting that can be now loaded in the Batch processing mode for automatic transcription site quantification for all images.
9. Save the results. From the menu select: Batch > Save > Summary nascent and mature mRNAs, which gives the number of spots in each cell. From the menu select: Batch > Save > Summary of All Thresholded spots, which give the information about the x, y, z position and intensity of each spot. Because these files are .txt files, the information can be easily copied to other analysis

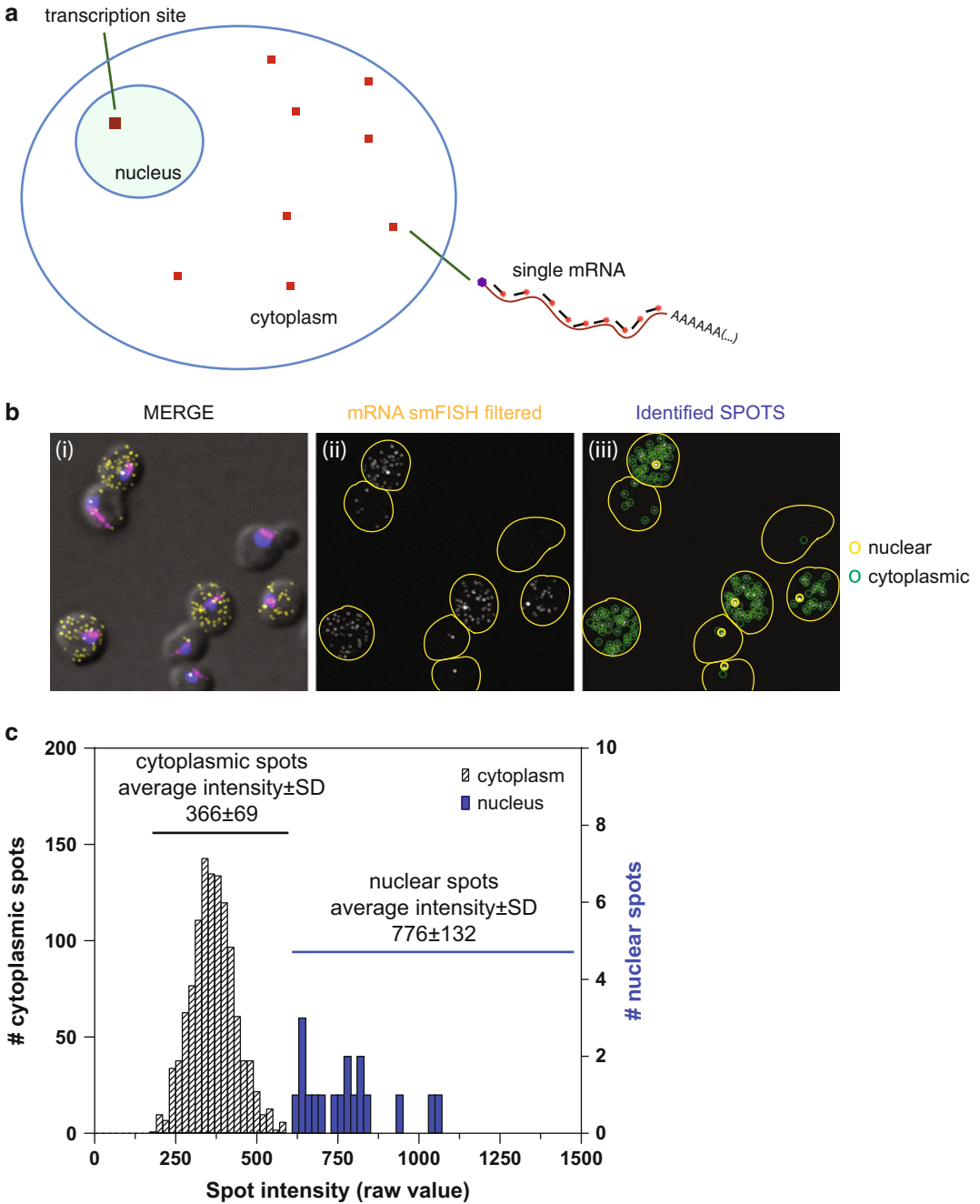


Fig. 6 Quantification of smFISH data. **(a)** Schematic representation of a cell where the single cytoplasmic mRNAs are represented as red squares and the transcription site is a larger and brighter spot co-localizing with the nuclear signal. **(b)** (i) Cropped image from Fig. 3b. Maximally projected image: *CLN2* mRNA smFISH Quasar 570 (yellow), tubulin IF Alexa 647 (magenta), and DAPI (blue) merged to a single-plane DIC image (gray). (ii) Maximally projected and filtered CY3 channel (*CLN2* mRNA smFISH). The outlines of the cells are shown in yellow. (iii) Cytoplasmic spots identified using FISH-quant are circled in green while the nuclear spots are circled in yellow. **(c)** Distribution of cytoplasmic (black histogram bars, left Y-axis) and nuclear (blue histogram bars, right Y-axis) spot intensities measured for 1176 *CLN2* mRNAs. The plotted intensities are raw intensities, before filtering

tools. If the smFISH worked well, the distribution of the intensities of the cytoplasmic spots should resemble a Gaussian distribution (Fig. 6c). Nuclear spots are usually brighter than cytoplasmic spots and they can be automatically filtered based on their intensity. The smFISH quantifications can be correlated with the IF, for instance, by creating outlines for specific stages of the cell cycle, based on the alpha-tubulin expression and pattern (Note 18).

4 Notes

1. FISH probes were custom designed against *ASH1* and *CLN2* by using the Stellaris RNA FISH Probe Designer (Biosearch Technologies) freely available online at <http://www.biosearchtech.com/stellarisdesigner>. Each smFISH probe mix is shipped as a dried set containing up to 48 individual smFISH probes, mixed in an equimolar ratio. We eliminate probes that have more than 85% homology with other mRNAs to avoid high background signal in the smFISH channel.
2. For smFISH imaging we use an Olympus BX-63 epifluorescence microscope equipped with Ultrasonic stage and UPlanApo 100 \times , 1.35NA oil-immersion objective (Olympus). An X-Cite 120 PC Lamp (EXFO), an ORCA-R2 Digital Interline CCD Camera (C10600-10B; Hamamatsu; 6.45 μ m-pixel size) mounted using U-CMT and 1X-TVAD Olympus c-Mount Adapters, and zero-pixel shift filter sets: DAPI-5060C-Zero, FITC-5050-000, Cy3-4040C-Zero, and Cy5-4040C-Zero from Semrock. We acquired data using 41 optical sections with a z-step size of 0.2 μ m. MetaMorph (Molecular Devices) software was used for instrument control as well as image acquisition.
3. For smFISH analysis we recommend using FISH-quant [31], a free software developed in the MATLAB programming language (MathWorks). Download the FISH-quant package (<http://code.google.com/p/fish-quant/>) together with the MCRInstaller, which allows one to run a MATLAB algorithm without separately installing MATLAB onto the computer.
4. For imaging processing we recommend the free software *Fiji* (Java software for image processing analysis; freely available at <https://fiji.sc/>) [32].
5. Keep the cells growing in exponential phase ($OD_{600} < 1$) at all times. At this density the autofluorescence of the cells is minimal.

6. Excessive fixation will reduce the efficiency of yeast cell wall removal during the Lyticase treatment.
7. Duration on Lyticase treatment varies with yeast strain and treatment. Over-digestion will damage cell morphology and will preclude accurate counting of single molecules.
8. 70% Ethanol allows to store the cells for several months. It also perforates the cell membrane helping the penetration of the smFISH probes during hybridization. Although a 20-min incubation in 70% ethanol at -20°C should be enough for cell membrane permeabilization, we usually do an overnight incubation.
9. At this stage a phase-contrast microscope should be used to check if the cells are well attached to the coverslip. If cells detach at this step from the coverslips, the coverslip may not have been completely dry after poly-L-lysine treatment.
10. The pre-hybridization and the hybridization solutions contain 10% (vol/vol) formamide in $2\times$ SSC. This formamide concentration is optimal for ~ 20 -nt-long probes. If using longer probes of 50 nt, the recommended formamide concentration is 50%.
11. To perform smFISH for two mRNAs simultaneously, add for each coverslip an equal amount ($0.125\ \mu\text{L}$ of a $25\ \mu\text{M}$ stock) of the two probe mixes in $5\ \mu\text{L}$ of the DNA/RNA competitor and lyophilize. Continue the protocol from paragraph Sub-heading **3.3, step 4**. If only one smFISH probe set is used we recommend the use of probes labeled with Quasar 570/Cy3 fluorophore. If a two-color smFISH is performed, we recommend the use of probes labeled with Quasar 670/Cy5 and Quasar 570/Cy3 dyes (Table 1).
12. Do not extend the washing time; otherwise the smFISH signal will reduce significantly.
13. As anti-alpha-tubulin antibody we use a mouse monoclonal antibody from Thermo Fisher (#236-10501). The use of polyclonal antibodies from other brands led to higher background in the IF channel under our conditions. Resuspend the lyophilized stock in 2 mM Na azide, 1% BSA, and PBS. The stock concentration is 160 ng/mL. Dilute the antibody 1:1000 in IF solution.
14. The secondary antibody stock concentration is 2 mg/mL. Dilute the antibody 1:1500 in IF solution.
15. Let nail polish dry before imaging by microscopy in order to avoid damaging the objective.
16. Slides can be stored at 4°C for a few days or at -20°C for months in the dark.

17. While acquiring the Z-stacks for the different channels, start imaging from the longest (CY5) to the shortest (DAPI) wavelengths and finish with the DIC. Long exposure times can cause photo-bleaching. To increase the signal of the smFISH, it is better to increase the number of probes specific for each mRNA rather than increasing the exposure time for signal imaging for longer than 1 s.
18. Three representative datasets and smFISH analysis files are available for download and are described in [33, 34].

Acknowledgments

We would like to thank Carolina Elisovich and Noura Ghazale for helpful discussion during the protocol development. This work was supported by NIH Grant GM57071 to R.H.S. E.T. was supported by Swiss National Science Foundation Fellowships P2GEP3_155692 and P300PA_164717.

Contributions: E.T. designed the protocol, performed the experiments, and analyzed the data. E.T. and R.H.S. wrote the manuscript.

References

1. Bruggeman FJ, Teusink B (2018) Living with noise: On the propagation of noise from molecules to phenotype and fitness. *Curr Opin Syst Biol* 8:144–150
2. Femino AM, Fay FS, Fogarty K, Singer RH (1998) Visualization of single RNA transcripts in situ. *Science* 280(5363):585–590
3. Zenklusen D, Larson DR, Singer RH (2008) Single-RNA counting reveals alternative modes of gene expression in yeast. *Nat Struct Mol Biol* 15(12):1263–1271. <https://doi.org/10.1038/nsmb.1514>
4. Raj A, Peskin CS, Tranchina D, Vargas DY, Tyagi S (2006) Stochastic mRNA synthesis in mammalian cells. *PLoS Biol* 4(10):e309. <https://doi.org/10.1371/journal.pbio.0040309>
5. Tutucci E, Livingston NM, Singer RH, Wu B (2018) Imaging mRNA in vivo, from birth to death. *Annu Rev Biophys* 47:85–106. <https://doi.org/10.1146/annurev-biophys-070317-033037>
6. Pichon X, Bastide A, Safeddine A, Chouaib R, Samacoits A, Basyuk E, Peter M, Mueller F, Bertrand E (2016) Visualization of single endogenous polysomes reveals the dynamics of translation in live human cells. *J Cell Biol* 214(6):769–781. <https://doi.org/10.1083/jcb.201605024>
7. Itzkovitz S, van Oudenaarden A (2011) Validating transcripts with probes and imaging technology. *Nat Methods* 8(4 Suppl):S12–S19. <https://doi.org/10.1038/nmeth.1573>
8. Farack L, Egozi A, Itzkovitz S (2018) Single molecule approaches for studying gene regulation in metabolic tissues. *Diabetes Obes Metab* 20(Suppl 2):145–156. <https://doi.org/10.1111/dom.13390>
9. Raj A, van den Bogaard P, Rifkin SA, van Oudenaarden A, Tyagi S (2008) Imaging individual mRNA molecules using multiple singly labeled probes. *Nat Methods* 5(10):877–879. <https://doi.org/10.1038/nmeth.1253>
10. Long X, Colonell J, Wong AM, Singer RH, Lionnet T (2017) Quantitative mRNA imaging throughout the entire Drosophila brain. *Nat Methods* 14(7):703–706. <https://doi.org/10.1038/nmeth.4309>

11. Pichon X, Lagha M, Mueller F, Bertrand E (2018) A growing toolbox to image gene expression in single cells: sensitive approaches for demanding challenges. *Mol Cell* 71 (3):468–480. <https://doi.org/10.1016/j.molcel.2018.07.022>
12. Vera M, Biswas J, Senecal A, Singer RH, Park HY (2016) Single-cell and single-molecule analysis of gene expression regulation. *Annu Rev Genet* 50:267–291. <https://doi.org/10.1146/annurev-genet-120215-034854>
13. Trcek T, Larson DR, Moldon A, Query CC, Singer RH (2011) Single-molecule mRNA decay measurements reveal promoter-regulated mRNA stability in yeast. *Cell* 147 (7):1484–1497. <https://doi.org/10.1016/j.cell.2011.11.051>
14. Long RM, Singer RH, Meng X, Gonzalez I, Nasmyth K, Jansen RP (1997) Mating type switching in yeast controlled by asymmetric localization of ASH1 mRNA. *Science* 277 (5324):383–387
15. Moor AE, Golan M, Massasa EE, Lemze D, Weizman T, Shenhav R, Baydatch S, Mizrahi O, Winkler R, Golani O, Stern-Ginossar N, Itzkovitz S (2017) Global mRNA polarization regulates translation efficiency in the intestinal epithelium. *Science* 357:1299–1303. <https://doi.org/10.1126/science.aan2399>
16. Buxbaum AR, Wu B, Singer RH (2014) Single beta-actin mRNA detection in neurons reveals a mechanism for regulating its translatability. *Science* 343(6169):419–422. <https://doi.org/10.1126/science.1242939>
17. Levisky JM, Shenoy SM, Pezo RC, Singer RH (2002) Single-cell gene expression profiling. *Science* 297(5582):836–840. <https://doi.org/10.1126/science.1072241>
18. Chen KH, Boettiger AN, Moffitt JR, Wang S, Zhuang X (2015) RNA imaging. Spatially resolved, highly multiplexed RNA profiling in single cells. *Science* 348(6233):aaa6090. <https://doi.org/10.1126/science.aaa6090>
19. Lubeck E, Cai L (2012) Single-cell systems biology by super-resolution imaging and combinatorial labeling. *Nat Methods* 9 (7):743–748. <https://doi.org/10.1038/nmeth.2069>
20. Lubeck E, Coskun AF, Zhiyentayev T, Ahmad M, Cai L (2014) Single-cell in situ RNA profiling by sequential hybridization. *Nat Methods* 11(4):360–361. <https://doi.org/10.1038/nmeth.2892>
21. Moffitt JR, Zhuang X (2016) RNA imaging with multiplexed error-robust fluorescence in situ hybridization (MERFISH). *Methods Enzymol* 572:1–49. <https://doi.org/10.1016/bs.mie.2016.03.020>
22. Wittenberg C, Sugimoto K, Reed SI (1990) G1-specific cyclins of *S. cerevisiae*: cell cycle periodicity, regulation by mating pheromone, and association with the p34CDC28 protein kinase. *Cell* 62(2):225–237
23. Bertrand E, Chartrand P, Schaefer M, Shenoy SM, Singer RH, Long RM (1998) Localization of ASH1 mRNA particles in living yeast. *Mol Cell* 2(4):437–445
24. Jansen RP, Dowzer C, Michaelis C, Galova M, Nasmyth K (1996) Mother cell-specific HO expression in budding yeast depends on the unconventional myosin myo4p and other cytoplasmic proteins. *Cell* 84(5):687–697
25. Long RM, Chartrand P, Gu W, Meng XH, Schaefer MR, Singer RH (1997) Characterization of transport and localization of ASH1 mRNA in yeast. *Mol Biol Cell* 8:2060–2060
26. Tutucci E, Vera M, Biswas J, Garcia J, Parker R, Singer RH (2018) An improved MS2 system for accurate reporting of the mRNA life cycle. *Nat Methods* 15(1):81–89. <https://doi.org/10.1038/nmeth.4502>
27. Cosma MP (2004) Daughter-specific repression of *Saccharomyces cerevisiae* HO: Ash1 is the commander. *EMBO Rep* 5(10):953–957. <https://doi.org/10.1038/sj.embor.7400251>
28. Pereira G, Schiebel E (2001) The role of the yeast spindle pole body and the mammalian centrosome in regulating late mitotic events. *Curr Opin Cell Biol* 13(6):762–769
29. Bayer LV, Batish M, Formel SK, Bratu DP (2015) Single-molecule RNA in situ hybridization (smFISH) and Immunofluorescence (IF) in the *Drosophila* egg chamber. *Methods Mol Biol* 1328:125–136. https://doi.org/10.1007/978-1-4939-2851-4_9
30. Eliscovich C, Shenoy SM, Singer RH (2017) Imaging mRNA and protein interactions within neurons. *Proc Natl Acad Sci U S A* 114(10):E1875–E1884. <https://doi.org/10.1073/pnas.1621440114>
31. Mueller F, Senecal A, Tantale K, Marie-Nelly-H, Ly N, Collin O, Basyuk E, Bertrand E, Darzacq X, Zimmer C (2013) FISH-quant: automatic counting of transcripts in 3D FISH images. *Nat Methods* 10(4):277–278. <https://doi.org/10.1038/nmeth.2406>
32. Schindelin J, Arganda-Carreras I, Frise E, Kaynig V, Longair M, Pietzsch T, Preibisch S, Rueden C, Saalfeld S, Schmid B, Tinevez JY, White DJ, Hartenstein V, Eliceiri K, Tomancak P, Cardona A (2012) Fiji: an open-source platform for biological-image analysis.

- Nat Methods 9(7):676–682. <https://doi.org/10.1038/nmeth.2019>
33. Maekiniemi A, Singer RH, Tutucci E (2020) Single molecule mRNA fluorescent in situ hybridization combined with immunofluorescence in *S. cerevisiae*: dataset and quantification. Data in Brief. <https://doi.org/10.1016/j.dib.2020.105511>
34. Tutucci E, Maekiniemi A, Singer RH (2020) Single molecule mRNA fluorescent in situ hybridization combined to immunofluorescence in *S. cerevisiae*: dataset and quantification. Mendeley Data, v4, <https://doi.org/10.17632/bcmm9cxys.4>

Part II

In Vivo Imaging of RNA Transport and Localization



Development and Applications of Fluorogen/Light-Up RNA Aptamer Pairs for RNA Detection and More

Michael Ryckelynck

Abstract

The central role of RNA in living systems made it highly desirable to have noninvasive and sensitive technologies allowing for imaging the synthesis and the location of these molecules in living cells. This need motivated the development of small pro-fluorescent molecules called “fluorogens” that become fluorescent upon binding to genetically encodable RNAs called “light-up aptamers.” Yet, the development of these fluorogen/light-up RNA pairs is a long and thorough process starting with the careful design of the fluorogen and pursued by the selection of a specific and efficient synthetic aptamer. This chapter summarizes the main design and the selection strategies used up to now prior to introducing the main pairs. Then, the vast application potential of these molecules for live-cell RNA imaging and other applications is presented and discussed.

Key words Fluorogen, Aptamer, RNA, Functional screening, SELEX, Live-cell imaging, Biosensing, Engineering

1 Introduction

RNA is a main actor of cell life mainly through its central role in gene expression and its regulation. Indeed, RNA has pleiotropic functions such as being the message (messenger RNA or mRNA) to be translated into protein, and the regulator of gene transcription, mRNA maturation, and/or translation (e.g., noncoding regulatory RNAs), as well as being the active component of key cellular machineries (e.g., ribosomal RNA, small nuclear RNAs, and RNase P). It is therefore of prime importance to be able to monitor the expression and ideally also the location of RNAs all along the cellular life span. Yet, for a long time, the detection of cellular nucleic acids was restricted to the use of nonspecific intercalating dyes (e.g., Hoechst [1] and cyanines [2]) and to in situ hybridization (ISH) methodologies [3], in which radioactively or fluorescently labeled oligonucleotides (DNA or RNA) are used to detect RNA molecules upon specific annealing of the probe. Whereas ISH

approaches allow detecting nucleic acids with great specificity and sensitivity, they also require cells to be fixed and permeabilized, which compromises live-cell imaging and leads to a significant loss of information on the dynamics of the biological system. Other probes and nanoparticles such as molecular beacons and nanoflares have been proposed as an alternative to fluorescent ISH (FISH) but these probes face cell entry and toxicity issues [4].

A first breakthrough in live-cell RNA imaging came with the introduction of the “RBP-FP” methods pioneered by Bertrand et al. in late 1990s with the so-called MS2-GFP system [5]. These approaches exploit the capacity of some RNA-binding proteins (RBP) to specifically recognize short RNA motifs herein used as RNA tags. The RNA to image is then expressed in cells in fusion (usually in the 3′ untranslated region of mRNAs) with an array of RNA tags (several tens of motifs tandemly repeated). In addition, a construct coding for the RBP specific to the RNA tag and fused with a fluorescent protein (FP), such as the green fluorescent protein (GFP), is also expressed in the same cell. As a consequence, upon synthesis, the target mRNA is rapidly decorated with tens of GFPs turning it into a highly fluorescent object that can be imaged with single-molecule resolution [6]. Yet, whereas this technology allowed collecting highly valuable data on mRNA synthesis, addressing, and distribution in the cell, it also suffers significant drawbacks linked to the large size of the tag array (up to 32 repeats of the RNA motif), especially when decorated by the RBP-FP, as well as the background coming from the constitutively expressed RBP-FP, though adding a nuclear localization sequence can be used to confine unbound RBP-FP into the nucleus. These features preclude the use of this technology for imaging small, yet highly relevant, noncoding RNAs but also its application to organisms deprived of internal compartments (e.g., bacteria). Yet, these major limitations can be overcome by reducing the length of RNA tag arrays and by exchanging the bulky fluorescent RBP-FP for a smaller pro-fluorescent molecule.

Conversely to proteins, no naturally fluorescent RNA has been discovered yet, making it necessary to use a pro-fluorescent cofactor. In 2003 the group of Roger Tsien reported that the so-called MGA RNA aptamer binds specifically to malachite green and other triphenylmethane dyes and that this interaction activates their fluorescence [7], making these dyes fluorogenic (Fig. 1). Since this pioneering work, a large variety of such dyes (“fluorogens”) and RNA aptamers (“light-up aptamers”) forming specific fluorogen/light-up aptamer pairs have been developed and they are still subject of a very active field of research today [8–10]. This chapter aims at reviewing and discussing the development of the main fluorogen/light-up aptamer pairs that are currently available. In addition, some of their applications in live-cell RNA imaging as well as in biosensing and nanotechnology are presented.

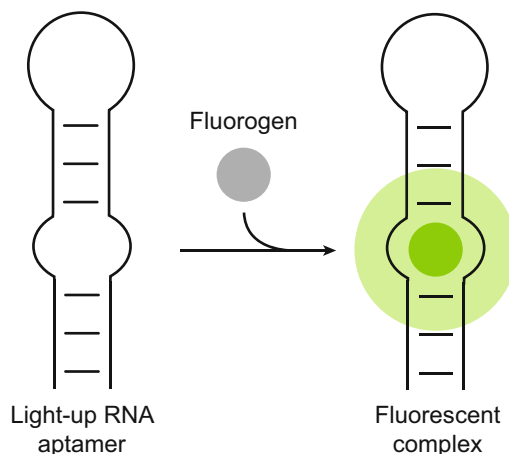


Fig. 1 Formation of a fluorogen/light-up aptamer fluorescent complex. In its free state, the fluorogen (gray) is poorly emissive. However, upon the proper accommodation into the fluorogen-binding site of a light-up RNA aptamer (black) the fluorescence capacity of the molecule is restored (green) and a fluorescent complex is formed

2 Development of Fluorogen/Light-Up RNA Aptamer Pairs

As highlighted above, RNA has no intrinsic fluorescence capacity, but it can acquire fluorescence through specific binding of a fluorogen. Ideally, this fluorogen cofactor should (1) emit no fluorescence in its free state, (2) bind the RNA aptamer with high affinity (sub-micromolar or even sub-nanomolar K_D), (3) produce strong fluorescence upon binding, and (4) be photostable. All these properties rely on both partners as demonstrated below. As a consequence, the development of an efficient fluorogen/aptamer pair is a long and complex multiparametric process in which the fluorogen should be properly designed and the RNA aptamer subsequently identified by using a suited selection strategy. This strategy led to the identification of several tens of pairs covering all the visible spectrums and displaying ever-improved properties (Table 1).

2.1 Design of the Fluorogen

Malachite green (MG) was the first fluorogen found to be specifically activated by an RNA aptamer [7]. This was rather an unexpected discovery, since the aptamer was originally developed to bind MG with the idea of producing reactive radicals aimed at cleaving RNA in close proximity [11]. The true development of dedicated fluorogens (most of them are shown in Fig. 2) started shortly after, leading to a first generation of molecules based on known nucleic acid-binding dyes such as Hoechst and cyanines like thiazole orange (TO) and oxazole orange (YO). These molecules are intrinsically pro-fluorescent. Indeed, Hoechst is an environment-sensitive molecule that does not emit fluorescence in

Table 1
Main fluorogen/RNA light-up aptamer pairs and their properties

Fluorogen	Light-up aptamer	Aptamer selection strategy	K_D (nM)	Ex./Em. (nm)	Abs. Coef. (ϵ)	Q.Y.	Brightness	Rel. Brightness	Reference
	cGFP	Natural molecule	/	490/508	39,200	0.68	26.60	1.00	[36]
OTB-SO3	Dir2s	SELEX	662	380/421	73,000	0.51	37.23	1.40	[17]
Hoescht-1c	Apt II-mini3-4	SELEX	35	345/470	n.a.	0.26	n.a.	n.a.	[12, 13]
DFHBI	Spinach	SELEX	540	469/501	24,300	0.72	17.50	0.65	[18]
DFHBI	iSpinach	μ IVC	920	442/503	n.a.	n.a.	n.a.	n.a.	[42]
DFHBI-1T	Spinach2	SELEX/design	560	482/505	31,000	0.94	29.10	1.10	[19]
DFHBI-1T	Broccoli	SELEX/FACS	360	472/507	29,600	0.94	27.80	1.04	[35]
TO1-Biotin	iMangoIII	μ IVC	4	506/527	77,500	0.64	49.6	1.86	[55]
RG-DN	DNB	SELEX	4480	507/534	37,350	0.32	11.90	0.44	[28]
TO1-Biotin	Mango	SELEX	3	510/535	77,500	0.14	10.85	0.40	[14]
TO1-Biotin	MangoII	μ IVC	1	510/535	77,500	0.21	16.28	0.61	[43]
TO1-Biotin	MangoIII	μ IVC	5	510/534	77,500	0.55	42.63	1.6	[43]
DMHBI+	Chili	SELEX/design	63	413/542	n.a.	0.40	n.a.	n.a.	[22]
DMHBI-Imi	Chili	SELEX/design	71	463/545, 594	n.a.	0.08	n.a.	n.a.	[22]
DFHO	Corn	SELEX	70	505/545	29,000	0.25	7.25	0.27	[21]
DFHO	Orange Broccoli	SELEX	230	513/562	34,000	0.28	9.52	0.36	[21]
CY3-BHQ1	BHQ apt (A1)	SELEX	n.a.	520/565	n.a.	n.a.	n.a.	n.a.	[31]
DFHO	Red-Broccoli	SELEX	206	518/582	35,000	0.34	11.90	0.44	[21]
TMR-DN	SRB2	SELEX	35	564/587	90,500	0.33	29.87	1.12	[29]
SR-DN	DNB	SELEX	800	572/591	50,250	0.98	49.24	1.85	[28]
DMHBO+	Chili	SELEX/design	12	456/592	n.a.	0.10	n.a.	n.a.	[22]
SR-DN	SRB2	SELEX	1340	579/596	85,200	0.65	55.38	2.08	[29]
Cbl-Atto590	Riboglow	Natural molecule	3-34	594/624	120,000	0.31	37.2	1.40	[32]
DIR	DIR apt	SELEX	86	600/646	134,000	0.26	34.80	1.30	[16]
Mal. Green	MGA	SELEX	117	630/650	150,000	0.19	28.00	1.05	[7, 11]
DIR-pro	DIR2s-Apt	SELEX	252	600/658	164,000	0.33	54.12	2.00	[17]
TO3-Biotin	Mango	SELEX	6-8	637/658	9,300	n.a.	n.a.	n.a.	[14]
SiR-DN	SiRA	SELEX	1000	650/662	n.a.	n.a.	n.a.	n.a.	[30]
Cbl-Cy5	Riboglow	Natural molecule	n.a.	646/662	271,000	0.26	70.46	2.65	[32]
Patent Blue	SRB apt	SELEX	23	n.a./665	n.a.	0.034	n.a.	n.a.	[7]
SiR-linker	SiRA	SELEX	430	649/666	86,000	0.98	84.28	3.16	[30]

its free state, but becomes highly fluorescent when bound to DNA [9]. On their side, TO and YO have the capacity to eliminate an excitation energy via intramolecular movements in their free state. However, binding to nucleic acids hinders intramolecular movements and the excitation energy is then eliminated by fluorescence emission. To serve as specific fluorogen, the nonspecific binding capacity of these dyes was strongly attenuated by introducing blocking chemical groups, leading to compounds with a potential to interact with nucleic acids but becoming fluorescent only upon binding to a specific sequence. This first set of fluorogens encompasses molecules like Hoechst derivative 1c [12, 13], TO1-Biotin [14], TO3-Biotin [14], YO3 [15], DIR [16], DIR-pro [17], and OTB-SO3 [17] (Table 1). In addition to these repurposed dyes, bio-inspired fluorogens (also behaving as molecular rotors) were designed by mimicking fluorophores found in fluorescent proteins. In doing so, the group of Samie Jaffrey introduced DFHBI (3,5-difluoro-4-hydroxybenzylidene imidazolinone) as the first GFP-mimicking fluorogen [18] together with DFHBI-1T, a brighter derivative [19]. Moreover, since green fluorescence may also originate from cell autofluorescence, several groups later developed red-emitting FP-mimicking fluorogens [20–22]. Interestingly, protonated forms of these FP-mimicking fluorogens (e.g., DMHBI⁺, DMHBI-Imi, and DMHBO⁺) represent large stokes-shift fluorogens, which are particularly attractive for Förster resonance energy transfer (FRET) applications [22]. This first generation of fluorogens already covered most of the visible spectrum (Fig. 2) and allowed a real breakthrough to begin in RNA imaging technologies (see below). However, these dyes suffer from a limited brightness (Table 1) and, in most of the cases, a low photostability—the most extreme case being encountered with the DFHBI and DFHBI-1 T (from now summarized as DFHBI(–1 T)) fluorogens that, when associated with their specific aptamer, produce fluorescence for less than a second before getting photobleached [23, 24].

The abovementioned limitations encouraged the development of a second set of fluorogens based on organic dyes known to be both bright and photostable (e.g., rhodamines, Atto, and Alexa). Yet, these molecules first needed to be converted into reversible non-emissive species (Fig. 2). To do so, the molecule is usually conjugated with a quenching moiety that prevents fluorescence emission by either contact quenching, FRET, or electron transfer [25]. For instance, direct addition of an aniline to an amino group of a sulforhodamine core led to ASR, a dye quenched by an electron transfer mechanism revertible upon aptamer binding [26]. Sulforhodamine B (SRB) can also be conjugated to dinitroaniline (DN) via a short polyethylene glycol (PEG) linker introduced at the level of a sulfone group, yielding a fluorogen (i.e., SR-DN) rendered non-emissive by a contact quenching phenomenon,

[27, 28]. The beauty of this approach is the possibility of generating a variety of dyes with different colors. Indeed, grafting DN-PEG to various dyes with xanthene-like cores (e.g., RG-DN and TMR-DN) allowed generating a rainbow of fluorogens [29] and led recently to the development of the very bright silicon rhodamine-DN fluorogen [30]. Interestingly, exploiting the internal spirocyclization (a spontaneous intramolecular cyclization event abrogating the fluorescence of the molecule but reversible by the binding to an aptamer) capacity of the silicon rhodamine even made the addition of the quencher moiety (i.e., SR linker) dispensable, yet at the expense of a lower fluorescence turn-on, thus leading to a lower contrast [30]. Alternative designs in which DN was exchanged for FRET quenchers like Black Hole Quencher 1 (e.g., Cy3-BHQ1) [31] and, more recently, cobalamin (e.g., Cbl-Cy5 and Cbl-Atto590) [32] were also described and enabled the development of multicolor imaging platforms. The use of cobalamin (Cbl) as a quencher is a very clever strategy as it exploits a natural compound for which several natural and specifically interacting RNA aptamer sequences were already identified in bacterial riboswitches. Fortunately, this interaction with Cbl is efficient enough to abrogate the quenching of the dye, making the *de novo* isolation of a dedicated aptamer dispensable.

2.2 Development and Properties of Artificial Light-Up RNA Aptamers

With the exception of Cbl-binding RNAs introduced above, no other natural light-up RNA aptamer has been described yet. While the absence of such molecule in cells limits the risk of unwanted background fluorescence resulting from a cross activation by endogenous sequences, it also requires the development of an artificial aptamer. Over the past decade, several strategies have been proposed to isolate and optimize light-up RNA aptamers.

2.2.1 Aptamer Isolation Strategies

Traditionally, artificial aptamers are obtained using an *in vitro* selection technology known as SELEX (Systematic Evolution of Ligands by EXponential enrichment) introduced in the early 1990s [33, 34]. In this approach, RNA (or DNA) molecules contained in large libraries made of 10^{14-15} different sequences are challenged to interact with an immobilized target, here, a fluorogen (Fig. 3a). Upon stringent washes, molecules displaying sufficient affinity for the target are recovered and the resulting enriched library is used to prime another round of selection. As a consequence, aptamers isolated by SELEX are likely to be specific and high-affinity binders. Consistent with this assumption, most of the aptamers recognize their fluorogen with nanomolar affinity (Table 1). The best systems described so far in this regard are the TO1-Biotin/Mango [14], DMHBO⁺/Chili [22], and TMR-DN/SRB2 systems showing K_D values of 3 nM, 12 nM, and 35 nM, respectively [29].

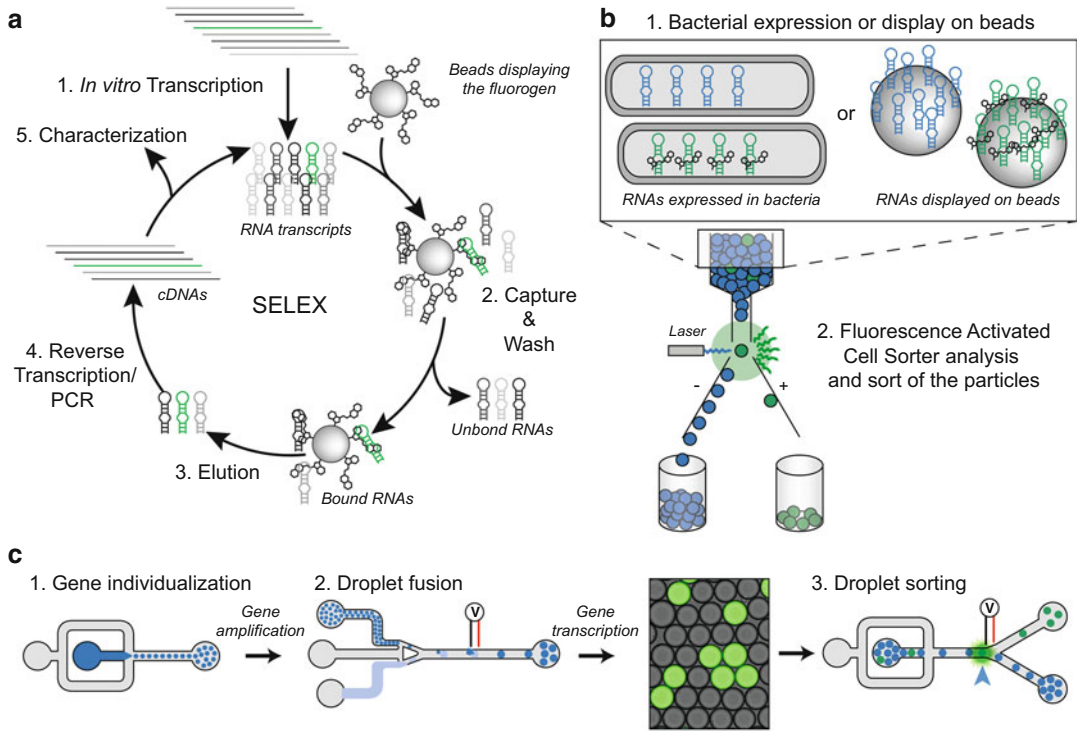


Fig. 3 Principal technologies available for selecting light-up RNA aptamers. **(a)** In vitro selection using Systematic Evolution of Ligands by EXponential enrichment (SELEX). Gene libraries are in vitro transcribed into RNAs later challenged to interact with a fluorogen immobilized on beads. Selection pressures are mainly applied to select aptamers able to bind the fluorogen with high affinity. This approach has been used to isolate most of the aptamers listed in Table 1. **(b)** Functional screening of aptamers using fluorescence-activated cell sorter (FACS). Gene libraries are expressed in RNAs either in bacteria [35] or at the surface of beads [37]. Upon incubation with the fluorogen, the fluorescence of the particles (bacteria or beads) is analyzed on a FACS and used to sort particles displaying the highest fluorescence and, therefore, contain/display efficient light-up aptamers. **(c)** Functional screening of aptamers using microfluidic-assisted in vitro compartmentalization (μ IVC). Genes contained in a library are individualized (step 1) together with a PCR amplification mixture in droplets (dark blue) carried by an oil phase (gray). Droplets are collected and thermocycled prior to being reinjected into a droplet fusion device where each DNA-containing droplet (dark blue) is fused to a larger droplet containing an in vitro transcription mixture (light blue) supplemented with fluorogen (step 2). Upon an incubation allowing amplified DNA to be in vitro transcribed, the fluorescence of each droplet is analyzed. To do so, droplets are reinjected into a sorting device in which the fluorescence of each droplet is measured and used to isolate droplets displaying the highest fluorescence and, thus, contain efficient light-up aptamers. This process was used to isolate several aptamers listed in Table 1 [42, 43, 56]

Yet, since during SELEX no selection pressure is applied for the capacity of the aptamer to turn on the fluorogen, isolated RNAs are not necessarily expected to be efficient light-up molecules. In agreement with this statement, it has been reported that within the final pool of DFHBI-binding aptamers, less than 1% of the molecules were actually fluorogenic [35]. Furthermore, except from SiRA (Table 1), all the SELEX-derived aptamers reported so

far form complexes of suboptimal brightness. The brightness of a fluorogen/aptamer complex results from the number of photons the fluorogen can absorb (quantified by the absorption coefficient ϵ) and from the number of photons re-emitted per absorbed photons (quantified by the quantum yield, QY). Therefore, to be as bright as possible, a complex should have both the highest possible ϵ value and a QY as close as possible to 1 (i.e., every absorbed photon is re-emitted). Consequently, even though DFHBI-1T/Spinach2 displays an excellent QY of 0.98, the low ϵ of the complex makes it just as bright as eGFP. On the contrary, complexes with much higher ϵ such as TO1-Biotin/Mango, DIR--Pro/DIR2s, and Cbl-Cy5/Riboglow are limited by their low QY (Table 1). Therefore, to be efficient, the aptamer selection pipeline should ideally include a screening step during which the capacity of each molecule to light up the fluorogen is also taken into account.

Following the strategy originally used to identify improved variants of GFP [36], the aptamer variants contained in a SELEX-enriched pool can be further selected for light-up aptamers upon expression in bacteria grown on agar plates supplemented with fluorogen and selecting colonies that are fluorescent [26]. However, this approach allows only analyzing a few hundreds of aptamers. Significant gain in throughput can be reached by analyzing bacteria with a fluorescence-activated cell sorter (FACS, Fig. 3b). Indeed, combining SELEX pre-enrichment with FACS screening of aptamer-expressing bacteria allowed to identify Broccoli, a DFHBI-binding aptamer optimized for imaging RNA in living cells [35]. While live-cell FACS screening allows to select aptamers with lighting-up capacity directly in the cellular context, it may also face significant drawbacks given by the cell-based system such as (1) limited bacteria transformation efficiency, (2) requirement of the fluorogen to be cell membrane permeable (dispensable for the development of extracellular probes), or (3) difficulty to apply harsh and controlled selection pressures. To overcome these limitations, aptamer libraries should ideally be screened *in vitro*. Such *in vitro* screening can be performed using gene-linked RNA aptamer particle (GRAP) display [37], a technology in which aptamer-coding genes contained in a library are first individualized at the surface of beads onto which they are then clonally amplified by emulsion PCR. Upon washing, beads are emulsified in a second set of droplets into which DNA is transcribed into RNA aptamers that are then captured on the bead surface. Finally, incubating beads with a fluorogen allows to fluorescently label the beads all the better the aptamer is efficient and makes it possible to FACS-sort them (Fig. 3b). Advantageously, this method enables to select for both brightness and affinity and was successfully used to isolate new MG-binding aptamers forming higher affinity or brighter complexes with the fluorogen. Such a screening would have been

extremely challenging to perform with living cells given the significant toxicity of the fluorogen [38]. Recently, the methodology was further improved by making the second emulsification step (in vitro transcription step) dispensable. Indeed, in the so-called R-CAMPS technology the RNA produced from DNA coupled on the bead surface is co-transcriptionally captured at the surface of the same bead via a specific sequence [39]. The functionality of this approach was demonstrated by screening small libraries of Baby Spinach aptamer. However, the significant polydispersity of the emulsions generated during PCR and in vitro transcription steps may affect the overall efficiency of the bead-based methods. Thus, a significant gain in accuracy could be reached by performing the amplification and transcription reactions in more homogenous emulsions.

An attractive way of producing highly identical water-in-oil droplets is to use microfluidics as it allows to generate and manipulate highly monodisperse emulsions and to gain control over selection conditions. In this view, we recently introduced microfluidic-assisted in vitro compartmentalization (μ IVC) as an alternative to the in vitro ultrahigh-throughput screening approach [40]. In μ IVC, genes contained in a library are individualized into small water-in-oil droplets (Fig. 3c) in which they are PCR amplified, expressed into RNA (or even protein), and analyzed for their properties (e.g., enzyme activity, capacity to light up a fluorogen). The droplets with the genes of interest are then sorted at rates of several millions per day. Such ultrahigh-throughput is primarily possible due to the extreme miniaturization of the reaction vessels (down to a few picoliters) and the use of microfluidic devices that allow to produce highly monodisperse emulsions and to manipulate (fusion, injection, and sorting) individual droplets with electricity (avoiding the use of moving parts that would limit the throughput) [41]. We first demonstrated μ IVC efficiency in light-up aptamer development by improving the folding and fluorescence properties of the light-up aptamer Spinach, which led to the isolation of iSpinach, an aptamer optimized for in vitro applications [42]. Yet, so far, the best illustration of μ IVC efficiency was obtained with the isolation of new Mango aptamers. Indeed, the original Mango aptamer was found to form a high-affinity complex with the fluorogen TO1-Biotin, but the complex also suffered from a low QY of 0.14, making it dimmer than half an eGFP (Table 1). Rescreening the SELEX-enriched library from which Mango was identified using a μ IVC procedure enabled us to identify three new Mango variants (Mango-II, -III, and -IV) [43]. Of these new aptamers, Mango-II displayed an improved affinity for TO1-Biotin while having unchanged lighting-up capacity, whereas Mango-III (the major sequence found at the end of process) had preserved affinity for the fluorogen while forming a complex with a nearly fourfold higher QY, making it significantly brighter than eGFP (Table 1).

Interestingly, Mango-III displays important differences with the other Mango aptamers both at the sequence and the structure level (see below). Moreover, Mango-III dominated the pool at the end of the screening process, whereas it was completely missed during the previous hand screenings [14]. Taken together, the case of Mango-III demonstrates how powerful the combined use of SELEX and μ IVC can be at identifying efficient light-up RNA aptamers.

Finally, also microarrays were used for in vitro functional screening of aptamers [44–46]. Upon DNA spotting onto a surface, genes are transcribed and captured either onto a functionalized coverslip [46] or into a dedicated micro-chamber [44]. Then, the RNA is incubated with the fluorogen and the array imaged. Moreover, using a microfluidic device it became possible to keep the array under perfusion of liquid and to vary the concentration of the fluorogen (or other compounds) while collecting thermodynamic data on the system [44]. Whereas array-based technologies operate at much lower throughput than μ IVC and are therefore less efficient at isolating optimal light-up aptamers from large pools, the possibility to directly associate each phenotype to the encoding genotype makes these techniques particularly well suited for the fine functional characterization of light-up aptamers via the screening of comprehensive single (if not double)-point mutant libraries.

2.2.2 Structure-Assisted Characterization and Optimization of Light-Up Aptamers

Once a light-up aptamer has been identified, the most efficient way to understand the molecular mechanism driving the recognition and the activation of the fluorogen is to solve the crystal structure of the fluorogen/aptamer complex. Moreover, such structural characterization is highly valuable to further engineer the system (e.g., to develop biosensors and supramolecular assemblies, see below). Thus, nearly half of the systems presented in Table 1 have been crystalized and their structure has been solved. Even though each aptamer adopts an idiosyncratic folding, they all share the presence of an extended platform made of a base-triple [47], a base-quadruple [48], or even a G-quartet [49–54] that accommodates the fluorogen [53]. Fluorogens are polycyclic compounds and their optimal activation is usually obtained by holding them in planar conformation while properly confining them within a binding pocket.

On a structural point of view, the original Mango aptamer possesses one of the simplest fluorogen-binding pockets, which consists of a G-quartet surmounted by three unpaired nucleotides (two As and a U) that belong to G-quadruplex propellers (Fig. 4a) [52]. As a consequence, one face of the fluorogen is still largely exposed to the solvent, explaining in part the low QY of the complex (Table 1). Moreover, both cycles of the TO1 fluorogen are rotated relative to each other instead of being coplanar as

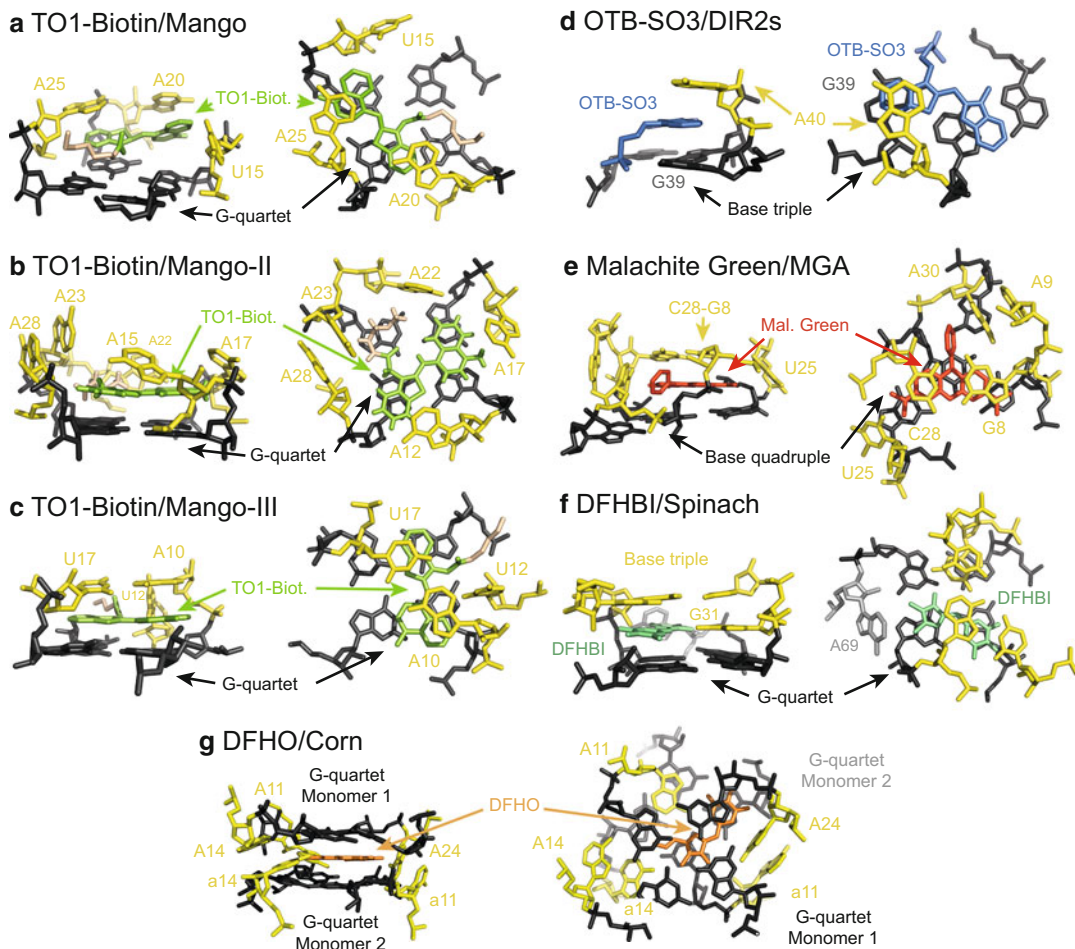


Fig. 4 Structural organization of the main fluorogen-binding sites. **(a)** Binding of TO1-Biotin to Mango aptamer. Based on model PDB 5V3F [52]. **(b)** Binding of TO1-Biotin to Mango-II aptamer. Based on model PDB 6C63 [54]. **(c)** Binding of TO1-Biotin to Mango-III aptamer. Based on model PDB 6E8S [55]. **(d)** Binding of OTB-SO3 to DIR2s aptamer. Based on model PDB 6DB8 [47]. **(e)** Binding of malachite green to MGA aptamer. Based on model PDB 1F1T [48]. **(f)** Binding of DFHBI to Spinach aptamer. Based on model PDB 4TS2 [50]. **(g)** Binding of DFHO to Corn aptamer. Based on model PDB 5BJO [62]. Nucleotides contributed by Monomer1 (upper case nucleotides) or distinguished from those contributed by Monomer2 (lower case nucleotides). In every model, only the elements in direct contact with the fluorogen are represented. For G-quadruplex-containing RNAs, only the proximal quartet is shown. For each fluorogen/aptamer pair a side (left picture) and top (right picture) view of the complex is represented. Elements are colored as follows: fluorogen-binding platform (G-quartet, base quadruple, or base triple) in dark gray, surrounding and capping residues in yellow, and fluorogen colored according to their emission wavelength (i.e., OTB-SO3 in blue, TO1-Biotin and DFHBI in green, DFHO in orange, and malachite green in red)

required to obtain maximal fluorescence emission. Mango-II shares the same overall structure except that five adenines are contributed by the G-quadruplex propellers and allow to better constrain and accommodate the fluorogen [54] without significantly modifying

the environment of the dye (Fig. 4b). Moreover, while held in planar conformation, the fluorogen is also slightly more exposed to the solvent. Taken together, these observations explained the increased affinity of Mango-II for TO1-Biotin (better accommodation of the fluorogen) while the brightness of the complex remained unchanged (no advantageous modification of the fluorogen environment). Mango-I and -II are both able to trigger TO1-Biotin fluorescence and to a lower extent that of the related, red-emitting analog TO3-Biotin. However, guided by the crystal structure, we identified a point mutant of Mango-II (Mango-II (A22U)) endowed with a better capacity to discriminate both fluorogens [54]. Interestingly, and as expected from the significant sequence differences, Mango-III displays a rather different structural organization [55]. Indeed, whereas the RNA still possesses a G-quadruplex of which the top quartet forms the fluorogen-binding platform, the aptamer has a much more compact and robust structure in which almost every residue is involved in hydrogen bonding. Moreover, and conversely to other Mangos, the G-quartet platform of Mango-III is not surmounted by unpaired nucleobases but is rather capped by a A-U base pair (A10-U17) that sandwiches the fluorogen and is stabilized by an intercalating U (U12) residue (Fig. 4c). As a direct consequence of this tight accommodation of TO1-Biotin between the G-quadruplex platform and the apical A-U base-pair, the QY of TO1-Biotin/Mango-III is almost four times higher than that of other Mango aptamers without significant change in affinity (Table 1). Moreover, we found out that Mango-III almost completely lost the capacity to trigger TO3-Biotin fluorescence, making this aptamer one of the most specific aptamer known to date. As before, guided by the crystal structure, we identified ten residues that could potentially be suboptimal [55]. We prepared a mutant library in which these ten positions were randomized, and we screened it for improved variants using μ IVC. Excitingly, this allowed us to identify iMango-III, an aptamer forming an even brighter complex with TO1-Biotin and with preserved affinity (Table 1). The overall structure of iMango-III is identical to that of Mango-III [55, 56], the main difference being the exchange of the A-U apical closing base pair for a U•U pair that was identified as being responsible for the increase in brightness of the complex.

Recently, the crystal structure of the DIR2s aptamer was solved in complex with the fluorogen OTB-SO₃ [47]. Interestingly, the fluorogen-binding platform of DIR2s consists only of a base triple, and the fluorogen is capped by a single adenine (A40, Fig. 4d). Moreover, the fluorogen establishes a specific interaction with a guanine (G39) of the platform via its sulfone moiety. Interestingly, it was proposed that the absence of G-quadruplex should render this aptamer less sensitive to the cellular G-quadruplex unfolding

machinery recently discovered [57]. However, the relaxed constraint exerted on the fluorogen has also two main drawbacks, i.e., a moderate brightness (moderate QY) and a lack of specificity of the complex (the aptamer was found to bind and trigger fluorescence not only of OTB-SO₃ but also of DIR-Pro and TO1-Biotin). Yet, both limitations could be overcome by re-exploring the SELEX-enriched libraries using a functional screening approach like μ IVC. Interestingly, the fluorogen-binding platform of MGA does not consist of a G-quartet either but instead consists of a base quadruple (G•G•A•C) that accommodates the fluorogen which is further capped by a G•C base pair (G8-C28) and surrounded by several unpaired residues (Fig. 4e) [48]. Despite this a priori tight accommodation, the complex is still characterized by a low QY (0.19), but recent experiments showed that this value could be significantly increased using in vitro functional screening [37].

Among the different structurally characterized light-up RNA aptamers, DFHBI(-1T)-binding Spinach aptamers (Spinach [18], Spinach2 [58], iSpinach [42]) possess the most elaborated fluorogen-binding pocket (Fig. 4f). Indeed, all the solved crystal structures showed that the fluorogen-binding platform is made of a G-quartet and that DFHBI(-1T) is accommodated between this platform and a base triple, while specific contacts are established with a side guanine (G31) [49–51]. Exploiting the crystal structure allowed to truncate Spinach to a much shorter aptamer called Baby-Spinach that preserves the properties of the parental molecule [50]. In addition to the Spinach family aptamers, it is very likely that the same DFHBI(-1T)-binding pocket is shared by Broccoli [35]. Indeed, even though no crystal structure has been solved for this aptamer, the close sequence proximity with Spinach strongly suggests that both molecules adopt the same folding [59–61]. However, despite the tight apparent accommodation of the fluorogen, all the known DFHBI(-1T)/aptamer complexes suffer from a very short fluorescence half-life (less than 1 s) [23]. This is likely due to the loose constraint applied to the imidazolinone moiety that stays free to eliminate part of the excitation energy through rapid photoisomerization.

The precursor of Broccoli was recently subjected to rounds of directed evolution and converted into Orange Broccoli and Red Broccoli, two aptamers able to light up DFHO, a red fluorescent protein-mimicking fluorogen, at different wavelengths [21]. Comparing the sequences of the three (the original, Orange and Red) Broccolis as well as considering their putative Spinach-like DFHBI(-1T)-binding pocket allowed to identify a single nucleotide responsible for the Broccoli spectral tuning [60]. While this feature makes Broccoli an interesting precursor for the development of multicolor tags, this aptamer family is still limited by the poor photostability and the limited brightness of the complex they form with their fluorogens [21]. However, significant gain in

photostability of the FP-mimicking fluorogens was recently reached with the isolation of Corn, a DFHO-binding aptamer protecting its fluorogen from the rapid photoisomerization encountered with Spinach and Broccoli families [21]. Interestingly, this impressive gain in photostability was not attributable to the fluorogen itself (which does not display such a stability when bound to Broccoli aptamers) but rather to the way the aptamer accommodates it. Indeed, the crystal structure of DFHO/Corn revealed that the RNA is organized around a G-quadruplex and that the DFHO is actually accommodated between the apical quartet of two monomers forming a complex with a fluorogen:aptamer stoichiometry of 1:2. (Fig. 4g) [62]. As a consequence, the DFHO is maintained in an emissive planar conformation by being sandwiched between both G-quartets while five unpaired adenines further restrict possible movement. Altogether, these elements prevent photoisomerization to take place and confer to DFHO/Corn a very high photostability.

3 Imaging and Sensing Applications Using Light-Up RNA Aptamers

As highlighted in the introduction of this chapter, one of the main motivations in developing fluorogens and light-up RNA aptamers was the possibility foreseen to directly monitor RNA synthesis, as well as the movement and location of RNA molecules within living cells, while overcoming limitations of RBP-FPs. The strong toxicity of malachite green for yeast and mammalian cells [38] largely prevented its use as a fluorogen for live-cell RNA imaging. On the contrary, all the other above-introduced fluorogens were found to be nontoxic, deprived of nonspecific interaction with cell components and most of them were further found to be cell membrane permeable. Therefore, most of these systems are well suited for live-cell imaging applications. Moreover, since nucleic acids are molecules highly amenable to engineering, these aptamers were rapidly converted into a variety of sensors with a wide application spectrum both in live cells and in vitro.

3.1 General Considerations Before Starting Live-Cell Applications

So far, DFHBI(-1T) has been the most broadly used fluorogen, as it is commercially available from several companies and is able to enter various cell types such as bacteria [18], yeast [63, 64], algae [65], and mammalian cells [18, 35, 58]. However, other fluorogens like DFHO and TO1-Biotin are also known to be cell permeable and are now commercialized (by Lucerna and Applied Biological Material, respectively), which will further ease their wide use in the near future. Because of the short half-life of short RNAs in cells and because of limited folding capacity, fluorescence can hardly be observed upon expressing Spinach or Broccoli family aptamers as free RNA molecules (Fig. 5a). Instead, aptamer RNAs

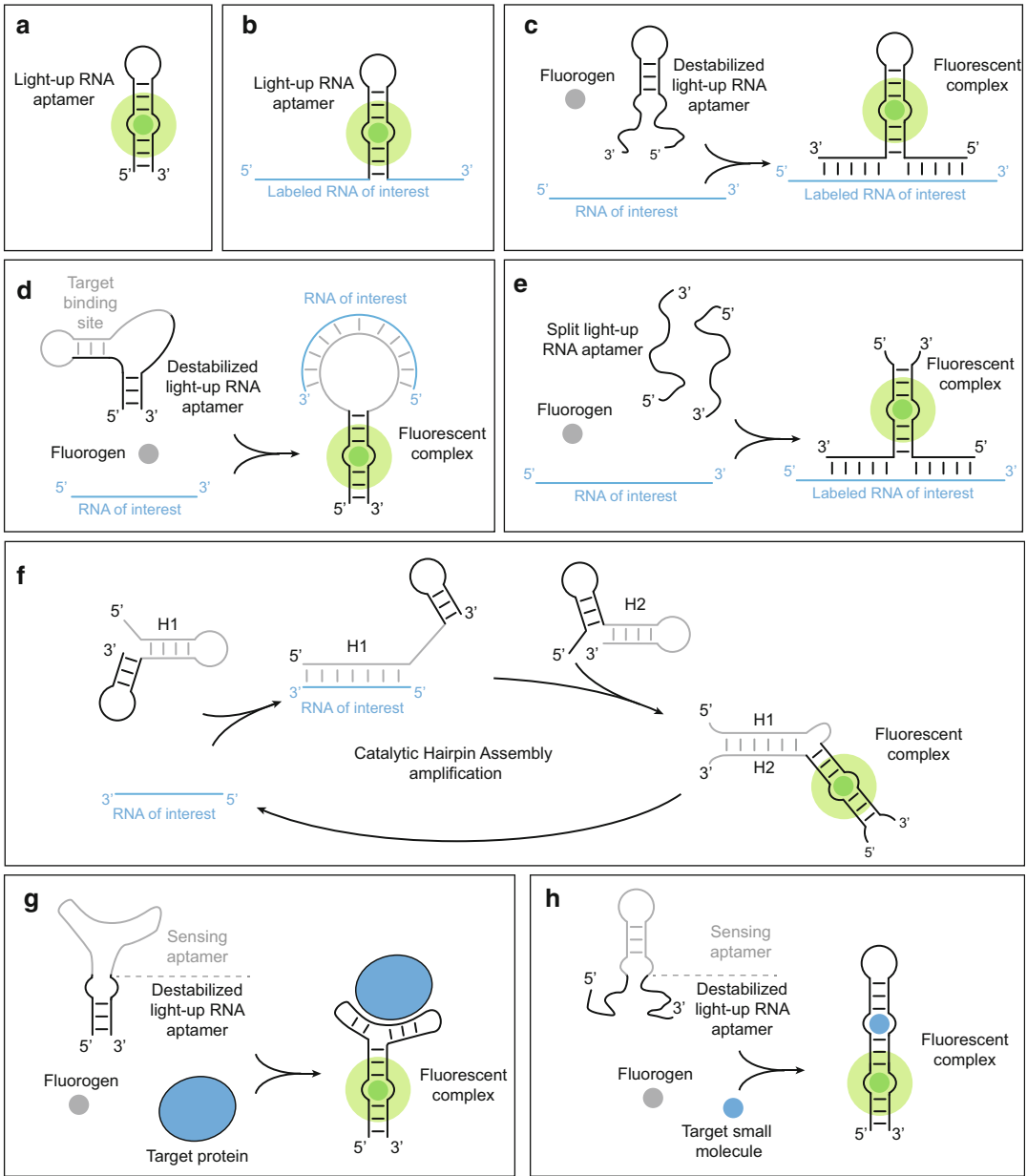


Fig. 5 Main labeling/sensing strategies using light-up RNA aptamers. **(a)** Light-up RNA aptamer with its fluorogen. **(b)** Light-up RNA aptamer directly inserted into the RNA of interest. **(c)** RNA-specific probe acting *in trans* based on transient structural destabilization. **(d)** RNA-specific probe acting *in trans* based on strand displacement/structural remodeling. **(e)** RNA-specific probe acting *in trans* based on a split light-up RNA aptamer. **(f)** RNA-specific probe acting *in trans* combining strand displacement and split light-up aptamers together with catalytic hairpin assemblies amplification circuit (CHARGE technology) [83]. **(g)** Protein sensor using light-up RNA aptamer transiently structurally stabilized as readout [109]. **(h)** Metabolite sensor using light-up RNA aptamer transiently structurally stabilized as readout [117]

should be transcribed in fusion to a tRNA [66] or an F30 scaffold [67] that assist in the proper folding and providing resistance to RNase degradation. An elegant alternative called Tornado was recently proposed in which the aptamer is flanked by a pair of ribozymes that undergo self-cleavage just after RNA synthesis leaving 5' and 3' extremities that are joined together by a cellular ligase, thus releasing a circular RNA (racRNA) endowed with an extremely long half-life [68]. To visualize these stabilized light-up RNA aptamers, they are usually expressed from strong promoters (i.e., T7 RNA polymerase promoter in prokaryotes and U6 polymerase III promoter in eukaryotes) to demonstrate both proper aptamer functionality in the cellular environment and capacity of the fluorogen to cross the plasma membrane [15, 18, 21, 27–32, 35, 43, 58]. Moreover, proper expression and integrity of the aptamer can also be assessed by extracting and analyzing total RNA by gel electrophoresis. Staining the gel with a fluorogen (DFHBI or TO1-Biotin) then allows to specifically detect RNAs labeled with the light-up aptamer [67, 69]. Yet, to be significant, the fluorogen/ aptamer pair should also enable imaging less abundant but more biologically relevant RNAs.

3.2 Live-Cell RNA Imaging Using Light-Up Aptamers Inserted into the Target RNA

An RNA of interest (ROI) can be imaged by expressing it in fusion with the light-up aptamer (Fig. 5b). This strategy was initially applied to abundant eukaryotic small noncoding RNAs transcribed by RNA polymerase III (pol. III). Indeed, labeling 5S rRNA and 7SK RNA with Spinach2 allowed visualizing them at the expected location (i.e., diffuse in the cytoplasm and in nuclear speckles, respectively) [58]. Moreover, using a construct in which 60 CGG repeats (the hallmark of some neurodegenerative diseases) were fused to Spinach2 allowed to recapitulate the aggregation process seen during the disease and to devise a drug screening strategy. Other small pol. III transcripts (i.e., 5S rRNA, U6 RNA, a box C/D scaRNA, or a tRNA) were also successfully detected at the expected location upon labeling with Mango-II [43] or Corn [21]. Extending this imaging strategy to less abundant pol. II transcripts (mRNAs and microRNAs) turned to be more complex because of the only moderate brightness and photostability of these first set of probes (see above). Indeed, it was possible to detect and track *STL1* mRNA fused to a single copy of Spinach aptamer in yeast using a sophisticated microscopy and image analysis pipeline [63]. However, whereas this work demonstrated the great potential of light-up RNA aptamers, the complexity of the approach prevented its wide use. Significant gain in signal was obtained by using an array of up to 64 tandem repeats of Spinach introduced into the 3' untranslated region of an ROI without affecting its life cycle [70]. Using brighter systems like TMR-DN/SRB2 allowed detecting CFP mRNA labeled with only 15 repeats of the aptamer in mammalian and GFP mRNA labeled with only 6 repeats in bacteria

[29]. The number of aptamer repeats was even further recently decreased by labeling β -actin mRNA with only four copies of the Riboglow aptamer while still being able to observe RNA relocation in stress granules with a signal quality outperforming the MS2-GFP method [32]. Recently, direct labeling of GFP mRNA by only five copies of the very bright SiRA aptamer allowed to detect RNA synthesis in bacteria and to gain in imaging accuracy using STED super-resolution imaging [30].

Recently, it has been reported that the direct insertion of the probe may lead to folding interference between the labeled mRNA and the light-up aptamer, as in the case of eGFP mRNA labeled with SRB2 aptamer [71]. Yet, such an adverse effect can be avoided by inserting a Dicer cleavage site between the mRNA and the aptamer so that, upon synthesis, Dicer physically separates both molecules and thereby restores the aptamer folding capacity. However, while still informative on the synthesis of the ROI, this approach compromises the chances to track the ROI in the cell. Another way of avoiding folding interference while reducing the required genetics is to use probes acting *in trans*.

3.3 Live-Cell RNA Imaging Using Light-Up Aptamers Acting In Trans

Besides the direct insertion of a light-up aptamer into the sequence of an ROI, the labeling can also be performed *in trans* (Fig. 5c–f). A first engineering strategy consists of transiently destabilizing a key structural element (e.g., a stem close to the fluorogen-binding site) of the aptamer by shortening and/or mutating it while appending sequences complementary to the ROI near the destabilized stem (Fig. 5c). In its free state, the RNA probe is unable to interact with the fluorogen and cannot form a fluorescent complex. However, upon interaction with the ROI, the light-up domain of the probe recovers its “active” folding together with its capacity to bind its fluorogen, resulting in the fluorescent labeling of the ROI. Such approach was successfully applied to endogenous mRNA visualization using engineered versions of the BHQ-1-binding aptamer [72] and of Spinach [73]. Recently, improved designs of Broccoli-derived probes with optimized sequences have been proposed and were shown to display superior performances to detect mRNA *in vitro* [61, 74]. Yet, these probes still need to be validated in live cells. Similar design was also exploited for the development of a probe called PANDAN aimed at detecting microRNA (miR), though this probe was not evaluated in living cells either [75].

Besides stem stabilization, aptamer activation can also take place through more important structural remodeling involving strand displacements (Fig. 5d). For instance, in FASTmiR technology, an engineered version of Spinach, is trapped in an inactive form and the successful binding of a target miR to a sensing domain induces, both *in vitro* and in live cells, several strand displacements eventually leading to the release of an active Spinach domain [76]. Substantial gain in sensitivity was later achieved by

engineering a domain of the SRB2 aptamer into a molecular beacon [77]. In this construct, the successful interaction between the sensing loop of the probe and the target miR leads to structural rearrangements activating SRB2, which in turn can bind and trigger the bright SR-DN fluorogen. More recently, a new concept in which the probe is made of an L-enantiomer of Mango-III supplied from outside the cell has been introduced [78]. L-enantiomers are naturally resistant to nuclease, making these probes extremely long-lasting in challenging media (e.g., extracellular space). Furthermore, coupling the probe to a cholesterol molecule and using a clever LNA-based blocker allowed cell entry of the probe and its activation by cellular miR (natural D-enantiomer).

Finally, a light-up aptamer can be converted into a probe acting *in trans* by splitting it and appending each half to a sequence complementary to the ROI (Fig. 5c). Therefore, a functional aptamer is reconstituted only in the presence of the target RNA that acts as a scaffold driving aptamer assembly. Split aptamer-based methodologies were shown to offer a very high specificity [79–81]. The recent application of this concept in live cells allowed mRNA to be detected from genetically encoded Spinach and Broccoli-derived probes with a decent sensitivity (minimum detectable concentration of 50–100 nM) in living cells [82]. Substantial gain in sensitivity was further obtained by combining the use of a split Broccoli aptamer and a catalytic hairpin assembly amplification circuit (a molecular amplification circuit derived from RNA nanotechnology). The resulting CHARGE technology (Fig. 5f) allows detecting the presence of as few as 2.5 nM of target RNAs in live cells in a digital manner (i.e., informs on the presence or absence of the target) [83]. Last but not least, split aptamers can also be expressed in cells and used to detect RNA-RNA interactions [84].

3.4 In Vitro Detection of RNA

The key implication of miRs in various diseases and disorders has stimulated the development of sensitive *in vitro* detection technologies for diagnostic applications. In this view, light-up RNA aptamers offer the great advantage of allowing to design cheap, label-free, and sensitive assays. Following the same concepts as for live-cell RNA imaging, the first generation of *in vitro* RNA sensors exploited transiently destabilized aptamers (e.g., PANDAN technology [75]) and split aptamer [81] strategies. However, the micromolar to high nanomolar sensitivity of these technologies was insufficient to detect low-abundant RNAs suggesting that an amplification step may be necessary. Several RNA-based molecular amplification circuits, including CHARGE, have been developed for *in vitro* applications [83, 85, 86] and could be used to increase detection sensitivity. However, an elegant alternative consisting of using the amplification capacity of the *in vitro* transcription reaction has recently been proposed and revealed to be extremely efficient for the sensitive detection of nucleic acids [87, 88] and other classes

of targets (see below). Briefly, the target miR interacts with two DNA molecules (one containing the T7 RNA polymerase promoter and the second containing the sequence coding for Spinach aptamer) and drives their specific ligation to form a full-length transcription template. Then, each template is transcribed into a large number of Spinach aptamers that become fluorescent in the presence of DFHBI(-1T). Such amplification-based detections allow the specific detection of miR with a low femtomolar limit of detection. In the latest format of these technologies, this limit was pushed down to the attomolar range (5 aMol) by replacing the ligation step by a primer extension coupled with a strand displacement amplification (SDA), adding a second amplification step to the process [89].

Being able to detect RNA *in vitro* allows also to set up new screening and analytical pipelines in which the *in vitro* transcription process can be monitored either alone [90] or in tandem with *in vitro* translation [91–93]. This ability to independently monitor RNA and protein (e.g., using fluorescent protein) synthesis permits to finely tune gene expression rates for applications in synthetic biology, for instance. Light-up RNA aptamers can also be used as reporters to aid in the development of catalytic RNAs endowed with self-cleaving [94] or RNA-modifying activities [95].

Finally, light-up RNA aptamers also offer the great opportunity to assist and validate the design of supramolecular assemblies in RNA nanotechnology. RNA nanotechnology aims at designing programmable molecular circuits (such as the catalytic hairpin assemblies introduced above) and supramolecular assemblies to achieve complex functions (e.g., computation using logic gates, channeling of catalysts on functionalized surfaces, drug delivery) *in vitro* or in living cells by genetically encoding the system. For instance, light-up aptamers can be used as output signal of a molecular circuit aiming at amplifying a signal [85, 96] or analyzing several inputs using logic gates as complex as half-adders [97]. Incorporating a monolithic light-up aptamer into supramolecular assemblies is also frequently used to assess that RNA elements grafted onto the assembly preserve their function as well as to track these nano-objects [98, 99]. Last but not least, split versions of MGA [100–103], Spinach [102, 104], or Broccoli [105, 106] revealed to be extremely useful to validate the proper assembly of multistrand RNA nanoparticles forming a variety of tiles [102, 103, 105] but also more elaborated shapes like cubes [100] and rings [104], just to name a few examples.

3.5 Detection of Other Biological Molecules and Ions

Beyond RNA detection, light-up RNA aptamers also found a wide range of applications allowing to specifically detect and quantify several other types of target. For instance, by inserting Spinach2 into sgRNAs, it is possible to precisely localize specific loci on genomic DNA using CRISPR-display technology [107]. In a

different way, fusing Spinach to the PP7 RNA sequence enables to bring the aptamer in close proximity to a PP7-mCherry fusion protein and, this way, to characterize RNA/protein interaction (e.g., affinity measurement) by monitoring FRET (Förster resonance emission transfer) between DFHBI/Spinach and mCherry fluorophores [108]. Specific protein/RNA interactions can also be established by fusing the light-up RNA to another aptamer that specifically targets a protein. This concept was applied to monitor EGFR (epidermal growth factor receptor) internalization by labeling the receptor with an EGFR-binding aptamer fused to the DIR2s aptamer [17]. As in the case described above for RNA detection, proteins can also be detected by using a bipartite probe made of a transiently destabilized light-up aptamer domain fused to a second aptamer binding specifically to the protein of interest (Fig. 5g). As before, the specific interaction between the protein and the sensing aptamer stabilizes the overall structure of the probe and restores the fluorogen-binding capacity of the light-up aptamer moiety. Such allosteric probes were successfully derived from Spinach and applied to the detection of a variety of proteins synthesized in *E. coli* [109]. Whereas such a direct labeling is particularly well suited to monitor protein synthesis in living cells, it does not offer sufficient sensitivity to detect low-abundant protein targets as potentially required for diagnostic purposes. Yet, combining conventional immunoassays like the proximity ligation assay (PLA) and ELISA with the Spinach transcription-based amplification strategy introduced above allowed to devise ultrasensitive assays able to detect proteins present at picomolar [110] and attomolar [111] concentrations. Interestingly, applying the same concept to the detection of whole bacteria allowed to devise an assay able to specifically identify the presence of as few as 77 *Staphylococcus aureus* per mL of food samples [112]. Light-up aptamers can also be used to monitor the activity of enzymes, such as Dicer [113], telomerase [114], or RNA-modifying enzymes [115]. These fluorogenic assays are compatible with high-throughput screening and are therefore suited for drug discovery applications, for example.

Light-up RNA aptamers also served as building blocks in the design of metabolite biosensors permitting to monitor the accumulation of a target metabolite in real time and in a noninvasive manner. Such genetically encoded biosensors were developed, for instance, to detect SAM [116], FMN [117], TPP, cyclic AMP [118], as well as various types of cyclic dinucleotides [119–125]. In general, these sensors are based on the transient destabilization strategy (Fig. 5h) similar to that described above for RNA and protein detection. These sensors are usually developed by using a trial-and-error approach, but optimal biosensors can also be

identified by employing high-throughput screening approaches such as the μ IVC-based procedure we recently described [126]. Alternative design strategies have been proposed using natural riboswitches and circularly permuted molecules. However, since these sensors and their development are out of the scope of this chapter, the reader is redirected to some excellent recent reviews on the topic [127–129]. While for a long time the use of these sensors in mammalian cells was challenged by the short half-life of small RNAs in these cells, the recent development of the Tornado technology allows to express these sensors as highly stable circular RNAs [68].

Exploiting RNA nanotechnology also led to the designing of a construct comprising Spinach and Mango aptamers positioned in such a way that FRET can occur between the fluorogens (respectively, DFHBI-1T and YO3) bound to each aptamer. Moreover, inserting a metabolite-sensing aptamer into the construct allows to couple the FRET signal to a metabolite-sensing event [15]. Interestingly, metabolite biosensors can also be used as extracellular probes in screening experiments aiming at identifying microbes with improved capacity to synthesize and secrete a target metabolite [130].

Last but not least, light-up aptamers can easily be converted into ion sensors. The two most prominent examples are silver and lead sensors. Indeed, simply converting a Watson-Crick base pair of Broccoli into a C•C mismatch allowed to transiently abrogate the fluorogen-binding capacity of the aptamer. However, in the presence of silver ions, a C-Ag⁺-C metallo base pair forms and restores aptamer capacity to bind and trigger DFHBI-1T fluorescence [131]. Expressing this sensor in living bacteria permitted to titrate the amount of silver that can actually enter and accumulate into the cells. The second example is lead detection. Indeed, it was found that the G-quadruplex structure contained in Spinach can strongly bind and get stabilized by Pb²⁺ ions, making Spinach an excellent sensor able to specifically detect as few as 6 nM Pb²⁺, a concentration far below the maximum permissible concentration (72 nM) [132]. Moreover, it was recently found that a 2'-fluorinated version of the sensor may offer even higher performance by protecting the sensor from RNase action and by enhancing the association with Pb²⁺ ions [133]. Interestingly, exploiting this Pb²⁺ binding capacity of Spinach enabled the development of a fluorescence-free liquid crystal sensor able to detect Pb²⁺ ions with similar selectivity and sensitivity [134], demonstrating how properties of light-up aptamers can even be used without exploiting their fluorescence capacity. In the same line, the very high affinity of Mango for TO1-Biotin can be exploited in experiments aiming to specifically isolate target RNAs and bound molecules by affinity capture [135].

4 Conclusions

Since the discovery that an RNA molecule may have the capacity to light up a fluorogen [7], many groups have started to develop highly efficient, bright, photostable, and cell-permeable fluorogens together with their specific aptamers. To this end, strong progresses were made in the chemistry of the fluorogen but also in the development of new technologies and methodologies for high-throughput functional screening of mutant gene libraries as well as for the stabilization of RNA probes both inside (e.g., Tornado [68]) and outside (e.g., use of 2'-fluorinated ribose [133] and L-enantiomers [78]) the cell.

While the main motivation in developing new efficient fluorogen/light-up aptamer pairs was mainly driven by the possibility of imaging RNA in living cells with high sensitivity, one can see that the application scope of these probes rapidly diversified toward the sensitive sensing of a variety of molecules (DNA, protein, metabolites, and ions) both in live cells and in vitro. Indeed, the development and the commercialization of ultrasensitive detection kits may have a profound impact on various fields such as healthcare and environment survey. Light-up aptamers may also play a role in drug discovery by allowing to set up high-throughput screening pipelines as well as by assisting the development of RNA nano-objects that could act, for instance, as drug delivery cargos.

As a conclusion, it is likely that even more efficient fluorogen/light-up aptamer pairs will be developed over the coming years and that additional types of molecules beyond RNA will be used for the development of light-up aptamers. Indeed, two DNA-based light-up aptamers have been described [12, 20] which may provide great advantages in terms of cost and backbone stability. Moreover, one can expect that the application spectrum of light-up aptamers will continue to grow far beyond RNA detection and that first analysis kits and devices using these molecules may appear on the market in a near future. Therefore, the story of light-up aptamers is just beginning.

References

1. Jin R, Breslauer KJ (1988) Characterization of the minor groove environment in a drug-DNA complex: bisbenzimidazole bound to the poly[d(AT)].poly[d(AT)]duplex. *Proc Natl Acad Sci U S A* 85(23):8939–8942
2. Armitage BA (2008) Cyanine dye–nucleic acid interactions. In: Strekowski L (ed) *Heterocyclic polymethine dyes: synthesis, properties and applications*. Springer, Berlin, pp 11–29. https://doi.org/10.1007/7081_2007_109
3. Tyagi S (2009) Imaging intracellular RNA distribution and dynamics in living cells. *Nat Methods* 6(5):331–338. <https://doi.org/10.1038/nmeth.1321>
4. Wang Z, Liu W, Fan C, Chen N (2019) Visualizing mRNA in live mammalian cells. *Methods*. <https://doi.org/10.1016/j.ymeth.2019.03.008>
5. Bertrand E, Chartrand P, Schaefer M, Shenoy SM, Singer RH, Long RM (1998)

- Localization of ASH1 mRNA particles in living yeast. *Mol Cell* 2(4):437–445
- Buxbaum AR, Haimovich G, Singer RH (2015) In the right place at the right time: visualizing and understanding mRNA localization. *Nat Rev Mol Cell Biol* 16(2):95–109. <https://doi.org/10.1038/nrm3918>
 - Babendure JR, Adams SR, Tsien RY (2003) Aptamers switch on fluorescence of triphenylmethane dyes. *J Am Chem Soc* 125(48):14716–14717. <https://doi.org/10.1021/ja037994o>
 - Ouellet J (2016) RNA fluorescence with light-up aptamers. *Front Chem* 4:29. <https://doi.org/10.3389/fchem.2016.00029>
 - Bouhedda F, Autour A, Ryckelynck M (2018) Light-up RNA aptamers and their cognate fluorogens: from their development to their applications. *Int J Mol Sci* 19(1):44. <https://doi.org/10.3390/ijms19010044>
 - Neubacher S, Hennig S (2019) RNA structure and cellular applications of fluorescent light-up aptamers. *Angew Chem Int Ed Engl* 58(5):1266–1279. <https://doi.org/10.1002/anie.201806482>
 - Grate D, Wilson C (1999) Laser-mediated, site-specific inactivation of RNA transcripts. *Proc Natl Acad Sci U S A* 96(11):6131–6136
 - Sando S, Narita A, Aoyama Y (2007) Light-up Hoechst-DNA aptamer pair: generation of an aptamer-selective fluorophore from a conventional DNA-staining dye. *Chembiochem* 8(15):1795–1803. <https://doi.org/10.1002/cbic.200700325>
 - Sando S, Narita A, Hayami M, Aoyama Y (2008) Transcription monitoring using fused RNA with a dye-binding light-up aptamer as a tag: a blue fluorescent RNA. *Chem Commun (Camb)* 44(33):3858–3860. <https://doi.org/10.1039/b808449a>
 - Dolgosheina EV, Jeng SC, Panchapakesan SS, Cojocaru R, Chen PS, Wilson PD, Hawkins N, Wiggins PA, Unrau PJ (2014) RNA mango aptamer-fluorophore: a bright, high-affinity complex for RNA labeling and tracking. *ACS Chem Biol* 9(10):2412–2420. <https://doi.org/10.1021/cb500499x>
 - Jepsen MDE, Sparvath SM, Nielsen TB, Langvad AH, Grossi G, Gothelf KV, Andersen ES (2018) Development of a genetically encodable FRET system using fluorescent RNA aptamers. *Nat Commun* 9(1):18. <https://doi.org/10.1038/s41467-017-02435-x>
 - Constantin TP, Silva GL, Robertson KL, Hamilton TP, Fague K, Waggoner AS, Armitage BA (2008) Synthesis of new fluorogenic cyanine dyes and incorporation into RNA fluoromodules. *Org Lett* 10(8):1561–1564. <https://doi.org/10.1021/ol702920c>
 - Tan X, Constantin TP, Sloane KL, Waggoner AS, Bruchez MP, Armitage BA (2017) Fluoromodules consisting of a promiscuous RNA aptamer and red or blue fluorogenic cyanine dyes: selection, characterization, and bioimaging. *J Am Chem Soc* 139(26):9001–9009. <https://doi.org/10.1021/jacs.7b04211>
 - Paige JS, Wu KY, Jaffrey SR (2011) RNA mimics of green fluorescent protein. *Science* 333(6042):642–646. <https://doi.org/10.1126/science.1207339>
 - Song W, Strack RL, Svensen N, Jaffrey SR (2014) Plug-and-play fluorophores extend the spectral properties of spinach. *J Am Chem Soc* 136(4):1198–1201. <https://doi.org/10.1021/ja410819x>
 - Feng G, Luo C, Yi H, Yuan L, Lin B, Luo X, Hu X, Wang H, Lei C, Nie Z, Yao S (2017) DNA mimics of red fluorescent proteins (RFP) based on G-quadruplex-confined synthetic RFP chromophores. *Nucleic Acids Res* 45(18):10380–10392. <https://doi.org/10.1093/nar/gkx803>
 - Song W, Filonov GS, Kim H, Hirsch M, Li X, Moon JD, Jaffrey SR (2017) Imaging RNA polymerase III transcription using a photostable RNA-fluorophore complex. *Nat Chem Biol* 13(11):1187–1194. <https://doi.org/10.1038/nchembio.2477>
 - Steinmetzger C, Palanisamy N, Gore KR, Hobartner C (2019) A multicolor large Stokes shift fluorogen-activating RNA aptamer with cationic chromophores. *Chemistry* 25(8):1931–1935. <https://doi.org/10.1002/chem.201805882>
 - Han KY, Leslie BJ, Fei J, Zhang J, Ha T (2013) Understanding the photophysics of the spinach-DFHBI RNA aptamer-fluorogen complex to improve live-cell RNA imaging. *J Am Chem Soc* 135(50):19033–19038. <https://doi.org/10.1021/ja411060p>
 - You M, Jaffrey SR (2015) Structure and mechanism of RNA mimics of green fluorescent protein. *Annu Rev Biophys* 44:187–206. <https://doi.org/10.1146/annurev-biophys-060414-033954>
 - Klymchenko AS (2017) Solvatochromic and fluorogenic dyes as environment-sensitive probes: design and biological applications. *Acc Chem Res* 50(2):366–375. <https://doi.org/10.1021/acs.accounts.6b00517>

26. Lee J, Lee KH, Jeon J, Dragulescu-Andrasi A, Xiao F, Rao J (2010) Combining SELEX screening and rational design to develop light-up fluorophore-RNA aptamer pairs for RNA tagging. *ACS Chem Biol* 5 (11):1065–1074. <https://doi.org/10.1021/cb1001894>
27. Sunbul M, Jaschke A (2013) Contact-mediated quenching for RNA imaging in bacteria with a fluorophore-binding aptamer. *Angew Chem Int Ed Engl* 52 (50):13401–13404. <https://doi.org/10.1002/anie.201306622>
28. Arora A, Sunbul M, Jaschke A (2015) Dual-colour imaging of RNAs using quencher- and fluorophore-binding aptamers. *Nucleic Acids Res* 43(21):e144. <https://doi.org/10.1093/nar/gkv718>
29. Sunbul M, Jaschke A (2018) SRB-2: a promiscuous rainbow aptamer for live-cell RNA imaging. *Nucleic Acids Res* 46(18):e110. <https://doi.org/10.1093/nar/gky543>
30. Wirth R, Gao P, Nienhaus GU, Sunbul M, Jaschke A (2019) SiRA: a silicon rhodamine-binding aptamer for live-cell super-resolution RNA imaging. *J Am Chem Soc* 141 (18):7562–7571. <https://doi.org/10.1021/jacs.9b02697>
31. Murata A, Sato S, Kawazoe Y, Uesugi M (2011) Small-molecule fluorescent probes for specific RNA targets. *Chem Commun (Camb)* 47(16):4712–4714. <https://doi.org/10.1039/c1cc10393h>
32. Braselmann E, Wierzba AJ, Polaski JT, Chrominski M, Holmes ZE, Hung ST, Batan D, Wheeler JR, Parker R, Jimenez R, Gryko D, Batey RT, Palmer AE (2018) A multicolor riboswitch-based platform for imaging of RNA in live mammalian cells. *Nat Chem Biol* 14(10):964–971. <https://doi.org/10.1038/s41589-018-0103-7>
33. Ellington AD, Szostak JW (1990) In vitro selection of RNA molecules that bind specific ligands. *Nature* 346(6287):818–822. <https://doi.org/10.1038/346818a0>
34. Tuerk C, Gold L (1990) Systematic evolution of ligands by exponential enrichment: RNA ligands to bacteriophage T4 DNA polymerase. *Science* 249(4968):505–510. <https://doi.org/10.1126/science.2200121>
35. Filonov GS, Moon JD, Svensen N, Jaffrey SR (2014) Broccoli: rapid selection of an RNA mimic of green fluorescent protein by fluorescence-based selection and directed evolution. *J Am Chem Soc* 136 (46):16299–16308. <https://doi.org/10.1021/ja508478x>
36. Heim R, Cubitt AB, Tsien RY (1995) Improved green fluorescence. *Nature* 373 (6516):663–664. <https://doi.org/10.1038/373663b0>
37. Gotrik M, Sekhon G, Saurabh S, Nakamoto M, Eisenstein M, Soh HT (2018) Direct selection of fluorescence-enhancing RNA aptamers. *J Am Chem Soc* 140 (10):3583–3591. <https://doi.org/10.1021/jacs.7b10724>
38. Kraus GA, Jeon I, Nilsen-Hamilton M, Awad AM, Banerjee J, Parvin B (2008) Fluorinated analogs of malachite green: synthesis and toxicity. *Molecules* 13(4):986–994. <https://doi.org/10.3390/molecules13040986>
39. Endoh T, Ohyama T, Sugimoto N (2019) RNA-capturing microsphere particles (R-CAMPs) for optimization of functional aptamers. *Small* 15(26):e1805062. <https://doi.org/10.1002/sml.201805062>
40. Ryckelynck M, Baudrey S, Rick C, Marin A, Coldren F, Westhof E, Griffiths AD (2015) Using droplet-based microfluidics to improve the catalytic properties of RNA under multiple-turnover conditions. *RNA* 21 (3):458–469. <https://doi.org/10.1261/rna.048033.114>
41. Autour A, Ryckelynck M (2017) Ultrahigh-throughput improvement and discovery of enzymes using droplet-based microfluidic screening. *Micromachines* 8(4):128. <https://doi.org/10.3390/mi8040128>
42. Autour A, Westhof E, Ryckelynck M (2016) iSpinach: a fluorogenic RNA aptamer optimized for in vitro applications. *Nucleic Acids Res* 44(6):2491–2500. <https://doi.org/10.1093/nar/gkw083>
43. Autour A, S CYJ ADC, Abdolhazadeh A, Galli A, Panchapakesan SSS, Rueda D, Ryckelynck M, Unrau PJ (2018) Fluorogenic RNA Mango aptamers for imaging small non-coding RNAs in mammalian cells. *Nat Commun* 9(1):656. <https://doi.org/10.1038/s41467-018-02993-8>
44. Ketterer S, Fuchs D, Weber W, Meier M (2015) Systematic reconstruction of binding and stability landscapes of the fluorogenic aptamer spinach. *Nucleic Acids Res*. <https://doi.org/10.1093/nar/gkv944>
45. Ketterer S, Gladis L, Kozica A, Meier M (2016) Engineering and characterization of fluorogenic glycine riboswitches. *Nucleic Acids Res* 44(12):5983–5992. <https://doi.org/10.1093/nar/gkw465>
46. Henderson CA, Rail CA, Butt LE, Vincent HA, Callaghan AJ (2019) Generation of small molecule-binding RNA arrays and their

- application to fluorogen-binding RNA aptamers. *Methods*. <https://doi.org/10.1016/j.ymeth.2019.04.021>
47. Shelke SA, Shao Y, Laski A, Koirala D, Weissman BP, Fuller JR, Tan X, Constantin TP, Waggoner AS, Bruchez MP, Armitage BA, Piccirilli JA (2018) Structural basis for activation of fluorogenic dyes by an RNA aptamer lacking a G-quadruplex motif. *Nat Commun* 9(1):4542. <https://doi.org/10.1038/s41467-018-06942-3>
 48. Baugh C, Grate D, Wilson C (2000) 2.8 Å crystal structure of the malachite green aptamer. *J Mol Biol* 301(1):117–128. <https://doi.org/10.1006/jmbi.2000.3951>
 49. Huang H, Suslov NB, Li NS, Shelke SA, Evans ME, Koldobskaya Y, Rice PA, Piccirilli JA (2014) A G-quadruplex-containing RNA activates fluorescence in a GFP-like fluorophore. *Nat Chem Biol* 10(8):686–691. <https://doi.org/10.1038/nchembio.1561>
 50. Warner KD, Chen MC, Song W, Strack RL, Thorn A, Jaffrey SR, Ferre-D'Amare AR (2014) Structural basis for activity of highly efficient RNA mimics of green fluorescent protein. *Nat Struct Mol Biol* 21(8):658–663. <https://doi.org/10.1038/nsmb.2865>
 51. Fernandez-Millan P, Autour A, Ennifar E, Westhof E, Ryckelynck M (2017) Crystal structure and fluorescence properties of the iSpinach aptamer in complex with DFHBI. *RNA* 23(12):1788–1795. <https://doi.org/10.1261/rna.063008.117>
 52. Trachman RJ 3rd, Demeshkina NA, Lau MWL, Panchapakesan SSS, Jeng SCY, Unrau PJ, Ferre-D'Amare AR (2017) Structural basis for high-affinity fluorophore binding and activation by RNA Mango. *Nat Chem Biol* 13(7):807–813. <https://doi.org/10.1038/nchembio.2392>
 53. Trachman RJ 3rd, Truong L, Ferre-D'Amare AR (2017) Structural principles of fluorescent RNA aptamers. *Trends Pharmacol Sci* 38(10):928–939. <https://doi.org/10.1016/j.tips.2017.06.007>
 54. Trachman R, Abdolhazadeh A, Andreoni A, Cojocar R, Knutson JR, Ryckelynck M, Unrau PJ, Ferre-D'Amare A (2018) Crystal structures of the Mango-II RNA aptamer reveal heterogeneous fluorophore binding and guide engineering of variants with improved selectivity and brightness. *Biochemistry*. <https://doi.org/10.1021/acs.biochem.8b00399>
 55. Trachman RJ 3rd, Autour A, Jeng SCY, Abdolhazadeh A, Andreoni A, Cojocar R, Garipov R, Dolgosheina EV, Knutson JR, Ryckelynck M, Unrau PJ, Ferre-D'Amare AR (2019) Structure and functional reselec-tion of the Mango-III fluorogenic RNA aptamer. *Nat Chem Biol* 15(5):472–479. <https://doi.org/10.1038/s41589-019-0267-9>
 56. Trachman RJ 3rd, Stagno JR, Conrad C, Jones CP, Fischer P, Meents A, Wang YX, Ferre-D'Amare AR (2019) Co-crystal structure of the iMango-III fluorescent RNA aptamer using an X-ray free-electron laser. *Acta Crystallogr F Struct Biol Commun* 75(Pt 8):547–551. <https://doi.org/10.1107/S2053230X19010136>
 57. Guo JU, Bartel DP (2016) RNA G-quadruplexes are globally unfolded in eukaryotic cells and depleted in bacteria. *Science* 353(6306). <https://doi.org/10.1126/science.aaf5371>
 58. Strack RL, Disney MD, Jaffrey SR (2013) A superfolder Spinach2 reveals the dynamic nature of trinucleotide repeat-containing RNA. *Nat Methods* 10(12):1219–1224. <https://doi.org/10.1038/nmeth.2701>
 59. Ageely EA, Kartje ZJ, Rohilla KJ, Barkau CL, Gagnon KT (2016) Quadruplex-flanking stem structures modulate the stability and metal ion preferences of RNA mimics of GFP. *ACS Chem Biol* 11(9):2398–2406. <https://doi.org/10.1021/acschembio.6b00047>
 60. Filonov GS, Song W, Jaffrey SR (2019) Spectral tuning by a single nucleotide controls the fluorescence properties of a fluorogenic aptamer. *Biochemistry* 58(12):1560–1564. <https://doi.org/10.1021/acs.biochem.9b00048>
 61. Furuhata Y, Kobayashi M, Maruyama R, Sato Y, Makino K, Michiue T, Yui H, Nishizawa S, Yoshimoto K (2019) Programmable RNA detection with a fluorescent RNA aptamer using optimized three-way junction formation. *RNA* 25(5):590–599. <https://doi.org/10.1261/rna.069062.118>
 62. Warner KD, Sjekloca L, Song W, Filonov GS, Jaffrey SR, Ferre-D'Amare AR (2017) A homodimer interface without base pairs in an RNA mimic of red fluorescent protein. *Nat Chem Biol* 13(11):1195–1201. <https://doi.org/10.1038/nchembio.2475>
 63. Guet D, Burns LT, Maji S, Boulanger J, Hersen P, Wente SR, Salamero J, Dargemont C (2015) Combining Spinach-tagged RNA and gene localization to image gene expression in live yeast. *Nat Commun* 6:8882. <https://doi.org/10.1038/ncomms9882>
 64. Zinskie JA, Roig M, Janetopoulos C, Myers KA, Bruist MF (2018) Live-cell imaging of small nucleolar RNA tagged with the broccoli

- aptamer in yeast. *FEMS Yeast Res* 18(8). <https://doi.org/10.1093/femsyr/foy093>
65. Guzman-Zapata D, Dominguez-Anaya Y, Macedo-Osorio KS, Tovar-Aguilar A, Castrejon-Flores JL, Duran-Figueroa NV, Badillo-Corona JA (2017) mRNA imaging in the chloroplast of *Chlamydomonas reinhardtii* using the light-up aptamer Spinach. *J Biotechnol* 251:186–188. <https://doi.org/10.1016/j.jbiotec.2017.03.028>
66. Ponchon L, Dardel F (2007) Recombinant RNA technology: the tRNA scaffold. *Nat Methods* 4(7):571–576. <https://doi.org/10.1038/nmeth1058>
67. Filonov GS, Kam CW, Song W, Jaffrey SR (2015) In-gel imaging of RNA processing using broccoli reveals optimal aptamer expression strategies. *Chem Biol* 22(5):649–660. <https://doi.org/10.1016/j.chembiol.2015.04.018>
68. Litke JL, Jaffrey SR (2019) Highly efficient expression of circular RNA aptamers in cells using autocatalytic transcripts. *Nat Biotechnol* 37(6):667–675. <https://doi.org/10.1038/s41587-019-0090-6>
69. Yaseen IM, Ang QR, Unrau PJ (2019) Fluorescent visualization of mango-tagged RNA in polyacrylamide gels via a poststaining method. *J Vis Exp* (148). <https://doi.org/10.3791/59112>
70. Zhang J, Fei J, Leslie BJ, Han KY, Kuhlman TE, Ha T (2015) Tandem Spinach Array for mRNA Imaging in Living Bacterial Cells. *Sci Rep* 5:17295. <https://doi.org/10.1038/srep17295>
71. Ying ZM, Yuan YY, Tu B, Tang LJ, Yu RQ, Jiang JH (2019) A single promoter system co-expressing RNA sensor with fluorescent proteins for quantitative mRNA imaging in living tumor cells. *Chem Sci* 10(18):4828–4833. <https://doi.org/10.1039/c9sc00458k>
72. Sato S, Watanabe M, Katsuda Y, Murata A, Wang DO, Uesugi M (2015) Live-cell imaging of endogenous mRNAs with a small molecule. *Angew Chem Int Ed Engl* 54(6):1855–1858. <https://doi.org/10.1002/anie.201410339>
73. Ong WQ, Citron YR, Sekine S, Huang B (2017) Live cell imaging of endogenous mRNA using RNA-based fluorescence “turn-on” probe. *ACS Chem Biol* 12(1):200–205. <https://doi.org/10.1021/acscchembio.6b00586>
74. Soni R, Sharma D, Krishna AM, Sathiri J, Sharma A (2019) A highly efficient Baby Spinach-based minimal modified sensor (BSMS) for nucleic acid analysis. *Org Biomol Chem* 17(30):7222–7227. <https://doi.org/10.1039/c9ob01414d>
75. Aw SS, Tang MX, Teo YN, Cohen SM (2016) A conformation-induced fluorescence method for microRNA detection. *Nucleic Acids Res* 44(10):e92. <https://doi.org/10.1093/nar/gkw108>
76. Huang K, Doyle F, Wurz ZE, Tenenbaum SA, Hammond RK, Caplan JL, Meyers BC (2017) FASTmiR: an RNA-based sensor for in vitro quantification and live-cell localization of small RNAs. *Nucleic Acids Res*. <https://doi.org/10.1093/nar/gkx504>
77. Ying ZM, Wu Z, Tu B, Tan W, Jiang JH (2017) Genetically encoded fluorescent RNA sensor for ratiometric imaging of microRNA in living tumor cells. *J Am Chem Soc* 139(29):9779–9782. <https://doi.org/10.1021/jacs.7b04527>
78. Zhong W, Sczepanski JT (2019) A mirror image fluorogenic aptamer sensor for live-cell imaging of microRNAs. *ACS Sens* 4(3):566–570. <https://doi.org/10.1021/acssensors.9b00252>
79. Kolpashchikov DM (2005) Binary malachite green aptamer for fluorescent detection of nucleic acids. *J Am Chem Soc* 127(36):12442–12443. <https://doi.org/10.1021/ja0529788>
80. Kikuchi N, Kolpashchikov DM (2016) Split spinach aptamer for highly selective recognition of DNA and RNA at ambient temperatures. *Chembiochem* 17(17):1589–1592. <https://doi.org/10.1002/cbic.201600323>
81. Kikuchi N, Kolpashchikov DM (2017) A universal split spinach aptamer (USSA) for nucleic acid analysis and DNA computation. *Chem Commun (Camb)* 53(36):4977–4980. <https://doi.org/10.1039/c7cc01540b>
82. Wang Z, Luo Y, Xie X, Hu X, Song H, Zhao Y, Shi J, Wang L, Glinsky G, Chen N, Lal R, Fan C (2018) In situ spatial complementation of aptamer-mediated recognition enables live-cell imaging of native RNA transcripts in real time. *Angew Chem Int Ed Engl* 57(4):972–976. <https://doi.org/10.1002/anie.201707795>
83. Karunanayake Mudiyanseilage A, Yu Q, Leon-Duque MA, Zhao B, Wu R, You M (2018) Genetically encoded catalytic hairpin assembly for sensitive RNA imaging in live cells. *J Am Chem Soc* 140(28):8739–8745. <https://doi.org/10.1021/jacs.8b03956>
84. Alam KK, Tawiah KD, Lichte MF, Porciani D, Burke DH (2017) A fluorescent split aptamer for visualizing RNA-RNA assembly in vivo.

- ACS Synth Biol. <https://doi.org/10.1021/acssynbio.7b00059>
85. Bhadra S, Ellington AD (2014) Design and application of cotranscriptional non-enzymatic RNA circuits and signal transducers. *Nucleic Acids Res* 42(7):e58. <https://doi.org/10.1093/nar/gku074>
86. Akter F, Yokobayashi Y (2015) RNA signal amplifier circuit with integrated fluorescence output. *ACS Synth Biol* 4(5):655–658. <https://doi.org/10.1021/sb500314r>
87. Tang X, Deng R, Sun Y, Ren X, Zhou M, Li J (2018) Amplified tandem spinach-based aptamer transcription enables low background miRNA detection. *Anal Chem* 90(16):10001–10008. <https://doi.org/10.1021/acs.analchem.8b02471>
88. Ying ZM, Tu B, Liu L, Tang H, Tang LJ, Jiang JH (2018) Spinach-based fluorescent light-up biosensors for multiplexed and label-free detection of microRNAs. *Chem Commun (Camb)* 54(24):3010–3013. <https://doi.org/10.1039/c8cc00123e>
89. Zhou M, Teng X, Li Y, Deng R, Li J (2019) Cascade transcription amplification of RNA aptamer for ultrasensitive microRNA detection. *Anal Chem* 91(8):5295–5302. <https://doi.org/10.1021/acs.analchem.9b00124>
90. Hofer K, Langejürgen LV, Jaschke A (2013) Universal aptamer-based real-time monitoring of enzymatic RNA synthesis. *J Am Chem Soc* 135(37):13692–13694. <https://doi.org/10.1021/ja407142f>
91. Pothoulakis G, Ceroni F, Reeve B, Ellis T (2013) The Spinach RNA aptamer as a characterization tool for synthetic biology. *ACS Synth Biol*. <https://doi.org/10.1021/sb400089c>
92. Chizzolini F, Forlin M, Cecchi D, Mansy SS (2014) Gene position more strongly influences cell-free protein expression from operons than T7 transcriptional promoter strength. *ACS Synth Biol* 3(6):363–371. <https://doi.org/10.1021/sb4000977>
93. Chizzolini F, Forlin M, Yeh Martin N, Berloff G, Cecchi D, Mansy SS (2017) Cell-free translation is more variable than transcription. *ACS Synth Biol* 6(4):638–647. <https://doi.org/10.1021/acssynbio.6b00250>
94. Auslander S, Fuchs D, Hurlemann S, Auslander D, Fussenegger M (2016) Engineering a ribozyme cleavage-induced split fluorescent aptamer complementation assay. *Nucleic Acids Res* 44(10):e94. <https://doi.org/10.1093/nar/gkw117>
95. Poudyal RR, Benslimane M, Lokugamage MP, Callaway MK, Staller S, Burke DH (2017) Selective inactivation of functional RNAs by ribozyme-catalyzed covalent modification. *ACS Synth Biol* 6(3):528–534. <https://doi.org/10.1021/acssynbio.6b00222>
96. Bhadra S, Ellington AD (2014) A Spinach molecular beacon triggered by strand displacement. *RNA* 20(8):1183–1194. <https://doi.org/10.1261/rna.045047.114>
97. Goldworthy V, LaForce G, Abels S, Khisamutdinov EF (2018) Fluorogenic RNA aptamers: a nano-platform for fabrication of simple and combinatorial logic gates. *Nanomaterials (Basel)* 8(12). <https://doi.org/10.3390/nano8120984>
98. Shu D, Shu Y, Haque F, Abdelmawla S, Guo P (2011) Thermodynamically stable RNA three-way junction for constructing multifunctional nanoparticles for delivery of therapeutics. *Nat Nanotechnol* 6(10):658–667. <https://doi.org/10.1038/nnano.2011.105>
99. Shu D, Khisamutdinov EF, Zhang L, Guo P (2014) Programmable folding of fusion RNA in vivo and in vitro driven by pRNA 3WJ motif of *Pbt29* DNA packaging motor. *Nucleic Acids Res* 42(2):e10. <https://doi.org/10.1093/nar/gkt885>
100. Afonin KA, Bindewald E, Yaghoubian AJ, Voss N, Jacovetty E, Shapiro BA, Jaeger L (2010) In vitro assembly of cubic RNA-based scaffolds designed in silico. *Nat Nanotechnol* 5(9):676–682. <https://doi.org/10.1038/nnano.2010.160>
101. Afonin KA, Viard M, Martins AN, Lockett SJ, Maciag AE, Freed EO, Heldman E, Jaeger L, Blumenthal R, Shapiro BA (2013) Activation of different split functionalities on re-association of RNA-DNA hybrids. *Nat Nanotechnol* 8(4):296–304. <https://doi.org/10.1038/nnano.2013.44>
102. Chopra A, Sagredo S, Grossi G, Andersen ES, Simmel FC (2019) Out-of-plane aptamer functionalization of RNA three-helix tiles. *Nanomaterials (Basel)* 9(4). <https://doi.org/10.3390/nano9040507>
103. Afonin KA, Danilov EO, Novikova IV, Leontis NB (2008) TokenRNA: a new type of sequence-specific, label-free fluorescent biosensor for folded RNA molecules. *Chembiochem* 9(12):1902–1905. <https://doi.org/10.1002/cbic.200800183>
104. O'Hara JM, Marashi D, Morton S, Jaeger L, Grabow WW (2019) Optimization of the split-Spinach aptamer for monitoring

- nanoparticle assembly involving multiple contiguous RNAs. *Nanomaterials* (Basel) 9(3). <https://doi.org/10.3390/nano9030378>
105. Torelli E, Kozyra JW, Gu JY, Stimming U, Piantanida L, Voitchovsky K, Krasnogor N (2018) Isothermal folding of a light-up bio-orthogonal RNA origami nanoribbon. *Sci Rep* 8(1):6989. <https://doi.org/10.1038/s41598-018-25270-6>
 106. Chandler M, Lyalina T, Halman J, Rackley L, Lee L, Dang D, Ke W, Sajja S, Woods S, Acharya S, Baumgarten E, Christopher J, Elshalia E, Hrebien G, Kublank K, Saleh S, Stallings B, Tafere M, Striplin C, Afonin KA (2018) Broccoli fluorets: split aptamers as a user-friendly fluorescent toolkit for dynamic RNA nanotechnology. *Molecules* 23(12). <https://doi.org/10.3390/molecules23123178>
 107. Shechner DM, Hacisuleyman E, Younger ST, Rinn JL (2015) Multiplexable, locus-specific targeting of long RNAs with CRISPR-Display. *Nat Methods* 12(7):664–670. <https://doi.org/10.1038/nmeth.3433>
 108. Roszyk L, Kollenda S, Hennig S (2017) Using a specific RNA-protein interaction to quench the fluorescent RNA Spinach. *ACS Chem Biol* 12(12):2958–2964. <https://doi.org/10.1021/acscchembio.7b00332>
 109. Song W, Strack RL, Jaffrey SR (2013) Imaging bacterial protein expression using genetically encoded RNA sensors. *Nat Methods* 10(9):873–875. <https://doi.org/10.1038/nmeth.2568>
 110. Ying ZM, Xiao HY, Tang H, Yu RQ, Jiang JH (2018) Light-up RNA aptamer enabled label-free protein detection via a proximity induced transcription assay. *Chem Commun (Camb)* 54(64):8877–8880. <https://doi.org/10.1039/c8cc04498h>
 111. Sim J, Byun JY, Shin YB (2019) Transcription immunoassay: light-up RNA aptamer-based immunoassay using in vitro transcription. *Chem Commun (Camb)* 55(25):3618–3621. <https://doi.org/10.1039/c9cc00514e>
 112. Sheng L, Lu Y, Deng S, Liao X, Zhang K, Ding T, Gao H, Liu D, Deng R, Li J (2019) A transcription aptasensor: amplified, label-free and culture-independent detection of food-borne pathogens via light-up RNA aptamers. *Chem Commun (Camb)*. <https://doi.org/10.1039/c9cc05036a>
 113. Rogers TA, Andrews GE, Jaeger L, Grabow WW (2015) Fluorescent monitoring of RNA assembly and processing using the split-spinach aptamer. *ACS Synth Biol* 4(2):162–166. <https://doi.org/10.1021/sb5000725>
 114. Zhou Y, Shen S, Lau C, Lu J (2019) A conformational switch-based fluorescent biosensor for homogeneous detection of telomerase activity. *Talanta* 199:21–26. <https://doi.org/10.1016/j.talanta.2019.02.018>
 115. Svensen N, Jaffrey SR (2016) Fluorescent RNA aptamers as a tool to study RNA-modifying enzymes. *Cell Chem Biol* 23(3):415–425. <https://doi.org/10.1016/j.chembiol.2015.11.018>
 116. Paige JS, Nguyen-Duc T, Song W, Jaffrey SR (2012) Fluorescence imaging of cellular metabolites with RNA. *Science* 335(6073):1194. <https://doi.org/10.1126/science.1218298>
 117. Stojanovic MN, Kolpashchikov DM (2004) Modular aptameric sensors. *J Am Chem Soc* 126(30):9266–9270. <https://doi.org/10.1021/ja032013t>
 118. Sharma S, Zaveri A, Visweswariah SS, Krishnan Y (2014) A fluorescent nucleic acid nano-device quantitatively images elevated cyclic adenosine monophosphate in membrane-bound compartments. *Small* 10(21):4276–4280. <https://doi.org/10.1002/sml.201400833>
 119. Nakayama S, Luo Y, Zhou J, Dayie TK, Sintim HO (2012) Nanomolar fluorescent detection of c-di-GMP using a modular aptamer strategy. *Chem Commun (Camb)* 48(72):9059–9061. <https://doi.org/10.1039/c2cc34379g>
 120. Kellenberger CA, Wilson SC, Sales-Lee J, Hammond MC (2013) RNA-based fluorescent biosensors for live cell imaging of second messengers cyclic di-GMP and cyclic AMP-GMP. *J Am Chem Soc* 135(13):4906–4909. <https://doi.org/10.1021/ja311960g>
 121. Kellenberger CA, Chen C, Whiteley AT, Portnoy DA, Hammond MC (2015) RNA-based fluorescent biosensors for live cell imaging of second messenger cyclic di-AMP. *J Am Chem Soc* 137(20):6432–6435. <https://doi.org/10.1021/jacs.5b00275>
 122. Kellenberger CA, Wilson SC, Hickey SF, Gonzalez TL, Su Y, Hallberg ZF, Brewer TF, Iavarone AT, Carlson HK, Hsieh YF, Hammond MC (2015) GEMM-I riboswitches from *Geobacter* sense the bacterial second messenger cyclic AMP-GMP. *Proc Natl Acad Sci U S A* 112(17):5383–5388. <https://doi.org/10.1073/pnas.1419328112>

123. Hallberg ZF, Wang XC, Wright TA, Nan B, Ad O, Yeo J, Hammond MC (2016) Hybrid promiscuous (Hypr) GGDEF enzymes produce cyclic AMP-GMP (3',3'-cGAMP). *Proc Natl Acad Sci U S A* 113(7):1790–1795. <https://doi.org/10.1073/pnas.1515287113>
124. Inuzuka S, Matsumura S, Ikawa Y (2016) Optimization of RNA-based c-di-GMP fluorescent sensors through tuning their structural modules. *J Biosci Bioeng* 122(2):183–187. <https://doi.org/10.1016/j.jbiosc.2016.01.011>
125. Wang C, Sinn M, Stifel J, Heiler AC, Sommershof A, Hartig JS (2017) Synthesis of all possible canonical (3'-5'-linked) cyclic dinucleotides and evaluation of riboswitch interactions and immune-stimulatory effects. *J Am Chem Soc* 139(45):16154–16160. <https://doi.org/10.1021/jacs.7b06141>
126. Autour A, Bouhedda F, Cubi R, Ryckelynck M (2019) Optimization of fluorogenic RNA-based biosensors using droplet-based microfluidic ultrahigh-throughput screening. *Methods* 161:46–53. <https://doi.org/10.1016/j.ymeth.2019.03.015>
127. Hallberg ZF, Su Y, Kitto RZ, Hammond MC (2017) Engineering and In Vivo Applications of Riboswitches. *Annu Rev Biochem* 86:515–539. <https://doi.org/10.1146/annurev-biochem-060815-014628>
128. Karunanayake Mudiyansele A, Wu R, Leon-Duque MA, Ren K, You M (2019) “Second-generation” fluorogenic RNA-based sensors. *Methods* 161:24–34. <https://doi.org/10.1016/j.ymeth.2019.01.008>
129. Sun Z, Nguyen T, McAuliffe K, You M (2019) Intracellular imaging with genetically encoded RNA-based molecular sensors. *Nanomaterials (Basel)* 9(2). <https://doi.org/10.3390/nano9020233>
130. Abatemarco J, Sarhan MF, Wagner JM, Lin JL, Liu L, Hassouneh W, Yuan SF, Alper HS, Abate AR (2017) RNA-aptamers-in-droplets (RAPID) high-throughput screening for secretory phenotypes. *Nat Commun* 8(1):332. <https://doi.org/10.1038/s41467-017-00425-7>
131. Yu Q, Shi J, Mudiyansele A, Wu R, Zhao B, Zhou M, You M (2019) Genetically encoded RNA-based sensors for intracellular imaging of silver ions. *Chem Commun (Camb)* 55(5):707–710. <https://doi.org/10.1039/c8cc08796b>
132. DasGupta S, Shelke SA, Li NS, Piccirilli JA (2015) Spinach RNA aptamer detects lead (II) with high selectivity. *Chem Commun (Camb)* 51(43):9034–9037. <https://doi.org/10.1039/c5cc01526j>
133. Savage JC, Shinde P, Bachinger HP, Davare MA, Shinde U (2019) A ribose modification of Spinach aptamer accelerates lead(ii) cation association in vitro. *Chem Commun (Camb)* 55(42):5882–5885. <https://doi.org/10.1039/c9cc01697j>
134. Verma I, Devi M, Sharma D, Nandi R, Pal SK (2019) Liquid crystal based detection of Pb (II) ions using Spinach RNA as recognition probe. *Langmuir* 35(24):7816–7823. <https://doi.org/10.1021/acs.langmuir.8b04018>
135. Panchapakesan SSS, Ferguson ML, Hayden EJ, Chen X, Hoskins AA, Unrau PJ (2017) Ribonucleoprotein purification and characterization using RNA Mango. *RNA* 23(10):1592–1599. <https://doi.org/10.1261/rna.062166.117>



Visualization of Transiently Expressed mRNA in Plants Using MS2

Eduardo José Peña and Manfred Heinlein

Abstract

RNA transport and localization are evolutionarily conserved processes that allow protein translation to occur at specific subcellular sites and thereby having fundamental roles in the determination of cell fates, embryonic patterning, asymmetric cell division, and cell polarity. In addition to localizing RNA molecules to specific subcellular sites, plants have the ability to exchange RNA molecules between cells through plasmodesmata (PD). Plant RNA viruses hijack the mechanisms of intracellular and intercellular RNA transport to establish localized replication centers within infected cells and then to disseminate their infectious genomes between cells and throughout the plant organism with the help of their movement proteins (MP). In this chapter, we describe the transient expression of the tobacco mosaic virus movement protein (TMV-MP) and the application of the MS2 system for the *in vivo* labeling of the MP-encoding mRNA. The MS2 method is based on the binding of the bacteriophage coat protein (CP) to its origin of assembly (OAS) in the phage RNA. Thus, to label a specific mRNA *in vivo*, a tandem repetition of a 19-nucleotide-long stem-loop (SL) sequence derived from the MS2 OAS sequence (MSL) is transcriptionally fused to the RNA under investigation. The RNA is detected by the co-expression of fluorescent protein-tagged MS2 CP (MCP), which binds to each of the MSL elements. In providing a detailed protocol for the *in vivo* visualization of TMV-MP mRNA tagged with the MS2 system in *Nicotiana benthamiana* epidermal cells, we describe (1) the specific DNA constructs, (2) *Agrobacterium tumefaciens*-mediated transfection for their transient expression in plants, and (3) imaging conditions required to obtain high-quality mRNA imaging data.

Key words RNA localization, RNA visualization, RNA transport, MS2 system, TMV, Movement protein

1 Introduction

The life of an mRNA begins when its 5' region emerges from a transcribed gene in the nucleus. The nascent pre-mRNA is sequentially associated with RNA-binding proteins (RBPs) that control every aspect of its life, such as its maturation, its transport through the nuclear pores and its localization to specific sites in the cytoplasm, its localized translation, and its degradation [1]. By determining the localization at which a protein is translated, RNA

transport and localization play a fundamental role in the determination of cell polarity and morphogenesis, asymmetric cell divisions, embryonic patterning, and cell migration [2]. Moreover, by localizing mRNAs to specific cellular target sites, the RNA localization processes prevent adverse effects that the proteins of localized mRNAs may have if translated elsewhere in the cell [3–5]. mRNA localization is evolutionarily conserved across the Eukarya and transcriptome-wide approaches have demonstrated that mRNA localization has a rather prominent than exceptional role in the spatial regulation of genome expression [6, 7]. However, the ability to target specific mRNA to subcellular sites is not limited to eukaryotes. In contrast to the conventional view of co-transcriptional translation in bacteria, *in vivo* studies show that *E. coli* also has the capacity to localize RNAs independent of and, thus, prior to translation [8].

Although the localization of RNAs is a rational solution for localized synthesis of the encoded proteins, the mechanisms by which the cell orchestrates the complex distribution of individual mRNAs to their respective subcellular compartments remain to be further studied. The development of *in vivo* RNA tagging methods and high-resolution fluorescent microscopy techniques have been fundamental for advancing the understanding of RNA transport. It is now accepted that mobile RNAs carry *cis*-acting “zipcode” sequences that are recognized by *trans*-acting RBPs, which together with their cognate target RNA molecules are assembled into ribonucleoprotein (RNPs) complexes termed “RNA granules.” The heterogeneity of mRNAs and RBPs complicates the identification of rules for RNA-protein interactions leading to RNA granule assembly. Nevertheless, we know today that these granules, which may contain only single mRNA copies [9], are transported by molecular motors along the elements of the cytoskeleton, and in a translationally repressed state, to their final destination [5, 10, 11].

In addition to transporting and localizing mRNA to different subcellular compartments [12–14], plants transport RNAs also between cells through plasmodesmata (PD), gateable membranous pores within the cell wall of neighboring cells. The PD provide cytoplasmic as well as plasma membrane and endoplasmic reticulum (ER) continuity between adjacent cells [15]. Moreover, the system of PD in leaves is connected to the phloem sieve elements in the stems and thus creates a cell-to-cell and long-distance communication network [16]. The profiling of heterografted plants led to the identification of thousands of mRNAs that are transported constitutively or in response to environmental stresses through the graft junction into distant tissues [17, 18].

However, little is known about the cellular machinery and the RNA features involved in cell-to-cell and long-distance RNA transport in plants. Although recent studies imply a role of RNA

methylation (m^5C) in systemic RNA transport [19], the intracellular mechanisms supporting mRNA transport to the PD are not well understood. One approach for identifying these mechanisms is by studying the cell-to-cell dissemination of single-stranded (ss) RNA virus infections [20, 21]. Most plant viruses are RNA viruses and all plant viruses disseminate infection by targeted movement through PD [21, 22]. Tobacco mosaic virus (TMV) has been a pioneer in this regard [23, 24]. This filamentous virus has a positive-sensed RNA genome that encodes two polymerase subunits (126 kDa and 183 kDa proteins) as well as a movement protein (30 kDa; MP) and a coat protein (17.5 kDa; CP) from subgenomic RNAs [25]. The CP is dispensable for cell-to-cell movement [26], thus indicating that the virus targets and moves its RNA genome through PD in the form of an RNP, independent of encapsidation by its CP. This feature positions TMV as an excellent model to study the intra- and intercellular transport of RNA complexes in plants.

The MP is essential for viral RNA transport [24]. Consistently, it binds to RNA in a sequence nonspecific manner [27] and also targets PD. During infection in *Nicotiana benthamiana*, the protein is transiently expressed and modifies the size exclusion limit (SEL) of PD between cells at the spreading infection front [28]. At later stages, thus in cell behind the front of infection, the protein is ubiquitinated and degraded through ER-associated degradation (ERAD) [29] by the 26S proteasome [30]. Infection foci in *N. benthamiana* leaves of TMV derivatives in which the CP gene was deleted and MP expressed as a fusion to a fluorescent protein reporter indeed show a fluorescent halo [31–33], indicating accumulation of MP at the infection front, thus during a short period of time. Microscopic observations in cells of such foci led to the discoveries that MP localizes to the ER-actin network and interacts with microtubules (MT) [31–33]. In the foremost line of cells at the virus front, MP accumulates at PD but is also a constituent of cortical ER-associated, mobile particles. Using conditional mutations within the MP, the mobile particles were functionally associated with the capacity of MP to support the cell-to-cell movement of the virus [33, 34]. Although these particles likely reflect the formation of early viral replication complexes (eVRCs) at cortical ER-MT junctions, similar particles are also observed upon transient expression of MP alone [35], thus indicating that the formation of these particles is a function of MP. Indeed, conditional mutations in MP that correlated the formation of these MP particles (eVRCs) and the ability of the virus to move between cells during infection also affected the formation of the MP particles in the noninfected, MP-transfected cells [35]. The MP particles in TMV-infected and MP-transfected cells are visible at cortical planes of the cells, and while many of them are anchored at ER-MT junctions, other particles disassociate from such sites and show a stop-and-go movement along the cortical ER-actin network, pausing their trajectories

when in contact or in the proximity of MTs and MT organizing centers [35–38]. The targeting of MP to PD and the spread of infection depend on myosin motor proteins [39] and can be inhibited by over-expression of actin-binding proteins [40]. Taken together, these observations led to the model that TMV forms eVRCs at cortical MT-associated ER sites (cMERs) [36] with the help of MP, and that myosin motor proteins (class VIII and class XI myosins) target the VRCs along the ER-actin network to PD and into adjacent cells to spread infection [21, 41].

The use of fluorescent protein fusions and their imaging with advanced fluorescent microscopy technologies allow single-molecule detection with sub-diffraction resolution *in vivo* [42]. However, unlike proteins, RNAs cannot be expressed as fluorescent molecules. Thus, new techniques for the *in vivo* detection of RNA molecules are under continuous development. RNA molecules may be imaged upon *in vitro* labeling with fluorochromes followed by introduction into cells by transfection or microinjection [43], or need to be visualized by indirect methods. Native RNAs can be detected either by hybridization with fluorescent probes delivered into the cell [44] or by using RBPs, such as the Pumilio family of RBPs, whose modular structure can be modified to recognize and bind virtually any RNA sequence of interest [45, 46]. More recently, nuclease-inactivated CRISPR-Cas9 systems modified to bind ssRNA have been applied [47]. Other approaches involve the modification of the studied RNA, for example, by the introduction of structural RNA elements called aptamers. These aptamers are capable of binding small molecules, like malachite green, or various types of recently developed fluorogens such as “spinach,” which gain fluorescence upon aptamer binding [48, 49]. RNAs of interest may also be modified by fusion to aptamers able to bind proteins. An example is the broadly used “MS2 system.” This system relies on the fusion of the RNA target with a tandem repetition of a sequence motif derived from the origin of assembly of the bacteriophage MS2. Upon transcription, these motifs adopt a stem-loop structure (MSL) that is specifically recognized and bound by the co-expressed and fluorescent protein-tagged MS2 coat protein (MCP), thus allowing RNA imaging through binding of an RBP to its cognate RNA-binding motif in the target RNA [50]. Other analogous aptamer/RBP-dependent RNA-labeling systems have been developed and most of them have been comprehensively described [51–53]. Moreover, their application to plant systems has been reviewed [54].

The MS2 system was first developed in yeast and has been extensively applied for the study of all aspects of RNA life and in a broad range of organisms, including plants [10, 35, 50, 55–57]. The successful application of the MS2 method for the study of a given mRNA molecule depends on several aspects that need to be considered. Zipcodes (usually located at the 3′ untranslated

region) in mRNAs actively participate in mRNA maturation, localization, and translation by interacting with cellular proteins and should not be modified. Moreover, retention of their activity should be verified after introducing the RBP-binding MSL aptamers into the target mRNA sequence. The fluorescent signal intensity emitted by the tagged target mRNA is directly proportional to the number of MSL aptamers added into the construct. Each MSL aptamer is recognized and bound by one MCP dimer. While 24 MSL copies are sufficient to detect a single mRNA molecule [58], this involves the incorporation of around 1.5 kb MSL RNA into the RNA under investigation, which possibly affects mRNA maturation and function. Moreover, given the repetitive identity of the incorporated material, each MSL copy increases the risk of recombination during cloning, which may impede the recovery of a functional construct. Due to these reasons, it is advisable to design different RNA constructs, each containing a specific number of MSL repetitions, and to test the activity of the MSL repetitions also at different positions within the construct, but avoiding insertion into any eventually identified zip code or regulatory element. Once plasmid constructs are obtained, the expected size of the mature transcript as well as normal mRNA accumulation kinetics and retention of the encoded protein function should be verified. It was recently shown that MCP molecules bound to their MSLs in the tagged mRNA can significantly modify the turnover of short-lived mRNAs in *Saccharomyces cerevisiae* [59, 60]. This problem was solved by modifying MCP-binding affinity and by enlarging the linker sequence between each element of the MSL tandem [61, 62], thus illustrating the effect which the MS2 system might have on the target mRNAs. The second element of the system, the MCP fused to a fluorescent protein (FP) reporter (MCP:FP), is frequently targeted to the nucleus by incorporation of a nuclear localization signal (NLS). This will decrease the cytoplasmic background and therefore increases the signal-to-noise ratio for the labeled RNAs [50]. The amount of expressed MCP must be sufficiently high to ensure proper binding to the MSL array. While not all MSL repeats are decorated with MCP [58], an overly increased MCP expression level augments cytoplasmic background and should be avoided. Therefore, rigorous controls must be conducted to verify that the amount of MCP:FP needed to visualize the MSL-tagged RNA indeed shows fluorescence only in the presence of MSL-tagged RNA but not in the presence of MSL-free control mRNA under the same conditions. In the absence of a specific MSL-tagged RNA, the MCP:FP should not aggregate or form other types of visible fluorescent particles that would strongly compromise the specific RNA signal [63].

Adding MSLs to the TMV genome resulted in the loss of infectivity. Thus, we decided to determine if the MP particles formed also in transiently MP-expressing cells contain RNA.

Because the MP binds RNA in a sequence nonspecific manner [27], it is probably designed to form a complex with RNA molecules in its vicinity. Thus, while the MP binds to nearby viral RNA within VRCs during infection, the MP may likely bind to the mRNA from which it is translated under transient expression conditions. Upon *Agrobacterium tumefaciens*-mediated transient expression, MP reproduces its typical cellular accumulation and turnover pattern seen during infection, thus forming mobile MP particles during early transient expression stages. To determine if these particles contain MP mRNA in addition to MP protein, we optimized the MS2 RNA visualization system for MP mRNA detection in *N. benthamiana* leaves. This allowed us to demonstrate that the mobile MP particles indeed contain MP mRNA and that the mRNA is also targeted together with MP to the PD [35].

Using the detection of MP mRNA as an example, we here provide a detailed protocol for the MS2-based in vivo visualization of mRNAs in plant cells. The protocol can be generally applied for the study of mRNA localization and transport in plants. It combines the simple and reliable use of agroinfiltration for transient expression in *N. benthamiana* leaves with the simplicity of Gateway[®] cloning.

2 Materials

2.1 Cloning of Plasmid Constructs

1. Standard thermal cycler (e.g., Biometra-Analytik Jena).
2. DNA polymerase for high-fidelity PCR amplification (e.g., Platinum[™] Taq DNA Polymerase High Fidelity, Thermo Fisher).
3. Agarose gel electrophoresis system.
4. Reagents for purification of DNA fragments from gels (e.g., PCR cleanup gel extraction kit, Macherey-Nagel).
5. PCR cloning system with plasmids and reagents (e.g., pGem[®]-T Easy, Promega).
6. *E. coli* cells for DNA cloning (e.g., DH5 α), competent for electro-transformation.
7. *E. coli* cells for the amplification of *ccdB*-expressing Gateway[®] plasmids (e.g., DB3.1), competent for electro-transformation.
8. Electroporator system (e.g., Gene Pulser Xcell, Bio-Rad) and electroporation cuvettes.
9. LB liquid medium: 10 g/L Bacto-tryptone, 5 g/L yeast extract, 85.6 mM NaCl, pH 7.0. Sterilize by autoclaving.
10. LB-agar plates: Add 15 g bacto-agar to 1.0 L of LB liquid medium, sterilize by autoclaving, and pour plates while the solution is still warm and not solidified.

11. Incubator for agar plates at 37 °C.
12. Sterile petri dishes.
13. Shaker for liquid cultures (15 mL Falcon tubes) for incubation at 180–200 rpm and 37 °C.
14. Sterile 15 mL Falcon tubes.
15. Antibiotics, 1000× stock solutions, sterilized by filtration through 0.22 μm pore-size membrane:
 - (a) Zeocin: 20 mg/mL (in water).
 - (b) Ampicillin: 100 mg/mL (in water).
 - (c) Kanamycin: 50 mg/mL (in water).
 - (d) Spectinomycin: 50 mg/mL (in water).
 - (e) Chloramphenicol: 34 mg/mL (in 100% ethanol).
16. For the color screening of bacterial colonies containing the desired plasmid with insert:
 - (a) IPTG solution: 0.1 M IPTG in water.
 - (b) X-gal solution: 50 mg/mL X-gal in dimethyl sulfoxide (DMSO).
17. Plasmid DNA isolation kit (e.g., NucleoSpin[®] Plasmid kit, Macherey-Nagel).
18. Benchtop centrifuge (able to hold 1.5 mL tubes and providing 15,000 × *g*).
19. *PacI* DNA restriction endonuclease.
20. *SacI* DNA restriction endonuclease.
21. T4 DNA ligase.
22. pSL-MS2 plasmids containing the MSL tandem sequence (6, 12, or 24 SL copies) and plasmid pMS2-GFP containing the MCP gene (*see Note 1*).
23. pDONR[™]/Zeo Vector (Thermo Fisher) and BP[™] and LR[™] clonase enzyme mixes (Thermo Fisher) for Gateway[®]-compatible cloning.
24. Binary Gateway[®] destination vector pMDC32 for propagation in *E. coli* and for use as vector for *A. tumefaciens*-mediated transient expression in plants [64] (*see Note 2*).
25. Oligonucleotide primers:
 - (a) MS2-12SLfw: 5' ttaattaacgggcctatatatggatcc
 - (b) MS2-12SLrev: 5' gagctccgctgatatcgatcgcgcg
 - (c) T7: 5' taatcactcactataggg
 - (d) SP6: 5' gatttaggtgacactatag
 - (e) ccdBfw: 5'-cacctataaaagagagagcc
 - (f) T-nosrev: 5'-aatcatcgcaagaccgg
 - (g) M13fw: 5'-tgtaaacgacggccagt

- (h) M13rev: 5'-caggaacagctatgac
- (i) MP-GV1rev: 5'-cagagaagcggacagaaaaccgctgacatcttcac
- (j) mRFPfw: 5'-gcctcctccgaggacgtc

2.2 Transient Gene Expression

1. *A. tumefaciens* strain GV3101 [65] competent for electrotransformation.
2. pB7-NLS-MCP:GFP, for the expression of MCP fused to eGFP and targeted to the nucleus [35].
3. Incubator for agar plates at 28 °C.
4. Shaker for liquid cultures (50 mL falcon tubes) for incubation at 180–200 rpm and 28 °C.
5. Sterile 50 mL falcon tubes.
6. Antibiotics, 1000× stock solutions, sterilized by filtration through 0.22 μm pore-size membrane:
 - (a) Rifampicin: 50 mg/mL (in DMSO).
 - (b) Gentamicin: 50 mg/mL (in water).
7. Spectrophotometer (to measure absorbance at 600 nm).
8. Centrifuge (compatible with 50 mL falcon tubes and 5000 × *g*).
9. Sterile distilled water.
10. Greenhouse or growth chamber for *N. benthamiana* plants (16 h/8 h day/night and 24 °C/22 °C day/night temperature).
11. *N. benthamiana* plants, 4–5 weeks old.
12. 1.0–2.5 mL Syringes without needle.
13. Hypodermic needles (e.g., blue or orange needles, 0.5–0.6 mm diameter, respectively).

2.3 Fluorescence Imaging

1. Epifluorescence, spinning-disk, or laser scanning confocal microscope equipped with (1) specific filtering for GFP and RFP fluorescence; (2) low-magnification objective (e.g., 10× or 20×) and high-magnification, high-optical-numerical-aperture objective (e.g., 60× or 100×); and (3) a detection system compatible with high-frame-rate time-lapse image acquisition.
2. Microscopy glass slides and coverslips (thickness compatible with available objectives).
3. Scotch tape (e.g., Magic™ Tape 1/2", 3 M).
4. Cork borer (0.7–1.0 cm diameter, for leaf disk preparation).
5. Vacuum pump with vacuum desiccator.
6. Sterile distilled water.
7. Microscope image acquisition and analysis software (e.g., ImageJ <https://imagej.nih.gov/ij/index.html>).

3 Methods

3.1 Cloning of Plasmid Constructs

The visualization of RNA with the MS2 system involves the co-expression of MSL-tagged RNA together with fluorescent protein-tagged MCP. Here we describe the insertion of 12 copies of the MSL into the 3'UTR sequences encoded by the Gateway[®] (see **Note 3**)-compatible plant expression vector pMDC32 to generate a MSL-tagged destination vector, and its application as destination vector for the expression of TMV MP fused to mRFP (MP: mRFP) and its MSL-tagged mRNA. The plasmid vector for the expression of NLS-tagged MCP fused to GFP (pB7-NLS:MCP: GFP) has been described elsewhere [35], and this plasmid is available upon request.

3.1.1 Cloning of the Destination Vector pMDC32-GW-12xMSL

1. Use a high-fidelity polymerase and the primers MS2-12SLfw and MS2-12SLrev to amplify a 708 bp long DNA fragment encoding 12 copies of the MSL of the plasmid pSL-MS2-12 (available at <http://www.addgene.org/27119/>). The primer sequences contain *PacI* and *SacI* restriction sites (underlined) required for further cloning steps.
2. Verify the expected size of the amplified DNA fragment by agarose electrophoresis and purify the DNA fragment from the gel using a DNA gel extraction kit following the manufacturer's instructions.
3. Insert the purified DNA fragment into a PCR cloning vector (e.g., pGem[®]-T Easy, Promega) using T4 DNA ligase according to the manufacturer's instructions. Transform competent *E. coli* cells with 1.0–3.0 µL of the ligation mix and plate them on petri dishes with antibiotic selection (100 µg/mL ampicillin for pGem[®]-T-Easy). Before plating the cells, distribute 5 µL of 0.5 mM IPTG and 25 µL of 80 µg/mL X-Gal onto the plate. Incubate the plates with bacteria overnight at 37 °C.
4. Isolate bacteria from 4 to 5 white colonies and propagate them overnight in 15 mL falcon tubes containing 4.0 mL of liquid LB medium with antibiotics (100 µg/mL ampicillin for pGem[®]-T Easy) at 37 °C with agitation (180–200 rpm).
5. Harvest bacteria by centrifugation and isolate plasmid DNA using a plasmid purification kit and following the manufacturer's instructions. Verify the presence and correct size of the inserted DNA by PCR amplification (using universal primers homologous to vector sequences, e.g., T7 and SP6 primers homologous to T7 and SP6 promoter sequences present in pGem[®]-T Easy) and agarose gel electrophoresis. Confirm the absence of mutations by DNA sequencing and select one of the verified plasmid clones to proceed with the following steps.

6. Excise the 12xMSL fragment by *PacI/SacI* digestion and purify the fragment from an agarose gel.
7. Digest plasmid pMDC32 with *PacI/SacI* and purify the linearized plasmid from an agarose gel.
8. Ligate the purified 12xMSL fragment into the linearized and purified pMDC32 plasmid with T4 DNA ligase to create pMDC32-MS2-12xMSL. Transform *E. coli* DB3.1 high-efficiency competent cells with 1.0–3.0 μL of the ligation mix and distribute the cells on petri dish with antibiotic selection (50 $\mu\text{g}/\text{mL}$ kanamycin and 34 $\mu\text{g}/\text{mL}$ chloramphenicol). Grow colonies overnight at 37 °C.
9. Isolate bacteria from 4 to 5 isolated colonies and propagate them overnight in 15 mL falcon tubes containing 4.0 mL of liquid LB medium with antibiotics (50 $\mu\text{g}/\text{mL}$ kanamycin and 34 $\mu\text{g}/\text{mL}$ chloramphenicol) at 37 °C with agitation (180–200 rpm).
10. Isolate the plasmid DNA (i.e., the destination vector pMDC32-GW-12xMSL) using a plasmid purification kit and confirm the correct insertion of the 12xMSL tandem by DNA sequencing with ccdBfw and T-nosrev primers.

3.1.2 Cloning of the RNA of Interest into pMDC32-GW-12xMSL

1. Design primers for PCR amplification of the DNA fragment encoding your RNA of interest and add *attB* sequences required for BPTM cloning (see **Note 4**).
2. Amplify the DNA fragment encoding your RNA of interest by PCR using a high-fidelity DNA polymerase and the appropriate DNA source as template (DNA or cDNA). Verify the correct size of the amplified DNA fragment by agarose gel electrophoresis and, subsequently, purify the fragment from the gel using an agarose gel extraction kit.
3. Perform a BPTM recombination reaction between the purified DNA fragment and pDONRTM/Zeo, with the BPTM clonase enzyme mix (Thermo Fisher) according to the manufacturer's instructions, to create your entry clone. Transform *E. coli* cells with 0.5–1.0 μL of the reaction and grow colonies overnight at 37 °C on LB plates under antibiotic selection (20 $\mu\text{g}/\text{mL}$ of zeocin for pDONRTM/Zeo).
4. Use 4–5 colonies for growing bacterial cultures in liquid LB medium with antibiotic selection (20 $\mu\text{g}/\text{mL}$ of zeocin for pDONRTM/Zeo) overnight at 37 °C with 180–200 rpm agitation.
5. Isolate the plasmid DNA (the entry vector), verify the presence, and correct cloning of your DNA by DNA sequencing (use universal primers homologous to vector sequences, e.g., M13fw and M13rev for pDONRTM/Zeo).

6. Use the LRTM clonase mix (follow the manufacturer's instructions) to perform separate LRTM reactions between the entry vector now containing the DNA of your RNA of interest and both (1) pMDC32 and (2) pMDC32-GW-12xMSL (*see* Sub-heading 3.1.1, step 10) to obtain the expression vectors pMDC32-RNA and pMDC32-RNA-12xMSL, respectively (follow the manufacturer's instructions). Transform *E. coli* cells and select them on LB agar plates with antibiotic selection (50 µg/mL kanamycin).
7. Start 4–5 liquid cultures from isolated bacterial colonies and grow them overnight under antibiotic selection (50 µg/mL kanamycin) at 37 °C with agitation (180–200 rpm).
8. Isolate the plasmids using a plasmid purification kit and verify proper vector assembly by DNA sequencing (for our destination vectors pMDC32-MP:mRFP and pMDC32-MP:mRFP-12xMSL we used internal fragment primers MP-GV1rev and mRFPfw).

3.2 Agrobacterium-Mediated Transient Expression of MSL-Tagged RNA and Fluorescent MCP in *N. benthamiana* Leaves

The Gateway[®] system destination vectors used in this protocol are binary vectors suitable for transformation of *Agrobacterium* and *Agrobacterium*-mediated transformation of plants. Infiltration of plant leaf tissues with diluted *agrobacteria* containing the destination expression vector of interest is a flexible and reliable method for the expression of foreign proteins in *N. benthamiana* leaves. By mixing two *Agrobacterium* cultures harboring two different expression vectors, two proteins of interest can be simultaneously expressed within the cells of the infiltrated leaf area [66]. Here, we apply this co-transfection method for expression of the MSL-tagged RNA together with fluorescent protein-tagged MCP in the same cells.

1. Transform separate aliquots of electrocompetent *A. tumefaciens* GV3101 cells with plasmids pMDC32-RNA, pMDC32-RNA-12xMSL, and pB7-NLS-MCP:GFP [35], respectively, by electroporation and grow colonies for 48 h at 28 °C on LB agar plates containing rifampicin and gentamicin (both at 50 µg/mL) and either (1) kanamycin (50 µg/mL) for pMDC32 vectors or (2) spectinomycin (50 µg/mL) for pB7-NLS-MCP:GFP.
2. Use individual colonies to start liquid cultures in 50 mL falcon tubes containing 5.0 mL of LB medium and under antibiotic selection as used for the plates in the previous step. Incubate the cultures overnight at 28 °C with agitation (180–200 rpm).
3. Harvest the bacteria by centrifugation at 5000 × *g* for 5 min and resuspend the bacterial pellets in sterile distilled water. Determine the optical density of the bacterial solution at 600 nm.

4. Dilute the bacterial solutions for the agroinfiltration experiment. Create a bacterial “solution A” by combining pB7-NLS-MCP:GFP-containing bacteria with pMDC32-RNA-SL-containing agrobacteria, and another bacterial “solution B” by combining pB7-NLS-MCP:GFP-containing bacteria with pMDC32-RNA-containing bacteria. Solution B is required as control in the RNA visualization experiment. The appropriate concentrations of the bacterial solutions to obtain a good RNA imaging result must be empirically determined (*see Note 5*).
5. To agroinfiltrate *N. benthamiana* plants with both solutions, start by using a needle to puncture two holes into the youngest fully expanded leaf at sites selected for agroinfiltration. Select single sites on the left and on the right of the major vein. Position a 1.0 mL or 2.5 mL syringe without needle and filled with solution A onto the abaxial side of the punctured site on the left and infiltrate the leaf blade with bacterial solution by applying pressure onto the plunger. Upon infiltration with the liquid, the infiltrated area acquires a darker color and thus can be easily distinguished from the non-infiltrated, light-green region. Infiltrate until the wetted, dark leaf area reaches the major vein. Repeat the same procedure for infiltration of the right side of the leaf blade with solution B.
6. Return the infiltrated plant(s) to their normal growing conditions in the greenhouse or growth chamber and incubate them for the needed time until the gene constructs reach desired expression levels suitable for microscopy (*see Note 6*).

3.3 Microscopy, Sample Preparation, and Conditions for the Visualization of MS2-Tagged RNA

1. Use a sharpened cork borer to excise samples from the leaf areas infiltrated with solution A and solution B, respectively.
2. Place the leaf disks on microscopic slides and cover them with a coverslip. The abaxial, infiltrated side of the disk should face the coverslip. Fix the coverslip to the slide with tape. Fill the airspace between coverslip and glass slide with sterile water.
3. To exchange the air present in intercellular spaces with water, place the slides into a vacuum desiccator and evacuate the air until the pressure reaches -0.8 to -1.0 bar. Subsequently, slowly release the pressure to allow slow water entry. During this process, the leaf disks should acquire a darker green color.
4. Analyze the leaf disk samples by microscopy. Start by using a low-magnification objective to verify tissue integrity and to determine if samples that were infiltrated with solution A and solution B, respectively, express similar levels of NLS:MCP:GFP. If the RNA under study encodes a fluorescently tagged protein, the two samples expressing this protein from MSL-tagged RNA and non-tagged RNA, respectively, should show similar expression levels for this protein (*see Note 7*).

5. Use a high-magnification objective to investigate the leaf disks that were infiltrated with solution A to visualize the cytoplasmic localization of the MSL-tagged RNA labeled by GFP fluorescence emitted from NLS:MCP:GFP bound to it. Specific cytoplasmic fluorescent signals that are due to specific binding of NLS:MCP:GFP to the MSL repeats in MSL-tagged RNA should be absent in the control samples that were infiltrated with solution B and in which the RNA lacks the MSL sequences required for NLS:MCP:GFP binding. Acquire images from cells expressing both samples and time-lapse videos at high sampling rates to capture the movements of detected RNA granules. Signal detection is facilitated in the abaxial epidermal pavement cells in which most of the volume is occupied by the vacuole, which compresses the cytoplasm toward the plasma membrane and cell wall.
6. Use ImageJ or similar software for image acquisition and analysis (e.g., colocalization, particle tracking, velocity measurement). Observations should finish within 30 min after leaf disks were excised. After this time, new samples need to be prepared.
7. Images of RNA granules formed by the mRNA of the TMV MP are seen in Fig. 1. In views focusing on the lateral cell walls of epidermal cells, the cytoplasm is condensed to a thin line along the wall, and MP:RFP fluorescence is detected at PD (Fig. 1a). Views focusing on the cortical cytoplasm just beneath the upper epidermal cell wall allow the observation of thin layers of cytoplasm, where the ER-actin network and the cortical MT array share the same focal plane below the plasma membrane. Here, RNA granules are detected and their lateral movement can be visualized (Fig. 1b) (*see Note 8*).

4 Notes

1. pSL-MS2 plasmids containing different numbers of MSL copies as well as plasmids expressing different MCP variants are available from the plasmid repository Addgene (https://www.addgene.org/Robert_Singer/).
2. pMDC32 is available from TAIR (<https://www.arabidopsis.org/servlets/TairObject?type=vector&id=501100106>).
3. Gateway[®] cloning is a versatile technology that allows the fast and precise exchange of DNA material, based on recombination. An entry clone contains your DNA of interest flanked by *attL* sequences, which allow recombination in a LRTM reaction with the *attR* site of the destination vector, to obtain the desired final expression plasmid.

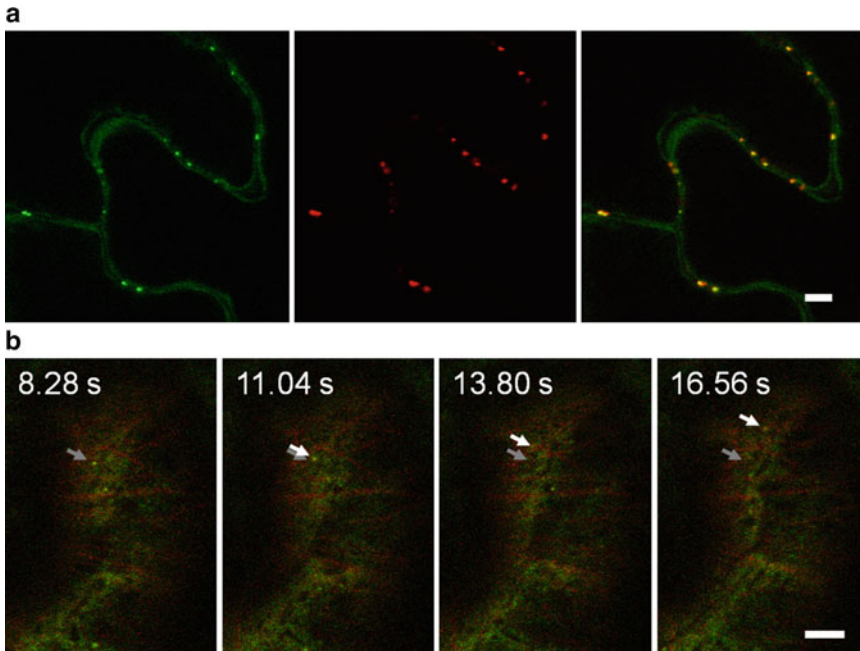


Fig. 1 Visualization of RNA granules formed by MP:mRFP and its mRNA by MS2 tagging in *N. benthamiana* epidermal cells. **(a)** MP:mRFP mRNA (labeled with NLS:MCP:GFP, green, left) and MP:mRFP (red, middle) coincide in small dots (presumably PD) at the cell wall (yellow, right). Size bar, 5 μ m. **(b)** Example of a time-lapse imaging study with video frames showing the co-localization of MP:mRFP and MP:mRFP mRNA (labeled by NLS:MCP:GFP) in mobile particles present in the cortical cytoplasm. Red and green channels are merged. The particles appear in yellowish color and the direction of their movements appears to be guided along microtubules, which are seen as red-colored filaments. Arrows highlight the movement of a particle. Gray arrows indicate the location of the mRNA particle observed in the first frame and white arrows indicate the new particle location in each subsequent time frame. Size bar, 5 μ m. The figure has been reproduced from [68], Elsevier

4. Entry clones can be obtained either by traditional restriction endonuclease/ligase methods, through a BPTM reaction in which the gene of interest is flanked by recombination sites by PCR and then recombined into a donor vector (pDONRTM), or by TOPOTM cloning. The three alternatives offer directional cloning, but special considerations are needed to design primers and ensure the desired cloning result. Please refer to <http://tools.thermofisher.com/content/sfs/manuals/gatewayman.pdf> for instructions for the design of primers appropriate for BP cloning into pDONRTM vectors, and to https://assets.thermofisher.com/TFS-Assets/LSG/manuals/pentr_dtopo_man.pdf for instructions for the design of primers suitable for TOPO[®] cloning into pENTRTM vectors.
5. For co-expression experiments, the bacterial cultures resuspended in sterile distilled water are mixed before infiltration. To obtain the desired expression level, the concentration of

each clone in the infiltration mixture and the time after infiltration for observation must be empirically determined. Higher concentration of the bacterial solutions used for agroinfiltration will lead to higher expression levels. For RNA labeling experiments, high expression of NLS:MCP:GFP induces fluorescence background while low expression compromises the sensitivity by which tagged RNA can be detected. For the visualization of TMV MP mRNA we use bacterial solutions with an $OD_{600} = 0.5$ for agrobacteria carrying pMDC32-RNA or pMDC32-RNA-SL and an of $OD_{600} = 0.1$ for agrobacteria carrying pB7-NLS-MCP:GFP.

6. The *Agrobacterium*-mediated transient expression level reaches a maximum after 3–4 days following infiltration and then decreases, which is, in part, due to posttranscriptional gene silencing. A more sustained expression can be obtained by co-expression of a viral silencing suppressor protein (e.g., P19 from tomato bushy stunt virus) [67]. In our experiments, we rely on the co-expression of P19 to reach desirable levels of the MSL-tagged clones [35]. Expression levels can also be increased by inducing the *A. tumefaciens vir* genes. This can be achieved by resuspending the bacteria in infiltration medium (10 mM MES pH 5.6, 10 mM NaCl₂, 150 μ M acetosyringone) followed by incubation for at least 2 h prior to infiltration.
7. In order to ensure a reliable MCP-mediated localization of the mRNA under investigation, the background of the system must be minimized. The MCP expression and localization pattern must be evaluated in the presence of both MSL tagged- or non-tagged mRNA.
8. The MP-containing mobile RNA granules shown in Fig. 1b were detected as early as 30–36 h post-agroinfiltration. Imaging the motility of these dually labeled, mRNA-containing granules required high-rate dual-color image acquisition over extended time intervals. Initially, we achieved this by using a standard epifluorescence microscope equipped with a dual-view beam splitter (Optical Insights) for simultaneous imaging of green and red fluorescence, and by image acquisition with a high-speed charge-coupled device (CCD) camera (CoolSnap HQ, Roper Scientific) [35]. Today, more modern dual-color split-view systems are available that allow simultaneous two-color imaging with two attached cameras (e.g., TuCam, Oxford Instruments). The images shown in Fig. 1b were taken with a confocal laser scanning microscope (Zeiss LSM780). The frequency of image acquisition was increased by reducing image size and resolution.

Acknowledgments

This work was supported by the Agence National de la Recherche (grant ANR-08-BLAN-244 to MH), the Consejo Nacional de Investigaciones Científicas y Técnicas (CONICET, grant PIP-0847 to EP), and by a binational CNRS-CONICET grant (PICS-2014 to MH and EP).

References

- Erickson SL, Lykke-Andersen J (2011) Cytoplasmic mRNP granules at a glance. *J Cell Sci* 124:293–297
- Palacios IM, St Johnston D (2001) Getting the message across: The intracellular localization of mRNAs in higher eukaryotes. *Annu Rev Cell Dev Biol* 17:569–614
- Martin KC, Ephrussi A (2009) mRNA localization: gene expression in the spatial dimension. *Cell* 136:719–730
- Wang ET, Taliaferro JM, Lee JA et al (2016) Dysregulation of mRNA localization and translation in genetic disease. *J Neurosci* 36:11418–11426
- Jung H, Gkogkas CG, Sonenberg N, Holt CE (2014) Remote control of gene function by local translation. *Cell* 157:26–40
- Lécuyer E, Yoshida H, Parthasarathy N et al (2007) Global analysis of mRNA localization reveals a prominent role in organizing cellular architecture and function. *Cell* 131:174–187
- Holt CE, Bullock SL (2009) Subcellular mRNA localization in animal cells and why it matters. *Science* 326:1212–1216
- Nevo-Dinur K, Nussbaum-Shochat A, Ben-Yehuda S, Amster-Choder O (2011) Translation-independent localization of mRNA in *E. coli*. *Science* 331:1081–1084
- Das S, Singer RH, Yoon YJ (2019) The travels of mRNAs in neurons: do they know where they are going? *Curr Opin Neurobiol* 57:110–116
- Buxbaum AR, Haimovich G, Singer RH (2015) In the right place at the right time: Visualizing and understanding mRNA localization. *Nat Rev Mol Cell Biol* 16:95–109
- Eliscovich C, Buxbaum AR, Katz ZB, Singer RH (2013) mRNA on the move: the road to its biological destiny. *J Biol Chem* 288:20361–20368
- Okita TW, Choi SB (2002) mRNA localization in plants: targeting to the cell's cortical region and beyond. *Curr Opin Plant Biol* 5:553–559
- Tian L, Chou H-L, Fukuda M et al (2020) mRNA localization in plant cells. *Plant Physiol* 182:97–109
- Chou HL, Tian L, Washida H et al (2019) The rice storage protein mRNAs as a model system for RNA localization in higher plants. *Plant Sci* 284:203–211
- Zambryski P, Crawford K (2000) Plasmodesmata: gatekeepers for cell-to-cell transport of developmental signals in plants. *Annu Rev Cell Dev Biol* 16:393–421
- Lucas WJ, Lee JY (2004) Plasmodesmata as a supracellular control network in plants. *Nat Rev Mol Cell Biol* 5:712–726
- Thieme CJ, Rojas-Triana M, Stecyk E et al (2015) Endogenous Arabidopsis messenger RNAs transported to distant tissues. *Nat Plants* 1:1–8
- Zhang Z, Zheng Y, Ham B-K et al (2016) Vascular-mediated signalling involved in early phosphate stress response in plants. *Nat Plants* 2:16033
- Yang L, Perrera V, Saplaoura E et al (2019) m5C methylation guides systemic transport of messenger RNA over graft junctions in plants. *Curr Biol* 29:2465–2476
- Peña EJ, Heinlein M (2012) RNA transport during TMV cell-to-cell movement. *Front Plant Sci* 3:1–10
- Heinlein M (2015) Plant virus replication and movement. *Virology* 479–480:657–671
- Heinlein M (2015) Plasmodesmata: channels for viruses on the move. *Methods Mol Biol* 1217:25–52
- Citovsky V (1999) Tobacco mosaic virus: a pioneer of cell-to-cell movement. *Philos Trans R Soc Lond Ser B Biol Sci* 354:637–643
- Deom CM, Oliver MJ, Beachy RN (1987) The 30-kilodalton gene product of tobacco mosaic virus potentiates virus movement. *Science* 237:389–394
- Goelet P, Lomonosoff GP, Butler PJ et al (1982) Nucleotide sequence of tobacco mosaic

- virus RNA. *Proc Natl Acad Sci U S A* 79:5818–5822
26. Holt CA, Beachy RN (1991) In vivo complementation of infectious transcripts from mutant tobacco mosaic virus cDNAs in transgenic plants. *Virology* 181:109–117
 27. Citovsky V, Knorr D, Schuster G, Zambryski P (1990) The P30 movement protein of tobacco mosaic virus is a single-strand nucleic acid binding protein. *Cell* 60:637–647
 28. Oparka KJ, Prior DAM, Santa Cruz S et al (1997) Gating of epidermal plasmodesmata is restricted to the leading edge of expanding infection sites of tobacco mosaic virus (TMV). *Plant J* 12:781–789
 29. Niehl A, Amari K, Gereige D et al (2012) Control of tobacco mosaic virus movement protein fate by cell-division-cycle protein48. *Plant Physiol* 160:2093–2108
 30. Reichel C, Beachy RN (2000) Degradation of tobacco mosaic virus movement protein by the 26S proteasome. *J Virol* 74:3330–3337
 31. Heinlein M, Epel BL, Padgett HS, Beachy RN (1995) Interaction of tobamovirus movement proteins with the plant cytoskeleton. *Science* 270:1983–1985
 32. Heinlein M, Padgett HS, Gens JS et al (1998) Changing patterns of localization of the tobacco mosaic virus movement protein and replicase to the endoplasmic reticulum and microtubules during infection. *Plant Cell* 10:1107–1120
 33. Boyko V, Ferralli J, Ashby J et al (2000) Function of microtubules in intercellular transport of plant virus RNA. *Nat Cell Biol* 2:826–832
 34. Boyko V, Hu Q, Seemanpillai M et al (2007) Validation of microtubule-associated tobacco mosaic virus RNA movement and involvement of microtubule-aligned particle trafficking. *Plant J* 51:589–603
 35. Sambade A, Brandner K, Hofmann C et al (2008) Transport of TMV movement protein particles associated with the targeting of RNA to plasmodesmata. *Traffic* 9:2073–2088
 36. Peña EJ, Heinlein M (2013) Cortical microtubule-associated ER sites: organization centers of cell polarity and communication. *Curr Opin Plant Biol* 16:764–773
 37. Boyko V, Ashby JA, Suslova E et al (2002) Intramolecular complementing mutations in tobacco mosaic virus movement protein confirm a role for microtubule association in viral RNA transport. *J Virol* 76:3974–3980
 38. Boyko V, Ferralli J, Heinlein M (2000) Cell-to-cell movement of TMV RNA is temperature-dependent and corresponds to the association of movement protein with microtubules. *Plant J* 22:315–325
 39. Amari K, Di Donato M, Dolja VV, Heinlein M (2014) Myosins VIII and XI play distinct roles in reproduction and transport of tobacco mosaic virus. *PLoS Pathog* 10:e1004448
 40. Hofmann C, Niehl A, Sambade A et al (2009) Inhibition of tobacco mosaic virus movement by expression of an actin-binding protein. *Plant Physiol* 149:1810–1823
 41. Pitzalis N, Heinlein M (2017) The roles of membranes and associated cytoskeleton in plant virus replication and cell-to-cell movement. *J Exp Bot* 69:117–132
 42. Shashkova S, Leake MC (2017) Single-molecule fluorescence microscopy review: shedding new light on old problems. *Biosci Rep* 37:BSR20170031
 43. Christensen N, Tilsner J, Bell K et al (2009) The 5' cap of tobacco mosaic virus (TMV) is required for virion attachment to the actin/endoplasmic reticulum network during early infection. *Traffic* 10:536–551
 44. Sokol DL, Zhang X, Lu P, Gewirtz AM (1998) Real time detection of DNA-RNA hybridization in living cells. *Proc Natl Acad Sci U S A* 95:11538–11543
 45. Cheong C-G, Hall TMT (2006) Engineering RNA sequence specificity of Pumilio repeats. *Proc Natl Acad Sci* 103:13635–13639
 46. Adamala KP, Martin-Alarcon DA, Boyden ES (2016) Programmable RNA-binding protein composed of repeats of a single modular unit. *Proc Natl Acad Sci U S A* 113:2579–2588
 47. Nelles DA, Fang MY, O'Connell MR et al (2016) Programmable RNA tracking in live cells with CRISPR/Cas9. *Cell* 165:488–496
 48. Paige JS, Wu KY, Jaffrey SR (2011) RNA mimics of green fluorescent protein. *Science* 333:642–646
 49. Babendure JR, Adams SR, Tsien RY (2003) Aptamers switch on fluorescence of triphenylmethane dyes. *J Am Chem Soc* 125:14716–14717
 50. Bertrand E, Chartrand P, Schaefer M et al (1998) Localization of ASH1 mRNA particles in living yeast. *Mol Cell* 2:437–445
 51. Urbanek MO, Galka-Marciniak P, Olejniczak M, Krzyzosiak WJ (2014) RNA imaging in living cells - methods and applications. *RNA Biol* 11:1083–1095
 52. George L, Indig FE, Abdelmohsen K, Gorospe M (2018) Intracellular RNA-tracking methods. *Open Biol* 8:180104
 53. van Gijtenbeek LA, Kok J (2017) Illuminating messengers: an update and outlook on RNA

- visualization in bacteria. *Front Microbiol* 8:1161
54. Tilsner J (2015) Techniques for RNA in vivo imaging in plants. *J Microsc* 258:1–5
 55. Tutucci E, Livingston NM, Singer RH, Wu B (2018) Imaging mRNA in vivo, from birth to death. *Annu Rev Biophys* 47:85–106
 56. Hamada S, Ishiyama K, Choi S-B et al (2003) The transport of prolamine RNAs to prolamine protein bodies in living rice endosperm cells. *Plant Cell* 15:2253–2264
 57. Luo K-R, Huang N-C, Yu T-S (2018) Selective targeting of mobile mRNAs to plasmodesmata for cell-to-cell movement. *Plant Physiol* 177:604–614
 58. Fusco D, Accornero N, Lavoie B et al (2003) Single mRNA molecules demonstrate probabilistic movement in living mammalian cells. *Curr Biol* 13:161–167
 59. Heinrich S, Sidler CL, Azzalin CM, Weis K (2017) Stem-loop RNA labeling can affect nuclear and cytoplasmic mRNA processing. *RNA* 23:134–141
 60. Garcia JF, Parker R (2015) MS2 coat proteins bound to yeast mRNAs block 5' to 3' degradation and trap mRNA decay products: implications for the localization of mRNAs by MS2-MCP system. *RNA* 21:1393–1395
 61. Tutucci E, Vera M, Biswas J et al (2018) An improved MS2 system for accurate reporting of the mRNA life cycle. *Nat Methods* 15:81–89
 62. Vera M, Tutucci E, Singer RH (2019) Imaging single mRNA molecules in mammalian cells using an optimized MS2-MCP system. *Methods Mol Biol* 2038:3–20
 63. Tutucci E, Vera M, Singer RH (2018) Single-mRNA detection in living *S. cerevisiae* using a re-engineered MS2 system. *Nat Protoc* 13:2268–2296
 64. Curtis MD, Grossniklaus U (2003) A gateway cloning vector set for high-throughput functional analysis of genes in planta. *Plant Physiol* 133:462–469
 65. Hellens R, Mullineaux P, Klee H (2000) Technical focus: a guide to *Agrobacterium* binary Ti vectors. *Trends Plant Sci* 5:446–451
 66. Kapila J, De Rycke R, Van Montagu M, Angenon G (1997) An *Agrobacterium*-mediated transient gene expression system for intact leaves. *Plant Sci* 122:101–108
 67. Voinnet O, Rivas S, Mestre P, Baulcombe D (2003) An enhanced transient expression system in plants based on suppression of gene silencing by the p19 protein of tomato bushy stunt virus. *Plant J* 33:949–956
 68. Peña EJ, Heinlein M (2016) In vivo RNA visualization in plants using MS2 tagging. *Methods Enzymol* 572:105–122



New Generations of MS2 Variants and MCP Fusions to Detect Single mRNAs in Living Eukaryotic Cells

Xavier Pichon, Marie-Cécile Robert, Edouard Bertrand, Robert H. Singer, and Evelina Tutucci

Abstract

Live imaging of single RNA from birth to death brought important advances in our understanding of the spatiotemporal regulation of gene expression. These studies have provided a comprehensive understanding of RNA metabolism by describing the process step by step. Most of these studies used for live imaging a genetically encoded RNA-tagging system fused to fluorescent proteins. One of the best characterized RNA-tagging systems is derived from the bacteriophage MS2 and it allows single RNA imaging in real-time and live cells. This system has been successfully used to track the different steps of mRNA processing in many living organisms. The recent development of optimized MS2 and MCP variants now allows the labeling of endogenous RNAs and their imaging without modifying their behavior. In this chapter, we discuss the improvements in detecting single mRNAs with different variants of MCP and fluorescent proteins that we tested in yeast and mammalian cells. Moreover, we describe protocols using MS2-MCP systems improved for real-time imaging of single mRNAs and transcription dynamics in *S. cerevisiae* and mammalian cells, respectively.

Key words MS2-MCP system, mRNA labeling, Single molecule, Single cell, *S. cerevisiae*, Mammalian cells, Gene expression, mRNA localization, Transcription

1 Introduction

Cells are the basic unit of life. Within a single cell, networks of molecules control how the environment is sensed through signaling and how cells adapt via metabolic changes and modulation of gene expression. Quantitative methods are required to model these fundamental processes, which often involve only tens or less molecules [1–3]. To detect variations in gene expression, one approach is to measure mRNA levels. Even though these are not always a proxy for protein expression, i.e., when a delay exists between

Electronic supplementary material: The online version of this chapter (https://doi.org/10.1007/978-1-0716-0712-1_7) contains supplementary material, which is available to authorized users.

mRNA accumulation and protein production [4], mRNA measurements provide information about the rate of transcription, accumulation, and decay, revealing modes of gene expression regulation. Bulk mRNA measurements, i.e., northern blots, quantitative PCR, and RNA sequencing, are informative to measure multiple mRNA species from a single RNA preparation and to perform relative comparisons of mRNA levels in different conditions. However, these approaches, which average millions of cells, have fundamental limitations when it comes to precisely measuring RNAs at the level of single cells, or within cellular compartments, i.e., nucleus vs. cytoplasm, cellular protrusions such as the bud of *S. cerevisiae*, the leading edge of fibroblast, or neuronal dendrites and axons.

To achieve quantitative subcellular mRNA measurements, several approaches based on fluorescence microscopy have been developed over the past decades. In fixed cells, a standard method to visualize and count individual mRNAs is single-molecule fluorescent in situ hybridization (smFISH) [5, 6]. Briefly, this approach allows detecting single endogenous mRNAs by hybridizing tens of fluorescently labeled DNA oligos onto the target molecule. By using sensitive digital cameras and wide-field microscopy, it is possible to detect single mRNAs as diffraction-limited spots, allowing their subcellular localization and quantification in thousands of cells. This method can be applied to single isolated cells (i.e., [7–13]) as well as to tissues [14–16]. Several modified smFISH protocols exist, which use DNA probes of different lengths and complexities (i.e., 20 mer, 50 mer, branched DNA, RNA scope [8, 10, 17]) or fluorescence amplification systems to detect weak signals (i.e., hybridization chain reaction, HCR [18]). An important difference between these techniques is whether the probes are fluorescently labeled or not, in which case they need to be detected with a secondary fluorescent oligo. A simple, reliable, and affordable protocol that uses indirect labeling has recently been published [19]. Furthermore, smFISH can be multiplexed to simultaneously visualize different mRNA species within single cells (up to 10,000; [15, 20–24]), or it can also be combined to protein detection by immunofluorescence (see refs. 25, 26 and this issue). These approaches revealed asymmetric RNA distribution within single cells, as well as significant cell-to-cell variability existing in tissue or even isogenic populations [27–32]. Furthermore, by using smFISH, other aspects of gene expression have been characterized, such as the “bursty” nature of transcription [8, 9, 33, 34], the mechanisms controlling mRNA export from the nucleus to the cytoplasm [35, 36], as well as the control of mRNA degradation [37, 38]. For more in-depth reviews see refs. 1, 2, 39; see also Chapter 1 by Bleckmann et al. and Chapter 4 by Tutucci and Singer.

However, fixed cells provide limited information about highly dynamic and rare events controlling mRNA metabolism. To follow mRNAs in living cells, several labeling strategies have been developed over the past decades. The best characterized system is a genetically encoded reporter based on the multimerization of RNA stem-loops derived from the bacteriophage MS2 [40–42]. To visualize single mRNAs in living cells, 24 MS2 stem-loops are used to tag an RNA of interest, which is then detected by co-expression of a specific RNA-binding protein, the MS2 coat protein (MCP), fused to fluorescent proteins (FP, i.e., eGFP, mCherry, tdTomato, HALO, photoactivatable proteins) [1, 39]. Several MS2 array variants are available, and the recommendation for using a particular one depends on the model organism, the mRNA, and the step of the mRNA life cycle under investigation [1, 43]. High-affinity MS2-MCP variants have been successfully used to measure the dynamics of mRNA transcription and splicing [44–46], export [47, 48], localization [49, 50], and translation in mammalian cells [51–55]. They are also recommended if the experimental setup involves FRAP. However, several groups reported that the high-affinity MS2-MCP variants are not optimal to visualize mRNAs in rapidly dividing organisms such as *S. cerevisiae* [56–59]. For this reason, we recently generated an improved MS2 array (MS2-binding sites V6, MBSV6) with decreased affinity for MCP. This allowed measuring the half-life of rapidly decaying mRNAs while preserving single-molecule mRNA detection in living cells [43, 58]. Low-affinity MS2-MCP variants have also been used to tag mRNAs in mammalian cells, specifically to generate arrays containing up to 128 MS2 stem-loops in a single transcript, with the aim of monitoring transcription with high temporal resolution for long periods of time and with minimal photo-bleaching [60].

To visualize more than one mRNA species at the time, in single living cells, several orthogonal systems are available. Another system was generated by multimerizing RNA stem-loops derived from the bacteriophage PP7, detected by the cognate protein PP7 coat protein (PCP) fused to fluorescent proteins [61]. This reporter has been used to study transcription dynamics [62], mRNA export [63], and translation [64, 65]. It has also been used to create a homozygous mice where the immediate early gene *Arc* was endogenously tagged with 24 PP7 loops, allowing to visualize its response to synaptic activity [66]. Alternative genetically encoded RNA labeling strategies use arrays generated from other RNA sequences, such as the BglG stem-loop [67], the λ BoxB RNA [68], and the U1A loop [69, 70]. Other RNA labeling methods are reviewed elsewhere [1, 43, 54].

The optimization of single mRNA visualization in living cells relies also on the expansion of the FP and fluorophore palette [71, 72]. In a recent publication, the brightness, photostability, pH resistance, and monomeric properties of more than 40 FP have

been systematically quantified [73]. These measurements are valuable to design mRNA imaging reporters with precise photochromatic properties. Furthermore, the development of fluorescent dyes partly bypasses some of the common problems encountered using fluorescent proteins, i.e., wide excitation and emission spectrum, sensitivity to photobleaching, tendency to multimerization since these molecules generally have small size, high brightness and photostability, and narrow spectrum.

In the following paragraphs we report our tests aimed at optimizing the visualization of single mRNAs in living eukaryotic cells. We tested several MCP variants in the model organism *S. cerevisiae* as well as multiple green FP fused to MCP both in *S. cerevisiae* and mammalian cell lines. These comparisons revealed that for efficient mRNA detection, MCP variants with high affinity for the RNA reporter remain the best option. In addition, we found that the green FP Envy shows improved brightness compared to other GFP variants, both in yeast and mammalian cells.

1.1 mRNA Detection Using Different MCP Variants

We previously demonstrated that it is possible to efficiently detect single mRNAs in *S. cerevisiae* by using the latest MS2 variant, MBSV6, in combination with the expression of MCP-NLS-2xyeGFP [43, 58] (Fig. 1a–d). To improve the long-term detection of single mRNAs in living cells (i.e., brightness and photostability) we generated other MCP constructs that we compared to MCP-NLS-2xyeGFP for their brightness and propensity to form aggregates. Even though we find that the MCP-NLS-2xyeGFP performs better than other constructs tested thus far, here we report the advantages and disadvantages of other tested reporters.

To improve the brightness of single mRNAs, we generated an MCP variant fused to 3xyeGFP. This plasmid was transformed in the yeast strain expressing *MDNI* tagged with 24xMBSV6 and Nup49-tdTomato (Fig. 1e, f). We compared the brightness of *MDNI* mRNAs detected with either MCP-2xyeGFP or MCP-3xyeGFP (Fig. 1g). As expected, mRNAs labeled with MCP-3xyeGFP shows a 25% increase in brightness compared to mRNAs labeled with MCP-2xyeGFP ($310,950 \pm 155,349$ a.u. and $263,373 \pm 109,890$ a.u., respectively). In addition, the number of *MDNI* mRNAs per cell counted with the MCP-3xyeGFP reporter is similar to the mRNAs counted with MCP-2xyeGFP or by smFISH (mean \pm S.D. 9.2 ± 6.1 mRNAs/cell, Fig. 1h). However, we found that the MCP-3xyeGFP reporter has the tendency to induce cytoplasmic aggregates, likely due to the propensity of GFP to multimerize (Fig. 1f, orange arrowheads). These aggregates are similar to the ones that we previously described [58] and that can lead to artifactual conclusions about mRNA localization in yeast. It may still be possible to use the MCP-3xyeGFP reporter for mRNAs that are less abundant than *MDNI*, but we recommend always comparing the live imaging results to smFISH to avoid false conclusions.

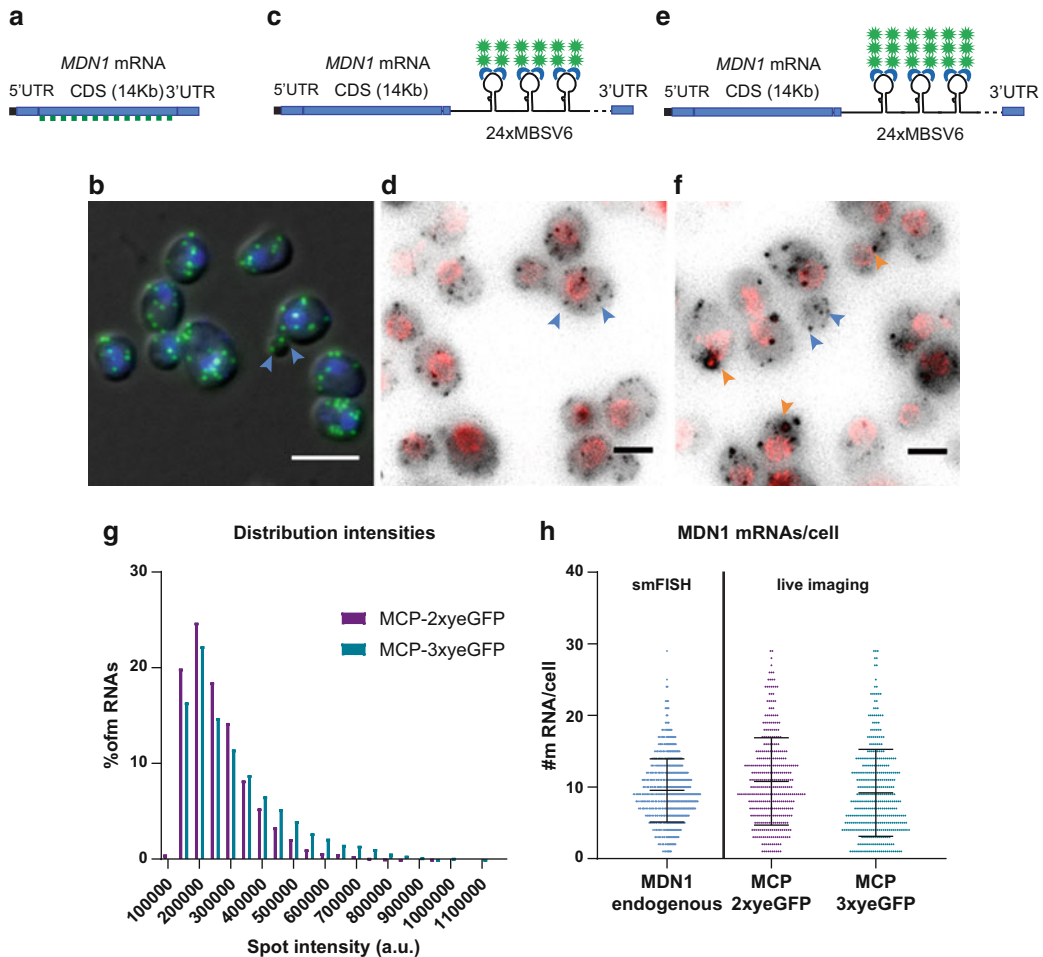


Fig. 1 *MDN1* mRNA detection using the MS2-MCP system in *S. cerevisiae*. **(a)** Schematic representation of the *MDN1* locus. smFISH probes labeled with Q760 anneal all along the CDS. Probe list is provided in [58]. **(b)** Overlap of the DAPI signal in the nucleus (blue), smFISH for the *MDN1* CDS (green) with the differential interference contrast (DIC) image. Single mRNAs are indicated with blue arrowheads. Scale bar 5 μ m. **(c)** Schematic representation of *MDN1* locus tagged at the 3'UTR with 24xMBSV6. mRNAs are detected in living cells by co-expression of the plasmid MCP-NLS-2xyeGFP. **(d)** *MDN1* mRNAs are shown in gray, and the nuclear pore protein Nup49 is shown in red. Max projection of a 15 Z-stack. Rolling average background subtraction (rolling ball radius = 50) was performed for the two channels. Single mRNAs are indicated by blue arrowheads. Scale bar 3 μ m. **(e)** Schematic representation of *MDN1* locus tagged at the 3'UTR with 24xMBSV6. mRNAs are detected by co-expression of the plasmid MCP-NLS-3xyeGFP. **(f)** *MDN1* mRNAs are shown in gray, and the nuclear pore protein Nup49 is shown in red. Max projection of a 15 Z-stack. Rolling average background subtraction (rolling ball radius = 50) was performed for the two channels. Selected single mRNAs are indicated by blue arrowheads. MCP-containing granules are indicated in orange arrowheads. Scale bar 3 μ m. **(g)** Distribution of *MDN1* mRNA intensities measured by live imaging in expressing cells. Purple bars, *MDN1* 24xMBSV6 co-expressing MCP-NLS-2xyeGFP. Mean \pm S.D. 263,373 \pm 109,890 a.u. number of spots = 4186. Green bars, *MDN1* 24xMBSV6 co-expressing MCP-NLS-3xyeGFP. Mean \pm S.D. 3,100,950 \pm 155,349 a.u. number of spots = 3414. **(h)** Comparison of *MDN1* mRNA/cell counted in fixed cells vs. live imaging. mRNAs per cell counted by smFISH in wild-type cells vs. *MDN1* mRNAs counted in cells expressing *MDN1* 24xMBSV6 co-expressing MCP-NLS-2xyeGFP (purple, $n = 368$) or *MDN1* 24xMBSV6 co-expressing MCP-NLS-3xyeGFP (green, $n = 390$)

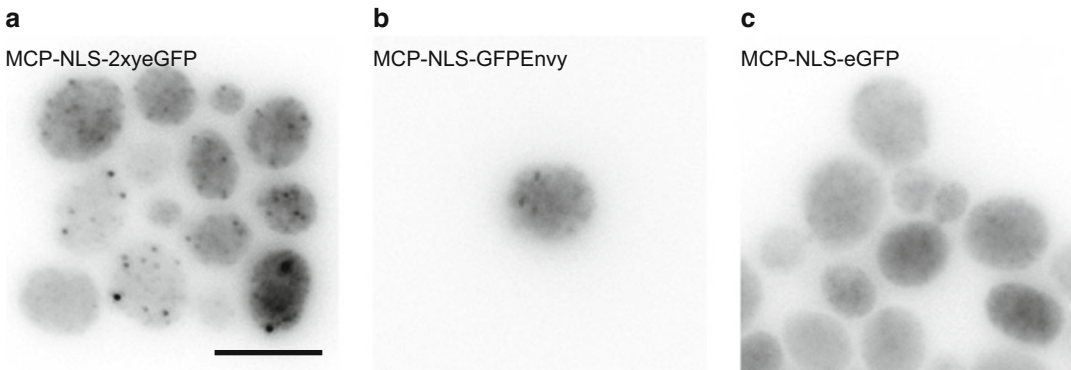


Fig. 2 Comparison of MCP-FP variants in yeast. Images are from yeast cells expressing the *DOA1* gene tagged with 24xMBSV6 transformed with (a) MCP-NLS-2xyeGFP plasmid, (b) MCP-NLS-GFPEnv plasmid, (c) MCP-NLS-eGFP plasmid. Panels are maximum intensity projections of Z-stacks. Scale bar 5 μm

1.2 Comparison of FP Variants in Yeast

Many FP variants now exist, and we tested a few promising ones to see whether this would improve the signal: sfGFP, mNG2, eGFP, muGFP, and EnvY. sfGFP is the superfolder GFP and muGFP is one of its ultrastable monomeric variants [74]. mNG is a bright and stable variant derived from a *Branchiostoma lanceolatum* fluorescent protein [75], and EnvY is an FP that performs particularly well in *S. cerevisiae* [76]. The cDNA coding for these fluorescent proteins was cloned into pET296, replacing the yeGFP tag, such that they are expressed as monomeric variants lacking NLS (MCP-1xFP). The plasmids were then transformed into yeast cells expressing the *DOA1* gene tagged with 24xMBSV6 as described in [58]. Cells were then grown, fixed, and observed under the microscope (Fig. 2a–c). We found that mRNAs were undetectable with MCP-1xeGFP, MCP-1xsfGFP, and MCP-1xmuGFP, while they were nicely visible with the MCP-1xEnvY and MCP-1xmNG2 (with best results for MCP-1xEnvY).

1.3 Comparison of Low- and High-Affinity MCP Variants in Yeast

The original MS2 system was designed with high-affinity variants of both the MBS and the MCP [40]. Indeed, this MCP variant carried the V29I mutation that enhances binding stability by 5–10-fold [77]. Since a too high affinity of the MCP-MBS interaction was found to cause artifacts in yeast [58], we tested the effect of reverting the V29I mutation. A plasmid expressing MCP-I29V-2xyeGFP was generated and transformed in yeast cells expressing the *DOA1* gene tagged with MBV6. No signals corresponding to single mRNAs could be detected, suggesting that the affinity of the MS2V6/MCP-I29V is probably too low for an efficient mRNA detection. Overall, MBSV6/MCP-V29I appears to have the best affinity compromise to allow for an artifact-free mRNA detection in yeast.

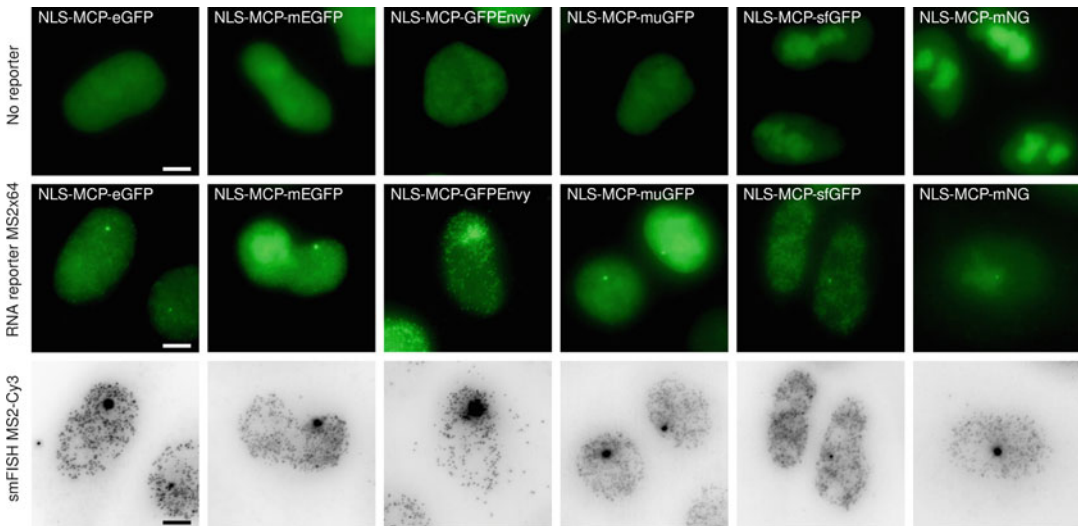


Fig. 3 Comparison of MCP-FP variants in mammalian cells. Images are maximum intensity projections from HeLa Flp-in cells transfected with the indicated NLS-MCP-FP variant constructs. Top panels: Images are from cells expressing the indicated NLS-MCP-FP variants without RNA reporter (parental HeLa H9 AAVS1-Tat cell line). Middle panels: Images are from cells expressing the indicated NLS-MCP-FP variant in HeLa H9 AAVS1-Tat cell line expressing the HIV-1 MS2x64 reporter. Bottom panels: Images are smFISH signals obtained with probes against the MS2 tag. Scale bar 5 μ m. Contrast adjustment is identical for all images of the top and middle panels

Table 1
List of the FP variants

NLS-MCP-FP variants	FP plasmid from	References for the FP
eGFP	Gift from Lionnet T./Singer RH	Cormack et al. (1996) [78]
mEGFP	Addgene #54610	Zacharias et al. (2002) [79]
sfGFP	Addgene #60907	Pedelacq et al. (2006) [80]
GFPEnv	Addgene #60782	Slubowski et al. (2015) [76]
muGFP	Gift from Scott DJ	Scott et al. (2018) [74]
mNG	pUC57-mNeonGreen	Shaner et al. (2013) [81]

1.4 Comparison of FP Variants in Mammalian Cells

MCP-FP variants displayed distinct performance in yeast, and we thus tested how these variants [74, 76, 78–81] performed in mammalian cells (Fig. 3 and Table 1). Transient transfections of the different NLS-MCP-FP variant constructs were evaluated in a HeLa H9 cell line without RNA reporter gene (Fig. 3, top panels). A diffuse fluorescent signal was seen in the nucleus, indicating a good solubility of all NLS-MCP-FP variant constructs. When the various NLS-MCP-FP were expressed in a derivative of this cell line expressing the HIV-1 MS2x64 RNA reporter (Figs. 3 and 4,

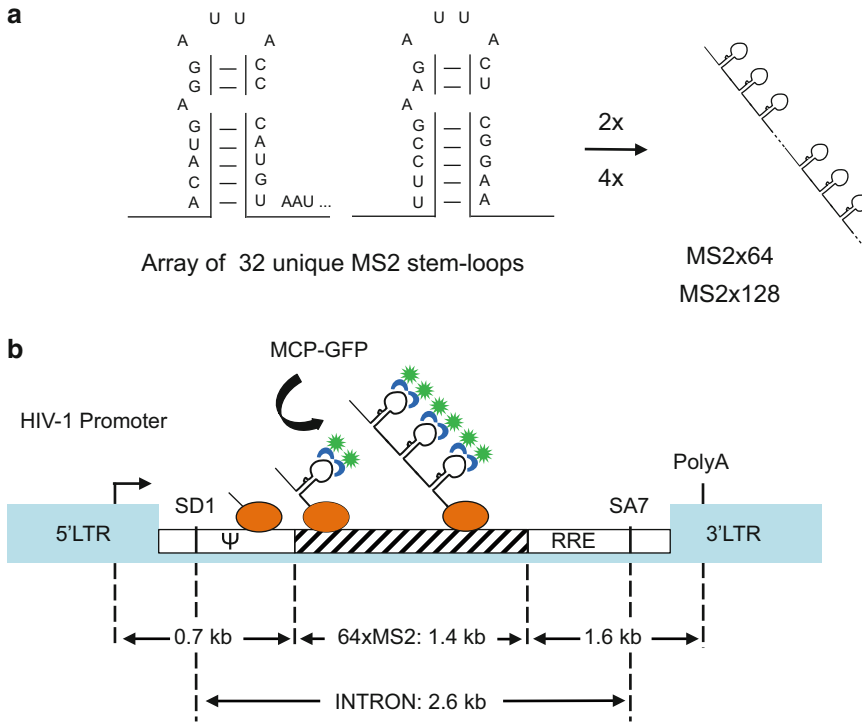


Fig. 4 Schematic representation of plntro-MS2x64 RNA reporter construct. **(a)** Generation of the MS2x64 RNA tag. The MS2x32 stem-loop sequence with low-affinity binding to MCP is multimerized to generate repeats of 64 and 128 stem-loops. **(b)** Schematic of the plntro-MS2x64 reporter construct. The striped box represents the MS2 repeat; the green spot represents the GFP fused to MCP (blue); the orange oval represents RNAPII with the nascent RNAs. *LTR* The HIV-1 long terminal repeat; *SD1* The major HIV-1 splice donor; *SA7* The last splice acceptor; *Ψ* Packaging sequence; *RRE* Rev-responsive element

middle panels), the NLS-MCP-GFP_{Envy} showed the highest contrast (see signal quantifications in Fig. 5), followed by the NLS-MCP-eGFP and NLS-MCP-sfGFP. Single RNA molecules were only barely detectable with the NLS-MCP-muGFP and NLS-MCP-mNG construct, while single RNA molecules were observed by smFISH (Fig. 3, bottom panels).

In light of these recent developments, we describe here protocols to visualize and quantify mRNAs labeled with the low-affinity MS2 systems that we recently developed both for *S. cerevisiae* and mammalian cells. By describing the visualization of mRNA in these model organisms, we highlight the general rules and recommendations that can improve live imaging of single mRNAs. While elsewhere we described in depth the steps required to endogenously tag an mRNA with the MS2 reporter in yeast [43, 58] or in mammalian cells [49], here we focused on the protocols used to perform live imaging and to quantify the number and the brightness of single mRNAs and transcription sites.

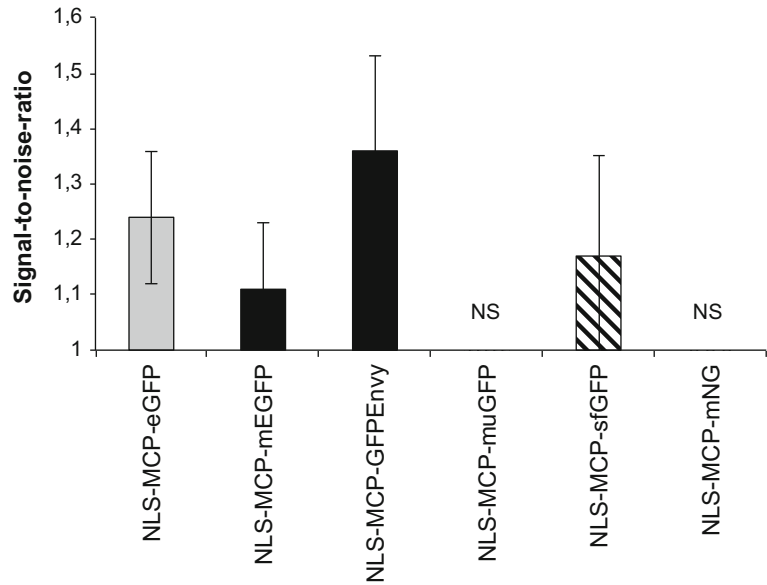


Fig. 5 Signal-to-noise ratio (SNR) of single RNA molecule detection with MCP-FP variants. The bar plots show the mean values of the SNR of single RNA molecules (error bar: standard deviation). NS: nonsignificant detection of single RNAs occurred with the NLS-MCP-muGFP and NLS-MCP-mNG constructs. To measure the intensity of single RNA molecules, a straight line with a width of 2 pixels was used, and the maximal value of the intensity plot was recorded. This value was divided over the mean gray value measured in the nucleus of the cell following the application of a Gaussian blur of 3 pixels (maximum intensity projected images). The background value (outside the cell nucleus) was subtracted from each of these values (total of 133 single molecules quantified per construct)

For *S. cerevisiae* we outline a protocol for the visualization of mRNAs labeled with the low-affinity 24xMBSV6 (*see* Subheadings 2.1 and 3.1). The constitutive and well-characterized mRNA *MDNI* is used as a model gene. *MDNI* was endogenously tagged with 24xMBSV6 as previously described in [58]. Here, we detail how to transform yeast cells with the constructs expressing MCP-FP (Subheading 3.1.1), grow cells for live imaging (Subheading 3.1.2), prepare the coated dishes (Subheading 3.1.3), perform live imaging (Subheading 3.1.4), and count single mRNAs in living cells (Subheading 3.1.5).

For mammalian cells, we outline a protocol for the visualization of mRNAs labeled with the low-affinity MS2x64 reporter, which is particularly useful to analyze transcription dynamics (*see* Subheadings 2.2 and 3.2). To this end, we used a stable HeLa H9 AAVS1-Tat cell line expressing the HIV-1 MS2x64 reporter gene [60]. Here, we describe how to produce lentiviruses encoding the MCP-FP (Subheading 3.2.1), how to generate a stable cell line expressing the MCP-FP construct (Subheading 3.2.2), how to

select a cell line with optimal MCP-FP expression (Subheading 3.2.3), how to prepare the cells (Subheading 3.2.4), and how to perform live image acquisition (Subheading 3.2.5).

2 Materials

2.1 Materials for Visualizing MBSV6-Labeled mRNAs in Yeast

1. Yeast cells: All strains used in this protocol are derived from the *S. cerevisiae* background BY4741 MATa; *his3Δ1*; *leu2Δ0*; *met15Δ0*; *ura3Δ0*.
2. YPD medium: 50 g/L of the YPD mix (i.e., Clonetechn). Sterilize by autoclaving.
3. LEU medium (dropout media lacking leucine): 6.7 g/L Yeast nitrogen base (YNB) with ammonium sulfate, dropout mix lacking leucine, 20 g/L glucose. Sterilize by autoclaving.
4. LEU plates (dropout agar plates): 6.7 g/L Yeast nitrogen base (YNB) with ammonium sulfate, dropout mix lacking leucine, 20 g/L glucose, 20 g/L of bacteriological agar. Sterilize by autoclaving.
5. 100% Glycerol stock: Sterilize by autoclaving. Store at room temperature, protected from light.
6. Plasmids: pET264-pUC 24xMS2V6 Loxp KANr Loxp (Addgene ID:104393), pET251-pUC 12xMS2V6 Loxp KANr Loxp (Addgene ID:104392); pET296-YcpLac111 CYC1p-MCP-NLS-2xyeGFP (yeast-optimized eGFP) (Addgene ID:104394); pET511-YcpLac111 CYC1p-MCP-NLS-3xyeGFP; pET518-YcpLac11-CYC1p-MCP-1x-eGFP; pET519-YcpLac11-CYC1p-MCP-1xEnvy; pET521-YcpLac11-CYC1p-MCP-1xmuGFP; pET522-YcpLac11-CYC1p-MCP-1xmNG; pET523-YcpLac11-CYC1p-MCP-1xsfGFP (constructs available upon request).
7. Lithium-TE: 100 mM LiAc, 10 mM Tris-HCl, pH 7.5, 1 mM EDTA. Sterilize by autoclaving.
8. Lithium-TE-PEG: 100 mM LiAc, 10 mM Tris, pH 7.5, 1 mM EDTA, 50% PEG 3350-4000. Sterilize by autoclaving.
9. Salmon sperm DNA (ssDNA): 10 mg/mL Lyophilized, sheared, organically extracted, and denatured ssDNA is resuspended in double-distilled water (DDW). Store 100 μL aliquots at -20 °C.
10. Centrifuges (table top): Up to 20,000 × g for samples 1.5 mL.
11. Heat blocks at 42 °C and 95 °C.
12. Temperature-controlled shaker for yeast cultures.
13. Temperature-controlled, Delta-T dishes (i.e., Bioptech Cat# 04200417C).

14. Concanavalin A (ConA) stock: 10 mg/mL in sterile DDW (10× stock). Store 500 μL aliquots at −20 °C.
15. ConA-coated plate activation solution: 50 mM CaCl₂, 50 mM MnCl₂ in DDW. Filter sterilize, store at room temperature.
16. Fluorescent wide-field microscope of choice for live-cell image acquisition (*see Note 1*).
17. Image analysis software: FISH-quant [82], free software developed in the MATLAB programming language (MathWorks). Download the FISH-quant package (<http://code.google.com/p/fish-quant/>) together with the MCRInstaller, which allows one to run a MATLAB algorithm without separately installing MATLAB onto the computer.
18. Image analysis software: Fiji (Java software for image-processing analysis; freely available at <https://fiji.sc/>).
19. Image analysis software: CellProfiler [83], for cell outline generation (freely available at <https://cellprofiler.org/>).
20. Image analysis software: For image deconvolution use a software such as the Huygens Software Suite (<https://svi.nl/HomePage>).

**2.2 Materials
for Visualizing
MS2-Labeled RNAs
in Mammalian Cells,
with a Focus
on Analyzing
Transcription
Dynamics**

1. Transcription reporter constructs containing MS2 stem-loop repeats: pIntro-MS2x64 and pIntro-MS2x128 [60]. These plasmids are available upon request (*see Fig. 4*).
2. Lentiviral plasmid for MCP fused to a fluorescent protein: pHAGE-Ubc-NLS-MCP-GFP (available upon request) or pHAGE-Ubc-NLS-tdMCP-GFP (Addgene #40649).
3. Packaging plasmids for lentivirus production (available upon request): pHDM-tat1b (helper plasmid for lentiviral vector, HIV tat driven by CMV promoter); pRC-CMV-rev1b (helper plasmid for lentiviral vector, rev1b driven by CMV promoter); pHDM-Hgpm2 (helper plasmid for lentiviral vector, has codon-optimized HIV gag-pol driven by CMV promoter); pHDM-G (helper plasmid for lentiviral vectors, VSV-G driven by CMV promoter).
4. XL1-Blue competent cells (*see Note 2*).
5. HeLa Flp-in H9 cell line [60], allowing the generation of isogenic stable cell lines by genomic integration in a single integrated Flp recombination target (FRT) site from pFRT/Lac Zeo, under zeocin selection (100 μg/mL) (*see Notes 3 and 4*).
6. DMEM + GlutaMAX supplemented with 10% fetal bovine serum (FBS) and penicillin/streptomycin (P/S; 10 U/mL), in a humidified CO₂ incubator at 37 °C for propagation conditions.

7. HEK-293T cell line for lentiviral production.
8. 1× Phosphate-buffered saline (PBS): 137 mM NaCl, 2.7 mM KCl, 8 mM Na₂HPO₄, and 2 mM KH₂PO₄ (without Ca²⁺ and Mg²⁺).
9. Trypsin (0.25%)/EDTA (1 mM).
10. Transfection reagent: JetPRIME[®] (Polyplus transfection).
11. Syringes for filtering (5 mL).
12. Sterile falcon tube (15 mL).
13. 0.45 μm Cellulose acetate or polyethersulfone filters.
14. Lenti-X[™] Concentrator (Clontech).
15. Polybrene.
16. 10% Bleach.
17. Live-cell imaging medium (showing lower background fluorescence) supplemented with 10% FBS.
18. 32% (w/v) Paraformaldehyde (PFA): Store at room temperature, protected from light.
19. Vectashield mounting medium with DAPI.
20. Glass microscopy slides.
21. Noncoated 22 × 22 mm coverslips.
22. 25 mm diameter non-coated coverslips (0.17 mm thick).
23. Epifluorescent microscope of choice for acquisition of still pictures (*see Note 5*).
24. Fluorescent microscope of choice for live-cell image acquisition (*see Note 6*).
25. smFISH analysis software (FISH-quant [82], *see above*) Fiji image-processing software (freely available at <https://fiji.sc/>).

3 Methods

3.1 Visualizing MBSV6-Labeled mRNAs in Yeast

3.1.1 Yeast Transformation

1. Grow yeast expressing the mRNA of interest tagged with 24xMBSV6 in 5 mL of YPD at 26 °C until an OD₆₀₀ of 0.6–0.8 is reached. Do not use cells grown over OD₆₀₀ >1. The transformation efficiency will be significantly reduced. The method to tag the mRNA with the MS2 system and to verify that the expression of the mRNA is not affected is described in more details in [43, 58] (*see Note 7*).
2. Centrifuge the cells for 3 min at 7000 × *g*. Discard the supernatant and resuspend the cells in 5 mL of lithium-TE.
3. Centrifuge for 3 min at 1000 × *g* and resuspend in 150 μL of lithium-TE.
4. Put 450 μL of lithium-TE-PEG in an Eppendorf tube.

5. Add 5 μL of 10 mg/mL ssDNA denatured at 95 °C for 10 min.
6. Add 500 ng–1 μg of plasmid expressing MCP-GFP (i.e., YcpLac111 MCP-NLS-2xyeGFP) for each transformation.
7. Add 150 μL of cells to the tube and mix by gentle vortexing (speed 5 out of 10).
8. Incubate at room temperature for 30 min.
9. Heat shock the cells at 42 °C for 15 min.
10. Centrifuge the cells for 3 min at 7000 $\times g$.
11. Discard the supernatant, resuspend the pellet in 100 μL of DDW, and plate the entire transformation on selective LEU plates.
12. Incubate at 26 °C for 3–4 days. The transformed cells can be used to start cultures for live imaging (*see Note 8*).

3.1.2 Growing Yeast Cells for Live Imaging

1. Grow a low-density culture of the yeast strain expressing the endogenously tagged mRNA and MCP-GFP in selective LEU medium overnight at 26 °C. Apply constant shaking at 210 rpm. It is important to keep the cells growing in exponential phase ($\text{OD}_{600} < 1$) at all times.
2. In the morning, dilute the cells with fresh medium to an $\text{OD}_{600} \sim 0.1$ and allow to grow until $\text{OD}_{600} 0.2\text{--}0.3$. At this concentration, the autofluorescence of the cells is minimal and the expression of the MCP is homogenous (*see Note 9*).

3.1.3 Coating of Delta-T Dishes and Plating of Cells

1. Incubate the Delta-T dishes with 400 μL of ConA at a final concentration 1 mg/mL for 10 min at room temperature.
2. Aspirate the excess and let the dish air-dry completely.
3. Activate the ConA coating, by incubating the dish with 400 μL of ConA activating solution, for 10 min at room temperature (*see Note 10*).
4. Aspirate the excess and let the dish air-dry completely.
5. Wash the dish twice with sterile DDW and let air-dry completely.
6. Plate 500 μL of cells at $\text{OD}_{600} 0.2\text{--}0.3$ (*see Note 11*).
7. Place the dish on the microscope stage and let the cells attach for at least 15–30 min. Using the Delta-T temperature control system, allow the temperature to stabilize at 26 °C. It is important to wait until cells attach and restart the cell cycle.

3.1.4 Live Imaging Acquisition

The live imaging conditions need to be adapted based on the expression of the mRNA under investigation. We recommend testing the mRNA of interest first by smFISH. Here, we outline the imaging conditions for the constitutive *MDNI* mRNA. We previously characterized the expression of this mRNA by smFISH

[8, 58] and this protocol is detailed in Chapter 4 of this book as well as in [43, 58]. Figure 1a, b shows an example of smFISH for the *MDN1* mRNA in wild-type cells, for side-by-side comparison with the live imaging results shown in Fig. 1c–f. For live imaging, the *MDN1* mRNA was tagged at the 3' UTR with 24xMBSV6 (Fig. 1c) [58]. To distinguish the nucleus from the cytoplasm, the nuclear pore protein Nup49 is endogenously fused to the red fluorescent protein tdTomato (YET443 MATa; his3 Δ 1; leu2 Δ 0; met15 Δ 0; ura3 Δ 0 NUP49::NUP49-tdTomato KAN- CRE recombined MDN1:: MDN1 3UTR 24MS2V6 KAN- CRE recombined; Ycp-Lac111 CYC1p MCP-NLS-2xyeGFP).

1. For short-term imaging and fast acquisition to follow mRNAs with high temporal resolution, stream one single Z-plane, 50 ms exposure. Detection of single mRNAs tagged with MCP-GFP is achieved by using 10% of 100 mW 491 laser (\sim 1–2 mW/cm² measured at the objective). To detect Nup49-tdTomato, use 1% of 50 mW 561 laser (\sim 0.5 mW/cm² measured at the objective). Under these conditions the mRNAs in the cytoplasm and the transcription sites in the nucleus can be visualized for 2–3 min before significant photobleaching occurs (*see* Supplementary Video 1).
2. For long-term imaging, i.e., over the course of a complete cell cycle, and to cover the whole cell width, take 15 Z-stacks every 0.5 μ m every 2 min (\sim 90 Z-stacks total). An exposure of 50 ms for each Z-plane was used under our conditions. To visualize MBSV6-MCP-NLS-2xyeGFP-labeled mRNAs use a 491 nm wavelength laser. For visualization of single mRNA molecules, set the laser to 10% power (\sim 1–2 mW/cm² measured at the objective). To detect Nup49-tdTomato, use 1% of 50 mW 561 laser (\sim 0.5 mW/cm² measured at the objective). Acquire Z-planes at different stage positions and use them to detect the number, the position, and the brightness of mRNAs in living cells (Fig. 1d and *see* Note 12).

3.1.5 Imaging Analysis

1. To improve the signal-to-noise ratio, restore the images using a deconvolution software such as the Huygens software package. Automatically compute the theoretical point spread function based on your microscope settings. Restore the images using the classic maximum likelihood estimation algorithm (i.e., number of iterations = 99; signal/noise ratio = 15).
2. To measure the number, position, and brightness of the mRNAs in single cells, use the freely available software FISH-quant running on Matlab [82]. Deconvolved images can be analyzed with FISH-quant without further filtering. Cell outlines can be created using FISH-quant or using the freely available software CellProfiler [83]. Recent versions of FISH-

quant have a built-in plug-in converting CellProfiler outlines for FISH-quant analysis. 3D gaussian fitting of the single spots generates a text file containing the x,y position, brightness, and number of spots identified in each cell. In our experiments, the counting of *MDNI* mRNA molecules per cell detected with MCP-2xyeGFP revealed a mean \pm S.D. = 10.8 ± 6.1 mRNAs/cell. Counting the *MDNI* mRNAs per cell by smFISH gave similar results, i.e., a mean \pm S.D. = 9.5 ± 4.4 mRNAs/cell (Fig. 1h). These results show that live imaging faithfully reports on *MDNI* mRNA expression.

3.2 Visualizing MS2-Labeled RNAs in Mammalian Cells, with a Focus on Analyzing Transcription Dynamics

3.2.1 Lentiviral Production of MCP-GFP

1. Seed HEK-293T cells at 4×10^6 cells in 100 mm tissue culture plate and incubate cells for 24 h.
2. Change HEK-293T cells into 5 mL of fresh medium without antibiotics.
3. Transfect HEK-293T cells with JetPRIME (Polyplus transfection; according to the supplier's recommendations) by preparing a mix of 10 μ g DNA total with 8 μ g of pHAGE-Ubc-NLS-MCP-GFP, 0.4 μ g of pHDM-Hgpm2, 0.4 μ g of pHDM-tat1b, 0.4 μ g of pRC-CMV-rev1b, 0.8 μ g of pHDM-G, and 500 μ L jetPRIME buffer.
4. Mix by vortexing, add 20 μ L of JetPRIME, vortex for 5 s, spin down briefly, and incubate for 10 min at room temperature.
5. Add the transfection mix dropwise onto the HEK-293T cells. Gently rock the plate back and forth and incubate at 37 °C for 24 h (*see Note 13*).
6. Harvest medium containing lentivirus, filter it through a 0.45 μ m filter into a sterile falcon tube, and keep it at 4 °C.
7. Add 5 mL of fresh medium without antibiotics to the packaging cells and incubate at 37 °C for 24 h for a new round of lentivirus production.
8. Repeat **steps 6** and **7** once. After the harvest of virus, discard the HEK-293T cells with 10% bleach.
9. Pool the viral harvests of this and the previous days.
10. To concentrate lentiviral stocks, add Lenti-X Concentrator (Clontech) to viral harvest and incubate at 4 °C for 30 min to overnight.
11. Centrifuge the mixture at low speed (1500 $\times g$ for 45 min at 4 °C) and discard the supernatant.
12. Resuspend the pellet in DMEM and aliquot for titration and single-use aliquots. Store at -80 °C (*see Note 14*).

3.2.2 *Generating Stable Cell Lines Expressing MCP-GFP in MS2x64 RNA Reporter Cell Line*

1. Seed MS2x64 RNA reporter cells (*see Note 4*) to a low density (5000 cells per well) in a 12-well plate.
2. Thaw a lentiviral single-use aliquot at 37 °C, prepare a range of virus dilutions (e.g., 1:10; 1:50; 1:100) in DMEM (the volume of 300 µL is enough to cover a 12 well-plate dish) without serum and 6 µg/mL of polybrene (*see Note 15*), and mix well.
3. Remove the medium from cells, rinse once with DMEM, remove and add the virus dilution, and incubate at 37 °C. Tilt the vessel back and forth to mix the virus every 20 min. After 2 h, add 1 mL of fresh medium with serum and allow cells to recover overnight.
4. Change medium the next day and treat all culture supernatant as hazardous waste for several days afterward (5 days). Expand and passage cells as normal for a week.

3.2.3 *Screening Polyclonal Population Expressing MCP-GFP*

1. Grow a fraction of the cells on 22 × 22 mm coverslips in a 6-well plate dish.
2. Wash briefly in 1 × PBS and fix the cells with PFA 4% in PBS for 20 min at room temperature.
3. Wash briefly in 1 × PBS, add 20 µL of Vectashield mounting medium on glass microscopy slides, and mount the coverslips upside down.
4. Using an epifluorescence microscope, select the pool of cells based on GFP expression (*see Note 16*).

3.2.4 *Growing Cells for Live Imaging*

1. Split the cells to 50% confluence 1 day before imaging on a 25 mm diameter coverslips or a glass-bottomed tissue culture plates (based on the microscope used).
2. Set up the incubator chamber of the microscope at 37 °C and 5% CO₂ 1 h before starting your experiment to avoid thermal fluctuation leading to optical instability and cellular stress.
3. Set up the coverslips on the microscopic chamber and 30 min before starting imaging replace the media with live-cell imaging medium supplemented with 10% FBS and P/S.

3.2.5 *Live Image Acquisition*

1. Determine experimental parameters for live-cell imaging. To minimize photobleaching, the light intensity and the exposure time need to be set to the lowest values allowing visualization of single pre-mRNA molecules in the nucleus. These parameters are dependent on the microscope used (*see Note 6*) and the light source and should be strictly determined when starting imaging (*see Note 17*). This should be done at the beginning of each experiment.
2. For each cell, determine the correct focal plane, as well as the boundaries of the Z-stacks (*see Note 18*). For transcriptional studies, two types of movies can be recorded: short movies (fast

acquisition) where one Z-stack is recorded every 3 s for 30 min and long movies where one Z-stack is recorded every 3 min for >8 h (*see Note 19*).

- Analyze the time-lapse movies of transcription sites with dedicated software tools that are available upon request (MS2-quant, RampFinder, RampFitter, ON-quant, *see ref. 60*) (*see Note 20*).

4 Notes

- Yeast microscopy experiments were performed on a home-built microscope built around an IX71 stand (Olympus). For excitation, a 491 nm laser (CalypsoTM, Cobolt) and a 561 nm laser (JiveTM, Cobolt) were combined and controlled by an acoustic-optic tunable filter (AOTF, AOTFnC-400.650-TN, AA Opto-electronic) before being coupled into a single-mode optical fiber (Qioptiq). The output of the fiber was collimated and delivered through the back port of the microscope and reflected into an Olympus 150x 1.45 N.A. oil immersion objective lens with a dichroic mirror (zt405/488/561rpc, 2 mm substrate, Chroma). The tube lens (180 mm focal length) was removed from the microscope and placed outside of the right port. A triple-band notch emission filter (zet405/488/561 nm) was used to filter the scattered laser light. A dichroic mirror (T560LPXR, 3 mm substrate, Chroma) was used to split the fluorescence onto two precisely aligned EMCCDs (Andor iXon, Model DU-897 U-CS0, pixel size 16 μm) mounted on alignment stages (x , y , z , θ -, and φ -angle). Emission filters FF03-525/50-25 and FF01-607/70-25 (Semrock) were placed in front of green and red channel cameras, respectively. The two cameras were triggered for exposure with a TTL pulse generated on a DAQ board (Measurement Computing). The microscope was equipped with a piezo stage (ASI) for fast z-stack and a Delta-T incubation system (Biotech) for live-cell imaging. The microscope (AOTF, DAQ, stage, and cameras) was automated with the software MetaMorph (Molecular Devices).
- XLI-blue competent cells are bacteria of choice for transformation of plasmid containing MS2 repeats. Note that the bacteria can be grown at 30 °C if the plasmid is unstable.
- Other Flp-in mammalian cell lines can be used.
- A stable Flag-Tat-expressing cell line was created by CRISPR genome editing using an AAVS1 repair vector [60] in HeLa Flp-in H9 cell line (available upon request). Individual clones were picked and analyzed by immunofluorescence with an anti-

Flag antibody. One clone was further characterized and used for the following experiments. Isogenic stable cell lines expressing the HIV-1 MS2x64 reporter gene were created using the Flp-in system in a HeLa H9 AAVS1-Tat cell line [60]. Flp-in integrants were selected on hygromycin (150 µg/mL). The MS2 tag is located in the intron of the reporter and thus labels only the pre-mRNA. Note that splicing of this reporter occurs post-transcriptionally and is not disturbed by the MS2 repeat [60]. We found that this setup was the most appropriate to visualize transcription because it allows the use of large tags without compromising the mRNA fate. Individual clones were picked and analyzed by *in situ* hybridization. One clone was further characterized and used for the following experiments.

5. A ZEISS Axioimager Z1 wide-field microscope equipped with a Plan Apochromat 63× objective, N.A. 1.4 oil-immersion objective (ZEISS), was used with a ZEISS VSG HBO 100/001.26E illuminating System, and Zyla 4.2 sCMOS Camera (2048 × 2048 pixels; 6.5 µm pixel size, from Andor). We acquire data using 21 optical sections with a z-step size of 0.3 µm. MetaMorph (Molecular Devices) software is used for instrument control as well as image acquisition.
6. An inverted OMX Deltavision microscope in time-lapse mode with temperature-controlled chamber with CO₂, together with a x100, N.A. 1.4 objective and EMCCD cameras Evolve 512 × 512, was used for live-cell imaging. Spinning disk confocal or HiLo microscopes equipped with 60× or 100× objectives with a N.A. >1.3 are also suitable.
7. To maximize the brightness of the tagged mRNAs, we recommend tagging the mRNA of interest with 24xMBSV6. However, as we discussed in previous publications [43, 58], for mRNAs that are strongly expressed and that have a short half-life (i.e., GAL1 mRNA), tagging with 24 stem-loops can be suboptimal. This is because when many mRNAs have to be rapidly degraded, the presence of 24 MS2 loops, even if they are low-affinity variant, can cause a delay in the degradation of the MS2 array. In this case the mRNAs can be tagged with 12xMBSV6. We recommend always testing whether the insertion of the MS2 loops affects the stability, the localization, and the expression of the mRNA of interest by comparing the tagged mRNA (with or without the expression of MCP) to the untagged mRNA by smFISH [43, 58].
8. Transformed cells can be frozen at this stage. Glycerol stocks can be prepared by mixing 1 mL of exponentially growing culture with 1 mL of 60% glycerol in YPD. Mix thoroughly and freeze in cryo-tubes at −80 °C. We did not notice a reduction in live imaging quality if the cells are thawed instead of using fresh transformations.

9. Background strains that are ADE2+, thus not producing the red pigment accumulating in mutant cells, show reduced cellular background during live imaging.
10. For short-term imaging, not requiring strict temperature control, other types of glass-bottom dishes can be used, i.e., MatTek.
11. High-quality and reproducible imaging is achieved only if the cells are imaged while growing exponentially.
12. The parameters for imaging single mRNAs in living cells (laser power, exposure time) can be modified to increase the fluorescence intensity of single mRNAs. Choose parameters that will keep the fluorescence intensity signal in the dynamic range of the camera while minimizing photo-bleaching of the sample.
13. At this point active lentivirus is being produced. Strict adherence to biosafety class II is necessary. All materials in contact with virus-containing liquid must be bleached prior to disposal.
14. Viruses may be stored at 4 °C for short periods (hours to days). For long-term storage, aliquots should be frozen at –80 °C.
15. Polybrene increases the efficiency of retrovirus-mediated gene transfer; the conditions should be optimized for each cell type.
16. Expression levels of the MCP-FP transgene should show a strong spot for the transcription site, smaller dots throughout the nucleus (single-molecule mRNA), and a low nuclear background of free unbound MCP-FP. If needed, the best pool can be re-sorted by FACS to obtain a more homogenous population. Positive cells can be FACS-sorted upon a single-cell clonal dilution to isolate pure clones. Select the most suitable sub-cloned cells that display the optimal signal-to-noise ratio for the live-cell imaging acquisition.
17. We recommend a stable integration of the MCP-GFP with viral infection followed by sorting a pool of low-expressing MCP-FP cells. This gives much better results than a crude transient transfection. Optimization of the MCP-GFP expression further improves the signal-to-noise ratio of single-molecule detection and enhances the quality of the data recorded.
18. We recommend stacks of 11 planes with a Z-spacing of 0.6 μm. This size allows accurate quantification of single mRNA molecules when using 100×, N.A. 1.4 objectives.
19. These short and long movies are important if one wants to capture the entire promoter dynamics (*see ref. 60*), and they are required since at high temporal resolution, bleaching limits the acquisitions to about 30 min.

20. After being processed, each movie should be checked to ensure that no drift or loss of focus happened during the acquisition (especially for long-term movies).

Acknowledgments

This work was supported by NIH Grant GM57071 to R.H.S., and by an ANRS Grant to E.B. E.T. was supported by Swiss National Science Foundation Fellowships P2GEP3_155692 and P300PA_164717. X.P. was supported by a fellowship from the Labex EpiGenMed Montpellier/Université de Montpellier, and E.B. had a travel grant from the Philippe Foundation.

Contributions: X.P. performed the experiments and wrote the protocol for mammalian cells. M.C.R. performed the experiments testing different FP in yeast. E.T. performed experiments and designed the protocol for yeast. E.T. wrote the manuscript with inputs from E.B. and R.H.S.

References

1. Tutucci E, Livingston NM, Singer RH, Wu B (2018) Imaging mRNA in vivo, from birth to death. *Annu Rev Biophys* 47:85–106. <https://doi.org/10.1146/annurev-biophys-070317-033037>
2. Vera M, Biswas J, Senecal A, Singer RH, Park HY (2016) Single-cell and single-molecule analysis of gene expression regulation. *Annu Rev Genet* 50:267–291. <https://doi.org/10.1146/annurev-genet-120215-034854>
3. Raj A, van Oudenaarden A (2008) Nature, nurture, or chance: stochastic gene expression and its consequences. *Cell* 135(2):216–226. <https://doi.org/10.1016/j.cell.2008.09.050>
4. Liu Y, Beyer A, Aebersold R (2016) On the dependency of cellular protein levels on mRNA abundance. *Cell* 165(3):535–550. <https://doi.org/10.1016/j.cell.2016.03.014>
5. Femino AM, Fay FS, Fogarty K, Singer RH (1998) Visualization of single RNA transcripts in situ. *Science* 280(5363):585–590
6. Femino AM, Fogarty K, Lifshitz LM, Carrington W, Singer RH (2003) Visualization of single molecules of mRNA in situ. *Methods Enzymol* 361:245–304
7. Gandhi SJ, Zenklusen D, Lionnet T, Singer RH (2011) Transcription of functionally related constitutive genes is not coordinated. *Nat Struct Mol Biol* 18(1):27–34. <https://doi.org/10.1038/nsmb.1934>
8. Zenklusen D, Larson DR, Singer RH (2008) Single-RNA counting reveals alternative modes of gene expression in yeast. *Nat Struct Mol Biol* 15(12):1263–1271. <https://doi.org/10.1038/nsmb.1514>
9. Senecal A, Munsky B, Proux F, Ly N, Braye FE, Zimmer C, Mueller F, Darzacq X (2014) Transcription factors modulate c-Fos transcriptional bursts. *Cell Rep* 8(1):75–83. <https://doi.org/10.1016/j.celrep.2014.05.053>
10. Raj A, van den Bogaard P, Rifkin SA, van Oudenaarden A, Tyagi S (2008) Imaging individual mRNA molecules using multiple singly labeled probes. *Nat Methods* 5(10):877–879. <https://doi.org/10.1038/nmeth.1253>
11. Yang L, Titlow J, Ennis D, Smith C, Mitchell J, Young FL, Waddell S, Ish-Horowicz D, Davis I (2017) Single molecule fluorescence in situ hybridisation for quantitating post-transcriptional regulation in Drosophila brains. *Methods* 126:166–176. <https://doi.org/10.1016/j.ymeth.2017.06.025>
12. Buxbaum AR, Wu B, Singer RH (2014) Single beta-actin mRNA detection in neurons reveals a mechanism for regulating its translatability. *Science* 343:419–422. <https://doi.org/10.1126/science.1242939>
13. Duncan S, Olsson TSG, Hartley M, Dean C, Rosa S (2016) A method for detecting single mRNA molecules in *Arabidopsis thaliana*. *Plant Methods* 12:13. <https://doi.org/10.1186/s13007-016-0114-x>

14. Moor AE, Golan M, Massasa EE, Lemze D, Weizman T, Shenhav R, Baydatch S, Mizrahi O, Winkler R, Golani O, Stern-Ginossar N, Itzkovitz S (2017) Global mRNA polarization regulates translation efficiency in the intestinal epithelium. *Science* 357:1299–1303. <https://doi.org/10.1126/science.aan2399>
15. Moffitt JR, Hao J, Bambach-Mukku D, Lu T, Dulac C, Zhuang X (2016) High-performance multiplexed fluorescence in situ hybridization in culture and tissue with matrix imprinting and clearing. *Proc Natl Acad Sci U S A* 113(50):14456–14461. <https://doi.org/10.1073/pnas.1617699113>
16. Long X, Colonell J, Wong AM, Singer RH, Lionnet T (2017) Quantitative mRNA imaging throughout the entire *Drosophila* brain. *Nat Methods* 14(7):703–706. <https://doi.org/10.1038/nmeth.4309>
17. Battich N, Stoeger T, Pelkmans L (2013) Image-based transcriptomics in thousands of single human cells at single-molecule resolution. *Nat Methods* 10(11):1127–1133. <https://doi.org/10.1038/nmeth.2657>
18. Choi HM, Chang JY, Trinh le A, Padilla JE, Fraser SE, Pierce NA (2010) Programmable in situ amplification for multiplexed imaging of mRNA expression. *Nat Biotechnol* 28(11):1208–1212. <https://doi.org/10.1038/nbt.1692>
19. Tsanov N, Samacoits A, Chouaib R, Traboulsi AM, Gostan T, Weber C, Zimmer C, Zibara K, Walter T, Peter M, Bertrand E, Mueller F (2016) smiFISH and FISH-quant - a flexible single RNA detection approach with super-resolution capability. *Nucleic Acids Res* 44(22):e165. <https://doi.org/10.1093/nar/gkw784>
20. Moffitt JR, Hao J, Wang G, Chen KH, Babcock HP, Zhuang X (2016) High-throughput single-cell gene-expression profiling with multiplexed error-robust fluorescence in situ hybridization. *Proc Natl Acad Sci U S A* 113(39):11046–11051. <https://doi.org/10.1073/pnas.1612826113>
21. Lubeck E, Coskun AF, Zhiyentayev T, Ahmad M, Cai L (2014) Single-cell in situ RNA profiling by sequential hybridization. *Nat Methods* 11(4):360–361. <https://doi.org/10.1038/nmeth.2892>
22. Shah S, Lubeck E, Zhou W, Cai L (2017) seqFISH accurately detects transcripts in single cells and reveals robust spatial organization in the hippocampus. *Neuron* 94(4):752–758. <https://doi.org/10.1016/j.neuron.2017.05.008>
23. Eng CL, Lawson M, Zhu Q, Dries R, Koulena N, Takei Y, Yun J, Cronin C, Karp C, Yuan GC, Cai L (2019) Transcriptome-scale super-resolved imaging in tissues by RNA seqFISH. *Nature* 568:235–239. <https://doi.org/10.1038/s41586-019-1049-y>
24. Shah S, Takei Y, Zhou W, Lubeck E, Yun J, Eng CL, Koulena N, Cronin C, Karp C, Liaw EJ, Amin M, Cai L (2018) Dynamics and spatial genomics of the nascent transcriptome by intron seqFISH. *Cell* 174(2):363–376. <https://doi.org/10.1016/j.cell.2018.05.035>
25. Bayer LV, Batish M, Formel SK, Bratu DP (2015) Single-molecule RNA in situ hybridization (smFISH) and immunofluorescence (IF) in the *Drosophila* egg chamber. *Methods Mol Biol* 1328:125–136. https://doi.org/10.1007/978-1-4939-2851-4_9
26. Elisavich C, Shenoy SM, Singer RH (2017) Imaging mRNA and protein interactions within neurons. *Proc Natl Acad Sci U S A* 114(10):E1875–E1884. <https://doi.org/10.1073/pnas.1621440114>
27. Buxbaum AR, Haimovich G, Singer RH (2015) In the right place at the right time: visualizing and understanding mRNA localization. *Nat Rev Mol Cell Biol* 16(2):95–109. <https://doi.org/10.1038/nrm3918>
28. Weil TT, Parton RM, Davis I (2010) Making the message clear: visualizing mRNA localization. *Trends Cell Biol* 20(7):380–390. <https://doi.org/10.1016/j.tcb.2010.03.006>
29. Martin KC, Ephrussi A (2009) mRNA localization: gene expression in the spatial dimension. *Cell* 136(4):719–730. <https://doi.org/10.1016/j.cell.2009.01.044>
30. Lecuyer E, Yoshida H, Parthasarathy N, Alm C, Babak T, Cerovina T, Hughes TR, Tomancak P, Krause HM (2007) Global analysis of mRNA localization reveals a prominent role in organizing cellular architecture and function. *Cell* 131(1):174–187. <https://doi.org/10.1016/j.cell.2007.08.003>
31. Samacoits A, Chouaib R, Safeddine A, Traboulsi AM, Ouyang W, Zimmer C, Peter M, Bertrand E, Walter T, Mueller F (2018) A computational framework to study sub-cellular RNA localization. *Nat Commun* 9(1):4584. <https://doi.org/10.1038/s41467-018-06868-w>
32. Das S, Singer RH, Yoon YJ (2019) The travels of mRNAs in neurons: do they know where they are going? *Curr Opin Neurobiol* 57:110–116. <https://doi.org/10.1016/j.conb.2019.01.016>

33. Bahar Halpern K, Tanami S, Landen S, Chapal M, Szlak L, Hutzler A, Nizhberg A, Itzkovitz S (2015) Bursty gene expression in the intact mammalian liver. *Mol Cell* 58 (1):147–156. <https://doi.org/10.1016/j.molcel.2015.01.027>
34. Raj A, Peskin CS, Tranchina D, Vargas DY, Tyagi S (2006) Stochastic mRNA synthesis in mammalian cells. *PLoS Biol* 4(10):e309. <https://doi.org/10.1371/journal.pbio.0040309>
35. Paul B, Montpetit B (2016) Altered RNA processing and export lead to retention of mRNAs near transcription sites and nuclear pore complexes or within the nucleolus. *Mol Biol Cell* 27(17):2742–2756. <https://doi.org/10.1091/mbc.E16-04-0244>
36. Bahar Halpern K, Caspi I, Lemze D, Levy M, Landen S, Elinav E, Ulitsky I, Itzkovitz S (2015) Nuclear retention of mRNA in mammalian tissues. *Cell Rep* 13(12):2653–2662. <https://doi.org/10.1016/j.celrep.2015.11.036>
37. Trcek T, Larson DR, Moldon A, Query CC, Singer RH (2011) Single-molecule mRNA decay measurements reveal promoter-regulated mRNA stability in yeast. *Cell* 147 (7):1484–1497. <https://doi.org/10.1016/j.cell.2011.11.051>
38. Trcek T, Sato H, Singer RH, Maquat LE (2013) Temporal and spatial characterization of nonsense-mediated mRNA decay. *Genes Dev* 27(5):541–551. <https://doi.org/10.1101/gad.209635.112>
39. Pichon X, Lagha M, Mueller F, Bertrand E (2018) A growing toolbox to image gene expression in single cells: sensitive approaches for demanding challenges. *Mol Cell* 71 (3):468–480. <https://doi.org/10.1016/j.molcel.2018.07.022>
40. Bertrand E, Chartrand P, Schaefer M, Shenoy SM, Singer RH, Long RM (1998) Localization of ASH1 mRNA particles in living yeast. *Mol Cell* 2(4):437–445
41. Peabody DS (1993) The RNA binding site of bacteriophage MS2 coat protein. *EMBO J* 12 (2):595–600
42. Fusco D, Bertrand E, Singer RH (2004) Imaging of single mRNAs in the cytoplasm of living cells. *Prog Mol Subcell Biol* 35:135–150
43. Tutucci E, Vera M, Singer RH (2018) Single-mRNA detection in living *S. cerevisiae* using a re-engineered MS2 system. *Nat Protoc* 13 (10):2268–2296. <https://doi.org/10.1038/s41596-018-0037-2>
44. Brody Y, Neufeld N, Bieberstein N, Causse SZ, Bohnlein EM, Neugebauer KM, Darzacq X, Shav-Tal Y (2011) The in vivo kinetics of RNA polymerase II elongation during co-transcriptional splicing. *PLoS Biol* 9(1): e1000573. <https://doi.org/10.1371/journal.pbio.1000573>
45. Darzacq X, Shav-Tal Y, de Turrís V, Brody Y, Shenoy SM, Phair RD, Singer RH (2007) In vivo dynamics of RNA polymerase II transcription. *Nat Struct Mol Biol* 14(9):796–806. <https://doi.org/10.1038/nsmb1280>
46. Schmidt U, Basyuk E, Robert MC, Yoshida M, Villemin JP, Auboeuf D, Aitken S, Bertrand E (2011) Real-time imaging of cotranscriptional splicing reveals a kinetic model that reduces noise: implications for alternative splicing regulation. *J. Cell Biol* 193(5):819–829. <https://doi.org/10.1083/jcb.201009012>
47. Grunwald D, Singer RH (2010) In vivo imaging of labelled endogenous beta-actin mRNA during nucleocytoplasmic transport. *Nature* 467(7315):604–607. <https://doi.org/10.1038/nature09438>
48. Smith C, Lari A, Derrer CP, Ouwehand A, Rossouw A, Huisman M, Dange T, Hopman M, Joseph A, Zenklusen D, Weis K, Grunwald D, Montpetit B (2015) In vivo single-particle imaging of nuclear mRNA export in budding yeast demonstrates an essential role for Mex67p. *J Cell Biol* 211 (6):1121–1130. <https://doi.org/10.1083/jcb.201503135>
49. Lionnet T, Czaplinski K, Darzacq X, Shav-Tal Y, Wells AL, Chao JA, Park HY, de Turrís V, Lopez-Jones M, Singer RH (2011) A transgenic mouse for in vivo detection of endogenous labeled mRNA. *Nat Methods* 8 (2):165–170. <https://doi.org/10.1038/nmeth.1551>
50. Park HY, Lim H, Yoon YJ, Follenzi A, Nwokafor C, Lopez-Jones M, Meng X, Singer RH (2014) Visualization of dynamics of single endogenous mRNA labeled in live mouse. *Science* 343(6169):422–424. <https://doi.org/10.1126/science.1239200>
51. Halstead JM, Lionnet T, Wilbertz JH, Wippich F, Ephrussi A, Singer RH, Chao JA (2015) Translation. An RNA biosensor for imaging the first round of translation from single cells to living animals. *Science* 347 (6228):1367–1671. <https://doi.org/10.1126/science.aaa3380>
52. Katz ZB, English BP, Lionnet T, Yoon YJ, Monnier N, Ovrin B, Bathe M, Singer RH (2016) Mapping translation ‘hot-spots’ in live cells by tracking single molecules of mRNA and ribosomes. *elife* 5:e10415
53. Morisaki T, Lyon K, DeLuca KF, DeLuca JG, English BP, Zhang Z, Lavis LD, Grimm JB, Viswanathan S, Looger LL, Lionnet T, Stasevich TJ (2016) Real-time quantification of

- single RNA translation dynamics in living cells. *Science* 352(6292):1425–1429. <https://doi.org/10.1126/science.aaf0899>
54. Pichon X, Bastide A, Safieddine A, Chouaib R, Samacoits A, Basyuk E, Peter M, Mueller F, Bertrand E (2016) Visualization of single endogenous polysomes reveals the dynamics of translation in live human cells. *J Cell Biol* 214(6):769–781. <https://doi.org/10.1083/jcb.201605024>
 55. Wu B, Elisavich C, Yoon YJ, Singer RH (2016) Translation dynamics of single mRNAs in live cells and neurons. *Science* 352(6292):1430–1435. <https://doi.org/10.1126/science.aaf1084>
 56. Garcia JF, Parker R (2015) MS2 coat proteins bound to yeast mRNAs block 5' to 3' degradation and trap mRNA decay products: implications for the localization of mRNAs by MS2-MCP system. *RNA* 21(8):1393–1395. <https://doi.org/10.1261/rna.051797.115>
 57. Haimovich G, Zabezhinsky D, Haas B, Slobodin B, Purushothaman P, Fan L, Levin JZ, Nusbaum C, Gerst JE (2016) Use of the MS2 aptamer and coat protein for RNA localization in yeast: A response to “MS2 coat proteins bound to yeast mRNAs block 5' to 3' degradation and trap mRNA decay products: implications for the localization of mRNAs by MS2-MCP system”. *RNA* 22(5):660–666. <https://doi.org/10.1261/rna.055095.115>
 58. Tutucci E, Vera M, Biswas J, Garcia J, Parker R, Singer RH (2018) An improved MS2 system for accurate reporting of the mRNA life cycle. *Nat Methods* 15(1):81–89. <https://doi.org/10.1038/nmeth.4502>
 59. Heinrich S, Sidler CL, Azzalin CM, Weis K (2017) Stem-loop RNA labeling can affect nuclear and cytoplasmic mRNA processing. *RNA* 23(2):134–141. <https://doi.org/10.1261/rna.057786.116>
 60. Tantale K, Mueller F, Kozulic-Pirher A, Lesne A, Victor JM, Robert MC, Capozzi S, Chouaib R, Backer V, Mateos-Langerak J, Darzacq X, Zimmer C, Basyuk E, Bertrand E (2016) A single-molecule view of transcription reveals convoying of RNA polymerases and multi-scale bursting. *Nat Commun* 7:12248. <https://doi.org/10.1038/ncomms12248>
 61. Chao JA, Patskovsky Y, Almo SC, Singer RH (2008) Structural basis for the coevolution of a viral RNA-protein complex. *Nat Struct Mol Biol* 15(1):103–105. <https://doi.org/10.1038/nsmb1327>
 62. Larson DR, Zenklusen D, Wu B, Chao JA, Singer RH (2011) Real-time observation of transcription initiation and elongation on an endogenous yeast gene. *Science* 332(6028):475–478. <https://doi.org/10.1126/science.1202142>
 63. Saroufim MA, Bensidoun P, Raymond P, Rahman S, Krause MR, Oeffinger M, Zenklusen D (2015) The nuclear basket mediates perinuclear mRNA scanning in budding yeast. *J Cell Biol* 211(6):1131–1140. <https://doi.org/10.1083/jcb.201503070>
 64. Wang C, Han B, Zhou R, Zhuang X (2016) Real-time imaging of translation on single mrna transcripts in live cells. *Cell* 165(4):990–1001. <https://doi.org/10.1016/j.cell.2016.04.040>
 65. Yan X, Hoek TA, Vale RD, Tanenbaum ME (2016) Dynamics of translation of single mRNA molecules In vivo. *Cell* 165(4):976–989. <https://doi.org/10.1016/j.cell.2016.04.034>
 66. Das S, Moon HC, Singer RH, Park HY (2018) A transgenic mouse for imaging activity-dependent dynamics of endogenous Arc mRNA in live neurons. *Sci Adv* 4(6):eaar3448. <https://doi.org/10.1126/sciadv.aar3448>
 67. Chen J, Nikolaitchik O, Singh J, Wright A, Bencsics CE, Coffin JM, Ni N, Lockett S, Pathak VK, Hu WS (2009) High efficiency of HIV-1 genomic RNA packaging and heterozygote formation revealed by single virion analysis. *Proc Natl Acad Sci U S A* 106(32):13535–13540. <https://doi.org/10.1073/pnas.0906822106>
 68. Lange S, Katayama Y, Schmid M, Burkacky O, Brauchle C, Lamb DC, Jansen RP (2008) Simultaneous transport of different localized mRNA species revealed by live-cell imaging. *Traffic* 9(8):1256–1267. <https://doi.org/10.1111/j.1600-0854.2008.00763.x>
 69. Brodsky AS, Silver PA (2002) Identifying proteins that affect mRNA localization in living cells. *Methods* 26(2):151–155. [https://doi.org/10.1016/S1046-2023\(02\)00017-8](https://doi.org/10.1016/S1046-2023(02)00017-8)
 70. Takizawa PA, Vale RD (2000) The myosin motor, Myo4p, binds Ash1 mRNA via the adapter protein, She3p. *Proc Natl Acad Sci U S A* 97(10):5273–5278. <https://doi.org/10.1073/pnas.080585897>
 71. Rodriguez EA, Campbell RE, Lin JY, Lin MZ, Miyawaki A, Palmer AE, Shu X, Zhang J, Tsien RY (2017) The growing and glowing toolbox of fluorescent and photoactive proteins. *Trends Biochem Sci* 42(2):111–129. <https://doi.org/10.1016/j.tibs.2016.09.010>
 72. Specht EA, Braselmann E, Palmer AE (2017) A critical and comparative review of fluorescent tools for live-cell imaging. *Annu Rev Physiol*

- 79:93–117. <https://doi.org/10.1146/annurev-physiol-022516-034055>
73. Cranfill PJ, Sell BR, Baird MA, Allen JR, Lavagnino Z, de Gruiter HM, Kremers GJ, Davidson MW, Ustione A, Piston DW (2016) Quantitative assessment of fluorescent proteins. *Nat Methods* 13(7):557–562. <https://doi.org/10.1038/nmeth.3891>
 74. Scott DJ, Gunn NJ, Yong KJ, Wimmer VC, Veldhuis NA, Challis LM, Haidar M, Petrou S, Bathgate RAD, Griffin MDW (2018) A novel ultra-stable, monomeric green fluorescent protein for direct volumetric imaging of whole organs using CLARITY. *Sci Rep* 8(1):667. <https://doi.org/10.1038/s41598-017-18045-y>
 75. Feng S, Sekine S, Pessino V, Li H, Leonetti MD, Huang B (2017) Improved split fluorescent proteins for endogenous protein labeling. *Nat Commun* 8(1):370. <https://doi.org/10.1038/s41467-017-00494-8>
 76. Slubowski CJ, Funk AD, Roesner JM, Paulissen SM, Huang LS (2015) Plasmids for C-terminal tagging in *Saccharomyces cerevisiae* that contain improved GFP proteins, Envy and Ivy. *Yeast* 32(4):379–387. <https://doi.org/10.1002/yea.3065>
 77. Lim F, Peabody DS (1994) Mutations that increase the affinity of a translational repressor for RNA. *Nucleic Acids Res* 22(18):3748–3752
 78. Cormack BP, Valdivia RH, Falkow S (1996) FACS-optimized mutants of the green fluorescent protein (GFP). *Gene* 173:33–38
 79. Zacharias DA, Violin JD, Newton AC, Tsien RY (2002) Partitioning of lipid-modified monomeric GFPs into membrane microdomains of live cells. *Science* 296(5569):913–916. <https://doi.org/10.1126/science.1068539>
 80. Pedelacq JD, Cabantous S, Tran T, Terwilliger TC, Waldo GS (2006) Engineering and characterization of a superfolder green fluorescent protein. *Nat Biotechnol* 24(1):79–88. <https://doi.org/10.1038/nbt1172>
 81. Shaner NC, Lambert GG, Chammas A, Ni Y, Cranfill PJ, Baird MA, Sell BR, Allen JR, Day RN, Israelsson M, Davidson MW, Wang J (2013) A bright monomeric green fluorescent protein derived from *Branchiostoma lanceolatum*. *Nat Methods* 10(5):407–409. <https://doi.org/10.1038/nmeth.2413>
 82. Mueller F, Senecal A, Tantale K, Marie-Nelly H, Ly N, Collin O, Basyuk E, Bertrand E, Darzacq X, Zimmer C (2013) FISH-quant: automatic counting of transcripts in 3D FISH images. *Nat Methods* 10(4):277–278. <https://doi.org/10.1038/nmeth.2406>
 83. Carpenter AE, Jones TR, Lamprecht MR, Clarke C, Kang IH, Friman O, Guertin DA, Chang JH, Lindquist RA, Moffat J, Golland P, Sabatini DM (2006) CellProfiler: image analysis software for identifying and quantifying cell phenotypes. *Genome Biol* 7(10):R100. <https://doi.org/10.1186/gb-2006-7-10-r100>



In Vivo Imaging of Mobile mRNAs in Plants Using MS2

Kai-Ren Luo, Nien-Chen Huang, and Tien-Shin Yu

Abstract

Multicellular organisms rely on systemic signals to orchestrate diverse developmental and physiological programs. To transmit environmental stimuli that perceived in the leaves, plants recruit many mobile molecules including mobile mRNAs as systemic signals for interorgan communication. The mobile mRNAs provide an efficient and specific remote control system for plants to cope with environmental dynamics. Upon being transcribed in local tissues, mobile mRNAs are selectively targeted to plasmodesmata for cell-to-cell and long-distance translocation. The mRNA labeling system based on the RNA-binding protein MS2 provides a useful tool to investigate intracellular trafficking of mobile mRNAs in plants. Here we describe the detailed protocol to visualize intracellular trafficking of plant mobile mRNAs by using the MS2 live-cell imaging system.

Key words MS2, Nucleus localization signal, Live-cell imaging, Mobile mRNA, Intracellular trafficking

1 Introduction

The discovery that mRNA can function non-cell-autonomously has launched a new era in investigating plant systemic signaling [1, 2]. These mobile mRNAs are transcribed in local tissues and delivered cell to cell and long distance to distal organs to regulate many developmental processes [3–8]. Evidence has suggested that many mobile mRNAs use phloem as a conduit for long-distance transport [5, 9, 10]. Extensive analysis of mRNA population in phloem exudates and interspecies grafting indicated that mobile mRNAs are widely spread among plant species [11–13]. The pivotal roles of mobile mRNAs in regulating plant development imply the presence of delicate mechanisms to fine-tune the mobility of these signaling transcripts [1]. Although computational model suggests that the movement of mobile mRNAs is determined by

Electronic supplementary material: The online version of this chapter (https://doi.org/10.1007/978-1-0716-0712-1_8) contains supplementary material, which is available to authorized users.

transcript abundance [14], grafting experiments show that mRNA mobility is independent of the abundance of transcripts [5, 15]. Further studies show that in many phloem mobile mRNAs, the t-RNA-like motifs are necessary and sufficient to mediate RNA movement [16]. Thus, it is possible that the movement of mobile mRNA is controlled by a yet-to-be-elucidated regulatory mechanism. The use of a mRNA live-imaging system provides an ideal approach to reveal underlying regulatory elements.

One of the most frequently used approaches for genetics-based mRNA live-cell imaging involves the use of the MS2 system [17]. In this system, the coat protein of bacteriophage MS2, which is an RNA-binding protein that specifically recognizes a stem-loop (SL) structure in the bacteriophage RNA, is fused with GFP and nuclear localization signal (NLS) from the SV40 virus. When this MS2_{SV40}-GFP fusion protein is co-expressed with target mRNA conjugated to multiple copies of the SL structure, the binding of MS2_{SV40}-GFP to SL-bearing mRNAs reveals the location of the tagged mRNA by fluorescence. The NLS in the MS2_{SV40}-GFP fusion protein is used to restrict unbound MS2_{SV40}-GFP to the nucleus and, thus, to reduce the cytoplasmic fluorescent background. The MS2 system has been widely used to study cellular mRNA metabolism in various species, including yeast, zebrafish, fly, mammals [18–21], and plants [22–25]. As compared with the accumulated data for RNA live imaging in yeast, mammals, and other systems, the data related to the MS2 system in plants are relatively limited [26]. The development of the plant MS2 system is mainly hindered by the cytoplasmic background issue. The use of SV40_{NLS} allows a slight amount of MS2_{SV40}-GFP fusion protein to diffuse from the nucleus to cytosol [27], thereby causing substantial fluorescent background in plant cells. This drawback is significant in mature cells with extensive vacuoles and restricted cytoplasmic space, such as leaf epidermal cells, which are usually used for *in vivo* imaging.

Recently, we optimized the MS2 system for tracking mobile mRNAs *in planta* [28]. Two improvements were achieved (1) by replacement of the SV40 NLS (MS2_{SV40}) with the NLS from a plant transcription factor FD (MS2_{FD}) to diminish the cytoplasmic fluorescent background and (2) by applying a specific sampling strategy to optimize the appropriate time point for observation (i.e., examining leaf cells at the boundary of the agrobacteria-infiltrated tissue patch that are close to the non-infiltrated surrounding tissues). Upon transient co-expression of MS2_{FD}-GFP and SL-bearing target mRNAs in *Nicotiana benthamiana* cells, the target mRNA is bound by MS2_{FD}-GFP and can be detected in the cytosol by confocal microscopy. On the contrary, upon co-expression of MS2_{FD}-GFP and target mRNAs without SL structures, the GFP fluorescence is exclusively detected in the nucleus. Exceptional signal-to-noise ratio in cytosol indicates that the MS2

system is a reliable strategy to dissect spatial and temporal regulation of mobile mRNAs in real time and under subcellular resolution.

2 Materials

2.1 Molecular Cloning

- The following plasmids are available upon request (*see Note 1*):
 - pCAMBIA1390-35S-MS2_{FD}-GFP (Fig. 1).
 - pCAMBIA1390-35S-FT (Fig. 1).
 - pBS-SL24 or pBS-SL48 plasmids (Fig. 2).
- Restriction enzymes and enzyme buffer: NotI, SalI, and XbaI.
- DNA polymerase I, large (*Klenow*) fragment.
- T4 DNA ligase and T4 DNA ligase buffer.
- TE buffer: 10 mM Tris pH 8.0, 1 mM EDTA.
- LB medium: 10 g/L NaCl, 10 g/L tryptone, 5 g/L yeast extract, supplemented with 50 µg/mL kanamycin.
- LB agar plate: LB medium with 15 g/L bacto-agar, supplemented with 50 µg/mL kanamycin.
- Equipment for agarose electrophoresis.

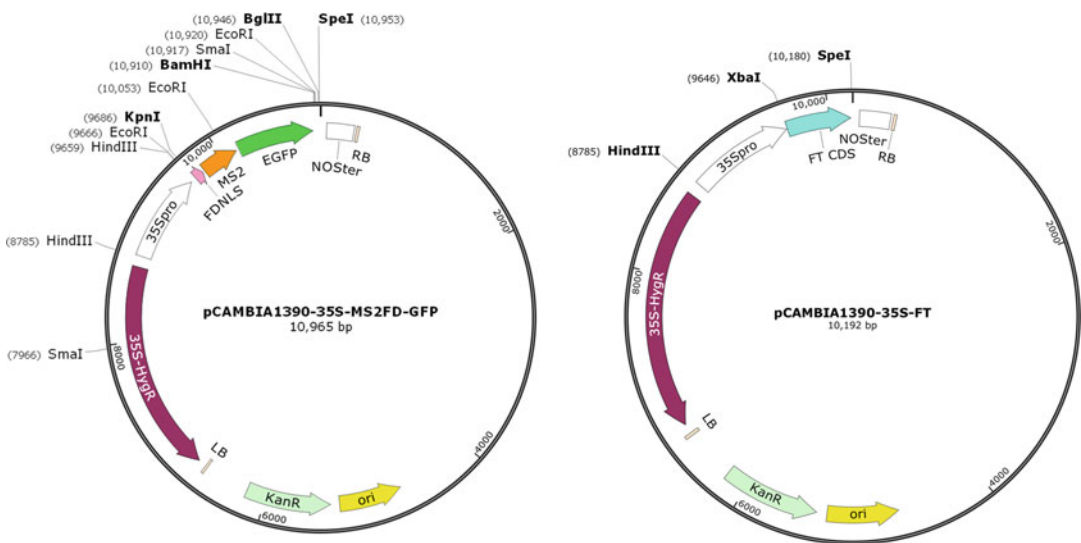


Fig. 1 Map of pCAMBIA1390-35S-MS2_{FD}-GFP and pCAMBIA1390-35S-FT. These plasmids are pCAMBIA-based binary vectors that contain MS2_{FD}-GFP or FT cDNA driven by the 35S promoter of cauliflower mosaic virus (35Spro). FDNLS, nuclear localization sequence from Arabidopsis FD; MS2, coat protein of bacteriophage MS2; EGFP: enhanced green fluorescent protein; NOSter, nopaline synthase terminator; 35S-HygR, hygromycin B phosphotransferase gene conferring resistance to hygromycin B in plants; KanR, aminoglycoside phosphotransferase gene conferring resistance to kanamycin in bacteria. RB and LB, right and left border sequences of T-DNA. The restriction enzymes that are used to excise individual DNA fragment are shown

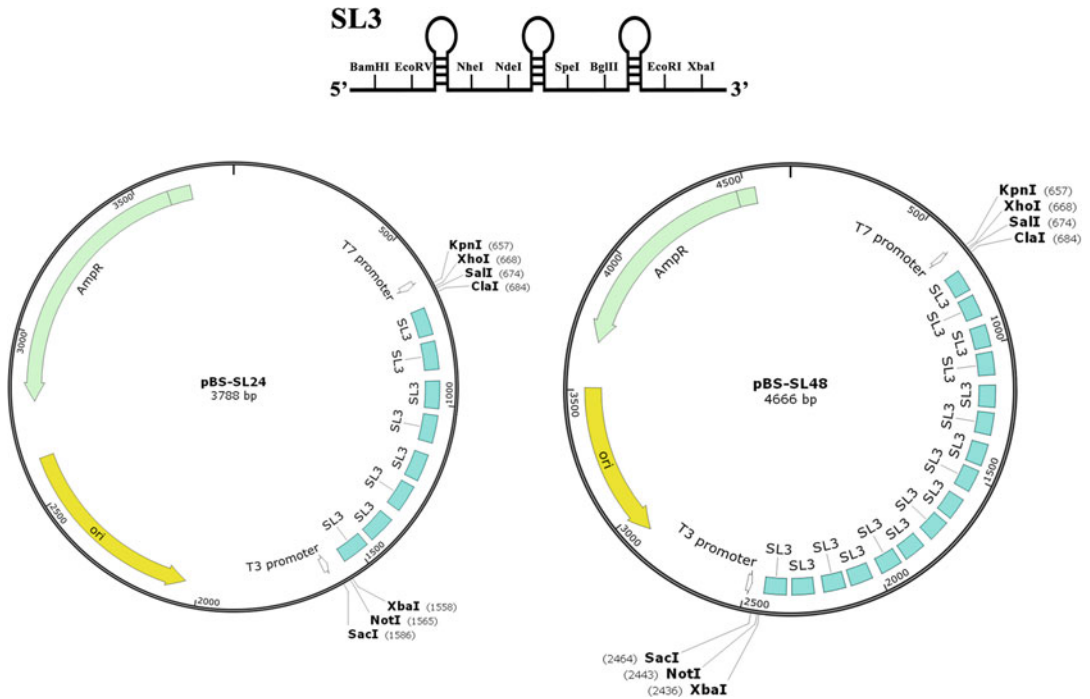


Fig. 2 Maps of SL3, pBS-SL24, and pBS-SL48. SL3 refers to a DNA fragment encoding three tandem repeats of the MS2 RNA stem-loop (SL) structure and is derived from AdMI-M3 [29]. pBS-SL24 and pBS-SL48 are pBluescript-based plasmids that contain 8 and 16 copies of SL3, respectively. The single-cut enzymes that are used to excise the SL24 or SL48 DNA fragments are shown

9. Agarose.
10. TAE buffer: 40 mM Tris, 1 mM EDTA, 20 mM acetic acid.
11. Sterilized water.
12. Commercialized *E. coli* or *Agrobacterium tumefaciens* competent cells.
13. DNA gel extraction kit.
14. DNA isolation kit.

2.2 Transient Expression

1. *Agrobacteria* (*Agrobacterium tumefaciens* strain AGL1) transformed with (see Note 1):
 - (a) pCAMBIA1390-35S-MS2_{FD}-GFP.
 - (b) pCAMBIA1390-35S-FT.
 - (c) pCAMBIA1390-35S-RFP.
 - (d) pCAMBIA1390-35S-FT_{SL24}.
 - (e) pCAMBIA1390-35S-RFP_{SL24}.
2. One-month-old *Nicotiana benthamiana* plants kept at 28 °C in 14-h/10-h light/dark cycle growth chambers.
3. Pipettes and compatible tips.

4. MES buffer: 0.1 M MES monohydrate, pH 5.7, stored at 4 °C after sterilization.
5. LB medium: 10 g/L NaCl, 10 g/L tryptone, 5 g/L yeast extract, supplemented with 50 µg/ml kanamycin.
6. Acetosyringone stock solution: 0.1 M Acetosyringone in ethanol. Store at -20 °C.
7. Inoculation medium: LB medium supplemented with 10 mM MES buffer and 20 µM acetosyringone (*see Note 2*).
8. Incubator with shaker set to 28 °C and 220 rpm.
9. Infiltration medium: 10 mM MES, 10 mM MgCl₂, and 200 µM acetosyringone in distilled water (*see Note 2*).
10. 125 mL Glass flask.
11. Glass test tubes (12 × 100 mm).
12. 15 and 50 mL Falcon polypropylene conical tubes.
13. Disposable 5 mL syringe without needle.

2.3 Imaging

1. Ophthalmic scissors (10 cm).
2. Blunt-headed forceps.
3. Pipettes and compatible tips.
4. Glass slides (76 × 26 mm).
5. Cover slides (18 × 18 mm, 175 ± 5 µm thick) (*see Note 3*).
6. Sterilized distilled water.
7. Kimwipes (Kimberly Clark, Irving, TX).
8. Confocal laser scanning microscope (e.g., LSM880 by Carl Zeiss, Oberkochen, Germany) equipped with 20×, 40×, and 63× magnification objectives.
9. Computer with software for image acquisition (e.g., the ZEN software developed by Carl Zeiss for LSM880 confocal laser scanning microscope).

3 Methods

3.1 Molecular Cloning

To track intracellular movement of mRNA, it is necessary to generate the plasmid containing the cDNA of the target mRNA fused with multiple repeats of the MS2 stem-loop (SL) structure. Here, we describe how to construct the plasmid encoding SL-tagged *FT*. We provide two pBluescript-based plasmids, pBS-SL24 (with 24 MS2 stem-loops) and pBS-SL48 (with 48 MS2 stem-loops), for restriction enzyme-based cloning of SL-tagged target mRNA (Fig. 2, *see Notes 1 and 4*).

1. Incubate 4 μL (2 μg) of pBS-SL24 plasmid DNA with 1 μL (20 units) of NotI, 1 μL (20 units) of SalI, 1 μL (5 units) of Klenow enzyme, 1 μL of 10 mM dNTP, 2 μL of enzyme buffer, and 10 μL of sterilized water at 37 °C for 2 h.
2. Incubate 4 μL (2 μg) of pCAMBIA1390-35S-FT plasmid DNA with 1 μL (20 units) of XbaI, 1 μL (5 units) of Klenow enzyme, 1 μL of 10 mM dNTP, 2 μL of enzyme buffer, and 11 μL of sterilized water at 37 °C for 2 h to create a linearized, blunt-ended vector.
3. Separate the DNA fragment of blunt-ended vector as well as the DNA fragment containing SL24 (841 bp) or SL48 (1719 bp) by electrophoresis through 0.8% agarose in TAE buffer. Purify the vector and DNA fragments from the gel with a gel extraction kit (*see Note 5*).
4. Mix 3 μL of the purified SL24/SL48 fragment with 1 μL of the purified linearized and blunt-ended vector as well as with 1 μL (400 units) T4 DNA ligase, 1 μL T4 DNA ligase buffer, and 4 μL sterilized water, and incubate at 16 °C overnight.
5. Mix the ligation mixture with 100 μL transformation-competent *E. coli* cells (*see Note 5*) and incubate on ice for 30 min. Select colonies of transformed bacteria on kanamycin-containing LB agar plates at 37 °C for overnight.
6. Use a single colony to inoculate 3 mL of kanamycin-containing LB medium and grow the bacteria at 37 °C on a shaker set to 220 rpm for 6–8 h. Purify plasmid DNA with a plasmid DNA isolation kit (*see Note 5*) and verify the insertion by sequencing or restriction enzyme digestion.
7. Incubate 100 μL transformation-competent *A. tumefaciens* cells (*see Note 5*) with 1 μL plasmid DNA carrying the SL24-tagged *FT* mRNA. Incubate the bacteria cells on ice for 30 min. Select colonies of transformed *A. tumefaciens* bacteria on kanamycin-containing LB agar plates at 28 °C for 2 days.

3.2 Transient Expression

The following plasmids are required for the RNA labeling experiment (*see Note 1*):

pCAMBIA1390-35S-FT_{SL24} (mobile *FT* mRNA with 24 repeats of SL).

pCAMBIA1390-35S-FT (negative control of mobile *FT* mRNA without SL).

pCAMBIA1390-35S-RFP_{SL24} (nonmobile *RFP* mRNA with 24 repeats of SL).

pCAMBIA1390-35S-RFP (negative control of nonmobile *RFP* mRNA without SL).

1. Use single colonies of transformed *A. tumefaciens* bacteria containing the abovementioned plasmids as well as bacteria containing pCAMBIA1390-35S-MS2_{FD}-GFP to separately inoculate 2 mL LB medium in test tubes. Incubate the bacterial cultures at 28 °C on a shaker set to 220 rpm for 24 h.
2. Transfer 200 µL of each overnight culture into a 125 mL glass flask containing 10 mL inoculation medium. Incubate the flasks at 28 °C on a shaker set to 220 rpm overnight.
3. Transfer the medium with bacteria from each flask to a 50 mL Falcon tube. Collect bacteria by centrifugation for 5 min at 9000 × *g* in the cold (4 °C). Resuspend the bacterial pellets in 3 mL infiltration medium and adjust the concentration of bacteria to OD₆₀₀ = 1 with infiltration medium.
4. Incubate the bacteria in the infiltration solution for 1 h at room temperature.
5. Set up the following mixtures by mixing equal volumes (1 mL for each solution) of the bacteria-containing infiltration solutions in a 15 mL Falcon tube:
 - (a) pCAMBIA1390-35S-MS2_{FD}-GFP with infiltration medium.
 - (b) pCAMBIA1390-35S-MS2_{FD}-GFP with pCAMBIA1390-35S-FT_{SL24}.
 - (c) pCAMBIA1390-35S-MS2_{FD}-GFP with pCAMBIA1390-35S-FT.
 - (d) pCAMBIA1390-35S-MS2_{FD}-GFP with pCAMBIA1390-35S-RFP_{SL24}.
 - (e) pCAMBIA1390-35S-MS2_{FD}-GFP with pCAMBIA1390-35S-RFP.
6. Use a 5 mL syringe without needle to infiltrate the abaxial side of *Nicotiana benthamiana* leaves (*see Note 6*) (Fig. 3a). Use 4-week-old *N. benthamiana* plants and infiltrate the fifth to seventh leaves (counted from the bottom of the plants). Incubate the infiltrated plants in a growth chamber set to 28 °C and a 14-h/10-h light/dark cycle for 24–48 h before analysis by confocal microscopy (*see Note 7*).

3.3 Imaging

1. Use a 10 cm ophthalmic scissor to remove a leaf disk (*see Note 8*) from the rim of the agroinfiltrated patch (Fig. 3b).
2. Place the leaf disk on a microscope glass slide with the adaxial side facing the glass. Use a plastic dropper to apply an appropriate amount of sterilized-distilled water onto the abaxial side of leaf disk. Cover the leaf disk with a cover slide. Gently press the cover slide and remove excess water with Kimwipes.

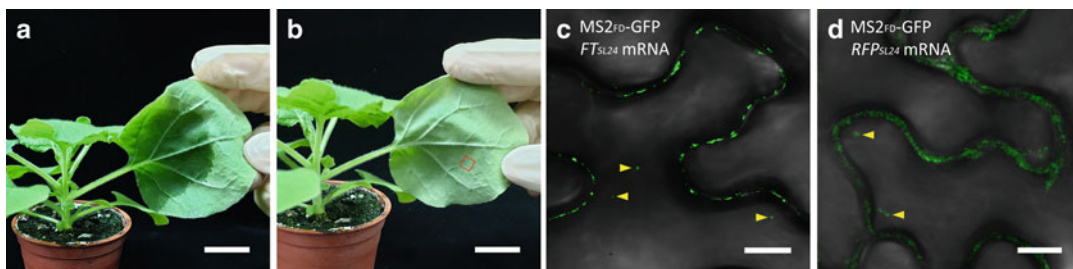


Fig. 3 The sampling strategy and live-cell imaging of mRNA. (a) Agro-infiltrated *N. benthamiana* leaf. (b) Two days after infiltration, a leaf disk is removed from the rim of the agro-infiltrated patch (indicated by red-dashed rectangle) and prepared for confocal microscopy. (c) Punctate distribution of MS2_{FD}-GFP-tagged *FT_{SL24}* mRNA. Arrowheads indicate the intracellular movement of *FT_{SL24}* mRNA. (d) The distribution of RFP_{SL24} mRNA in cytosol. In mature leaf cells, the majority of cytoplasmic space is occupied by vacuoles, which compresses the cytosol in a thin layer along the cell. Arrowheads indicate the intracellular movement of RFP_{SL24} mRNA. (a and b) Bar = 2 cm. (c and d) Bar = 10 μ m

3. Observe samples by confocal microscopy. Use a 20 \times objective to locate the area of interest (i.e., the boundary area of the agroinfiltrated patch) (*see Note 9*).
4. Use 40 \times or 63 \times objectives to optimize microscopy settings to differentiate the following four sample types:
 - (a) Set I: samples expressing pCAMBIA1390-35S-MS2_{FD}-GFP only.
 - (b) Set II: samples expressing pCAMBIA1390-35S-MS2_{FD}-GFP and pCAMBIA1390-35S-FT_{SL24}.
 - (c) Set III: samples expressing pCAMBIA1390-35S-MS2_{FD}-GFP and pCAMBIA1390-35S-FT (non-tagged mRNA control).
 - (d) Set IV: samples expressing pCAMBIA1390-35S-MS2_{FD}-GFP and pCAMBIA1390-35S-RFP_{SL24} (nonmobile mRNA control).
5. Use 40 \times or 63 \times objectives to record Z-stack or time-series images (*see Note 10*) with support by the microscope software (e.g., ZEN by Carl Zeiss, Oberkochen, Germany).
6. Process and analyze the acquired images with image processing software (Fig. 3c and d; Supplementary Movies S1 and S2; *see Note 11*).

4 Notes

1. The author responsible for distribution of plasmids is Tien-Shin Yu (tienshin@gate.sinica.edu.tw).
2. The inoculation and infiltration media must be freshly prepared before use.

3. Use cover slides with minimal thickness to obtain high-resolution images.
4. Figure 2 shows the map of pBS-SL24 and pBS-SL48, which are pBluescript-based plasmids that encode 8 and 16 copies of the SL3 structure, and the enzymes that are used to excise the DNA fragments encoding the SL repeats. Note that the fragments are oriented from KpnI to SacI (5' to 3') to fuse the SL repeats to the RNA encoded by the target construct in correct orientation. Although the number of SL3 structures used for tagging the target mRNA may enhance fluorescent signals, a higher SL3 copy number may also affect the stability and transport of the SL-tagged mRNA.
5. Commercialized plasmid DNA extraction system (for extraction of plasmid DNA from bacteria) and gel extraction system (for extraction of DNA fragments from agarose gels) are utilized for efficient cloning. Commercialized competent cells of *E. coli* and *A. tumefaciens* strains are applied for transformation.
6. Infiltrate the abaxial side of the leaves. Infiltration creates an “infiltrated patch” on the leaves. Cells at the margin between infiltrated and non-infiltrated tissues should be used for analysis by confocal microscopy (Fig. 3b).
7. Watering should be avoided within 24 h after infiltration.
8. The removed leaf disks should be smaller than 5 × 5 mm and contain no large veins.
9. High expression of SL-tagged mobile mRNAs can interfere in specific subcellular distribution of mobile mRNAs. The critical mRNA abundance within a cell occurs within a short time after agrobacteria infiltration. The cells at the boundary area display lower expression of mobile mRNAs as compared to the cells in the center of the infiltrated area. The boundary area represents the margin between agroinfiltrated and non-infiltrated tissues, which can be distinguished by observing GFP signals under confocal microscopy. Cells located within the agroinfiltrated patch exhibit extensive GFP fluorescence, whereas GFP fluorescence is not detected in cells outside the patch. The boundary area is the area where the two types of cells encounter. The cells in boundary area usually exhibit moderate GFP fluorescence (bright nucleolus and faint fluorescence in the nucleoplasm). In our experience, selective PD targeting of mobile mRNA is detected in the cells within or adjacent to the boundary area [28].
10. Considering the dynamic distribution of mobile mRNA, images should be captured as fast as possible, by using a low number of scans (e.g., 1) for each pixel line.

11. We used the ZEN software for Z-stack image acquisition and time series live-imaging recording. ZEN also offers embedded image export and movie export tools to process raw data acquired by Carl Zeiss LSM880 confocal microscopy.

Acknowledgments

This work was supported by the Thematic Research Program of the Academia Sinica, Taiwan (AS-105-TP-B03).

References

1. Lucas WJ, Yoo BC, Kragler F (2001) RNA as a long-distance information macromolecule in plants. *Nat Rev Mol Cell Biol* 2:849–857
2. Kehr J, Kragler F (2018) Long distance RNA movement. *New Phytol* 218:29–40
3. Kim M, Canio W, Kessler S, Sinha N (2001) Developmental changes due to long-distance movement of a homeobox fusion transcript in tomato. *Science* 293:287–289
4. Banerjee AK, Chatterjee M, Yu Y, Suh SG, Miller WA, Hannapel DJ (2006) Dynamics of a mobile RNA of potato involved in a long-distance signaling pathway. *Plant Cell* 18:3443–3457
5. Haywood V, Yu TS, Huang NC, Lucas WJ (2005) Phloem long-distance trafficking of *GIBBERELLIC ACID-INSENSITIVE* RNA regulates leaf development. *Plant J* 42:49–68
6. Lu KJ, Huang NC, Liu YS, Lu CA, Yu TS (2012) Long-distance movement of Arabidopsis *FLOWERING LOCUS T* RNA participates in systemic floral regulation. *RNA Biol* 9:653–662
7. Huang NC, Jane WN, Chen J, Yu TS (2012) *Arabidopsis thaliana* *CENTRORADIALIS* homologue (*ATC*) acts systemically to inhibit floral initiation in Arabidopsis. *Plant J* 72:175–184
8. Huang NC, Luo KR, Yu TS (2018) Mobility of antiflorigen and PEBP mRNAs in tomato-tobacco heterografts. *Plant Physiol* 178:783–794
9. Ruiz-Medrano R, Xoconostle-Cázares B, Lucas WJ (1999) Phloem long-distance transport of *CmNACP* mRNA: implications for supracellular regulation in plants. *Development* 126:4405–4419
10. Huang NC, Yu TS (2009) The sequences of Arabidopsis *GA-INSENSITIVE* RNA constitute the motifs that are necessary and sufficient for RNA long-distance trafficking. *Plant J* 59:921–929
11. Notaguchi M, Higashiyama T, Suzuki T (2015) Identification of mRNAs that move over long distances using an RNA-Seq analysis of Arabidopsis/Nicotiana benthamiana heterografts. *Plant Cell Physiol* 56:311–321
12. Thieme CJ, Rojas-Triana M, Stecyk E, Schudoma C, Zhang W, Yang L, Miñambres M, Walther D, Schulze WX, Paz-Ares J, Scheible W-R, Kragler F (2015) Endogenous Arabidopsis messenger RNAs transported to distant tissues. *Nat Plants* 1:15025
13. Yang Y, Mao L, Jittayasothorn Y, Kang Y, Jiao C, Fei Z, Zhong GY (2015) Messenger RNA exchange between scions and rootstocks in grafted grapevines. *BMC Plant Biol* 15:251
14. Calderwood A, Kopriva S, Morris RJ (2016) Transcript abundance explains mRNA mobility data in *Arabidopsis thaliana*. *Plant Cell* 28:610–615
15. Xia C, Zheng Y, Huang J, Zhou X, Li R, Zha M, Wang S, Huang Z, Lan H, Turgeon R, Fei Z, Zhang C (2018) Elucidation of the mechanisms of long-distance mRNA movement in a *Nicotiana benthamiana*/tomato heterograft system. *Plant Physiol* 177:745–758
16. Zhang W, Thieme CJ, Kollwig G, Apelt F, Yang L, Winter N, Andresen N, Walther D, Kragler F (2016) tRNA-related sequences trigger systemic mRNA transport in plants. *Plant Cell* 28:1237–1249
17. Bertrand E, Chartrand P, Schaefer M, Shenoy SM, Singer RH, Long RM (1998) Localization of ASH1 mRNA particles in living yeast. *Mol Cell* 2:437–445
18. Edelman FT, Schlundt A, Heym RG, Jenner A, Niedner-Boblentz A, Syed MI, Pailart JC, Stehle R, Janowski R, Sattler M, Jansen

- RP, Niessing D (2017) Molecular architecture and dynamics of ASH1 mRNA recognition by its mRNA-transport complex. *Nat Struct Mol Biol* 24:152–161
19. Herbert AL, Fu MM, Drerup CM, Gray RS, Harty BL, Ackerman SD, O'Reilly-Pol T, Johnson SL, Nechiporuk AV, Barres BA, Monk KR (2017) Dynein/dynactin is necessary for anterograde transport of Mbp mRNA in oligodendrocytes and for myelination in vivo. *Proc Natl Acad Sci U S A* 114: E9153–E9162
 20. Brendza RP, Serbus LR, Duffy JB, Saxton WM (2000) A function for kinesin I in the posterior transport of oskar mRNA and Staufén protein. *Science* 289:2120–2122
 21. Rook MS, Lu M, Kosik KS (2000) CaMKII α 3' untranslated region-directed mRNA translocation in living neurons: visualization by GFP linkage. *J Neurosci* 20:6385–6393
 22. Zhang F, Simon AE (2003) A novel procedure for the localization of viral RNAs in protoplasts and whole plants. *Plant J* 35:665–673
 23. Sambade A, Brandner K, Hofmann C, Seemanpillai M, Mutterer J, Heinlein M (2008) Transport of TMV movement protein particles associated with the targeting of RNA to plasmodesmata. *Traffic* 9:2073–2088
 24. Peña E, Heinlein M, Sambade A (2015) In vivo RNA labeling using MS2. *Methods Mol Biol* 1217:329–341
 25. Hamada S, Ishiyama K, Choi SB, Wang C, Singh S, Kawai N, Franceschi VR, Okita TW (2003) The transport of prolamine RNAs to prolamine protein bodies in living rice endosperm cells. *Plant Cell* 15:2253–2264
 26. Urbanek MO, Galka-Marciniak P, Olejniczak M, Krzyzosiak WJ (2014) RNA imaging in living cells - methods and applications. *RNA Biol* 11:1083–1095
 27. Köhler RH (1998) GFP for in vivo imaging of subcellular structures in plant cells. *Trends Plant Sci* 3:317–320
 28. Luo KR, Huang NC, Yu TS (2018) Selective targeting of mobile mRNAs to plasmodesmata for cell-to-cell movement. *Plant Physiol* 177:604–614
 29. Zhou Z, Sim J, Griffith J, Reed R (2002) Purification and electron microscopic visualization of functional human spliceosomes. *Proc Natl Acad Sci U S A* 99:12203–12207



RNA Imaging with RNase-Inactivated Csy4 in Plants and Filamentous Fungi

David Burnett, Alexander Lichius, and Jens Tilsner

Abstract

Subcellular localizations of RNAs can be imaged *in vivo* with genetically encoded reporters consisting of a sequence-specific RNA-binding protein (RBP) fused to a fluorescent protein. Several such reporter systems have been described based on RBPs that recognize RNA stem-loops. Here we describe RNA tagging for imaging with an inactive mutant of the bacterial endonuclease Csy4, which has a significantly higher affinity for its cognate stem-loop than alternative systems. This property allows for sensitive imaging with only few tandem copies of the target stem-loop inserted into the RNA of interest.

Key words Csy4, RNA stem-loop, RNA imaging, Live-cell imaging, RNA virus, Plant virus, Filamentous fungi, *Neurospora crassa*

1 Introduction

The subcellular localizations of various types of RNA are intimately related to their functions. Functional localizations can include highly localized translation or recruitment to various types of RNA granules [1–3]. Viral RNA (vRNA) genomes are localized at sites of replication, translation, and encapsidation, and in plants some types of RNA are also transported between cells [4, 5]. In filamentous fungi, targeted delivery of RNAs provides essential means of spatial control over their respective function within the elaborate hyphal network [6, 7].

Multiple systems have been developed that enable sequence-specific tracking of RNA molecules in living cells [8, 9]. Genetically encoded RNA reporters are particularly well suited for RNA imaging in organisms with a cell wall, as they do not necessitate delivery of additional molecules into cells. Generally, they consist of a sequence-specific RNA-binding protein (RBP) translationally fused to a fluorescent protein. Unbound and RNA-bound reporter can be distinguished either by directing the unbound fusion protein to the nucleus, from where it is recruited by cytoplasmic RNAs, or by

bimolecular fluorescence complementation between two RBP fusion proteins bound to the same RNA. Some RBPs used for RNA imaging can be engineered to bind to a sequence of choice, enabling detection of native, unaltered RNAs [4]. However, the effects of artificially altered sequence specificity on RNA affinity can be hard to predict [10]. Alternatively, the RNA of interest can be genetically tagged with a sequence motif bound by a suitable RBP. This allows for the use of well-characterized protein-RNA interactions, and sensitivity can easily be increased by using multiple tandem copies of the recognition motif. The latter approach has been implemented with several stem-loop-binding RBPs, first with the capsid protein of bacteriophage MS2 and later with several similar systems [8, 9 and references therein]. The dissociation constants of the respective protein-RNA complexes vary between about 1 nM and 3 μ M. In order to achieve sensitive RNA imaging, typically 6–24 stem-loops are inserted into the RNA of interest, although as few as 4 and as many as 96 have been employed [8, 9 and references therein]. The extensive secondary structures formed by these tags can interfere with RNA processing, localization, and translation [11, 12]. For imaging of viral genomes, multiple tandem stem-loops are particularly problematic, as RNA viruses rely on native secondary structures and short- and long-range intramolecular base pairing for regulation of their RNA replication and gene expression.

Here, we describe RNA tagging for imaging with the bacterial endonuclease Csy4 (21.4 kDa), which recognizes its cognate, 15 bp stem-loop (Fig. 1a) with exceptionally high affinity (k_D 0.05 nM) [13]. Csy4 normally functions in the processing of CRISPR pre-crRNAs, which it cleaves specifically immediately after the recognized stem-loop. This endonuclease activity can be removed with a single-point mutation in the active site, H29A, which does not affect RNA affinity [14, 16]. By fusing Csy4 [H29A] (Csy4*) to GFP and tagging RNAs of interest with two cognate stem-loops, highly sensitive imaging of Potato virus X (PVX) vRNA was achieved in infected *Nicotiana benthamiana* leaf epidermal cells (Burnett & Tilsner, in preparation), while the distribution of messenger RNAs tagged with 12 stem-loops was visualized in hyphae of the filamentous fungus *Neurospora crassa* (Tilsner & Lichius, in preparation).

2 Materials

Novel and published plasmids described in this chapter are available upon request for noncommercial academic research.

2.1 Construction of Csy4* Expression Plasmids for Imaging in Plants

1. Synthesized gene fragment of *Pseudomonas aeruginosa* UCBPP-PA14 Csy4* open reading frame (https://www.ncbi.nlm.nih.gov/nuccore/NC_008463.1?from=2927517&to=2928080) without the stop codon (*see Note 1*). Following

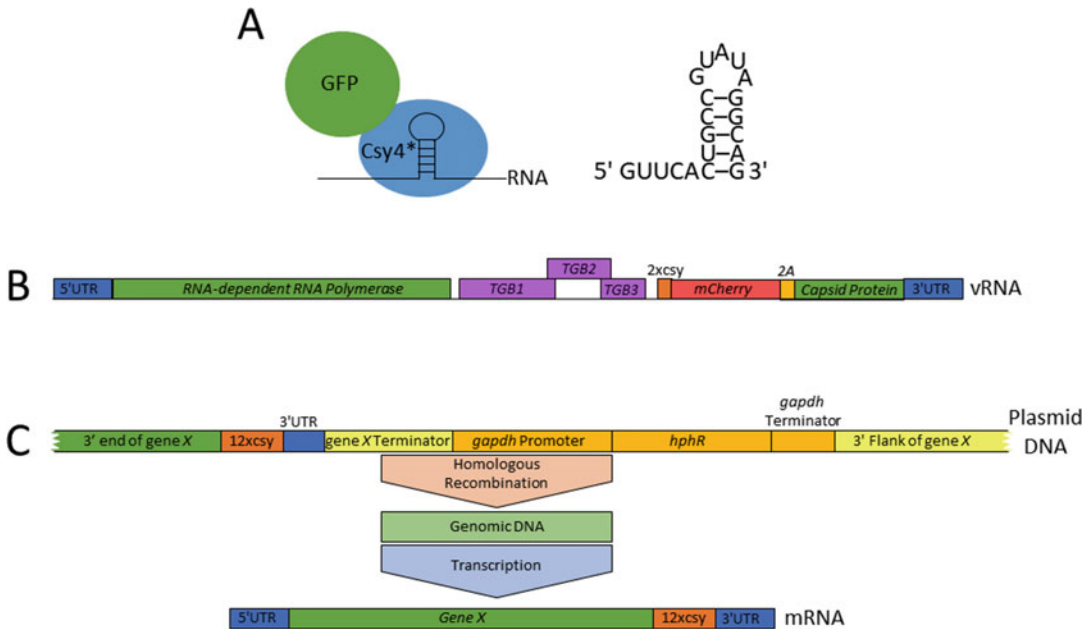


Fig. 1 RNA tagging for live-cell imaging with inactivated Csy4 (Csy4*). **(a)** Schematic representation of a Csy4*-GFP fusion binding to its cognate 15 bp csy stem-loop. For RNA tagging, 5 nucleotides upstream of the stem-loop are included [13, 14]. **(b)** Position of csy stem-loops in the tagged Potato virus X vRNA genome carrying an mCherry infection marker [15]. Two stem-loops are sufficient for imaging (TGB1–3, triple-gene block 1–3 movement proteins; 2A, linker peptide from Foot and mouth disease virus mediating partial co-translational separation of mCherry and capsid protein). **(c)** Diagram of the knock-in cassette for insertion of 12xcsy stem-loops between the stop codon and 3'UTR of a gene of interest “X” in the *N. crassa* genome through homologous recombination, and the resulting tagged mRNA (*gapdh*, glyceraldehyde 3-phosphate dehydrogenase; *hphR*, hygromycin B resistance gene). Genetic elements shown approximately to scale

the last Csy4* codon, a glycine codon is inserted and then a SV40 nuclear localization signal flanked by two in-frame *KpnI* sites: 5'-GGA-GGTACC-CCTAAGAAAAAGCGTAAAGGTTGGTACC-3'. The entire cassette is flanked by Gateway attB1 and attB2 sites at the 5' and 3' ends, respectively (attB1-Csy4*-*KpnI*-NLS-*KpnI*-attB2).

2. Gateway BP Clonase II (Invitrogen).
3. Gateway LR Clonase II (Invitrogen).
4. pDONR221 Gateway donor vector (Invitrogen).
5. pGWB405 destination vector (Addgene #74799, [17]).
6. *KpnI* restriction enzyme and 10× buffer.
7. T4 DNA ligase.
8. Electroporator and electroporation cuvettes with 0.2 cm electrode gap width.
9. *Escherichia coli* XL1 Blue MRF' electrocompetent cells.
10. *Agrobacterium tumefaciens* AGL1 electrocompetent cells.

11. LB liquid medium: 10 g Tryptone, 10 g NaCl, and 5 g yeast extract per 1 L, pH 7.0.
12. LB agar plates (prepared using LB liquid medium with the addition of 15 g/L agar) containing 50 µg/mL kanamycin or 100 µg/mL spectinomycin, respectively.
13. LB liquid medium containing 50 µg/mL kanamycin or 100 µg/mL spectinomycin, respectively.
14. LB agar plates (*see* Subheading 2.1, **item 12**) containing 100 µg/mL spectinomycin and 50 µg/mL rifampicin.
15. LB liquid medium containing 100 µg/mL spectinomycin and 50 µg/mL rifampicin.
16. 37 °C Incubator.
17. 37 °C Shaking incubator.
18. Plasmid miniprep kit.
19. PCR purification kit with a size exclusion limit ≥ 50 bp (i.e., smaller DNA fragments are removed).
20. 28 °C Incubator.
21. 28 °C Shaking incubator.
22. Glycerol, sterilized by autoclaving.
23. DNA oligonucleotide primers DONRfor (5'-CTGGCAGTTC CCTACTCTCG-3'), DONRrev (5'-ATGTAACATCAGAGATTTTGAGACACG-3'), attB1 adapter (5'-GGGGACAAGTTTGTACAAAAAAGCAGGCT-3'), and attB2 adapter (5'-GGGACCCTTTGTACAAGAAAGCTGGGT-3').

2.2 Tagging of the PVX Genome

1. Synthesized gene fragment provided in a cloning vector and containing two 20 bp Csy4 cognate recognition sequences (consisting of the 15 bp stem-loop-forming sequence and 5 upstream bases to maximize protein-RNA affinity [13, 14]) (pMA-RQ.*NheI*-2xcsy-*NheI*). The two repeats are separated by an *EcoRI* restriction site, and flanked on both sides by *NheI* sites (*see* **Note 2**) (5'-GCTAGCGTTC**ACTGCCGTA-TAGGCAGAAATTCGTTCACTGCCGTATAGGCAGGC-TAGC**-3'; stem-loop-forming sequences in bold, restriction sites italicized). Ligation into a single restriction site allows for the easy generation of tandem copies of the two stem-loop cassettes.
2. Plasmid pTRA.PVX.mCherry-2A-CP containing a PVX genome with mCherry translationally fused to the capsid protein via a Foot and mouth disease virus 2A ribosomal “skipping” sequence under the control of a Cauliflower mosaic virus 35S promoter [15].
3. *NheI* and *EcoRI* restriction enzymes and corresponding 10× buffers.

4. T4 DNA ligase.
5. Electroporator and electroporation cuvettes with 0.2 cm electrode gap width.
6. *E. coli* XL1 Blue MRF' electrocompetent cells.
7. LB liquid medium (*see* Subheading 2.1, item 11).
8. LB liquid medium (*see* Subheading 2.1, item 11) containing 100 µg/mL ampicillin.
9. LB agar plates (*see* Subheading 2.1, item 12) containing 100 µg/mL ampicillin.
10. Calf intestinal phosphatase (CIP).
11. For agarose gel electrophoresis:
 - Agarose.
 - TBE buffer: 89 mM Tris, 89 mM boric acid, 2 mM ethylenediaminetetraacetic acid (EDTA).
 - Ethidium bromide.
 - Sample loading buffer (6×): 60% glycerol, 0.3 mg/mL bromophenol blue, 0.03 mg/mL xylene cyanol in 20 mM Tris-HCl pH 8.
 - DNA molecular weight ladder.
 - Agarose gel tank.
 - Power supply.
 - UV transilluminator.
12. 37 °C Incubator.
13. 37 °C Shaking incubator.
14. Plasmid miniprep kit.
15. PCR clean up kit.
16. DNA gel extraction kit.
17. Primer PVX5539F (5'-TGTGTCATCAAGATTACTGG-3').

2.3 Inoculation of *N. benthamiana* with Tagged PVX by Microprojectile Bombardment

1. *N. benthamiana* plants and growth facilities suitable for handling of transgenic plants and genetically modified plant pathogens under containment conditions.
2. Plasmid pTRA.PVX.2xcsy.mCherry-2A-CP (*see* Subheading 3.2).
3. 1 mg/mL Gold particles (1 µm, BioRad 1652263) in ethanol.
4. Free-standing [18] or handheld (BioRad Helios™ 1652432) microprojectile gun allowing microprojectile bombardment of leaves without removing them from plants. Descriptions in Subheading 3.3 are based on the former, which uses Swinnex 13 mm syringe filter holders (Sigma-Aldrich SX0001300) as sample holders.

2.4 Agro-Infiltration of *N. benthamiana* with *Csy4 Expression Plasmids**

1. *A. tumefaciens* AGL1 strains transformed with pGWB405.Csy4*-NLS-GFP or pGWB405.Csy4*-GFP plasmids (*see* Subheading 3.1).
2. Glycerol stock of *A. tumefaciens* AGL1 strain transformed with a plasmid for expression of the Tomato bushy stunt virus p19 silencing suppressor, e.g., pDGB3alpha2_35S:P19:Tnos (GB1203) (Addgene #68214 [19]).
3. LB liquid medium (*see* Subheading 2.1, item 11) containing 100 µg/mL spectinomycin and 50 µg/mL rifampicin.
4. LB liquid medium (*see* Subheading 2.1, item 11) containing 50 µg/mL kanamycin and 50 µg/mL rifampicin.
5. 28 °C Shaking incubator.
6. Infiltration buffer: 10 mM morpholino ethane sulfonic acid (MES), 10 mM MgCl₂, 67 mM acetosyringone.
7. UV spectrophotometer.
8. 1 mL Syringes.
9. 25G Needle.

2.5 Visualization of Tagged PVX vRNA in *N. benthamiana* Leaf Epidermal Cells

1. Upright confocal laser scanning microscope equipped with 10× long-distance and 40× water-dipping lenses, and capable of detecting GFP and mCherry.
2. Glass slide.
3. Double-sided tape.
4. Leaf prepared as per Subheadings 3.3 and 3.4.

2.6 Construction of *Csy4 Expression Plasmid for RNA Imaging in *N. crassa***

1. pDONR221.Csy4* (*see* Subheading 3.1), template for Csy4*.
2. pLS3 [20], template for mBasicGFP.
3. pAB261 [21] (*see* Note 3), template for expression vector backbone.
4. Oligonucleotide primers Csy4-IF-F (5'-CAGCACATCAACC GTCAAAGATATCATGGACCATTACCTCGAC-3'), Csy4-IF-R (5'-GCCTCCGCCTCCGCCTCCGCCGCCTCCGCC GAACCAAGGAACGAAACC-3'), GFP-IF-F (5'-GGCGG AGGCGGCGGAGGCGGAGGCGGAGGCATGGTGAGCAA GGGCG-3'), GFP-IF-R (5'-GTTCGACGGTATCGATAAGC TTTTACTTGACAGCTCGTCCATGC-3'), pAB261-lin-F (5'-AAGCTTATCGATACCGTC-3'), and pAB261-lin-R (5'-GATATCTTTGACGGTTGATG-3').
5. High-fidelity DNA polymerase.
6. 10 mM dNTP mixture.
7. PCR thermocycler.
8. Components for agarose gel electrophoresis (*see* Subheading 2.2, item 11).

9. *DpnI* restriction enzyme and 10× buffer.
10. PCR cleanup kit.
11. NEBuilder HiFi DNA Assembly Master Mix (NEB E2621S).
12. *E. coli* chemically competent cells (any standard cloning strain suitable).
13. LB liquid medium (*see* Subheading 2.1, item 11).
14. LB liquid medium (*see* Subheading 2.1, item 11) containing 100 µg/mL ampicillin.
15. LB agar plates (*see* Subheading 2.1, item 12) containing 100 µg/mL ampicillin.
16. 37 °C Incubator.
17. 37 °C Shaking incubator.
18. Plasmid miniprep kit.

2.7 Construction of the 12xcsy Stem-Loop Knock-In Cassette for RNA Imaging in *N. crassa*

1. pTRA.PVX.12xcsy.mCherry-2A-CP (*see* Subheading 3.2), template for 12xcsy stem-loops.
2. *N. crassa* strain FGSC6103 genomic DNA, purified by gDNA quick extraction protocol [22].
3. pLS3 [20], template for hygromycin B resistance cassette.
4. pAL12-Lifeact [23], template for AmpR-ORI plasmid backbone.
5. Oligonucleotide primers for PCR-based recombinational cloning: NC-xxx-IF-F (5'-CCTGATTCTGTGGATAACCGTTAA TTAA-[*target gene-specific sequence*]-3'); NC-xxx-IF-R (5'-G TGAACGCTAGCTGGTGCTGACCTCT-[*target gene-specific sequence*]-3'); 12xcsySL-F (5'-AGAGGTCAGCACCAGCTA GC-3'); 12xcsySL-R (5'-GGCCGGATCGATGCTAG-3'); NC-Txxx-IF-F (5'-GCAGCTAGCATCGATCCGGCC-[*target gene-specific sequence*]-3'); NC-Txxx-IF-R (5'-GCCATATTGA TGTAAGGTAGCTCTC-[*target gene-specific sequence*]-3'); Pgapdh-F (5'-GAGAGCTACCTTACATCAA-3'); Tgapdh-R (5'-GGTACTATGGCTTAGATGG-3'); NC-xxx-3'flank-F (5'-GGTATTCATCTAAGCCATAGTACC-[*target gene-specific sequence*]-3'); NC-xxx-3'flank-R (5'-GTTATTGTCTCATGAG CGGATACTTAATTAA-[*target gene-specific sequence*]-3'); AmpR-F (5'-GTATCCGCTCATGAGACAATA-3'); ORI-R (5'-CGGTTATCCACAGAATCAG-3'). *PacI* sites italicized (*see* Subheadings 3.7 and 3.10).
6. High-fidelity (HiFi) DNA polymerase.
7. 10 mM dNTP mixture.
8. PCR thermocycler.
9. Components for agarose gel electrophoresis (*see* Subheading 2.2, item 11).

10. *DpnI* restriction enzyme and 10× buffer.
11. PCR cleanup kit.
12. NEBuilder HiFi DNA Assembly Master Mix (NEB E2621S).
13. *E. coli* chemically competent cells (any standard cloning strain suitable).
14. LB liquid medium (*see* Subheading 2.1, item 11).
15. LB liquid medium (*see* Subheading 2.1, item 11) containing 100 µg/mL ampicillin.
16. LB agar plates (*see* Subheading 2.1, item 12) containing 100 µg/mL ampicillin.
17. 37 °C Incubator.
18. 37 °C Shaking incubator.
19. Plasmid miniprep kit.

2.8 Preparation of Electrocompetent *Conidia* of *N. crassa* FGSC6103

1. *N. crassa* strain FGSC6103 (*see* Note 4).
2. 1 M Sorbitol in distilled water, sterile filtered.
3. Vogel's minimal medium [24].
4. 25 mg/mL L-Histidine in distilled water, sterile filtered.
5. 500 mL Conical flask, sterilized by autoclaving.
6. 30 °C Shaking incubator.
7. Miracloth, autoclaved.
8. Funnel, autoclaved.
9. 50 mL Screw-cap tubes, sterile.
10. Refrigerated benchtop centrifuge suitable for 50 mL screw-cap tubes.
11. Vortex mixer.

2.9 Electro-Transformation of *Csy4 Expression Plasmid into *N. crassa***

1. pAL13.*Csy4**-GFP plasmid (*see* Subheading 3.6).
2. *SspI* and *PciI* restriction enzymes with corresponding 10× buffers.
3. PCR cleanup kit.
4. *N. crassa* strain FGSC6103 electrocompetent conidia (*see* Subheading 3.8).
5. 1 M Sorbitol in distilled water, sterile filtered.
6. Electroporator and electroporation cuvettes with 0.2 cm electrode gap width.
7. Yeast extract.
8. 50 µM SCR7 pyrazine in dimethyl sulfoxide (DMSO).
9. 15 mL Screw-cap tubes, sterile.

10. Vogel's minimal medium top agar (prepared using Vogel's minimal liquid medium as per Subheading 2.4, **item 3**, with the addition of 7 g/L agar), molten, and kept liquid at 55 °C.
11. Vogel's minimal medium bottom (thinly poured) agar plates (prepared using Vogel's minimal liquid medium as per Subheading 2.4, **item 3**, with the addition of 15 g/L agar).
12. Vogel's minimal medium agar plates (prepared using Vogel's minimal liquid medium as per Subheading 2.4, **item 3**, with the addition of 15 g/L agar).
13. 30 °C Incubator.
14. 30 °C Shaking incubator.

2.10 Electro-Transformation of the 12xcsy Stem-Loop Knock-In Cassette into *N. crassa*

1. Plasmid pAL15.X-12xcsySL containing 12xcsy stem-loop knock-in cassette (*see* Subheading 3.7).
2. *PacI* restriction enzyme with corresponding 10× buffer.
3. PCR cleanup kit.
4. *N. crassa* transformant strain expressing Csy4*-GFP from *his3* locus (*see* Subheading 3.9).
5. 1 M Sorbitol in distilled water, sterile filtered.
6. Electroporator and electroporation cuvettes with 0.2 cm electrode gap width.
7. Yeast extract.
8. 50 μM SCR7 pyrazine in DMSO.
9. 15 mL Screw-cap tubes, sterile.
10. Vogel's minimal medium top agar (*see* Subheading 2.9, **item 10**) supplemented with 50 μg/mL hygromycin B, molten, and kept liquid at 55 °C.
11. Vogel's minimal medium bottom (thinly poured) agar plates (*see* Subheading 2.9, **item 11**) supplemented with 250 μg/mL hygromycin B.
12. Vogel's minimal medium agar plates (*see* Subheading 2.9, **item 12**) supplemented with 200 μg/mL hygromycin B.
13. 30 °C Incubator.
14. 30 °C Shaking incubator.

2.11 Visualization of Tagged mRNA in *N. crassa*

1. Inverted confocal laser scanning microscope equipped with 40× and 63× oil immersion lenses, capable of imaging GFP.
2. Colony of *N. crassa* transformant strain expressing Csy4*-GFP from *his3* locus (*see* Subheading 3.9) and 12xcsy-tagged mRNA (*see* Subheading 3.10) cultivated on Vogel's minimal medium agar plates (*see* Subheading 2.9, **item 9**) supplemented with 200 μg/mL hygromycin B.

3. 24 × 60 mm Cover glass.
4. Physiological salt solution: 0.9% NaCl.
5. 30 °C Incubator.

3 Methods

3.1 Construction of *Csy4** Expression Plasmids for Imaging in Plants

1. Recombine the attB1-*Csy4**-*KpnI*-NLS-*KpnI*-attB2 gene fragment with pDONR221 using Gateway BP Clonase II according to the manufacturer's instructions.
2. Electroporate 1 μL BP recombination reaction into 50 μL XL1 Blue MRF' cells, and then incubate cells in 1 mL LB medium without antibiotics at 37 °C for 1 h.
3. Plate 100 μL transformed cells on LB-agar plates containing 50 μg/mL kanamycin, and incubate overnight at 37 °C.
4. The next day, inoculate several well-separated colonies into 5 mL LB liquid medium containing 50 μg/mL kanamycin each, and incubate overnight at 37 °C with shaking.
5. Purify pDONR221.*Csy4**-*KpnI*-NLS-*KpnI* plasmid DNA from each culture using a plasmid miniprep kit according to the manufacturer's instructions.
6. Verify the correct insert by DNA sequencing with primers DONRfor and DONRrev.
7. With the miniprep DNA of one correct clone, set up the following restriction digest according to the manufacturer's instructions and incubate at 37 °C for 2 h: 10 μL pDONR221.*Csy4**-*KpnI*-NLS-*KpnI*, 5 μL 10× buffer, and 1 μL *KpnI*, and make up to 50 μL with water.
8. Purify the DNA from the restriction digests with a PCR cleanup kit according to the manufacturer's instructions. A size cutoff of greater than 50 bp will ensure that the excised NLS fragment passes through the column.
9. Re-ligate 2 μL of the purified digested plasmid in a total volume of 20 μL using T4 DNA ligase according to the manufacturer's instructions.
10. Electroporate 2 μL ligation reaction into 50 μL XL1 Blue MRF' cells, and then incubate cells in 1 mL LB medium without antibiotics at 37 °C for 1 h (*see Note 5*).
11. Plate 25 μL transformed cells on LB-agar plates containing 50 μg/mL kanamycin, and incubate overnight at 37 °C.
12. The next day, inoculate several 5 mL aliquots of LB liquid medium containing 50 μg/mL kanamycin with a well-separated colony each, and incubate overnight at 37 °C with shaking.

13. Purify pDONR221.Csy4* plasmid DNA from each culture using a plasmid miniprep kit according to the manufacturer's instructions.
14. Verify the removal of the NLS by DNA sequencing with primer DONRrev.
15. Recombine the following constructs in two separate Gateway LR Clonase II reactions according to the manufacturer's instructions:
 - (a) pDONR221.Csy4* and pGWB405 to make pGWB405.Csy4*-GFP.
 - (b) pDONR221.Csy4*-*KpnI*-NLS-*KpnI* and pGWB405 to make pGWB405.Csy4*-NLS-GFP.
16. Electroporate 1 μ L of each LR recombination reaction into 50 μ L aliquots of XL1 Blue MRF' cells, and then incubate cells in 1 mL LB medium without antibiotics at 37 °C for 1 h.
17. Plate 100 μ L of each transformation on LB-agar plates containing 100 μ g/mL spectinomycin, and incubate overnight at 37 °C.
18. The next day, inoculate several 5 mL aliquots of LB liquid medium containing 100 μ g/mL spectinomycin with a well-separated colony each, and incubate overnight at 37 °C with shaking.
19. Purify pGWB405.Csy4*-GFP and pGWB405.Csy4*-NLS-GFP plasmids from each culture using a plasmid miniprep kit according to the manufacturer's instructions.
20. Verify the presence of the Csy4* inserts by DNA sequencing with primers attB1 adapter and attB2 adapter.
21. Electroporate 0.5 μ L of a verified pGWB405.Csy4*-GFP and pGWB405.Csy4*-NLS-GFP plasmid, respectively, into 50 μ L aliquots of *A. tumefaciens* AGL1 cells each, and then incubate cells in 1 mL LB medium without antibiotics at 28 °C for 2 h.
22. Plate 10–25 μ L of each transformation on LB-agar plates containing 100 μ g/mL spectinomycin and 50 μ g/mL rifampicin, and incubate at 28 °C for 2–3 days.
23. Inoculate separate 5 mL aliquots of LB liquid medium containing 100 μ g/mL spectinomycin and 50 μ g/mL rifampicin with one well-separated colony from each plate, and incubate at 28 °C with shaking for 2 days.
24. Prepare a glycerol stock from each culture by mixing 750 μ L culture with 750 μ L sterile glycerol and shock-freezing in liquid nitrogen. Store the glycerol stocks at –80 °C.

3.2 Tagging of the PVX Genome

1. Digest 25 μ L of each of the plasmids pTRA.PVX.mCherry-2A-CP and pMA-RQ.*NheI*-2xcsy-*NheI* with *NheI* in separate

50 μL reactions for 2 h at 37 °C according to the manufacturer's instructions.

2. Add 1 μL calf intestinal phosphatase to the pTRA.PVX.mCherry-2A-CP *NheI* digest and incubate for 1 h at 37 °C.
3. Purify the digested pTRA.PVX.DsRed-2A-CP with a PCR cleanup kit according to the manufacturer's instructions.
4. Prepare a 2% agarose gel containing 0.05 $\mu\text{L}/\text{mL}$ ethidium bromide.
5. Apply the entire pMA-RQ.*NheI*-2xcsy-*NheI* *NheI* digest to the gel, perform electrophoresis, and excise the 56 bp *NheI*-2xcsy-*NheI* tag band.
6. Purify the *NheI*-2xcsy-*NheI* tag DNA from the excised gel slice using a gel extraction kit, eluting in the smallest volume possible, according to the manufacturer's instructions.
7. Ligate the *NheI*-2xcsy-*NheI* tag into the linearized, dephosphorylated pTRA.PVX.mCherry-2A-CP, using a 10:1 molar insert-to-vector ratio (*see Note 6*) in a total volume of 20 μL with T4 DNA ligase according to the manufacturer's instructions (*see Note 7*).
8. Transform 50 μL XL1 Blue MRF³ cells with 3 μL of the ligation reaction by electroporation, and then incubate cells in 1 mL LB medium without antibiotic at 37 °C for 1 h.
9. Plate 100 μL of the transformation on LB-agar plates containing 100 $\mu\text{g}/\text{mL}$ ampicillin, and incubate overnight at 37 °C.
10. The next day, inoculate several 5 mL aliquots of LB liquid medium containing 100 $\mu\text{g}/\text{mL}$ ampicillin with a well-separated colony each, and incubate overnight at 37 °C with shaking.
11. Purify pTRA.PVX.[2xcsy]_n.mCherry-2A-CP (*see Fig. 1b*) plasmids from each culture using a plasmid miniprep kit according to the manufacturer's instructions.
12. Set up *EcoRI* restriction digests with 2.5 μL of each plasmid DNA in 20 μL total volume according to the manufacturer's instructions and incubate at 37 °C for 1 h.
13. Prepare a 1% agarose gel containing 0.05 $\mu\text{L}/\text{mL}$ ethidium bromide.
14. Separate the whole DNA restriction reaction by agarose gel electrophoresis. Plasmid pTRA.PVX.mCherry-2A-CP should fragment into approximately 0.8, 2.6, and 10.7 kb bands. The insertion of one or more 2xcsy tags will cause the further fragmentation of the 10.7 kb band into approximately 2.1 and 7.7 kb products, which are diagnostic for successful insertions.

15. Verify the presence, number, and orientation of 2xcsy stem-loop tags by DNA sequencing with primer PVX5539F (*see Note 8*).

3.3 Inoculation of *N. benthamiana* with Tagged PVX by Microprojectile Bombardment

1. Thoroughly vortex the ethanol-suspended gold particles until the gold is evenly distributed throughout the solution, visible by the dark color.
2. Immediately pipette 7 μL of the gold suspension into a clean 1.5 mL tube.
3. Add 3 μL of pTRA.PVX.2xcsy.mCherry-2A-CP plasmid DNA and vortex immediately and thoroughly.
4. Add 12 μL of ethanol and vortex immediately and thoroughly.
5. Set the nitrogen gas pressure on the gene gun to 20–25 psi at the regulator valve, and the intensity dial of the trigger to 20.
6. Hold the tube with the DNA-gold mixture by the side with the lid open and vortex. While vortexing, pipet 5 μL DNA-gold mixture and dispense them onto the grid of a Swinnex 13 mm syringe filter holder. Screw the top onto the filter holder, and then screw the filter holder into the nozzle of the gene gun.
7. Place a *N. benthamiana* leaf below the gene gun nozzle so that the lower opening of the cartridge sits 2–3 cm above the leaf. Gently turn the leaf to make the lower surface face upward.
8. Bombard the lower surface twice, moving the leaf a few centimeters in between.
9. For inoculating additional leaves, repeat with a fresh 5 μL aliquot of DNA-gold mixture for each leaf.

3.4 Agro-Infiltration of *N. benthamiana* with Csy4* Expression Plasmids

1. On the same day as the PVX inoculation (Subheading 3.3), inoculate 5 mL LB liquid medium containing 100 $\mu\text{g}/\text{mL}$ spectinomycin and 50 $\mu\text{g}/\text{mL}$ rifampicin with *A. tumefaciens* AGL1 transformed with either pGWB405.Csy4*-GFP or pGWB405.Csy4*-NLS-GFP from a glycerol stock (from Subheading 3.1, step 24) (*see Note 9*), and incubate at 28 °C with shaking for 2–3 days.
2. Also inoculate 5 mL LB liquid medium containing 50 $\mu\text{g}/\text{mL}$ kanamycin and 50 $\mu\text{g}/\text{mL}$ rifampicin with *A. tumefaciens* AGL1 transformed with pDGB3alpha2_35S:P19:Tnos (GB1203) from a glycerol stock, and incubate as above.
3. Centrifuge the liquid cultures at $3000 \times g$ for 15 min to pellet the cells.
4. Decant the liquid medium and resuspend each cell pellet in 2 mL of infiltration buffer.

5. Dilute the *Agrobacterium* suspensions 1:10 in infiltration medium and measure their optical density at 600 nm using a spectrophotometer.
6. Rest cells for 1 h in the dark at room temperature.
7. Adjust the optical density of each (undiluted) *Agrobacterium* suspension to 0.2 using infiltration buffer, and then mix a strain transformed with a Csy4* reporter and the strain carrying p19 1:1, so that the final optical density for each individual AGL1 strain is 0.1.
8. Gently turn a leaf previously inoculated with tagged PVX (Subheading 3.3) to expose the underside, support with your hand, and with extreme care use the 25G needle to pierce only the lower epidermis of the leaf in several spots about 1–2 cm apart (*see* **Note 10**).
9. Fill a 1 mL syringe (without a needle) with the *Agrobacterium* suspension and while supporting the leaf from the opposite side, press the syringe mouth firmly against one of the incisions and depress the plunger of the syringe; the leaf tissue will change color as the air space is filled with the *Agrobacterium* suspension (*see* **Note 11**).
10. Repeat until the entire leaf area has been infiltrated. This requires about 1–2 mL suspension.
11. Label the plant and return to the growth facility for 3–5 days before imaging.

3.5 Visualization of Tagged PVX vRNA in *N. benthamiana* Leaf Epidermal Cells

1. Imaging should be performed 3–4 days after agro-infiltration (Subheading 3.4), and 4–6 days after PVX inoculation (Subheading 3.3).
2. Detach a virus-inoculated and agro-infiltrated leaf from a plant and attach it to a glass slide using double-sided tape with the lower epidermis facing upwards.
3. Image epidermal cells on an upright confocal laser scanning microscope. A 10× long-distance air lens is suitable for identifying mCherry-expressing infection sites. For imaging of sub-cellular vRNA localization, a 40× water-dipping lens is required, with a drop of water placed directly onto the leaf epidermis. Use sequential imaging for optimal channel separation. GFP is excited at 488 nm and detected at 495–525 nm; mCherry is excited at 594 nm and detected at 600–630 nm (*see* **Note 12**).

3.6 Construction of Csy4* Expression Plasmid for RNA Imaging in *N. crassa*

1. Amplify the open reading frames of Csy4* from pDONR221. Csy4* (Subheading 3.1) and mBasicGFP from pLS3 by PCR with primer pairs Csy4-IF-F/Csy4-IF-R and GFP-IF-F/GFP-IF-R, respectively. Use HiFi DNA polymerase according to the

manufacturer's instructions, and NEB Tm Calculator (<https://tcalculator.neb.com>) to select annealing temperatures (see **Note 13**).

2. Amplify a linear recipient vector backbone from pAB261 by PCR with primer pair pAB261-lin-F/pAB261-lin-R, using HiFi DNA polymerase as above.
3. Determine the correct size of the generated amplicons by electrophoresis in a 1% agarose gel containing 0.05 $\mu\text{L}/\text{mL}$ ethidium bromide.
4. Use *DpnI* restriction digestion according to the manufacturer's instructions to remove methylated template plasmids.
5. Purify all DNA amplicons with a PCR cleanup kit according to the manufacturer's instructions.
6. Assemble the three DNA fragments seamlessly *via* their overlapping ends using the NEBuilder Assembly master mix according to the manufacturer's recommendations.
7. Transform 50 μL *E. coli* competent cells with 2 μL NEBuilder reaction using a standard heat shock protocol, and allow cells to recover in 1 mL LB medium without antibiotics for 1 h at 37 °C.
8. Plate 100 μL transformed cells on LB agar plates containing 100 $\mu\text{g}/\text{mL}$ ampicillin and incubate at 37 °C overnight.
9. Identify positive *E. coli* clones by colony PCR with primers Csy4-IF-F/GFP-IF-R and inoculate 5 ml LB liquid medium containing 100 $\mu\text{g}/\text{mL}$ ampicillin with positive colonies; incubate at 37 °C overnight with shaking.
10. Purify resulting pAL13.Csy4*-GFP plasmids from each culture using a plasmid miniprep kit according to the manufacturer's instructions.
11. Confirm correct inserts by DNA sequencing with the primers used to amplify the Csy4* and GFP inserts.

3.7 Construction of the 12xcsy Stem-Loop Knock-In Cassette for RNA Imaging in *N. crassa*

1. Amplify by PCR with HiFi DNA polymerase according to the manufacturer's instructions: (1) A 5' genomic flanking region for homologous recombination comprising the 1 kb sequence upstream from the 3'-end (incl. stop codon) of the desired target gene ORF from genomic DNA (primers NC-xxx-IF-F/NC-xxx-IF-R), (2) the 12xcsy-stem-loop repeat from p35S.PVX.12xcsy.mCherry-2A-CP (primers 12xcsySL-F/12xcsySL-R), (3) the 500–650 bp terminator region of your target gene from genomic DNA (primers NC-Txxx-IF-F/NC-Txxx-IF-R), (4) the hygromycin B resistance cassette from pLS3 (primers Pgpdh-F/Tgpdh-R), (5) a 1 kb 3' genomic flanking region for homologous recombination comprising the terminator region of the desired target gene from genomic

DNA (primers NC-xxx-3'flank-F/NC-xxx-3'flank-R), and (6) the AmpR-ORI fragment from pAL12-Lifeact (primers AmpR-F/ORI-R). Use NEB Tm Calculator (<https://tmcalsculator.neb.com>) to select annealing temperatures.

2. Determine the correct size of the generated amplicons by electrophoresis in a 1% agarose gel containing 0.05 $\mu\text{L}/\text{mL}$ ethidium bromide.
3. Use *DpnI* restriction digestion according to the manufacturer's instructions to remove methylated template plasmids.
4. Purify all DNA amplicons with a PCR cleanup kit according to the manufacturer's instructions.
5. Assemble the six DNA fragments seamlessly via their overlapping ends using the NEBuilder Assembly master mix according to the manufacturer's recommendations. This will place the 12xcsy stem-loops between the stop codon and 3'UTR of your target gene and a hygromycin B expression cassette downstream of the terminator of your target gene (*see* Fig. 1c). The entire cassette for homologous recombination is flanked by *PacI* sites for release from the plasmid backbone.
6. Transform 50 μL *E. coli* competent cells with 2 μL NEBuilder reaction using a standard heat shock protocol, and allow cells to recover in 1 mL LB medium without antibiotics for 1 h at 37 °C.
7. Plate 100 μL transformed cells on LB agar plates containing 100 $\mu\text{g}/\text{mL}$ ampicillin and incubate at 37 °C overnight.
8. Identify positive *E. coli* clones by colony PCR with primers NC-xxx-IF-F/NC-xxx-3'flank-R and inoculate 5 mL LB liquid medium containing 100 $\mu\text{g}/\text{mL}$ ampicillin with positive colonies; incubate at 37 °C overnight with shaking.
9. Purify the resulting pAL15.X-12xcsySL plasmids from each culture using a plasmid miniprep kit according to the manufacturer's instructions.
10. Confirm correct inserts by DNA sequencing with the primers used to amplify the knock-in cassette.

3.8 Preparation of Electrocompetent *Conidia* of *N. crassa* FGSC6103

1. Supplement 100 mL Vogel's minimal medium with 0.5 mg/mL L-histidine in a 500 mL conical flask and inoculate with *N. crassa* strain FGSC6103.
2. Incubate for 3 days at 30 °C in the dark and for another 4–6 days at room temperature on the bench in daylight, until intensively orange conidia have developed.
3. Harvest the conidia by rinsing the flask culture with 40 mL ice-cold 1 M sorbitol and transfer the spore suspension into a 50 mL screw-cap tube.

4. Vigorously vortex the cell suspension for several minutes, and then filter through four layers of sterile Miracloth fixed in a sterile plastic funnel into a fresh 50 mL screw-cap tube.
5. Pellet conidia by centrifugation for 5 min at $600 \times g$ and 4°C , decant supernatant, and keep cell pellet on ice.
6. Wash the conidia twice in 45 mL of ice-cold 1 M sorbitol with centrifugation for 5 min at $800 \times g$ and 4°C , and finally drain off supernatant by inverting the tube onto a paper towel.
7. Resuspend the conidia by gently vortexing the pellet in remaining runoff supernatant which should result in a viscous and deeply orange cell suspension. If it is not possible to properly pipette the cell suspension through a 200 μL pipette tip, dilute with 1 M sorbitol.
8. Prepare 90 μL aliquots in pre-chilled 1.5 mL tubes and keep on ice for immediate use.

3.9 Electro-Transformation of Csy4* Expression Plasmid into *N. crassa*

1. Release the *his3*-targeted Csy4* expression cassette from the pAL13.Csy4*-GFP plasmid (Subheading 3.6) by *SspI/PciI* double digestion according to the manufacturer's instructions (*see Note 14*).
2. Purify DNA with a PCR cleanup kit according to the manufacturer's instructions.
3. Add 10 μL of transforming DNA solution (1 $\mu\text{g}/\mu\text{L}$) to 90 μL of electrocompetent conidia (Subheading 3.8) and incubate for 15 min on ice.
4. Transfer the 100 μL transformation mixture into a pre-chilled (-20°C) electroporation cuvette and remove possible air bubbles from between the electrodes by gently tapping the cuvette on the bench surface.
5. Wipe the outside of the cuvette dry before placing it into the shocking pod and apply one electroshock with the following settings: exponential decay, 1.5 kV with 0.2 cm gap width (resulting in 7.5 kV/cm field strength), 600 Ω and 25 μF (resulting in an optimal time constant of 13.4 ms).
6. Add 900 μL of ice-cold 1 M sorbitol solution into the cuvette immediately after the shock, and transfer the cell suspension back into its original tube and onto ice.
7. Add 1 mL electroporated conidia to 5 mL liquid Vogel's minimal medium supplemented with 0.01 g/mL yeast extract and 50 μM SCR7 pyrazine (*see Note 15*) in a 15 mL screw-cap tube, and incubate for 3 h at 30°C with gentle shaking at 150 rpm (place the tube horizontally into a shaking incubator).

8. Pellet the germlings for 3 min at $700 \times g$, remove the supernatant, and wash once with 5 mL liquid Vogel's minimal medium. Repeat the centrifugation and remove the supernatant.
9. Resuspend the germling pellet in 1 mL liquid Vogel's minimal medium, add into 30 mL liquid (55 °C) Vogel's minimal medium top agar, and then mix by gently inverting the tube 2–3 times.
10. Distribute 5 mL top agar aliquots onto six individual pre-warmed (30 °C) Vogel's minimal medium bottom agar plates and wait for the top agar to solidify.
11. Incubate the plates at 30 °C in the dark, and watch for emerging colonies after 3 days.
12. Transfer emerging colonies onto fresh Vogel's minimal medium agar plates.

3.10 Electro-Transformation of the 12xcsy Stem-Loop Knock-In Cassette into *N. crassa*

1. Release the 12xcsy stem-loop knock-in cassette from the pAL15.X-12xcsySL plasmid (Subheading 3.7) by *PacI* restriction digestion according to the manufacturer's instructions.
2. Purify the DNA with a PCR cleanup kit according to the manufacturer's instructions.
3. Follow the electroporation protocol **steps 3–8** as explained above (Subheading 3.9).
4. Resuspend the germling pellet in 1 mL liquid Vogel's minimal medium, add to 30 mL liquid (55 °C) Vogel's minimal medium top agar supplemented with 50 µg/mL hygromycin B, and then mix by gently inverting the tube 2–3 times.
5. Distribute 5 mL top agar aliquots onto six individual pre-warmed (30 °C) Vogel's minimal medium bottom agar plates supplemented with 250 µg/mL hygromycin B and wait for the top agar to solidify.
6. Incubate the plates at 30 °C in the dark and watch for emerging colonies after 3 days.
7. Transfer emerging colonies onto fresh Vogel's minimal medium agar plates supplemented with 200 µg/mL hygromycin B.

3.11 Visualization of Tagged mRNA in *N. crassa*

1. Pre-culture a medium-size (approx. 4–5 cm diameter) fungal colony of the final transformant strain generated in Subheading 3.10 by incubation on Vogel's minimal medium agar supplemented with 200 µg/mL hygromycin B at 30 °C for 12–14 h.
2. Use the inverted agar block method [25] to mount a $1.5 \times 1.5 \text{ cm}^2$ sample from the colony edge on a glass cover slide using 15 µL of physiological salt solution as mounting medium.

3. Following the standard procedure for the confocal laser scanning microscope in use search the growing hyphae for expression of GFP-tagged Csy4* associated to its cognate stem-loop repeat of the target mRNA.

4 Notes

1. The ORF can be codon-optimized depending on the target organism: see <http://www.kazusa.or.jp/codon/> [26].
2. The restriction sites are chosen so that the one separating the stem-loops does not occur or is unique in the target vRNA, to allow easy identification of tagged constructs by restriction digest. The flanking sites correspond to a unique site in the vRNA where the insertion does not disrupt any open reading frames or regulatory elements. If a different vRNA is to be tagged, sites need to be chosen accordingly. If no suitable insertion site is present, it can be engineered by PCR mutagenesis.
3. Vector pAB261 and the resulting pAL13.Csy4*-GFP are based on the *N. crassa* expression vector pMF272 [27] which contains flanking sequences for homologous integration at the *his-3* locus (NCU03139) of *N. crassa*. Expression of Csy4*-GFP is under the control of the constitutive *Ptef-1* promoter of *N. crassa*.
4. *N. crassa* strain FGSC6103 (see www.fgsc.net strain list) is a histidine auxotrophic mutant due to the truncation of the essential *his-3* locus. Integration of the transformation cassette from pAL13.Csy4*-GFP complements *his-3* and allows selection of positive transformants on standard Vogel's minimal medium, i.e., on medium that is not supplemented with 0.5 mg/mL L-histidine.
5. Transforming bacteria with 2 μ L of a 1:10 dilution of the digested plasmid without re-ligation will provide an estimate of what percentage of colonies is due to incompletely digested plasmid, rather than re-ligation and, thus, approximately how many colonies should be screened to identify clones without the NLS.
6. Increasing the insert/vector ratio will increase, whereas reducing it will decrease, the number of tandem inserts obtained on average, and can be optimized depending on the desired number of inserts. There is no control over the orientation of the insertions, but we have found that the large majority of clones obtained contain all inserts in the same, either sense or anti-sense orientation, though it remains unclear why that is the case.

7. Setting up and transforming a negative control ligation reaction with the same amount of linearized plasmid without insert will provide an estimate of what percentage of colonies is due to incompletely digested or empty re-ligated plasmid and thus approximately how many colonies should be screened to identify tagged clones.
8. A single insertion (two stem-loops) in sense orientation, i.e., with the Csy4 cognate RNA recognition motifs in the (+) sense vRNA, is sufficient for imaging. 2–8 stem-loops (1–4 insertions) are tolerated with little to no attenuation of virus infectivity, whereas the insertion of 12 stem-loops (6 insertions) render the virus noninfectious.
9. Targeting the Csy4* reporter to the nucleus reduces nonspecific cytoplasmic fluorescence, but also reduces overall cytoplasmic signal. Therefore, either Csy4*-NLS-GFP or Csy4*-GFP may be better suited depending on the experiment.
10. Utilizing the side of the needle tip like a scalpel can be helpful to creating incisions that do not pierce entirely through the leaf.
11. Avoid pressing too hard to prevent damage to the leaf. Additionally, face protection may be desired, as if too much pressure is used the *Agrobacterium* suspension can spray back at the user.
12. We find that PVX infection largely suppresses the expression of agro-infiltrated constructs. Optimal imaging conditions, where both virus and Csy4* reporter are present, are therefore most easily found at the leading edge of the growing infection sites. Using a silencing suppressor to boost the expression of Csy4* fusions makes it easier to find suitable imaging conditions. Nevertheless, GFP-expressing cells can also be identified deeper within infection sites. Due to the extremely bright fluorescence of the PVX-expressed mCherry, they may not be visible through the eye piece under UV illumination, but will be apparent in confocal scanning mode.
13. We have found that the presence of an NLS significantly reduces the expression of the Csy4* reporter in *N. crassa*; therefore only the cloning of a cytoplasmic Csy4*-GFP construct is described. With the primers in this protocol, a Gly₁₀ linker is inserted between Csy4* and mBasicGFP.
14. Transformation and subsequent integration into the fungal genome are considerably more efficient when using linearized DNA compared to circular plasmids.
15. SCR7 pyrazine suppresses nonhomologous end-joining (NHEJ) repair of double-strand breaks, thereby significantly increasing the efficiency of homologous recombination for the

targeted integration of transforming DNA fragments [28]. The authors use this as an alternative approach to genetic inhibition of the NHEJ pathway employing $\Delta ku70/\Delta ku80$ ortholog mutants of *N. crassa* which would require backcrossing for strain purification.

Acknowledgments

David Burnett and Alexander Lichius contributed equally to this work.

References

- Chin A, Lécuyer E (2017) RNA localization: making its way to the center stage. *BBA-Gen Subjects* 1861:2956–2970. <https://doi.org/10.1016/j.bbagen.2017.06.011>
- Ryder PV, Lerit DA (2018) RNA localization regulates diverse and dynamic cellular processes. *Traffic* 19:496–502. <https://doi.org/10.1111/tra.12571>
- Suter B (2018) RNA localization and transport. *Biochim Biophys Acta Gene Regul Mech* 1861:938–951. <https://doi.org/10.1016/j.bbagr.2018.08.004>
- Tilsner J, Linnik O, Christensen NM, Bell K, Roberts IM, Lacomme C, Oparka KJ (2009) Live-cell imaging of viral RNA genomes using a pumilio-based reporter. *Plant J* 57:758–770. <https://doi.org/10.1111/j.1365-313X.2008.03720.x>
- Chitwood DH, Nogueira FTS, Howell MD, Montgomery TA, Carrington JC, Timmermans MCP (2009) Pattern formation via small RNA mobility. *Genes Dev* 23:549–554. <https://doi.org/10.1101/gad.177009>
- Zarnack K, Feldbrügge M (2007) mRNA trafficking in fungi. *Mol Gen Genomics* 278:347–359. <https://doi.org/10.1007/s00438-007-0271-8>
- König J, Baumann S, Koepke J, Pohlmann T, Zarnack K, Feldbrügge M (2009) The fungal RNA-binding protein Rrm4 mediates long-distance transport of ubi1 and rho3 mRNAs. *EMBO J* 28:1855–1866. <https://doi.org/10.1038/emboj.2009.145>
- Christensen NM, Oparka KJ, Tilsner J (2010) Advances in imaging RNA in plants. *Trends Plant Sci* 15:196–203. <https://doi.org/10.1016/j.tplants.2010.01.005>
- Chao JA, Lionnet T (2018) Imaging the life and death of mRNAs in single cells. *Cold Spring Harb Perspect Biol* 10:a032086. <https://doi.org/10.1101/cshperspect.a032086>
- Cheong C-G, Tanaka Hall TM (2006) Engineering RNA sequence specificity of pumilio repeats. *Proc Natl Acad Sci U S A* 103:13635–13639. <https://doi.org/10.1073/pnas.0606294103>
- Cerny RE, Qi Y, Aydt CM, Huang S, Listello JJ, Fabbri BJ, Conner TW, Crossland L, Huang J (2003) RNA-binding protein-mediated translational repression of transgene expression in plants. *Plant Mol Biol* 52:357–369. <https://doi.org/10.1023/a:1023953130574>
- Heinrich S, Sidler CL, Azzalin CM, Weis K (2017) Stem-loop RNA labeling can affect nuclear and cytoplasmic mRNA processing. *RNA* 23:134–141. <https://doi.org/10.1261/rna.057786>
- Sternberg SH, Haurwitz RE, Doudna JA (2012) Mechanism of substrate selection by a highly specific CRISPR endoribonuclease. *RNA* 18:661–672. <https://doi.org/10.1261/rna.030882.111>
- Lee HY, Haurwitz RE, Apffel A, Zhou K, Smart B, Wenger CD, Laderman S, Bruhn L, Doudna JA (2013) RNA–protein analysis using a conditional CRISPR nuclease. *Proc Natl Acad Sci U S A* 110:5416–5421
- Shukla S, Dickmeis C, Nagarajan AS, Fischer R, Commandeur U, Steinmetz NF (2014) Molecular farming of fluorescent virus-based nanoparticles for optical imaging in plants, human cells and mouse models. *Biomater Sci* 2:784–797. <https://doi.org/10.1039/c3bm60277j>
- Haurwitz RE, Jinek M, Wiedenheft B, Zhou K, Doudna JA (2010) Sequence- and structure-specific RNA processing by a CRISPR endonuclease. *Science* 329:1355–1358. <https://doi.org/10.1126/science.1192272>

17. Nakagawa T, Suzuki T, Murata S, Nakamura S, Hino T, Maeo K, Tabata R, Kawai T, Tanaka K, Niwa Y, Watanabe Y, Nakamura K, Kimura T, Ishiguro S (2007) Improved Gateway binary vectors: high-performance vectors for creation of fusion constructs in transgenic analysis of plants. *Biosci Biotechnol Biochem* 71:2095–2100. <https://doi.org/10.1271/bbb.70216>
18. Gal-On A, Meiri E, Elman C, Gray DJ, Gaba V (1997) Simple hand-held devices for the efficient infection of plants with viral-encoding constructs by particle bombardment. *J Virol Methods* 64:103–110. [https://doi.org/10.1016/s0166-0934\(96\)02146-5](https://doi.org/10.1016/s0166-0934(96)02146-5)
19. Sarrion-Perdigones A, Vazquez-Vilar M, Palací J, Castelijn B, Forment J, Ziarsolo P, Blanca J, Granell A, Orzaez D (2013) GoldenBraid 2.0: a comprehensive DNA assembly framework for plant synthetic biology. *Plant Physiol* 162:1618–1631. <https://doi.org/10.1104/pp.113.217661>
20. Salzmann L (2017) Generation of live-cell imaging markers for mycoparasitism in *Trichoderma atroviride*. Master Thesis, University of Innsbruck, Austria
21. Berepiki A, Lichius A, Shoji J-Y, Tilsner J, Read ND (2010) F-actin dynamics in *Neurospora crassa*. *Eukaryot Cell* 9:547–557. <https://doi.org/10.1128/EC.00253-09>
22. Tripathy SW, Maharana M, Ithape DM, Lenka D, Mishra D, Prusti A, Swain D, Mohanty MR, Raj KRR (2017) *Int J Curr Microbiol App Sci* 6:951–960. <https://doi.org/10.20546/ijcmas.2017.603.113>
23. Lichius A, Read ND (2010) A versatile set of Lifeact-RFP expression plasmids for live-cell imaging of F-actin in filamentous fungi. *Fungal Genet Rep* 57:8–14. <https://doi.org/10.4148/1941-4765.1070>
24. Vogel HJ (1956) A convenient growth medium for *Neurospora* (Medium N). *Microb Genet Bull* 13:42–43
25. Hickey PC, Swift SR, Roca MG, Read ND (2004) Live-cell imaging of filamentous fungi using vital fluorescent dyes and confocal microscopy. In: Savidge T, Charalabos P (eds) *Microbial imaging, Methods in microbiology*, vol 34. Academic Press, Cambridge, MA, pp 63–87. [https://doi.org/10.1016/S0580-9517\(04\)34003-1](https://doi.org/10.1016/S0580-9517(04)34003-1)
26. Nakamura Y, Gojbori T, Ikemura T (2000) Codon usage tabulated from the international DNA sequence databases: status for the year 2000. *Nucleic Acids Res* 28:292. <https://doi.org/10.1093/nar/28.1.292>
27. Freitag M, Hickey PC, Raju NB, Selker EU, Read ND (2004) GFP as a tool to analyze the organization, dynamics and function of nuclei and microtubules in *Neurospora crassa*. *Fungal Genet Biol* 41:897–910. <https://doi.org/10.1016/j.fgb.2004.06.008>
28. Srivastava M, Nambiar M, Sharma S, Karki SS, Goldsmith G, Hegde M, Kumar S, Pandey M, Singh RK, Ray P, Natarajan R, Kelkar M, De A, Choudhary B, Raghavan SC (2012) An inhibitor of non-homologous end-joining abrogates double-strand break repair and impedes cancer progression. *Cell* 151:1474–1487. <https://doi.org/10.1016/j.cell.2012.11.054>

Part III

Imaging and Analysis of RNA Uptake and Transport Between Cells



Utilizing Potato Virus X to Monitor RNA Movement

Zhiming Yu, Sung Ki Cho, Pengcheng Zhang, Yiguo Hong,
and David J. Hannapel

Abstract

Mobility assays coupled with RNA profiling have revealed the presence of hundreds of full-length non-cell-autonomous messenger RNAs that move through the whole plant via the phloem cell system. Monitoring the movement of these RNA signals can be difficult and time consuming. Here we describe a simple, virus-based system for surveying RNA movement by replacing specific sequences within the viral RNA genome of *potato virus X* (PVX) that are critical for movement with other sequences that facilitate movement. PVX is a RNA virus dependent on three small proteins that facilitate cell-to-cell transport and a coat protein (CP) required for long-distance spread of PVX. Deletion of the CP blocks movement, whereas replacing the CP with phloem-mobile RNA sequences reinstates mobility. Two experimental models validating this assay system are discussed. One involves the movement of the *flowering locus T* RNA that regulates floral induction and the second involves movement of *StBEL5*, a long-distance RNA signal that regulates tuber formation in potato.

Key words *Potato virus X*, RNA mobility assay, *FT*, *BEL5*

1 Introduction

Plants have evolved a unique long-distance signaling system that utilizes cell-to-cell plasmodesmatal connections and a specialized phloem cell network. In addition to its function in the transport of sugars from source to sink organs, the phloem is an important conduit for moving signals that mediate responses to stress and processes of development [1]. Phloem sap profiling has now confirmed that the phloem functions in a dynamic process to deliver signals that respond to internal and environmental cues. Numerous full-length mRNAs have been identified in the sieve element system of several plant species [2–6]. Using heterografts and movement assays, several mRNAs have been identified that are transported through the vascular system. It is now clear that RNA trafficking plays an important role in systemic signaling that controls plant development and defense [7]. Using a heterograft system between

different plant species and RNA-Seq, Notaguchi et al. [8] identified 138 transcripts of *Arabidopsis* that were mobile across an *Arabidopsis*/tobacco graft union. Approximately ten of these were RNAs that encode transcription factors (TFs), including transcripts from a BEL1-like and a KNOX-type TFs. In another study, using variant ecotype transcript profiling in heterografts, 2006 genes producing mobile RNAs were identified in *Arabidopsis* [9]. Many of these mobile transcripts followed the phloem-dependent sugar allocation pathway from leaves to roots, but a high number of transcripts also moved in a root-to-shoot direction. Despite these valuable insights, mobile RNAs with an established function or phenotype are still rare. Some of the best examples of these latter types include *StBEL5*, *-11*, *-29* [10, 11], and *POTH1* [12] of potato; *CmGAI* of pumpkin [13]; *PPF-LeT6* from tomato [14]; and *AUX/IAA* [15], *FLOWERING LOCUS T* (FT), and *CENTRORADIALIS* [16–18] from *Arabidopsis*. Molecular tools for assaying movement are critical for elucidating the function of these numerous phloem-mobile transcripts.

Potato virus X (PVX), a member of the Potexvirus genus, has a positive-sense single-stranded RNA genome encoding five open reading frames (ORFs) [19, 20]. The first ORF at the 5'-terminus encodes the 166 kDa RNA-dependent RNA polymerase gene and the last one at the 3'-terminus for the coat protein (CP). Between them is the triple-gene block of three overlapping ORFs, which encode proteins of 25, 12, and 8 kDa (Fig. 1). These three proteins and the CP are required for cell-to-cell movement, and CP is important for long-distance spread of PVX; but these proteins are dispensable for replication. The p25 protein is also involved in suppression of the antiviral RNA silencing defense mechanism [21]. PVX has been modified as a plasmid vector that is widely used for foreign gene expression and as a functional tool to activate RNA silencing that specifically targets and suppresses foreign RNA invading plant cells [22, 23]. It has also been used to monitor RNA movement [24].

Two mobile RNAs that have been clearly implicated in regulating developmental processes are *FT* in floral induction and *StBEL5* in tuber formation. The regulatory RNA movement sequences have been identified in both. *FT* movement depends on a stretch of 102 nucleotides (nt) present in the coding sequence [24] and for *StBEL5*, the mobility sequence consists of specific cytosine/uracil (CU) motifs present in the 3' untranslated region (UTR) [10, 25, 26]. In potato, specific RNA-binding proteins, designated StPTB1 and StPTB6, bind to the CU motifs present in the 3' UTR to stabilize and mobilize transcripts of *StBEL5* [26]. Based on this information, an RNA mobility assay was developed using the PVX vector to investigate long-distance signaling by *FT* mRNA [16, 24] and *StBEL5* mRNA [10] movement in flowering induction and tuberization, respectively. In both cases, deletion of the coat

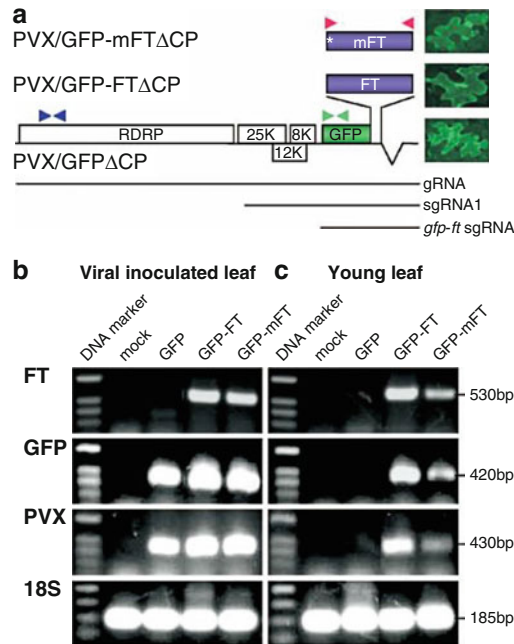


Fig. 1 PVX-based FT RNA mobility assay (RMA). **(a)** PVX-based PVX 7.0 kb genomic gRNA, 2.6 kb subgenomic sgRNA1, and 1.4 kb GFP-FT sgRNA are indicated. The coat protein (CP) gene was deleted. PVX functions with the RNA-dependent RNA polymerase (RDRP), an enzyme that catalyzes the replication of RNA from a RNA template. The positions of a stop codon (*) replacing FT start codon in PVX/GFP-mFT Δ CP, and three sets of primers for detection of FT (red arrows), GFP (green arrows), and PVX (blue arrows) RNAs are indicated. Individual epidermal cells expressing free GFP or GFP-FT fusion proteins show green fluorescence. **(b and c)** RT-PCR analysis of FT, GFP, and PVX RNA and 18S ribosomal RNA in inoculated and newly growing systemic young leaves, including shoot apices of *N. benthamiana*. RNAs were extracted from leaves of plants mock inoculated (mock) or inoculated with PVX/GFP Δ CP (GFP), PVX/GFP-FT Δ CP (GFP-FT), or PVX/GFP-mFT Δ CP (GFP-mFT). The 1.0 Kb DNA ladder and sizes of RT-PCR products are indicated. This experiment demonstrates that wild-type or mutated FT mRNA (* panel **a**) can promote the long-distance spread of PVX/GFP-FT Δ CP (GFP-FT), or PVX/GFP-mFT Δ CP (GFP-mFT), respectively, from virus-inoculated source leaves to systemic new leaves. This figure is taken from Li et al. [24] with permission of the publisher

protein gene (PVX/ Δ CP) or (PVX/GFP Δ CP) resulted in immobile PVX. Insertion of key *FT* or *StBEL5* sequences into the RNA genome of PVX/ Δ CP or PVX/GFP Δ CP, however, led to recovery of movement-deficiency of PVX/GFP-FT Δ CP (Fig. 1) or PVX/BEL5 Δ CP (Fig. 2).

Here, we describe the PVX-based RNA movement assay to identify RNA sequences that facilitate movement, using the *FT* (Fig. 1) or *StBEL5* (Fig. 2) model systems as examples. This protocol outlines easy steps for cloning the target RNA as cDNA into the

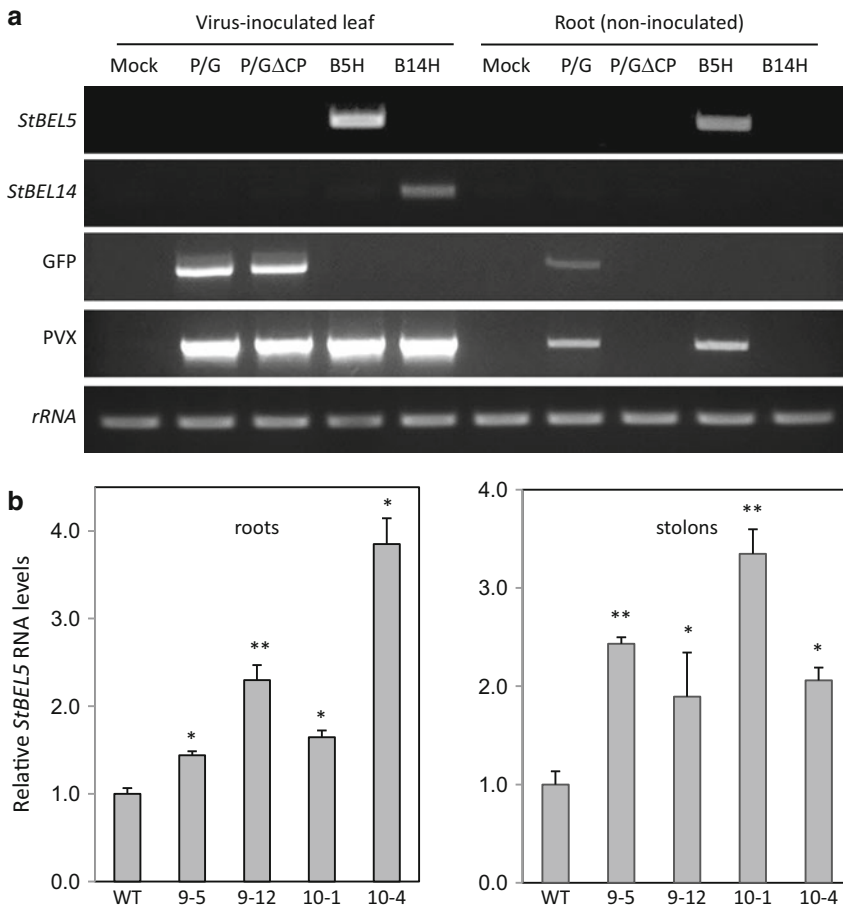


Fig. 2 Analysis of RNA movement using a PVX-vector system in WT potato cultivar Désirée **(a)**. PVX-based *StBEL5* RNA (full length plus both UTRs) movement into target roots and stolons of StPTB transgenic over-expression lines, 8d post-viral inoculation of leaves **(b)**. *StBEL5* RNA movement is enhanced in correlation with StPTB1 and –6 over-expression [26]. StPTB1 and –6 are RNA-binding proteins that bind to specific motifs present in the 3' untranslated region of *StBEL5* RNA [26]. No movement is observed for the nonmobile control RNA, *StBEL14* **(a)**. RNA was extracted and quantitative real-time RT-PCR with gene-specific primers was used to calculate the relative amounts of *StBEL5* RNA **(b)**. For RT-qPCR, the qScript One-Step SYBR Green qRT-PCR kit (Quanta Biosciences) with the Eco Real-Time PCR system (Illumina) was used. Each sample was measured and normalized against *StActin8* RNA. RNA values were calculated as the $2^{-\Delta\Delta Ct}$ value relative to the mean values obtained from WT samples [27]. StPTB1 and –6 OE lines are designated #9 and #10, respectively. Standard deviations of the means of two biological replicates with two technical replicates are shown with one and two asterisks indicating significant differences ($p < 0.05$, $p < 0.01$, respectively) using a Student's *t*-test. For panel **a**, mock, inoculation with water; P/G, PVX vector with coat protein and GFP (mobile); P/GΔCP, PVX vector with GFP but no coat protein (nonmobile); B5H, PVX vector with full-length *StBEL5* plus histidine tag but no GFP or coat protein; B14H, PVX vector with full-length *StBEL14* plus histidine tag but no GFP or coat protein. Ribosomal RNA (rRNA) was used as a loading control in panel **a**. This figure was used in accordance with a copyright agreement with Oxford University Press [26]

virus vector using RT-PCR. Upon linearization, the RNA is synthesized to large scale by using *in vitro* transcription. The RNA of interest is then incorporated into tobacco leaves through direct inoculation to be tested for mobility. Gel-based analysis of the RT-PCR product can be used to confirm movement of any RNAs of interest (Fig. 1). Quantitative RT-PCR (RT-qPCR) is utilized to monitor RNA movement or test elements that mediate movement. This simple protocol may be used for any RNA sequence of interest to assess its capacity for long-distance transport from source leaves to distal target organs.

2 Materials

Prepare all solutions using high-purity deionized water and analytical grade reagents. Prepare and store all reagents at room temperature unless otherwise noted. Follow all safety regulations when disposing of waste or biohazardous materials.

2.1 Plasmid Preparation

1. Sterile distilled water.
2. RNase-free water.
3. Bovine serum albumin (BSA).
4. Phenol.
5. Chloroform.
6. 3.0 M NaAc (sodium acetate) pH 5.2.
7. PVX/CP vector (obtained from Yiguo Hong).
8. PVX/ Δ CP vector (obtained from Yiguo Hong).
9. *Mlu*I enzyme (10 units/ μ L).
10. *Mlu*I 1 \times buffer: 100 mM NaCl, 50 mM Tris-HCl, 10 mM MgCl₂ 100 μ g/mL BSA (pH 7.9).
11. *Eco*RV enzyme (20 units/ μ L).
12. *Eco*RV 1 \times buffer: 100 mM NaCl, 50 mM Tris-HCl, 10 mM MgCl₂ 100 μ g/mL BSA (pH 7.9).
13. *E. coli* strain **DH5 α** .

2.2 *In Vitro* Transcription and RT-qPCR

1. Total RNA extraction kit.
2. RNase-free DNase: 30 Kunitz units per RNA prep.
3. 10 \times DNase buffer: 100 mM Tris-HCl, 25 mM MgCl₂, 5.0 mM CaCl₂ (pH 7.6).
4. 70% Ethanol.
5. 100% Ethanol.
6. One-Step SYBR Green Master Mix.
7. qScript One-Step Reverse Transcriptase.

8. High-Fidelity PCR Master Mix.
9. *SpeI* enzyme (10 units/ μ L).
10. *SpeI* 10 \times reaction buffer: 500 mM Potassium acetate, 200 mM Tris-acetate, 100 mM magnesium acetate, 100 μ g/mL BSA (pH 7.9).
11. RNasin (40 units/ μ L).
12. NTP mix: 20 mM each of ATP, CTP, UTP, and 2.0 mM GTP.
13. 20 mM GTP.
14. 5.0 mM Cap analog (m7GpppG).
15. T7 RNA polymerase (50 units/ μ L).
16. TBE: 90 mM Tris-borate/2.0 mM EDTA, pH 8.0.
17. Appropriate gene-specific primers for selected mobile RNAs.

2.3 Plant Inoculation and Molecular Analysis of RNA Long-Distance Trafficking

1. *Nicotiana benthamiana* seeds.
2. 6-in. plastic pots.
3. Carborundum dust.
4. Agarose.

2.4 Equipment

1. Bench-top microcentrifuge.
2. Real-time PCR thermocycler.
3. 37 °C Incubator.
4. Growth chamber.
5. NanoDrop spectrophotometer.

3 Methods

3.1 Cloning into the PVX Vector

The coat protein (CP) of PVX is required for PVX movement and without it, the PVX RNA is immobile. PVX vectors with and without the coat protein have been previously designed and tested [23, 24]. Without its CP, PVX cannot move systemically in infected plants and it has been shown that replacing the CP with phloem-mobile RNA sequences reinstates systemic mobility [24, 26]. The purpose of this section is to prepare RNA sequences of interest (ROI) and to clone derived cDNA into the CP-deficient PVX vector to determine if the ROI contains sequences for systemic transport and thus for mobilizing PVX for systemic infection. The PVX plasmid vectors (PVX/CP with CP and PVX/ Δ CP without CP) can be obtained from the co-author, Yiguo Hong. The protocol involves the cloning of derived cDNA (from the ROI) into the multiple cloning site (MCS) just downstream of the three viral movement proteins (Fig. 1). This cDNA represents ROI from the gene sequence of interest (GOI). It is the GOI that is cloned into

the MCS of the PVX vector. In most cases, the GOI is not a full-length gene (Fig. 1). This cloning strategy was used for the BEL RNAs of potato (Fig. 2), *StBEL5* (mobile) and *StBEL14* (nonmobile). These were cloned after RT-PCR amplification into the *Mlu*I and *Eco*RV sites of the PVX/ Δ CP vector to create PVX/BEL5 RNA Δ CP and PVX/BEL14 RNA Δ CP fusions [26]. Figure 1 shows PVX/ Δ CP constructs in which FT RNA was fused to the RNA for GFP (designated PVX/GFP-FT Δ CP), thus allowing the monitoring of the mobilized viral RNA via fluorescence emitted from the encoded GFP protein. Inclusion of the GFP fusion is not critical for the movement assay and will not be discussed in this protocol. Only cloning of the cDNA of the ROI into the *Mlu*I and *Eco*RV sites of the PVX/ Δ CP vector will be described here (Fig. 3).

1. Extract RNAs from selected plant samples expressing your ROI using a commercial kit following the manufacturer's protocol (*see Note 1*).
2. To prevent genomic DNA contamination, treat two micrograms of purified RNA with RNase-free DNase. Mix 2 μ g of RNA with 10 μ L 10 \times DNase buffer and 1 μ L DNase (30 units) and bring volume to 100 μ L with sterile distilled water.

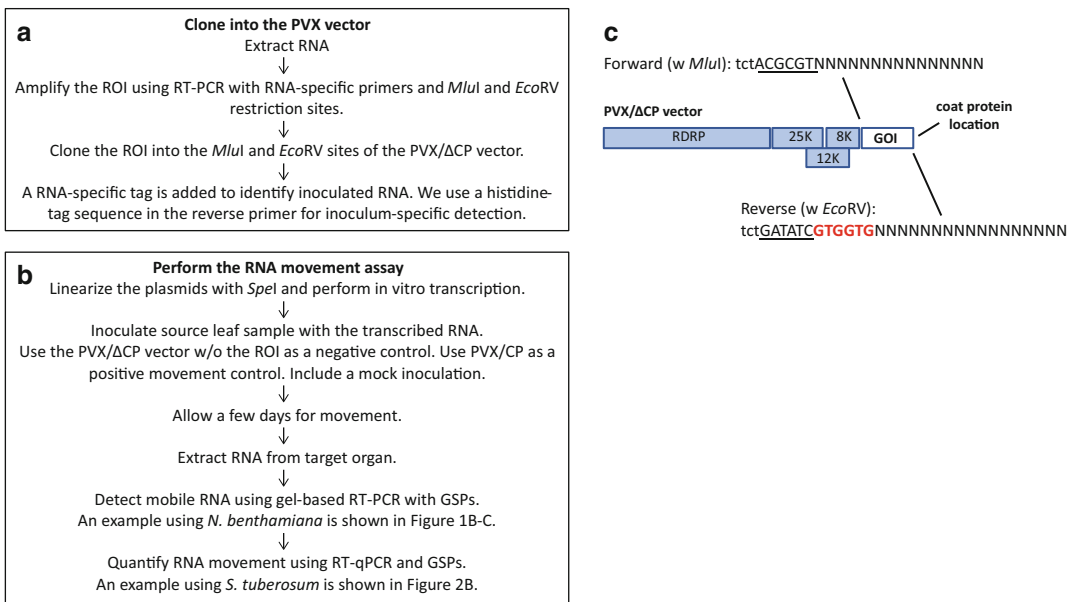


Fig. 3 Summary of the cloning and inoculation strategy for the RNA movement assay (**a** and **b**). The coat protein (CP) of PVX is required for PVX movement and without it, the PVX RNA is immobile. The PVX plasmid vectors discussed in this protocol are designated PVX/CP (plus CP) and PVX/ Δ CP (minus CP), respectively [23]. Primer design for cloning a cDNA from the ROI into PVX/ Δ CP (**c**). The forward primer contains the *Mlu*I site (underlined) and gene-specific sequence (N). The reverse primer contains the *Eco*RV site (underlined), a histidine tag (in red), and gene-specific sequence (N). ROI, RNA of interest; RDRP, RNA-dependent RNA polymerase; 25 K, 12 K, and 8 K represent three proteins required for PVX function; GOI, gene sequence of interest; GSPs, gene-specific primers. Both vectors may be obtained by request from the co-author, Yiguo Hong

3. Mix gently and centrifuge briefly for $1000 \times g$.
4. Incubate at $37\text{ }^{\circ}\text{C}$ for 20 min.
5. Add 100 μL 1:1 phenol/chloroform, vortex for 30 s, and centrifuge at $16,000 \times g$ at $25\text{ }^{\circ}\text{C}$ for 3 min.
6. Transfer 100 μL of the upper aqueous phase to a new 1.5 mL tube.
7. Add 100 μL chloroform, vortex for 30 s, and centrifuge at $16,000 \times g$ at $25\text{ }^{\circ}\text{C}$ for 3 min.
8. Transfer 100 μL of the upper aqueous phase to a new 1.5 mL tube.
9. Add 10 μL of 3 M NaAc (pH 5.2) (0.1 volume of the total water phase) and 250 μL of 100% ethanol (2.5 volumes of the total water phase) and mix well.
10. Centrifuge at $16,000 \times g$ at $25\text{ }^{\circ}\text{C}$ for 15–20 min.
11. Carefully discard the supernatant, add 100 μL of 70% ethanol to wash the small pellet (do not pipette or vortex), and centrifuge at $16,000 \times g$ at $25\text{ }^{\circ}\text{C}$ for 5 min.
12. Carefully remove the supernatant with a pipette and allow the pellet to air-dry for 5–10 min.
13. Dissolve RNA in 40 μL RNase-free water (pH 7.0). RNA is now ready for amplification by RT-PCR.
14. For amplification, set up a 15 μL RT-PCR reaction by adding 7.5 μL of One-Step SYBR Green Master Mix and 0.3 μL of qScript One-Step Reverse Transcriptase to 50 ng of the isolated plant RNA and 200 nM of GOI-specific forward and reverse primers. Use GOI primers designed to contain the DNA sequence encoding the RNA to be tested, the appropriate restriction site for cloning into the PVX vector (*Mlu*I and *Eco*RV sites), and a gene-specific tag to distinguish leaf-inoculated mRNA from WT RNA. We use a histidine-tag sequence in the reverse primer for inoculum-specific detection (Fig. 3). Use standard PCR thermocycling conditions.
15. Clone the amplified cDNA of the ROI into the *Mlu*I and *Eco*RV sites within the MCS of the PVX vector using standard cloning methods.
16. Transform the recombinant plasmid DNA into *E. coli* strain DH α . Grow the bacteria under ampicillin selection and isolate the plasmid DNA using a miniprep kit from any commercial source. We commonly use the Qiagen miniprep kit, but other commercial brands are suitable.
17. Verify the plasmid by DNA sequencing.
18. Measure the concentration of the plasmid DNA with a nano-drop spectrophotometer using standard methods.

3.2 Preparation of Linear DNA Template for In Vitro Transcription

The purpose of this part of the protocol is to linearize the recombinant DNA template in preparation for in vitro transcription. Include both negative (PVX/ Δ CP) and positive (PVX/CP) RNA movement controls.

1. Mix 10 μ L of 10 \times *SpeI* restriction enzyme buffer with 10 μ L of 10 \times BSA (1 mg/mL), 10.5 μ g of plasmid DNA, and 3 μ L of *SpeI* (10 units/ μ L) with sterile distilled water to make 100 μ L in total.
2. Incubate at 37 °C for 3 h.
3. Add an equal volume (100 μ L) of phenol/chloroform, vortex for 30 s, and centrifuge at 16,000 $\times g$ at 25 °C for 3 min.
4. Transfer 100 μ L of the upper aqueous phase to a new 0.5 mL tube.
5. Repeat steps 3 and 4.
6. Add an equal volume (100 μ L) of chloroform, vortex for 30 s, and centrifuge at 16,000 $\times g$ at 25 °C for 3 min.
7. Transfer 100 μ L of the upper aqueous phase to a new 1.5 mL tube.
8. Add 10 μ L of 3 M NaAc (pH 5.2) (0.1 volume of the total water phase) and 250 μ L of 100% ethanol (2.5 volumes of the total water phase), mix well, incubate at -70 °C for at least 1 h, and centrifuge at 16,000 $\times g$ at 25 °C for 15–20 min.
9. Carefully discard the supernatant, add 100 μ L of 70% ethanol to wash the small pellet (do not pipette or vortex), and centrifuge at 16,000 $\times g$ at 25 °C for 5 min.
10. Carefully pipette out the supernatant and dissolve the small pellet in 40 μ L sterile distilled water to make a final concentration of 0.25 μ g/ μ L linearized plasmid DNA.

3.3 In Vitro Transcription (See Note 2)

This section outlines the steps for in vitro transcription of the linearized DNA to produce high-quality RNA inoculum for plant infection and monitoring RNA mobility.

1. Mix 10 μ L of linearized PVX DNA containing the RNA of interest (0.25 μ g/ μ L) with 20 μ L RNase-free water, 5 μ L 10 \times buffer, 1 μ L RNasin (40 units/ μ L), 5 μ L 10 \times NTPs (20 mM each of ATP, CTP, UTP, 2.0 mM GTP), and 5 μ L of 5 mM Cap analog (m7GpppG). Include linearized control plasmids for PVX/CP and PVX/ Δ CP. RNAs transcribed from these plasmids will provide positive (+CP) and negative (no CP) controls, respectively.
2. Incubate at 37 °C for 5 min.
3. Add 4 μ L of T7 RNA polymerase (50 units/ μ L) to the mixture.
4. Incubate at 37 °C for 25 min.

5. Add 5 μL of 20 mM GTP.
6. Incubate at 37 °C for 35 min.
7. Add 45 μL of 10 mM Tris, pH 8.5, to the mixture.
8. Purify the in vitro-transcribed RNA by following **steps 5** through **12** of the protocol described under Subheading **3.1**.
9. Dissolve the RNA in 40 μL RNase-free water (pH 7.0). RNA is now ready for plant inoculation.

3.4 Plant Inoculation and Molecular Analysis of RNA Long-Distance Trafficking Using RT-PCR

This section describes the inoculation of plant leaves with the in vitro-transcribed RNA and analysis of transported RNA by RNA isolation and RT-PCR.

1. Sow *Nicotiana benthamiana* seeds on soil in 6-in. plastic pots.
2. Cover the soil with transparent film (*see Note 3*).
3. Germinate the seeds in a growth chamber with the temperature at 25 °C under 16-h light/8-h dark and allow plantlets to grow for approximately 14 days.
4. Transfer individual plantlets to individual pots and keep plants growing under the same conditions.
5. At the six-leaf stage and with plants still in the growth chamber, apply a thin layer of fine carborundum onto two small leaves (*see Note 4*).
6. Drop 5 μL of RNA transcripts prepared by in vitro transcription (*see Subheading 3.3*) onto each of the two carborundum-dusted small leaves.
7. Wear clean gloves and gently rub the RNA droplet across the entire lamina of the leaves.
8. Spray water onto the inoculated plants (*see Note 5*).
9. Incubate plants in a growth chamber at 25 °C under 16-h light/8-h dark for 7–14 days.
10. Collect the inoculated leaves and samples of target organs for RNA extraction (*see Note 6*). Pool samples from three independent plants each of (1) inoculated leaves and other organs and (2) the same leaves of non-inoculated or buffer-inoculated control plants. Repeat **steps 7–12** including tissue sampling two times to create samples from a total of three biological replicate experiments (*see Note 7*).
11. Extract RNAs from samples using a commercial kit following the manufacturer's protocol (*see Note 1*).
12. Use 150 ng total RNA from each sample for RT-PCR assays using a commercial kit (*see Note 8*).
13. Using a UV light source, visualize the amplified products resolved by agarose gel electrophoresis through a 1.2% agarose gel in TBE buffer (Figs. **1b, c**, and **2a**).

3.5 Quantifying RNA Movement

The following section describes how to quantify RNA movement using the PVX movement assay. For effective monitoring of movement, the ROI-containing viral RNA should be tagged to distinguish it from native, plant-encoded RNA (Fig. 3). RT-qPCR reactions with gene-specific primers are utilized to score RNA levels in both the source leaf and the target organ. Control and test reactions will provide quantitative data on the movement of viral RNA with and without the ROI. Results may be interpreted with a simple statistical test for significance (*see* Fig. 2 for an example).

1. Clone and tag transcribed RNAs to be inoculated with a unique sequence to distinguish them from native transcripts (*see* **Notes 9** and **10**; Fig. 3).
2. Perform inoculation, harvest of samples, and RNA extraction as described in Subheading 3.4, **steps 1–11**. In addition to RNA samples from plants inoculated with the ROI-expressing virus, RNA samples should include control samples derived from plants inoculated with (1) water, (2) PVX vector with its coat protein (mobile), and (3) the PVX vector with no coat protein and without the ROI (nonmobile).
3. Treat two micrograms of each RNA samples with RNase-free DNase (*see* Subheading 3.1, **steps 2–13**).
4. Set up RT-qPCR reactions by combining 50 ng of total DNA-free RNA sample with 7.5 μ L of One-Step SYBR Green Master Mix, 0.3 μ L of qScript One-Step Reverse Transcriptase, and target-specific primers (200 nM) in a total volume of 15 μ L.
5. Perform qPCR reactions with a real-time PCR thermocycler (*see* **Note 11**). All reactions should be performed in triplicate with internal standards for normalization (detection of RNA transcripts of “housekeeping” genes, such as *Actin8* or *GAPDH* using gene-specific primers). Fast quantitative PCR cycling parameters for complementary DNA (cDNA) synthesis are 50 °C, 5 min. Taq activation: 95 °C for 2 min, followed by 40 cycles of 95 °C for 15 s and 60 °C for 30 s. Conditions for qPCR may vary slightly depending on the primer design and the internal standard employed.
6. Check PCR specificity using melting curve analysis and calculate RNA values as the $2^{-\Delta\Delta C_t}$ value relative to the mean values of control samples [27]. Obtain standard deviations of the means of three biological replicates with two technical replicates and implement statistical analysis using the Student’s *t*-test using GraphPad Prism (6.0 version) [28].

4 Notes

1. Kits may be purchased from Qiagen, Promega, Ambion, Biolabs, Invitrogen, or any other numerous commercial kits available. We used the Qiagen Plant RNeasy Purification Kit.
2. Add each of the individual components as described in this protocol. There are in vitro transcription kits available from different companies. We assemble reaction components using reagents purchased from Biolabs and Promega, which are less expensive.
3. This step is important to maintain high humidity to increase seed germination.
4. Avoid applying too much carborundum on leaves. Excessive contact can lead to severe damage of leaves after finger-rubbing them during inoculation.
5. This minimizes desiccation and enhances the inoculation.
6. Plant material may be stored at -80°C for later use.
7. Leaf inoculation also works well on potato cultivars.
8. For RT-PCR, kits may be purchased from Qiagen, Promega, Ambion, Biolabs, Invitrogen, or any other company. We commonly use the One-Step RT-PCR kit from Promega or the Next High-Fidelity $2\times$ PCR Master Mix from NEB. Using the same commercial kit for all RT-PCR assays ensures consistency and quality control.
9. See Table S5 in the Supplemental files of [26] for examples of primers designed for the quantitative analysis of a mobile RNA, *StBEL5*, and an immobile negative control, *StBEL14*, by RT-qPCR.
10. In the example shown in Fig. 2, reverse primers for creation of the *StBEL* constructs were designed to include a histidine-tag sequence for specific ROI detection (Fig. 3).
11. For RT-qPCR, we commonly use the qScript One-Step SYBR Green qRT-PCR kit (Quanta Biosciences) with the Eco Real-Time PCR thermocycler (Illumina). However, any other RT-qPCR real-time system may be used.

Acknowledgments

This work was in part funded by Ministry of Science and Technology of China (National Key R&D Program 2017YFE0110900), Ministry of Agriculture of China (National Transgenic Program 2016ZX08009001-004), the National Natural Science Foundation of China (31872636, 31370180), Zhejiang Provincial Natural

Science of Foundation (LY19C020002), Hangzhou Normal University (Sino-EU Plant RNA Signaling S&T Platform Initiative 9995C5021841101), and a NSF Plant Genome Research Program award no. DBI-0820659 to DH.

References

- Lucas WJ, Groover A, Lichtenberger R, Furuta K, Yadav SR, Helariutta Y, He XQ, Fukuda H, Kang J, Brady SM, Patrick JW, Sperry J, Yoshida A, López-Millán AF, Grusak MA, Kachroo P (2013) The plant vascular system: evolution, development and functions. *J Integr Plant Biol* 55:294–388
- Asano T, Masumura T, Kusano H, Kikuchi S, Kurita A, Shimada H, Kadowaki K (2002) Construction of a specialized cDNA library from plant cells isolated by laser capture microdissection: Toward comprehensive analysis of the genes expressed in the rice phloem. *Plant J* 32:401–408
- Vilaine F, Palauqui JC, Amselem J, Kusiak C, Lemoine R, Dinant S (2003) Towards deciphering phloem: a transcriptome analysis of the phloem of *Apium graveolens*. *Plant J* 36:67–81
- Omid A, Keilin T, Glass A, Leshkowitz D, Wolf S (2007) Characterization of phloem-sap transcription profile in melon plants. *J Exp Bot* 58:3645–3656
- Deeken R, Ache P, Kajahn I, Klinkenberg J, Bringmann G, Hedrich R (2008) Identification of *Arabidopsis thaliana* phloem RNAs provides a search criterion for phloem-based transcripts hidden in complex datasets of microarray experiments. *Plant J* 55:746–759
- Gaupels F, Buhtz A, Knauer T, Deshmukh S, Waller F, van Bel AJE, Kogel KH, Kehr J (2008) Adaptation of aphid stylectomy for analyses of proteins and mRNAs in barley phloem sap. *J Exp Bot* 59:3297–3306
- Lough TJ, Lucas WJ (2006) Integrative plant biology: role of phloem long-distance macromolecular trafficking. *Annu Rev Plant Biol* 57:203–232
- Notaguchi M, Higashiyama T, Suzuki T (2015) Identification of mRNAs that move over long distances using a RNA-Seq analysis of *Arabidopsis/Nicotiana benthamiana* heterografts. *Plant Cell Physiol* 56:311–321
- Thieme CJ, Rojas-Triana M, Stecyk E, Schudoma C, Zhang W, Yang L, Miñambres M, Walther D, Schulze WX, Paz-Ares J, Scheible WR, Kragler F (2015) Endogenous *Arabidopsis* messenger RNAs transported to distant tissues. *Nat Plants* 1:15025
- Banerjee AK, Chatterjee M, Yu Y, Suh SG, Miller WA, Hannapel DJ (2006) Dynamics of a mobile RNA of potato involved in a long-distance signaling pathway. *Plant Cell* 18:3443–3457
- Ghate TH, Sharma P, Khondare KR, Hannapel DJ, Banerjee AK (2017) The mobile RNAs, StBEL11 and StBEL29, suppress growth of tubers in potato. *Plant Mol Biol* 93:563–578
- Mahajan A, Bhogle S, Kang IH, Hannapel DJ, Banerjee AK (2012) The mRNA of a Knotted1-like transcription factor of potato is phloem mobile. *Plant Mol Biol* 79:595–608
- Haywood V, Yu TS, Huang NC, Lucas WJ (2005) Phloem long-distance trafficking of gibberellic acid-insensitive RNA regulates leaf development. *Plant J* 42:49–68
- Kim M, Canio W, Kessler S, Sinha N (2001) Developmental changes due to long distance movement of a homeobox fusion transcript in tomato. *Science* 293:287–289
- Notaguchi M, Wolf S, Lucas WJ (2012) Phloem-mobile Aux/IAA transcripts target to the root tip and modify root architecture. *J Integr Plant Biol* 54:760–772
- Li C, Gu M, Shi N, Zhang H, Yang X, Osman T, Liu Y, Wang H, Vatissh M, Jackson S, Hong Y (2011) Mobile FT mRNA contributes to the systemic florigen signalling in floral induction. *Sci Rep* 1:73
- Lu KJ, Huang NC, Liu YS, Lu CA, Yu TS (2012) Long-distance movement of *Arabidopsis* flowering locus T RNA participates in systemic floral regulation. *RNA Biol* 9:653–662
- Huang NC, Jane WN, Chen J, Yu TS (2012) *Arabidopsis* centroradialis homologue acts systemically to inhibit floral initiation in *Arabidopsis*. *Plant J* 72:175–184
- Baulcombe D, Gilbert J, Goulden M, Köhm B, Cruz SS (1994) Molecular biology of resistance to potato virus X in potato. *Biochem Soc Symp* 60:207–218
- Lico C, Benvenuto E, Baschieri S (2015) The two-faced potato virus X: from plant pathogen to smart nanoparticle. *Front Plant Sci* 6:1009

21. Van Wezel R, Hong Y (2004) Virus survival of RNA silencing without deploying protein-mediated suppression in *Nicotiana benthamiana*. *FEBS Lett* 562:65–70
22. Hong Y, Saunders K, Stanley J (1997) Transactivation of dianthin transgene expression by African cassava mosaic virus AC2. *Virology* 228:383–387
23. Van Wezel R, Dong X, Liu H, Tien P, Stanley J, Hong Y (2002) Mutations of three cysteine residues in Tomato yellow leaf curl virus-China C2 protein causes dysfunction in pathogenesis and posttranscriptional gene silencing suppression. *Mol Plant-Microbe Interact* 15:203–208
24. Li C, Zhang K, Zeng X, Jackson S, Zhou Y, Hong Y (2009) A cis element within Flowering Locus T mRNA determines its mobility and facilitates trafficking of heterologous viral RNA. *J Virol* 83:3540–3548
25. Banerjee AK, Lin T, Hannapel DJ (2009) Untranslated regions of a mobile transcript mediate RNA metabolism. *Plant Physiol* 151:1831–1843
26. Cho SK, Sharma P, Butler NM, Kang IH, Shah S, Rao AG, Hannapel DJ (2015) Polypyrimidine tract-binding proteins of potato mediate tuberization through an interaction with StBEL5 RNA. *J Exp Bot* 66:6835–6847
27. Livak KJ, Schmittgen TD (2001) Analysis of relative gene expression data using real-time quantitative PCR and the 2^{(-Delta Delta C (T))} method. *Methods* 25:402–408
28. Wirjanata G, Handayani I, Zaloumis SG, Chalfein F, Prayoga P, Kenangalem E, Poesprodjo JR, Noviyanti R, Simpson JA, Price RN, Marfurt J (2016) Analysis of ex vivo drug response data of *Plasmodium* clinical isolates: the pros and cons of different computer programs and online platforms. *Malar J* 15:137



A Protocol for Non-biased Identification of RNAs Transferred Between Heterologous Mammalian Cell Types Using RNA Tagging, Cell Sorting, and Sequencing

Sandipan Dasgupta and Jeffrey E. Gerst

Abstract

Intercellular communication is a major hallmark of multicellular organisms and is responsible for coordinating cell and tissue differentiation, immune responses, synaptic transmission, and both paracrine and endocrine signaling, for example. Small molecules, peptides, and proteins have all been studied extensively as mediators of intercellular communication; however, RNAs have also been shown recently to transfer between cells. In mammalian cells, microRNAs, tRNAs, short noncoding RNAs, mRNA fragments, as well as full-length mRNAs have all been shown to transfer between cells either by exosomes or by membrane nanotubes. We have previously described nanotube-mediated cell-cell transfer of specific mRNAs between heterologous mammalian cell types cultured *in vitro*. Here, we describe a simple method for the unbiased and quantitative identification of the complete range of transferred mRNAs (i.e., the mRNA transferome) in one population of mammalian cells following co-culture with another population. After co-culture, the individual cell populations are sorted by magnetic bead-mediated cell sorting and the transferred RNAs are then identified by downstream analysis methods, such as RNA sequencing. Application of this technique not only allows for determination of the mRNA transferome, but can also reveal changes in the native transcriptome of a cell population after co-culture. This can indicate the effect that co-culture and intercellular transfer of mRNA have upon cell physiology.

Key words mRNA, MS2, MS2-binding sequence, β -Actin, Magnetic sorting, MACS, RNA sequencing, Co-culture, RNA transfer, Membrane nanotubes, miRNA, lncRNA

1 Introduction

Multicellular organisms are complex entities composed of multiple cell types and to ensure functional operation of the organism the various cell types need to communicate with one another. The languages in which cells talk to each other include those of secreted peptides and proteins (e.g., hormones, cytokines, chemokines, cell adhesion molecules), small molecules (e.g., nitric oxide, carbon monoxide, neurotransmitters, steroids), and nucleic acids (e.g., DNA). In addition, it has been recently shown that RNAs can be

used to transfer information between cells [1, 2]. The gamut of transferred RNAs includes microRNAs (miRNAs), tRNAs, small noncoding RNAs (sncRNAs), Y RNAs, long noncoding RNAs (lncRNAs), fragments of mRNAs, and full-length mRNAs [3–14]. RNAs have been shown to undergo transfer by both contact-independent (i.e., via extracellular vesicles, such as exosomes) and contact-dependent routes (i.e., via long thin cytoplasmic projections called membrane nanotubes; mNTs) [13–15]. The transfer of RNAs has been shown to affect the transcriptome of downstream acceptor cells by either miRNA or lncRNA regulation or direct transfer of mRNA [8, 10, 13, 16, 17]. Although several studies profiled the RNAs contained in the exosomes by employing DNA microarrays or RNA sequencing (RNA-seq), no systematic study has been done to identify the transferred RNAs present in downstream acceptor cells after transfer [18–20]. Hence, the scope of RNA transfer has not been fully understood due to the lack of unbiased and quantitative approaches to study transferred RNAs.

In our work, we have demonstrated the direct intercellular transfer of full-length mRNAs in a contact-dependent manner, via mNTs [13]. mNT-mediated mRNA transfer was observed between adherent mammalian cells in culture, including between heterologous cell types [e.g., mouse embryonic fibroblasts (MEFs), HEK293, U2OS, and HeLa cells] and cell states (i.e., primary-primary, primary-immortalized, and immortalized-immortalized). mRNA transfer largely correlated with gene expression and, while a number of mRNAs were shown to undergo transfer (e.g., mouse β -actin and human cyclin D1, BRCA1, MT2A), we employed MS2 aptamer-tagged mouse β -actin (β -actin-MBS) to show that transfer is mNT (and not EV) mediated, regulated by stress, and can be visualized using either single-molecule fluorescent in situ hybridization (smFISH) or live imaging using the MS2 coat protein fused to GFP. While numerous questions abound, the intercellular transfer of mRNA appears to be a common phenomenon of adherent cells in in vitro culture. However, before determining whether this phenomenon also occurs in vivo it is important to first examine the extent of transfer, i.e., which species of mRNAs undergo transfer, and at what levels, and whether transferred mRNAs have common *cis*-acting determinants that allow for their selection for transfer to, and translation in, acceptor cells.

In this chapter, we put forth a simple method to elucidate the entire spectrum of transferred RNAs after the co-culture of two heterologous cell populations (i.e., “donor” and “acceptor” cells) in a non-biased and quantitative fashion. Briefly, donor and acceptor cell lines are cultured together in the same dish, following which the different cell types are sorted into their component cell populations using cell surface antigen-based magnetic sorting. Total RNA from the sorted populations is collected and checked for integrity and quality, and the RNA samples are subjected to RNA-seq to

identify the transferred RNAs, as well as to measure the native transcriptome of the acceptor cell. As a negative control, donor and acceptor monocultures are mixed together after harvesting and immediately sorted prior to RNA-seq analysis. A pre-validated transferred mRNA is used as a positive control using reverse transcription-polymerase chain reaction (RT-PCR) to first check for the efficiency of cell sorting. This protocol is scalable to allow for the rapid collection of large numbers of cells and can be applied to study RNA transfer in systems having multiple cell types both in vitro (e.g., organoids) and in vivo (e.g., tumor or tissue samples) (see **Notes 1** and **2**).

2 Materials

The following protocol is established for the co-culture of 3×10^6 human and mouse cells each per biological replicate (see **Note 3**). In this protocol, the following specific cell types used are:

1. Mouse embryonic fibroblasts (MEFs) tagged with 24 repeats of the MS2 coat protein (MCP)-binding sequence (MBS) RNA aptamer between the ORF and the 3' UTR of both endogenous alleles of β -actin (referred to here as “MBS-MEFs”) (see Fig. 1 and [21]): The β -actin-MBS gene serves as a specific marker for the MEFs, while its message serves as a marker for RNA transfer to the recipient human cells.

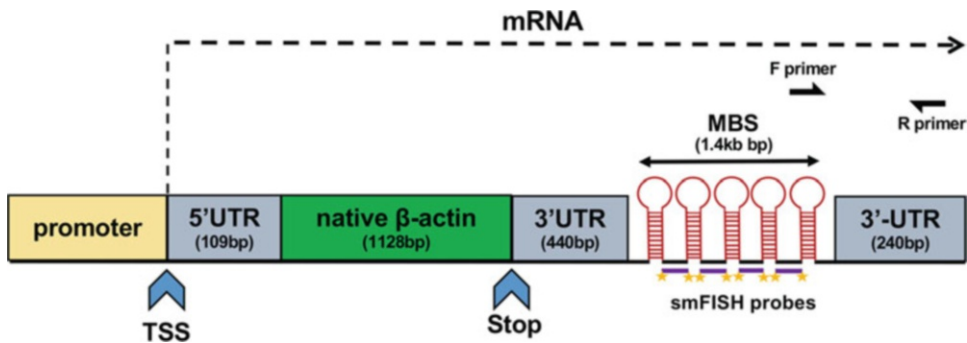


Fig. 1 Schematic of the MS2 aptamer-tagged β -actin alleles expressed in MBS-MEFs. A schematic representing aptamer tagging of both genomic loci of the mouse β -actin gene by insertion of MBS sequence in the 3'UTR [21]. The MBS sequence consists of 12 repeats of a unit, each unit consisting of a dimer of MS2 stem-loops and three linker regions, thus containing 24 MS2 stem-loops in total. This MBS sequence is inserted 441 bp downstream of the stop codon of β -actin ORF. The expressed mRNA is shown as dashed arrow. Fluorescent (Cy3)-labeled DNA probes complementary to the linker regions between each dimer of MS2 stem-loops are used to detect β -actin-MBS mRNA by single-molecule FISH [21]. Forward (F) and reverse (R) primers to detect the presence of the β -actin-MBS gene, as well as the smFISH probes are illustrated. TSS, transcription start site; stop, stop codon; UTR, untranslated region; MBS, MS2 bacteriophage stem-loop sequence/MS2 coat protein-binding sequence

2. Human breast carcinoma (MCF7) cells:

Although the protocol does not depend on using tagged RNAs, we strongly recommend to check the efficiency of the sorting protocol by verifying the transfer of a *bona fide* transferred mRNA. In this protocol, β -actin-MBS mRNA is used as a model transferred mRNA from MBS-MEF (donor) to MCF7 (acceptor) cells.

It is important to note that the protocol can be adapted for use with other pairs of heterologous adherent mammalian cells, as well as with other co-culture models (*see* **Notes 1** and **2**). In addition, the protocol can be scaled up to sort a higher number of cells, as per the intended design of the experiment. If available, use of a pre-validated transferred mRNA is highly recommended to determine the efficiency of transfer.

2.1 Cell Culture

1. Dulbecco's modified Eagle medium (DMEM) high-glucose culture medium.
2. Composite penicillin-streptomycin antibiotic solution: 10,000 units/mL penicillin G, 10 mg/mL streptomycin.
3. 11 mg/mL (100 mM) Sodium pyruvate solution.
4. European-grade fetal bovine serum.
5. Trypsin-EDTA solution: 0.25% Trypsin, 0.02% EDTA.
6. 150 mm Sterile cell culture dishes.
7. 0.5–1 mg/mL Fibronectin from bovine plasma: Dilute the stock solution of fibronectin to a working solution of 0.5 μ M in warm PBS.
8. 1 \times Phosphate-buffered saline (PBS): 0.137 M NaCl, 0.0027 M KCl, 0.01 M Na₂HPO₄, 0.0018 M KH₂PO₄.
9. Hemocytometer or cell counter.

2.2 Magnetic Sorting

1. 15 mL Volume conical tubes.
2. 40 μ m Nylon cell strainer.
3. Temperature-controlled centrifuge for spinning 15 mL volume tubes.
4. MidiMACS Separator for separating up to 10⁹ cells (Miltenyi Biotec).
5. MACS MultiStand (Miltenyi Biotec).
6. LS Columns (Miltenyi Biotec).
7. Human CD326 (epithelial cell adhesion molecule; EpCAM) magnetic microbeads (Miltenyi Biotec).
8. Alexa Fluor[®] 488-labeled anti-human CD326 (EpCAM) antibody (Biolegend).
9. 7-Aminoactinomycin D (7-AAD) for monitoring cell viability.

10. Flow cytometer with 488 nm and 560 nm filters for detection of green and red fluorescence (or as is appropriate for the fluorophore used).
11. Sorting buffer: 0.5% Bovine serum albumin (BSA), 2 mM EDTA, in PBS, pH 7.2, degassed and cooled to 4–8 °C before use.
12. Complete culture media (DMEM, supplemented with sodium pyruvate and penicillin-streptomycin), cooled to 4–8 °C before use.
13. R-phycoerythrin (PE)-anti-mouse CD321 (Jam1) antibody (BD-Pharmingen).

2.3 RNA Extraction and Quality Control

1. Commercial RNA extraction kit for extracting up to 100 µg of total RNA.
2. NanoDrop microvolume spectrophotometer.
3. Agilent TapeStation (for checking RNA integrity).

2.4 Reverse Transcription-Polymerase Chain Reaction

1. 1.7 mL Microcentrifuge tubes.
2. 200 µL PCR tubes.
3. Commercial RNase-free DNase I kit.
4. First-strand cDNA synthesis kit.
5. Commercial PCR mix, consisting of Taq polymerase, reaction buffers, and dNTP mixture.
6. PCR thermal cycler.
7. Primers to detect the transfer of a validated mRNA: In this protocol, forward and reverse primers were designed to specifically detect the MS2 aptamer-tagged β -actin mRNA, which is known to transfer from MBS-MEFs to MCF7 cells and serves as a positive control for the transfer of RNA (Fig. 1).
8. Molecular biology-grade agarose.
9. SB running buffer: 0.8% NaOH, 4.5% boric acid (H_3BO_3) in double-distilled water (DDW).
10. Ethidium bromide.
11. Power supply (300 V).

2.5 Deep Sequencing

1. Library preparation kit: The kit is selected with respect to the experimental design in mind (i.e., detection of the transfer of mRNA, miRNA, or lncRNA). For example, commercial kits for the preparation of the different types of RNA for sequencing are available.
2. Sequencing kit and the platform, selected according to experimental design.

3 Methods

An overall scheme of the experiment is given in Fig. 2.

3.1 Cell Culture and Harvesting

The following protocol is written for a co-culture of 3×10^6 MBS-MEFs and MCF7 cells each to be cultured in a single 150 mm petri dish. A typical total RNA yield for such a plate is 30–50 μg —for a larger amount of RNA the number of plates can be increased proportionately.

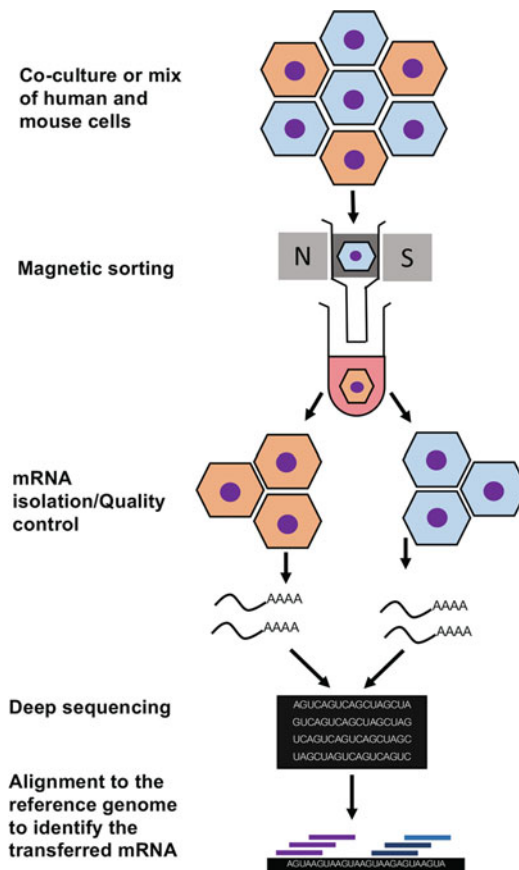


Fig. 2 Schematic representation of magnetic bead-based sorting and RNA detection to identify mRNAs transferred between two cell types. Human and mouse (e.g., MCF7 cells and MBS-MEFs, respectively) are either co-cultured or only mixed before cell sorting. The heterologous cell population is then sorted using magnetic microbeads conjugated to antibodies (e.g., anti-CD326) specific to one of the two cell types (i.e., human MCF7 cells in this case). The sorted cells are then analyzed by RNA-sequencing to identify the transferred RNAs. *N* north pole of the magnetic column; *S* south pole

3.1.1 Preparation of Culture Medium and Fibronectin-Coated Plates

1. Prepare complete culture medium to reach a final concentration of 10% FBS, 1% sodium pyruvate solution, and 1% penicillin-streptomycin solution in DMEM.
2. Coat the 150 mm dishes with fibronectin: Rinse the 150 mm dishes with 10 mL PBS. Add 10 mL of the fibronectin working solution to each dish and incubate at 37 °C for 20 min. After incubation, rinse the dish with 10 mL PBS.

3.1.2 Preparation of “Mix” Control Samples

As a control for the transfer of RNA between cells in co-culture, we strongly recommend having a negative control of the two cell types mixed together (“mix”) and immediately sorted (*see* Subheading 3.2). Proceed as follows:

1. Culture the different cell types in fibronectin-coated dishes, prepared as described in Subheading 3.1.1.
2. Harvest the separately cultured MBS-MEF and MCF7 cells by trypsinization for 5 min (we recommend using 3 mL trypsin-EDTA added per plate) at 37 °C.
3. Neutralize trypsin-EDTA by adding 3–5 mL of complete DMEM medium.
4. Pass the cell suspension through a 40 µm cell strainer.
5. Count cells by a hemocytometer or cell counter and mix 3×10^6 cells of each cell type in a pre-chilled 15 mL tube (*see* **Note 4**).
6. (Optional, but highly recommended) At this point, in order to check for the efficiency of sorting, an aliquot of approximately $5\text{--}10 \times 10^4$ of the “mix” cell populations can be saved for analysis by flow cytometry.
7. Spin down the cells in a centrifuge at $350 \times g$ for 10 min at 4 °C and aspirate the medium carefully.
8. Resuspend the cells in 400 µL of cold DMEM and proceed to magnetic bead-mediated cell sorting.

3.1.3 Preparation of “Co-culture” Samples

1. Harvest one cell type, which can be designated as the “acceptor” cells, from a standing culture (e.g., here we chose MCF7 cells, *see* **Note 5**). Following trypsinization, neutralize by adding complete DMEM, and count the cells using a hemocytometer or automatic cell counter (*see* **Note 6**).
2. Add 3×10^6 MCF7 cells to 20 mL complete medium in a fibronectin-coated dish and incubate for 3–4 h.
3. After 3–4 h, add 3×10^6 cells of the “donor” line (e.g., here we chose the MBS-MEFs) to the same dish and co-culture for the required duration of time. For example, we found that 12 h of co-culture leads to the transfer of ~2% of β-actin-MBS mRNA from MBS-MEFs to MCF7 cells (*see* **Note 7**).

4. Harvest the co-culture by incubating with 3 mL trypsin-EDTA solution at 37 °C for 5 min followed by neutralization with 3–5 mL of complete medium.
5. Pass the cell suspension through a 40 µm cell strainer.
6. (Optional, but highly recommended) In order to check for the efficiency of cell sorting, an aliquot of $\sim 5\text{--}10 \times 10^4$ cells of the “co-culture” sample can be saved for analysis by flow cytometry.
7. Spin down the cells in a centrifuge at $350 \times g$ for 10 min at 4 °C and aspirate the media carefully.
8. Resuspend the cells in 400 µL of cold DMEM and proceed to magnetic bead-mediated cell sorting.

3.2 Magnetic Bead-Mediated Cell Sorting

1. Add human CD326-conjugated magnetic microbeads to cell suspensions prepared above (Subheadings 3.1.2 and 3.1.3). In the current protocol, MCF7 cells display surface antigen CD326 (EpCAM). By using microbeads conjugated to anti-CD326 antibodies, the MCF7 cells can be selected for and the MBS-MEF cells, which do not possess the CD326 surface marker, selected against. Use the microbeads at a concentration recommended by the manufacturer.
2. Incubate the cell suspension as per the manufacturer’s instructions. For anti-CD326 microbeads, the recommended duration is 30 min on ice.
3. After 30 min of incubation, attach the MidiMACS Separator to the MACS MultiStand.
4. Insert the LS Column into the MidiMACS Separator and add 3 mL of cold complete media or the sorting buffer to the LS column. Allow the media/buffer to elute through the column into a tube placed underneath the separator.
5. Place a 15 mL tube under the separator to collect the eluate (the negatively selected fraction of the cells, i.e., the MBS-MEF cells in this case).
6. Add the cell suspension (after incubation with the microbeads) to the separator and let it pass through the column.
7. Wash the column twice with 1 mL of ice-cold medium or sorting buffer. Remove the tubes with the eluate and keep on ice (*see Note 4*).
8. Place another 15 mL tube under the separator to collect the positively selected fraction of cells from the suspension (i.e., the MCF7 cells in this case).
9. Add 3 mL of cold medium/sorting buffer to the column. **Immediately** recover the positive fraction with the help of a plunger (as supplied with the column, *see Note 8*).
10. (Optional) In order to check for the efficiency of cell sorting, an aliquot of $\sim 5\text{--}10 \times 10^4$ cells of the sorted cell populations

corresponding to the “mix” and “co-culture” samples can be saved for analysis by flow cytometry.

11. Place the tubes on ice and spin down the cells at $350 \times g$ for 10 min at 4 °C.
12. Aspirate the supernatant and flash-freeze until RNA extraction or proceed to RNA extraction immediately.
13. Purify total RNA using a kit of choice according to the manufacturer’s instructions (*see Note 9*). Quantify total RNA using a Nano Drop microvolume spectrophotometer. Treatment with DNase is NOT recommended if intending to check the sorting efficiency later (*see Subheading 3.3.2*).

3.3 Quality Control for Cell Sorting

3.3.1 Quality Control for Cell Sorting by Flow Cytometry

We recommend two methods to determine the efficiency of sorting—by flow cytometry and by DNA-PCR.

As mentioned in the previous section, aliquots of samples—“mix” and “co-culture”—obtained both before and after sorting can be saved for analysis by flow cytometry. It is helpful if the cells used have a genetic fluorescent marker (e.g., GFP, RFP). If such cell line is not available, the cells can be counterstained using an antibody against a specific surface marker suitable for flow cytometry. If both cells express fluorescently labeled proteins (i.e., in two different excitation and emission spectra), they can be directly analyzed by a flow cytometer. If even one type of the cells requires labeling with an antibody, the following steps can be followed as described below:

1. Prepare cell suspensions having between 5 and 10×10^5 cells in 50–100 μL of complete culture (DMEM) medium or sorting buffer.
2. Add the first antibody (per the recommended dilution) and incubate on ice for 30 min (if the first antibody is fluorescently labeled, incubation should be performed in the dark).
3. Spin down the cells at $350 \times g$ for 5 min at 4 °C. Wash twice by resuspending the cells in 500 μL of cold medium and spinning down at $350 \times g$ for 5 min at 4 °C after each wash.
4. Add the second antibody (per the recommended dilution) and incubate on ice for 30 min in the dark.
5. Spin down the cells at $350 \times g$ for 5 min at 4 °C. Wash once by resuspending in 500 μL of cold medium and spinning down at $350 \times g$ for 5 min at 4 °C. Resuspend the cells in 500 μL of cold medium.
6. Incubate with 0.25 μg PI or 7-AAD per 10^6 cells for 10 min at room temperature.
7. Transfer to FACS tubes and analyze on a flow cytometer. *See Fig. 3a* for representative results.

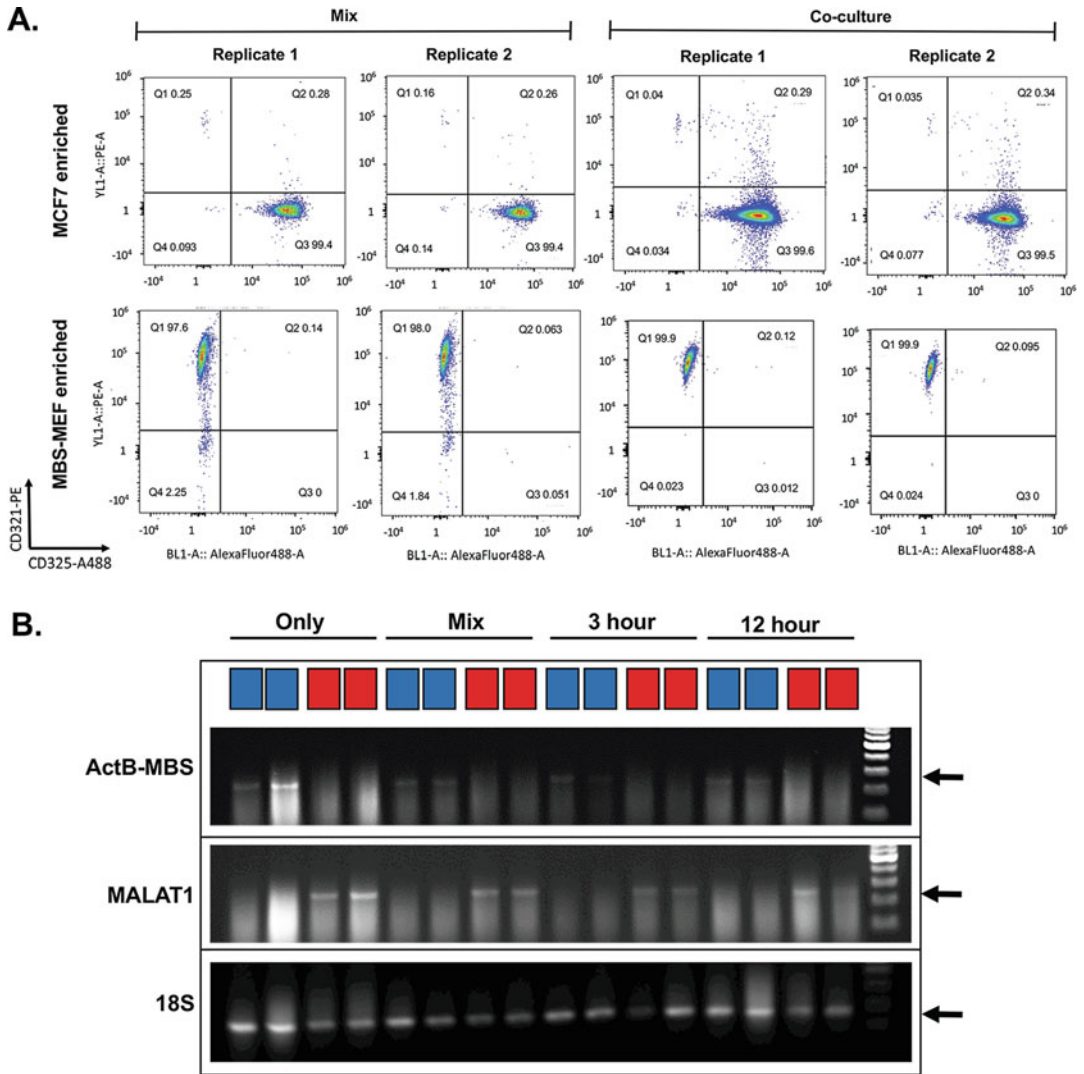


Fig. 3 Sorting of MBS-MEF and MCF7 cells using magnetic beads. **(a)** Flow cytometry data to determine the efficiency of magnetic bead-mediated sorting. An equal number of unlabeled MCF7 cells and MBS-MEFs that expressed a red membrane marker (palmitoylated TagRFP) were either mixed or co-cultured for 12 h in two replicates. Afterwards, they were magnetically sorted according to the presence of the CD326 cell surface antigen only on MCF7 cells and not on MEFs. Post-sorting, the cell suspensions were counterstained with a CD326-Alexa 488 and CD321-PE antibodies that label specifically MCF7 and MBS-MEF cell, respectively. The unsorted and sorted cell populations were analyzed by flow cytometry using the Alexa Fluor-488 and PE windows. The left-hand panels show the profile of mixed and co-cultured cells prior to cell sorting. After quantification, the MBS-MEF-enriched samples (bottom panels) were found to be 99.86% pure, while the MCF7 cells (top panels) were sorted to 99.91% purity (for “co-culture”) and 99.7% purity (for “mix”). **(b)** Verification of the sorting by DNA-PCR. MBS-MEF and MCF7 cells cultured as monocultures (*Only*), mixed in equal proportions without co-culture (*Mix*), and co-cultured for 3 or 12 h (*3 h* and *12 h*) were sorted and RNA was extracted from the samples. After the extraction of total RNA (and without treating the samples with DNase), DNA-PCR was performed for 25 cycles to determine the purity of the sorted MBS-MEF and MCF7 cells. Test amplicons specific for each cell type were chosen (e.g., the sequence corresponding to the MBS-3’UTR junction of β -actin-MBS

3.3.2 Quality Control
for Cell Sorting by
DNA-PCR

As mentioned above, total RNA extracted from the “mix” and “co-culture” samples contains genomic DNA contaminants, as they have not been treated with DNase I. Therefore, DNA amplification by PCR can be readily used to check the efficiency of sorting, in addition to flow cytometry method described above.

1. Choose test amplicons for genes specific to the different cell types. For example, in the co-culture system of MBS-MEF and MCF7 cells, we use forward and reverse primers that can specifically detect either the MBS-3'UTR junction sequence of the β -actin-MBS gene (present only in MBS-MEF cells) or the human MALAT1 (present only in MCF7 cells). Thus, we expect that the purified mouse cell fractions should contain only the β -actin-MBS band (and not MALAT1), while purified human cell fractions should have only the MALAT1 band (and not β -actin-MBS). Presence of MALAT1 in the mouse cell fraction and β -actin-MBS in the human cell fraction indicates that the samples are not pure. This may result in a high occurrence of nonspecific reads during deep sequencing (*see Note 10*).
2. Set up the PCR reaction in a 20 μ L reaction volume using gene-specific primer pairs described above (i.e., \sim 20 bp each, 50–60% GC content and melting temperature 55–60 $^{\circ}$ C), as recommended by the manufacturer of PCR reaction mix employed. The following calculation for reaction mix can be used as a reference: premade PCR mix—at a concentration recommended by the manufacturer; forward and reverse primers—final concentration of 0.8 μ M; and genomic DNA template—1 μ L; fill the rest of the reaction volume with nuclease-free water to 20 μ L.
3. Perform the reaction according to the following conditions: melting—95 $^{\circ}$ C for 30 s; annealing—55–60 $^{\circ}$ C for 1 min; elongation—72 $^{\circ}$ C for 1 min; and number of recommended cycles—less than 30. We recommend 28 cycles to reduce the nonspecific amplification.
4. Check the amplification results by running the reaction in a 1% (w/v) agarose gel for 20 min at 200 V prior to staining with ethidium bromide. *See Fig. 3b* for representative results.

Fig. 3 (continued) gene is used to test for MBS-MEFs (Fig. 1) and a human specific long noncoding RNA gene, MALAT1, for MCF7 cells). 18S rRNA was amplified as an internal control. As expected, the β -actin-MBS band was detected only in mouse cells, while MALAT1 was detected only in human cells, indicating a high degree of purity of magnetic sorting. Blue boxes—MBS-MEF mouse cells, red boxes—MCF7 human cells

3.4 RT-PCR Verification of RNA Transfer (Optional)

If a validated RNA which is known to undergo transfer is available, it can be used as a positive control for the experiment. For example, in the co-culture system of MBS-MEF cells and MCF7 cells, we know that β -actin-MBS mRNA transfers from mouse to human cells. Using sm-FISH, we detected about 30 copies of β -actin-MBS mRNA (~2% of donor mRNAs) that are transferred from MBS-MEF to MCF7 by 12 h of co-culture (Fig. 4). Thus, the transferred β -actin-MBS mRNA is expected to be present in the human cell fraction after sorting post-co-culture. The transfer can be verified using reverse transcription and polymerase chain reaction (RT-PCR) with specific primers to detect the presence of β -actin-MBS mRNA.

1. Treat 1–5 μ g of total RNA with about 2 Units DNase I in an appropriate buffer for 30 min at 37 °C (or as per the manufacturer's instructions).
2. Perform reverse transcription to produce the cDNA by using 1–5 μ g of DNase-treated total RNA and random hexamers as provided in the cDNA preparation kit, as per the manufacturer's protocol.
3. Set up the PCR reaction in a 20 μ L reaction volume with primers specific for the gene whose mRNA is known to be transferred (i.e., ~20 bp each, 50–60% GC content and melting temperature 55–60 °C) as recommended by the manufacturer of the PCR mix. Forward and reverse primers can be used at a final concentration of 0.8 μ M per 2 μ L from the reverse-transcribed RNA used as template.
4. Perform the reaction according to the following conditions: melting—95 °C for 30 s; annealing—55–60 °C for 1 min; elongation—72 °C for 1 min; and number of recommended cycles—23–28. We recommend performing the PCR reaction in the semiquantitative range to reduce the amplification of nonspecific bands (*see Note 11*).
5. Check the amplification results by running the reaction in a 1% (w/v) agarose gel for 20 min at 200 V prior to staining with ethidium bromide. *See Fig. 5* for representative results.

3.5 Bioanalyzer Analysis and Deep Sequencing

Prior to sending RNA samples for deep sequencing, it is highly recommended to check the quality and integrity of the RNA samples using a bioanalyzer. We use and recommend the Agilent TapeStation 2200 system, as per the manufacturer's recommended protocol. The output of the analysis is in the form of the **RNA Integrity Number (RIN)**. Typically, RIN scores of >8 are good for sequencing experiments.

Finally, for the sequencing of the RNA samples, it is recommended to choose a library preparation kit, sequencing kit, and platform based on the overall objective of the experiment. In

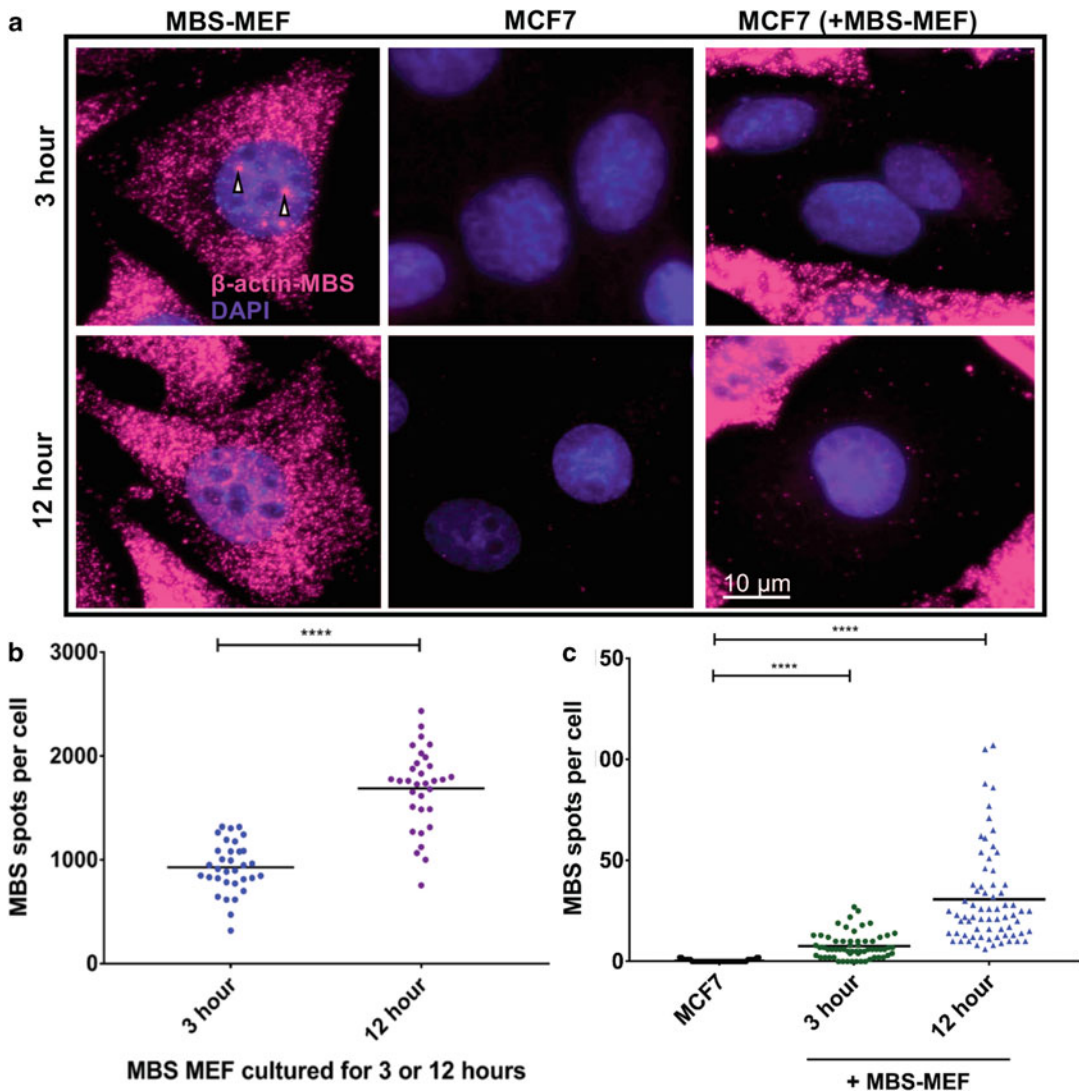


Fig. 4 Detection of β -actin-MBS mRNA transferred from MBS-MEF to MCF7 cells by smFISH. Donor cells (MBS-MEFs) were co-cultured with MCF7 cells together in the ratio of 1:1 for either 3 or 12 h according to the protocol previously described [13, 27]. Following co-culture, the cells were fixed and smFISH was performed using Cy3-labeled oligonucleotide probes specific for the MBS sequence (see Note 7). The transfer of mRNAs was detected by wide-field microscopy and quantified using a MATLAB program, FISH-Quant [28]. (a) smFISH images. Representative smFISH images of MBS-MEF and MCF7 single cultures, and MCF7 cells in co-culture with MBS-MEFs after either 3 or 12 h of co-culture. Labels: magenta, Cy3-labeled MBS probes; blue, DAPI staining of the nucleus. Donor and acceptor cells were distinguished by the presence of brightly labeled transcription sites (arrowheads) in the nucleus of the donor MBS-MEF cells only. (b) Distribution of β -actin-MBS mRNA in donor MBS-MEF cells. Donor MBS-MEFs were cultured alone for either 3 or 12 h and the endogenous level of β -actin-MBS mRNA transcription was detected by smFISH. Each dot in *b* (and *c*) represents the number of β -actin-MBS mRNAs detected in a single cell, as measured by FISH-Quant. Horizontal lines represent the average number of mRNAs detected in a given condition (c) Distribution of β -actin-MBS mRNA in MCF7 cells alone or in co-culture with MBS-MEFs for 3 or 12 h. As shown, at 3 h co-culture, on average, only 7 copies of mRNAs are transferred ($\sim 0.7\%$ of endogenous mRNAs in donor) while at 12 h, about 30 copies are transferred ($\sim 2\%$ of endogenous mRNAs in donor). Details of number of cells scored, average number of spots (mRNA scored), and *P*-values are given in Table 1

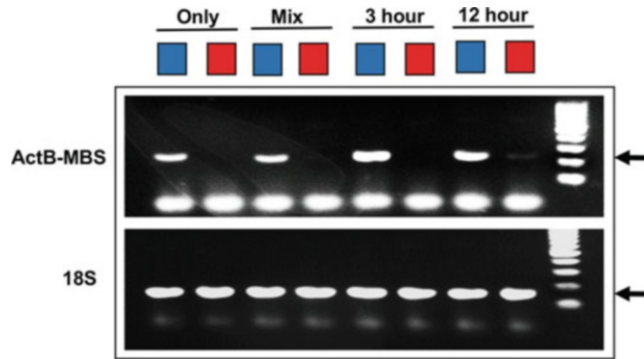


Fig. 5 Validation of RNA transfer by RT-PCR. The transfer of β -actin-MBS mRNA from MBS-MEFs to MCF7 cells in co-culture was validated by RT-PCR. Total RNA from one replicate of each of the “Only,” “Mix,” “3 h,” and “12 h” conditions was collected for analysis by semiquantitative RT-PCR (22 cycles) using primers specific for β -actin-MBS. 18S rRNA was amplified as an internal control. Blue box—mouse cells, red box—human cells. A band corresponding to β -actin-MBS RNA can be seen in the MCF7 cells after 12 h of co-culture, but not in the Mix or in the 3-h co-culture experiment, indicating that the transfer of mRNA (indicated) is detected only after 3 h. This is in good agreement with smFISH data shown in Fig. 4

Table 1
smFISH quantification of MS2-aptamer-tagged beta-actin mRNA in cells under mono- and co-culture conditions

Image	Sample/columnn	Number of cells scored	Average number of MBS spots per cell	P-value
4B	MBS-MEF - 3 h	33	927.8	
	MBS-MEF - 12 h	32	1687.3	<0.00001 ^a
4C	MCF7	48	0.3	
	MCF7 (+MBS-MEF) 3-h co-culture	62	7.6	<0.00001 ^b
	MCF7 (+MBS-MEF) 12-h co-culture	69	30.6	<0.00001 ^c

P-values calculated from Mann-Whitney U test between:

^aMBS-MEF alone (3 h) and MBS-MEF alone (12 h)

^bMCF7 (+MBS-MEF)—3-h co-culture and MCF7 cells alone

^cMCF7 (+MBS-MEF)—12-h co-culture and MCF7 cells alone

general, if a high degree of specificity is desired, it is recommended to use long, paired-end reads. If the query RNAs are less abundant, sequencing at a higher level of coverage is preferred. For example, transferred RNAs in vitro typically represent <2% of the total for a given species of RNA in MEFs (Fig. 4) [14]. Thus, given the

relative rarity of transferred RNAs it is highly recommended to sequence on the order of 100–150 million paired-end reads that are at least 75 bp in length. However, that can be adapted based on the particular experimental design (*see Note 12*).

Another point to be considered is the length and type of fragment (single or paired ends). Due to the high degree of homology between the human and mouse transcriptomes, using suboptimal length reads may lead to the mapping of human reads to the mouse genome and vice versa. To determine the optimum length and type of fragment end, we did an *in silico* simulation of mapping 25, 50, 75, and 100 bp long single- and paired-end reads from the human transcriptome to the mouse transcriptome. We observed that 25 bp, single-end reads have a very high (>85%) nonspecific alignment with the mouse genome (Fig. 6 and Table 2). This nonspecific alignment decreases drastically when using longer reads. A similar analysis was done for mouse reads aligned to the human genome. Based on this analysis, we recommend using 75 bp paired-end reads when performing human-mouse cell co-cultures.

3.6 Identification of Transferred RNAs

To identify human RNAs transferred from MCF7 to MBS-MEF cells, the sequenced reads from MBS-MEF-enriched fraction of the “co-culture” sample are aligned to the human reference genome (e.g., hg38). *Bona fide* transferred human RNAs from co-cultured cells will have more reads that align to the human reference genome as compared to the “mix” sample, wherein the human and mouse cells were mixed and immediately sorted. A similar analysis can be done to detect mouse RNAs transferred from MBS-MEF to MCF7 cells by aligning the reads from MCF7-enriched fraction to a reference mouse genome (e.g., mm10). For identifying RNAs that are enriched in the “co-culture” samples, as compared to the “mix” samples, any statistical package designed for differential gene expression analysis can be used. We use DESeq2 [22, 23]. Other packages for similar analysis include edgeR, DSS, and EBSec [24–26]. Since we know that β -actin-MBS mRNA robustly transfers from MBS-MEFs to MCF7 cells, it can be used as a positive control for analysis of the sequencing data.

4 Notes

1. The protocol can be adapted for studying RNA transfer in “in vivo” systems such as chimeric (mosaic) tissue, tumors, and organoids. For example, chimeric tissues or tumor xenografts can be made by injecting human cells into immunosuppressed mice. After sacrificing and harvesting of the tissue, the same protocol can be used to sort the cells and perform the required downstream analysis. In addition, this protocol can also be scaled up to analyze higher numbers of cells, if so required.

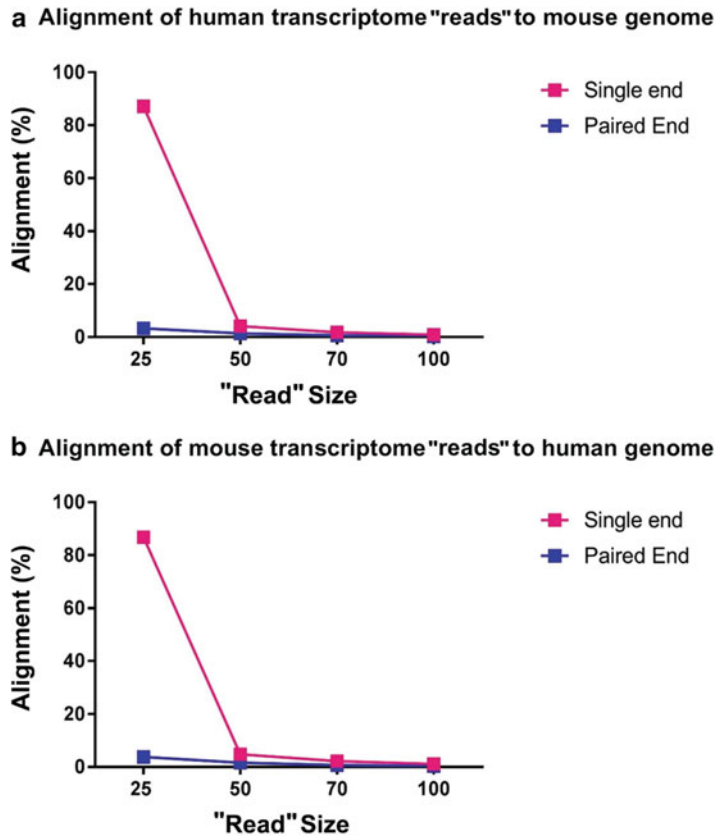


Fig. 6 In silico simulation of the alignment of human and mouse transcriptome "reads" to cross-reference genomes. **(a)** The complete human transcriptome derived from the hg38 reference genome was divided into 250 bp fragments having 200 bp overlaps with each other. From each fragment, in silico single- or paired-end "reads" were generated corresponding to 25, 50, 75, or 100 bps in length from the ends of the fragments. Each of the resulting "reads" was mapped to the mouse reference genome (mm10), using STAR 2.4.0 (parameters: "--alignEndsProtrude 15 ConcordantPair") [28]. The percentage of aligned "reads" (i.e., unique aligned + multiple aligned) was calculated out of the total "reads" generated. A similar analysis was done with the mouse transcriptome "reads," which were aligned to the human reference genome. As shown, 25 bp single-end "reads" yield a nonspecific alignment of about 86–87%. Nonspecific alignment decreases rapidly with increasing "read" length and using paired-end "reads." Details of this analysis are given in Table 2

- Depending on the design of the experiment, this method can also be employed to study RNA transfer in co-culture systems involving more than two cell types. For example, in co-culture system of three cell types, it will be essential to find magnetic microbeads specific for at least two of them. Following the harvesting and incubation with the microbeads, the cell suspension needs to be sequentially sorted two times to retrieve the pure cell populations.

Table 2
In silico simulation of human and mouse read alignments to cross-referenced genomes

Alignment of mouse transcriptome “reads” to human genome				
“Read” length and end type^a	Number of “reads”	Unique aligned “reads”	Multiple aligned “reads”	% Alignment^b
25 SE	13,421,394	4,412,268	7,231,840	86.8
50 SE	13,421,372	600,135	44,607	4.8
75 SE	13,420,606	279,012	15,989	2.2
100 SE	13,419,864	140,156	4425	1.1
25 PE	6,710,697	240,825	12,344	3.8
50 PE	6,710,686	106,495	3083	1.6
75 PE	6,710,303	47,091	1122	0.7
100 PE	6,709,932	25,407	558	0.4

Alignment of human transcriptome reads to mouse genome				
“Read” length and end type^a	Number of “reads”	Unique aligned “reads”	Multiple aligned “reads”	% Alignment^b
25 SE	20,868,680	6,794,310	11,373,252	87.1
50 SE	20,868,646	810,783	51,943	4.1
75 SE	20,867,026	357,552	15,409	1.8
100 SE	20,864,540	174,668	4688	0.9
25 PE	10,434,340	329,694	17,527	3.3
50 PE	10,434,323	139,438	4562	1.4
75 PE	10,433,513	59,135	1975	0.6
100 PE	10,432,270	30,842	792	0.3

^aSE Single-end “reads”; PE paired-end “reads”

^b% Alignment is calculated as (Unique aligned + multiple aligned “reads”)/number of reads × 100

3. We recommend having multiple biological replicates (at least two) to ensure reproducibility.
4. It is important that all the reagents, media, tubes, etc. that are used after harvesting are chilled to 4 °C and free of RNases to prevent the degradation of RNA.
5. We have found in certain cases, such as transfer of mRNA through nanotubes, that the efficiency of mRNA transfer is higher when the acceptor cells are allowed to adhere first to

the dish after which the donor cells are added. Thus, we recommend seeding the acceptor cells earlier than the donor cells. A typical time gap between the plating of the acceptor cells and the donor cells is about 3.5–4 h.

6. It is essential to collect as many cells as possible after trypsinization. Thus, we recommend incubating with trypsin for about 5 min in the incubator, with occasional shaking, to detach as many cells as possible. It is recommended to use an inverted light microscope to determine if cells have been effectively detached. The trypsinization time can vary with cell types.
7. To visualize the transfer of individual mRNA in co-culture of adherent cells, one can employ single-molecule FISH using fluorescent mRNA probes specific for the gene of interest, as described in [27]. Using Cy3-labeled probes specific for the MS2 loops (comprising 35 end-labeled 5' and 3' amino-allyl oligonucleotides [21]), we found that about 0.7% (~7 copies per cell) of β -actin-MBS mRNA transfers from MBS-MEF to MCF7 during 3 h. However, by 12 h, about 2% of β -actin-MBS mRNA (~30 copies per cell) underwent transfer (Fig. 4).
8. After allowing the cell suspension to pass through the magnetic column, the negatively selected fraction is collected in the eluate. To collect the positively selected fraction of high purity, it is essential to press the plunger through the column immediately after adding media to the column. If the media is allowed to passively elute through the column, the efficiency of recovery of the positively selected cells (MCF7) may decrease.
9. The amount of RNA collected can vary between cell types, cell numbers, and kits used. For reference, we use the Qiagen RNeasy mini kit, which allowed us to extract up to 32 μ g of total RNA from 3×10^6 MBS-MEF cells and 38 μ g of total RNA from 3×10^6 MCF7 cells. When using Macherey-Nagel NucleoSpin[®] RNA, we could collect 49 μ g and 50 μ g of total RNA from same number of MBS-MEF and MCF7 cells, respectively.
10. The presence of any nonspecific band is detected using DNA-PCR, such as the human MALAT1 band in the MBS-MEF-enriched fraction post-sorting, would indicate that sorting was not sufficiently efficient and the resulting human and mouse cell fractions are not pure. Under this situation, we recommend passing magnetic microbead-labeled cell suspension through a new LS column for one or more times, as described in Subheading 3.2.
11. For the verification of RNA transfer using RT-PCR, we recommend to use a high amount of input RNA for the first-strand cDNA synthesis (1–5 μ g) to be able to detect the less abundantly transferred RNAs by semiquantitative PCR. If no PCR

products are detected, the number of PCR cycles can be increased. However, we do not recommend going higher than 32 cycles. We also recommend to include a positive control for each primer pair (e.g., cDNA collected from MBS-MEF or MCF7 single cultures).

12. This protocol is not suitable for analysis of RNA transfer using single-cell RNA-seq. The detection of a low level of transferred RNAs requires the isolation of a high amount of RNA from multiple cells (Fig. 4) [13].

Acknowledgments

The authors thank Tsviya Olender for the simulation of human and mouse “read” alignments. This work was funded by grants to J.E.G. from the Joel and Mady Dukler Fund for Cancer Research, the Jean-Jacques Brunschwig Fund for the Molecular Genetics of Cancer, a Proof-of-Principle Grant from the Moross Integrated Cancer Center (Weizmann Institute of Science), the German-Israel Foundation (GIF; I-1461-412.13/2018) and the US-Israel Binational Science Foundation-National Science Foundation (#2015846).

References

1. Morel O, Toti F, Hugel B, Freyssinet JM (2004) Cellular microparticles: a disseminated storage pool of bioactive vascular effectors. *Curr Opin Hematol* 11:156–164
2. Ramachandran S, Palanisamy V (2012) Horizontal transfer of RNAs: exosomes as mediators of intercellular communication. *Wiley Interdiscip Rev RNA* 2:286–293
3. Kim G, LeBlanc ML, Wafula EK, dePamphilis CW, Westwood JH (2014) Genomic-scale exchange of mRNA between a parasitic plant and its hosts. *Science* 345:808–881
4. Shimizu K, Shinga J, Yamasaki S, Kawamura M, Dörrie J et al (2015) Transfer of mRNA encoding invariant NKT cell receptors imparts glycolipid specific responses to T cells and $\gamma\delta$ T cells. *PLoS One* 10(6):e0131477
5. Chen J, Hu C, Pan P (2017) Extracellular vesicle microRNA transfer in lung diseases. *Front Physiol* 8:1028
6. Nguyen MA, Karunakaran D, Geoffrion M, Cheng HS, Tandoc K et al (2018) Extracellular vesicles secreted by atherogenic macrophages transfer microRNA to inhibit cell migration. *Arterioscler Thromb Vasc Biol* 38:49–63
7. Das S, Halushka MK (2015) Extracellular vesicle microRNA transfer in cardiovascular disease. *Cardiovasc Pathol* 24:199–206
8. Ma P, Pan Y, Li W, Sun C, Liu J, Xu T, Shu Y (2017) Extracellular vesicles-mediated non-coding RNAs transfer in cancer. *J Hematol Oncol* 10(1):57
9. Takahashi K, Yan IK, Wood J, Haga H, Patel T (2014) Involvement of extracellular vesicle long noncoding RNA (linc-VLDLR) in tumor cell responses to chemotherapy. *Mol Cancer Res* 10:1377–1387
10. Takahashi K, Yan IK, Kogure T, Haga H, Patel T (2014) Extracellular vesicle-mediated transfer of long non-coding RNA ROR modulates chemosensitivity in human hepatocellular cancer. *FEBS Open Biol* 4:458–467
11. Cai Q, Qiao L, Wang M, He B, Lin FM, Palmquist J, Huang SD, Jin H (2018) Plants send small RNAs in extracellular vesicles to fungal pathogen to silence virulence genes. *Science* 360:1126–1129
12. Maida Y, Takakura M, Nishiuchi T, Yoshimoto T, Kyo S (2015) Exosomal transfer of functional small RNAs mediates cancer-stroma communication in human endometrium. *Cancer Med* 5(2):304–314
13. Haimovich G, Ecker CM, Dunagin MC, Eggan E, Raj A, Gerst JE, Singer RH (2017) Intercellular mRNA trafficking via membrane

- nanotube-like extensions in mammalian cells. *Proc Natl Acad Sci U S A* 114(46):9873–9882
14. Shurtleff MJ, Yao J, Qin Y, Nottingham RM, Temoche-Diaz MM et al (2017) Broad role for YBX1 in defining the small noncoding RNA composition of exosomes. *Proc Natl Acad Sci U S A* 114(43):8987–8995
 15. Mittelbrunn M, Gutiérrez-Vázquez C, Villarroya-Beltri C, González S, Sánchez-Cabo F et al (2011) Unidirectional transfer of microRNA-loaded exosomes from T cells to antigen-presenting cells. *Nat Commun* 2:282
 16. Villarroya-Beltri C, Gutiérrez-Vázquez C, Sánchez-Madrid F, Mittelbrunn M (2013) Analysis of microRNA and protein transfer by exosomes during an immune synapse. *Methods Mol Biol* 1024:41–51
 17. Jiang H, Li Z, Li X, Xia J (2015) Intercellular transfer of messenger RNAs in multiorgan tumorigenesis by tumor cell-derived exosomes. *Mol Med Rep* 11:4657–4663
 18. Valadi H, Ekström K, Bossios A, Sjöstrand M, Lee JJ, Lötvall JO (2007) Exosome-mediated transfer of mRNAs and microRNAs is a novel mechanism of genetic exchange between cells. *Nat Cell Biol* 9:654–659
 19. Ekström K, Valadi H, Sjöstrand M, Malmhäll C, Bossios A et al (2012) Characterization of mRNA and microRNA in human mast cell-derived exosomes and their transfer to other mast cells and blood CD34 progenitor cells. *J Extracell Vesicles* 1(10):3402
 20. Eirin A, Riester SM, Zhu XY, Tang H, Evans JM et al (2014) MicroRNA and mRNA cargo of extracellular vesicles from porcine adipose tissue-derived mesenchymal stem cells. *Gene* 551:55–64
 21. Lionnet T, Czaplinski K, Darzacq X, Shav-Tal Y, Wells AL et al (2011) A transgenic mouse for in vivo detection of endogenous labeled mRNA. *Nat Methods* 8:165–170
 22. Love MI, Huber W, Anders S (2014) Moderated estimation of fold change and dispersion for RNA-seq data with DESeq2. *Genome Biol* 15:550
 23. Link for DeSeq2: <https://bioconductor.org/packages/release/bioc/html/DESeq2.html>
 24. Robinson MD, McCarthy DJ, Smyth GK (2010) edgeR: a bioconductor package for differential expression analysis of digital gene expression data. *Bioinformatics* 26(1):139–140
 25. Wu H, Wang C, Wu Z (2013) A new shrinkage estimator for dispersion improves differential expression detection in RNA-seq data. *Biostatistics* 2:232–243
 26. Leng N, Kendziorski C (2019) EBSeq: An R package for gene and isoform differential expression analysis of RNA-seq data. R package version 1.22.1
 27. Haimovich G, Gerst JE (2018) Single-molecule fluorescence in situ hybridization (smFISH) for RNA detection in adherent animal cells. *Bio-protocol* 8(21):e3070
 28. Dobin A, Gingeras TR (2016) Optimizing RNA-Seq Mapping with STAR. *Methods Mol Biol* 1415:245–262



Synthesizing Fluorescently Labeled dsRNAs and sRNAs to Visualize Fungal RNA Uptake

Rachael Hamby, Ming Wang, Lulu Qiao, and Hailing Jin

Abstract

Fungal pathogens are responsible for severe crop losses worldwide. Defending crops against fungal disease is critical for global food security; however, most current disease management approaches rely on chemical fungicides that can leave dangerous residues in the environment. RNA interference (RNAi) is an important process through which RNA molecules target and silence complementary genes, regulating gene expression during both transcription and translation. Recently, it has been discovered that some species of fungi can efficiently take up RNAs originating from their host plant and the environment. If these RNAs are complementary to fungal genes, this can lead to the targeting and silencing of fungal genes, termed “cross-kingdom RNAi,” if the RNA originated from a plant host, or “environmental RNAi,” if the RNA originated from the environment. These discoveries have inspired the development of spray-induced gene silencing (SIGS), an innovative crop protection strategy involving the foliar application of RNAs which target and silence fungal virulence genes for plant protection against fungal pathogens. The effectiveness of SIGS is largely dependent on the ability of fungi to take up environmental RNAs. Here, we describe the protocols used to label and visualize RNAs which are taken up by *Botrytis cinerea*. This protocol could easily be adapted for use across various fungal species. Determining the efficiency of RNA uptake by a specific fungal species is a critical first step to determining if SIGS approaches could be an effective control strategy for that fungus.

Key words Fungicides, RNA uptake, RNA interference, Environmental RNAi, Cross-kingdom RNAi, dsRNA, RNA labeling, Spray-induced gene silencing (SIGS), Crop protection

1 Introduction

Plants are constantly under attack by pathogens, pests, and parasites. Of the various classes of plant pathogens, fungi are among the most devastating. Alarming, drug resistance has been reported in each major class of fungicide used in agriculture [1]. Due to this and other reasons, the development of novel crop protection strategies is critical for global food security. The utilization of existing pathways within the host or pathogen can be an effective method for designing new approaches to combat disease.

Environmental RNA interference (RNAi), initially discovered in the nematode *Caenorhabditis elegans*, refers to the systemic gene silencing in an organism induced by the uptake of environmental RNAs [2]. Similar to *C. elegans*, the aggressive fungal pathogen, *Botrytis cinerea*, is also able to take up RNAs from the environment [3]. Further, a series of recent discoveries revealed a new mechanism of communication between plants and fungi. This phenomenon is known as cross-kingdom RNAi, in which plants send sRNAs into the fungus to silence and target virulence genes, and in turn, the fungus sends sRNAs into the plant host to target and silence defense genes [4, 5]. Combined, these discoveries inspired the development of spray-induced gene silencing (SIGS), a crop protection approach involving the foliar application of RNAs which target and silence fungal pathogen genes.

Foliar application of RNAs has been a successful approach in protecting several plants from fungal diseases, including barley leaves from *Fusarium graminearum* [6], postharvest material such as fruits and flowers from *B. cinerea* [3], and *Brassica napus* plants from *Sclerotinia sclerotiorum* [7]. The ability of these fungi to take up environmental RNAs is crucial for RNA-based control strategies to be effective. In order to establish best protocols for using RNA to control specific fungal diseases, the uptake efficiency of the fungi across types and treatments of environmental RNA must be established. Additionally, research into fungal RNA uptake may help to elucidate the mechanisms of cross-kingdom RNAi. Here, we present a protocol for observing the uptake efficiency of both double-stranded RNAs (dsRNAs) and small RNAs (sRNAs) using *B. cinerea* as an example, though these methods can be easily adapted across fungal species.

2 Materials

2.1 *In Vitro* Synthesis of Fluorescein-Labeled Double-Stranded RNAs

1. Phusion[®] High-Fidelity DNA Polymerase.
2. 5× Phusion HF buffer.
3. 2.5 mM dNTPs.
4. 10 μM Forward primer, with T7 promoter sequence [5'-TAATACGACTCACTATAG-3'] appended to 5' end.
5. 10 μM Reverse primer, with T7 promoter sequence [5'-TAATACGACTCACTATAG-3'] appended to 5' end.
6. Nuclease-free water.
7. Fluorescein RNA Labeling Mix Kit.
8. T7 RNA polymerase.
9. T7 RNA polymerase reaction buffer, 10×, supplied with T7 RNA polymerase.

10. 0.2 M Ethylenediaminetetraacetic acid (EDTA), pH 8.0.
11. 100% Ethanol.
12. 3 M Sodium acetate (pH 5.5).
13. 75% Ethanol.
14. NanoDrop™ 2000/2000c Spectrophotometer.
15. PCR thermocycler.
16. 0.2 mL PCR tubes.
17. 1.5 mL Microcentrifuge tubes.
18. Benchtop centrifuge capable of speeds up to $13,000 \times g$.
19. Agarose.
20. $1\times$ Tris-acetate-EDTA (TAE) buffer: 40 mM Tris-acetate and 1 mM EDTA.
21. $6\times$ Loading dye.
22. 1 kb DNA ladder.
23. 10 mg/mL Ethidium bromide.
24. Erlenmeyer flask.
25. Microwave.
26. Equipment and supplies for running an agarose gel including gel casting mold, well combs, and horizontal electrophoresis chamber.
27. Voltage source.
28. UV light source.
29. $-20\text{ }^{\circ}\text{C}$ Freezer.
30. $4\text{ }^{\circ}\text{C}$ Refrigerator.
31. Incubator set to $37\text{ }^{\circ}\text{C}$.

2.2 Preparation of Fluorescent sRNAs

1. ShortCut® RNase III.
2. $10\times$ ShortCut reaction buffer.
3. 200 mM MnCl_2 .
4. 250 mM Ethylenediaminetetraacetic acid (EDTA).
5. 100% Ethanol.
6. 80% Ethanol.
7. Nuclease-free water.
8. NanoDrop™ 2000/2000c Spectrophotometer.
9. Incubator set to $37\text{ }^{\circ}\text{C}$.
10. 40% Acrylamide solution for polyacrylamide gel electrophoresis (PAGE).
11. $10\times$ TBE buffer: 890 mM Tris base, 30 mM EDTA, pH 8.0, 890 mM boric acid.

12. Equipment and supplies for preparing and running a PAGE gel, including glass plates, casting frame, casting stand and combs, voltage source, gel holder cassettes, and vertical electrophoresis chamber.
13. *N,N,N',N'*-tetramethylethylenediamine (TEMED).
14. Urea.
15. 10 bp DNA ladder.
16. 5× RNA loading buffer.
17. 10% Ammonium persulfate solution (APS).
18. Dry block incubator capable of reaching temperatures of 95 °C.
19. EtBr staining solution: 0.5× TBE + 1 µg/mL ethidium bromide.
20. Voltage source.
21. UV light source.
22. −20 °C Freezer.
23. Benchtop centrifuge capable of speeds up to 13,000 × *g*.

2.3 Visualization of RNA Trafficking into *B. cinerea* Mycelium

1. MEA medium: 20 g/L Malt extract, 10 g/L Bacto™ proteose peptone no. 2, 15 g/L agar.
2. *Botrytis cinerea* spores stored in −80 °C freezer.
3. Nuclease-free water (sterile).
4. Microscope slides (sterile).
5. Petri dish (sterile).
6. 50 mL Falcon tubes (sterile).
7. 70 µm Nylon mesh sterile cell strainer.
8. Benchtop binocular microscope with 10× objective.
9. Hemocytometer.
10. Micrococcal nuclease.
11. Laser scanning confocal microscope.
12. Sterile hood.

3 Methods

3.1 In Vitro Synthesis of Fluorescein-Labeled Double-Stranded RNAs

1. Prepare DNA template with opposing T7 promoters at the 5' ends of each strand by performing PCR on the DNA target of interest and with primers that each contain the T7 promoter sequence [5'-TAATACGACTCACTATAG-3'] appended to each 5' end. For a 50 µL PCR reaction, add the following components to a PCR tube on ice (*see Note 1*) (Step A, Fig. 1):

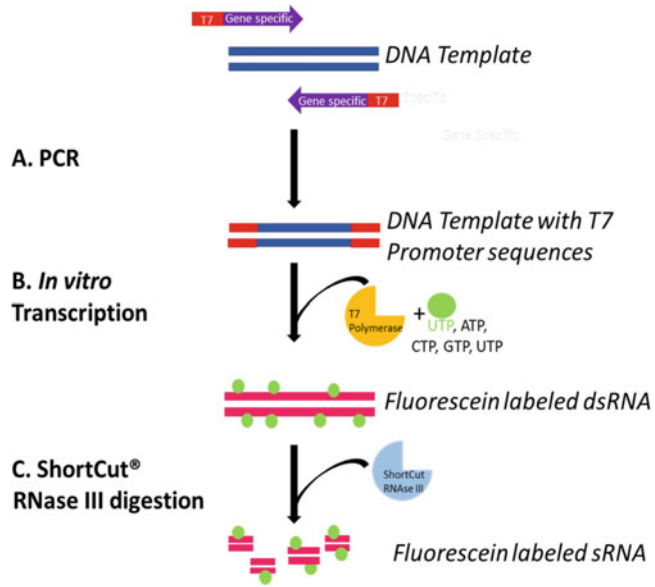


Fig. 1 Key steps in the synthesis of fluorescein-labeled dsRNA and sRNAs

Reagent	Volume (μL)
Template DNA, final amount recommended should be between 50 and 250 ng if genomic, 1–10 ng if using a plasmid template	x
5× HF buffer	10
10 μM Forward primer	2.5
10 μM Reverse primer	2.5
2.5 μM dNTP	4
Phusion high-fidelity DNA polymerase	0.5
Add nuclease-free water to a final volume of 50 μL	x

2. Place in a thermocycler and run the following program, optimized for specific target DNA:

1. 98 °C for 1 min
2. 98 °C for 10 s
3. 45–72 °C for 3 s
4. 72 °C for 15–30 s (depends on the length of PCR product, 30 s per 1 kb for Phusion polymerase)
5. Repeat steps 2–4 35×
6. 72 °C for 5 min

3. Confirm that the PCR product is unique and of the expected size of the target DNA + two T7 promoter sequences by agarose gel electrophoresis (*see Note 2*). Prepare a 1% agarose gel by adding 1 g agarose per 100 mL TAE buffer in a 500 mL Erlenmeyer flask. Specific amounts vary based on the size of gel mold. Microwave for sufficient time to completely dissolve agarose. Add ethidium bromide to a final concentration of 0.3 $\mu\text{g}/\text{mL}$. Briefly swirl to mix and pour into gel mold. Add comb and let set for about 30 min.
4. When gel is solidified, place it into the horizontal electrophoresis chamber. Fill the chamber with $1\times$ TAE until the gel is covered. Add 2 μL $6\times$ loading dye to a 10 μL aliquot of PCR product and load into gel. Add 8 μL of 1 kb DNA ladder as molecular marker. Run the gel at 180 V/cm for 15–30 min.
5. Place the gel on a UV light source after electrophoresis. There should be a single band of a size consistent with that of target DNA + two T7 promoter sequences.
6. Pool all PCR products into a single 1.5 mL tube and add 2.5 volumes of 100% ethanol and 0.1 volumes of 3 M sodium acetate (pH 5.5).
7. Precipitate the DNA at $-20\text{ }^{\circ}\text{C}$ overnight.
8. Centrifuge the tube at $4\text{ }^{\circ}\text{C}$ for 15 min at $13,000\times g$.
9. Discard the supernatant and add 700 μL of cold 75% ethanol to wash.
10. Centrifuge again for 5 min at $13,000\times g$.
11. Discard the supernatant, air-dry the pellet, and resuspend the DNA in 30 μL of nuclease-free water.
12. Run a small aliquot on an agarose gel, as described above, to check the quality of the product and use Nanodrop spectrophotometry to estimate the concentration.
13. Thaw frozen reagents of the fluorescein RNA labeling mix kit needed for in vitro labeling reaction at room temperature before placing on ice.
14. For a 20 μL reaction, add amounts listed in the table below to a microcentrifuge tube on ice (Step B, Fig. 1):

Reagent	Volume (μL)
1 μg Linearized plasmid DNA or 100–200 ng PCR product	x
Fluorescein RNA-labeling mix, $10\times$	2
$10\times$ Transcription buffer	2
Add nuclease-free water to a final volume of 18 μL	x
T7 RNA polymerase	2

15. Mix reaction by flicking the tube or pipetting the mixture up and down, and then briefly spin to collect the mixture at the bottom of the tube.
16. Incubate at 37 °C for 2 h.
17. Stop the reaction by adding 2 µL of 0.2 M EDTA, pH 8.0.
18. To purify the dsRNA, add 2.5 volumes of 100% ethanol and 0.1 volumes of 3 M sodium acetate (pH 5.5) and precipitate at –20 °C overnight.
19. Centrifuge at 4 °C for 15 min at 13,000 × *g*.
20. Discard supernatant and add 700 µL of cold 75% ethanol to wash.
21. Centrifuge for 5 min at 13,000 × *g*.
22. Discard supernatant and resuspend dsRNA pellet in 30 µL of nuclease-free water.
23. Run a small aliquot on an agarose gel, as described above, to check the quality of the product and use Nanodrop spectrophotometry to estimate the concentration.
24. Use immediately or store at –80 °C.

3.2 Preparation of Fluorescent sRNAs

1. Use the fluorescent dsRNA synthesized in **step 1** and combine the following in a microcentrifuge tube on ice to produce a 100 µL reaction (Step C, Fig. 1):

Reagent	Volume (µL)
10 µg dsRNA	x
10× ShortCut [®] Reaction Buffer	10
ShortCut [®] RNase III	10
200 mM MnCl ₂	10
Nuclease-free water to a final volume of 100 µL	x

2. Gently mix the volume with a pipette and incubate at 37 °C for 20 min.
3. To stop the reaction, add 10 µL of 250 mM EDTA (*see Note 3*).
4. To precipitate the digestion product, transfer it to a 1.5 mL tube and add 2 µL RNase-free glycogen, 3 volumes of cold 100% ethanol, and 0.1 volumes of 3 M sodium acetate (pH 5.5) (*see Note 4*).
5. Precipitate at –20 °C overnight.
6. Centrifuge at 4 °C for 15 min at 13,000 × *g*.

7. Discard supernatant and add 700 μL of cold 80% ethanol to wash.
8. Centrifuge for 5 min at $13,000 \times g$.
9. Discard supernatant and air-dry the sRNA pellet.
10. Resuspend sRNA pellet in 20 μL of nuclease-free water.
11. Check the quality of the sRNA products using PAGE (*see Note 5*). Prepare a 20% polyacrylamide/urea gel by mixing 5 mL of 40% acrylamide solution, 1 mL of $10\times$ TBE, and 10 mL nuclease-free water. Dissolve 5 g of urea in this mixture at room temperature and then add 80 μL 10% APS and 10 μL TEMED immediately before pouring between glass plates set up on a gel-casting frame, leaving enough room to insert comb without overflow. Insert comb and allow to polymerize for about 30 min.
12. When gel is solidified, remove glass plates and gel from the casting frame, move to gel holder cassette, and place in vertical electrophoresis chamber. Fill both the inner and outer reservoirs with $0.5\times$ TBE. Remove comb and rinse wells with $0.5\times$ TBE using a micropipette with a fine tip.
13. Take a small aliquot of purified sRNA pellet, heat for 5 min at 95°C , then chill on ice for 5 min, and add appropriate amount of loading buffer. Load into gel along with 10 bp DNA ladder and run at 130 V for approximately 2 h.
14. After completion of PAGE, transfer the gel to EtBr staining solution and incubate on a platform rotator for 5–25 min, depending on the amount of RNA used. Once staining is complete, the RNA can be visualized using a UV light source.
15. Use gel to verify the quality of the sRNA preparation and use Nanodrop spectrophotometry to estimate the concentration.
16. Use immediately or store at -80°C .

3.3 Visualization of RNA Trafficking into *B. cinerea* Mycelium

1. Store *B. cinerea* B05.0 spores at -80°C , and culture on plates with solidified malt extract agar (MEA) medium.
2. When petri dish is covered with sporulating fungus, approximately 10 days after plating, pour 5 mL of sterile water onto the surface and suspend the spores in water using a sterile loop as aid.
3. Strain the liquid into a 50 mL Falcon tube through a 70 μm nylon mesh sterile cell strainer.
4. Count spore numbers present in the liquid using a hemocytometer and a benchtop binocular microscope equipped with a $10\times$ objective.
5. Dilute the liquid with sterile water to 1×10^5 spores/mL.

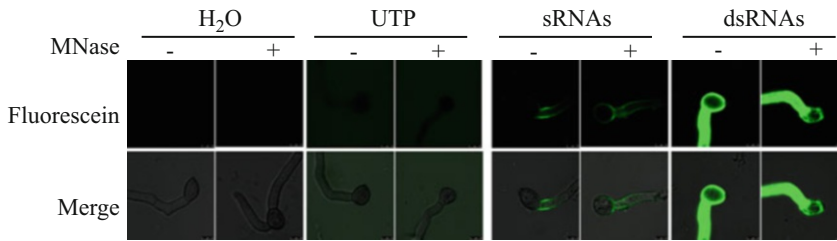


Fig. 2 Uptake of external fluorescein-labeled dsRNAs and sRNAs by *B. cinerea* cells. MNase, micrococcal nuclease treatment. Merge, the merge of mycelium structure and fluorescein signals

- In a sterile hood, pipette 1 mL hot liquid MEA medium (at around 60 °C) onto each sterile microscope slide and allow the MEA to be evenly and fully distributed onto each slide (*see Note 6*).
- Wait about 5–10 min for the MEA medium to solidify.
- Add 4 μL of 100 ng/μL fluorescent sRNAs or dsRNAs to 4 μL of the 1×10^5 spores/mL suspension. As a control, add 4 μL of sterile water and 4 μL of properly diluted fluorescein (*see Note 7*) to 4 μL of the 1×10^5 spores/mL suspension (*see Note 8*).
- Directly apply these solutions to the MEA microscope slides.
- Incubate the microscope slides in a sterile petri dish covered with aluminum foil to prevent direct exposure to the light at room temperature for 12 h (*see Note 9*).
- Treat mycelium with 20 μL 75 U micrococcal nuclease at 37 °C for 30 min to degrade any fluorescent dsRNA and sRNAs outside of the fungal mycelium.
- Analyze fluorescent signal with a laser scanning confocal microscope (*see Note 10*), as shown in Fig. 2.

4 Notes

- It is recommended that at least eight 50 μL PCR reactions are made in this step to generate a sufficient quantity of DNA product for the in vitro transcription reaction.
- If having trouble avoiding primer-dimerization or amplification of nonspecific bands, it is also possible to run the entire PCR product on the gel, cut the specific band from the gel, and use a gel purification kit to obtain specific purified DNA product. This decreases yield, however, compared to following Subheading 3.1, steps 3–9. In this case, it is important to accumulate more PCR reactions for the purification to create enough DNA template for use in in vitro transcription.

3. Do not stop the reaction by heating, as this would reduce the yield of sRNAs.
4. Adding 3 volumes instead of 2.2 volumes of 100% ethanol improves the efficiency of sRNA precipitation.
5. To verify the sRNA quality and quantity, we suggest using a 20% PAGE gel instead of a highly concentrated agarose gel, because PAGE gels are much more effective at sRNA separation and detection.
6. It is best to prepare MEA slides in a sterile petri dish by placing one side of the microscope slide on the edge of the petri dish and the other side down to the bottom. This creates a slope that allows the liquid MEA medium to evenly flow down the microscope slide when pipetting the MEA medium along the upper side.
7. In the fluorescent dsRNA synthesis step, 2 μL of fluorescein mix was added to the reaction, which was then eluted into 30 μL of dsRNA. Therefore, we recommend preparing the fluorescein control by adding 1 μL of fluorescein into 15 μL of nuclease-free water, and then to apply any dilution steps used on the fluorescein-RNA mixture also to this control.
8. We recommend using around 400 spores total on each MEA microscope slide, which will lead to growth of separated individual mycelium after 12 h. If too many spores are used, individual mycelia could be difficult to distinguish, and if too few spores are used, the mycelium can be difficult to find under the microscope.
9. For the whole procedure in Subheading 3.3, work in sterile conditions in a sterile hood to avoid the growth of bacteria on the MEA microslides.
10. To correct for artificial/autofluorescence of fungal mycelium, adjust the confocal microscope settings using water-treated control samples of mycelium and use the same settings for the rest of the samples.

References

1. Fisher MC, Hawkins NJ, Sanglard D, Gurr SJ (2018) Worldwide emergence of resistance to antifungal drugs challenges human health and food security. *Science* 360(6390):739–742
2. Whangbo JS, Hunter CP (2008) Environmental RNA interference. *Trends Genet* 24(6):297–305
3. Wang M, Weiberg A, Lin FM, Thomma BP, Huang HD, Jin H (2016) Bidirectional cross-kingdom RNAi and fungal uptake of external RNAs confer plant protection. *Nat Plants* 2:16151
4. Weiberg A, Wang M, Lin FM, Zhao H, Zhang Z, Kaloshian I, Huang HD, Jin H (2013) Fungal small RNAs suppress plant immunity by hijacking host RNA interference pathways. *Science* 342(6154):118–123
5. Cai Q, Qiao L, Wang M, He B, Lin FM, Palmquist J, Huang SD, Jin H (2018) Plants send small RNAs in extracellular vesicles to

- fungal pathogen to silence virulence genes. *Science* 360(6393):1126–1129
6. Koch A, Biedenkopf D, Furch A, Weber L, Rossbach O, Abdellatef E, Linicus L, Johansmeier J, Jelonek L, Goesmann A, Cardoza V, McMillan J, Mentzel T, Kogel KH (2016) An RNAi-based control of *Fusarium graminearum* infections through spraying of long dsRNAs involves a plant passage and is controlled by the fungal silencing machinery. *PLoS Pathog* 12:e1005901
 7. McLoughlin AG, Wytinck N, Walkee PL, Girard IJ, Rashid KY, de Kievit T, Fernando WGD, Whyard S, Belmonte MF (2018) Identification and application of exogenous dsRNA confers plant protection against *Sclerotinia sclerotiorum* and *Botrytis cinerea*. *Sci Rep* 8:7320



Chapter 13

Labeling of dsRNA for Fungal Uptake Detection Analysis

Matteo Galli, Jafargholi Imani, and Karl-Heinz Kogel

Abstract

Double-stranded RNA (dsRNA) plays an essential role in many biological processes and has a great potential for agronomic applications in disease and pest control. A simple and effective method to monitor dsRNA uptake by fungi is crucial for the use of dsRNA as alternative fungicide. The protocol reported in this chapter describes an efficient method to detect and localize labeled dsRNA in fungal hyphae. We use the fungal *Verticillium longisporum*, a fungal plant pathogen that commonly infects rapeseed and other *Brassica* species, to explain the procedure, though we have validated the method in a broad spectrum of fungi. Hereafter we elucidate step-by-step the production, fluorescence labeling, as well as detection of dsRNA via fluorescence microscopy in fungal mycelium.

Key words dsRNA detection, Fluorescent dsRNA, Environmental RNAi, Hyphae

1 Introduction

Double-stranded RNA (dsRNA) is an essential molecule in various cellular processes, from eukaryotic organisms to viruses. In plants, dsRNA is fundamental to triggering of gene silencing through RNA interference (RNAi) through production of small RNAs (sRNAs), including microRNAs (miRNAs) and small interfering RNAs (siRNAs) [1, 2]. In this process, the dsRNA is cut into short 21–24 nucleotide (nt) RNA duplexes by DICER-like (DCL) endonuclease III enzymes. Subsequently, short RNA duplexes are loaded onto ARGONAUTE (AGO) enzymes and associated proteins that together form the RNA-induced silencing complex (RISC). One strand of the RNA duplex is discarded, while the remaining guide strand guides the RISC to complementary mRNAs through base-pairing. Upon matching, AGO cleaves the target mRNA, causing its rapid degradation. Recent reports suggest that dsRNAs are also fundamental components controlling the outcome of plant host-pathogen interactions. This phenomenon is called cross-kingdom RNAi, where dsRNA is bidirectionally transferred between host and microbe to eventually target

corresponding genes in a sequence-specific manner. In this way, dsRNAs positively or negatively regulate genes involved in plant defense or fungal virulence, respectively [3–5]. Successful translational research has led to agronomic application of this natural phenomenon. Crop protection techniques have been established, where artificial dsRNA is either expressed in plants to target interacting pathogens or pest (host-induced gene silencing, HIGS) or applied directly on plants by spraying (spray-induced gene silencing, SIGS), also called environmental RNAi [6, 7]. Both technologies have been already used to control a vast number of pathogens, including *Botrytis cinerea*, *Verticillium dahliae*, *Sclerotinia sclerotiorum*, *Fusarium spec.*, and pests, including *Diabrotica virgifera virgifera* [8–12, 14]. Nonetheless, not all plant pathogens can be targeted and controlled through HIGS or SIGS. A recent example is *Zymoseptoria tritici*, a major fungal pathogen of wheat: all current RNAi-mediated crop protection techniques failed to protect wheat plants against this fungal pathogen [13]. Hence, for further analysis of the amenability of a fungal species to disease control by dsRNA, it is of vital importance to investigate its ability to take up and process exogenous dsRNA. The method described in detail in this section portrays one possible approach to easily produce, deliver, and detect labeled RNA duplexes in germinating fungal mycelia. We present here a case study on *Verticillium longisporum* (VL), an economically important fungal plant pathogen of *Brassicaceae*. Application of the labeling strategy described herein indicates a strong ability of this fungus to take up dsRNA.

2 Materials

Prepare all solutions and buffers using deionized water at room temperature (RT). Prepare and store all reagents at RT (unless indicated otherwise by the manufacturer). The waste of residual materials should be in accordance with safety regulations.

2.1 Fungus Culture and Propagation

1. *Verticillium longisporum* wild-type strain VL41 (Institute of Plant Pathology and Crop Protection, Georg August University, Göttingen, Germany).
2. Potato dextrose broth (PDB): 20 g/l Glucose, 4 g/l potato extract, pH 5.6 ± 0.2 at 25 °C (see Note 1).
3. Potato dextrose agar (PDA): 20 g/l Glucose, 4 g/l potato extract, 17 g/l agar, pH 5.6 ± 0.2 at 25 °C (see Note 1).
4. Sterilized lab ware (scalpel, bottles, flasks, cork borer, glass funnel, and Petri dishes).
5. Orbital flask shaker (3 μmol photons/m²/s).
6. Fungal growing chamber (70 μmol photons/m²/s).

**2.2 Total RNA
Extraction, DNase
Treatment, and cDNA
Synthesis**

1. Fungal mycelium (*V41*).
2. 50 mL Falcon tubes.
3. Cooled laboratory centrifuge.
4. Mortar and pestle.
5. Water bath.
6. Spectrophotometer.
7. 1.5 and 2 mL Eppendorf Safe-Lock Tubes.
8. Liquid nitrogen.
9. Filter sheet (pore size: 22–25 μm).
10. RNase- and DNase-free water.
11. TRIzol (guanidinium thiocyanate, store at RT) (*see Note 2*).
12. Chloroform (use it under chemical hood).
13. Isopropanol.
14. 70% Ethanol.
15. DNase I-free RNase (1 U/ μL).
16. 10 \times DNase I buffer: 100 mM Tris-HCl, 25 mM MgCl₂, 1 mM CaCl₂, pH 7.5.
17. 50 mM Ethylenediaminetetraacetic acid (EDTA), pH 7.
18. Reverse transcriptase.
19. 10 \times Reverse transcriptase buffer: 100 mM Tris-HCl, 500 mM KCl, 1% Triton-X-100, pH 9.0.
20. Thermocycler.
21. PCR mix: 1.5 mM MgCl₂, Taq polymerase (0.5 U) with specific buffer, 4 mM deoxynucleotides (dNTPs), and 0.1–0.5 μM of primers.
22. Agarose powder.
23. Tris/borate/EDTA buffer: 109.03 g/l (0.9 M) Tris base, 55.0 g/l (0.9 M) boric acid, 9.31 g/l (0.025 M) EDTA.
24. DNA ladder for gel electrophoresis.
25. Horizontal gel electrophoresis apparatus and power supply.
26. Ethidium bromide.
27. PCR cleanup kit.
28. Membrane-binding solution: 5.5 M Guanidine hydrochloride, 20 mM Tris-HCl, pH 6.6.
29. Membrane wash solution: 20 mM NaCl, 2 mM Tris-HCl, 80% ethanol V/V, pH 7.5.
30. Silica-membrane spin column (for DNA purification).

2.3 Labeled dsRNA Production and In Vitro Assay Detection

1. Fungal conidia (*V41*).
2. Spore-counting chamber (e.g., Fuchs-Rosenthal, Germany).
3. Bright-field microscope.
4. Si-Fi v21 software (siRNA finder, <http://labtools.ipk-gatersleben.de>).
5. Primers flanked by T7 promoter sequences (5'-TAATACGACTCACTATAGGG-3').
6. Atto 488 RNA Labeling Kit (Jena Bioscience, Germany).
7. Silica-based membrane columns for RNA purification.
8. RNA wash buffer: 1 mM EDTA, 10 mM Tris-HCl, ethanol 80% V/V, pH 8.
9. DNase/RNase-free water.
10. RNase-free 1.5 mL tube.
11. 96 Microtiter well plates.
12. Microscope glass slides.
13. Fluorescence microscope.
14. Digital image processing software (*see Note 3*).

3 Methods

In the following, the fungus *V. longisporum* *V41* is taken as an example to demonstrate the labeling strategy and to demonstrate the ability of a fungus to take up dsRNA. Nevertheless, the technique described here can be applied to a vast array of fungi [7, 11, 13, 14].

Carry out all procedures at RT unless otherwise specified.

3.1 Fungal *V41* Culture and Selection of the Target Template

1. *V41* culture: Prepare a fungal stock on PDA Petri dish plates and incubate at 25 °C in 16/8-h light period (light intensity: 70 $\mu\text{mol photons/m}^2/\text{s}$). For maintenance, the fungus should be routinely subcultured within an interval of 3 weeks on new Petri dishes or stored in the dark at 4 °C. In sterile conditions, punch an agar block (diameter 0.5 cm^2) with a sterilized cork borer, transfer the agar block to a freshly prepared PDA plate, and seal the plate with parafilm.
2. *V41* broth culture: All steps should be performed under sterile conditions. Punch an agar block (diameter 0.5 cm^2) with a sterilized cork borer and transfer it into flasks containing PDB medium. Incubate on an orbital shaker (100 rpm) under constant illumination from one near-white-light tube (3 $\mu\text{mol photons/m}^2/\text{s}$) at RT.

3. Select target sequence: Choose a cDNA sequence (circa 400 nt in length), which derives from a potential fungal target gene sequence and is likely to generate a good number of silencing-efficient siRNAs. To determine this last parameter, perform in silico analysis using si-Fi v21 software (program designed for RNAi off-target analysis and silencing efficiency predictions). Paste the target sequence into the software and analyze it against the DNA database of the pathogen tested. Use as database the complete genome of the fungus or the DNA sequence of the gene used to produce the approximately 400 nt long fragment sequence. The program will calculate the possible number of efficient siRNAs hits (as a number) based upon the contextual similarity between the two sequences and the predicted thermodynamic stability analysis, and it will show the results in a chart (see Fig. 1). For generation of labeled dsRNA use the 400 bp sequence which produces the highest number of efficient siRNAs hits (see Fig. 2) (see Note 4).

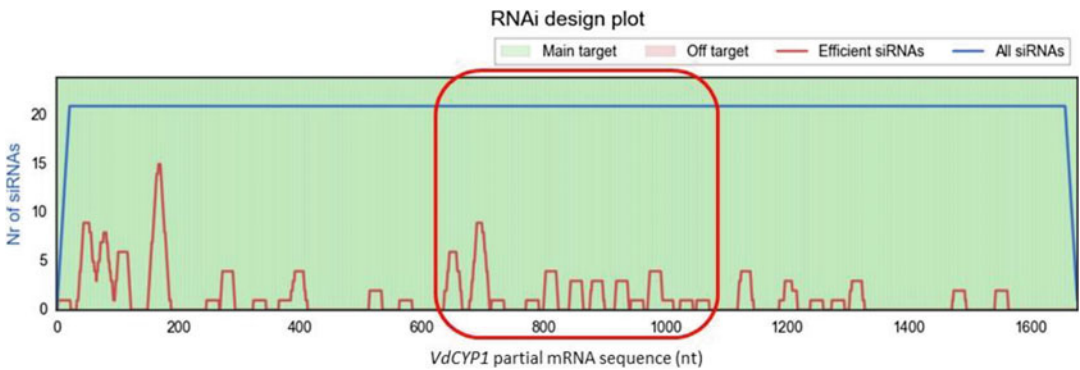


Fig. 1 Graphical output of the predicted total and efficient siRNA hits in the *Verticillium dahliae* CYP1 mRNA (*VdCYP1*) calculated via the si-Fi v21 software. The red box accounts for the sequence used to generate the *VICYP1* fragment for the production of labeled dsRNA

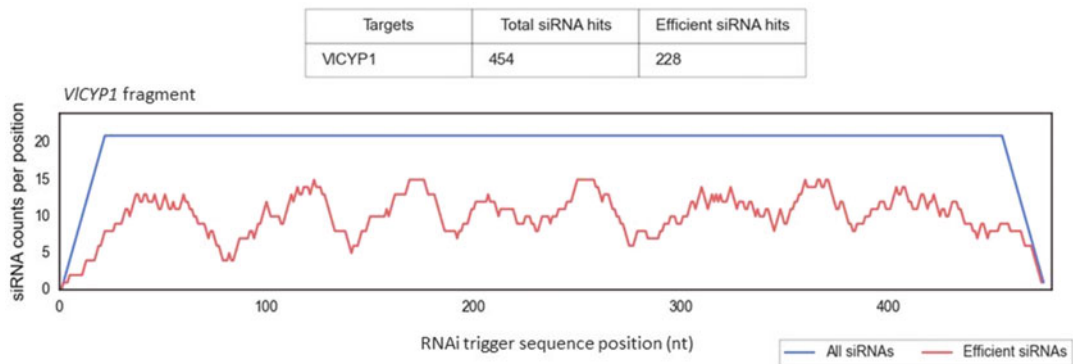


Fig. 2 In silico prediction of total and efficient siRNA hits in *VICYP1* fragment as determined by the si-Fi v21 software

3.2 Production of Labeled dsRNA_{A488}

Work described in this subchapter can be completed within 2 days. This includes total RNA extraction, cDNA synthesis, and amplification followed by purification of the target template flanked by T7 promoter sequences on day 1, and production, washes, and quantification of the labeled dsRNA_{A488} on day 2.

1. For total RNA extraction, start by collecting 1-week-old mycelium (*V41*) grown in a PDB flask in a 50 mL Falcon tube and centrifuge at $3000 \times g$ for 10 min.
2. Discard the supernatant and homogenize the pellet using mortar and pestle in liquid nitrogen.
3. Collect the homogenized sample into 2 mL Eppendorf Safe-Lock Tubes (50 to 100 mg of tissue). Samples can be immediately used or stored at $-80\text{ }^{\circ}\text{C}$ for a longer period.
4. Under a chemical fume hood add 1 mL of TRIzol reagent to the 2 mL collection tube, mix well, and incubate at RT for 5 min.
5. Add 200 μL of chloroform to the sample mix, shake vigorously for 15 s, incubate at RT for 2–3 min followed by centrifugation at $12,000 \times g$ for 15 min at $4\text{ }^{\circ}\text{C}$. After centrifugation, the TRIzol mix will separate into a lower red phenol-chloroform phase, an interphase, and a colorless upper aqueous phase.
6. Place the upper aqueous phase carefully in a new 2 mL collection tube and, always under a chemical fume hood, add 0.5 mL isopropanol to the mix. Incubate at RT for 10 min followed by centrifugation at $12,000 \times g$ for 10 min at $4\text{ }^{\circ}\text{C}$.
7. Discard the supernatant and wash the pellet with 1 mL of 75% ethanol. Briefly vortex the sample and centrifuge it at $7500 \times g$ for 5 min at $4\text{ }^{\circ}\text{C}$. Discard the ethanol solution and allow the pellet to air-dry for 5 min.
8. Finally, dissolve the pellet in 50 μL RNase-free water by heating in a water bath at $55\text{--}60\text{ }^{\circ}\text{C}$ for 15 min and measure the total RNA concentration via spectrophotometric analysis (absorption wavelength 260/230 nm). Proceed with the cDNA synthesis or store the RNA at $-80\text{ }^{\circ}\text{C}$ (*see Note 5*).
9. For removal of genomic DNA mix 2 μg of the RNA with 1 μL of DNase I (1 U/ μL), 1 μL of DNase buffer (10 \times), and 8 μL of RNase-free water to reach the total volume of 10 μL . Incubate at $37\text{ }^{\circ}\text{C}$ for 30 min.
10. Add 2 μL of EDTA (50 mM) and heat the sample at $65\text{ }^{\circ}\text{C}$ for 10 min in a water bath to stop any DNase activity.
11. For cDNA synthesis, set up a 20 μL total volume reaction by placing $\sim 1\text{ }\mu\text{g}$ of the RNA (5 μL from the previous step), 1 μL reverse transcriptase, 5 μL reverse transcriptase buffer (1 \times final concentration), and RNase-free water. Incubate the reaction in

a thermocycler at 22 °C for 5 min followed by 42 °C for 30 min and a final step at 85 °C for 5 min. Store the newly formed cDNA at -20 °C.

12. For the production of a DNA fragment flanked by T7 promoter sequences perform a simple PCR with the T7 primers (the T7 sequence 5'-TAATACGACTCACTATAGGG-3' must be attached at the 5' ends of each primer to permit the association of T7 polymerase with the DNA fragment and the latter production of labeled dsRNA). As the template for the PCR with these primers use the cDNA previously produced. In a PCR collection tube mix around 500 ng of genomic templates with 0.1–0.5 μM of T7-primers, 1.5 mM of MgCl₂, 0.5 U of Taq polymerase plus buffer, 4 mM deoxynucleotides (dNTPs), and RNase-free water to reach a total volume of 25 μL (*see Note 6*).
13. Set up cycler parameters (annealing temperature, denaturation, and extension time) according to your primers, length of the amplicon, and Taq polymerase (*see Note 7*).
14. After completion of the PCR reaction, run the total PCR amplicon on an agarose gel (1.2%) to verify the correct length of the DNA fragment.
15. Extract the DNA fragment from the gel with the help of a scalpel, and place it in a 2 mL centrifuge micro-collection tube.
16. For purifying the DNA fragment use any PCR cleanup kit: add 10 μL of membrane-binding solution per 10 mg of gel slice, vortex briefly, and incubate at 55 °C until the gel is completely dissolved.
17. Place a silica membrane spin column into a collection tube, transfer the dissolved gel mixture into it, incubate for 1 min, centrifuge at 16,000 × *g* at RT for 1 min, and discard the flow-through.
18. Perform two washing steps with membrane wash solution (the first one with 700 μL and the second one with 500 μL) each followed by centrifugation (16,000 × *g* at RT for 2 min). Discard again the flow-through, and dry the membrane with a final centrifugation (16,000 × *g* at RT for 1 min).
19. Finally, add 50 μL of nuclease-free water to the silica membrane spin column and centrifuge for a last time (16,000 × *g* at RT for 1 min). Keep the purified DNA at 4 °C for a short time or store it at -20 °C.
20. For labeling of dsRNA: Apply approximately 1 μg of linearized T7 DNA template for bidirectional *in vitro* transcription (*see Note 8*) in the presence of fluorescent Atto₄₈₈ UTP to create Atto₄₈₈-UTP-tagged dsRNA. Using components of an Atto488 RNA Labeling Kit and following the instruction

protocol provided by the manufacturer, mix in a nuclease-free microtube placed on ice 4 μL T7 reaction buffer ($5\times$), 4 μL labeling mix ($5\times$), 0.25 μL RNase inhibitor (40 U/ μL), and 0.25 μL T7 RNA polymerase (200 U/ μL), and add linearized T7-template-DNA (up to 1 μg) and RNase-free water to a total volume of 20 μL . Incubate the mix at 37 °C for 30 min in a water bath in darkness.

21. Remove the DNA template by DNase (*see* procedure **steps 9–11**) and purify the probe through silica-based membrane columns: transfer the labeled dsRNA_{A488} mix to a silica-based membrane column, incubate at RT for 1 min, and centrifuge at $13,000 \times g$ for 30 s. Wash two times with 700 μL of RNA wash buffer followed each time by centrifugation at $13,000 \times g$ for 30 s. Ensure the complete removal of the RNA wash buffer via centrifugation at $13,000 \times g$ for 2 min. Finally transfer the column into a RNase-free 1.5 mL tube, elute the labeled dsRNA_{A488} with 25 μL of DNase/RNase-free water, and centrifuge at $13,000 \times g$ for 30 s. Perform these steps in a semi-dark room to avoid degradation of the probe due to light (*see* **Note 9**).
22. Quantify the labeled dsRNA concentration via spectrophotometric analysis (e.g., using NanoDrop nanospectrometry equipment) and conserve the mix at -80 °C.

3.3 Labeled dsRNA Feeding to Fungus and Detection of Fluorescent Signal

1. Isolate conidia from 5- to 7-day-old fungal broth culture in sterile conditions (*see* **Notes 10** and **11**). To separate the mycelia from the conidia, filtrate the broth culture through two layers of a sterilized filter sheet (pore size: 22–25 μm) positioned on a sterilized glass funnel. Collect the conidia in a 50 mL Falcon tube and count the conidia with a counting chamber under a bright-field microscope. Set the final concentration to 20,000 conidia per ml of PDB. Conidia can be stored in PDB at 4 °C up to 2 days after isolation (*see* **Note 12**) or at -80 °C in deionized water for a longer period. In the case of a low conidia yield, smash mycelia bulk bodies prior to filtration. This technique will free the conidia trapped in the mycelia. Use freshly isolated vital conidia for the *in vitro* assay.
2. Into each well of a flat-bottom microplate (96-well), add 500 freshly isolated conidia, 250–500 ng of labeled dsRNA, and PDB up to 100 μL of total volume. For the control sample, place an equal volume of nuclease-free water as for labeled dsRNA added into the test samples.
3. Place the microplate on a shaker at low speed (20 g) for 2 days at RT (*see* **Note 13**). During this time, keep the microplate in a darkroom, to avoid the loss of fluorescence of labeled dsRNA due to light.

4. Forty-eight hours after inoculation of labeled dsRNA, transfer 10 μ l of conidia suspension onto a glass slide and take images of growing mycelia in darkness with a fluorescence microscope using appropriate filtering for Atto488 imaging (excitation at 482–514 nm and emission at 520 nm). Take pictures with either a fluorescent microscope equipped with a 10 \times /20 \times objective (Plan-Apochromat 10 \times /20 \times 0.8) (*see* Fig. 3a, b), or a confocal microscope equipped with the 488 nm laser line of an argon multiline laser (11.5 mW) and a water immersion objective (HCX APO L40x0.80 W U-V-l objective) (*see* Fig. 3c–f).

4 Notes

1. For PDB and PDA production, mix the ingredients with 1 L dH₂O and autoclave for 15 min at 121 °C with a pressure of approximately 15 pounds per square inch (PSI). To make PDA plates, pour the still hot (~50 °C) PDA medium into Petri dishes under sterile conditions. Petri dishes can be stacked one on top of another to dissipate the condensation heat.
2. TRIzol is toxic to skin and can give nausea if inhaled. Use TRIzol only with gloves and under a chemical hood.
3. Digital images can be processed with imaging processing software (e.g., Adobe Photoshop) to optimize brightness, contrast, and color and to enable an overlay of the photomicrographs.
4. In our case we selected the *Vl41 Cytochrome P450 monooxygenase* (*VICYPI*) as target for labeled dsRNA. The *VICYPI* mRNA sequence is not available in the literature. The closest conceivable homologous sequence is the *Verticillium dahliae* *Cytochrome P450 monooxygenase* (*VdCYP1*; VDAG_05890 in VdLs.17 genome; 11). Therefore, after analyzing *VdCYP1* for efficient siRNA hits (*see* Fig. 1), we amplified with primers based upon *VdCYP1* sequence a 475 nt fragment of *VICYPI* (*see* Fig. 2), which supposedly had the highest number of efficient siRNA hits. The primers (a) and the *VICYPI* partial sequence used as the template to generate the labeled dsRNA (b, 228 efficient siRNA hits) are listed below:
 - (a) *VICYPI* primers:
 - *VICYPI*_F: 5'- AGAACCGCCTCATTGAGCAT-3'
 - *VICYPI*_R: 5'- ATCGCTCGGGATCAAATACCT-3'

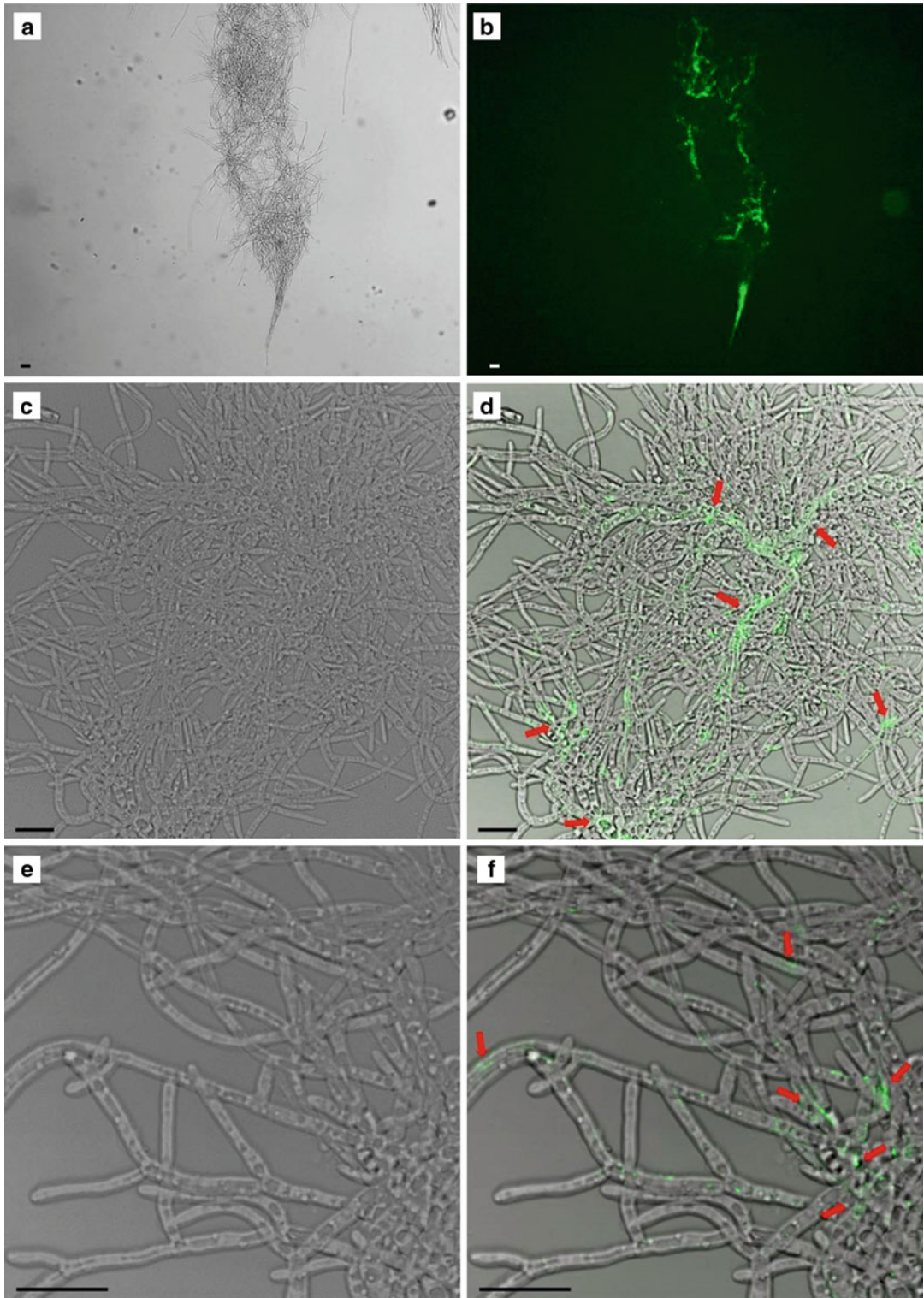


Fig. 3 Detection of ATTO 488-labeled CYP1-dsRNA_{A488} (green) in *V. longisporum* VI41 axenic mycelia growing in PDB 48 h after inoculation (**a–f**). (**a** and **b**) Detection of CYP1-dsRNA₄₈₈ (green) by fluorescent microscopy (Leica DMRE). (**c–f**) Detection of CYP1-dsRNA_{A488} (red arrows) by confocal microscopy (Leica TCS SP2). Scale bars: 25 μm

(b) Partial *VICYPI* DNA sequence (475 nt):

• GGCAGACAAC TACGTGATGG AGTCGAGCAA
 ACGCTCCGAT CCGTCTCCAT TCACGCTGCT
 CAGCCGATTG CACGAGAAGG CGGCAGCGAG
 TGGCGGCACC CTAGACCAGG CGGACATGGC
 AGGAGAGTGT CTTGATCACA TGGCGGCCGG
 CATTGACACA ACGGGCGATG GCCTTTGTTT
 CCTAATGTGG CAGCTGTGCG AGCCATCGTC
 GATGCACTGC CAGGAGAAGC TGCAGCAGGA
 GCTGCGCAAC AACCCAGATG TCGACTTTGA
 CAAGCTGCCC TATCTGGATG CCGTGATCCA
 GGAAGGCCTG CGATGCTTCC CTCCCATCCC
 CATGTGCGCTT CCCCGACGAG TGCCGCAGGG
 CGGAAAGGTC GTGGACGGCT TCTTCGTGCC
 CGGAGGCACC ATCGTCAGCT GCCAAGCGTA
 CTCTGTGCAC ACAATCAACA GCCAGGTATT
 CCCTGAGCCG GAGGTATTTG ATCCC

5. Keep clean conditions when dealing with RNA to avoid degradation by ribonucleases. Avoid repetitive RNA freezing and thawing cycles.
6. Increasing the total volume of the reaction to 50–100 μL and/or the PCR number of cycles can lead to improving the yield of amplicon copies especially for short DNA sequences.
7. Set different annealing temperatures for the PCR. The beginning cycles, 5–6 cycles, should have a lower melting temperature (T_m) (around 5 $^{\circ}\text{C}$ lower) to allow the primers to bind to the gene-specific portion. Subsequent primer annealing events (cycle 6 and thereafter) use the entire primer site and can have a higher T_m to avoid the synthesis of spurious PCR products.
8. For a higher yield of labeled dsRNA, clone the DNA fragment into a plasmid vector (e.g., pGEM[®]-T Easy). This step will allow a higher and easier production of the purified DNA template, leading to a higher production of labeled dsRNA.
9. After purification, observe 1 μL of the mix with a fluorescence microscope using the proper filtering for Alexa Fluor 488 (482–514 nm for excitation and 520 nm for emission) to be sure that the labeling was correctly performed. The drop should emit green light.
10. Both agar and broth cultures can be used for the isolation of conidia; however, the broth culture is preferred because it leads to higher conidia yield in a shorter time period (3–5 days) and the conidia are easier to isolate (just filter through a membrane (pore size: 22–25 μm)).
11. Avoid the use of old broth cultures, which in the case of *V141* may contain a mix of microsclerotia and conidia. Microsclerotia

are big melanized multicellular survival structures and tend to form aggregates resulting in more difficult and imprecise conidia count.

12. Stored conidia will start to germinate after 1 or 2 days at 4 °C. To conserve them for a longer period, resuspend conidia in distilled water (centrifuge at $3000 \times g$ at RT for 10 min and replace PDB with dH₂O). Place the conidia solution after immediate freezing in liquid nitrogen at –80 °C.
13. To avoid loss of material due to evaporation and/or wrong handling, 96-well plates can be sealed with a plastic transparent sticky foil like the one used for sealing qPCR well plates.

References

1. Baulcombe D (2004) RNA silencing in plants. *Nature* 431:7006
2. Castel SE, Martienssen RA (2013) RNA interference in the nucleus: roles for small RNAs in transcription, epigenetics and beyond. *Nat Rev Genet* 14(2):100–112
3. Weiberg A, Wang M, Lin FM, Zhao H, Zhang Z, Kaloshian I, Jin H (2013) Fungal small RNAs suppress plant immunity by hijacking host RNA interference pathways. *Science* 342(6154):118–123
4. Cai Q, He B, Kogel KH, Jin H (2018) Cross-kingdom RNA trafficking and environmental RNAi-nature’s blueprint for modern crop protection strategies. *Curr Opin Microbiol* 46:58–64
5. Zanini S, Šečić E, Busche T, Kalinowski J, Kogel KH (2019) Discovery of interaction-related sRNAs and their targets in the *Brachypodium distachyon* and *Magnaporthe oryzae* pathosystem. *BioRxiv* 631945. <https://doi.org/10.1101/631945>
6. Nowara D, Gay A, Lacomme C, Shaw J, Ridout C, Douchkov D, Schweizer P (2010) HIGS: host-induced gene silencing in the obligate biotrophic fungal pathogen *Blumeria graminis*. *Plant Cell* 22(9):3130–3141
7. Koch A, Biedenkopf D, Furch A, Weber L, Rossbach O, Abdellatef E, Lincus L, Johannismeier J, Jelonek L, Goesmann A, Cardoza V, McMillan T, Mentzel T, Kogel KH (2016) An RNAi-based control of *Fusarium graminearum* infections through spraying of long dsRNAs involves a plant passage and is controlled by the fungal silencing machinery. *PLoS Pathog* 12(10):e1005901
8. Koch A, Kumar N, Weber L, Keller H, Imani J, Kogel KH (2013) Host-induced gene silencing of cytochrome P450 lanosterol C14- α -demethylase-encoding genes confers strong resistance to *Fusarium* species. *Proc Natl Acad Sci U S A* 110(48):19324–19329
9. Head GP, Carroll MW, Evans SP, Rule DM, Willse AR, Clark TL, Meinke LJ (2017) Evaluation of SmartStax and SmartStax PRO maize against western corn rootworm and northern corn rootworm: efficacy and resistance management. *Pest Manag Sci* 73(9):1883–1899
10. McLoughlin AG, Wytinck N, Walker PL, Girard IJ, Rashid KY, Kievit T, Belmonte MF (2018) Identification and application of exogenous dsRNA confers plant protection against *Sclerotinia sclerotiorum* and *Botrytis cinerea*. *Sci Rep* 8(1):7320
11. Zhang DD, Wang XY, Chen JY, Kong ZQ, Gui YJ, Li N, Bao YM, Dai XF (2016) Identification and characterization of a pathogenicity-related gene *VdCTP1* from *Verticillium dahliae*. *Sci Rep* 6:27979
12. Niehl A, Soiminen M, Poranen MM, Heinlein M (2018) Synthetic biology approach for plant protection using dsRNA. *Plant Biotechnol J* 16(9):1679–1687
13. Kettles GJ, Hofinger BJ, Hu P, Bayon C, Rudd JJ, Balmer D, Courbot M, Hammond-Kosack KE, Scalliet G, Kanyuka K (2019) sRNA profiling combined with gene function analysis reveals a lack of evidence for cross-kingdom RNAi in the wheat – *Zymoseptoria tritici* Pathosystem. *Front Plant Sci* 10:892
14. Koch A, Höfle L, Timo Werner B, Imani J, Schmidt A, Jelonek L, Kogel KH (2019) SIGS vs HIGS: a study on the efficacy of two dsRNA delivery strategies to silence genes in infected host and non-host plants. *Molecular Plant Pathology* 20(12):1636–1644

Part IV

Identification and Analysis of RNA-Binding Proteins



Using RNA Affinity Purification Followed by Mass Spectrometry to Identify RNA-Binding Proteins (RBPs)

Mengge Shan and Brian D. Gregory

Abstract

RNA-binding proteins (RBPs) perform key functions in posttranscriptional regulation, adding complexity to the RNA life cycle. RNA interactome capture techniques have been applied to various organisms of interest and detected hundreds of RBPs, some with uncharacterized functions. However, even in many well-studied organisms, the primary sequence motif for most RBPs remains unknown. Here, we describe a 3-day protocol where users couple an RNA sequence of interest that is known to be bound by an RBP (s) with agarose beads, incubate the now tagged RNA sequence with protein lysate, and then pull down the proteins bound to the RNA. Subsequent mass spectrometry allows users to profile the RNA sequence-interacting proteome and pick out any enriched proteins as RBPs of interest. This protocol allows researchers to match sequences to their RBPs and even often identify novel RBPs or new functions for known RBPs.

Key words RNA tagging, RNA-binding proteins

1 Introduction

RNA-binding proteins (RBPs) are key players in posttranscriptional regulatory processes, and perform diverse functions such as stabilization, localization, splicing, and transport of bound RNAs [1]. Research has shown that interactions between RBPs and target RNAs impact every part of the RNA life cycle, from polyadenylation to degradation. This is because RBPs bind to specific target RNAs to form ribonucleoprotein complexes (RNPs), which then progress through the events of the RNA life cycle. The binding of an RBP to its target RNA molecule can depend on the RNA's primary nucleotide sequence, its RNA secondary structure, and oftentimes both of these features. The importance of these interactions makes it no surprise that defects in the RBP-RNA binding can disrupt important regulatory networks and ultimately result in diseases such as cancer, autoimmune problems, and metabolic and neurological disorders [2–4].

To date, research has identified the binding sequences of more than 400 RBPs in humans and mice model systems [5]. Exploratory computational analysis in human cells puts the number of human RBPs at over 1500, or approximately 7.5% of the human proteome [6]. In *Arabidopsis*, interactome capture techniques have tentatively identified 1145 RBPs, with 550 of them known to have RNA binding potential and 595 novel candidates [7]. Many identified RBPs have functions that are tissue or timepoint specific, prompting further research to categorize their functions in post-transcriptional regulatory processes.

The development of recent techniques such as genome-wide UV cross-linking immunoprecipitation followed by sequencing (gCLIP-seq) [8] and protein interaction profile sequencing (PIP-seq) [9] enable researchers to identify the interaction sites of RBPs on a transcriptome-wide scale. However, the proteins that interact with the identified RBP-bound sequences are not known. Therefore, subsequent RNA-tagging-based techniques can help identify the specific RBPs that bind to unique target sequences identified by these high-throughput techniques. To do this, the identified protein-interacting sequences are used as bait to form RNP complexes with RBPs that bind these sequences in a protein lysate of interest. These probe-bound RBPs are then eluted and identified using mass spectrometry. The process is based on the propensity of RBPs to bind to specific sequences, which enables researchers to identify proteins that are enriched in a purification experiment as likely RBP candidates for further validation.

The protocol described in this chapter (Fig. 1) is one such approach for identifying RBPs where RNA sequences of interest are covalently tagged to adipic acid dihydrazide agarose beads through their 3' hydroxyl groups. Each tagged RNA sequence is then combined with a protein lysate so that the RBPs that recognize and interact with the RNA sequence of interest are isolated and then subsequently identified using mass spectrometry. We have successfully used this technique multiple times with results from the model plant *Arabidopsis* to identify a novel nuclear function for an RBP that had previously been annotated to be localized specifically in the chloroplast [10] as well as SERRATE and GLYCINE-RICH RNA-BINDING PROTEIN8 (GRP8) as RBPs with novel functions in regulating hair root cell development [11].

2 Materials

2.1 Equipment

1. Centrifuge.
2. Microcentrifuge.
3. SpeedVac.

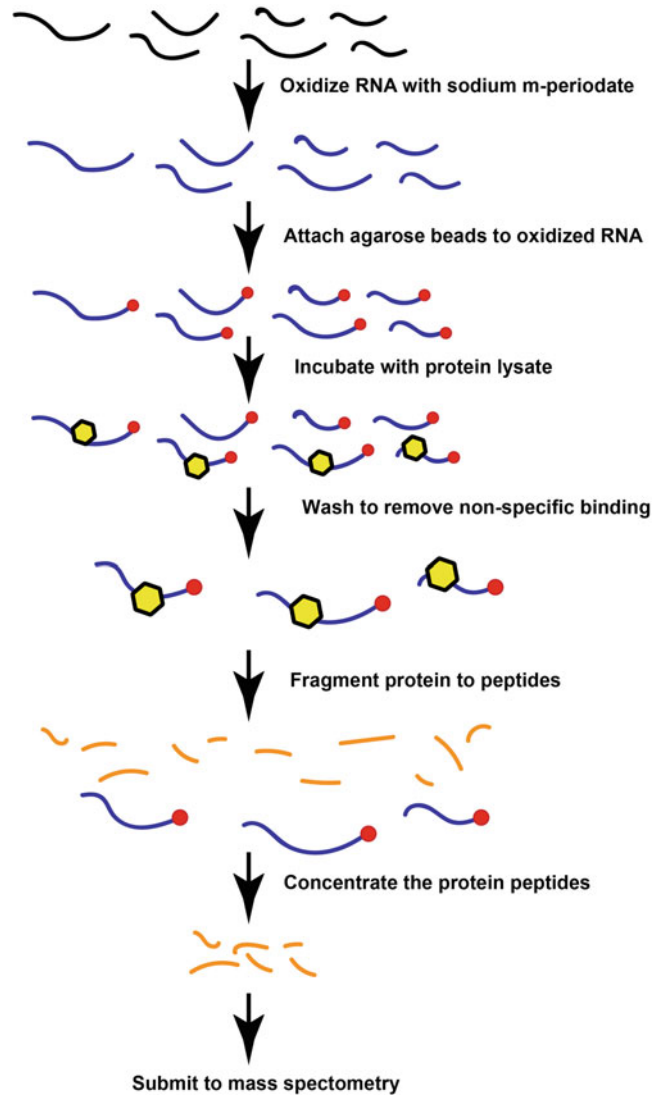


Fig. 1 An overview of RNA-affinity pulldown. After oxidation, RNA probes are covalently tagged with agarose beads. Incubation of the tagged RNA probes and protein lysates encourages the formation of RNPs. After several washes to remove nonspecific binding, the RNP complex is pulled down and the proteins that interact with the RNA sequence of interest are subsequently identified using mass spectrometry

4. Rotator.
5. Incubator at 37 °C.
6. Freezer at -80 °C.
7. Cold room at 4 °C.
8. Mass spectrometer.

2.2 Solutions

1. 100 μM RNA probe sequences (*see Note 1*).
2. 100 μM Scrambled RNA probe sequence as control.
3. Ribonuclease (RNase)-free water.
4. 3 M NaOAc.
5. 0.1 M NaOAc.
6. 5 mM Sodium m-periodate in 0.1 M NaOAc (*see Note 2*).
7. 100 mM ATP.
8. 0.25 $\mu\text{g}/\mu\text{L}$ Yeast tRNA in BC100 (*see Subheading 2.3, item 3*).
9. 6 ng/ μL Modified trypsin, sequencing grade (*see Note 3*).
10. 13% Polyvinyl alcohol (PVA) (*see Note 4*).
11. 1 \times TE: 10 mM Tris-HCl, 1 mM EDTA, pH 8.0.
12. 0.02 \times TE: TE diluted 1:50 with RNase-free water.
13. 100 mM KCl.
14. 200 mM KCl.
15. 80 mM MgCl_2 .
16. 6 mM MgCl_2 .
17. 2 M NaCl.
18. 100 mM NaCl.
19. 400 mM NaCl.
20. 0.5 M Creatine phosphate.
21. Adipic acid dihydrazide agarose beads in 50% solution (*see Note 5*).
22. 20 mM Tris-HCl, pH 7.5.
23. 100% Ethanol.
24. 80% Ethanol.
25. 5 mg/mL Glycogen.
26. 100 mM NH_4CO_3 .
27. Protein lysate (45–50 μg per reaction; *see Subheading 3.2*).

2.3 Buffers

1. GFB100: 0.02 \times TE, 100 mM KCl.
2. GFB200+ 6 mM MgCl_2 : 0.02 \times TE, 200 mM KCl, 6 mM MgCl_2 .
3. BC100: 0.02 \times TE, 100 mM NaCl.
4. BC400: 0.02 \times TE, 400 mM NaCl.
5. Binding buffer (per reaction): 397.5 μL BC100, 316.5 μL RNase-free water, 150 μL BC400, 150 μL 13% PVA, 150 μL 10 mM ATP, 150 μL 0.25 $\mu\text{g}/\mu\text{L}$ tRNA in BC100, 60 μL 80 mM MgCl_2 , 60 μL 0.5 M creatine phosphate, 45–50 μg protein lysate (no more than 60 μL).

The 5 mM sodium m-periodate and binding buffer must always be made fresh as the former is light sensitive and the latter contains protein lysates. The other buffers can be stored longer, but the use of fresh buffer is always advised whenever possible.

2.4 Miscellaneous

1. 2 mL Eppendorf tubes ($2 \times$ number of reactions).
2. 1.5 mL Eppendorf tubes ($2 \times$ number of reactions).
3. 15 mL Falcon tubes ($1 \times$ number of reactions).
4. 50 mL Falcon tubes or other sterilized containers for storing buffers.

3 Methods

3.1 Designing Probe Sequences

Since RBPs can bind to their target RNAs in a sequence-specific manner, RNA sequences used as probes in the protocol should be significantly enriched at suspected RBP-binding sites as those sequences are likely to correspond to the binding motif of an RBP. To identify binding sites, users can use techniques such as gCLIP-seq [8] or PIP-seq [9]. gCLIP-seq identifies the binding sites of RBPs throughout the genome based on protein-RNA cross-linking resulting in mutations and truncated read ends in the resulting high-throughput sequencing data. PIP-seq is an antibody-independent sequencing technique that uses RNase digestion in the presence compared to the absence of bound RBPs to identify transcriptome-wide RBP-binding sites. Thus, both protocols allow researchers to unbiasedly survey RBP-binding sites on a transcriptome-wide scale. However, researchers will not be able to identify the RBPs that bind to each identified RBP-bound site based simply on the data from these approaches alone. From the total collection of identified RBP-binding sites, users can identify enriched sequences using motif enrichment analysis tools such as MEME [12] or HOMER [13] (Fig. 2) (*see Note 6*).

Figure 2 provides a general overview of motif enrichment and selection. In more detail, both MEME and HOMER operate under the same general principle of scanning through a collection of sequences and identifying consensus sequences that occur multiple times. As part of that process, the algorithm will compare sequence representation against a background distribution of all possible *n-mers*. While both algorithms provide a default background model as a starting point, users can also supply their own custom background sequences to better fine-tune results. For example, users can create organism-specific background models or classify sequences of interest into untranslated regions (UTRs), CDS, introns, etc. and then supply the relevant custom background. This has the advantage of correcting for species-specific biases in

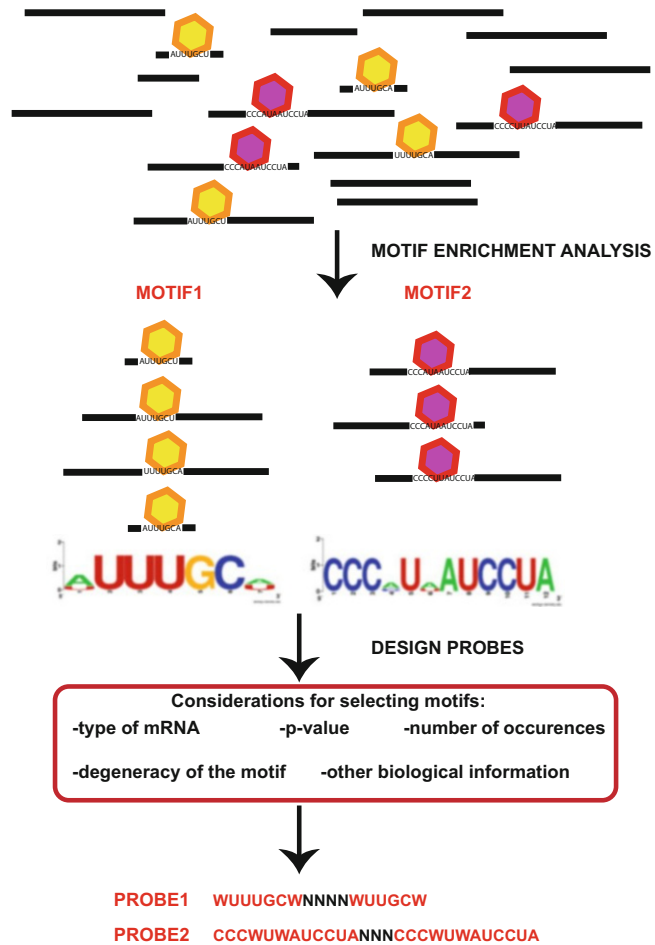


Fig. 2 Identifying enriched motifs and designing RNA probes. Motif enrichment tools can identify overrepresented sequence motifs present in a collection of sequences such as putative RBP-binding sites. Users can elect motifs based on several criteria and generate RNA probes. For RNA sequence motifs <20 nucleotides in length, the sequence should be duplicated and separated by several random nucleotides to minimize the possibility of proteins binding and occluding the site through chance

GC content or sequences that are only overrepresented in certain gene regions.

Often motif enrichment tools will detect more than one enriched sequence and users have to identify the relevant motifs of interest. To that end, both MEME and HOMER supply a statistical p-value, which can be used as a criterium to select enriched motifs. Additional considerations could include the number of times a sequence has been detected, which mRNAs contain the motif, the degeneracy of the sequence, as well as any other biological context. While <http://homer.ucsd.edu/homer/>

[introduction/practicalTips.html](#) is geared toward HOMER users, the general principles discussed regarding background selection, motif size restriction, etc. is applicable to other motif enrichment tools.

Once you select the motifs of interest for identifying the specific interacting RBPs, they need to be synthesized as an RNA molecule for subsequent tagging with agarose beads and ultimately identification of interacting protein. We tend to choose motif sequences that are relatively short (i.e., <20 nucleotides) in nature, which allows us to develop an RNA probe that consists of a duplex of the motif sequence of interest separated by random nucleotides. We recommend designating these random nucleotides as a sequence of Ns (Fig. 2). The inclusion of these random spacer regions is to minimize the risk of the binding site being masked by the bead [14].

3.2 Protein Lysate Collection

The RNA affinity purification protocol is cell culture independent and can therefore be easily adapted to suit any organism of interest. Standard protein collection protocol should be employed to collect protein samples, keeping in mind that each reaction requires 45–50 μg of protein at a minimum concentration of 0.75 $\mu\text{g}/\mu\text{L}$ (see Note 7).

3.3 RNA Affinity Purification

The following RNA affinity purification protocol takes 3 days and is written for a single reaction. If using the same RNA probe on multiple samples, we recommend treating each probe-lysate pair separately. For example, if probe A is to be used in four samples, make four probe A samples as opposed to adding four times the volumes of buffers to a bigger tube and then splitting the resulting probe sample four ways.

Though the numerous washing steps should alleviate much of the nonspecific protein binding that can pose a challenge in the RNA affinity protocol, suitable controls such as scrambled RNA probe and/or non-RNA probe should still be included in your experiments to eliminate any nonspecific proteins that generally bind RNA or that are found in high concentration and tend to contaminate mass spectrometry analyses (e.g., ribosomal subunit proteins). In the downstream analysis, RBPs that are enriched in the test probe when compared to the control probe(s) should be considered as candidates for further analysis and follow-up studies.

3.3.1 Tagging RNA with Agarose Beads

In order to make the execution of the protocol smoother, users should (1) reconstitute the RNA probe in RNase-free water and (2) make up ~ 42 mL/probe worth of 0.1 M NaOAc (see Note 8) before starting. The following steps will oxidize the RNA probe at the 3' end before precipitating the oxidized RNA with ethanol and then tagging the RNA sequences with agarose beads.

1. Transfer 5 μL of 100 μM stock of RNA probe to a new 2 mL tube (*see Note 9*).
2. Add 35 μL of RNase-free water.
3. Add 360 μL of 5 mM sodium m-periodate in 0.1 M NaOAc (*see Note 10*).
4. Incubate for 1 h in the dark at room temperature (*see Note 11*).
5. Add 3 μL of 5 mg/mL glycogen, 23 μL 3 M NaOAc, and 1 mL 100% EtOH.
6. Shake vigorously and then centrifuge down.
7. Store at $-80\text{ }^{\circ}\text{C}$ > 2 h (*see Note 12*).
8. Centrifuge at max speed for >80 min at $4\text{ }^{\circ}\text{C}$ (*see Note 13*).
9. Aspirate supernatant.
10. Wash with 750 μL 80% ethanol.
11. Spin for 5 min at max speed at room temperature in a micro-centrifuge, remove supernatant, and let air-dry until only the pellet remains (*see Note 14*).
12. During ethanol washing (**step 11**), prepare and label new 2 mL tubes.
13. Resuspend pellet in 290 μL RNase-free water and transfer the content to a new tube.
14. Add 10 μL 3 M NaOAc for a final volume and concentration of 300 μL in 0.1 M NaOAc.
15. During centrifuging step (**step 8**), transfer 100 μL of adipic acid dihydrazide agarose beads in 50% solution to a 15 mL tube, one for each sample (*see Note 15*).
16. Wash 4 \times with 10 mL 0.1 M NaOAc; each spin is at 1439 rcf for 5 min.
17. Resuspend beads in 900 μL /probe 0.1 M NaOAc (*see Note 16*).
18. Add beads to the RNA, cover each tube with tinfoil, and let rotate at $4\text{ }^{\circ}\text{C}$ overnight.

If possible, calculate and make up enough of the buffers for day 2. Buffers can be stored for short term at room temperature.

3.3.2 Incubating Tagged RNA with Protein Lysate

During the previous day, RNA probes were tagged with agarose beads. At the successful completion of the following steps, the tagged RNAs will be incubated with protein lysates to encourage the binding of RBPs to the RNA sequences of interest. The various washes will remove nonspecific protein binding before the reaction is digested with trypsin overnight to fragment the bound proteins into peptide fragments.

To prepare for the protocol, users should (1) make all the buffers and store them in sterilized containers and (2) thaw/make up ATP, tRNA, and creatine phosphate. Please note that **steps 1–3** are best done in 4 °C cold rooms while the rest of the protocol can be done at room temperature. At a minimum, the microcentrifuge needs to be chilled to 4 °C and kept at that temperature during **steps 1–3**. In addition, depending on the downstream mass spectrometry protocol, users may choose to add a reduction and alkylating step before digesting with trypsin; these additions will replace **step 11** and are discussed in further detail in the Notes section below.

Steps 1–3 are done at 4 °C.

1. Spin beads at $1,702 \times g$ for 5 min in a microcentrifuge and remove supernatant (*see Note 17*).
2. Wash beads 2× with 2 M NaCl, 1 mL each time. Each spin is at $958 \times g$ for 5 min in a microcentrifuge.
3. Wash beads 2× with GFB-100.

The rest of the protocol is done at room temperature.

4. Add 1.5 mL binding solution (which contains the protein lysate of interest) to the bead/RNA mix and let rotate at room temperature for 90 min (*see Note 18*).
5. Spin samples at $958 \times g$ for 5 min in a microcentrifuge.
6. Remove supernatant and add 1 mL GFB-200 + 6 mM MgCl₂.
7. Let rotate for 5 min, and spin samples at $958 \times g$ for 5 min in a microcentrifuge.
8. Repeat **steps 6–7** three additional times for a total of four washes.
9. Wash with 20 mM Tris-HCl [pH = 7.5]; spin for 5 min at $958 \times g$ in a microcentrifuge.
10. Wash with 100 mM NH₄HCO₃; spin for 5 min at $958 \times g$ in a microcentrifuge.
11. Resuspend in 100 μL 100 mM NH₄HCO₃ (*see Note 19*).
12. Add 35 μL of 6 ng/μL trypsin.
13. Incubate at 37 °C overnight.

3.3.3 Isolating Enriched Proteins

After trypsin digestion, the proteins of interest exist as peptide fragments in the supernatant. The last portion of the protocol separates the supernatant from the beads and RNA fragments and concentrates the peptides into a form that is usable for downstream mass spectrometry.

1. Spin down (5 min at $958 \times g$ in a microcentrifuge) and transfer supernatant to a new tube.

2. Spin down (5 min at $958 \times g$ in a microcentrifuge) and transfer supernatant to a new tube.
3. Concentrate in the SpeedVac for >2 h at room temperature. Check the samples approximately once every hour until all the liquid has evaporated, leaving behind a solid powder at the bottom of the tube (*see Note 20*).
4. Store at -20 °C and submit for liquid chromatography-mass spectrometry.

3.3.4 Mass Spectrometry

RNA affinity purification should be followed by liquid chromatography-mass spectrometry to identify enriched protein candidates. The liquid chromatography-mass spectrometry (LC-MS) technique uses liquid chromatography principles to separate peptides and then identifies them with mass spectrometry. For well-characterized model organisms, label-free methods such as the iBAQ system can be used in the mass spectrometry portion [15]. Other mass spectrometry methods include stable isotope labeling methods [16] or selective reaction monitoring [17]. Based on the analysis of protein sequence similarity and RNA-binding motif similarity, proteins with $>70\%$ amino acid sequence similarity are likely to have very similar RNA sequence specificity [18], so users should expect several candidate proteins to be identified after mass spectrometry analysis.

3.3.5 Further Validation

Once mass spectrometry analysis has identified possible RBP candidates of interest, further possible validation experiments include western blots, knockout/knockdown experiments, CLIP-seq to validate that the protein interacts with the motif that was used to pull it down, etc.

4 Notes

1. RNA oligos can be purchased from services such as IDT. In general, we recommend probe sequences of >20 bases. The oligo comes as lyophilized content and will need to be reconstituted with ribonuclease (RNase)-free water. To make up $100 \mu\text{M}$ of the RNA probe, add in $x \mu\text{L}$ of nuclease-free water where x is $10 \times$ the concentration of the oligo in nmoles. For example, if the probe is 89.4 nmol , add $894 \mu\text{L}$ of RNase-free water to reconstitute to $100 \mu\text{M}$. Properly stored at -20 °C, probes can be stable for up to 2 years. For longer term storage, probes should be aliquoted and kept at -80 °C.
2. Sodium m-periodate is light sensitive and should be stored in the dark and the solution made fresh daily.

3. The trypsin needs to be of sequencing grade. Regular trypsin used for cell culture is not an appropriate substitute. Reconstitute trypsin ahead of time and aliquot as needed. The trypsin type listed here needs to be reconstituted with needle and gauge and then heated at 30 °C for 15 min before use.
4. Dissolving PVA in water is best done with gradual heating and mechanical stirring. This process can take several hours so it is recommended to prepare the required 13% PVA ahead of time.
5. Streptavidin-coated beads, such as Dynabeads M-280 Streptavidin, can also be used in RNA affinity purifications with minor adjustments to the protocol.
6. The motif discovery tool MEME is available as an online and command-line version. For more information, please visit the tutorial at http://meme-suite.org/doc/meme.html?man_type=web. HOMER is available as a command-line tool; installation instructions and tutorial are available at <http://homer.ucsd.edu/homer/motif/>.
7. At least two replicates with follow-up studies is the recommended standard. When collecting lysates, please ensure that there is enough for all replicates. In addition, because the binding buffer only allows for 60 µL of lysates to be added, it is better to have a concentrated sample that can be diluted with RNase-free water.
8. Always make up a few extra mLs of buffer as a precaution.
9. While 1.5 mL tubes are suitable for this part, 2 mL tubes are preferred as they give users some extra room to work with.
10. Usually only a small amount of sodium m-periodate is needed to make enough of the solution. Rather than trying to accurately measure out the small amount needed, it is easier to make up more solution than necessary and dispose of the extra. Given the light-sensitive nature of sodium m-periodate, do not store the solution for more than 24 h.
11. Sodium m-periodate is light sensitive, so tubes should be placed on a rack and the rack be completely wrapped in tinfoil and then shut in a drawer.
12. After 2 h at –80 °C, the solution may freeze but should thaw out very quickly once out of –80 °C. In addition, there should be no distinct layers; if the ethanol has formed a layer of its own, wait for solution to thaw, and repeat **steps 6** and **7**.
13. If there is no dedicated 4 °C centrifuge, the equipment should be chilled down while the samples are in –80 °C.
14. The best practice is to remove most of the supernatant with a pipette and then air-dry the sample with the cap open. At the end, there should be a small pellet at the bottom of the tube.

15. There should be one 15 mL tube with beads for each probe sample. For example, if there are four samples total, then there should be four tubes with 100 μ L of beads in each instead of one tube with 400 μ L of beads.
16. The resuspended beads can be stored at 4 °C until needed.
17. The agarose beads can be difficult to visualize. Users can use a pipette and remove a little bit less than the amount of liquid put in during previous steps. For example, if the previous step added in 1 mL of liquid, remove 900 μ L. Use a new pipette tip for each tube to minimize cross-contamination. Tilting the tube slightly can also help visualize the concentration of beads at the bottom of the tube.
18. Depending on the concentration of the lysate, the binding buffer may not be exactly 1.5 mL. Users can make up the difference with additional RNase-free water.
19. Some mass spectrometry protocols will recommend adding a reduction and alkylating step at this point to improve the quality of downstream mass spectrometry data. If so, instead of resuspending in 100 μ L 100 mM NH_4HCO_3 , resuspend in 100 μ L of 10 mM DTT in 100 mM NH_4HCO_3 and then incubate for 1 h at 56 °C. After cooling the sample to room temperature, add iodoacetamide to a final concentration of 50 mM and incubate in the dark for 45 min. Iodoacetamide is unstable and light sensitive, which means 1 M stock needs to be made fresh every day and kept in the dark for as much time as possible when performing the experiments, especially once it is in solution.
20. Depending on the number of samples and the room humidity, concentrating the samples can take longer than 2 h. As long as the vacuum is operating normally and the liquid is evaporating, simply monitor the samples until the supernatant has evaporated.

Acknowledgments

The authors would like to thank members of the Gregory lab both past and present for helpful discussions. This work was funded by NSF grants MCB-1243947, MCB-1623887, and IOS-1444490 to B.D.G.

References

1. Glisovic T, Bachorik JL, Yong J, Dreyfuss G (2008) RNA-binding proteins and post-transcriptional gene regulation. *FEBS Lett* 582:1977–1986
2. Lukong KE, Chang K, Khanjian EW, Richard S (2008) RNA-binding proteins in human genetics disease. *Trends Genet* 24:416–425

3. Cooper TA, Wan L, Dreyfuss G (2009) RNA and disease. *Cell* 136:777–793
4. Darnell RB (2010) RNA regulation in neurologic disease and cancer. *Cancer Res Treat* 42:125–129
5. Cook KB, Kazan H, Zuberi K, Morris Q, Hughes TR (2011) RBPDB: a database of RNA-binding specificities. *Nucleic Acids Res* 39:D301–D308
6. Gerstberger S, Hafner M, Tuschl T (2014) A census of human RNA-binding proteins. *Nat Rev Genet* 15:829–845
7. Marondedze C, Thomas L, Serrano NL, Lilley KS, Gehring L, Gehring S (2016) The RNA-binding protein repertoire of *Arabidopsis thaliana*. *Sci Rep* 6:29766
8. Stork C, Zheng S (2016) Genome-wide profiling of RNA-protein interactions using CLIP-seq. *Methods Mol Biol* 1421:137–151
9. Foley S, Gregory BD (2016) Protein interaction profile sequencing (PIP-seq). *Curr Protoc Mol Biol* 116:27.5.1–27.5.15
10. Goasi SJ, Foley SW, Wang D, Silverman IM, Selamoglu N, Nelson AD, Beilstein MA, Daldal F, Deal RB, Gregory BD (2015) Global analysis of the RNA-protein interaction and RNA secondary structure landscapes of the *Arabidopsis* nucleus. *Mol Cell* 57:376–388
11. Foley S, Gosai SJ, Wang D, Selamoglu N, Solitti AC, Koster T, Steffen A, Lyons E, Daldal F, Garcia BA, Staiger D, Deal RB, Gregory BD (2017) A global view of RNA-protein interactions reveals novel root hair cell fate regulators. *Dev Cell* 41:204–220
12. Bailey TL, Elkan C (1994) Fitting a mixture model by expectation maximization to discover motifs in biopolymers. *Proceedings of the second international conference on intelligent systems for molecular biology*, pp 28–36
13. Heinz S, Brenner C, Spann N, Bertolino E, Lin YC, Laslo P, Cheng JX, Murre C, Singh H, Glass CK (2010) Simple combinations of lineage-determining transcription factors prime cis-regulatory elements required for macrophage and B cell identities. *Mol Cell* 38:576–589
14. Smith CWJ (ed) (1998) *RNA-protein interactions: a practical approach*. Oxford University Press, Oxford
15. Schwanhäusser B, Busse D, Dittmar G, Schuchhardt J, Wolf J, Chen W, Selbach M (2011) Global quantification of mammalian gene expression control. *Nature* 473:337–342
16. Chahrour O, Cobice D, Malone J (2015) Stable isotope labelling methods in mass spectrometry-based quantitative methods. *J Pharm Biomed Anal* 113:2–20
17. Vidova V, Spacil Z (2017) A review on mass spectrometry-based quantitative proteomics: targeted and data independent acquisition. *Anal Chim Acta* 964:7–23
18. Ray D, Kazan H, Cook KB, Weirauch MT, Li X, Gueroussov S, Albu M, Zheng H, Yang A, Na H, Irimia M, Matzat LH, Dale RK, Smith SA, Yarosh CA, Kelly SM, Nabet B, Mecnas D, Li W, Laishram RS, Qiao M, Lipshitz HD, Piano F, Corbett AH, Carstens RP, Frey BJ, Anderson RA, Lynch KW, Penalva LOF, Lei EP, Fraser AG, Blencowe BJ, Morris QD, Hughes TR (2013) A compendium of RNA-binding motifs for decoding gene regulation. *Nature* 499(7457):172–177



Plant Individual Nucleotide Resolution Cross-Linking and Immunoprecipitation to Characterize RNA-Protein Complexes

Tino Köster and Dorothee Staiger

Abstract

In recent years, it has become increasingly recognized that regulation at the RNA level pervasively shapes the transcriptome in eukaryotic cells. This has fostered an interest in the mode of action of RNA-binding proteins that, via interaction with specific RNA sequence motifs, modulate gene expression. Understanding such posttranscriptional networks controlled by an RNA-binding protein requires a comprehensive identification of its *in vivo* targets. In metazoans and yeast, methods have been devised to stabilize RNA-protein interactions by UV cross-linking before isolating RNA-protein complexes using antibodies, followed by identification of associated RNAs by next-generation sequencing. These methods are collectively referred to as CLIP-Seq (cross-linking immunoprecipitation-high-throughput sequencing). Here, we present a version of the individual nucleotide resolution cross-linking and immunoprecipitation procedure that is suitable for use in the model plant *Arabidopsis thaliana*.

Key words RNA immunoprecipitation, iCLIP, Posttranscriptional, RNA-binding protein

1 Introduction

Upon transcription, pre-mRNAs undergo a suite of processing steps including alternative splicing, 3' end formation, modification, export from the nucleus, and degradation. RNA-binding proteins (RBPs) control each of these steps through dynamic interaction with *cis*-regulatory motifs on their RNA targets [1–6]. To identify RNAs associated with RBPs *in vivo*, endogenously assembled RNA-protein complexes are stabilized by cross-linking and captured from cellular extracts with immobilized antibodies against the RBP. Subsequently, target mRNAs are identified in the RNA fraction isolated from the immunoprecipitated complexes.

In vivo cross-linking stabilizes transient and weak RNA-protein complexes and thus allows more stringent washing conditions to be applied. Moreover, it prevents reconfiguration or RNA-protein complexes upon tissue disruption [7]. In *Arabidopsis*, chemical

cross-linking through formaldehyde fixation has been mostly used [8–11]. Of note, formaldehyde also cross-links proteins so that transcripts may also coprecipitate due to binding to an interacting protein. In contrast, UV cross-linking immunoprecipitation and cross-linking (CLIP) use 254 nm UV light which only cross-links nucleic acids and proteins.

UV light cross-linking has only recently been used in plants for genome-wide determination of RBP targets [12, 13]. It was also used in recent mRNA interactome capture experiments [14–17]. For a detailed discussion of the use of UV light to cross-link RNA and protein in *Arabidopsis thaliana* we refer to [18].

In CLIP techniques, during construction of libraries from coprecipitated RNAs, RNA adapters are ligated at both the 5' and 3' ends before reverse transcription. Reverse transcriptase stalls at the cross-linked nucleotide in >90% of the cases [18] and CLIP can identify sequences only when reverse transcriptase is able to pass through the cross-link site. This property has been explicitly used to map cross-link sites in individual nucleotide resolution and immunoprecipitation (iCLIP) (Fig. 1). After ligation of an RNA linker to the 3' end, a two-part cleavable DNA adapter serves as primer for RT. The sequencing primer is moved to the 5' end via circularization and relinearization of the cDNAs, thus capturing cDNAs terminating at the site where the bound protein has been cross-linked.

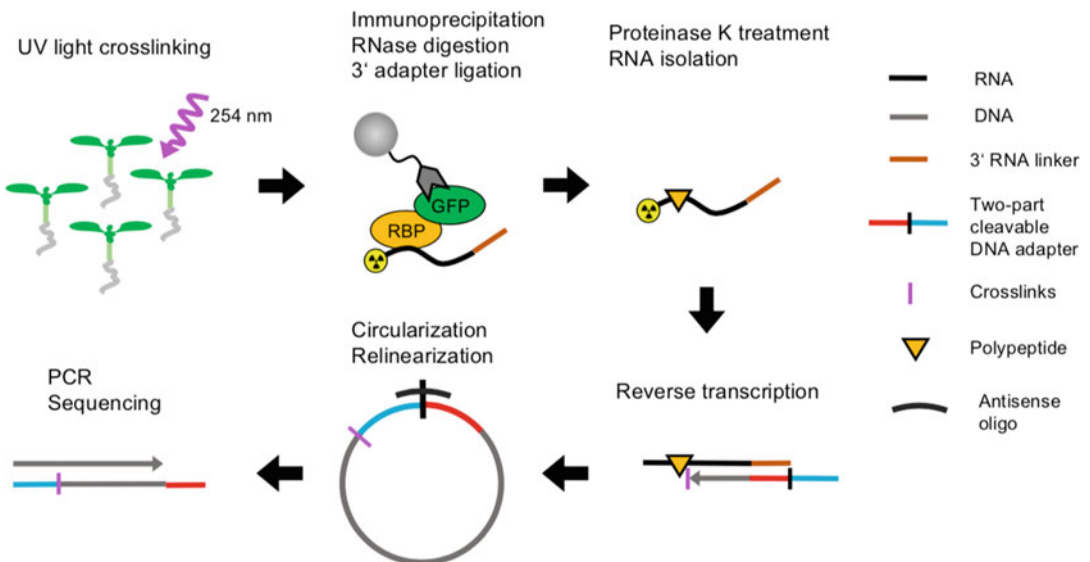


Fig. 1 Scheme of the iCLIP procedure. Plants are subjected to UV cross-linking (see Subheading 3.2), followed by immunoprecipitation of the RNA-protein complexes from the lysates, RNase digestion, and 3' adapter ligation (see Subheadings 3.5–3.8), and proteinase K treatment and RNA isolation (see Subheading 3.12). Reverse transcription, circularization, relinearization, PCR amplification to generate sequencing libraries, as well as high-throughput sequencing are performed as described in (23)

We have adapted the individual nucleotide resolution and immunoprecipitation (iCLIP) procedure developed by the Ule laboratory so that it is suitable for use in the model plant *Arabidopsis thaliana* [12, 19–22].

Transgenic expression of an epitope-tagged version of the RBP allows the recovery of RNA-protein complexes by virtue of commercially available antibodies of high specificity and high affinity for the tag. To obtain a realistic picture of the *in vivo* targets expressed in the same cell type as the RBP, the endogenous promoter should be used to drive the expression of the epitope-tagged protein. It is recommended to include the authentic *cis*-regulatory sequences within the transcribed part of the gene, i.e., untranslated regions and introns. It is imperative to demonstrate that the fusion protein retains *in vivo* functionality, most conveniently through complementation of a loss-of-function mutant.

In parallel to the experimental transgenic plant line expressing the RBP-GFP fusion protein, control lines can be generated that express an RNA-binding deficient variant of the RBP or the GFP moiety by itself, both driven by the identical regulatory elements of the RBP gene. A comparative analysis of experimental and control lines is then performed using GFP Trap beads for samples as well as controls.

Alternatively, control precipitations can be performed with GFP antibodies in wild-type plants lacking the RBP-GFP fusion protein [8] or by mock treatment of the extract with an unrelated antibody, e.g., RFP Trap beads.

Here, we describe the adaptation of UV cross-linking, recovery of RNA-protein complexes, and retrieval of the RNA from gel-purified complexes for plant tissue. Subsequent generation of cDNA libraries, high-throughput sequencing, and bioinformatics determination of binding targets and cross-link sites are done according to published protocols.

2 Materials

2.1 Plant Growth

1. Agar plates: 2.2 g Murashige-Skoog (MS) powder, 0.5 g morpholinoethane sulfonate (MES), 50 g sucrose. Add water to 1 L, adjust to pH 5.7 using 1 M KOH, add 10 g plant growth agar, and autoclave. Distribute the sterilized medium into agar plates and allow to cool under sterile conditions.

2.2 UV Light Fixation

1. Liquid nitrogen.
2. UV cross-linker equipped with 254 nm lamps.
3. Mortar and pestle.
4. 2 mL Tubes with punctured lid.

2.3 Preparation of Beads

1. IP lysis buffer w/o inhibitors: 50 mM Tris-HCl pH 7.5, 150 mM NaCl, 4 mM MgCl₂, 0.25% Igepal, 0.25% sodium desoxycholate, 1% SDS. Add 5 mM DTT before use.
2. Sepharose beads.
3. GFP-Trap[®] agarose beads (Chromotek).
4. End-over-end rotator.
5. DNA LoBind[®] tubes (Eppendorf).

2.4 Total Extract Preparation

1. Liquid nitrogen.
2. 0.1 M Phenylmethylsulfonyl fluoride (PMSF) in isopropanol.
3. IP lysis buffer: 50 mM Tris-HCl pH 7.5, 150 mM NaCl, 4 mM MgCl₂, 0.25% Igepal, 0.25% sodium desoxycholate, 1% SDS. Add 5 mM DTT, 100 U RiboLock/mL, 1 mM PMSF, as well as protease inhibitor tablets, as suggested by the supplier before use.
4. Steel balls ø 4 mm.
5. 0.45 µM Syringe filter.
6. 5 mL Syringe.
7. Thermomixer (e.g., Eppendorf).

2.5 Immuno-precipitation

1. IP wash buffer: 50 mM Tris-HCl pH 7.5, 500 mM NaCl, 2 M urea, 4 mM MgCl₂, 0.5% Igepal, 0.5% sodium desoxycholate, 1% SDS. Add 2 mM DTT and protease inhibitor tablets as suggested by the supplier before use.
2. PNK wash buffer (pH 7.4): 20 mM Tris-HCl, pH 7.4, 10 mM MgCl₂, 0.2% Tween 20.
3. End-over-end rotator.
4. DNA LoBind[®] tubes (Eppendorf).

2.6 RNase Digest

1. RNase I (100 U/µL).
2. PNK wash buffer (pH 7.4) (*see* Subheading 2.5).
3. Turbo DNase (Thermo Fisher Scientific).

2.7 Dephosphorylation

1. 5× PNK buffer (pH 6.5): 350 mM Tris-HCl, pH 6.5, 50 mM MgCl₂, 25 mM DTT (*see* Note 1).
2. T4 polynucleotide kinase.
3. RiboLock RNase Inhibitor (Thermo Fisher Scientific).
4. PNK wash buffer (pH 7.4) (*see* Subheading 2.5).
5. High-salt buffer: 50 mM Tris-HCl, pH 7.4, 1 M NaCl, 1 mM EDTA, 1% Igepal, 0.1% SDS, 0.5% sodium desoxycholate.
6. Thermomixer (e.g., Eppendorf).

2.8 Linker Ligation

1. 4× Ligation buffer: 200 mM Tris-HCl, pH 7.8, 40 mM MgCl₂, 40 mM DTT.
2. T4 RNA ligase 1 (30,000 U/mL).
3. 50% Polyethylene glycol 8000 (PEG8000).
4. RiboLock RNase Inhibitor (Thermo Fisher Scientific).
5. 20 μM Pre-adenylated L3 adapter (rAppAGATCGGAA-GAGCGGTTCAG/ddC/).
6. High-salt buffer (*see* Subheading 2.7).

2.9 Radioactive Labeling of RNA

1. 4× NuPAGE™ LDS sample buffer (Thermo Fisher Scientific).
2. T4 polynucleotide kinase (T4 PNK) and 10× buffer A (Thermo Fisher Scientific).
3. [γ -³²P] ATP (370 MBq/mL).
4. RiboLock RNase Inhibitor (Thermo Fisher Scientific).
5. PNK wash buffer (pH 7.4) (*see* Subheading 2.5).

2.10 SDS PAGE

1. 20× 3-(N-Morpholino)propanesulfonic acid (MOPS) SDS running buffer: 50 mM MOPS, 50 mM Tris, 0.1% SDS, 1 mM EDTA, pH 7.7 (*see* Note 2).
2. Precast 4–12% NuPAGE Bis-Tris gel (Thermo Fisher Scientific) (*see* Note 3).
3. XCell SureLock™ Mini-Cell Electrophoresis System (Thermo Fisher Scientific).
4. Prestained protein ladder.

2.11 Blot and Isolation of RNA-Protein Complexes

1. Transfer buffer: 25 mM Tris, 192 mM glycine, 0.05% SDS, 10% (v/v) methanol (add freshly).
2. 10× Phosphate-buffered saline (PBS): 79 mM Na₂HPO₄, 145 mM KH₂PO₄, 5 mM MgCl₂ x 6 H₂O, 27 mM KCl, 1.37 M NaCl.
3. XCell SureLock™ Mini-Cell Electrophoresis System (Thermo Fisher Scientific).
4. XCell II Blot Module (Thermo Fisher Scientific).
5. Whatman filter paper.
6. Protran BA-85 nitrocellulose membrane (Sigma-Aldrich).
7. Saran wrap.
8. Autoradiography exposure cassette.
9. Fluorescent ruler.
10. X-ray film.
11. Standard X-ray film processing chemicals/equipment (e.g., Kodak).
12. Clean scalpels.

2.12 RNA Isolation

1. Proteinase K buffer: 100 mM Tris-HCl pH 7.4, 50 mM NaCl, 10 mM EDTA.
2. Proteinase K (Roche): 20 mg/mL in 10 mM Tris-HCl, pH 7.4.
3. Proteinase K urea buffer: 100 mM Tris-HCl, pH 7.4, 50 mM NaCl, 10 mM EDTA, 7 M urea.
4. Tri-reagent: 0.8 M Guanidinium thiocyanate, 0.4 M ammonium thiocyanate, 4.35% (w/v) glycerol, 0.1 M sodium acetate, pH 5.0, 38% (v/v) acidic phenol.
5. Chloroform:isoamyl alcohol (24:1).
6. Isopropanol.
7. 70% (v/v) Ethanol pre-chilled at $-20\text{ }^{\circ}\text{C}$.
8. Ambion[®] GlycoBlue[™] (Invitrogen).
9. 3 M Sodium acetate, pH 5.5.
10. 100% Ethanol, pre-chilled.
11. Thermomixer.
12. Phase Lock Gel heavy tubes (VWR).

3 Methods
3.1 Plant Growth

1. Grow Arabidopsis plants of the appropriate genotypes for 2–3 weeks on agar plates under the chosen experimental conditions.

3.2 UV Light Fixation and Plant Harvest

1. Place agar plates on ice inside the UV cross-linker.
2. Subject plants to cross-linking, starting with a dose of $500\text{ mJ}/\text{cm}^2$ (*see Note 4*).
3. Harvest plants and immediately transfer to liquid nitrogen.
4. Grind frozen plant material to a fine powder in liquid nitrogen.
5. Transfer 0.5 g ground plant material to pre-chilled 2 mL tubes with punctured lid. Use $2 \times 0.5\text{ g}$ distributed to two 2 mL tubes. Store at $-80\text{ }^{\circ}\text{C}$ until further use.

3.3 Preparation of Beads

1. To prepare sepharose beads for preclearing (*see Note 5*), pipette 100 μL of sepharose beads (50% slurry) (*see Note 6*) in a 1.5 mL tube and add 1 mL of ice-cold IP lysis buffer w/o inhibitors. Incubate for 5 min at $4\text{ }^{\circ}\text{C}$ in an end-over-end rotator. Centrifuge for 1 min at $500 \times g$. Repeat this washing step in IP lysis buffer twice. Store at $4\text{ }^{\circ}\text{C}$ until use.
2. To prepare GFP-Trap[®] beads for immunoprecipitation, wash 20 μL GFP-Trap[®] beads (50% slurry) with 1 mL of ice-cold IP lysis buffer in a 1.5 mL LoBind[®] tube for 5 min at $4\text{ }^{\circ}\text{C}$

(see **Note 7**). Centrifuge for 1 min at $500 \times g$. Repeat this washing step in IP lysis buffer twice. Store at 4°C until use.

3.4 Total Extract Preparation

1. Remove tubes with frozen plant material from liquid nitrogen and add $750\ \mu\text{L}$ of IP lysis buffer prewarmed to 40°C (see **Note 8**).
2. Add steel ball and replace punctured lid by an intact lid of a new tube. Invert several times.
3. Incubate briefly at 40°C and 1400 rpm in a thermomixer until you get a homogenous lysate.
4. Centrifuge for 10 min at maximal speed at 4°C and transfer supernatant to a fresh 1.5 mL tube. Combine supernatants.
5. Filter lysate using a 5 mL syringe and a $0.45\ \mu\text{m}$ syringe filter.
6. Add 1.0–1.5 mL lysate to the washed sepharose beads and vortex.
7. Incubate on an end-over-end rotator for 1 h at 4°C .

3.5 Immunoprecipitation

1. Remove any remaining buffer from the GFP-Trap[®] beads.
2. Centrifuge precleared samples from Subheading 3.4, step 7, for 2 min at $500 \times g$ and 4°C to pellet the sepharose beads.
3. Transfer the precleared lysate to the GFP-Trap[®] beads and incubate on an end-over-end rotator for 1 h at 4°C .
4. Centrifuge for 1 min at $500 \times g$ at 4°C and discard supernatants.
5. Wash beads with $850\ \mu\text{L}$ of ice-cold IP wash buffer for 10 min at 4°C and rotate on an end-over-end rotator (see **Note 9**).
6. Centrifuge for 1 min at $500 \times g$ at 4°C and discard supernatants.
7. Repeat washing three more times.
8. Transfer beads to new LoBind[®] tubes.
9. Wash beads twice with $850\ \mu\text{L}$ of ice-cold PNK wash buffer (pH 7.4) for 1 min at 4°C and rotate on an end-over-end rotator during each washing step.
10. After each washing step, centrifuge for 1 min at $500 \times g$ at 4°C and discard supernatant.

3.6 RNase Digest

1. Resuspend beads in $100\ \mu\text{L}$ PNK wash buffer (pH 7.4).
2. Add $2\ \mu\text{L}$ of Turbo DNase and $5\ \mu\text{L}$ of RNase I dilution (see **Note 10**) to the beads and incubate for 10 min in a thermomixer at 37°C and 1100 rpm.
3. Transfer the reaction for more than 3 min on ice.
4. Centrifuge for 2 min at $500 \times g$ and discard supernatants.

3.7 Dephosphorylation

1. Prepare 1 × PNK buffer (pH 6.5) from 5 × stock.
2. Wash beads with 850 μL of ice-cold 1 × PNK buffer (pH 6.5) by inverting several times.
3. Centrifuge for 1 min at 500 × *g* and discard supernatant.
4. Resuspend beads in 20 μL of PNK mix (4 μL 5 × PNK buffer (pH 6.5), 0.5 μL T4 PNK, 0.5 μL RiboLock, 15 μL H₂O).
5. Incubate for 20 min at 37 °C at 1100 rpm in a thermomixer.
6. Wash beads twice with ice-cold 850 μL of PNK wash buffer (pH 7.4) for 1 min by inverting several times.
7. Centrifuge for 1 min at 500 × *g* and discard supernatant.
8. Wash beads once with 850 μL ice-cold high-salt buffer for 1 min by inverting several times.
9. Centrifuge for 1 min at 500 × *g* and discard supernatant.
10. Wash beads twice with 850 μL of PNK wash buffer (pH 7.4) for 1 min by inverting several times.
11. After each washing step, centrifuge for 1 min at 500 × *g* and discard supernatant.

3.8 Linker Ligation

1. Prepare 1 × ligation buffer from 4 × stock.
2. Wash beads once with 850 μL of ice-cold 1 × ligation buffer for 1 min by inverting several times.
3. Centrifuge for 1 min at 500 × *g* and discard supernatant.
4. Resuspend beads in 20 μL ligation mix (9 μL H₂O, 4 μL 4 × ligation buffer, 1 μL RNA ligase, 0.5 μL RiboLock, 4 μL 50% PEG8000).
5. Add 1.5 μL of pre-adenylated L3 adapter (20 μM).
6. Mix thoroughly and centrifuge briefly.
7. Incubate for at least 16 h at 16 °C and 1100 rpm in a thermomixer.
8. Add 500 μL PNK wash buffer (pH 7.4) and mix thoroughly.
9. Centrifuge for 1 min at 500 × *g* and remove supernatant.
10. Wash beads twice with 850 μL of ice-cold high-salt buffer for 5 min under constant rotation.
11. After each washing step, centrifuge for 1 min at 500 × *g* and discard supernatant.
12. Wash beads with 1 mL of ice-cold PNK wash buffer (pH 7.4) for 5 min under constant rotation.
13. Centrifuge for 1 min at 500 × *g* and discard supernatant.
14. Repeat washing step and leave second wash including beads behind (do not centrifuge).

3.9 Radioactive Labeling of RNA

1. Mix beads thoroughly and transfer 200 μL (20%) of the second wash including beads to a new 1.5 mL LoBind[®] tube.
2. Keep the remaining 800 μL (80%) of the second wash including beads and store on ice until **step 11**.
3. Centrifuge for 1 min at $500 \times g$ and discard supernatant.
4. Resuspend beads in 18 μL PNK mix (2 μL 10 \times buffer A, 14.5 μL H₂O, 1 μL T4-PNK, 0.5 μL RiboLock).
5. Add 2 μL [γ -³²P] ATP.
6. Incubate for 20 min at 37 °C and 1100 rpm in a thermomixer.
7. Wash three times with 800 μL of ice-cold PNK wash buffer (pH 7.4) for 1 min under constant agitation.
8. After each washing step, centrifuge for 1 min at $500 \times g$ and discard supernatant.
9. Bring 4 \times NuPAGE[™] LDS sample buffer to room temperature and dilute it to 2 \times with ddH₂O.
10. Add 20 μL of 2 \times NuPAGE[™] LDS sample buffer to the beads and mix carefully by pipetting (*see Note 11*).
11. Remove supernatant from the remaining cold beads from **step 2** and add the 20% radioactively labeled beads to the 80% cold beads.
12. Incubate at 95 °C for 10 min.
13. Place tube on ice and centrifuge briefly to precipitate the beads.
14. Collect the supernatant and store it on ice until loading of the gel.

3.10 SDS-PAGE

1. Prepare 1 \times MOPS SDS running buffer by diluting 20 \times stock solution with ddH₂O.
2. Set up a precast 4–12% NuPAGE Bis-Tris gel according to the manufacturer's instructions.
3. Load the supernatant of the beads from Subheading 3.9, **step 14**, on the gel (*see Note 12*).
4. Load 5 μL of prestained protein ladder.
5. Run the gel for 60 min at 180 V in 1 \times MOPS SDS running buffer according to the manufacturer's instructions.
6. Remove the gel front (~0.5 cm) and discard as solid radioactive waste (contains free radioactive [γ -³²P] ATP).

3.11 Blot and Isolation of RNA-Protein Complexes

1. Set up the XCell II Blot Module according to the manufacturer's instructions.
2. Prepare transfer buffer (*see Subheading 2.11*) by freshly adding 10% methanol.

3. Equilibrate Whatman paper and nitrocellulose membrane (8.0 × 6.5 cm each) in transfer buffer (do not soak the gel in transfer buffer).
4. Remove the wells of the gel using a razor blade.
5. Transfer the gel onto the nitrocellulose membrane. Therefore, place a pre-soaked Whatman paper on top of the gel. Remove the air bubbles and turn the plate over. Place the pre-soaked membrane on the gel. Again, remove the air bubbles and add a pre-soaked Whatman paper on top.
6. Fill the inner chamber with transfer buffer containing 10% methanol and the outer chamber with cold ddH₂O.
7. Transfer for 1 h at 30 V.
8. After blotting, disassemble the XCell II Blot Module and measure radioactivity in the gel and the membrane to verify efficient transfer.
9. Rinse the membrane in 1 × PBS buffer.
10. Wrap membrane in saran wrap and place it into an X-ray cassette along with a fluorescent ruler.
11. Expose the membrane to an X-ray film at -80 °C for 3 h or overnight and develop the film in the darkroom using standard X-ray film processing chemicals (Fig. 2).
12. Draw marker bands onto the film.

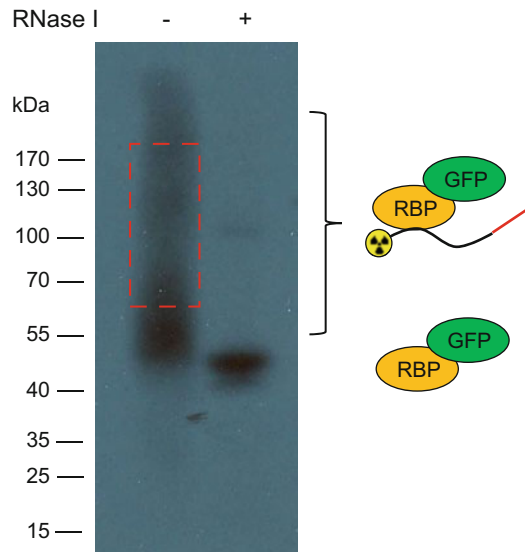


Fig. 2 Autoradiogram of RNA-protein complexes separated on an SDS-PAGE and blotted onto a nitrocellulose membrane. Samples with and without RNase treatment are shown. The region above the RNA-binding protein (apparent molecular weight 55 kDa) represents protein with associated RNAs and is cut out (indicated by the broken line) for RNA isolation and library preparation

13. Use a scalpel and a ruler to cut the desired sizes (15–80 kDa above the expected molecular weight of the precipitated protein) from the film.
14. Adjust the film to the membrane and use clean scalpels to excise the desired membrane fragments (*see Note 13*).
15. Transfer the membrane fragments into 1.5 mL tubes.

3.12 RNA Isolation

1. Add 200 μL of proteinase K buffer and 10 μL proteinase K to the membrane pieces.
2. Incubate tubes in the thermomixer for 20 min at 37 °C and at 1100 rpm.
3. Add 200 μL of PK urea buffer and incubate for another 20 min at 37 °C and 1100 rpm.
4. Collect the supernatant and transfer to a new tube. If necessary, centrifuge tubes briefly and add remaining solution to the supernatant sample (*see Note 14*).
5. Prespin Phase Lock Gel heavy tubes for 30 s at 12,000 $\times g$ to collect the gel at the bottom of the tubes.
6. Add 400 μL of Tri-reagent to the solution collected from the membrane.
7. Incubate for 5 min at 30 °C and 1100 rpm.
8. Add 400 μL chloroform/isoamyl alcohol (24:1), mix thoroughly by pipetting, and transfer the solution to a 2 mL Phase Lock tube.
9. Incubate for 5 min at 30 °C and 1100 rpm (do not vortex!).
10. Centrifuge for 5 min at 12,000 $\times g$ at room temperature.
11. Transfer the aqueous layer into a new tube. Be careful not to touch the gel with the pipette.
12. Add 0.8 μL of GlycoBlue and 40 μL 3 M sodium acetate (pH 5.5) and vortex thoroughly.
13. Add 850 μL of pre-chilled 100% EtOH, mix thoroughly, and precipitate overnight at -20 °C.
14. RNA is ready for preparation of cDNA libraries for high-throughput sequencing as described in [23].

4 Notes

1. Freeze aliquots of the buffer at -20 °C and thaw only once.
2. NuPAGE MOPS SDS running buffer is commercially available (Thermo Fisher Scientific).
3. We recommend to use precast 4–12% NuPAGE Bis-Tris gels as the NuPAGE buffer system ensures a stable pH around 7.0

throughout the run and prevents alkaline hydrolysis of the coprecipitated RNA.

4. The optimal dose of UV light is determined by inspection of the autoradiograms of the RNA-protein complexes separated on SDS polyacrylamide gels (*see* Subheadings 3.10 and 3.11). The optimal size of fragmented RNA ranges between 30 and 300 nucleotides, which corresponds to 15–80 kDa above the expected molecular weight of the precipitated protein (Fig. 2).
5. Binding of contaminating RNAs to the beads is minimized by preclearing the cellular lysate with plain beads.
6. Cut off the end of the tips when pipetting beads.
7. Use LoBind tubes (Eppendorf) to avoid unspecific binding of proteins and nucleic acids to the walls of the tube during IP. Change tubes during IP to remove residual proteins and nucleic acids which bind nonspecifically to the walls.
8. In case of high RNase activity in the total extract, the use of additional RNase inhibitors like vanadyl-ribosyl complex (VRC) or heparin sodium salt might be necessary.
9. Washing conditions have to be established carefully to reduce unspecific binding as much as possible but to avoid dissociation of the specific RNA-protein interactions and of the RBP-antibody interaction. Stringency of washing buffer can be changed by adjusting the concentration of NaCl, urea, or other chaotropic salts, e.g., LiCl.
10. Optimal RNase I conditions are crucial and have to be titrated for each RBP individually. Therefore, RNase I dilutions ranging from 1:100 to 1:6000 have to be tested. The efficiency of the RNase treatment can be monitored by visualization of the RNA-protein complexes via SDS-PAGE and autoradiography (*see* Note 3) (Fig. 2).
11. Pipette carefully as LDS easily produces foam.
12. Leave lanes free between the samples.
13. Use different scalpels for the different samples and controls to avoid cross-contamination.
14. Measure radioactivity on the beads. Above 90% of the radioactivity should be removed after digestion.

Acknowledgments

We greatly appreciate valuable suggestions on the protocol by Drs. Julian König, Kathi Zarnack, and Michaela Müller Mc-Nicoll. This work was supported by the DFG (STA 653/6, STA653/9, and STA653/14).

References

1. Singh G, Pratt G, Yeo GW et al (2015) The clothes make the mRNA: past and present trends in mRNP fashion. *Annu Rev Biochem* 84:325–354
2. Staiger D (2001) RNA-binding proteins and circadian rhythms in *Arabidopsis thaliana*. *Philos Trans R Soc Lond B Biol Sci* 356:755–1759
3. Kupsch C, Ruwe H, Gusewski S et al (2012) Arabidopsis chloroplast RNA binding proteins CP31A and CP29A associate with large transcript pools and confer cold stress tolerance by influencing multiple chloroplast RNA processing steps. *Plant Cell* 24:4266–4280
4. Kang H, Park SJ, Kwak KJ (2013) Plant RNA chaperones in stress response. *Trends Plant Sci* 18:100–106
5. Lewinski M, Hallmann A, Staiger D (2016) Genome-wide identification and phylogenetic analysis of plant RNA binding proteins comprising both RNA recognition motifs and contiguous glycine residues. *Mol Gen Genomics* 291:763–773
6. Rataj K, Simpson GG (2014) Message ends: RNA 3' processing and flowering time control. *J Exp Bot* 65:353–363
7. Mili S, Steitz JA (2004) Evidence for reassociation of RNA-binding proteins after cell lysis: implications for the interpretation of immunoprecipitation analyses. *RNA* 10:1692–1694
8. Xing D, Wang Y, Hamilton M et al (2015) Transcriptome-wide identification of RNA targets of Arabidopsis SERINE/ARGININE-RICH45 uncovers the unexpected roles of this RNA binding protein in RNA processing. *Plant Cell* 27:3294–3308
9. Köster T, Meyer K (2018) Plant ribonomics: proteins in search of RNA partners. *Trends Plant Sci* 23:352–365
10. Köster T, Staiger D (2014) RNA-binding protein immunoprecipitation from whole-cell extracts. *Methods Mol Biol* 1062:679–695
11. Köster T, Haas M, Staiger D (2014) The RIPper case: identification of RNA-binding protein targets by RNA immunoprecipitation. *Methods Mol Biol* 1158:107–121
12. Meyer K, Köster T, Nolte C et al (2017) Adaptation of iCLIP to plants determines the binding landscape of the clock-regulated RNA-binding protein AtGRP7. *Genome Biol* 18:204
13. Zhang Y, Gu L, Hou Y et al (2015) Integrative genome-wide analysis reveals HLP1, a novel RNA-binding protein, regulates plant flowering by targeting alternative polyadenylation. *Cell Res* 25:864–876
14. Maronedze C, Thomas L, Serrano NL et al (2016) The RNA-binding protein repertoire of Arabidopsis thaliana. *Sci Rep* 6:29766
15. Reichel M, Liao Y, Rettel M et al (2016) In planta determination of the mRNA-binding proteome of Arabidopsis etiolated seedlings. *Plant Cell* 28:2435–2452
16. Zhang Z, Boonen K, Ferrari P et al (2016) UV crosslinked mRNA-binding proteins captured from leaf mesophyll protoplasts. *Plant Methods* 12:42
17. Köster T, Maronedze C, Meyer K et al (2017) RNA-binding proteins revisited – the emerging Arabidopsis mRNA interactome. *Trends Plant Sci* 22:512–526
18. Köster T, Reichel M, Staiger D (2019) CLIP and RNA interactome studies to unravel genome-wide RNA-protein interactions in vivo in *Arabidopsis thaliana*. *Methods*. <https://doi.org/10.1016/j.ymeth.2019.09.005>
19. Sugimoto Y, König J, Hussain S et al (2012) Analysis of CLIP and iCLIP methods for nucleotide-resolution studies of protein-RNA interactions. *Genome Biol* 13:R67
20. König J, Zarnack K, Rot G et al (2010) iCLIP reveals the function of hnRNP particles in splicing at individual nucleotide resolution. *Nat Struct Mol Biol* 17:909–915
21. Wang Z, Kayikci M, Briese M et al (2010) iCLIP predicts the dual splicing effects of TIA-RNA interactions. *PLoS Biol* 8:e1000530
22. Zarnack K, König J, Tajnik M et al (2013) Direct competition between hnRNP C and U2AF65 protects the transcriptome from the exonization of alu elements. *Cell* 152:453–466
23. Huppertz I, Attig J, D'Ambrogio A et al (2014) iCLIP: Protein-RNA interactions at nucleotide resolution. *Methods* 65:274–287



A Single-Molecule RNA Mobility Assay to Identify Proteins that Link RNAs to Molecular Motors

Varun Bhaskar, Min Jia, and Jeffrey A. Chao

Abstract

mRNA transport and localization is a key aspect of posttranscriptional gene regulation. While the transport of many mRNAs is thought to occur through the recruitment of molecular motors, it has been a challenge to identify RNA-binding proteins (RBPs) that directly interact with motors by conventional assays. In order to identify RBPs and their specific domains that are responsible for recruiting a motor to transport granules, we have developed a single-molecule RNA mobility assay that enables quantifying the effect of a tethered RBP on the movement of an RNA. We demonstrate that tethering of RNAs to myosin or kinesin through their well-characterized interacting proteins results in quantitative differences in RNA mobility. This methodology provides a framework for identifying RBPs that mediate associations with motors.

Key words Tethering assay, Myosin, Kinesin, RNA transport, Single-molecule RNA imaging, Live cell

1 Introduction

mRNA transport and cytoplasmic localization is a key aspect of posttranscriptional gene regulation. While multiple mechanisms have been described that result in asymmetric RNA localization, active transport is thought to be the predominant mode by which mRNAs achieve specific subcellular localization [1–6]. Active transport of an mRNA involves the assembly of a ribonucleoprotein particle and its subsequent transport by a molecular motor including the kinesin, dynein, and myosin family of motors [7–11]. Therefore, the active transport of mRNA necessitates physical linking of the target mRNA to a molecular motor for its transport and subsequent anchoring at its destination [7–11]. Due to the complex architecture of the transport granule and the presence of multiple RNA-binding proteins (RBPs) within the granule, it has been a challenge to identify RBPs that directly bind to motors by conventional assays [9]. In order to identify RBPs and their specific domains that are responsible for recruiting a motor to a transport

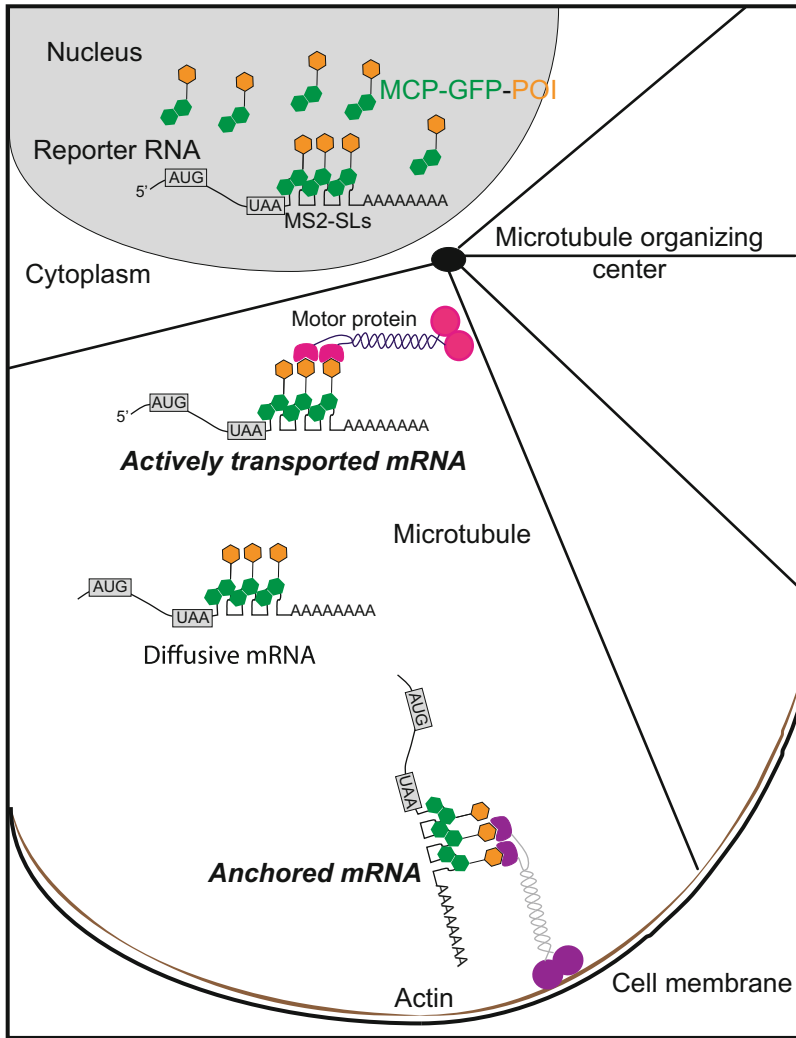


Fig. 1 Schematic diagram of the tethering assay for RNA mobility. The reporter RNA containing the MS2 stem-loops are bound by MCP-GFP (shown in green) fused to the protein of interest (POI, orange). The mobility of reporter RNA is altered depending on the interaction of POI with a molecular motor (magenta) or an anchor (purple)

granule, we have developed a single-molecule RNA mobility assay that enables the effect of a tethered protein on the movement of an RNA to be quantified within living cells (Fig. 1).

Tethering assays have been employed to study the role of specific proteins in different posttranscriptional regulatory pathways including translation and mRNA degradation [12–15]. These assays artificially connect the functional domain of a protein to a reporter RNA using a heterologous RNA-protein interaction such as the ones based upon the MS2 and PP7 coat proteins or the lambda N peptide and their cognate RNA hairpins

[12–16]. This is particularly useful when the *cis*-acting elements, necessary to recruit the RBP to a transcript, are not well known or if the protein functions within a complex whose components have not been fully characterized. Tethering of a protein of interest affects the properties of the reporter RNA that can then be measured using an appropriate readout. Since proteins could have more than one cellular function, it is generally preferred to tether a single functional domain of a protein to the reporter. Importantly, tethering of an individual domain helps to study its role in isolation and minimizes any secondary effects arising due to binding of the protein of interest to its endogenous targets.

In this tethering assay (Fig. 1), the reporter is composed of a Renilla luciferase coding sequence followed by 24x-MS2 stem-loops in its 3'UTR. The reporter is stably integrated into HeLa cells and is placed under a doxycycline-inducible promoter [17, 18]. The cells are transfected with a plasmid expressing the fusion protein of MS2 coat protein (MCP) fused to green fluorescent protein (GFP) and a protein or protein domain of interest (POI). The reporter can be visualized using the GFP signal in living cells and its movement can be measured by single-particle tracking (SPT). Since the reporter transcripts lack any known *cis*-acting elements that promote RNA localization, the mRNAs predominantly undergo diffusional movement (Fig. 1). When the protein domain that is fused to MCP-GFP recruits a molecular motor, its mobility gets altered and can be measured by calculating the mean squared displacements, diffusion coefficients, and velocity of the reporter RNA molecule (Fig. 1). In order to establish the assay, it is necessary to quantify the effect of tethering known motor-interacting domains to a transcript. For monitoring actin-based transport, the RILPL2 RH1 domain was chosen because of its well-characterized interaction with myosin Va [19]. For microtubule-based transport, the N-terminal domain of SKIP that has been shown to bind to kinesin light chain 2 (KLC2) was selected [20].

This chapter contains instructions on how to perform the tethering assay for RNA mobility. It describes how to acquire single-mRNA imaging data and analyze the images in order to quantify RNA mobility. We conclude with a description of the analysis of the positive controls (RILPL2-RH1 and SKIP).

2 Materials

2.1 Sample Preparation

1. HeLa cells stably expressing a reporter mRNA carrying 24x-MS2 stem-loops in the 3' untranslated region, under a doxycycline-inducible promoter [17, 18].

2. Plasmid expressing the chimeric fusion protein of MCP tandem dimer, 2x-GFP, and RBP (full-length/domain of interest). The domain of interest can be cloned at either the N- or the C-terminus of the fusion protein (*see Note 1*).
3. Cell culture incubator.
4. Dulbecco's modified Eagle medium (DMEM) supplemented with 10% (v/v) Tet-free fetal bovine serum (FBS) and 1% (v/v) penicillin and streptomycin (pen/strep).
5. DMEM supplemented with 10% (v/v) Tet-free FBS without pen/strep.
6. Phosphate-buffered saline (PBS).
7. Trypsin-EDTA solution.
8. 35 mm Cell culture dish or 6-well plate.
9. CYTOO coverslips with cross-bow printed pattern (CYTOO SA, CW-M-A X18, or CW-L-A X18).
10. CYTOO chamber (CYTOO SA, 30-010).
11. 40 µg/mL Fibronectin.
12. Automated cell counter and counting slides.
13. 1 mg/mL Doxycycline.
14. Lipofectamine 2000.
15. Opti-MEM.
16. 40 µm Cell strainer.

2.2 Imaging System

1. Wide-field or spinning disk confocal microscope (*see Note 2*).
2. 100 × 1.45NA PlanApo TIRFM oil immersion objective.
3. Back-illuminated EMCCD camera.
4. Emission filter for GFP fluorescence.
5. Solid-state laser (100 mW 491 nm).
6. Motorized X, Y, Z-piezo controlled stage.
7. Incubation box around microscope providing heating and CO₂ regulation.

2.3 Image Analysis

1. Fiji software with TrackMate plug-in [21, 22].
2. Diff2fit [18].
3. HMM-Bayes [23].
4. All code and analysis tools are available from the Chao lab (<https://data.fmi.ch/PublicationSupplementRepo/?group=gchao>).

3 Methods

3.1 Preparation of Cells and Transfection

Day 1

1. Seed 600,000 HeLa cells in a 35 mm dish with a final volume of 2 mL of DMEM + 10% FBS + 1% Pen/Strep and keep it at 37 °C with 5% CO₂.

Day 2

2. Remove the medium from the dish and add 2 mL of fresh prewarmed DMEM + 10% FBS without Pen/Strep.
3. Dilute 1 µg of the plasmid encoding the MCP-GFP-RBP fusion protein in 250 µL of Opti-MEM. Simultaneously, dilute 10 µL of Lipofectamine 2000 in 250 µL of Opti-MEM (*see Note 3*).
4. After 5 min, mix the two solutions and incubate at room temperature for 25 min.
5. Subsequently, add the transfection mixture to the cells in a dropwise manner.
6. Incubate the cells at 37 °C with 5% CO₂ for 6 h.
7. Split the cells using standard cell culture techniques, seed 350,000 cells in a new 35 mm dish, and place it at 37 °C with 5% CO₂.

3.2 Seeding of Cells on the CYTOO Coverslips for Imaging

Day 4

1. Coating the CYTOO chip with fibronectin:
 - (a) Place the CYTOO chip in a 35 mm dish such that the micropattern surface is facing upwards.
 - (b) Thaw 2 mL of 40 µg/mL fibronectin and add to the 35 mm dish containing the CYTOO chip. Additionally, add 2 mL of PBS. Make sure that the chip is fully immersed in the solution.
 - (c) Incubate the dish for 2 h at room temperature.
 - (d) Wash the chip by adding 4 mL of PBS to the existing solution and then by removing 4 mL of the final solution. Repeat this step three times and place the chip with PBS in the sterile CYTOO chamber.
2. Seeding cells on the CYTOO chip:
 - (a) Prepare a HeLa cell suspension at a density of 60,000 cells/mL by trypsinization of the transfected cells and filter them using a 40 µm cell strainer to ensure single cells.
 - (b) Seed 2 mL of cell solution in the CYTOO chamber (after removing PBS) (*see Note 4*).

- (c) Incubate for 10 min at room temperature and then for 20 min at 37 °C and 5% CO₂.
- (d) Subsequently, wash two times with 2 mL DMEM + 10% FBS + 1% Pen/Strep to remove unattached cells.
- (e) Incubate for 1 h at 37 °C and 5% CO₂.
- (f) Aspirate the media, add 2 mL of fresh DMEM + 10% FBS + 1% Pen/Strep containing 1 µg/mL doxycycline, and incubate for 1 h at 37 °C and 5% CO₂.

3.3 Image Acquisition

1. Equilibrate microscope imaging chamber to 37 °C and 5% CO₂ prior to imaging.
2. Select cells for imaging using GFP channel by identifying cells that contain well-resolved diffraction-limited RNA particles at densities that facilitate single-particle tracking. Use low laser power to reduce photobleaching when selecting cells for imaging (*see Note 5*).
3. Exposure times of 40–50 ms are generally applicable for single-mRNA tracking. Adjust laser power and camera gain for optimal signal-to-noise of RNA particles while minimizing photobleaching.
4. Collect short streaming image series (50 frames) in a single plane.

3.4 Image Analysis

Due to the difference in mobility between RNA particles that are tethered to distinct motors, it might be necessary to perform SPT with different parameters.

1. For static and diffusing RNA particles:
 - (a) Particle tracking is generally performed for five frames in the region of interest (cytoplasm). To do this, open the file in Fiji and use the *Image > Stacks > Tools > Slice Keeper* option to generate five frame movies.
 - (b) Draw the region of interest (cytoplasm) using the *Free-hand selections* tool from the toolbar.
 - (c) In case of low signal-to-noise ratio, use *Process > FFT > Bandpass Filter* in Fiji to filter out noise that is below 3 pixels and above 40 pixels.
 - (d) Go to *Image > Properties* and set the values for number of channels, number of frames, and pixel size (in µm). Click the box for the *global* option at the bottom of the pop-up window for applying these calibrations to all images.
 - (e) Use *Plugins > Tracking > TrackMate* to launch Trackmate and confirm that the number of frames, pixel size, dimensions of the region of interest, and time interval are correctly read by Trackmate.

- (f) Detect spots using the Laplacian of Gaussian (LoG) detector in Trackmate. Spot size (0.36–0.4 μm) and thresholds should be optimized empirically.
 - (g) Detected spots are joined into trajectories using simple linear assignment problem (LAP) tracker in Trackmate. The parameters for tracking such as linking max distance, gap-closing max distance, and gap-closing max frame gap should be optimized empirically. Typical values for these parameters are 0.4 μm , 0.7 μm , and 1 frame, respectively. Any tracks that are less than three frames should be discarded.
 - (h) Visually inspect the tracks to ensure appropriate tracking.
 - (i) Export tracking data as a spreadsheet.
2. For RNA particles undergoing directed movement:
- (a) Particle tracking is generally performed for typically 40 frames in the region of interest (cytoplasm) (similar to **steps 1a** and **1b** of previous section; the only exception is to change the option in the *Slice Keeper* to 40 frames instead of 5 frames).
 - (b) FFT band-pass filter in Fiji can be used to filter out noise that is below 3 pixels and above 40 pixels (similar to **step 1c** of previous section).
 - (c) Go to *Image > Properties* and set the values for number of channels, number of frames, and pixel size (in μm). Click the box for the *global* option at the bottom of the pop-up window for applying these calibrations to all images.
 - (d) Use *Plugins > Tracking > TrackMate* to launch Trackmate and confirm that the number of frames, pixel size, dimensions of the region of interest, and time interval are correctly read by Trackmate.
 - (e) Detect spots using the Laplacian of Gaussian (LoG) detector in Trackmate. Spot size (0.36–0.4 μm) and thresholds should be optimized empirically.
 - (f) Detected spots are joined into trajectories using the linear motion LAP tracker in Trackmate. The parameters for tracking such as initial search radius, search radius, and max frame gap should be optimized empirically. Typical values for these parameters are 0.4 μm , 0.7 μm , and 0 frame, respectively. Any tracks that are less than 20 frames should be discarded.
 - (g) Visually inspect the tracks to ensure appropriate tracking.
 - (h) Export tracking data as a spreadsheet.

3.5 Quantification

1. For static and diffusing RNA particles:
 - (a) Organize the tracking data as spreadsheets in the .xlsx format for all the cells (including the tracking data for the controls) in a single folder.
 - (b) In Matlab, add the Diff2fit folder containing the scripts and the folder containing the tracking data to the path.
 - (c) Execute Diff2fit by calling the “Diff2fit.m” script and choose the folder containing the tracking data.
 - (d) This script quantifies the tracking data as:
 - Diffusion coefficients based on either single- or two-population fit along with percentage of the particles exhibiting the corresponding movement, r^2 value, and goodness of fit for each cell. The abovementioned values are stored in the file “tracking filename _diffusion_coefficients_fit_results.txt” and the plot visualizing the single- and two-population fit is stored as “tracking filename_fit.tif” (Figs. 2a, b).
 - Instantaneous diffusion coefficients for each displacement window (three displacements over four frames) are calculated and stored in the file “tracking filename _IDC_all1.txt.” The plot visualizing the instantaneous diffusion coefficients is stored as “tracking filenameInstantaneous_Diffusion_Coefficients.tif.”
 - (e) Use the diffusion coefficients, percentage of the particles exhibiting the corresponding movement, or instantaneous diffusion coefficients elucidated from multiple cells to quantify the type of movement exhibited by the corresponding RNA (Figs. 2c, d).
2. For RNA particles undergoing directed movement:
 - (a) Organize the tracking data as spreadsheets in the .xlsx format for each cell in a way that each track is a separate sheet (see test.xlsx file inside the HMM-analysis folder from <https://data.fmi.ch/PublicationSupplementRepo/?group=gchao>).
 - (b) Download the HMM-Bayes package from <http://hmm-bayes.org/> and add the following files available from the Chao lab (*see* Subheading 2.3)
 - hmm_skeleton_MultiTrajip_SingleTrajProcess.m
 - hmm_skeleton_singletraj.m
 - XlsReadTraj.m
 to the Democode folder inside the HMM-Bayes folder.

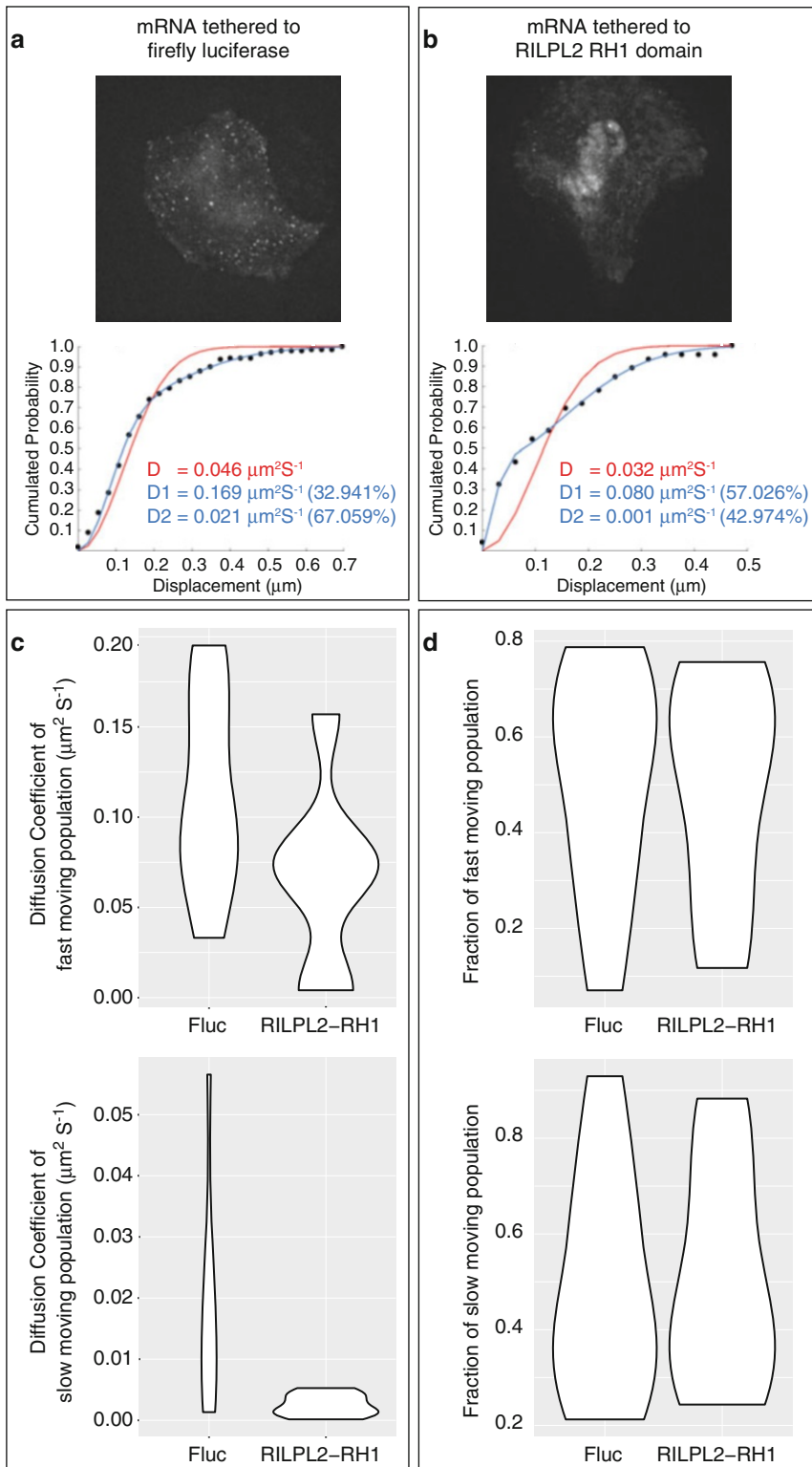


Fig. 2 Analysis and quantification of mobility of RNA particles that are undergoing diffusive and/or restricted motion. **(a)** Top panel shows a representative image of a cell that is transfected with the MCP-GFP-Firefly

- (c) In Matlab, add the HMM-Bayes folder containing the scripts and the folder containing the tracking data to the path.
- (d) Open the “hmm_skeleton_MultiTrajip_SingleTrajProcess.m” file in Matlab, add the input filename and full path after XlsReadtraj inside the bracket on line 7, and save this file, e.g., [*Multitrack, sheet*] = XlsReadTraj(‘**H:\MATLAB\test.xlsx**’).
- (e) Execute “hmm_skeleton_MultiTrajip_SingleTrajProcess.m” by calling the script. This script analyzes each track and the output plot contains the values of different parameters that best explains the movement of trajectory being analyzed, which can be used to quantify the type of movement exhibited by the corresponding RNA (Fig. 3). The output plot for each track is stored inside the folder Democode/data as “analysis_output_figure_-tracknumber.tif.” Copy the results to a new folder before starting the analysis for the next cell.

3.6 Summary of RILPL2-RH1 and SKIP Tethering Experiments

In cells, precise localization of mRNA is thought to be achieved by its interaction with specific RBPs. These RBPs exert this effect mainly by recruiting other cellular factors such as molecular motors or anchoring proteins that restrict the free diffusion of a transcript and alter its mobility. Tethering of the RH1 domain of RILPL2 leads to decreased mobility of the reporter RNA ($D < 0.01 \mu\text{m}^2/\text{S}$) when compared to a freely diffusing RNA (Fig. 2). In contrast, tethering of the N-terminal domain of SKIP protein leads to directed movement of the reporter RNA with an average velocity of $1.6 \mu\text{m}/\text{S}$, which is consistent with the previously observed speed of kinesin-1-based transport (Fig. 3). Thus, tethering of motor-interacting proteins can alter the mobility of a reporter RNA and this method could further be extended to evaluate the effect of distinct RNA-binding proteins on mRNA transport and localization.

Fig. 2 (continued) luciferase (MCP-GFP-FLuc) plasmid. Bottom panel shows a cumulative probability plot of particles from the cell shown above undergoing the corresponding displacements. Single (red)- and two (blue)-component fit is used to calculate displacement coefficients. **(b)** Top panel shows a representative image of a cell that is transfected with the MCP-GFP-RILPL2-RH1 plasmid. Bottom panel shows a cumulative probability plot of particles from the cell shown above undergoing the corresponding displacements. Single (red)- and two (blue)-component fit is used to calculate displacement coefficients. **(c)** Quantification of diffusion coefficients of two RNA populations from cells transfected with either MCP-GFP-FLuc or MCP-GFP-RILPL2-RH1 plasmids is shown. **(d)** Fraction of particles showing either fast or slow movement from cells transfected with either MCP-GFP-FLuc or MCP-GFP-RILPL2-RH1 plasmids is shown

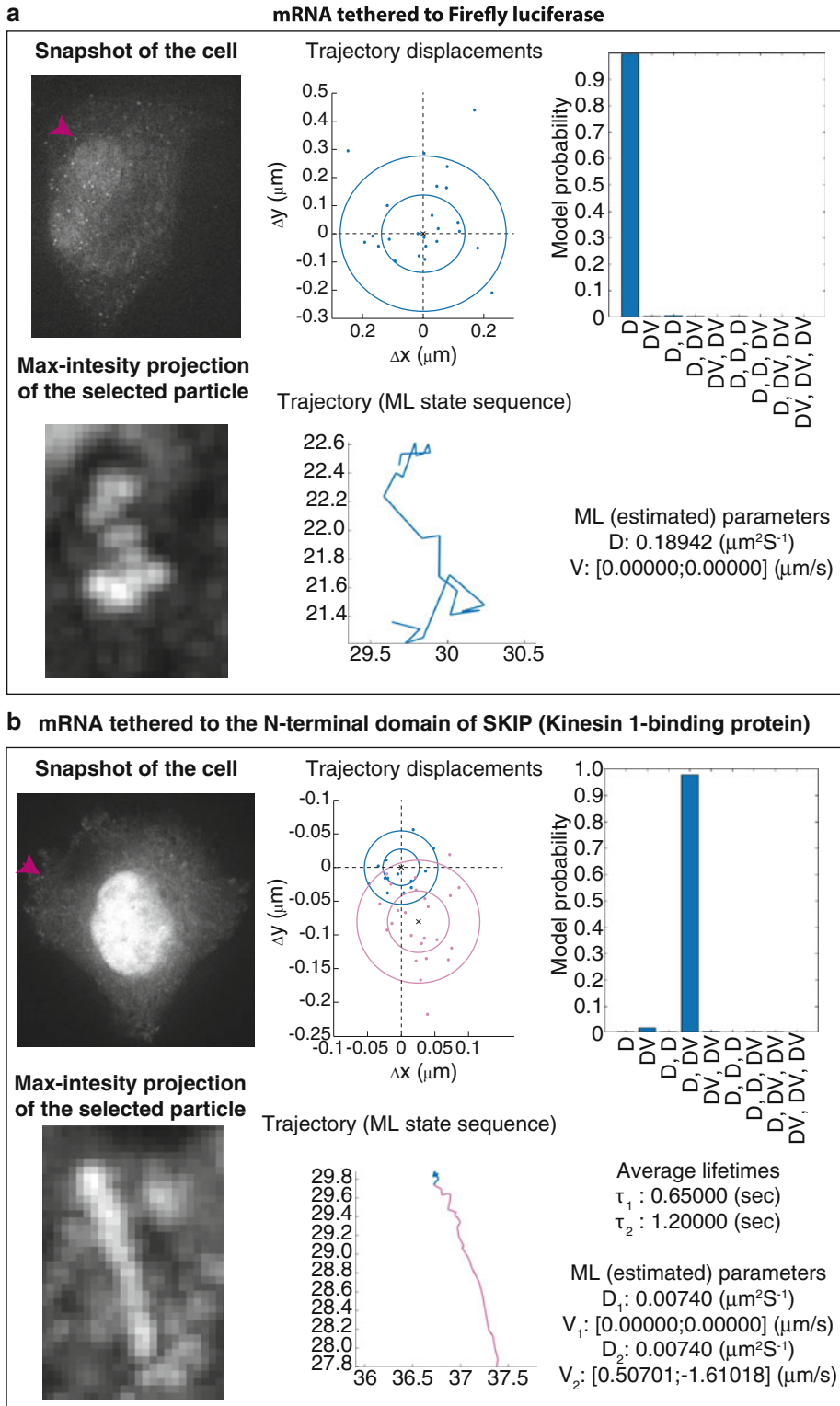


Fig. 3 Analysis and quantification of mobility of particles undergoing directed motion. **(a)** A representative image of a cell that is transfected with the MCP-GFP-FLuc plasmid is shown. **(b)** A representative image of a

4 Notes

1. The DNA encoding HA-tagged 2x-MCP-2x-GFP was cloned into the pOPINF vector belonging to the pOPIN vector suite (<https://www.oppf.rc-harwell.ac.uk/OPPF/protocols/cloning.jsp>) between the NcoI and KpnI restriction sites using conventional cloning. This plasmid was used as a vector to generate plasmids expressing the chimeric fusion protein of POI and 2x-MCP-2x-GFP by inserting the DNA encoding POI between the KpnI and HindIII sites using ligation-free cloning. This plasmid as well as the plasmids for expression of 2x-MCP-2x-GFP-RILPL2-RH1 and 2x-MCP-2x-GFP-SKIP N-terminal domain are available from the Chao lab upon request.
2. This assay can be performed on a variety of microscope configurations. Here, we provide the details of the microscope used in the described experiments. Images were acquired on an Olympus IX81 inverted microscope (Olympus) equipped with a Yokogawa CSU-X1 scanhead (Yokogawa) and Borealis modification (Andor). Our setup consists of a single band-pass filter or dichroic beam splitter in the scanhead (Semrock Di01-T488/568-13x15x0.5). For image acquisition, the emitted light was passed through an emission filter for GFP (Semrock, FF01-525/40-25) fluorescence and captured using a back-illuminated Evolve Delta EMCCD cameras (Photometrics).
3. Efficient transfection is key to obtain enough cells for imaging. This protocol is optimized for Lipofectamine 2000, to obtain efficient transfection without significant cell death. Hence, it is imperative to optimize for efficient transfection in case a different transfection reagent is used.
4. Seeding of the cells in CYTOO chips is a crucial step for obtaining enough cells with the desired cellular architecture for imaging. Seeding too many cells or extremely mild washing leads to multiple cells attaching to a single pattern eventually inhibiting the spreading of the cytoplasm of a single cell on the micropattern. On the other hand, seeding too few cells or extremely harsh washing leads to detachment of cells from the micropattern eventually leaving too few cells to image.

Fig. 3 (continued) cell that is transfected with the MCP-GFP-SKIP plasmid is shown. **(a and b)** For each image, the arrow indicates the particle being analyzed and the maximum intensity projection of this particle is shown underneath. The different panels on the right show the output of the HMM-Bayes program including the schematic of the track being analyzed, the distribution of displacements from the same track, and the evaluated probability for different modes of movements occurring in this track. The average lifetime for each type of movement (denoted by τ_1 and τ_2) and the respective diffusion coefficients (D , D_1 , and D_2) and velocities in x and y directions (V , V_1 , and V_2) are displayed. Note that for purely diffusive particle, the velocity is zero

5. Transient transfection leads to highly heterogeneous levels of expression of the fluorophore (MCP-GFP-RBP protein). Thus, there will be few cells which are extremely bright and some that are extremely faint. Particle tracking in these cells is extremely challenging due to low signal-to-noise ratio. Hence, for single-molecule imaging select cells that have a high signal-to-noise ratio for optimal single-particle tracking.

Acknowledgments

The authors would like to thank T. Lionnet (NYU) for helpful discussion and all members of the Chao lab for their input and the Facility for Advanced Imaging and Microscopy at the Friedrich Miescher Institute for Biomedical Research for data acquisition and image analysis support. Research in the Chao lab is funded by the Novartis Research Foundation (J.A.C.), a Swiss National Science Foundation (SNF) grant 31003A_182314 (J.A.C.), the SNF-NCCR RNA & Disease (J.A.C.), and a Synapsis Foundation grant 2017 CDA 01 (V.B.).

References

1. Tekotte H, Davis I (2002) Intracellular mRNA localization: motors move messages. *Trends Genet* 18:636–642
2. Gagnon JA, Mowry KL (2011) Molecular motors: directing traffic during RNA localization. *Crit Rev Biochem Mol Biol* 46:229–239. <https://doi.org/10.3109/10409238.2011.572861>
3. Bullock SL, Nicol A, Gross SP, Zicha D (2006) Guidance of bidirectional motor complexes by mRNA cargoes through control of dynein number and activity. *Curr Biol* 16:1447–1452. <https://doi.org/10.1016/j.cub.2006.05.055>
4. Bullock SL (2011) Messengers, motors and mysteries: sorting of eukaryotic mRNAs by cytoskeletal transport. *Biochem Soc Trans* 39:1161–1165. <https://doi.org/10.1042/BST0391161>
5. Holt CE, Bullock SL (2009) Subcellular mRNA localization in animal cells and why it matters. *Science* 326:1212–1216. <https://doi.org/10.1126/science.1176488>
6. St Johnston D (2005) Moving messages: the intracellular localization of mRNAs. *Nat Rev Mol Cell Biol* 6:363–375. <https://doi.org/10.1038/nrm1643>
7. McCaffrey MW, Lindsay AJ (2012) Roles for myosin Va in RNA transport and turnover. *Biochem Soc Trans* 40:1416–1420. <https://doi.org/10.1042/BST20120172>
8. Heym RG, Zimmermann D, Edelmann FT, Israel L, Ökten Z, Kovar DR, Niessing D (2013) In vitro reconstitution of an mRNA-transport complex reveals mechanisms of assembly and motor activation. *J Cell Biol* 203:971–984. <https://doi.org/10.1083/jcb.201302095>
9. Kanai Y, Dohmae N, Hirokawa N (2004) Kinesin transports RNA: isolation and characterization of an RNA-transporting granule. *Neuron* 43:513–525. <https://doi.org/10.1016/j.neuron.2004.07.022>
10. Lazzaretti D, Bono F (2017) mRNA localization in metazoans: A structural perspective. *RNA Biol* 14:1473–1484. <https://doi.org/10.1080/15476286.2017.1338231>
11. Jansen R-P, Niessing D (2012) Assembly of mRNA-protein complexes for directional mRNA transport in eukaryotes—an overview. *Curr Protein Pept Sci* 13:284–293. <https://doi.org/10.2174/138920312801619493>
12. Collier J, Wickens M (2002) Tethered function assays using 3' untranslated regions. *Methods* 26:142–150. [https://doi.org/10.1016/S1046-2023\(02\)00016-6](https://doi.org/10.1016/S1046-2023(02)00016-6)
13. Pillai RS, Artus CG, Filipowicz W (2004) Tethering of human Ago proteins to mRNA mimics

- the miRNA-mediated repression of protein synthesis. *RNA* 10:1518–1525. <https://doi.org/10.1261/rna.7131604>
14. Vasudevan S, Steitz JA (2007) AU-rich-element-mediated upregulation of translation by FXR1 and Argonaute 2. *Cell* 128:1105–1118. <https://doi.org/10.1016/j.cell.2007.01.038>
 15. Katz ZB, Wells AL, Park HY, Wu B, Shenoy SM, Singer RH (2012) β -Actin mRNA compartmentalization enhances focal adhesion stability and directs cell migration. *Genes Dev* 26:1885–1890. <https://doi.org/10.1101/gad.190413.112>
 16. Buxbaum AR, Haimovich G, Singer RH (2015) In the right place at the right time: visualizing and understanding mRNA localization. *Nat Rev Mol Cell Biol* 16:95–109. <https://doi.org/10.1038/nrm3918>
 17. Weidenfeld I, Gossen M, Löw R, Kentner D, Berger S, Görlich D, Bartsch D, Bujard H, Schönig K (2009) Inducible expression of coding and inhibitory RNAs from retargetable genomic loci. *Nucleic Acids Res* 37:e50–e50. <https://doi.org/10.1093/nar/gkp108>
 18. Halstead JM, Lionnet T, Wilbertz JH, Wippich F, Ephrussi A, Singer RH, Chao JA (2015) Translation. An RNA biosensor for imaging the first round of translation from single cells to living animals. *Science* 347:1367–1671. <https://doi.org/10.1126/science.aaa3380>
 19. Lisé M-F, Srivastava DP, Arstikaitis P, Lett RL, Sheta R, Viswanathan V, Penzes P, O'Connor TP, El-Husseini A (2009) Myosin-Va-interacting protein, RILPL2, controls cell shape and neuronal morphogenesis via Rac signaling. *J Cell Sci* 122:3810–3821. <https://doi.org/10.1242/jcs.050344>
 20. Rosa-Ferreira C, Munro S (2011) Arl8 and SKIP act together to link lysosomes to kinesin-1. *Dev Cell* 21:1171–1178. <https://doi.org/10.1016/j.devcel.2011.10.007>
 21. Tinevez J-Y, Perry N, Schindelin J, Hoopes GM, Reynolds GD, Laplantine E, Bednarek SY, Shorte SL, Eliceiri KW (2017) TrackMate: an open and extensible platform for single-particle tracking. *Methods* 115:80–90. <https://doi.org/10.1016/j.ymeth.2016.09.016>
 22. Schindelin J, Arganda-Carreras I, Frise E, Kaynig V, Longair M, Pietzsch T, Preibisch S, Rueden C, Saalfeld S, Schmid B, Tinevez J-Y, White DJ, Hartenstein V, Eliceiri K, Tomancak P, Cardona A (2012) Fiji: an open-source platform for biological-image analysis. *Nat Methods* 9:676–682. <https://doi.org/10.1038/nmeth.2019>
 23. Monnier N, Barry Z, Park HY, Su K-C, Katz Z, English BP, Dey A, Pan K, Cheeseman IM, Singer RH, Bathe M (2015) Inferring transient particle transport dynamics in live cells. *Nat Methods* 12:838–840. <https://doi.org/10.1038/nmeth.3483>



***Proximity-CLIP* Provides a Snapshot of Protein-Occupied RNA Elements at Subcellular Resolution and Transcriptome-Wide Scale**

Daniel Benhalevy and Markus Hafner

Abstract

The distribution of messenger RNAs (mRNAs) to specific subcellular locations has been studied for the past two decades. Technically, studies of RNA localization are lagging those related to protein localization. Here we provide a detailed protocol for *Proximity-CLIP*, a method recently developed by our group, that combines proximity biotinylation of proteins with photoactivatable ribonucleoside-enhanced protein-RNA cross-linking to simultaneously profile the proteome including RNA-binding proteins (RBPs) and the RBP-bound transcriptome in any given subcellular compartment. The approach is fractionation independent and also enables studying localized RNA-processing intermediates, as well as the identification of regulatory *cis*-acting elements on RNAs occupied by proteins in a cellular compartment-specific manner.

Key words RNA-protein interactions, RNA localization, RNA regulatory elements, RNA-processing intermediates, Subcellular RNA biology

1 Introduction

The location of molecular factors within the cell is crucial for their regulation and function [1–3]. Excellent tools allow high-resolution mapping of proteins within cells, where fractionation-independent approaches, such as fluorescence microscopy and more recently also proximity labeling coupled to high-throughput proteomics, profiled the localized proteome at subcellular resolution [4–9]. In contrast, studies comprehensively describing subcellular resolution data for RNA remain limited. Some of the reasons for this include the following: (1) RNAs are often short lived due to degradation or to maturation by sequential cleavage events. (2) Massive unregulated RNA degradation occurs upon cell lysis by released cellular RNases, complicating fractionation-based approaches. (3) Imaging of RNA in intact cells is limited by sensitivity, specificity, and bias. (4) Next-generation sequencing of RNA subspecies varying in size or in 5' or 3' features requires distinct

protocols. Recently, proximity-based approaches to study RNA localization have emerged that however do not fully overcome these or additional hurdles [5, 10–12].

We developed *Proximity-CLIP* [13, 14] that overcomes these barriers and pinpoints RNA elements occupied by proteins at a subcellular level. Our proof-of-concept experiments in HEK293 cells recapitulated many RNA biological phenomena that previously could only be detected using specialized approaches, and allowed us to generate hypotheses about RNA biology at the cell-cell interface [13, 15].

Proximity-CLIP relies on the well-supported assumption that most cellular RNAs are protein bound throughout their life cycle, including transcription, processing, transport, translation, and degradation [16]. *Proximity-CLIP* combines cellular compartment-specific protein biotinylation (*see Note 1*) [4] with photoreactive ribonucleoside-enhanced cross-linking to covalently and irreversibly cross-link RNA with RNA-binding proteins (RBPs) in intact cells [17, 18] (Fig. 1). Our approach enables determination of the localized proteome that includes RNA-binding proteins (RBPs) using mass spectrometry, and the profiling of localized transcripts

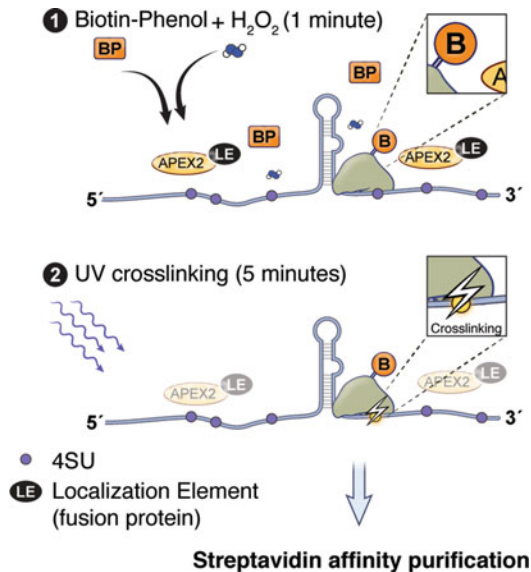


Fig. 1 Scheme of *Proximity-CLIP*. *Proximity-CLIP* relies on the assumption that cellular RNA is protein bound throughout its life cycle. APEX2 is targeted to a compartment of interest by fusion to a localization element (LE), and nascent RNAs labeled with 4SU. Cells are incubated with biotin-phenol (BP) for 30 min, and APEX2-mediated BP oxidation is induced by addition of hydrogen peroxide for 1 min. Biotin radicals are created locally and either covalently tag APEX2-proximate proteins or rapidly decay ($t_{1/2} < 1$ ms). Immediately after, the oxidation reaction is quenched under UV light ($\lambda > 312$ nm) for protein-RNA cross-linking. Then, cells are lysed and compartment-specific proteins and ribonucleoproteins are captured by streptavidin affinity chromatography

using RNAseq. Importantly, *Proximity-CLIP* reveals hot spots of protein occupancy along the RNA sequence, which often relates to elements of crucial functional and regulatory significance and facilitates studying short-lived and degradation-susceptible RNAs due to the stabilizing effect of cross-linking to their associated RBPs.

The covalent bonds between biotin, RBPs, and RNA render the RNP complexes resistant to stringent purification steps, maximizing the signal-to-noise ratio in the downstream high-throughput proteomic and transcriptomic analyses. The approach is fractionation independent and allows for the isolation of compartments that are inaccessible to biochemical purification. Furthermore, the use of stringent extraction conditions promotes the preservation of the isolated cellular components. Finally, UV cross-linking of 4-thiouridine (4SU)-labeled RNA to interacting proteins leads to a structural change at the photoreactive nucleoside, resulting in nucleotide misincorporation during reverse transcription and a characteristic T-to-C mutation in the corresponding cDNA libraries. This feature allows for efficient computational removal of contaminating sequences derived from non-cross-linked fragments of abundant cellular RNAs, further increasing the specificity of *Proximity-CLIP* by reducing the false-positive detection rate.

The workflow of *Proximity-CLIP* comprises the following steps (Fig. 1): (1) 4SU labeling of RNAs in living cells expressing specifically localized APEX2 (engineered ascorbate peroxidase); (2) biotinylation of APEX2-proximate proteins by incubation of cells (*see Note 1*) with biotin-phenol, followed by activation of the peroxidase reaction with hydrogen peroxide (H₂O₂) for 1 min, and reaction quenching using sodium ascorbate, Trolox, and sodium azide; (3) *in vivo* cross-linking of RNA and proteins using UVA or UVB light ($\lambda > 310$ nm) during the quenching step; and (4) isolation of localized, biotinylated, and cross-linked ribonucleoprotein (RNP) complexes by affinity chromatography.

In summary, *Proximity-CLIP* allows for (1) the determination of the localized proteome in general and the RBPome in particular using mass spectrometry; (2) the profiling of localized transcripts using RNA-seq; and (3) the identification and quantification of RBP-occupied *cis*-acting elements on transcripts, by isolation of RNase-resistant footprints that are converted into next-generation sequencing-compatible cDNA libraries.

2 Materials

2.1 Cells and Basic Culture Media

This chapter can be adapted to any adherent mammalian cell line and its growth medium. In addition to the cells expressing APEX2 targeted to the compartment of interest, cells expressing APEX2 in a control compartment, as well as the parental cell line, which does not express APEX2, are required (*see* more on cell line selection and cell types in **Note 1**).

2.2 Labeling

1. 500 mM 4-Thiouridine (4SU). Store at -20°C .
2. 500 mM Biotin-phenol (BP) in DMSO (may need to be sonicated to dissolve, store 50 μL aliquots at -80°C).
3. 1 M Sodium azide: For long term store aliquots at -20°C .
4. Sodium ascorbate (powder, needed fresh).
5. Trolox (6-hydroxy-2,5,7,8-tetramethylchroman-2-carboxylic acid) (powder, needed fresh).
6. 30% wt/wt Hydrogen peroxide stock: Needed fresh, do not prepare diluted solution in advance.
7. Any standard fixative to process cells for imaging by fluorescence microscopy. In our hands 16% PFA freshly diluted to 4% in PBS performed better than methanol at -20°C .
8. Phosphate-buffered saline (PBS) pH 7.4: 0.144 g/L KH_2PO_4 , 9 g/L NaCl, 0.795 g/L $\text{Na}_2\text{HPO}_4 \cdot 7\text{H}_2\text{O}$.
9. 10 \times PBS pH 7.4: 1.44 g/L KH_2PO_4 , 90 g/L NaCl, 7.95 g/L $\text{Na}_2\text{HPO}_4 \cdot 7\text{H}_2\text{O}$.
10. DMSO.
11. UV cross-linker equipped with far-UV light bulbs (wavelength >310 nm, preferably 365 nm).
12. Sonicator with probe that fits into a microcentrifuge tube.

2.3 Cell Extraction and Streptavidin Affinity Purification

1. DEPC-treated double-distilled water (will be referred in the Methods as water).
2. RIPA extraction buffer: 50 mM Tris-HCl, 150 mM NaCl, 0.1% (wt/vol) SDS, 0.5% (wt/vol) sodium deoxycholate, 1% (wt/vol) Triton X-100. Adjust pH to 7.5 with HCl. Can be stored at 4°C for many months.
3. 100 mM PMSF in ethanol.
4. Protease inhibitor cocktail without EDTA.
5. Sodium ascorbate (powder, needed fresh).
6. Trolox (**6-hydroxy-2,5,7,8-tetramethylchroman-2-carboxylic acid**) (powder, needed fresh).
7. 1 M Sodium azide.
8. Pierce 660 nm protein assay reagent.
9. Ponceau S solution.
10. Streptavidin-coupled horseradish peroxidase.
11. Streptavidin-coupled magnetic beads.
12. Magnetic rack for 1.5 mL tubes.
13. 1 M KCl.
14. 0.1 M Na_2CO_3 .
15. Urea (powder, needed fresh).

16. 10 mM Tris-HCl pH 8.
17. 6× Protein sample buffer: 300 mM Tris-HCl pH 6.8, 30% glycerol, 6% SDS, 600 mM DTT, 0.01% bromophenol blue.
18. 3× Protein sample buffer supplemented with 2 mM biotin and 20 mM DTT.
19. DMSO.

**2.4 On-Beads
Trypsinization (See
Note 2)**

1. Iodoacetamide, single use.
2. Dithiothreitol (DTT), No-Weigh™ Format.
3. Sequencing-grade modified trypsin.
4. 250 mM NH₄HCO₃ stock solution.

**2.5 RNA
Manipulations**

1. RNase T1 buffer: 20 mM Tris pH 7.4, 150 mM NaCl, 2 mM EDTA, 1% NP40.
2. RNase T1.
3. Dephosphorylation buffer (based on the calf intestinal phosphatase buffer): 50 mM Potassium acetate, 20 mM Tris-acetate, 10 mM magnesium acetate, 0.1 mg/ml BSA, pH 7.9. Make a 10× stock.
4. Calf intestinal phosphatase.
5. T4 polynucleotide kinase (PNK) buffer without DTT: 70 mM Tris-HCl, 10 mM MgCl₂, pH 7.6.
6. PNK buffer with DTT: 70 mM Tris-HCl, 10 mM MgCl₂, 5 mM DTT, pH 7.6. Prepare a 10× stock.
7. PNK.
8. γ -³²P-ATP 10 mCi/mL, 1.6 μ M.
9. Proteinase K buffer: 50 mM Tris pH 7.5, 75 mM NaCl, 6.25 mM EDTA, 1% SDS.
10. Proteinase K.
11. 10 mg/mL Glycogen or a stained glycogen product.
12. Acidic phenol-chloroform (pH 4.5).
13. Water-saturated chloroform.
14. Nucleic acid low-binding 1.5 mL tubes.
15. Truncated and mutated RNA ligase 2, T4 Rnl2(1-249)K227Q (1 mg/mL) (NEB).
16. T4 RNA ligase, T4 Rnl1 (1 mg/mL).
17. 50% DMSO.
18. Low-melting-point agarose.
19. SuperScript™ Reverse Transcriptase (III or IV).
20. *Taq* DNA polymerase.

21. 2× Formamide gel-loading solution: 95% Formamide, 0.02% (w/v) bromophenol blue, 0.01% (w/v) xylene cyanol, 10 mM EDTA.
22. Urea-PAGE (*see Note 3*).
23. Gel breaker tubes.
24. 5 μm Filter tube.
25. Pippin Prep and 3% Pippin gel cassettes (Sage Science) (*see Note 4*).
26. DNA clean and concentrate kit.
27. Phenol:chloroform:isoamyl alcohol 25:24:1, saturated with 10 mM Tris, pH 8.0, 1 mM EDTA.
28. Stranded, random hexamer primed RNA Library Prep Kit (we use NEBNext Ultra™ II directional RNA Library prep kit for Illumina).
29. Ribosomal RNA depletion kit (we use NEBNext rRNA depletion kit).
30. Magnetic rack for 96-well plate.
31. Agilent TapeStation with DNA D1000 and RNA ScreenTapes, or Bioanalyzer (less recommended).

3 Methods

3.1 Setting Up and Procedures Before Proximity Labeling and UV Cross-Linking

1. Accurately count and split cells ~36 h prior to proximity labeling and cross-linking. All cells should be in a similar growth state and confluence at the day of experiment. Balance the need for cell number with the requirement of cells to be rapidly growing for efficient 4SU incorporation (*see Note 1* and Fig. 2).
2. 16 h Before cross-linking, add 4-thiouridine (4SU) to the cell culture media at a final concentration of 100 μM. The stock concentration might be too high; calculate the required amount and prepare an intermediate 50 mM 4SU solution. Then add at 2 μL per ml of medium. It is not necessary to add 4SU to the media of cells grown for immunofluorescence validations. Read more on 4SU labeling in the Notes section (*see Note 5*).
3. Prepare stock solutions and buffers as described in Subheading 2.2.

3.2 Proximity Biotinylation and UV Cross-Linking

1. Bring cell media to 37 °C and PBS to room temperature, label 1.5 mL tubes and pre-chill them on ice, have liquid N₂ on hand for snap freezing cell samples, and an accessible sonicator (in case Trolox does not dissolve). Weigh (but do not dissolve) required amounts of sodium ascorbate and Trolox.

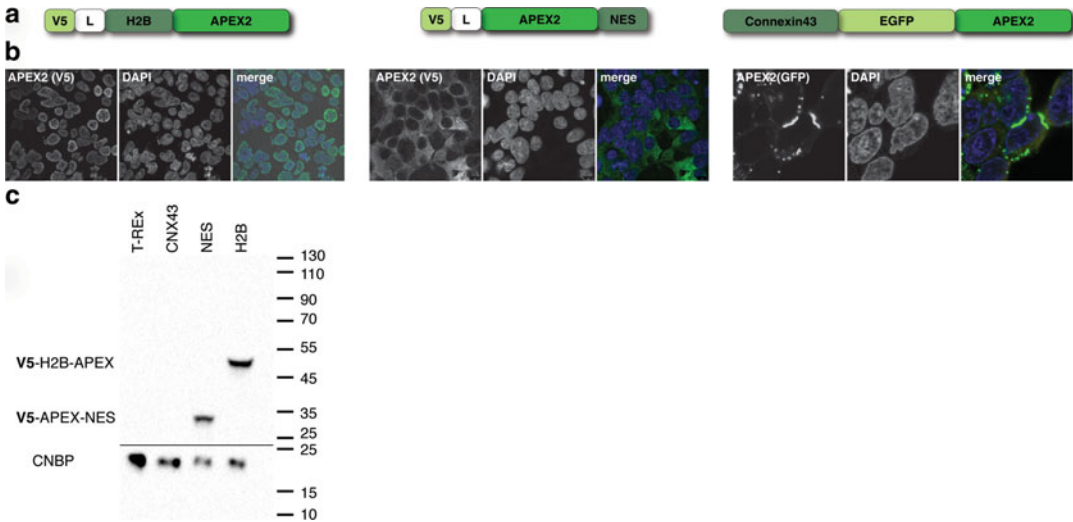


Fig. 2 Validation of cell lines expressing localized APEX2-fusion proteins prior to *Proximity-CLIP*. **(a)** Schemes of V5- or EGFP-tagged APEX2 constructs. L-linker, H2B is a histone protein targeting APEX2 to the nucleus, NES-nuclear export signal restricting APEX2 to the cytoplasm, Connexin43 is a gap junction protein targeting APEX2 to cell-cell interface. **(b)** Immunofluorescence analysis of HEK293 T-Rex stable cell lines expressing APEX2-fusion proteins from constructs depicted in **a**. **(c)** Example of Western blot validation of expression of V5-tagged APEX2-fusion proteins, using an anti-V5 antibody. Anti-CNBP Western blot analysis was used as loading control. The parental cell line HEK293 T-Rex and cells expressing the CNX43-APEX2 fusion protein that is not V5-tagged serve as negative controls. See Fig. 3f for Western blot analysis of the CNX43-APEX2-expressing cell line

2. Dilute the required amount of the BP stock solution 1:50 in prewarmed media to generate a 10 mM working stock. Immediately add to cell plates (except to –BP controls) 50 μ L of the 10 mM BP working stock per 1 mL of media for a final concentration of 500 μ M BP. Gently swirl and return plates to the incubator for 30 min.
3. During the 30-min BP incubation: Dilute the 16% PFA to 4% in PBS (use 10 \times PBS to account for the 16% PFA volume). Dilute hydrogen peroxide (most come as 30% wt/wt, which is \sim 10 M) to 100 mM in PBS. Dissolve sodium ascorbate to 1 M (in water) and Trolox to 500 mM (in DMSO, sonicate if necessary). Prepare fresh quencher solution (PBS supplemented with 10 mM sodium ascorbate, 5 mM Trolox, and 10 mM sodium azide).
4. Bring the plates from the incubator to the bench, add the 100 mM hydrogen peroxide stock into growth medium for a final concentration of 1 mM (except for the controls without hydrogen peroxide), swirl, and incubate for 1 min. Proceed immediately, and shorten rather than extend this incubation time to minimize the labeling time window.

5. Discard the labeling cell medium by decanting (or aspiration from the cells growing on cover glass for immunofluorescence microscopy), and quickly wash the plates three times in quenching solution (not less than 1 mL per 3 cm² surface area per wash). Pre-aliquot quenching solution into tubes and rapidly, but carefully pour wash solutions to ensure quick and efficient quenching of the reaction. Consider recruiting an extra pair of hands and streamline this step, in order to minimize the time gap between proximity biotinylation and UV cross-linking.
6. Leave quenching solution on cells growing on cover glasses, which will not undergo UV cross-linking while handling the other samples.
7. Decant quenching solution from cell plates for UV cross-linking and ensure that cells are covered by a liquid film to avoid them from drying out. If necessary, add 750 μ L (not more, because cells will need to be scraped and collected into 1.5 mL tubes) of quenching solution to cells growing in plates, remove lids, and cross-link cells with at least 0.15 J/cm² of >310 nm UV light. (Note: Mark cell plates and not only the lids, to avoid any switching of samples.)
8. While samples are cross-linking, return to aspirate the last quenching solution wash, off the cells growing on cover glasses for control immunofluorescence, and fix cells by fixative of choice. After fixation, wash cells three times in PBS, and store them in PBS at 4 °C, for later further processing and imaging. *See Note 6* on fluorescence microscopy cell imaging.
9. When UV cross-linking is completed (on our instrument after 5 min) cover plates and place them on ice. Scrape the cells off using a rubber policeman and collect them with the remaining quenching solution into pre-chilled 1.5 mL tubes. Pellet cells at 300 g, remove the supernatant, snap freeze cell pellets in liquid N₂, and store at -80 °C.

3.3 Processing of Cells from Control Plates

1. Transfer tubes with the cell pellets from 6 cm control plates from -80 °C storage to ice and resuspend pellets in 300 μ L of cold RIPA buffer supplemented with 1 mM PMSF, 1 \times protease inhibitors cocktail, 10 mM sodium azide, 10 mM sodium ascorbate, and 5 mM Trolox (sodium ascorbate and Trolox should be fresh and can be weighed and directly dissolved in the appropriate amount of RIPA buffer).
2. Incubate the resuspended cells in RIPA buffer on ice for 2 min, and then clear the extracts by centrifugation at 15,000 \times *g* for 10 min at 4 °C. Carefully transfer the clarified extract without disturbing the precipitated debris into new pre-chilled tubes.

3. Quantify protein concentration in the extracts using the Pierce 660 nm protein assay. In our hands, with HEK293 cells, protein concentrations average around 1.2 $\mu\text{g}/\mu\text{L}$.
4. Wash streptavidin-coupled magnetic beads twice with RIPA buffer. Then incubate 150 μg of each of the cell extracts with $\sim 15 \mu\text{L}$ (*see Note 7*) of washed beads under rotation overnight at 4 °C or for 1 h at room temperature. Make sure that beads and extracts are mixed well during rotation; if necessary, increase the volume by addition of RIPA buffer. Store the remaining cell extract for Western blot analysis.
5. Collect magnetic beads using a magnetic rack and transfer the supernatant into pre-labeled and chilled tubes. The supernatant should be kept for Western blot analysis (Fig. 3d).
6. Wash beads with 1 mL volume of the following ice-cold solutions: twice with RIPA buffer, once with 1 M KCl, once with 0.1 M Na_2CO_3 , once with 2 M urea in 10 mM Tris-HCl pH 8 (freshly prepared), and again twice with RIPA buffer.
7. Elute by adding 60 μL 3 \times protein sample buffer supplemented with 2 mM biotin and 20 mM DTT, followed by 10-min incubation at 97 °C under vigorous shaking (*see Note 7*). Quickly spin down and place the tubes on the magnetic rack. Collect the eluates in fresh pre-labeled tubes.
8. Analyze cell extracts, bead supernatant, and eluate by Western blotting using streptavidin-coupled HRP (Fig. 3a–d). Western blot for the APEX2-fusion protein should also be performed on the cell extracts, to confirm its expression and detect possible proteolytic cleavage events (*see Figs. 2c and 3f*) (*see Note 8*). Stain the nitrocellulose membranes by Ponceau S as a loading control (Fig. 3a).

3.4 Processing of Cells from Preparative Plates

1. Transfer tubes with cell pellets from 15 cm preparative plates from $-80 \text{ }^\circ\text{C}$ storage to ice and resuspend pellets in 800 μL of cold RIPA buffer supplemented with 1 mM PMSEF, 1 \times protease inhibitors cocktail, 10 mM sodium azide, 10 mM sodium ascorbate, and 5 mM Trolox (sodium ascorbate and Trolox should be fresh and can be weighed and directly dissolved in the RIPA buffer).
2. Incubate the resuspended cells in RIPA buffer on ice for 2 min, and then clear the extracts by centrifugation at 15,000 $\times g$ for 10 min at 4 °C. Carefully transfer the clarified extract without disturbing the precipitated debris into new pre-chilled tubes.
3. Quantify protein concentration of the extracts using the Pierce 660 nm protein assay. In our hands, with HEK293 cells, protein concentrations average around 3 $\mu\text{g}/\mu\text{L}$.

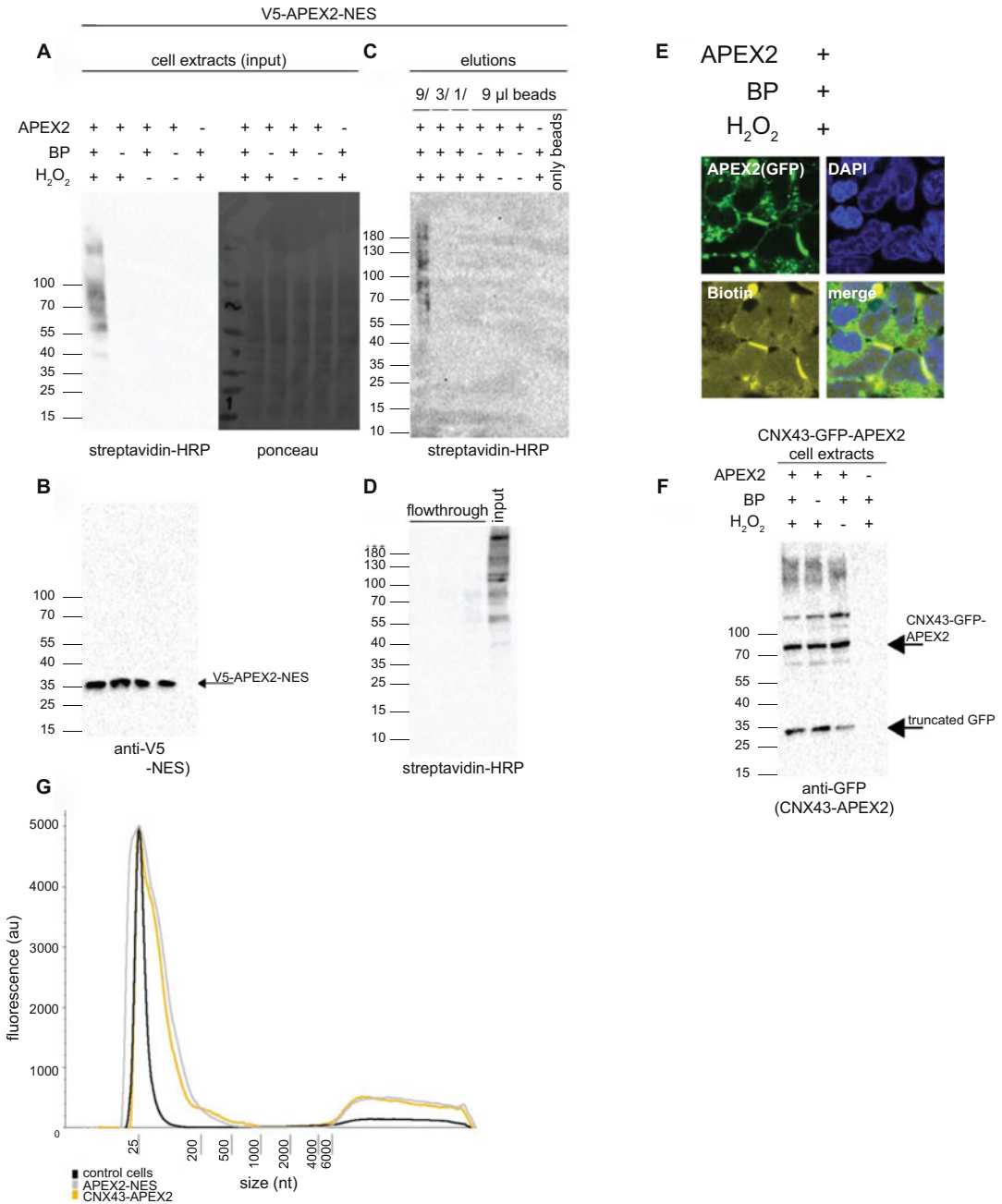


Fig. 3 Proximity-CLIP checkpoints and controls. (a–d) Control cells (growing on 6 cm plates) expressing an APEX2-fusion protein (V5-APEX2-NES) and supplemented with biotin-phenol (BP) and hydrogen peroxide (H₂O₂) or devoid of at least one of the three components were extracted and underwent proximity biotinylation. (a) Horseradish peroxidase (HRP)-coupled streptavidin Western blot analysis of protein biotinylation in cells expressing an APEX2-fusion protein and supplemented with biotin-phenol (BP) and hydrogen peroxide (H₂O₂), or devoid of at least one of the three components. Ponceau stain is used as a loading control. (b) Western blot validation of APEX2-fusion protein expression. (c and d) Validation of pull-down efficiency combined with calibration of the optimal ratio between amounts of beads and cell extract. (c) HRP-coupled streptavidin

4. Wash streptavidin-coupled magnetic beads twice with RIPA buffer. Then incubate with rotation 1.5 mg total protein of the cell extracts with ~60 μL of washed beads (*see Note 7*) for 1 h at room temperature. Keep 30 μL of the extract sample for total RNA extraction and store the rest for Western blot analyses.
5. Collect the beads using a magnetic rack and transfer the supernatant into pre-labeled and chilled tubes.
6. Wash beads with 1 mL volume of the following ice-cold solutions: twice with RIPA buffer, once with 1 M KCl, once with 0.1 M Na_2CO_3 , once with 2 M urea in 10 mM Tris-HCl pH 8 (freshly made), and again twice with RNase T1 buffer (*see Subheading 2.4*).
7. Use the last wash to split the beads from each cell sample to three non-equal aliquots: 30% for mass spectrometric analysis. Reduce liquid volume to minimum and keep on ice. 20% for RNA-seq of intact bound RNAs; collect beads on a magnetic rack, discard supernatant, and store at -80°C (note that this will spoil the magnetic beads). Keep the remaining 50% of the beads for RNA footprinting and small RNA cDNA library preparation. At this point it is necessary to continue with the beads for RNA footprints and proteomic analysis. We recommend proceeding first with Subheading 3.6, steps 1–12, and then returning to perform Subheading 3.5, steps 1–5, before pausing.

Fig. 3 (continued) Western blot analysis as in **a** of the eluted material (Subheading 3.3, step 7), using decreasing volumes of beads per identical volume of extract. **(d)** Western blot analysis as in **c** of the unbound material with different volumes of beads used (Subheading 3.3, step 5), relative to the input (cell extract). **(e)** Immunofluorescence analysis of cells expressing a CNX43-EGFP-APEX2 fusion protein. Note that while biotinylation (in yellow, detected by fluorophore-coupled neutravidin) is concentrated as expected at cell-cell interfaces, the GFP signal is also highly detected in cytoplasmic foci. **(f)** Anti-GFP Western blot analysis of cells as in **e**, illustrating that while the intact fusion protein is expressed, additional shorter product suggests proteolytic cleavage. The relative specificity of biotinylation to cell-cell interface suggests that the majority of cleavage events result in nonfunctional APEX2, while a free EGFP product remains stable. **(g)** TapeStation analysis of the intact RNA (not RNase treated) eluted from beads (Subheading 3.7, step 9) after Proximity-CLIP in HEK293 T-Rex cells that do not express APEX2 and of cells that express either NES and CNX43 APEX2-fusion proteins. Signal over 25 nt length represents the internal control of the TapeStation analysis. It is essential to sequence the RNA eluted from negative control cells even though quantitatively the amount of eluted RNA appears lower

3.5 *On-Beads Protein Trypsinization*

1. Transfer the beads (30% aliquot kept on ice) to the magnetic rack to discard the remaining supernatant and resuspend the beads in 30 μL freshly prepared 25 mM NH_4HCO_3 and 20 mM DTT. Shake for 30 min at 25 $^\circ\text{C}$, then for 20 min at 37 $^\circ\text{C}$, and finally for 10 min at 56 $^\circ\text{C}$.
2. Add 6 μL of 200 mM iodoacetamide in 25 mM NH_4HCO_3 and shake for 1 h at 25 $^\circ\text{C}$.
3. Collect liquid from tube caps by briefly spinning on a tabletop centrifuge and transfer the tubes to a magnetic rack. Discard the supernatant and wash the beads three times with 200 μL of 1 mM DTT in 25 mM NH_4HCO_3 , to quench any remaining iodoacetamide and to ensure full depletion of NP40.
4. Dissolve 20 μg of trypsin in 1 mL of 25 mM NH_4HCO_3 .
5. Add 98 μL of 25 mM NH_4HCO_3 and 2 μL of the trypsin dilution (40 ng) to the beads. Shake overnight at 37 $^\circ\text{C}$; if possible cover vortex with a heated lid to minimize condensation on tube lid.
6. Collect liquid from tube caps by briefly spinning on a tabletop centrifuge and transfer the tubes to a magnetic rack. Collect the liquid, which contains the proteolyzed peptides to clean tubes. Peptides are ready for final cleanup and processing for mass spectrometric analysis.

3.6 *Preparation of Small RNA cDNA Libraries from RNP Footprints for NGS (General Scheme in Fig. 4a)*

1. Transfer the beads (50% aliquot kept on ice) to the magnetic rack, discard the remaining supernatant, and resuspend the beads in 100 μL RNase T1 buffer.
2. Add RNase T1 to a final concentration of 1 U/ μL and incubate at 22 $^\circ\text{C}$ for 15 min. Then immediately cool the reaction on ice.
3. Wash beads twice with RNase T1 buffer and once with dephosphorylation buffer.
4. Resuspend the beads in 60 μL of dephosphorylation buffer supplemented with 30 units of calf intestine phosphatase (CIP). Incubate at 37 $^\circ\text{C}$ for 10 min with shaking.
5. Wash beads twice with 1 mL of dephosphorylation buffer.
6. Wash beads twice with PNK buffer without DTT.
7. Resuspend beads in 60 μL of ^{32}P 5' labeling reaction mix: PNK buffer (with DTT) supplemented with 60 units of PNK and 0.5 μCi γ - ^{32}P -ATP.
8. Incubate at 37 $^\circ\text{C}$ for 30 min with shaking.
9. Add nonradioactive ATP to a final concentration of 100 μM and incubate at 37 $^\circ\text{C}$ for additional 5 min.
10. Spin down and place tubes in a magnetic rack. Keep 50 μL of the supernatant, add into it 50 μL denaturing 2 \times formamide gel-loading solution to be used later to mark gel edges during

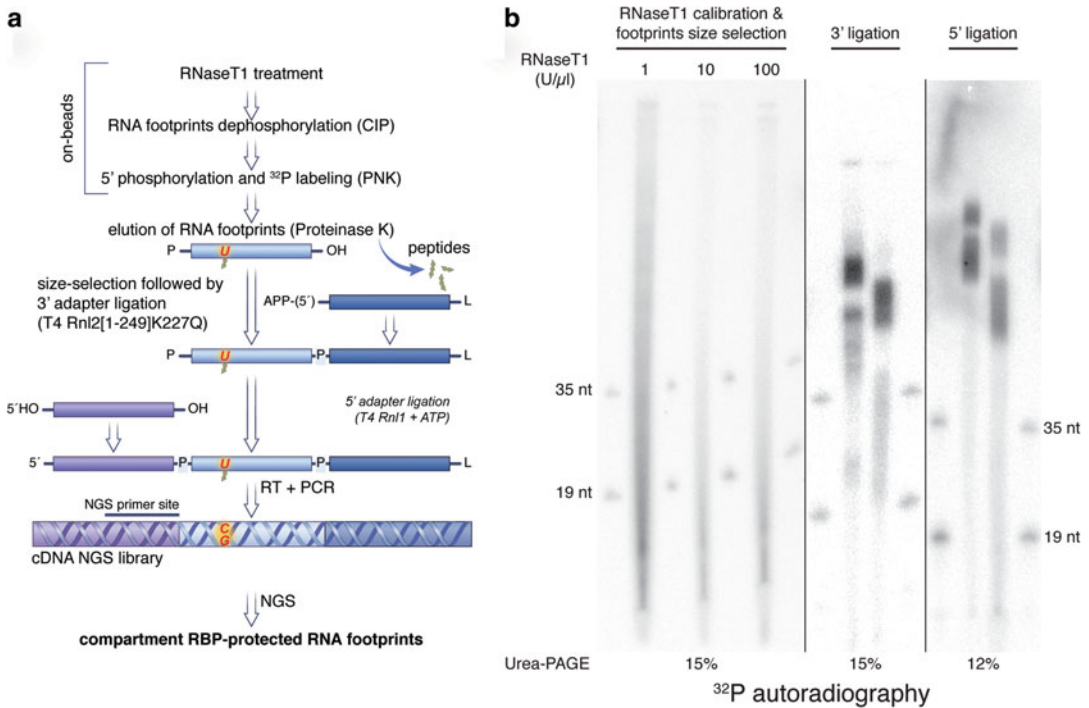


Fig. 4 Illustration and demonstration of steps along the production of small RNA cDNA libraries (Subheading 3.6). **(a)** Scheme of the molecular procedures succeeding streptavidin affinity purification. **(b)** Autoradiographs of the three denaturing gel steps along the procedure: Left, step 21—size selection of RNA footprints. Middle, step 27—purification of 3'-ligated footprints and depletion of excess non-ligated 3' adapter. Right, step 33—purification of 3'- and 5'-ligated footprints and depletion of excess non-ligated 5' adapter

urea-PAGE gel autoradiography for alignment (*see* **Notes 3** and **9**), and properly discard the rest.

11. Wash the beads five times with 1 mL of PNK buffer without DTT.
12. At this point the beads can be stored at $-20\text{ }^{\circ}\text{C}$. Note that the beads are also radioactive and make sure to follow radiation safety guidelines for storage.
13. Elute the RNA footprints by triple proteinase K digestions:
 - (a) Add 1.2 mg/mL proteinase K in 200 μL of proteinase K buffer. Incubate at $50\text{ }^{\circ}\text{C}$ under vigorous shaking for 30 min.
 - (b) Add 0.75 mg/mL proteinase K in 150 μL proteinase K buffer. Incubate at $50\text{ }^{\circ}\text{C}$ under vigorous shaking for 30 min.
 - (c) Add 0.75 mg/mL proteinase K in 150 μL proteinase K buffer. Incubate at $50\text{ }^{\circ}\text{C}$ under vigorous shaking for 30 min.
14. Collect liquid from tube caps by briefly spinning on a tabletop centrifuge and place in a magnetic rack. Transfer the supernatant, which contains the eluted RNA footprints, into a new 1.5 mL low-bind microcentrifuge tube.

15. To extract the RNA, add 30 μL of 5 M NaCl and 300 μL acidic phenol-chloroform (pH 4.5) to the 500 μL of supernatant, vortex well, and incubate for 10 min.
16. Centrifuge at $12,000 \times g$ for 10 min and transfer $\sim 300 \mu\text{L}$ of the top aqueous phase to a new 1.5 mL microcentrifuge tube.
17. Add 300 μL water-saturated chloroform, vortex well, and centrifuge at $12,000 \times g$ for 10 min. Transfer the aqueous phase to a new 1.5 mL microcentrifuge tube containing $\sim 10 \mu\text{g}$ of glycogen and mix.
18. Precipitate the RNA by adding 3 volumes of ethanol, incubating at -80°C for >1 h, and centrifuging at $>12,000 \times g$ for 20 min at 4°C .
19. Remove the ethanol as thoroughly as possible and air-dry the pellet by leaving the tubes open on the bench for 5 min. Do not let the pellet overdry.
20. Dissolve the RNA pellet in 20 μL of water, add 20 μL denaturing $2\times$ formamide gel loading solution, incubate at 90°C for 1 min, and load on a 15% denaturing urea-PAGE, with RNA size markers for reference (Table 1, *see* **Notes 3** and **9**).
21. Visualize the RNA footprint size distribution using autoradiography by exposing the gel to a film (*see* **Note 3**, Fig. 4b). Before exposure, use $\sim 0.1 \mu\text{L}$ volumes of the radioactive waste (Subheading 3.6, **step 10**) to pinch three marks to serve as reference points into the gel (make sure that reference points are far from sample lanes within the gel). Align a printout of the autoradiograph to the gel and excise gel fragments containing footprints 20–40 nt long and longer footprints as well if required.
22. Transfer the excised gel pieces in a gel breaker tube and extract the RNA as follows: (1) Centrifuge at maximum speed for 1 min. (2) Add 350 μL of 0.3 M NaCl and shake at 60°C for 1 h. (3) Transfer the suspension into filter tubes and centrifuge at $5000 \times g$ for 1 min. (4) Add $\sim 10 \mu\text{g}$ of glycogen and 1200 μL of 100% ethanol, vortex, and incubate at -80°C for >1 h. (5) Centrifuge at $>12,000 \times g$ for 15 min, discard the supernatant, and add 0.5 mL of 75% ethanol. Without mixing, centrifuge at max. speed for 7 min, thoroughly remove the supernatant, and air-dry the pellet by leaving the tubes open on the bench for 5 min. Do not let the pellet overdry.
23. Resuspend the RNA pellet in 8.7 μL of water.
24. For 3' adapter ligation to each 8.7 μL RNA add 8.3 μL mix containing 6 μL 50% DMSO, 2 μL $10\times$ RNA ligase buffer without ATP, and 0.3 μL of ^{32}P -labeled 19 nt and 35 nt RNA marker mix. Then add 2 μL of 10 μM sample-specific indexed 29-nucleotide adenylated 3' adapter (Table 1).

Table 1
Oligonucleotides

<i>RNA size markers</i>	
19 nt RNA size marker	5' CGUACGCGGGUUUAAAACGA
35 nt RNA size marker	5' CUCAUCUUGGUCGUACGCGGAAUAGUUUAAACUGU
<i>RNA 5' adapter</i>	
GUUCAGAGUUCUACAGUCCGACGAUC	
<i>DNA barcoded 3' adapters (barcodes underlined)</i>	
29.01	App- <u>NNTGACTGTGGAATTCTCGGGTGCCAAGG</u> -L
29.02	App- <u>NNACACTCTGGAATTCTCGGGTGCCAAGG</u> -L
29.03	App- <u>NNACAGAGTGGAATTCTCGGGTGCCAAGG</u> -L
29.04	App- <u>NNGCGATATGGAATTCTCGGGTGCCAAGG</u> -L
29.49	App- <u>NNATAGTATGGAATTCTCGGGTGCCAAGG</u> -L
29.50	App- <u>NNTCATAGTGGAATTCTCGGGTGCCAAGG</u> -L
App: 5' terminal adenosine residue connected via a 5',5'-diphosphate bridge to the 5'OH of the 5' nucleotide; L: 3' aminohexyl blocking group.	
<i>DNA Reverse transcription primer</i>	
GCCTTGGCACCCGAGAATTCCA	
<i>DNA 5' PCR primer</i>	
AATGATACGGCGACCACCGAGATCTACACGTTTCAGAGTTCTACAGTCCGA	
<i>DNA 3' barcoded PCR primers (indices underlined)</i>	
RP11	CAAGCAGAAGACGGCATA <u>CGAGATCGTGATGTGACTGGAGTTCC</u> TTGGCACCCGAGAATTCCA
RP12	CAAGCAGAAGACGGCATA <u>CGAGATACATCGGTGACTGGAGTTCC</u> TTGGCACCCGAGAATTCCA
RP13	CAAGCAGAAGACGGCATA <u>CGAGATGCCTAAGTGACTGGAGTTCC</u> TTGGCACCCGAGAATTCCA
RP14	CAAGCAGAAGACGGCATA <u>CGAGATTGGTCAGTGACTGGAGTTCC</u> TTGGCACCCGAGAATTCCA
RP15	CAAGCAGAAGACGGCATA <u>CGAGATCACTGTGTGACTGGAGTTCC</u> TTGGCACCCGAGAATTCCA
RP16	CAAGCAGAAGACGGCATA <u>CGAGATATTGGCGTGACTGGAGTTCC</u> TTGGCACCCGAGAATTCCA
RP17	CAAGCAGAAGACGGCATA <u>CGAGATGATCTGGTGACTGGAGTTCC</u> TTGGCACCCGAGAATTCCA
RP18	CAAGCAGAAGACGGCATA <u>CGAGATTCAAGTGTGACTGGAGTTCC</u> TTGGCACCCGAGAATTCCA

25. Incubate at 90 °C for 1 min and return the tubes to ice. Once chilled add 1 μL of T4 Rnl2(1-249)K227Q (1 $\mu\text{g}/\mu\text{L}$), mix gently, and incubate on ice overnight (place the ice bucket in a refrigerator).
26. Terminate 3' ligation by adding 20 μL of denaturing 2 \times formamide gel loading solution and incubating at 90 °C for 1 min.
27. Load samples on a 15% denaturing urea-PAGE gel, image by autoradiography as described in **step 21** (Fig. 4b, *see Note 3*), and excise ligated footprints (Fig. 4) using the ligated RNA size markers as reference.
28. Transfer the excised gel pieces in a gel breaker tube and extract the RNA as follows: (1) Centrifuge at maximum speed for 1 min. (2) Add 350 μL of 0.3 M NaCl and shake at 60 °C for 1 h. (3) Transfer the suspension into filter tubes and Centrifuge at 5000 $\times g$ for 1 min. (4) Add ~10 μg of glycogen and 1200 μL of 100% ethanol, vortex, and incubate at -80 °C for >1 h. (5) Centrifuge at maximum speed for 15 min, discard the supernatant, and add 0.5 mL of 75% ethanol. Without mixing, centrifuge at >12,000 $\times g$ for 7 min, thoroughly remove the 75% ethanol, and air-dry the pellet by leaving the tubes open on the bench for 5 min. Do not let the pellet overdry.
29. Resuspend the RNA pellet in 9 μL of water.
30. For 5' adapter ligation to each 9 μL RNA add 9 μL mix containing 6 μL 50% DMSO, 2 μL 10 \times RNA ligase buffer with ATP, and 1 μL of 100 μM RNA 5' adapter (Table 1).
31. Incubate at 90 °C for 1 min and return the tubes to ice. Once chilled, add 2 μL of T4 Rnl1 (1 $\mu\text{g}/\mu\text{L}$), mix gently, and incubate at 37 °C for 1 h.
32. Terminate 5' adapter ligation by adding 20 μL of denaturing 2 \times formamide gel loading solution and incubating at 90 °C for 1 min.
33. Load samples on a 12% denaturing urea-PAGE gel, image by autoradiography overnight as described in **step 21** (Fig. 4b, *see Note 3*), and excise ligated footprints (Fig. 4) using the ligated RNA size markers as reference.
34. Put the excised gel pieces in a gel breaker tube and extract the RNA as follows: (1) Centrifuge at maximum speed for 1 min. (2) Add 350 μL of 0.3 M NaCl and shake at 60 °C for 1 h. (3) Transfer the suspension into filter tubes and centrifuge at 5000 $\times g$ for 1 min. (4) Add ~10 μg of glycogen and 1200 μL of 100% ethanol, vortex, and incubate at -80 °C for >1 h. (5) Centrifuge at maximum speed for 15 min, discard the supernatant, and add 0.5 mL of 75% ethanol. Without mixing, centrifuge at >12,000 $\times g$ for 7 min, thoroughly remove the supernatant, and air-dry the pellet by leaving the tubes open on the bench for 5 min. Do not let the pellet overdry.

35. Resuspend the RNA pellet in 4.6 μL of water.
36. For reverse transcription denature the RNA at 90 $^{\circ}\text{C}$ for 1 min, then reduce the temperature to 50 $^{\circ}\text{C}$, and add 10.4 μL master mix comprised of 1.5 μL of 100 mM DTT, 3 μL of 5 \times first-strand buffer (Thermo), 4.2 μL of 2 mM dNTPs, 1 μL of 100 μM RT primer (Table 1), and 0.7 μL Superscript III.
37. Incubate at 50 $^{\circ}\text{C}$ for 1 h.
38. Dilute the cDNA by adding 85 μL water, reaching a volume of 100 μL .
39. Use 6 μL of the diluted cDNA for calibration PCR by adding 0.6 μL of 100 μM multiplexed reverse PCR primer (Table 1) and a mix comprised of 38.6 μL of water, 6 μL of 10 \times buffer without Mg^{2+} , 1.8 μL of 50 mM MgCl_2 , 6 μL of 2 mM dNTPs, 0.6 μL 100 μM forward PCR primer (Table 1), and 0.42 *Taq* polymerase.
40. Split the 60 μL reaction mix into 6 tubes and load on a PCR 19-cycle program. Remove one of the tubes after 9, 11, 13, 15, 17, and 19 cycles, and load the PCR products on a 2.5% agarose gel for electrophoresis.
41. Image the gel to select the optimal number of PCR cycles, where amplification of the library is favored relative to that of linker-linker products derived from directly ligated 3' and 5' adapters.
42. Use the same reagents to set up an identical PCR with reaction volume of 300 μL . Split the reaction to three 100 μL tubes and run with the previously determined optimal number of cycles.
43. Clean and concentrate the PCR product using a standard column-based purification kit and elute in 70 μL of water.
44. Load 30 μL of the purified PCR product for a Pippin Prep size selection to deplete ligated 3'–5' adapters (126 bp long) and enrich insert-containing library products. For footprints of lengths 20–40 nt, the expected library size is 146–166 bp.
45. Use TapeStation with a D1000 ScreenTape to measure the library final concentration and average length.

3.7 Transformation of Intact RNA into RNA-seq Libraries

1. Obtain the -80°C -stored 20% of beads for RNA-seq of intact bound RNAs (Subheading 3.4, step 7).
2. Elute the bound RNA by triple proteinase K digestions:
 - (1) Add 1.2 mg/mL proteinase K in 200 μL of proteinase K buffer. Incubate at 50 $^{\circ}\text{C}$ under vigorous shaking for 30 min.
 - (2) Add 0.75 mg/mL proteinase K in 150 μL proteinase K buffer. Incubate at 50 $^{\circ}\text{C}$ under vigorous shaking for 30 min.
 - (3) Add 0.75 mg/mL proteinase K in 150 μL proteinase K buffer. Incubate at 50 $^{\circ}\text{C}$ under vigorous shaking for 30 min.

3. Collect liquid from tube caps by briefly spinning on a tabletop centrifuge and place the tubes in a magnetic rack. Transfer the supernatant, which contains the eluted RNA, into a new 1.5 mL low-bind microcentrifuge tube.
4. To extract the RNA, add 30 μL of 5 M NaCl and 300 μL of acidic phenol-chloroform (pH 4.5) to the 500 μL supernatant, vortex well, and incubate for 10 min.
5. Centrifuge at $12,000 \times g$ for 10 min and transfer $\sim 300 \mu\text{L}$ of the top aqueous phase to a new 1.5 mL microcentrifuge tube.
6. Add 300 μL water-saturated chloroform, vortex well, and centrifuge at $12,000 \times g$ for 10 min. Transfer the aqueous phase to a new 1.5 mL microcentrifuge tube containing $\sim 10 \mu\text{g}$ of glycogen and mix.
7. Precipitate the RNA by adding three volumes of ethanol, incubating at -80°C for >1 h, and centrifuging at $>12,000 \times g$ for 20 min at 4°C .
8. Discard the supernatant and add 0.5 mL of 75% ethanol. Without mixing, centrifuge at $>12,000 \times g$ for 7 min, thoroughly remove the supernatant, and air-dry the pellet by leaving the tubes open on the bench for 5 min. Do not let the pellet overdry.
9. Dissolve the bound intact RNA pellet in 20 μL of water (Fig. 3f). Optional: Use TapeStation and an RNA ScreenTape to analyze the size distribution and concentration of the eluted RNA.
10. Obtain the cell extract 30 μL samples saved for total RNA analysis (Subheading 3.4, step 4).
11. To the 30 μL samples add 370 μL water and immediately after 400 μL of phenol:chloroform:isoamyl alcohol 25:24:1 mixture. Vortex, incubate on the bench for 15 min, and centrifuge at maximum speed for 10 min.
12. Transfer 200 μL of the top aqueous phase to a new tube, add the same volume of water-saturated chloroform, vortex, and centrifuge at maximum speed for 10 min.
13. Transfer 100 μL of the top aqueous phase to a new tube; add 7 μL of 3 M NaAc pH 5.3, $\sim 10 \mu\text{g}$ of glycogen, and 400 μL of cold 100% ethanol; vortex; and incubate at -80°C for >1 h.
14. Spin at maximum speed for 15 min in a pre-chilled centrifuge. Discard the supernatant and add 0.5 mL of 75% ethanol. Without mixing, centrifuge at maximum speed for 7 min, thoroughly remove the supernatant, and air-dry the pellet by leaving the tubes open for 5 min. Do not let the pellet overdry.

15. Dissolve the total RNA pellet in 20 μ L of water. Optional: Use TapeStation and an RNA ScreenTape to analyze the integrity of eluted RNA (RIN, RNA Integrity Number).
16. Use your preferred kit to transform the total and bound intact RNA samples into cDNA libraries for RNA-seq. For the bound RNA samples avoid ribosomal RNA depletion and use mild RNA fragmentation conditions.

4 Notes

1. APEX2 is an engineered soy ascorbate peroxidase that can oxidize biotin-phenol in the presence of hydrogen peroxide, thus generating rapidly decaying biotin-phenoxy radicals ($t_{1/2} < 1$ ms) [4]. The majority of radicals decay by reacting with water, but some will react with APEX2-proximal proteins at aromatic amino acids and biotinylate them. Therefore, compartment-specific proteins can be biotinylated and isolated by affinity chromatography by fusing localization signals to APEX2 and targeting it to a given cellular compartment.

Although the protocol is currently designed for adherent cells, adjustments could be made to fit cells in suspension. Cells that are weakly adherent, such as HEK293 cells, require additional caution during the numerous washing steps to avoid loss of cells. To employ *Proximity-CLIP* in other, nonmammalian or non-cell culture, systems the following requirements must be met: (1) Cells need to be expressing APEX2. (2) 4-Thiouridine or 4-thiouracil needs to be taken up by cells and metabolized into 4-thioUTP. (3) Cells need to be accessible for UV cross-linking and for administration of BP, hydrogen peroxide, and antioxidative quenching. Mediating proximity biotinylation by a biotin ligase such as TurboID [19] instead of APEX2 may be preferable in cases where a shorter labeling radius is required, which is particularly relevant in smaller cell systems, such as yeast and bacteria. It would also obviate the requirement for BP, hydrogen peroxide, and administration of quenching solution, but will add the requirement of accessibility for administration of biotin. Essentially, a good indication that a system is amenable to *Proximity-CLIP* would be the identification of successful PAR-CLIP and either APEX2- or biotin ligase-mediated labeling experiments in the literature.

In terms of cell density, to balance the need for high cell number with the requirement of cells to be rapidly growing for efficient 4SU incorporation (*see Note 5*) we aimed for 90% confluence on the day of the experiment. This requires careful calibration per cell line. We aimed to have at least $\sim 25 \times 10^6$

HEK293 cells in a similar growth stage 36 h prior to the experiment. This sufficed in our hands for seeding one 15 cm preparative plate, three 6 cm plates (+BP and hydrogen peroxide, and –BP and –hydrogen peroxide controls) for Western blot analyses (*see also Note 8*), and four cover glasses (–BP and –hydrogen peroxide controls and two +BP and hydrogen peroxide glasses) for immunofluorescence analyses. The additional +BP and hydrogen peroxide glass is usually required for “no primary antibody” or another technical control.

The compartment to which control APEX2 is targeted to should be selected based on where signal from the compartment of interest is expected to diffuse to; often this would be the cytoplasm. APEX2 fusion proteins should be detectable by fluorescence microscopy, by immunostaining, or by fusion to a fluorescent protein. Staining procedures should be optimized beforehand (Fig. 2), and homogenic APEX2 expression as well as proper localization in all expressing cells should be verified.

2. Although mass spectrometry is often outsourced, we recommend performing on-beads trypsinization and the preceding steps in-house. Due to relatively low amounts of input material, it is advisable to minimize the amount of added trypsin, to strictly avoid contamination of samples with skin proteins, and to use high-grade reagents. We used Pierce single-use/no-weigh iodoacetamide and DTT (Thermo Scientific 90034 and 20291, respectively) and sequencing-grade modified trypsin (Promega V5111).
3. Urea-PAGE, autoradiography, and excision of gel sections to obtain RNA:

Urea-polyacrylamide gels can be mixed and cast in-house. We use premixed solutions (SequaGel UreaGel 29:1 Denaturing Gel System, by National Diagnostics) and cast 16 cm long gels (length includes 2 cm for loading wells). Prior to loading either pure RNA or a reaction mix on gel, samples should be mixed in a 1:1 ratio with 2× formamide gel loading solution and incubated at 90 °C for 1 min. As a rule of thumb, samples should be loaded with at least one empty lane between them to avoid cross-contamination and facilitate image analysis in case autoradiography signals are dramatically different in their intensity. Once gels are assembled on the apparatus, use a syringe to wash wells with running buffer in order to remove urea precipitations, and pre-run prior to loading the samples for about 30 min to warm the gels. Repeat the wash of urea precipitations immediately prior to loading your samples. Once samples are loaded, we run our gels at 450 V for 45–70 min. Once the run has ended, dismantle the gel while leaving it attached to one of the glass plates. Mark three corners of the gel at locations distant from the sample lane with ~0.1 µL of

radioactive waste (Subheading 3.6, step 10), pinched into the gel using the pipette tip. This will enable alignment of the gel with a printout of the autoradiograph. Wrap the gel in Saran wrap and expose a pre-blanked phosphorimager screen to the gel in a dedicated cassette at $-20\text{ }^{\circ}\text{C}$ to avoid diffusion of the nucleic acids in the gel. Print the image in its original size and position the gel above the printed paper by aligning the signal and blue color of the radioactive waste. Cut gel sections that contain the required RNAs and collect them into gel breaker tubes.

4. Pippin Prep and 3% Pippin gel cassettes (Sage Science) are used for agarose gel size separation and extraction of the amplified sRNA cDNA sequencing library. This step is necessary because directly ligated 3' and 5' adapters ("empty library") are a common side reaction that can overwhelm the library during PCR. If Pippin Prep is not available it is possible to use standard 3% agarose gel electrophoresis to size-separate the two PCR products. An alternative to gel extraction of the amplified library would be to follow the following steps: (1) Run the gel at 90 V for ~90 min. (2) Position the gel on a UV imager and manually carve a well right below the band corresponding to the library. (3) Return the gel to the running apparatus, lower the buffer height so it is just below the top of the gel, empty the liquid off the carved well, and fill it with clean running buffer. (4) Continue to run the gel for 5 min while every 1 min collecting the buffer from the well into a fresh tube and quickly replacing it with fresh buffer. (5) Reimage the gel to validate that the library band no longer appears and use TapeStation and a D1000 ScreenTape to assess in which of the tubes the library eluted, and to measure its concentration and average length.
5. Nascent RNAs incorporate 4SU during transcription; therefore in most cases overcrowding of cells should be avoided to maintain a metabolically active culture. The 16-h labeling time window can be increased for slow-growing cells, or decreased for labeling of transient events, as required.
6. Fluorescence microscopy imaging should be performed according to the standard procedures applied per lab, cells, and experimental system. It is essential to image both the APEX2-fusion protein and biotinylated proteins in all conditions (labeled and -BP, -hydrogen peroxide, and -APEX2 controls). Note that immunological detection of the APEX2-fusion protein may vary after labeling due to self-biotinylation. Biotinylated proteins can be labeled by fluorophore-coupled neutravidin or an alternative (we use Alexa-Fluor-647-coupled neutravidin). The main goals of imaging are (1) to confirm that APEX2 is expressed and localized as expected; (2) to confirm

that biotinylation is dependent upon APEX2, BP, and hydrogen peroxide; and (3) to probe how well localization of biotinylated proteins correlates to APEX2 localization.

7. It is recommended to calibrate per each APEX2-fusion protein expressing cell line the optimal ratio of bead volume to cell extract total protein. While insufficient quantity of beads may result in loss of biotinylated material that remains in solution, use of too many beads can increase the experiment background. Only ~15% of bound material is eluted from streptavidin beads upon incubation with protein-loading dye (*see* Subheading 2.3, step 18, and Subheading 3.3, step 7). Therefore, Western blot analysis of the unbound material after incubation of cell extracts with the beads may be the best indication for full depletion of biotinylated proteins from the cell extracts (Fig. 3c, d). Finally, when working with beads or resin, make sure that either wide or cut tips are used to maintain their integrity.
8. Seeding three 6 cm plates per cell line enables biochemical control of the proximity biotinylation (Fig. 3). Western blot analysis of cell extracts and eluates with HRP-coupled streptavidin controls for the dependence of the reaction in APEX2, BP, and hydrogen peroxide. Similarly, analysis of the unbound material and eluates will confirm that biotinylated proteins were fully collected from the cell extracts and are concentrated on the beads. Finally, Western blot analysis to confirm the expression of the APEX2-fusion protein is vital to rule out the expression of truncated versions of the protein.
9. The radiolabeled 19 nt and 35 nt RNA size markers (Table 1) are essential as size markers on urea-PAGE gels, for RNA footprint size selection, and for monitoring 3' and 5' adapter ligations. We recommended loading non-ligated size markers on all urea-PAGE gels, as well as introduction of the RNA size markers into 3' ligation reaction mix, and their carryover through gel extraction into the 5' ligation reaction. Radiolabel 10 pmol of each size marker individually at 37 °C for 15 min in 10 µL reaction volumes of PNK buffer with DTT, 10 U T4 PNK, and 50 µCi γ -³²P-ATP. Terminate the reaction by addition of 10 µL 2× formamide gel loading solution and incubation at 90 °C for 1 min. To purify the labeled markers from the free γ -³²P-ATP load and run them through a 15% urea-PAGE with at least one empty lane between samples. Optional: To reduce the amount of radioactive waste a small RNA column purification kit (we use Zymo) can be used to clear the reaction mix off the γ -³²P-ATP prior to gel separation. Image the gels by autoradiography, excise, extract, purify, and solubilize each labeled marker in 10 µL of water. Finally, pool the markers together; if the radioactive signal of the markers appeared

significantly different, mix them at a ratio that equalizes their signal strength. Use a 1:100 dilution of the marker mix as your working stock. At each step estimate an appropriate marker that needs to be used to fit the signal in your samples. Marker signal decays with time at ^{32}P half-life rate ($t_{1/2} \sim 2$ weeks).

References

1. Wilk R, Hu J, Blotsky D, Krause HM (2016) Diverse and pervasive subcellular distributions for both coding and long noncoding RNAs. *Genes Dev* 30:594–609. <https://doi.org/10.1101/gad.276931.115>
2. Kejiou NS, Palazzo AF (2017) mRNA localization as a rheostat to regulate subcellular gene expression. *Wiley Interdiscip Rev RNA*:e1416. <https://doi.org/10.1002/wrna.1416>
3. Lécuyer E, Yoshida H, Parthasarathy N et al (2007) Global analysis of mRNA localization reveals a prominent role in organizing cellular architecture and function. *Cell* 131:174–187. <https://doi.org/10.1016/j.cell.2007.08.003>
4. Hung V, Udeshi ND, Lam SS et al (2016) Spatially resolved proteomic mapping in living cells with the engineered peroxidase APEX2. *Nat Protoc* 11:456–475. <https://doi.org/10.1038/nprot.2016.018>
5. Li Y, Aggarwal MB, Ke K et al (2018) Improved analysis of RNA localization by spatially restricted oxidation of RNA-protein complexes. *Biochemistry* 57:1577–1581. <https://doi.org/10.1021/acs.biochem.8b00053>
6. Fernández-Suárez M, Chen TS, Ting AY (2008) Protein-protein interaction detection in vitro and in cells by proximity biotinylation. *J Am Chem Soc* 130:9251–9253. <https://doi.org/10.1021/ja801445p>
7. Yang J, Jaramillo A, Shi R et al (2004) In vivo biotinylation of the major histocompatibility complex (MHC) class II/peptide complex by coexpression of BirA enzyme for the generation of MHC class II/tetramers. *Hum Immunol* 65:692–699. <https://doi.org/10.1016/j.humimm.2004.04.001>
8. de Boer E, Rodriguez P, Bonte E et al (2003) Efficient biotinylation and single-step purification of tagged transcription factors in mammalian cells and transgenic mice. *Proc Natl Acad Sci U S A* 100:7480–7485. <https://doi.org/10.1073/pnas.1332608100>
9. O'callaghan CA, Byford MF, Wyer JR et al (1999) BirA enzyme: production and application in the study of membrane receptor-ligand interactions by site-specific biotinylation. *Anal Biochem* 266:9–15. <https://doi.org/10.1006/abio.1998.2930>
10. Fazal FM, Han S, Kaewsapsak P, et al (2018) Atlas of subcellular RNA localization revealed by APEX-seq. *bioRxiv* 454470. <https://doi.org/10.1101/454470>
11. Kaewsapsak P, Shechner DM, Mallard W et al (2017) Live-cell mapping of organelle-associated RNAs via proximity biotinylation combined with protein-RNA crosslinking. *elife* 6:623. <https://doi.org/10.7554/eLife.29224>
12. Padron A, Iwasaki S, Ingolia N (2018) Proximity RNA labeling by APEX-Seq reveals the organization of translation initiation complexes and repressive RNA granules. *bioRxiv* 454066. <https://doi.org/10.1101/454066>
13. Benhalevy D, Anastasakis DG, Hafner M (2018) Proximity-CLIP provides a snapshot of protein-occupied RNA elements in subcellular compartments. *Nat Methods* 15:1074–1082. <https://doi.org/10.1038/s41592-018-0220-y>
14. Benhalevy D, Anastasakis D, Hafner M (2018) Proximity-CLIP. *Protoc Exch*. <https://doi.org/10.1038/protex.2018.115>
15. Koch L (2019) Proximity-CLIP - close encounters of the RNA kind. *Nat Rev Genet* 20:68–69. <https://doi.org/10.1038/s41576-018-0086-y>
16. Choder M (2011) mRNA imprinting: additional level in the regulation of gene expression. *Cell Logist* 1:37–40. <https://doi.org/10.4161/cl.1.1.14465>
17. Hafner M, Landthaler M, Burger L et al (2010) Transcriptome-wide identification of RNA-binding protein and microRNA target sites by PAR-CLIP. *Cell* 141:129–141. <https://doi.org/10.1016/j.cell.2010.03.009>
18. Benhalevy D, McFarland HL, Sarshad AA, Hafner M (2016) PAR-CLIP and streamlined small RNA cDNA library preparation protocol for the identification of RNA binding protein target sites. *Methods* 118–119:41–49. <https://doi.org/10.1016/j.jymeth.2016.11.009>
19. Branon TC, Bosch JA, Sanchez AD et al (2018) Efficient proximity labeling in living cells and organisms with TurboID. *Nat Biotechnol* 36:880–887. <https://doi.org/10.1038/nbt.4201>



Double-Stranded RNA Pull-Down to Characterize Viral Replication Complexes in Plants

Marco Incarbone and Christophe Ritzenthaler

Abstract

Plant RNA viruses are obligate intracellular parasites that hijack specific cellular membranes to replicate their genomes in what are commonly known as viral replication complexes (VRC). These contain host- and virus-encoded proteins and viral RNA. Double-stranded RNA (dsRNA) is a mandatory intermediate of RNA replication and a hallmark feature of VRCs. We have recently developed a method to isolate viral dsRNA and its associated proteins through pull-down of an ectopically expressed dsRNA-binding protein (B2:GFP) from infected *Arabidopsis thaliana* plants. After mass spectrometry analysis to identify the dsRNA-associated proteins, resulting candidate proteins of interest are tagged with a red fluorescent protein and their subcellular localization in relation to VRCs is assessed by transient expression within leaves of B2:GFP-transgenic *Nicotiana benthamiana* plants. In this chapter we describe in detail these experimental procedures to allow investigators to characterize the replication complexes of their plant RNA virus of interest.

Key words Virus replication complex, dsRNA, Immunoprecipitation, Mass spectrometry, North-western blot, Laser confocal microscopy

1 Introduction

RNA replication is a key step in the infection cycle of RNA viruses. This process involves both virus- and host-encoded proteins, and takes place in endo-membrane invaginations/vesicles [1, 2]. While the specific proteins and membranes involved in the formation of virus replication complexes depend on the virus and host species, the presence of dsRNA, as a product of the viral RNA-dependent RNA polymerase, is a hallmark of infection. The precise molecular composition of replication complexes remains poorly characterized for most plant viruses, although the question has been approached for a few model plant RNA viruses through different experimental approaches. These include genetic screens on yeast as a surrogate host [3] and *in planta* pull-down of viral proteins [4–6]. These approaches yielded seminal results, but were limited to the use of

specific viral proteins or virus species. We have recently shown that the dsRNA-binding domain of Flock House virus B2 protein can be used to efficiently detect virus-derived dsRNA in extracts from plant tissues infected with a variety of RNA viruses [7]. Furthermore, we showed that the same protein, when genetically fused with GFP (B2:GFP) and ectopically expressed in *N. benthamiana* plants, re-localizes to viral replication complexes upon infection by a variety of RNA viruses [7]. Based on these findings, we developed a protocol for the isolation of (i) viral replicating dsRNA and (ii) the proteins associated to it, through the immunoprecipitation of B2:GFP from infected plants [8] (Fig. 1). This protocol is based on a study with *A. thaliana* plants infected with *tobacco rattle virus* (TRV) as a model, but since dsRNA is an intermediate in the

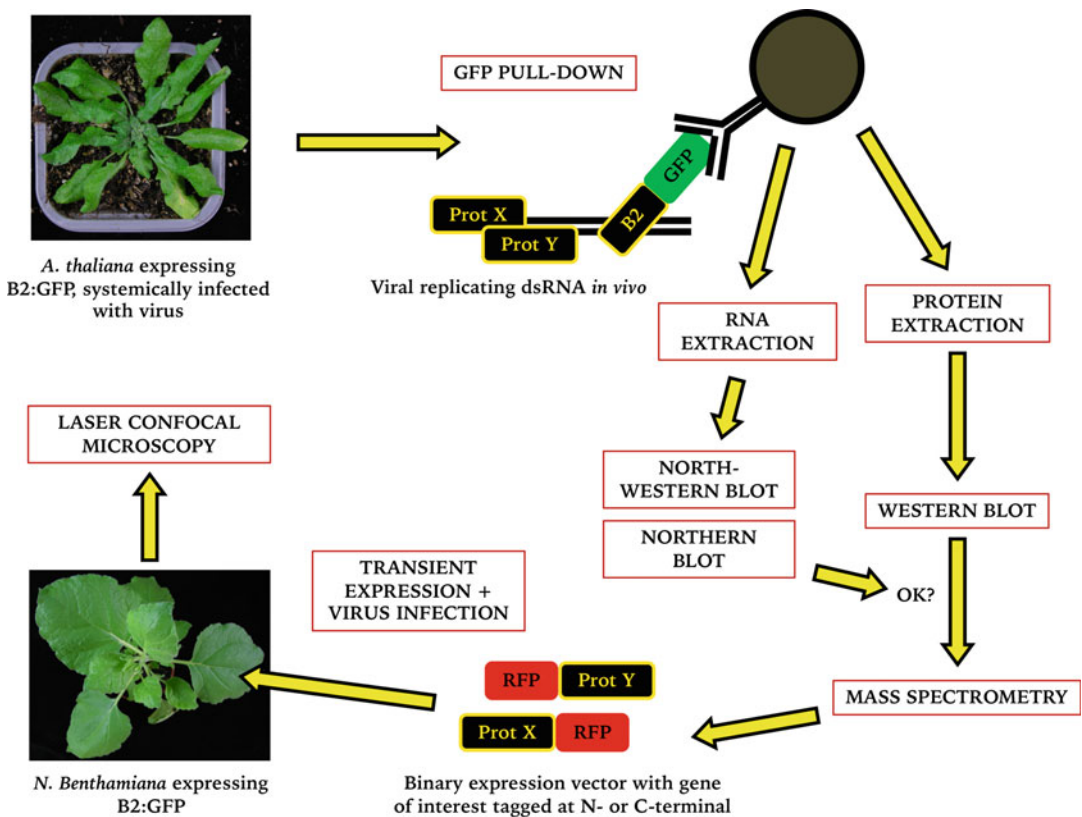


Fig. 1 Schematic diagram of experimental steps to characterize proteins associated with viral replicating dsRNA and VRCs. Virus-infected B2:GFP-expressing Arabidopsis is used for GFP pull-down. The immunoprecipitated fractions are subject to RNA and protein extraction. North-western blot, northern blot, and western blot analyses are used to confirm the presence of dsRNA, viral RNA, and B2:GFP, respectively. Protein extracts are then analyzed by mass spectrometry. Resulting genes encoding potential dsRNA-binding/VRC-associated proteins are cloned as N- or C-terminal fusions with a red-fluorescent tag into binary vectors for ubiquitous and abundant transient expression in virus-infected B2:GFP-expressing *N. benthamiana*. Analysis by confocal microscopy is used to determine the subcellular localization of the candidate protein(s) in relation to the B2:GFP-labeled dsRNA/VRCs

replication of all RNA viruses, this approach can potentially be used for any RNA virus able to infect *N. benthamiana* or *A. thaliana*, for which transgenic lines expressing B2:GFP are available. In this chapter, we describe in detail how to perform dsRNA pull-down and how to assess the quality of the experiment. In addition, we provide an overview of how to rapidly verify subcellular localization of potential VRC-associated proteins identified through mass spectrometry analysis of the dsRNA pull-down. We do not describe LC-MS/MS mass spectrometry analysis and processing of the resulting data, which should be outsourced to specialists.

2 Materials

2.1 dsRNA Pull-Down

1. *A. thaliana* Col-0 plants expressing the 35S:B2:GFP cassette [8] and systemically infected with the RNA virus of interest. As a negative control, virus-infected 35S:GFP/Col-0 plants can be used [8]. The 35S:B2:GFP/Col-0 and 35S:GFP/Col-0 lines are available upon request.
2. Sample collection tubes for -80°C storage.
3. Liquid nitrogen, mortar, pestle.
4. Cold lysis buffer (4°C or on ice): 50 mM Tris-HCl pH 8, 50 mM NaCl, 1% Triton X-100. Just before the experiment, add protease inhibitor cocktail and RNase inhibitor in amounts suggested by the manufacturer.
5. Sterile, RNase-free 1.5 mL centrifuge tubes.
6. Rotating wheel at 4°C able to hold 1.5 mL tubes.
7. Tabletop centrifuge capable of $12,000 \times g$ at 4°C .
8. Anti-GFP magnetic beads and magnetic stand for capture (in ref. 8 the Miltenyi μMACS kit was used, containing colloidal magnetic beads).

2.2 RNA Isolation

1. TRIzol (TRI reagent).
2. Sterile, RNase-free 1.5 mL centrifuge tubes.
3. Chloroform.
4. Vortex.
5. Tabletop centrifuge capable of providing $16,000 \times g$ at 4°C .
6. Isopropanol (ice cold).
7. RNA-grade glycogen.
8. 80% Ethanol (ice cold).
9. RNase-free water.

2.3

North-Western Blot

1. 10× HEPES buffer: 200 mM HEPES, 10 mM EDTA. Adjust to pH 7.8 with 1 M KOH, and sterilize by filtration.
2. Agarose (molecular biology grade).
3. 4× RNA-loading buffer: 50% Glycerol, 50 mM Tris-HCl pH 7.5, 5 mM EDTA, bromophenol blue, 50 µg/mL ethidium bromide.
4. Gel-running tank at 4 °C.
5. Power generator.
6. Gel documentation and analysis equipment (e.g.: Gel Doc).
7. Capillary transfer apparatus.
8. 20× SSC: 3 M NaCl, 0.3 M sodium citrate. Sterilize by filtration.
9. Blotting paper.
10. Nylon membrane, gel sized (e.g.: Amersham HyBond™ N+).
11. Stack of paper towels.
12. Approximately 1 kg weight.
13. 2× SSC.
14. UV cross-linker.
15. Crystal box large enough to accommodate the nylon membrane.
16. 1× PBS: 137 mM NaCl, 2.7 mM KCl, 10 mM Na₂HPO₄, 1.8 mM KH₂PO₄. Adjust to pH 7.4 with HCl.
17. PBS/Tween: 1× PBS, 0.1% Tween.
18. PBS/Tween/milk: 1× PBS, 0.1% Tween, 5% powdered milk.
19. Benchtop oscillator.
20. Recombinant B2:StrepTagII [7]: The plasmid to produce this protein is available upon request.
21. StrepTactin conjugated to horseradish peroxidase (IBA Life Sciences Strep-Tactin®-HRP conjugate).
22. Transparent plastic folder.
23. ECL chemiluminescence substrate.
24. Equipment to detect chemiluminescence (film or digital appliance).

2.4 Northern Blot

1. Subheadings 2.3, items 1–3 and 5–15.
2. Gel electrophoresis tank.
3. Formaldehyde.
4. RNA denaturing loading buffer: 1× HEPES buffer, 50% formamide, 6% formaldehyde, 20% glycerol, 0.05% (w/v) bromophenol blue, 50 µg/mL ethidium bromide.

5. Thermal block for 1.5 mL tubes.
6. Hybridization tube.
7. Hybridization oven.
8. Hybridization buffer (e.g., PerfectHyb™ Plus, Sigma-Aldrich).
9. DNA oligonucleotide complementary to viral sequence of interest, with a calculated melting temperature (in water) of around 55–60 °C. Generally, this oligonucleotide should be 20–25 nucleotides long. Crucially, this oligonucleotide should give no signal when used as probe in Northern blot on virus-free samples.
10. Polynucleotide kinase (PNK) labeling kit.
11. ³²P-γATP, along with all materials, protective gear, and authorizations required to handle radioactive isotopes and to dispose of radioactive waste.
12. Filter tips.
13. Paper towel cut into small squares of 5 × 5 cm and folded twice.
14. 20% SDS solution.
15. Wash buffer: 2% SDS, 2× SSC.
16. Tweezers.
17. Transparent plastic envelope.
18. Radioactivity-detection equipment of choice: Cassette with radiation-reflecting screens and autoradiographic film, or phosphor-imager screen and detector.

2.5 Western Blot

1. 4× Protein-loading buffer: 250 mM Tris–HCl pH 6.8, 40% glycerol, 8% SDS, 20% (v/v) 2-β-mercaptoethanol.
2. Protein resuspension buffer: 62.3 mM Tris–HCl pH 8, 10% glycerol, 3% SDS.
3. Heating block for 1.5 mL tubes.
4. Tabletop centrifuge capable of providing 16,000 × *g* at 4 °C.
5. Acetone (ice cold).
6. 80% Acetone (ice cold).
7. SDS-PAGE gel-casting system.
8. Glass plates for SDS-PAGE gels.
9. Well combs for SDS-PAGE gels.
10. Acrylamide/bis-acrylamide 37.5/1.
11. Resolving buffer: 1.1 M Tris–HCl, 0.4% SDS, pH 8.8.
12. Stacking buffer: 0.6 M Tris–HCl, 0.4% SDS, pH 6.8.
13. 10% Ammonium persulfate (APS).

14. TEMED.
15. Ethanol.
16. Blotting paper.
17. SDS-PAGE gel-running tank.
18. 10× Tris-glycine buffer: 250 mM Tris base, 1.92 M glycine.
19. SDS solution.
20. Migration buffer: 1× Tris-glycine, 0.1% SDS.
21. SDS-PAGE protein size ruler/marker.
22. Power generator.
23. PVDF membrane, gel sized.
24. 80% Ethanol.
25. Blotting paper, gel sized.
26. SDS-PAGE electro-transfer system.
27. Transfer buffer: 1× Tris-glycine, 20% ethanol.
28. Magnetic stir bar.
29. Magnetic stirrer at 4 °C.
30. Crystal box large enough to fit PVDF membrane.
31. 1× PBS (*see* Subheading 2.2).
32. PBS/Tween: 1× PBS, 0.1% Tween.
33. Benchtop oscillator.
34. PBS/Tween/milk: 1× PBS, 0.1% Tween, 5% powdered milk.
35. Anti-GFP antibody (as in ref. 8, or commercially available antibodies).
36. Appropriate secondary antibody coupled to horseradish peroxidase.
37. Transparent plastic envelope/pouch.
38. ECL chemiluminescence substrate.
39. Equipment to detect chemiluminescence (film or digital appliance).
40. Coomassie Brilliant Blue R-250.
41. Glacial acetic acid.
42. Coomassie staining buffer: 40% Ethanol, 10% glacial acetic acid, 0.1% Coomassie Brilliant Blue R-250.
43. Destaining buffer: 40% Ethanol, 10% glacial acetic acid.

2.6 Subcellular Localization of dsRNA-associated Protein Candidates

1. *N. benthamiana* plants expressing the 35S:B2:GFP cassette [7]: These plants are available upon request. Plants should be 3–4 weeks old and not watered for 1–2 days prior to infiltration.

2. *A. tumefaciens* carrying a plasmid driving abundant and ubiquitous expression of a protein of interest, genetically fused to a red fluorescent protein (e.g., tagRFP or mCherry).
3. Inoculum of the virus of interest, here in the form of *A. tumefaciens* carrying a virus-encoding plasmid for agroinfection.
4. 50 mL Falcon tubes.
5. Centrifuge able to spin 50 mL Falcon tubes at $3000 \times g$.
6. 200 mM Acetosyringone.
7. MMA buffer: 10 mM MES pH 5.6, 10 mM MgCl₂, 200 μM acetosyringone.
8. Spectrophotometer to measure optical density at 600 nm (OD₆₀₀).
9. Syringes without needle.
10. Microscopy glass slides.
11. Coverslips.
12. Vacuum pump.
13. Confocal laser fluorescence microscope.

3 Methods

3.1 dsRNA Pull-Down

All steps should be performed at 4 °C or on ice, and as rapidly as possible while pipetting and handling gently.

1. Harvest 0.5 g or more of systemically infected leaves from GFP- and B2:GFP-expressing plants and place them into collection tubes in liquid nitrogen. Break the leaves into a coarse powder and store at -80 °C.
2. Place 0.1 g of tissue powder into a mortar pre-chilled with liquid nitrogen (keep an aliquot of tissue powder aside for use as total tissue sample during later analysis; *see* Subheading 3.2) (*see* **Note 1**). Grind the tissue to a fine powder with a pestle, add 0.5 mL cold lysis buffer, homogenize with pestle, and add again 0.5 mL cold lysis buffer. Transfer the homogenate to a 1.5 mL Eppendorf and incubate for 10 min on a rotating wheel at 4 °C.
3. Centrifuge at 4 °C for 5–10 min at $12,000 \times g$ and transfer the supernatant to a new tube (*see* **Note 2**). Transfer 60 μL of the solution into fresh tube and set aside on ice. This aliquot will be used as “input” in the later analysis of the pull-down experiment.
4. Add anti-GFP magnetic beads to the main solution. The quantity of beads depends on the product used and on

manufacturer's instructions. Incubate for 30 min on a rotating wheel at 4 °C.

5. Place the tube on a magnetic stand to isolate the beads from the solution (*see Note 3*). Once the beads have been removed, take 60 µL from the remaining solution, put into fresh tube, and set aside on ice. This aliquot will be used as “flow-through” in the later analysis of the pull-down experiment.
6. Wash the beads three times in cold lysis buffer (*see Note 4*).

Once the washes have been completed, the beads are ready to be processed as described in the two sections below, depending on the analysis required (RNA: *see* Subheadings 3.2–3.4; proteins: *see* Subheading 3.5). It is advised to proceed immediately to RNA isolation or protein analysis, and store samples only after Subheadings 3.2, **step 4**, or 3.5, **steps 1** and **2**.

3.2 RNA Isolation

In parallel to the magnetic bead-bound RNA (IPed RNA), also total RNA from the aliquots of tissue samples set aside (*see* Subheading 3.1, **step 2**) should be isolated, processed, and analyzed. All steps should be carried out under a fume hood.

1. To isolate RNA from the beads, add 1 mL TRIzol to the magnetic beads (*see Note 5*). To isolate RNA from total tissue, grind 0.1 g of frozen tissue powder as described in Subheading 3.1, **step 2**, and homogenize in 1 mL TRIzol. Vortex, add 400 µL chloroform, and vortex for 15–20 s.
2. Centrifuge at 4 °C for 10 min at 16,000 × *g*, transfer supernatant into a new tube (do not discard the tubes containing the pink phenolic phase; set them aside for protein extraction and Western blot—*see* Subheading 3.5, **step 2**), add 1 volume isopropanol and 1.5 µL RNA-grade glycogen (do not add glycogen for total RNA samples), mix by inversion, and incubate overnight at –20 °C.
3. Centrifuge at 4 °C for 10 min at 16,000 × *g* and remove supernatant. Pay attention not to discard the small RNA/glycogen pellet. Add 400 µL ice-cold 80% ethanol, centrifuge for 5 min at 16,000 × *g*, remove supernatant, and allow the pellet to dry (do not dry excessively).
4. Resuspend the pellet in 10–20 µL RNase-free water (use 40–50 µL RNase-free water to resuspend total RNA samples) and store at –20 °C (*see Note 6*).

3.3 North-Western Blot

To determine if the IPed and total RNA fractions contain dsRNA, a north-western blot should be performed. This technique relies on the binding of recombinant B2 dsRNA-binding domain purified from *E. coli* to dsRNA immobilized on a nylon membrane [7]. Figure 2 shows the detection of dsRNA in the IPed fraction from

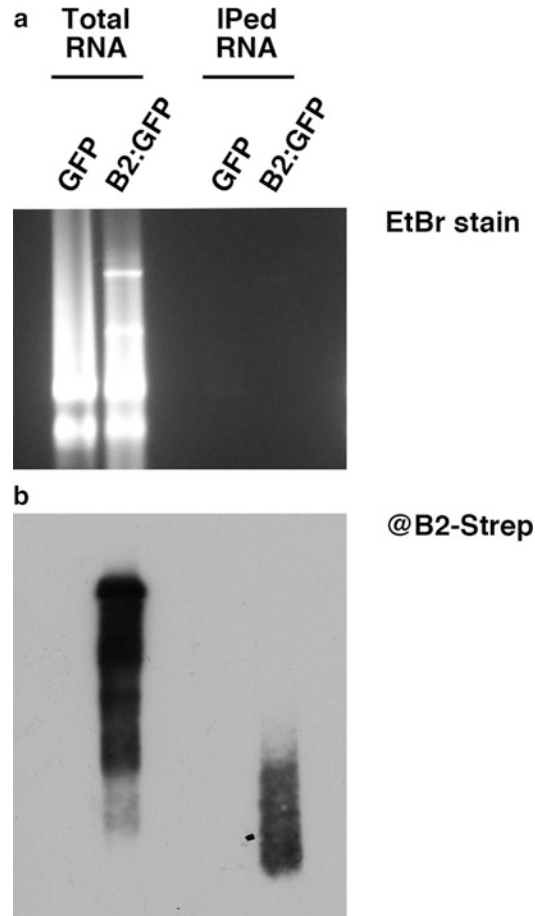


Fig. 2 North-western blot analysis for the detection of dsRNA in total RNA (two lanes on the left) and IPed (two lanes on the right) fractions. The experiment shown was performed with GFP (35S:*GFP*/Col-0)- and B2:GFP (35S:*B2:GFP*/Col-0)-transgenic *A. thaliana* infected with *tobacco rattle virus*. **(a)** Non-denaturing agarose gel showing equal loading of RNA samples and RNA quality. **(b)** North-western blotting: same samples transferred from gel in **a** onto nylon membrane and probed with recombinant B2-Strep. This north-western blot demonstrates that dsRNA was co-immunoprecipitated with B2:GFP, but not with GFP

infected B2:GFP-expressing plants, but not in the IPed fraction of GFP-expressing plants, thus showing that dsRNA was isolated along with B2:GFP in the GFP pull-down experiment.

1. Cast a non-denaturing agarose gel by boiling 1× HEPES with 1% agarose powder until agarose has totally melted. Allow the solution to cool to about 60 °C and pour it into a gel-casting apparatus (*see Note 7*).
2. Once the agarose gel has solidified (allow at least 15 min at room temperature) place it into an electrophoresis tank filled with 1× HEPES at 4 °C.

3. Prepare RNA samples by pipetting a fixed quantity of total RNA (e.g., 10 μg) and a fixed volume of IPed RNA (e.g., 10 μL) into fresh tubes, bring all samples to the same volume with RNase-free water, and add the appropriate amount of 4 \times RNA-loading buffer. Vortex and centrifuge briefly, and then keep on ice until loading.
4. Load the samples into the wells of the agarose gel and allow migration at 50–60 V at 4 $^{\circ}\text{C}$ (*see Note 8*).
5. Photograph the gel under UV light to visualize the quality and quantity of the RNA samples separated in the gel (Fig. 2a).
6. Assemble a capillary transfer apparatus to transfer the RNA from the gel to a nylon membrane in 20 \times SSC. To do so, fill the tank with 20 \times SSC and create a flat surface emerging from the buffer with plastic/glass plates. Place a strip of blotting paper (wider than the gel) on the emerging surface, with both ends immersed in the tank, and wet it with 20 \times SSC. Remove bubbles and cover the apparatus with a plastic layer of any kind (except for a gel-sized area on the blotting paper) to prevent buffer bypassing the gel. Place the gel on the blotting paper, the membrane on the gel, and two layers of blotting paper imbibed with 20 \times SSC onto the membrane. Carefully remove bubbles, and then place stacks of paper towels onto the top of the blotting paper, making sure that they are flat and evenly distributed. Place a flat object (e.g., a tray) onto the stacks of blotting paper and a 1 kg weight finally on top. Allow RNA transfer overnight, after which the stack of paper towels on top of the transfer assembly should have become wet and soaked with 20 \times SSC.
7. Disassemble the transfer apparatus, place the membrane on 2 \times SSC-imbibed blotting paper to prevent dehydration of the membrane, and cross-link the RNA to the membrane by UV irradiation in a Stratalinker (apply at least 120 mJ).
8. Rinse the membrane for 5 min in PBS/Tween in a crystal box, discard liquid, add PBS/Tween/milk to completely immerse the membrane, and incubate for 30 min with gentle oscillation at room temperature.
9. Add 0.13 μg purified B2:StrepTagII for each mL of PBS/Tween/milk, mix, and incubate for at least 1 h with gentle oscillation at room temperature.
10. Discard the liquid, add fresh PBS/Tween, and incubate for 10 min with oscillation. Repeat this step twice more.
11. Add PBS/Tween/milk containing a 1:5000 dilution of Strep-Tactin conjugated to horseradish peroxidase. Incubate for 1 h with gentle oscillation at room temperature.
12. Perform three washes as in **step 10**.

13. Remove the membrane from the box, briefly allow solution to drip off, and place it into a transparent plastic envelope (*see Note 9*).
14. Add ECL substrate to the membrane and reveal chemiluminescence with film or appropriate equipment (Fig. 2b).

3.4 Northern Blot

The same samples analyzed by north-western blot should be analyzed by conventional northern blot to detect viral RNA. In the cases where north-western blot analysis is successful (i.e., dsRNA is detected in the B2:GFP IPed samples), northern blot can provide confirmation that the IPed RNA is of viral origin (Fig. 3). In cases where north-western blot analysis fails or cannot be performed, detection of viral RNA in the B2:GFP IPed samples by northern blot still validates the pull-down experiment. Since formaldehyde is toxic, Subheading 3.4, steps 1 through 6, must be carried out under a fume hood. Subheading 3.4, steps 8 to 13 must be carried out in a room equipped for use of radioactive isotopes, using appropriate protection.

1. Cast a denaturing agarose gel by boiling 1× HEPES with 1% agarose powder until agarose has melted. Allow the solution to cool to about 60 °C, add formaldehyde to a final concentration of 6%, mix well, and pour the solution into a gel-casting apparatus.
2. Once gel has formed (allow at least 15 min at room temperature), place it into an electrophoresis tank filled with 1× HEPES.
3. Prepare RNA samples by pipetting a fixed quantity of total RNA (e.g., 10 µg) and a fixed volume of IPed RNA (e.g., 10 µL) into fresh tubes, bring all samples to the same volume with RNase-free water, and add 3 volumes of RNA denaturing loading buffer. Vortex and centrifuge briefly, incubate for 10 min at 65 °C, place on ice for 2 min, spin down the liquid, and keep on ice.
4. Load the samples into the wells of the agarose gel and allow migration at 50–60 V (*see Note 10*).
5. Photograph the gel under UV light to visualize quality and quantity of the RNA samples separated in the gel (Fig. 3a).
6. Assemble the capillary transfer apparatus as in Subheading 3.3, step 6, and then cross-link as in Subheading 3.3, step 7.
7. Rinse the membrane in water and place it in a hybridization tube with 10–15 mL hybridization buffer. Place in the hybridization oven with tube rotation and incubate at 42 °C for at least 30 min.
8. Create a DNA oligonucleotide probe. To do so, add 3–5 µL of a 10 µM stock of the oligonucleotide (able to detect viral RNA

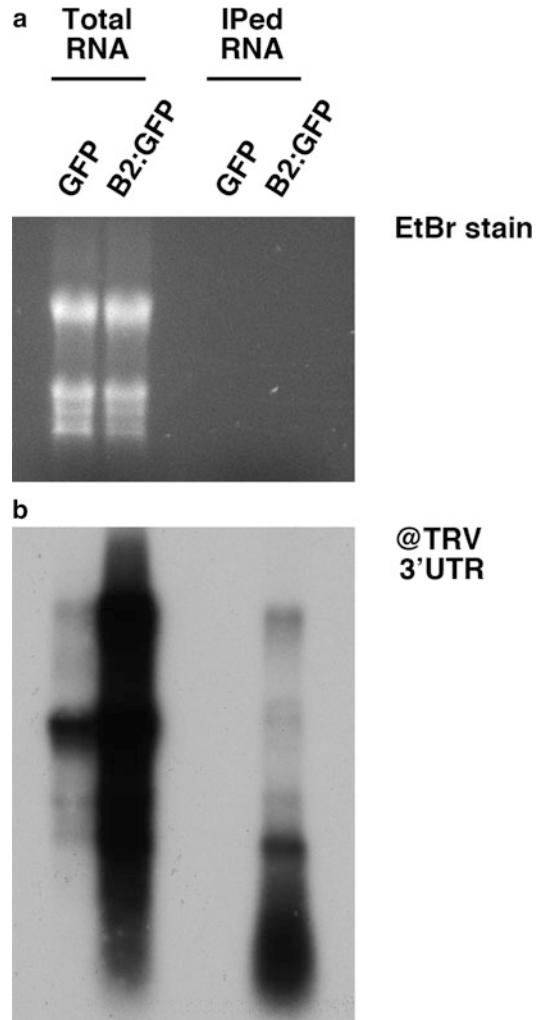


Fig. 3 Northern blot analysis to detect *tobacco rattle virus* (TRV) RNA in total RNA (two lanes on the left) and IPed (two lanes on the right) fractions. The experiment shown was performed with GFP (35S:*GFP/Col-0*)- and B2:GFP (35S:*B2:GFP/Col-0*)-transgenic *A. thaliana* infected with TRV. (a) Denaturing agarose gel showing equal RNA loading and quality before RNA transfer to membrane. (b) Autoradiographic film exposed to the membrane after hybridization with a radioactive ^{32}P isotope-labeled DNA oligomer complementary to sequences in the 3' end that are common to the two genomic RNAs of TRV. This northern blot demonstrates that TRV RNA was co-immunoprecipitated with B2:GFP, but not with GFP

by hybridization) to a PNK labeling reaction prepared according to the manufacturer's instructions. Using filter tips, add the ^{32}P -labeled γATP , mix by pipetting, and incubate the mix at 37 °C for 1 h. Prepare a sepharose column and remove liquid according to the manufacturer's instructions. Place the column

into a 1.5 mL tube, pipette the labeling mix into the column, and centrifuge as above. Following this step, the labeled probe is in the bottom of the tube while the column contains the unincorporated radioactive nucleotides. Discard the column and denature the probe by placing it at 95 °C for 2 min and then on ice.

9. Add the probe to the hybridization buffer in the hybridization tube containing the membrane. Return the tube to the hybridization oven and incubate under rotation at 42 °C for at least 4 h.
10. Open the tube and discard the hybridization buffer containing the labeled probe (*see Note 11*).
11. Add 20 mL wash buffer and incubate the membrane for 10–15 min in the hybridization oven at 50 °C with rotation.
12. Discard the wash buffer.
13. Repeat **steps 11** and **12** two more times.
14. Use a pair of tweezers to remove the membrane from the hybridization buffer and place it to dry on a paper towel. Once dry, place the membrane in a plastic envelope, and then place the envelope into a radioactivity-detection instrument of choice (cassette and autoradiographic film, or phosphor-imager screen and detector) (Fig. 3b).

3.5 Western Blot

The presence of proteins in the pull-down fraction should be verified before these are analyzed by mass spectrometry. Since B2:GFP is the bait protein through which dsRNA was pulled down, at least the presence of B2:GFP should be confirmed. Furthermore, the amount of B2:GFP should be confirmed as being (i) consistent between technical replicates and (ii) comparable to the amount of GFP pulled down in control samples. This quality control can be easily carried out by performing Western blot analysis of the bait GFP/B2:GFP proteins in the input and IPed (bead-bound) fractions using anti-GFP antibodies (Fig. 4) (*see Note 12*).

1. For samples to use for mass spectrometry, from pull-downs performed in triplicate, resuspend the magnetic beads in a solution consisting of three parts protein resuspension buffer and one part protein-loading buffer, preheated to 95 °C (*see Note 5*, but using the buffer instead of TRIzol). In parallel, add a ¼ volume of protein-loading buffer to the input and flow-through fractions collected during the pull-down experiment and vortex. Denature all samples by heating them for 2–3 min to 95 °C and then placing them for 5 min on ice. Samples can now be stored at –20 °C.
2. To provide a complete analysis of the pull-down experiment used for northern and north-western blot (*see Subheadings 3.3*

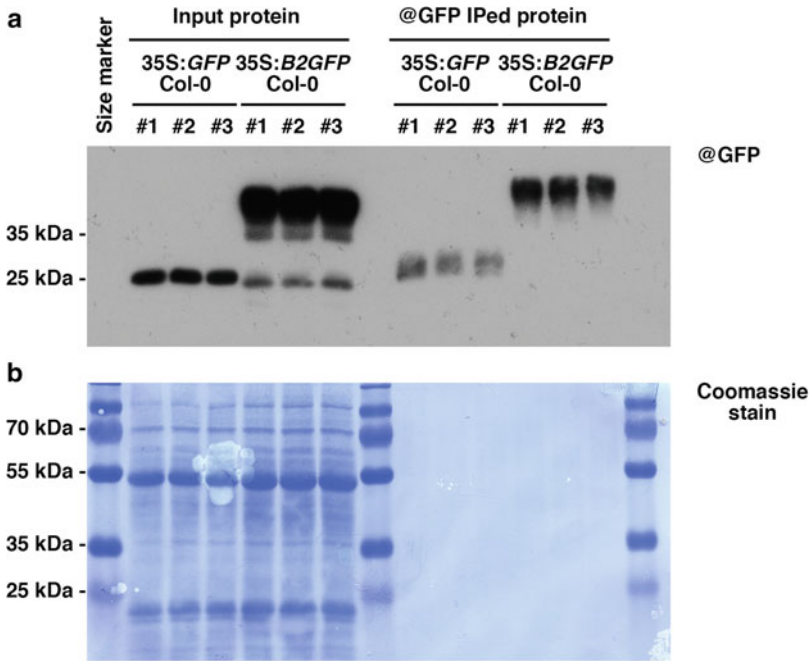


Fig. 4 Western blot analysis to detect GFP in the input (left) and in the GFP-immunoprecipitated (IPed) fraction (right). This experiment was performed with GFP (35S:GFP/Col-0)- and B2:GFP (35S:B2:GFP/Col-0)-transgenic *A. thaliana* plants that were not infected with virus. While these samples cannot obviously be used to characterize virus replication complexes, this western blot is shown as an example of a successful and homogenous pull-down experiment. For each sample, three technical replicates (#1, #2, #3) of the pull-down experiment were performed. **(a)** Western blot with GFP antibody. The similar intensity of the bands among technical replicates in the input attests to reproducible sample preparation, while the different intensities of the GFP vs. B2:GFP bands are likely due to differential accumulation of these proteins within the plant tissue. The clear and homogenous bands seen in the analysis of the IPed fractions demonstrate the efficient pull-down of the GFP and B2:GFP bait proteins, with little variation between replicates. **(b)** Coomassie staining of the membrane shown in **a** showing equal loading of protein extracts

and 3.4), proteins co-purified with dsRNA should be purified and analyzed by Western blot. Start with the phenolic phase obtained after TRIzol/chloroform extraction of the beads (*see* Subheading 3.2, step 2). Place 300 μ L of this phenolic phase into a new 1.5 mL tube. Add 4–5 volumes of ice-cold acetone, mix by inversion, and incubate overnight at -20°C . Centrifuge at 4°C for 30 min at $16,000 \times g$ and remove the supernatant, paying attention not to discard the small red pellet. Add 400 μ L ice-cold 80% acetone, centrifuge for 5 min at $16,000 \times g$, remove supernatant, and allow the pellet to dry. Resuspend the pellet in 30 μ L protein resuspension buffer, add 10 μ L protein-loading buffer, vortex, and denature as described in Subheading 3.5, step 1. The sample may be stored at -20°C .

3. Cast a 12% SDS-PAGE gel under a fume hood. To do so, prepare the resolving gel mix (10 mL of 30% acrylamide/bis-acrylamide 37.5/1, 8.3 mL of resolving buffer, and 6.7 mL of water—enough for 3 gels if using the standard 7×10 cm BioRad plates with spacers for 1.5 mm thickness). Mix well, then add 250 μ L of 10% APS, mix well again, add 25 μ L TEMED, and briefly mix once more. Quickly pour/pipette the liquid between the glass plates in the gel-casting system up to $2/3$ or $3/4$ of the height. Rapidly overlay the solution with 500 μ L ethanol to flatten its surface and seal it from air. Let the solution polymerize for 15 min, then pour out the ethanol, and carefully dry the top of the gel with blotting paper. Prepare the stacking gel mix (2 mL of 30% acrylamide/bis-acrylamide 37.5/1, 3 mL of stacking buffer, and 10 mL of water). Mix well, add 150 μ L of 10% APS, mix well again, add 15 μ L TEMED, and briefly mix once more. Quickly pour/pipette the liquid between the glass plates on the resolving gel until it is filled up to the top and insert the comb. Allow gel polymerization for 10–15 min at room temperature.
4. Place the glass plates containing the gel into the running tank filled with migration buffer and carefully remove the comb. Load the samples (10 μ L each) and the protein size marker (5 μ L) into the different wells of the gel, and then perform the electrophoresis at 80 V until the proteins reach the resolving part of the gel. Increase the voltage to 120–150 V and continue electrophoresis until the 25–30 kDa protein of the size marker has migrated into the lower third of the gel. Open the gel container to remove the gel.
5. Immerse the PVDF membrane, previously cut to the size of the gel, in 80% ethanol for 5 min. Imbibe two gel-sized pieces of blotting paper in transfer buffer. Assemble the transfer “sandwich” provided with the electro-transfer system: open the holder and place sponge, blotting paper, gel, and membrane in this order. Carefully remove all bubbles and then place the other blotting paper and sponge on top. Close the sandwich holder and place it into the transfer tank (with the gel oriented toward the cathode and the membrane oriented toward the anode) along with the provided ice container. Connect to the power supply and allow proteins to migrate from the gel onto the membrane at 4 °C for 90 min at 80 V. Stir the buffer by placing a stir bar into the tank and the tank onto a magnetic stirrer in order to homogenize the buffer composition and temperature during transfer.
6. Remove the membrane from transfer apparatus, place it into a crystal box containing PBS/Tween, and allow gentle oscillation for 5 min.

7. Discard the liquid, add PBS/Tween/milk (enough to immerse the membrane), and incubate for 30 min at room temperature with gentle oscillation. Add anti-GFP antibody and incubate (*see Note 13*).
8. Discard the antibody solution and wash the membrane 3–4 times for 5 min in PBS/Tween.
9. Add PBS/Tween/milk containing the appropriate secondary antibody conjugate (*see Note 14*) and incubate for 1 h with gentle oscillation at room temperature.
10. Discard the antibody solution and wash the membrane 3–4 times for 5 min in PBS/Tween.
11. Remove the membrane from the box, briefly allow the solution to drip off, and place it into a transparent plastic pouch (*see Note 9*).
12. Add ECL substrate to the membrane and expose the chemiluminescent signal to film or appropriate imaging equipment (Fig. 4a).
13. After imaging, the membrane should be incubated overnight with Coomassie staining buffer with gentle oscillation, then washed twice with destaining buffer (1 min per wash), rinsed well with water, and allowed to dry. The blue staining allows to assess the total protein content in each lane (Fig. 4b).

If the result of the western blot confirms the reproducibility of the IPed protein samples (as in Fig. 4), these can be sent for mass spectrometry and subsequent statistical analysis. Please refer to ref. 8 for an example of methods used. However, we highly recommend to outsource this phase of the experiment to specialists.

3.6 Subcellular Localization of dsRNA-Associated Protein Candidates

Following the identification of *A. thaliana* proteins isolated together with dsRNA by mass spectroscopy, it is important to verify their localization relative to virus replication complexes *in vivo*. To achieve this, the proteins of interest are genetically fused with a red fluorescent protein and transiently expressed in *N. benthamiana* plants stably and ubiquitously expressing B2:GFP [7], the same protein used in *A. thaliana* to pull down dsRNA (*see* Subheading 3.1). In the absence of viral infection, B2:GFP shows a diffuse nucleocytoplasmic subcellular localization. However, upon infection with a variety of RNA viruses the localization of B2:GFP changes dramatically, concentrating in bright and clearly visible cytoplasmic foci [7, 8], which correspond to the dsRNA-containing virus replication complexes. Transient expression of the RFP-tagged dsRNA-binding protein candidates in these plants and analysis by laser confocal microscopy allows to determine their localization relative to the B2:GFP-labeled viral replication complexes (Fig. 5).

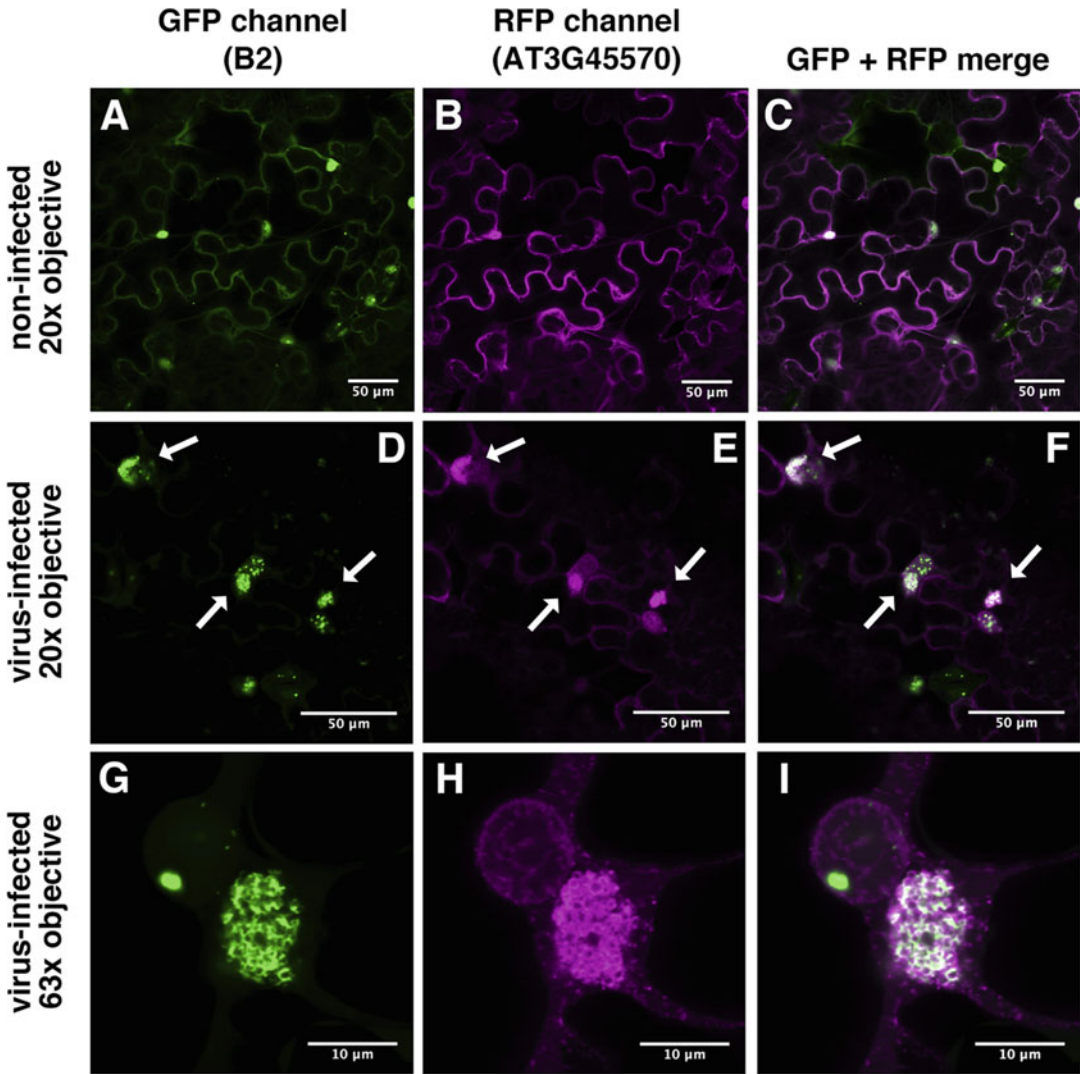


Fig. 5 Laser confocal microscopy of leaf disks from B2:GFP (35S:B2:GFP)-transgenic *N. benthamiana* transiently expressing an RFP-tagged *A. thaliana* dsRNA-binding protein candidate identified in the pull-down experiment followed by mass spectrometry (gene accession number AT3G45570—see ref. 8). Image acquisitions of the same leaf area with GFP-exciting laser (wavelength: 488 nm—represented in green) (a, d, g) and RFP-exciting laser (wavelength: 561 nm—represented in magenta) (b, e, h) as well as merged images of the two channels (c, f, i) are shown. Noninfected plants show nucleocytoplasmic localization for B2:GFP [7, 8] (a) and a mostly cytoplasmic localization for AT3G45570 (b), whereas TRV-infected plants show B2:GFP (d) and AT3G45570 (e) colocalized to dsRNA-containing TRV replication complexes (indicated by white arrows). The white areas of green/magenta overlap (f, i) show the colocalization of the two proteins at and within these sites. Observation at higher magnification allows to gain a more detailed picture of the localization patterns of the candidate protein relative to the replication complexes (g, h, i)

Before proceeding with this experiment, the genomic DNA or cDNA encoding the proteins of interest should be cloned in translational fusion with a red fluorescent protein of choice, under the

control of a promoter driving abundant and ubiquitous expression. Golden Gate or GreenGate systems provide rapid and seamless cloning into binary vectors suitable for *Agrobacterium*-mediated transformation [8, 9]. The binary plasmids should be verified by DNA sequencing before transformation into *A. tumefaciens*, which can then be used for transient expression in noninfected and virus-infected 35S:B2:GFP/*N. benthamiana* leaves. The virus itself can be delivered either by *A. tumefaciens*-mediated transient expression of an infectious clone or by rub inoculation with a crude extract of infected plant tissue or purified virus. The former method will be described here, since it is the one used in ref. 8. Also, since the virus clones are delivered via *A. tumefaciens* in the same solution containing the *A. tumefaciens* for transient protein expression, it can be expected that all the cells expressing the dsRNA-binding protein candidate will also be infected.

1. Grow a culture of *A. tumefaciens* containing the binary plasmid of interest in 10 mL LB medium with appropriate antibiotic selection on a shaker in the dark for 24 h at 28 °C in 50 mL Falcon tubes. In parallel, grow the *A. tumefaciens* containing a plasmid encoding the virus of interest.
2. Pellet the bacteria by centrifugation for 10 min at $3000 \times g$, discard the liquid, and resuspend in MMA buffer. Measure the absorbance (A) of the suspension at 600 nm (OD_{600}) with a spectrophotometer. Prepare two separate bacterial solutions in MMA buffer, one containing only the *A. tumefaciens* for expression of the protein of interest at final A of 0.2 (noninfected sample) and the other containing both *A. tumefaciens* for expression of the protein of interest at final A of 0.2 and *A. tumefaciens* containing the virus infection plasmid at final A of 0.01 or less (virus-infected sample). Incubate in the dark for 1 h.
3. Use a syringe without needle to infiltrate the *A. tumefaciens* solution into the abaxial side of young expanded leaves. To aid in infiltration, punch a small hole into the abaxial side of the leaf with a pipette tip. Place the tip of the syringe on the hole and a finger on the other side of the leaf and gently press the finger against the syringe tip so it is well in contact with the hole. Gently infiltrate the bacterial solution into the leaf through the hole. After completing the infiltration, water the plants and return them to the growth chamber/greenhouse (see **Note 15**).
4. 4 days after *A. tumefaciens* infiltration (see **Note 16**), collect leaf disks from the infiltrated areas, place them with their lower adaxial side oriented upwards onto a microscope slide, cover them with a coverslip, add water, and vacuum-infiltrate to replace the air in the intercellular spaces with the water.

5. The leaf disks can now be observed by laser confocal microscopy to detect B2:GFP (GFP channel) and RFP-tagged protein of interest (RFP channel), in noninfected tissues and virus-infected tissues. The high protein expression levels provided by the strong gene promoters should allow easy observation (*see Note 17*). An example of such an experiment is shown in Fig. 5.

4 Notes

1. If mass spectrometry analysis is planned, it is highly advisable to perform at least three technical replicates for each sample/condition.
2. This step can optionally be repeated for further clearing of the lysate.
3. This can be done by placing the tube on a magnetic stand and letting the bead cluster on a side (non-colloidal beads) or by letting the solution flow through a magnetic column (colloidal beads), depending on the kit used.
4. The washing method depends on the kind of beads used. If using non-colloidal beads, resuspend the beads in 500 μL cold lysis buffer by gentle inversion and incubate them on the rotating wheel for 5 min, after which the tubes are again placed on the magnetic stand to remove the beads and the buffer is removed. If using colloidal beads (such as those in the Miltenyi μMACS kit used here), let 500 μL lysis buffer flow through the column by gravity. In all cases, the buffer should be removed from the beads after the last wash.
5. If using non-colloidal beads, add Trizol to the tube containing the beads. If using colloidal beads, remove the column from the stand and pass the Trizol through the magnetic column into a 1.5 mL tube, gently pushing with a Pasteur pipette if necessary.
6. If colloidal beads are used for pull-down, some may be carried over into the final purified RNA suspension. In our experience, these beads did not interfere with the further analysis.
7. All material used for electrophoresis and transfer should be clean or treated with soap, rinsed, and cleaned with 70% EtOH.
8. Electrophoresis should continue until the blue dye migrated to the middle of the gel. Optionally, a dsRNA ladder such as the Phi6 dsRNA ladder [7] can be used to monitor dsRNA sizes and their separation during electrophoresis.
9. The membrane must not dry.

10. Electrophoresis should continue until the blue dye migrated to the middle of the gel.
11. The hybridization buffer containing the labeled probe can be appropriately stored and used again, taking into account the radioactive decay.
12. Optionally, western blot analysis can include the “flow-through” samples collected during the pull-down experiment. Western blot analysis of “input” and “flow-through” samples on the same gel/membrane allows to assess the pull-down efficiency by comparing the amount of B2:GFP present in the lysate before and after the IP. For an example of such an analysis *see* ref. 8.
13. Antibody dilution and time of incubation depend on the antibody used. For the study in ref. 8, a rabbit polyclonal antibody raised against GFP was used. The antibody was applied in 1:30,000 to 1:60,000 dilution and used for incubation overnight. If using commercially available monoclonal antibodies, follow the instructions of the manufacturer.
14. Incubation with a secondary antibody is not necessary if the primary GFP antibody is coupled to horseradish peroxidase.
15. If clones for agroinfection are not available, infection should be carried out by rub inoculation with a crude extract of infected tissue or with purified virus. This should be performed 24 h after agro-infiltration of the plasmid encoding the protein candidate of interest. Prepare the viral inoculum appropriately according to the virus, sprinkle celite/carborundum on the adaxial side of the agroinfiltrated leaves, and gently rub the viral inoculum with a gloved finger. After 10–15 min, rinse the leaves with water and return the plants to the growth chamber/greenhouse. Remember also to use some of the plants as noninfected/mock-treated controls.
16. In case the virus was delivered by rub inoculation, it is advisable to perform the observation at 3 days after virus infection. This time is needed for infection foci to form.
17. Virus infection may interfere with the expression of the dsRNA-binding protein candidate. This was observed for many candidates that were tested in ref. 8. While we do not know the reason for this phenomenon, a possible explanation is that infected tissues undergo a process similar to the previously described host gene shutoff [10]. In our hands, this phenomenon worsened with the time after virus infection. Therefore, it is advisable to evaluate the leaf disks as soon as possible after the appearance of the first infection foci.

References

1. Laliberté J-F, Zheng H (2014) Viral manipulation of plant host membranes. *Annu Rev Virol* 1:237–259. <https://doi.org/10.1146/annurev-virology-031413-085532>
2. Wang A (2015) Dissecting the molecular network of virus-plant interactions: the complex roles of host factors. *Annu Rev Phytopathol* 53:45–66. <https://doi.org/10.1146/annurev-phyto-080614-120001>
3. Nagy PD (2016) Tombusvirus-host interactions: co-opted evolutionarily conserved host factors take center court. *Annu Rev Virol* 3:491–515. <https://doi.org/10.1146/annurev-virology-110615-042312>
4. Dufresne PJ, Thivierge K, Cotton S, Beauchemin C, Ide C, Ubalijoro E, Laliberté J-F, Fortin MG (2008) Heat shock 70 protein interaction with Turnip mosaic virus RNA-dependent RNA polymerase within virus-induced membrane vesicles. *Virology* 374:217–227. <https://doi.org/10.1016/j.virol.2007.12.014>
5. Lohmus A, Varjosalo M, Makinen K (2016) Protein composition of 6K2-induced membrane structures formed during Potato virus A infection. *Mol Plant Pathol* 17:943–958. <https://doi.org/10.1111/mpp.12341>
6. Wang X, Cao X, Liu M, Zhang R, Zhang X, Gao Z, Zhao X, Xu K, Li D, Zhang Y (2018) Hsc70-2 is required for Beet black scorch virus infection through interaction with replication and capsid proteins. *Sci Rep* 8:4526. <https://doi.org/10.1038/s41598-018-22778-9>
7. Monsion B, Incarbone M, Hleibieh K, Poignavent V, Ghannam A, Dunoyer P, Daeflter L, Tilsner J, Ritzenthaler C (2018) Efficient detection of long dsRNA in vitro and in vivo using the dsRNA binding domain from FHV B2 protein. *Front Plant Sci* 9:70. <https://doi.org/10.3389/fpls.2018.00070>
8. Incarbone M, Monsion B, Kuhn L, Scheer H, Poignavent V, Dunoyer P, Ritzenthaler C (2019) Immunocapture of dsRNA-bound proteins provides insight into Tobacco rattle virus replication complexes. *bioRxiv*. <https://doi.org/10.1101/842666>
9. Lampropoulos A, Sutikovic Z, Wenzl C, Maegele I, Lohmann JU, Forner J (2013) GreenGate - A novel, versatile, and efficient cloning system for plant transgenesis. *PLoS One* 8:e83043. <https://doi.org/10.1371/journal.pone.0083043>
10. Wang D, Maule AJ (1995) Inhibition of host gene expression associated with plant virus replication. *Science* 267:229–231. <https://doi.org/10.1126/science.267.5195.229>

Part V

RNAs as Guides for Genome Editing and Imaging of Chromosome Loci



CRISPR Guide RNA Design Guidelines for Efficient Genome Editing

Patrick Schindele, Felix Wolter, and Holger Puchta

Abstract

The simple applicability and facile target programming of the CRISPR/Cas9-system abolish the major boundaries of previous genome editing tools, making it the tool of choice for generating site-specific genome alterations. Its versatility and efficacy have been demonstrated in various organisms; however, accurately predicting guide RNA efficiencies remains an organism-independent challenge. Thus, designing optimal guide RNAs is essential to maximize the experimental outcome. Here, we summarize the current knowledge for guide RNA design and highlight discrepancies between different experimental systems.

Key words Genome editing, CRISPR, Cas9, gRNA design, gRNA secondary structure, Mismatch tolerance, CRISPR prediction tool

1 Introduction

1.1 Genome Editing with CRISPR/Cas9

Targeted manipulation of DNA through site-specific double-strand breaks (DSBs) embodies the cornerstone of modern biotechnology. The challenge to target sites of interest continuously decreased over time with the discovery and development of novel tools, such as engineered nucleases [1]. The CRISPR/Cas9 system with its two-component setup accompanied by the simple target programming constitutes the current gold standard within the available toolbox. In this system, a complex of the Cas9 nuclease and a guide RNA (gRNA) mediates DSB induction at a selected target site. The gRNA is of major relevance, mediating target DNA recognition and binding on the one hand and activation of target DNA cleavage by Cas9 on the other hand [2]. The variable region of the gRNA (guide) determines the site of target DNA binding and can be adjusted to the sequence of interest. Employing this system, applications such as single and multiplex editing, epigenetic and transcriptional regulation, visualization of genomic loci, and base editing are feasible within a large number of organisms (for details *see* reviews [3–6]). The target selection solely requires an

abundant protospacer adjacent motif (PAM), apparently providing a wide variety of potential target sites, and gRNAs. However, indiscriminately selecting gRNAs can minimize and even prevent experimental success. Thus, optimization of gRNA design is required for improving target specificity and maximizing editing efficiency. Pre-experimental procedures therefore often involve the screening of different guides to determine the optimal target site. While animal cell lines allow high-throughput screenings, evaluating gRNA-editing efficiency in other organisms can be an elaborate process demanding longer periods for the generation of transgenic individuals. Especially for many crops like maize and wheat, generation of transgenic plants is very time and cost intensive, and being able to estimate gRNA efficiency before engaging in the laborious process of transgenic plant production would be most desirable. For this very reason, guidelines helping to define efficient gRNAs are of tremendous importance to ensure an optimal experimental progress. Both target site and gRNA features determine the on-target and off-target activity of the CRISPR nuclease. Length and sequence composition or structural features of the guide and target, respectively, have been reported as main contributors to overall efficiency.

1.2 Guide Length Variation for Reduced Off-Target Activity

The various Cas9 orthologs put different demands on PAM composition and guide length, yet, for each individual ortholog, an optimal PAM and guide length required for maximum on-target activity were identified [7]. Based on this observation, the most commonly used *Streptococcus pyogenes* Cas9 (SpCas9) is employed combining a 20-nt guide and the 5'-NGG-3' PAM. However, due to the abundance of the PAM and a certain tolerance toward mismatches, off-target activity was frequently detected in human and animal cell lines [8, 9]. More recent studies on human 293T cells and *Drosophila* reported strongly reduced off-target activity by employing truncated guides of 17 to 18 nt in length while maintaining the editing efficiency of full-length guides [10–12]. The strong decrease in off-target activity can presumably be explained by a much stronger disruptive impact of mismatches on truncated guides. Unfortunately, contradictory results have been reported in stem cells and plants where truncated guides were less efficient than full-length guides [13, 14]. Apart from that, full-length guides are highly precise in plants and off-target effects only detectable for highly similar targets or targets with PAM distal mismatches [15–19].

1.3 Effects of Nucleotide Composition and Identity on Guide Efficiency

Concerning the effect of the nucleotide composition of the guide and target, rather inconsistent results have been published. It is agreed that guides having a very low or very high GC content are less effective [20–22]. However, analysis about the optimal GC content strongly vary between different organisms. In animal cell lines, a preferable GC content of 40–60% was reported [23]. In

plants, analysis of a significant amount of validated gRNAs revealed a spacious GC content ranging from 30% to 80% [22]. Though rather marginal, guides with a GC content of more than 50% showed slightly higher efficiencies than guides with a GC content under 50% [24]. The same was reported for *Drosophila*, where a GC content over 50% within the 6 nt proximal to the PAM was reported as beneficial, an effect that was also detected concerning germline transmission rates of heritable mutations [12]. A similar inconsistency is prevalent regarding nucleotide preferences. In animal and human cell lines, efficient gRNAs strongly prefer purines at the very 3'-end of the guide [21]. Whereas guanine is favored at positions 1 and 2 proximal to the PAM, thymine and cytosine are restrictive for efficient editing [20, 25]. Cytosine is also disfavored at position 18 distal to the PAM, however, strongly preferred at positions 3 and 5 proximal to the PAM and as variable nucleotide of the PAM (5'-CGG-3' PAM), respectively. Adenine preference was detected in the midsection of the guide [20, 25]. In contrast, for plants no significant nucleotide preferences could be validated [22]. Merely an increased occurrence for guanine at the very 5'-end of the guides was detected, although this quite likely can be attributed to the common use of the U6 small nuclear RNA promoter constraining the first nucleotide to a guanine, at least if a one-nucleotide "G" overhang of the gRNA is not desired. Interestingly, irregular targets starting with H nucleobases still show comparable efficiencies in plants [24]. Analysis on target strand preference also provides contradictory results [20, 21].

1.4 Influence of Mismatch Nature and Position on Cleavage Activity

Off-target activity is largely determined by mismatch tolerance. Early studies showed that cleavage activity of Cas9 is preferentially abolished through mismatches in the PAM-proximal region [2, 26]. However, studies in human cells also revealed a strong impact of nucleotide identity on cleavage activity [9, 27]. Whereas a G:T mismatch between gRNA and target DNA in the PAM-proximal region only minimally affects cleavage, activity is barely detectable for a C:C mismatch between gRNA and target DNA [9]. The data from this study also indicate toward a significant relevance of nucleotides 5–7 proximal to the PAM with high levels of cleavage disruption independent of nucleotide identity. Consistent with this indication, a recent publication defined a new core region comprising nucleotides 4–7 proximal of the PAM with even single mismatches abolishing the majority of cleavage activity [27]. Crucial but rather neglected features concerning on-target and off-target activity are RNA and DNA bulges. These structures are formed when unpaired nucleotides reside in the otherwise consistent guide or target, respectively. In human cells, Cas9 can tolerate DNA bulges of 1 nt all along the target sequence, though exact positions are inconsistent between different gRNAs [11]. RNA bulges of 1 nt can also be tolerated; however, abolish

Cas9 cleavage when located in the PAM-proximal region. In contrast, DNA bulges of 2 or more nt completely abolish Cas9 cleavage independent of position, whereas larger RNA bulges at least outside the PAM-proximal region can be tolerated to a certain degree [11]. Guide-internal base pairs interfere with DNA target binding, as well. In plants, at least a certain degree of tolerance toward these pairings can be detected [22].

1.5 Preservation of gRNA Secondary Structure Is Essential for Proper Function

The structural characteristics of the gRNA are essential for interaction with the Cas protein. Structural analysis in human cell lines regarding SpCas9 revealed that an intact repeat:anti-repeat duplex and stem-loop 1 of the gRNA are of major relevance for Cas9 recognition, being less tolerant toward mismatches than stem-loop 2 and 3 [28]. Interestingly, structure analysis of validated gRNAs in plants revealed a minor relevance of stem-loop 1, indicating a disparity concerning the structural requirements in different species [22]. Mismatches or substitutions maintaining the stem-loop structures of the gRNA barely affect Cas9 function, rather emphasizing the significance of the global structure of the gRNA [28, 29]. Due to the variable nature of the guide sequence, base pairing and thus interference with gRNA secondary structure can occur (Fig. 1). Consequently, evaluating the guide-dependent gRNA secondary structure is inevitable. Structure analysis of various gRNAs in plants demonstrated a certain degree of tolerance toward base pairing between guide sequence and gRNA, with 12 base pairs or 7 consecutive base pairs, respectively, being sustainable for single gRNAs [22].

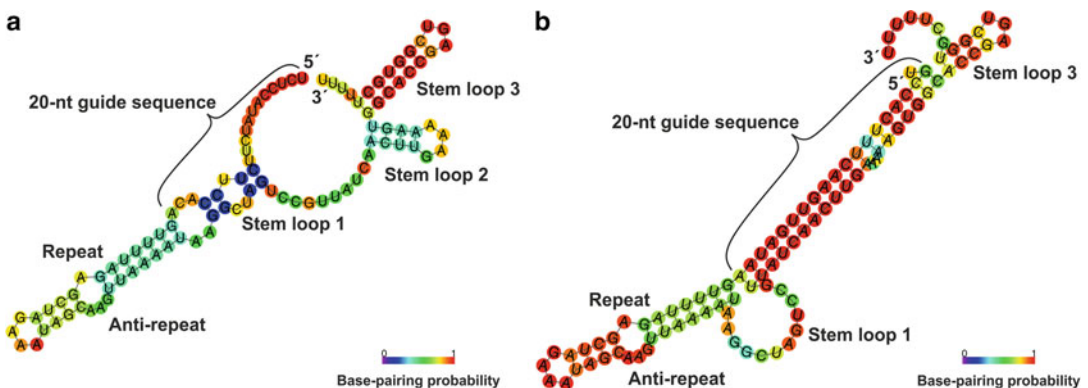


Fig. 1 Impact of guide sequence on gRNA secondary structure. (a) Illustration of a gRNA with intact secondary structure features. Guide sequence and gRNA exhibit marginal interactions only, not affecting the essential stem-loop structures of the gRNA. (b) Illustration of a gRNA with impaired secondary structure features. Guide sequence and gRNA exhibit a significant level of base pair interactions, compromising the formation of essential stem-loop structures (in this example stem-loop 2). The color scale displays the base-pairing probability. The RNA secondary structure was predicted using the RNAfold web server (<http://rna.tbi.univie.ac.at/cgi-bin/RNAWebSuite/RNAfold.cgi>)

1.6 Chromatin Accessibility Affects Genome Editing Efficiency

Epigenetic modifications influence chromatin state and thus accessibility of DNA; hence, they are a major factor affecting genome targeting ability. Restrictions due to epigenetic repression were already hypothesized for previous site-specific nucleases such as zinc-finger nucleases (ZFNs) and transcription activator-like effector nucleases (TALENs) [30, 31]. For SpCas9, *in vitro* and *in vivo* analysis demonstrated no restriction in cleavage activity when targeting methylated DNA [9, 32]. However, *in vitro* analysis revealed an impact of nucleosome occupancy on Cas9-mediated cleavage. A correlation between Cas9 binding and low nucleosome occupancy also indicates toward a contribution *in vivo* [33, 34]. Further experiments in human cells also demonstrated an impairment of genome editing at an epigenetically repressed reporter locus and data from zebrafish also suggests a negative correlation between chromatin accessibility and genome editing efficiency [35–37]. Additionally, the open chromatin state associated with transcriptionally active regions can have its own positive effect on Cas9 editing by displacing Cas9, thereby increasing the rate at which cleaved ends are exposed and accessible for DNA repair. On the other hand, this might have a negative effect for dCas9-based applications where extended binding is beneficial [32].

1.7 CRISPR Prediction Tools for Approving Target Selection

Applying *in silico* tools may assist in predicting on-target and minimizing off-target activity. However, some tools do not necessarily cover all contributing factors by the current state of knowledge. Furthermore, depending on the experimental system the data are based on, discrepancies between prediction and outcome can occur. To obtain an optimal consensus, the use of multiple prediction tools is recommended. For RNA secondary structure prediction, free-available online tools, such as Mfold [38] and RNAfold [39], are reliable to exclude potential issues from RNA structure. Computational prediction tools for the identification of optimal guide sequences are available on a large scale; however, they might differ concerning their parameters. While SSC [25] only allows for variation between different guide lengths, CRISPR-P 2.0 [40] and CCTop [41] allow the choice of a variety of CRISPR orthologs and target organisms. CRISPR RGEN Tools [42, 43] additionally offers crucial off-target prediction criteria such as RNA and DNA bulges. While these tools are highly useful to assist in target site selection, their limitations should always be kept in mind. Predictive power is often limited and efficiency prediction is based solely on the target sequence, whereas local chromatin context cannot be taken into account [44].

1.8 Nontrivial Considerations for Designing CRISPR Knockout Experiments

As extensively described above, designing efficient gRNAs is one of the major concerns when conducting CRISPR experiments. However, depending on the experimental goal, further criteria have to be taken into account. As the perhaps most frequent used CRISPR application, the following paragraph concentrates on the

prerequisites for designing knockout experiments. The majority of knockout mutants are generated through nonhomologous end joining (NHEJ)-mediated DSB repair and therefore based on the introduction of Indel mutations. Thus, selecting pertinent target sites within exons is of major concern. In particular, mutagenesis within exons aims for either mutations in essential protein domains or generation of frameshift mutations, the latter one being preferred when aiming for complete knockouts. Targeting regions too close to the C- or N-terminus of the encoded protein is not recommended, either increasing the probability of maintaining the majority of essential domains or, if the start codon is compromised, resulting solely in a minor displacement of transcription initiation. Nevertheless, mutations in the encoded N-terminal region are preferred for frameshift mutations, affecting the majority of the coding sequences and impeding a distortion through potential splice variants.

In the following, the design of a gRNA will be explained in detail comprising helpful bioinformatic design tools and guide sequence requirements based on current knowledge of gRNA design.

2 Materials

2.1 *Bioinformatic Online Tools*

1. CCTop.
2. CRISPR RGEN tools.
3. RNAfold.

2.2 *Sequence Information*

1. Query sequence.

3 Methods

3.1 *Guide Sequence Selection for CRISPR-Mediated Mutagenesis Using Bioinformatic Tools*

The first and essential step of designing the CRISPR experiment is the identification of the optimal guide sequence. Due to the variety of criteria to be considered for this purpose, the use of online tools is recommended. These tools cover the majority of the design criteria and thereby definitely help to choose the optimal guide sequence. To obtain an optimal consensus, the use of multiple prediction tools is recommended. In the following, the online tools CCTop and Cas-Designer (CRISPR RGEN tools) are employed, both comprising a solid extent of selectable options to prevent off-target activity and promote on-target activity.

3.1.1 *CCTop*

1. Go to <https://crispr.cos.uni-heidelberg.de/> to open the CCTop tool.

2. Enter your gene/sequence of interest into the query sequence field. For knockout experiments, concentrate on the exons of the gene (*see* Subheading 1.8).
3. Select the PAM type. The PAM depends on the employed CRISPR/Cas-system and respective Cas ortholog (e.g., 5'-NGG-3' for *Streptococcus pyogenes* Cas9).
4. Select the guide length of the respective CRISPR ortholog. This sequence corresponds to the nucleotides upstream of the PAM for Cas9 (*see* **Note 1**).
5. Optional: Enter 5' and 3' target site limitations. Dependent on the promoter and/or experimental system, the occurrence of specific nucleotides at these positions increases editing efficiency (*see* Subheading 1.3).
6. Optional: Specify the 5' guide sequence overhangs. Cloning of the guide is commonly realized via oligonucleotide annealing and sticky-end ligation (*see* **Note 2**).
7. For off-target prediction, select the number of total mismatches between guide and target site to be considered. Recommendation: Select four (*see* Subheading 1.4) (*see* **Note 3**).
8. Optional: Define the core length of the respective CRISPR ortholog and the number of total core mismatches between guide and target site to be considered. Recommendation: seven for core length and two for core mismatches (*see* Subheading 1.4) (*see* **Note 3**).
9. Select the target genome and submit the request.
10. Choose the guide(s) with the best efficacy score/off-target ratio (*see* **Note 4**). Compare the results with Cas-Designer to identify the optimal guide(s).

3.1.2 CRISPR RGEN Tools: Cas-Designer

1. Go to <http://www.rgenome.net/cas-designer/> to open the Cas-Designer tool.
2. Select the PAM type. The PAM depends on the employed CRISPR/Cas-system and respective Cas ortholog (e.g., 5'-NGG-3' for *Streptococcus pyogenes* Cas9).
3. Select the target genome.
4. Enter your target gene/sequence of interest into the query sequence field. For knockout experiments, concentrate on the exons of the gene (*see* Subheading 1.8).
5. Select the guide length (here: crRNA length) of the respective CRISPR ortholog (*see* **Note 1**).
6. Optional: Allow integration of 1 nt bulge for off-target analysis (*see* Subheading 1.4). However, this is not recommended in this step (*see* **Note 5**).
7. Submit the request.

8. Select a GC content of 25–75% and submit the filter (*see* Subheading 1.3).
9. Choose the guide(s) with a “out-of-frame score” above 66 (*see* **Note 6**) and with no potential mismatch targets (*see* **Note 7**). Compare with CCTop results to identify the optimal guide(s).

3.2 **Extended Off-Target Analysis**

Online tools for guide sequence selection often include mismatches only for off-target prediction. However, DNA and RNA bulges also contribute to off-target activity. Therefore, an extended off-target analysis using tools including these criteria might be useful to improve off-target prediction even further.

3.2.1 *CRISPR RGEN* Tools: *Cas-OFFinder*

1. Go to <http://www.rgenome.net/cas-offfinder/> to open the Cas-OFFinder tool.
2. Select the PAM type. The PAM depends on the employed CRISPR/Cas-system and respective Cas ortholog (e.g., 5'-NGG-3' for *Streptococcus pyogenes* Cas9).
3. Select the target genome.
4. Enter the guide sequence(s) into the query sequence field. The guide sequence(s) equal the guide(s) selected with CCTop/Cas-Designer.
5. Select the number of total mismatches and the DNA/RNA bulge size between guide and target site to be considered. Recommendation: Select three for number of total mismatches, two for DNA bulge, and one for RNA bulge (*see* Subheading 1.4) (*see* **Note 8**).
6. Submit the request.
7. Choose the guide(s) with no off-target sites or at least high discrepancy to the predicted off-target sites (*see* **Notes 3 and 8**).

3.3 **Analysis of gRNA Secondary Structure**

The secondary structure of the gRNA considerably contributes to overall activity. Being strongly affected by the variable guide sequence, verification of the secondary structure is inevitable.

3.3.1 *RNAfold*

1. Go to <http://rna.tbi.univie.ac.at/cgi-bin/RNAWebSuite/RNAfold.cgi> to open the RNAfold tool.
2. Enter the complete gRNA sequence including the guide (s) determined by the previous analysis into the sequence query field. The guide is upstream of the gRNA backbone.
3. Keep the default settings.
4. Submit the request.

5. Analyze the predicted gRNA secondary structure by comparing it to its optimal structure (Fig. 1) (*see* Subheading 1.5) (*see* Note 9).
6. Guide(s) of suitable gRNAs can subsequently be used for cloning of the CRISPR constructs and experimental procedure.

4 Notes

1. The optimal guide length depends on the employed CRISPR/Cas-system, respective Cas ortholog, as well as experimental system. The most commonly used SpCas9 and SaCas9 show solid efficiency among the majority of experimental systems with a 20-nt guide.
2. Cloning of the guide is commonly realized by its synthesis as oligonucleotides with subsequent oligonucleotide annealing and ligation into the linearized gRNA expression vector. The addition of 5'-overhangs to the oligonucleotides enables sticky-end cloning which guarantees integration of the guide in the correct orientation.
3. In general, a total amount of ≥ 4 mismatches between guide and target site or ≥ 2 mismatches between guide and target site within the first seven nucleotides proximal to the PAM is sufficient to prevent the majority of cleavage activity. Thus, if the amount of total mismatches is ≤ 4 , at least two mismatches should be inside this so-called core region to prevent off-target activity. The “core” region is defined as the region being the most sensitive toward mismatches.
4. A high efficacy score is desirable. If off-target sites exist, ≥ 4 mismatches in total or ≥ 2 mismatches in the “core” region prevent the majority of cleavage. Select the target(s) that have the highest efficacy score while showing the lowest likelihood for off-target activity.
5. This option is only available for the Cas-Designer tool and consequently complicates the comparison between the CCTop and Cas-Designer results in this step.
6. The “out-of-frame score” describes the likelihood for the emergence of out-of-frame mutations caused by the microhomology-mediated end-joining pathway. Out-of-frame mutations are desired for knockout experiments.
7. Targets with two mismatches within the “core” region can still be selected.
8. Prevent selecting targets that show potential off-target sites by only having one 1 nt DNA bulge in total or one 1 nt RNA bulge outside the “core” region. One 2 nt DNA bulge in total

or one 1 nt RNA bulge within the “core” region is sufficient to prevent cleavage. If at least three mismatches in total are present, additional bulges should abolish cleavage.

9. Efficient gRNAs show only few interactions between the guide sequence and gRNA backbone. Furthermore, intact stem-loop structures are crucial for high activity.

5 Conclusion

Many considerations and useful tools are available to aid for the selection of suitable CRISPR targets. However, a considerable inconsistency is reported between experimental systems and currently available prediction tools are far from predicting gRNA efficiency with high fidelity. While transient protoplast assays can also give relatively high levels of confidence, experimental validation inducing heritable changes in individuals remains the only way to achieve certainty regarding gRNA efficiency.

References

1. Urnov FD (2018) Genome editing B.C. (Before CRISPR): lasting lessons from the “old testament”. *CRISPR J* 1(1):34–46. <https://doi.org/10.1089/crispr.2018.29007.fyu>
2. Jinek M, Chylinski K, Fonfara I et al (2012) A programmable dual-RNA-guided DNA endonuclease in adaptive bacterial immunity. *Science* 337(6096):816–821. <https://doi.org/10.1126/science.1225829>
3. Doudna JA, Charpentier E (2014) Genome editing the new frontier of genome engineering with CRISPR-Cas9. *Science* 346(6213):1258096. <https://doi.org/10.1126/science.1258096>
4. Knott GJ, Doudna JA (2018) CRISPR-Cas guides the future of genetic engineering. *Science* 361(6405):866–869. <https://doi.org/10.1126/science.aat5011>
5. Schindele P, Wolter F, Puchta H (2018) Transforming plant biology and breeding with CRISPR/Cas9, Cas12 and Cas13. *FEBS Lett* 592(12):1954–1967. <https://doi.org/10.1002/1873-3468.13073>
6. Kümlehn J, Pietralla J, Hensel G et al (2018) The CRISPR/Cas revolution continues: from efficient gene editing for crop breeding to plant synthetic biology. *J Integr Plant Biol* 60(12):1127–1153. <https://doi.org/10.1111/jipb.12734>
7. Cebrian-Serrano A, Davies B (2017) CRISPR-Cas orthologues and variants: optimizing the repertoire, specificity and delivery of genome engineering tools. *Mamm Genome* 28(7–8):247–261. <https://doi.org/10.1007/s00335-017-9697-4>
8. Fu Y, Foden JA, Khayter C et al (2013) High-frequency off-target mutagenesis induced by CRISPR-Cas nucleases in human cells. *Nat Biotechnol* 31(9):822–826. <https://doi.org/10.1038/nbt.2623>
9. Hsu PD, Scott DA, Weinstein JA et al (2013) DNA targeting specificity of RNA-guided Cas9 nucleases. *Nat Biotechnol* 31(9):827–832. <https://doi.org/10.1038/nbt.2647>
10. Fu Y, Sander JD, Reyon D et al (2014) Improving CRISPR-Cas nuclease specificity using truncated guide RNAs. *Nat Biotechnol* 32(3):279–284. <https://doi.org/10.1038/nbt.2808>
11. Lin Y, Cradick TJ, Brown MT et al (2014) CRISPR/Cas9 systems have off-target activity with insertions or deletions between target DNA and guide RNA sequences. *Nucleic Acids Res* 42(11):7473–7485. <https://doi.org/10.1093/nar/gku402>
12. Ren X, Yang Z, Xu J et al (2014) Enhanced specificity and efficiency of the CRISPR/Cas9 system with optimized sgRNA parameters in *Drosophila*. *Cell Rep* 9(3):1151–1162. <https://doi.org/10.1016/j.celrep.2014.09.044>
13. Zhang J-P, Li X-L, Neises A et al (2016) Different effects of sgRNA length on CRISPR-

- mediated gene knockout efficiency. *Sci Rep* 6:28566. <https://doi.org/10.1038/srep28566>
14. Sugano SS, Nishihama R, Shirakawa M et al (2018) Efficient CRISPR/Cas9-based genome editing and its application to conditional genetic analysis in *Marchantia polymorpha*. *PLoS One* 13(10):e0205117
 15. Peterson BA, Haak DC, Nishimura MT et al (2016) Genome-wide assessment of efficiency and specificity in CRISPR/Cas9 mediated multiple site targeting in Arabidopsis. *PLoS One* 11(9):e0162169. <https://doi.org/10.1371/journal.pone.0162169>
 16. Feng C, Su H, Bai H et al (2018) High-efficiency genome editing using a dmc1 promoter-controlled CRISPR/Cas9 system in maize. *Plant Biotechnol J* 16(11):1848–1857. <https://doi.org/10.1111/pbi.12920>
 17. Lee K, Zhang Y, Kleinstiver BP et al (2019) Activities and specificities of CRISPR/Cas9 and Cas12a nucleases for targeted mutagenesis in maize. *Plant Biotechnol J* 17(2):362–372. <https://doi.org/10.1111/pbi.12982>
 18. Tang X, Liu G, Zhou J et al (2018) A large-scale whole-genome sequencing analysis reveals highly specific genome editing by both Cas9 and Cpf1 (Cas12a) nucleases in rice. *Genome Biol* 19(1):84. <https://doi.org/10.1186/s13059-018-1458-5>
 19. Zhang Q, Xing H-L, Wang Z-P et al (2018) Potential high-frequency off-target mutagenesis induced by CRISPR/Cas9 in Arabidopsis and its prevention. *Plant Mol Biol* 96(4-5):445–456. <https://doi.org/10.1007/s11103-018-0709-x>
 20. Doench JG, Hartenian E, Graham DB et al (2014) Rational design of highly active sgRNAs for CRISPR-Cas9-mediated gene inactivation. *Nat Biotechnol* 32(12):1262–1267. <https://doi.org/10.1038/nbt.3026>
 21. Wang T, Wei JJ, Sabatini DM et al (2014) Genetic screens in human cells using the CRISPR-Cas9 system. *Science* 343(6166):80–84. <https://doi.org/10.1126/science.1246981>
 22. Liang G, Zhang H, Lou D et al (2016) Selection of highly efficient sgRNAs for CRISPR/Cas9-based plant genome editing. *Sci Rep* 6:21451. <https://doi.org/10.1038/srep21451>
 23. Liu X, Homma A, Sayadi J et al (2016) Sequence features associated with the cleavage efficiency of CRISPR/Cas9 system. *Sci Rep* 6:19675. <https://doi.org/10.1038/srep19675>
 24. Ma X, Zhang Q, Zhu Q et al (2015) A robust CRISPR/Cas9 system for convenient, high-efficiency multiplex genome editing in monocot and dicot plants. *Mol Plant* 8(8):1274–1284. <https://doi.org/10.1016/j.molp.2015.04.007>
 25. Xu H, Xiao T, Chen C-H et al (2015) Sequence determinants of improved CRISPR sgRNA design. *Genome Res* 25(8):1147–1157. <https://doi.org/10.1101/gr.191452.115>
 26. Le C, Ran FA, Cox D et al (2013) Multiplex genome engineering using CRISPR/Cas systems. *Science* 339(6121):819–823. <https://doi.org/10.1126/science.1231143>
 27. Zheng T, Hou Y, Zhang P et al (2017) Profiling single-guide RNA specificity reveals a mismatch sensitive core sequence. *Sci Rep* 7:40638. <https://doi.org/10.1038/srep40638>
 28. Nishimasu H, Ran FA, Hsu PD et al (2014) Crystal structure of Cas9 in complex with guide RNA and target DNA. *Cell* 156(5):935–949. <https://doi.org/10.1016/j.cell.2014.02.001>
 29. Konermann S, Brigham MD, Trevino AE et al (2015) Genome-scale transcriptional activation by an engineered CRISPR-Cas9 complex. *Nature* 517(7536):583–588. <https://doi.org/10.1038/nature14136>
 30. Sander JD, Dahlborg EJ, Goodwin MJ et al (2011) Selection-free zinc-finger-nuclease engineering by context-dependent assembly (CoDA). *Nat Methods* 8(1):67–69. <https://doi.org/10.1038/nmeth.1542>
 31. Sanjana NE, Le C, Zhou Y et al (2012) A transcription activator-like effector toolbox for genome engineering. *Nat Protoc* 7(1):171–192. <https://doi.org/10.1038/nprot.2011.431>
 32. Verkuijl SA, Rots MG (2019) The influence of eukaryotic chromatin state on CRISPR-Cas9 editing efficiencies. *Curr Opin Biotechnol* 55:68–73. <https://doi.org/10.1016/j.copbio.2018.07.005>
 33. Horlbeck MA, Witkowsky LB, Guglielmi B et al (2016) Nucleosomes impede Cas9 access to DNA in vivo and in vitro. *elife* 5:e12677. <https://doi.org/10.7554/eLife.12677>
 34. Wu X, Scott DA, Kriz AJ et al (2014) Genome-wide binding of the CRISPR endonuclease Cas9 in mammalian cells. *Nat Biotechnol* 32(7):670–676. <https://doi.org/10.1038/nbt.2889>
 35. Daer RM, Cutts JP, Brafman DA et al (2017) The impact of chromatin dynamics on Cas9-mediated genome editing in human cells. *ACS*

- Synth Biol 6(3):428–438. <https://doi.org/10.1021/acssynbio.5b00299>
36. Uusi-Mäkelä MIE, Barker HR, Bäuerlein CA et al (2018) Chromatin accessibility is associated with CRISPR-Cas9 efficiency in the zebrafish (*Danio rerio*). PLoS One 13(4): e0196238. <https://doi.org/10.1371/journal.pone.0196238>
 37. Jensen KT, Fløe L, Petersen TS et al (2017) Chromatin accessibility and guide sequence secondary structure affect CRISPR-Cas9 gene editing efficiency. FEBS Lett 591(13):1892–1901. <https://doi.org/10.1002/1873-3468.12707>
 38. Zuker M (2003) Mfold web server for nucleic acid folding and hybridization prediction. Nucleic Acids Res 31(13):3406–3415. <https://doi.org/10.1093/nar/gkg595>
 39. Hofacker IL (2003) Vienna RNA secondary structure server. Nucleic Acids Res 31(13):3429–3431. <https://doi.org/10.1093/nar/gkg599>
 40. Liu H, Ding Y, Zhou Y et al (2017) CRISPR-P 2.0: an improved CRISPR-Cas9 tool for genome editing in plants. Mol Plant 10(3):530–532. <https://doi.org/10.1016/j.molp.2017.01.003>
 41. Stemmer M, Thumberger T, Del Sol KM et al (2015) CCTop: an intuitive, flexible and reliable CRISPR/Cas9 target prediction tool. PLoS One 10(4):e0124633. <https://doi.org/10.1371/journal.pone.0124633>
 42. Bae S, Park J, Kim J-S (2014) Cas-OFFinder: a fast and versatile algorithm that searches for potential off-target sites of Cas9 RNA-guided endonucleases. Bioinformatics 30(10):1473–1475. <https://doi.org/10.1093/bioinformatics/btu048>
 43. Park J, Bae S, Kim J-S (2015) Cas-Designer: a web-based tool for choice of CRISPR-Cas9 target sites. Bioinformatics 31(24):4014–4016. <https://doi.org/10.1093/bioinformatics/btv537>
 44. Lee CM, Davis TH, Bao G (2018) Examination of CRISPR/Cas9 design tools and the effect of target site accessibility on Cas9 activity. Exp Physiol 103(4):456–460. <https://doi.org/10.1113/EP086043>



Live-Cell CRISPR Imaging in Plant Cells with a Telomere-Specific Guide RNA

Solmaz Khosravi, Steven Dreissig, Patrick Schindele, Felix Wolter, Twan Rutten, Holger Puchta, and Andreas Houben

Abstract

Chromatin organization is highly dynamic in living cells. Therefore, it might have a regulatory role over biological mechanisms like transcription, replication, and DNA repair. To elucidate how these mechanisms are regulated, it is required to establish imaging methods to visualize the chromatin dynamic in living cells. Here, we provide a protocol for a live plant cell imaging technique based on application of two orthologs of the bacterial clustered regularly interspaced short palindromic repeats (CRISPR)-associated protein 9 (Cas9) from *Streptococcus pyogenes* and *Staphylococcus aureus*. This technique uses the inactive variants of Cas9 combined with different fluorescent proteins (GFP and mRuby) and telomere-specific guide RNA to target telomeric repeats in *Nicotiana benthamiana*. Our immuno-FISH data revealed that signals arising from the CRISPR/dCas9 method are specifically belonging to telomeric regions.

Key words Chromatin organization, Live-cell imaging, CRISPR/dCas9, Telomere, *Nicotiana benthamiana*, Guide RNA

1 Introduction

Structural and spatial organization of chromatin affects gene regulation and pivotal processes like recombination and DNA repair mechanisms. Eventually, studying chromatin structural changes in different tissues over time has always been of interest to decipher these regulatory mechanisms [1]. Our knowledge about the 3D organization of chromatin is mainly based on fixed specimens. Although imaging methods including fluorescence in situ hybridization (FISH) have been well applied to study subnuclear dynamics, harsh treatment of cells during FISH like heat-based denaturation could provide data only from perturbed chromatin structure which is not indicative of its structure in living cells [2]. To overcome this problem, live chromatin imaging techniques were developed to enable studying of biological compartments in their native context [3].

Live-cell imaging was boosted with the application of GFP-fused chromatin proteins including histones, condensins, and others [4]. Nonetheless, this method is unable to detect specific genomic loci. Later, fluorescent repressor/operator systems were used to allow specific labeling of genomic regions in comparison to chromatin proteins [5]. In plants, this technique was applied to *A. thaliana* to compare the ploidy level of guard cells and elongated epidermal root cells [6]. However, this method is not able to label predefined genomic regions as a random insertion of the tandem operator repeats into the genome occurs after plant transformation. In addition, methylation at operator insertion sites and subsequent alteration of the chromatin dynamics have been reported [7].

Subsequently, new live-cell imaging techniques were established that are based on the use of programmable DNA-binding proteins, including zinc finger protein (ZFP), transcription activator-like effector (TALE), and, more recently, clustered regularly interspaced short palindromic repeats (CRISPR)/CRISPR-associated protein 9 (Cas9) (Fig. 1). The major advantage of programmable DNA-binding proteins is that target regions like RNA or genomic DNA are recognized and marked in a sequence-specific way.

ZFP fused with GFP under the control of ribosomal protein 5S A promoter (*RPS5Ap*) was first used to label the 180 bp tandem repeats of the centromere in the root meristems of *A. thaliana* [8]. However, the ZFP system could not be used for imaging of specific loci, such as 5S rDNA or *HPT* gene. Since the genomic and chromatin content around the target region along with the context-dependent interactions with neighboring zinc fingers affects the DNA sequence recognition ability of ZFP for different genomic targets [9, 10], the further application of ZFP for live-cell imaging was substituted with TALEs. Similar to ZFPs, TALEs can be programmed to detect specific DNA sequences [11, 12]. Using this feature, TALEs were successfully fused to the GFP to visualize repetitive sequences in *A. thaliana* including telomeric sequences and centromeric 180 bp repeats [13]. However, being a time-consuming and laborious method due to reengineering of TALE proteins for the targeting of each new genomic region, the live-cell imaging techniques were improved to use a more user-friendly method called CRISPR/Cas9.

The application of CRISPR/Cas9 for chromatin imaging was first reported for the dynamic imaging of genomic loci in human cell cultures [14]. The CRISPR/Cas9 consists of a Cas9 protein and guide RNA (gRNA) scaffold. The gRNA is a fusion of crRNA (CRISPR RNAs) and tracrRNA (trans-activating crRNA). Part of crRNA which binds as a complementary strand to the foreign target sequence is called protospacer. tracrRNA has a stem-loop structure and supports the stability of Cas protein. The Cas9 protein contains

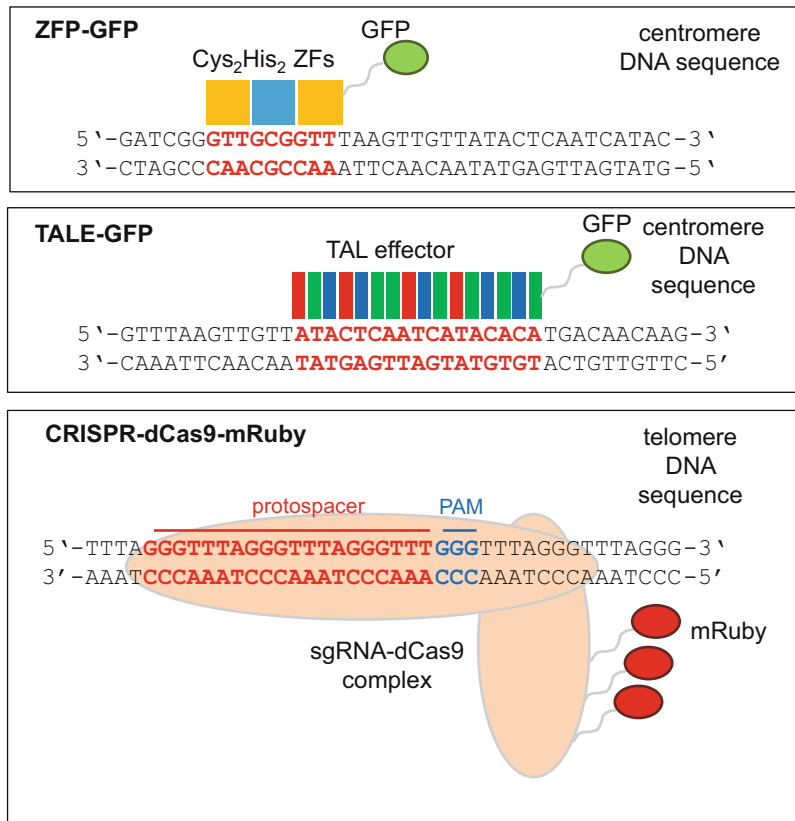


Fig. 1 Programmable DNA-binding proteins for live-cell imaging. **(a)** Zinc finger protein attached to GFP. Each protein can recognize just three base pairs in DNA. To recognize 9 bp, three ZFPs should be fused. **(b)** TALE protein fused to GFP. Each RVD region in TALE can recognize one base pair in DNA. **(c)** CRISPR/dCas9. A DNA cleavage-defective variant of Cas9 (dCas9) fused to GFP can be easily programmed for recognizing 20 base pairs in DNA

two HNH and RuvC-like domains and recognizes specific sequences within the genome called protospacer adjacent motif (PAM). Each Cas protein has specificity for a specific PAM sequence. When Cas protein recognizes the specific PAM and attaches to the genome, the protospacer base pairs with the target sequence and allows the HNH domain to cut the DNA strand complementary to crRNA, and the RuvC-like domain cleaves the other DNA strand [15]. Nevertheless, the nuclease activity of the Cas9 protein is not necessary for live-cell imaging. Therefore, in a deactivated Cas9 protein (dCas9) variant, this activity has been removed by the induction of two-point mutations in the HNH and RuvC-like domains [16]. CRISPR/dCas9 was successfully used for visualizing of telomere repeats in human cells, pericentric and centric sequences in mouse cells, 45S rDNA in yeast, or even a single chromosomal locus in *Xenopus* egg extracts [14, 17–19]. The application of this method for studying the dynamic of

telomeres in living plant cells has been accomplished in transiently transformed *Nicotiana benthamiana* and *N. tabacum* plants [20, 21]. For *N. benthamiana*, dCas9 from two different bacterial sources, *Streptococcus pyogenes* and *Staphylococcus aureus*, was employed. Accordingly, both orthologs of Cas9 could visualize telomeric regions with equal efficiency [20].

In this chapter, the protocol of using different dCas9 orthologs in combination with target-specific gRNA for live-cell imaging of telomeres in *N. benthamiana* leaves is explained in detail. To start live-cell imaging of telomeres with CRISPR/Cas, pChimera and pEn-Sa-Chimera vectors are used to express gRNA from *S. pyogenes* and *S. aureus*, respectively. The dCas9-eGFP/mRuby2 vector is used for the expression of dCas9 from *S. pyogenes* (pCAS9-TP-Sp-dCAS9-eGFP/mRuby2) or *S. aureus* (pCAS9-TP-Sa-dCAS9-eGFP/mRuby2) fused with a fluorescent protein, either GFP or mRuby2 (*see Note 1*).

The protocol starts by designing the protospacers for labeling of telomeres and annealing them to the pChimera vectors. Next, the gRNA from pChimera vectors is cloned next to dCas9-eGFP/mRuby2 with the help of conventional cloning. The resulting vector is agro-infiltrated into *N. benthamiana* leaves for the visualization of telomeres by confocal laser scanning microscopy. Subsequently, the specificity of observed signals is confirmed by immunostaining and FISH.

2 Materials

2.1 Material Used to Prepare CRISPR/Cas9 Constructs

1. gRNA expression vectors (here pChimera and pEn-Sa-Chimera) which express gRNA from *S. pyogenes* and *S. aureus*, respectively (*see Note 1*).
2. dCas9-eGFP/mRuby2 expression vectors (*see Note 1*):
 - (a) pCAS9-TP-Sp-dCAS9-eGFP/mRuby2, referred to as pSpCas in this chapter.
 - (b) pCAS9-TP-Sa-dCAS9-eGFP/mRuby2, referred to as pSaCas in this chapter.
3. *E. coli* NEB5 α , DH5 α derivative.
4. LB medium pH 7: 10 g Tryptone, 10 g sodium chloride (NaCl), 5 g yeast extract dissolved in 1 /L distilled water, supplement with 100 mg/L ampicillin or 100 mg/L spectinomycin.
5. Restriction enzymes *Bbs*I, *Mlu*I, *Avr*II, and respective restriction enzyme buffers.
6. T4 DNA ligase and T4 DNA ligase buffer.
7. Plasmid DNA isolation kit.
8. PCR purification kit.



Fig. 2 Final CRISPR/dCas9 live-cell imaging construct. LB: left border, Ubi-4 p: ubiquitin promoter for constitutive expression of Cas 9 protein, NLS: nuclear localization signal importing the expressed Cas9 protein to nucleus, 3× GFP/mRuby: fluorescent proteins, Pea3A T: terminator, AtU26-P: U6 promoter from *A. thaliana* for expression of gRNA, sgRNA telomere: sgRNA-containing telomere-targeting protospacer

2.2 Material Used for Agroinfiltration of *N. benthamiana*

1. Healthy 2–4-week-old *N. benthamiana* plants grown in a greenhouse under 16/8-h light/dark conditions and 22 °C temperature.
2. *Agrobacterium* strain harboring the imaging expression construct (Fig. 2).
3. LB medium with 100 mg/L spectinomycin and 50 mg/L rifampicin.
4. 100 mM Acetosyringone stock solution in ethanol, stored at –20 °C.
5. 0.5 M 2-(N-morpholino) ethanesulfonic acid buffer (MES-K), adjusted to pH 5.6 with KOH.
6. Resuspension solution: 10 mM MgCl₂, 10 mM MES-K.
7. Centrifuge for 50 mL tubes.
8. Spectrometer.
9. 5 mL Syringe.

2.3 Material Necessary for Microscopy of Plant Leaves

1. Confocal laser scanning microscope (e.g., LSM780, Carl Zeiss).
2. Phosphate buffer: 20 mM KH₂PO₄/Na₂PO₄, 0.01% Triton X100, pH 7.0.
3. Caulking gun.
4. 50 mL Syringe.
5. 76 × 26 mm Glass slides.
6. 40 × 24 mm Coverslips.
7. Sticking tape.
8. Fixogum rubber cement, Marabu GmbH, Germany.

2.4 Material Required for Immunostaining and FISH

1. Epifluorescence microscope (e.g., BX61, Olympus) equipped with a camera (e.g., Orca ER, Hamamatsu).
2. Cytocentrifuge (Shandon CytoSpin3, *see Note 2*).
3. Cytology funnels for cytocentrifuge.
4. 5 mL Polystyrene round-bottom tube with cell strainer cap (*see Note 3*).
5. Razor blade.

6. 4% (vol/vol) Paraformaldehyde solution (*see Note 4*).
7. LB01 lysis buffer: 15 mM Tris, 2 mM Na₂EDTA, 0.5 mM spermine tetrahydrochloride, 80 mM KCL, 20 mM NaCl, 15 mM β-mercaptoethanol, 0.1% (vol/vol) Triton X-100. Adjust pH to 7.5 with 1 M NaOH. Filtrate the buffer through 0.22 μm filter to sterilize it for longer storage.
8. 4% (vol/vol) Bovine serum albumin (BSA) solution.
9. PBS pH 7.4: 137 mM NaCl, 2.7 mM KCl, 10 mM Na₂HPO₄, 1.8 mM KH₂PO₄.
10. 4',6-Diamidino-2'-phenylindole dihydrochloride (DAPI) solution (*see Note 5*).
11. VECTASHIELD antifade mounting medium (Vector Laboratories) (*see Note 6*).
12. Ethanol solutions: 70, 90, 100%.
13. Fixation solution: (1:3) glacial acetic acid: 100% Ethanol.
14. Denaturation solution: 0.2 M NaOH in 70% ethanol.
15. FISH hybridization solution: 50% (vol/vol) Formamide, 10% (vol/vol) dextran sulfate in 2× SSC.
16. 2× Saline sodium citrate (SSC): 0.30 M Sodium citrate, 0.030 M NaCl, pH 7.0.
17. GFP antibody (directly labeled GFP mouse antibody Dylight 488; Rockland).
18. 5'-Cy5-labeled oligonucleotide probe (5'-Cy5-GGGTTTAGGGTTTAGGGTTT-3').
19. Sucrose buffer: 100 mM Tris, 50 mM KCl, 2 mM MgCl₂, 0.05% Tween, 5% sucrose.

3 Methods

3.1 Preparation of the Protospacer and Cloning of the CRISPR/Cas9-gRNA Vectors

1. Select a 20 nt protospacer for the telomere sequence upstream of 5'-NGG-3' and 5'-NNGRRT-3' PAM sequences for Cas9 from *S. pyogenes* and *S. aureus*, respectively (*see Note 7*).
2. Synthesize the protospacer as oligonucleotides with appropriate overhangs for cloning into the gRNA expression vector (5'-ATTG-protospacer-3' and 5'-AAAC-rev-com-protospacer-3') (*see Note 8*) (Fig. 3c).
3. Mix the oligonucleotides with a final concentration of 2 μM each in a final volume of 50 μL and anneal them by incubation at 95 °C for 5 min and subsequent incubation at room temperature for 20 min (*see Note 9*).

12. Transform 5 μ L of the ligation in 100 μ L competent *E. coli* DH5 α cells via the heat-shock method, plate 100 μ L on LB medium supplemented with 100 mg/L spectinomycin, and grow overnight at 37 °C.
13. Verify successful transformation via colony PCR, inoculate a single colony in 5 mL LB medium supplemented with the 100 mg/L spectinomycin, and grow overnight at 37 °C.
14. Isolate the plasmid DNA and verify successful cloning via sequencing. Adjust the DNA concentration to 100 ng/ μ L.
15. The vectors are ready for transformation into *Agrobacterium* strain GV3101.

3.2 Plant Material Preparation and Agrobacterium-Mediated Transformation

1. Grow *N. benthamiana* seeds in a greenhouse under 16/8-h light/dark conditions and 22 °C temperature for 2–4 weeks.
2. Use a single colony of *Agrobacterium* (**step 15** from Subheading 3.1) to inoculate 5 mL LB with 100 mg/L spectinomycin and 50 mg/L rifampicin and grow overnight at 28 °C.
3. Use 1 mL of the overnight culture to inoculate 25 mL LB medium with 100 mg/L spectinomycin and 50 mg/L rifampicin and grow overnight.
4. Measure the optical density (OD₆₀₀) of the overnight culture with a spectrometer.
5. Precipitate the bacteria in 50 mL tubes by centrifugation at 5000 $\times g$ for 15 min.
6. Meanwhile, prepare the resuspension solution by adding 100 μ M acetosyringone. Acetosyringone should always be added to the resuspension solution after autoclaving and before injection of leaves.
7. Resuspend the bacterial pellet in resuspension solution and adjust the final A₆₀₀ to 0.4.
8. Leave the bacterial suspension solution on the bench at room temperature for 2–3 h (or overnight) before infiltration.
9. Perform the infiltration with syringe. Simply press the syringe (without needle) on the abaxial surface of the leaf and exert a counter-pressure with finger on the other side (Fig. 4). Press the plunger of the syringe and allow the liquid to enter the leaf tissue. Successful infiltration is often observed as a spreading “wetting” area in the leaf.
10. Keep the injected plants in the greenhouse at 16/8-h light/dark conditions and 22 °C temperature for 48 h.
11. Look for the occurrence of fluorescent signals with a microscope 2–4 days after injection (Fig. 5) (*see Note 12*).



Fig. 4 Agroinfiltration of a *N. benthamiana* leaf. The infiltrated bacterial solution causes the spreading of a wet area in the leaf

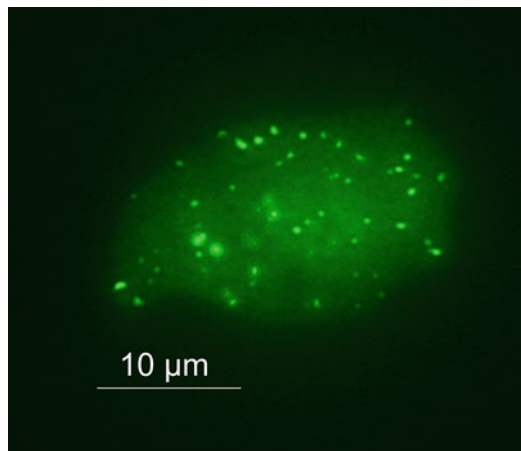


Fig. 5 Signal observation in living leaf tissue of *N. benthamiana* by fluorescence microscopy. The GFP signals emitted from telomeres can be detected 48 h after infiltration

3.3 Imaging of Telomeric Fluorescence Signals

3.3.1 Degassing of Leaf Samples

1. Remove the plunger from the 50 mL plastic syringe and seal the adaptor end of the funnel in a flame.
2. Fill the funnel with 15 mL 20 mM phosphate buffer/0.01% Triton X100.
3. While avoiding large veins, cut out a 15 × 8 mm rectangular piece of leaf tissue with a razor blade. Position the sample dorsal side up and remove part of the right upper corner to distinguish dorsal from ventral side.
4. Transfer the leaf sample into the funnel and install the plunger again.
5. Place the 50 mL syringe into the caulking gun and increase the pressure until the leaf sample is no longer afloat. The presence of 0.01% Triton X100 reduces surface tension and facilitates buffer infiltration.

6. Leave the syringe for 15 min in the caulking gun to ensure that residual air is replaced by buffer solution. Repeat if necessary.
7. Place degassed leaf sample ventral side up (position of cutoff corner on the left upper side) on a glass slide.
8. Add a droplet of buffer solution before covering the sample with a 40 × 24 mm coverslip.
9. Fix the short ends of the coverslip with sticking tape.
10. Remove air inclusions between sample and coverslip by careful tapping with the blunt end of a tweezer.
11. Fill empty space between coverslip and glass slide with buffer, and then seal the long ends with fast drying and easily removable fixogum.

3.3.2 Analysis of Telomeric GFP Signals

1. Place the slide in the microscope and examine with a 40× NA 1.2 water objective.
2. Select appropriate locations without air inclusions since the latter interfere with signal recording.
3. Select optimal resolution settings to avoid over- or undersampling.
4. GFP is excited with a 488 nm laser line and emission is detected over a range of 490–540 nm.
5. Collect telomeric GFP distribution as Z-stacks.

3.4 Combination of Immunostaining and FISH for Confirming the Specificity of CRISPR/dCas9-Caused Signals

1. Cut a 1 cm³ piece of leaf from the infiltrated area, transfer into 4% paraformaldehyde solution, and fix on ice for 5 min under vacuum followed by 30 min under atmospheric pressure (*see Note 13*).
2. Remove the paraformaldehyde solution and wash twice in PBS.
3. In a drop of LB01 lysis buffer in a petri dish, finely chop the leaf using a sharp razor blade (*see Note 14*).
4. Add 500 μL LB01 lysis buffer to the homogenate and transfer into 35 μm cell suspension filter tube.
5. Apply 200 μL of the homogenate to a cytology funnel and centrifuge for 5 min at 450 rpm in a cytocentrifuge (*see Note 2*).
6. Wash slides two times in PBS for 5 min and add 60 μL of 4% BSA followed by incubation at room temperature for 45 min in a high-humidity plastic box. Carefully cover slides with parafilm tape.
7. Wash slides two times in PBS for 5 min and add 60 μL of GFP antibody solution (2% (vol/vol) BSA in PBS, GFP antibody in 1:2500 dilution) followed by incubation at room temperature for 1 h in a high-humidity plastic box. Carefully cover slides with parafilm tape.

8. Wash slides two times in PBS for 5 min and fix in fixation solution for 24 h in darkness.
9. Perform sequential dehydration in 70, 90, and 100% ethanol for 2 min each and leave to dry for 30 min.
10. Afterwards, perform pre-hybridization at 37 °C for 1 night by adding 15 μ L FISH hybridization solution and cover slides with coverslip. Store slides in a high-humidity plastic box.
11. Wash slides twice in 2 \times SSC for 5 min and perform sequential dehydration in 70, 90, and 100% ethanol for 2 min each. Leave slides to dry for 30 min.
12. Perform DNA denaturation in denaturation solution at room temperature for 10 min followed by sequential dehydration in 70, 90, and 100% ethanol for 2 min each. Leave slides to dry for 15 min.
13. Meanwhile, prepare the FISH hybridization solution by mixing 0.5 μ L of the 5'-labeled oligonucleotide probe (10 μ M) with 14.5 μ L of FISH hybridization solution per slide.
14. Incubate the mixture at 95 °C for 5 min followed by rapid transfer onto ice for 5 min.
15. Apply 15 μ L of the mixture per slide and hybridize at 37 °C for 1 night. Cover slides with coverslips and store in a high-humidity plastic box.
16. Wash slides two times in 2 \times SSC for 5 min followed by sequential dehydration in 70, 90, and 100% ethanol for 2 min each. Leave slides to dry for 30 min.
17. Apply 10 μ L VECTASHIELD solution containing DAPI (1:1000) and analyze slides by fluorescence microscopy (Fig. 6).

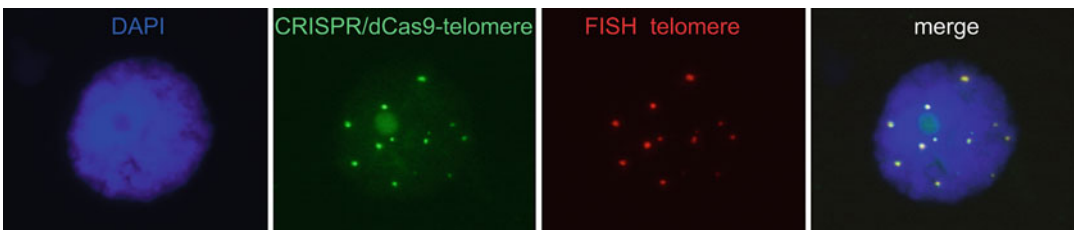


Fig. 6 *N. benthamiana* nuclei after CRISPR/dCas9-based staining of telomeres and subsequent FISH with a telomere-specific probe. From left to right: DAPI staining of nuclei (blue); GFP signals coming from CRISPR imaging vector targeting telomeres (green); FISH signals from telomere probe (red); co-localization of CRISPR and FISH signals demonstrating the specificity of CRISPR signals (merge)

4 Notes

1. All Cas9 expression vectors are based on the vector pCAS9-TPC [22, 23]. The vectors mentioned in this protocol are available from the Botanical Institute, Karlsruhe Institute of Technology, POB 6980, 76049 Karlsruhe, Germany. Vector information can be found on the respective webpage (<https://www.botanik.kit.edu/molbio/1057.php>).
2. This centrifuge is used to precipitate leaf nuclei onto a microscopic slide. It enables to obtain purified leaf nuclei at high density without any remaining cytoplasm. It is crucial to remove any cytoplasm for a successful immunostaining and FISH. If a cytocentrifuge is not available, the following alternative method could be used to prepare microscopic slides carrying nuclei. Drop 12 μL sucrose buffer on a clean glass slide, add 12 μL of nuclei suspension obtained after filtration of chopped leaf, and gently mix both types of drops with the pipette tip. Let slides dry overnight.
3. This tube contains a 35 μm nylon mesh to filtrate the extracted nuclei from leave debris.
4. Prepare 4% paraformaldehyde solution by diluting 37% ready-to-use paraformaldehyde solution.
5. DAPI solution is usually prepared by diluting 1 μL DAPI (stock) in 999 μL VECTASHIELD antifade mounting medium. Mix well by vortexing.
6. VECTASHIELD is used to prevent immediate fading of fluorescent signals during microscopy.
7. The PAM sequences which are recognized by the specific Cas9 proteins of *S. pyogenes* and *S. aureus* are 5'-NGG-3' and 5'-NNGRRT-3', respectively. The protospacers have to be selected 20 bp upstream of the respective PAM sequence. There are web pages like DeskGen (<https://www.deskgen.com/landing/#/>), WU-CRIPSR (<http://crispr.wustl.edu/>), and CRISPOR (<http://crispor.tefor.net/>) available for selecting a suitable protospacer for the target telomere sequence of interest (Fig. 7).



Fig. 7 Protospacer design for pCAS9-TP-Sp-dCAS9-eGFP/mRuby2 and pCAS9-TP-Sa-dCAS9-eGFP/mRuby2 to target telomere DNA sequence. The protospacer has to be selected 20 bp upstream of the respective PAM sequence. Target sequence is shown in red. The NGG protospacer adjacent motif (PAM) for Sp-cCas9 is indicated in blue, whereas *NNGRRT* PAM for Sa-dCas9 is indicated in green

8. The appropriate *overhangs* are added to the 5' end of selected **protospacer** for targeting telomeres in *N. benthamiana*:
 - (a) Forward sequence: 5'-*attg***GGGTTTAGGGTTTAGGG TTT**-3'
 - (b) Reverse sequence: 5'-*aaac***AAACCCTAAACCCTAAA CCC**-3'
9. To guarantee a proper annealing of the oligonucleotides, do not decrease the incubation time at room temperature.
10. Mere heat inactivation of the digestion reaction to linearize the gRNA expression vector is not recommended to prevent religation of the excised fragment. However, due to the small size of the excised fragment, a PCR purification kit is sufficient for the purification of the linearized gRNA expression vector.
11. To guarantee a proper ligation, an incubation time of at least 1 h is recommended.
12. The signals can be detected even up to 4 days after injection; however, the number of nuclei showing signals decreases over time.
13. Optimal fixation conditions may vary between species or tissue types. The durations described here are working well for *N. benthamiana* leaves. However, if the quality of the immunostaining is not as desired, an increase or decrease of fixation time might have an impact on how well the structure of the nuclei is preserved.
14. Chop by quickly moving the razor blade up and down in a steady rhythm. It is important not to squeeze the leaf, as this does not release nuclei. The LB01 buffer should only turn green as a result of homogenization, not squeezing the leaf.

References

1. Meldi L, Brickner JH (2011) Compartmentalization of the nucleus. *Trends Cell Biol* 21:701–708
2. Hoshi Y, Yagi K, Matsuda M, Matoba H, Tagashira N, Pläder W, Malepszy S, Nagano K, Morikawa A (2011) A comparative study of the three cucumber cultivars using fluorescent staining and fluorescence in situ hybridization. *Cytologia* 76:3–10
3. Bystricky K (2015) Chromosome dynamics and folding in eukaryotes: insights from live cell microscopy. *FEBS Lett* 589:3014–3022
4. Kanda T, Sullivan KF, Wahl GM (1998) Histone-GFP fusion protein enables sensitive analysis of chromosome dynamics in living mammalian cells. *Curr Biol* 8:377–385
5. Belmont AS, Straight AF (1998) In vivo visualization of chromosomes using lac operator-repressor binding. *Trends Cell Biol* 8:121–124
6. Kato L (2001) Detection of chromosomes tagged with green fluorescent protein in live *Arabidopsis thaliana* plants. *Genome Biol* 2: research0045
7. Jovtchev G, Borisova B, Kuhlmann M, Fuchs J, Watanabe K, Schubert I, Mette MF (2011) Pairing of lacO tandem repeats in *Arabidopsis thaliana* nuclei requires the presence of hypermethylated, large arrays at two chromosomal positions, but does not depend on H3-lysine-9-dimethylation. *Chromosoma* 120:609–619
8. Lindhout BI, Fransz P, Tessoro F, Meckel T, Hooykaas PJJ, Zaai BJ (2007) Live cell

- imaging of repetitive DNA sequences via GFP-tagged polydactyl zinc finger proteins. *Nucleic Acids Res* 35:e107
9. Sanjana NE, Cong L, Zhou Y, Cunniff MM, Feng G, Zhang F (2012) A transcription activator-like effector toolbox for genome engineering. *Nat Protoc* 7:171–192
 10. Gaj T, Gersbach CA, Barbas CF (2013) ZFN, TALEN, and CRISPR/Cas-based methods for genome engineering. *Trends Biotechnol* 31:397–405
 11. Miyanari Y, Ziegler-Birling C, Torres-Padilla M-E (2013) Live visualization of chromatin dynamics with fluorescent TALEs. *Nat Struct Mol Biol* 20:1321–1324
 12. Ma H, Reyes-Gutierrez P, Pederson T (2013) Visualization of repetitive DNA sequences in human chromosomes with transcription activator-like effectors. *Proc Natl Acad Sci U S A* 110:21048–21053
 13. Fujimoto S, Sugano SS, Kuwata K, Osakabe K, Matsunaga S (2016) Visualization of specific repetitive genomic sequences with fluorescent TALEs in *Arabidopsis thaliana*. *J Exp Bot* 67:6101–6110. <https://doi.org/10.1093/jxb/erw371>
 14. Chen B, Gilbert LA, Cimini BA, Schnitzbauer J, Zhang W, Li GW, Park J, Blackburn EH, Weissman JS, Qi LS, Huang B (2013) Dynamic imaging of genomic loci in living human cells by an optimized CRISPR/Cas system. *Cell* 155:1479–1491. <https://doi.org/10.1016/j.cell.2013.12.001>
 15. Chen H, Choi J, Bailey S (2014) Cut site selection by the two nuclease domains of the Cas9 RNA-guided endonuclease. *J Biol Chem* 289:13284–13294. <https://doi.org/10.1074/jbc.M113.539726>
 16. Qi LS, Larson MH, Gilbert LA, Doudna JA, Weissman JS, Arkin AP, Lim WA (2013) Repurposing CRISPR as an RNA-guided platform for sequence-specific control of gene expression. *Cell* 152:1173–1183
 17. Lane AB, Strzelecka M, Ettinger A, Grenfell AW, Wittmann T, Heald R (2015) Enzymatically generated CRISPR libraries for genome labeling and screening. *Dev Cell* 34:373–378. <https://doi.org/10.1016/j.devcel.2015.06.003>
 18. Anton T, Bultmann S, Leonhardt H, Markaki Y (2014) Visualization of specific DNA sequences in living mouse embryonic stem cells with a programmable fluorescent CRISPR/Cas system. *Nucleus* 5:163–172. <https://doi.org/10.4161/nucl.2848>
 19. Xue Y, Murat A (2018) Live-cell imaging of chromatin condensation dynamics by CRISPR. *iScience* 4:216–235. <https://doi.org/10.1016/j.isci.2018.06.001>
 20. Dreissig S, Schiml S, Schindele P, Weiss O, Rutten T, Schubert V, Gladilin E, Mette MF, Puchta H, Houben A (2017) Live-cell CRISPR imaging in plants reveals dynamic telomere movements. *Plant J* 91:565–573
 21. Fujimoto S, Matsunaga S (2017) Visualization of chromatin loci with transiently expressed CRISPR/Cas9 in plants. *Cytologia* 82:559–562
 22. Fauser F, Schiml S, Puchta H (2014) Both CRISPR/Cas-based nucleases and nickases can be used efficiently for genome engineering in *Arabidopsis thaliana*. *Plant J* 79:348–359
 23. Steinert J, Schiml S, Fauser F, Puchta H (2015) Highly efficient heritable plant genome engineering using Cas9 orthologues from *Streptococcus thermophilus* and *Staphylococcus aureus*. *Plant J* 84:1295–1305



Live-Cell Imaging of Genomic Loci Using CRISPR/Molecular Beacon Hybrid Systems

Xiaotian Wu, Yachen Ying, Shiqi Mao, Christopher J. Krueger, and Antony K. Chen

Abstract

The ability to monitor the behavior of specific genomic loci in living cells can offer tremendous opportunities for deciphering the molecular basis driving cellular physiology and disease evolution. Toward this goal, clustered regularly interspersed short palindromic repeat (CRISPR)-based imaging systems have been developed, with tagging of either the nuclease-deactivated mutant of the CRISPR-associated protein 9 (dCas9) or the CRISPR single-guide RNA (sgRNA) with fluorescent protein (FP) molecules currently the major strategies for labeling. Recently, we have demonstrated the feasibility of tagging the sgRNA with molecular beacons, a class of small molecule dye-based, fluorogenic oligonucleotide probes, and demonstrated that the resulting system, termed CRISPR/MB, could be more sensitive and quantitative than conventional approaches employing FP reporters in detecting single telomere loci. In this chapter, we describe detailed protocols for the synthesis of CRISPR/MB, as well as its applications for imaging single telomere and centromere loci in live mammalian cells.

Key words CRISPR, Molecular beacons, Chromatin dynamics, Fluorogenic probes

1 Introduction

Over the past several decades, increasing evidence has suggested that many fundamental cellular processes, including DNA replication, DNA damage repair, and gene expression, are highly regulated by chromatin dynamics [1, 2]. Consequently, much effort has been devoted to developing methods to enable direct visualization of single chromatin loci in living cells, with many approaches developed based on gene-editing tools [3, 4]. One such tool is the clustered regularly interspaced short palindromic repeat (CRISPR) system [5], which consists of two components: the CRISPR-associated protein 9 (Cas9) DNA nuclease and a chimeric single-guide RNA possessing a Cas9-binding motif and a spacer sequence complementary to the target DNA sequence of interest [6]. To edit a specific sequence, the sgRNA recruits Cas9 to form a stable

complex that can transiently bind to a short DNA sequence known as the protospacer adjacent motif (PAM) and locally unwind the DNA duplex [7–9]. Complementation of the sgRNA spacer sequence with the DNA sequence of the genomic protospacer stabilizes binding between the complex and the target sequence [9], allowing Cas9 to introduce double-stranded breaks that subsequently elicit error-prone repair by nonhomologous end joining to result in generation of new sequences [10–12].

Cas9 modified to eliminate nuclease activity (dCas9) can still bind specific DNA sequences in a sgRNA-guided fashion. This has spurred the development of various CRISPR/dCas9-based probes for live-cell fluorescent labeling of genomic loci, with either the dCas9 protein or the sgRNA modified to allow tagging by fluorescent proteins (FPs) [13–22], small-molecule dyes [23–26], oligonucleotide probes [27], or quantum dots [28] in a manner that does not appear to disrupt DNA targeting capacities. In this chapter, we describe the synthesis and applications of one such probe that was developed in our laboratory, termed the CRISPR/molecular beacon (MB) hybrid system (CRISPR/MB) [27]. Molecular beacons are a class of stem-loop-forming, fluorogenic oligonucleotide probes that possess a dye and a quencher at the two termini [29]. In the absence of target, the short arm sequences at the two termini self-anneal to form a duplex stem, holding the dye and the quencher in close spatial proximity, causing the MBs to emit a low fluorescence signal. Hybridization of target sequence to the MB disrupts the stem, separating the dye from the quencher to restore MB fluorescence. To image a genomic locus in living cells using CRISPR/MB (*see* Fig. 1), dCas9 and an sgRNA engineered to harbor a unique MB target sequence (sgRNA-MTS) are first co-expressed. After sufficient time is given to allow dCas9-sgRNA-MTS complex to bind a target locus, MBs are delivered into the cells by microporation. Collective hybridization of the MBs to the dCas9-sgRNA-MTS complexes tiling across the target locus can cause the locus to appear as a bright fluorescent spot, indicative of a single genomic locus, when imaged via fluorescence microscopy. Protocols used for live-cell imaging and tracking of single telomere and centromere loci are provided.

2 Materials

2.1 Plasmids

1. pSLQ1658-dCas9-EGFP that encodes the nuclease-deactivated *Streptococcus pyogenes* Cas9 protein (dCas9), fused to EGFP, is available on Addgene, a nonprofit plasmid repository (Code #51023).
2. pU6-SL2-sgTelo-MTSa and pU6-SL2-sgSat-MTSb (*see* **Note 1**): These two plasmids containing genomic-targeting sgRNAs harboring two orthogonal MTSs, named MTSa and

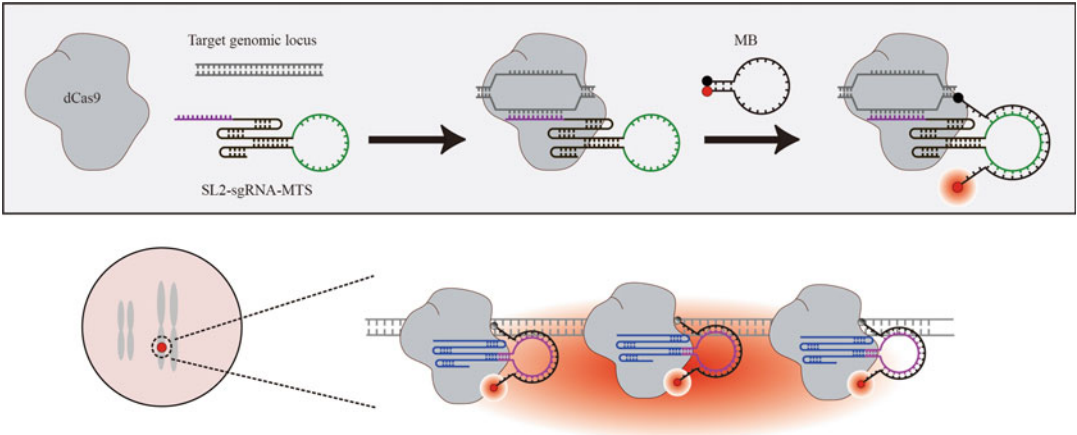


Fig. 1 Schematic of the CRISPR/MB labeling strategy and workflow. The CRISPR/MB system consists of dCas9, an MB, and an sgRNA scaffold (SL2-sgRNA-MTS) harboring a unique MB target sequence (MTS) (green). After the dCas9-sgRNA-MTS complex binds to target DNA, hybridization of the MB to the MTS will illuminate the specific chromatin locus. This figure was created by modifying Fig. 1 of [27] with permission in accordance with the [Creative Commons Attribution Non-Commercial \(CC BY-NC 4.0\) License](https://creativecommons.org/licenses/by-nc/4.0/)

MTSb, were custom-made by a genomics service provider. They can be used simultaneously for dual-color labeling or used, respectively, for single labeling. The two sgRNA sequences are listed below (the spacer sequence is bold, MTS is bold italicized, the stem sequence is italicized):

(a) SL2-sgTelo-MTSa targeting telomere (*see Note 2*):
GTTAGGGTTAGGGTTAGGGTTAGTTTGAGAGC
 TATGCTGGAACAGCATAGCAAGTTCAAATAAGG
 CTAGTCCGTTATCAACTTGGCCCCGGAGCAGAA
 CGACAGGAGTT***GTTTGTGGACGAAGAGCCTG***
 CAGTCTGCTCCGGGGCCAGTGGCACCAGTTCGG
 TGCTTTTTTT.

(b) SL2-sgSat-MTSb targeting centromere (*see Note 2*):
GAATCTGCAAGTGGATATTGTTTGAGAGCTATG
 CTGGAAACAGCATAGCAAGTTCAAATAAGGCTAG
 TCCGTTATCAACTTGGCCCCGGAGCAGAAGACG
TCACGACATCACTTACGCTGAGTAGCTGCAGTC
TGCTCCGGGGCCAGTGGCACCAGTTCGGTGCTT
 TTTTT.

3. pEGFP-C1 (Clontech) and pmTagBFP2-C1 plasmid (Evrogen).

2.2 Materials for Cloning

1. Polymerase chain reaction (PCR) master mix (*see Note 3*).
2. A thermocycler.
3. An electrophoresis system.

4. 1× TAE buffer for electrophoresis: 40 mM Tris base, 20 mM acetic acid, 1 mM EDTA sodium salt dihydrate (prepared by diluting 50× TAE stock in nuclease-free water).
5. 1% Agarose gel: 1% (w/v) Agarose diluted in 1× TAE buffer.
6. Gel extraction and PCR cleanup kits.
7. AgeI, BamHI, and AseI restriction enzymes.
8. Gibson assembly reaction mixture [30] (*see Note 4*).

2.3 Primer Pairs Used for Cloning

1. dCas9-Forward: 5'-GCTACCGGTCGCCACCATGGTGCC CAAAAAGAAGAGGAAAGTGG-3'; dCas9-Reverse: 5'-ACT GCTGGATCCGTGGAAC ACCTACCTTGCGCTTTTTC TTGGGA-3'.
2. U6-sgTelo-MTSa-Forward: 5'-ATTAATAGTTATTAGAGGG CCTATTTC CC-3'; U6-sgTelo-MTSa-Reverse: 5'-ATGACC CCGTAATTGATTACTATTAATCGGTTGGCAGTGACTC CGTCTC-3'.
3. EGFP-Forward: 5'-ATTACCGCCATGCATTAGTTATTACG CGTTACATAACTTACGGTAAATG-3'; EGFP-Reverse: 5'-AATAGGCCCTCTA ATAACTATTAATAAGATACATTGATGAGTTTGGAC-3'.
4. BFP-Forward: 5'-ATTACCGCCATGCATTAGTTATTACGC GTTACATAACTTACGGTAAATG-3'; BFP-Reverse: 5'-AAT AGGCCCTCTAATAACTATTAATAAGATACATTGATGAG TTTGGAC-3'.
5. U6-sgSat-MTSb-Forward: 5'-ATTAATAGTTATTAGAGGG CCTATTTC-3'; U6-sgSat-MTSb-Reverse: 5'-ATGACC CCGTAATTGATTACTATTACTCGTCGGTCCCGGCATC CGAT-3'.

2.4 MBs

MTS-targeting MBs with a backbone composed of 2'-O-methyl RNA (2Me) and a fully phosphorothioate (PS)-modified loop domain can be synthesized by an oligonucleotide synthesis service provider (*see Note 5*). Sequences of MBs used in our experiments are listed below (*see Note 6*) (m represents 2Me modification, * represents PS linkage modification):

1. AMTSa-targeting MB labeled with an ATTO647N fluorophore at the 5' end and an Iowa Black RQ quencher at the 3' end (*see Note 7*) has the sequence: 5'-mCmUmUmCmG*mU*mC*mC*mA*mC*mA*mA*mA*mC*mA*mC*mA*mA*mC*mU*mC*mC*mU*mGmAmAmG-3'.
2. MTSb-targeting MB labeled with an Iowa Black FQ quencher at the 5' end and an ATTO488 fluorophore at the 3' end (*see Note 7*) has the sequence: 5'-mCmUmCmAmG*mC*mG*mU*mA*mA*mG*mU*mG*mA*mU*mG*mU*mC*mG*mU*mG*mA*mCmUmGmAmG-3'.

2.5 Cell Culture

1. HEK293 cells (American Type Culture Collection) (*see Note 8*).
2. Cell culture medium: Dulbecco's modified Eagle's medium (DMEM) without phenol red and antibiotics, supplemented with 10% (v/v) fetal bovine serum (FBS) and 2 mM L-glutamine.
3. Phosphate-buffered saline (PBS): 0.2 g/L KCl, 0.24 g/L KH_2PO_4 , 8 g/L NaCl, and 1.44 g/L Na_2HPO_4 (anhydrous) in nuclease-free water.
4. Trypsin: Phenol red-free solution of 0.25% (w/v) trypsin diluted in PBS.
5. 6-Well plates.

2.6 Microporation
(*See Note 9*)

1. Microporator.
2. PBS.
3. Electroporation buffer (*see Note 9*).
4. Electrolytic buffer (*see Note 9*).
5. Electroporation chamber (*see Note 9*).
6. Electroporation tube (*see Note 9*).
7. Cell culture medium (as in Subheading 2.5, *see Note 10*).
8. 8-Well chambered cover glass.
9. 10 $\mu\text{g}/\text{mL}$ Fibronectin.
10. Refrigerated microcentrifuge.
11. Cell-counting device.

2.7 Fluorescence In Situ Hybridization (FISH)

1. Nuclease-free water.
2. 4% PFA: 4% (w/v) Paraformaldehyde diluted in PBS.
3. 0.5% NP-40: 0.5% (v/v) Nonyl phenoxyethoxyethanol in PBS.
4. SSC buffer: $2\times/1\times/0.2\times$ Saline sodium citrate, pH 7 (prepared by diluting $20\times$ saline sodium citrate containing 3 M sodium chloride and 0.3 M sodium citrate in nuclease-free water).
5. Wash buffer: 10% (v/v) Formamide in $2\times$ SSC buffer.
6. Hybridization buffer: 1% (v/v) Tween 20, 10% (v/v) dextran sulfate, 50% (v/v) formamide, 500 ng/mL salmon sperm DNA in $2\times$ SSC buffer.
7. Telomere leading strand-targeting FISH probes labeled with carboxytetramethylrhodamine (TAMRA) that are optically distinct from MTSa-targeting MBs (*see Note 11*). The FISH probe sequence is TAMRA-CCCTAACCCCTAACCCCTAA.

8. RNase/DNase-free pipette tips.
9. DAPI: 100 ng/mL 4',6-Diamidino-2-phenylindole diluted in PBS.
10. Sealing film.

2.8 Immuno-fluorescence (IF)

1. Nuclease-free water.
2. 4% PFA: 4% (w/v) Paraformaldehyde diluted in PBS.
3. 0.5% TritonX-100: 0.5% (v/v) TritonX-100 diluted in PBS.
4. 0.05% TritonX-100: 0.05% (v/v) TritonX-100 diluted in PBS.
5. Blocking buffer: 1% (w/v) BSA, 10% (v/v) FBS in PBS.
6. Human anti-centromere antibodies (*see Note 12*).
7. Anti-human secondary antibodies labeled with Alexa647 that are optically distinct from MTSb-targeting MBs (*see Note 12*).
8. RNase/DNase-free pipette tips.
9. DAPI: 100 ng/mL 4',6-Diamidino-2-phenylindole diluted in PBS.

2.9 Microscope and Imaging Software

1. Inverted wide-field fluorescence microscope equipped for high-magnification digital imaging.
2. A CCD camera.
3. Proper filter sets for DAPI, EGFP, TRITC, Cy5, TAMRA, and ATTO647N imaging.
4. A filter set enabling simultaneous dual-color imaging (*see Note 13*).
5. Image acquisition software.
6. Image analysis software such as Fiji [31] (*see Note 14*).
7. MATLAB (Version R2014b 64-bit, MathWorks) (*see Note 14*).

3 Methods

3.1 Cloning

For efficient co-transfection and co-expression of all system components (sgRNA-MTS, a transfection indicator (EGFP or BFP), and dCas9) in HEK293 cells, a single plasmid containing all three components should be generated. The steps and details are as follows:

1. Generate pdCas9-C1 by inserting the PCR product of dCas9 from pSLQ1658-dCas9-EGFP into AgeI/BamHI-digested pEGFP-C1 vector (*see Subheading 2.3, Primer pair 1*).
2. For telomere labeling, generate a mammalian expression vector termed SL2-sgTelo-MTSa/EGFP/pdCas9-C1, in which sgRNA, EGFP, and dCas9 are expressed under the control of

separate promoters. Amplify the U6-sgRNA cassette from pU6-SL2-sgTelo-MTSa (*see* Subheading 2.3, Primer pair 2) and the CMV-EGFP cassette from pEGFP-C1 (*see* Subheading 2.3, Primer pair 3). Use Gibson Assembly to simultaneously clone the two PCR products into AseI-digested pdCas9-C1 to create SL2-sgTelo-MTSa/EGFP/pdCas9-C1. Generate SL2-sgTelo-MTSa/BFP/pdCas9-C1 similarly with the CMV-BFP cassette PCR amplified from pmTagBFP2-C1 plasmid (*see* Subheading 2.3, Primer pair 4).

3. For centromere labeling, SL2-sgSat-MTSb/BFP/pdCas9-C1 should be similarly generated as SL2-sgTelo-MTSa/BFP/pdCas9-C1. The U6-sgRNA cassette is PCR amplified from pU6-SL2-sgSat-MTSb (*see* Subheading 2.3, Primer pair 5).

3.2 Cellular Delivery of MBs

Deliver MBs into transfected HEK293 cells by microporation. The detailed protocol is as follows:

Day 0:

Seed the proper number of HEK293 cells into a 6-well plate with cell culture medium such that cells will reach 50–70% confluency on day 1 for transfection.

Day 1:

1. Add 200 μ L fibronectin into each well of the 8-well chambered cover glass and incubate at 37 °C overnight (*see* **Note 15**).
2. Transfect the cells seeded in the 6-well plate with 2 μ g of SL2-sgTelo-MTSa/EGFP/pdCas9-C1 for telomere labeling or SL2-sgSat-MTSb/BFP/pdCas9-C1 for centromere labeling. Transfect the cells with SL2-sgTelo-MTSa/BFP/pdCas9-C1 and SL2-sgSat-MTSb/BFP/pdCas9-C1 at a 1:1 ratio (1 μ g each) for dual labeling (*see* **Note 16**).

Day 2:

1. Aspirate the cell culture medium and incubate the cells with 1 mL pre-warmed PBS at room temperature (RT) for 2 min.
2. Aspirate the PBS and add 0.5 mL of trypsin. Incubate for 1 min at RT.
3. Aspirate the trypsin (leaving a trace amount). Incubate at 37 °C until all cells are detached from the plate surface.
4. Neutralize the remaining trypsin with ~1 mL of cell culture medium and gently pipette to resuspend the cells (*see* **Note 17**).
5. Transfer the cell suspension to a 1.5 mL microcentrifuge tube and pellet the cells by centrifugation at $400 \times g$ for 5 min at 4 °C (*see* **Note 18**).
6. Aspirate the medium and gently resuspend the cell pellet with 1 mL of PBS.

7. Count the cells.
8. Pellet the appropriate number of cells by centrifugation at $400 \times g$ for 5 min at 4 °C.
9. Aspirate the PBS carefully and resuspend the cell pellet in electroporation buffer at 5000 cells per μL .
10. For single-color labeling, add 1 μL of the 10 μM MTSa-targeting or MTSb-targeting MB solution for every 10 μL of cells to achieve a final MB concentration of 1 μM . For dual-color labeling, add 1 μL of the MTSa-targeting MB solution and 1 μL of the MTSb-targeting MB solution for every 10 μL of cells to achieve a final MB concentration of 2 μM .
11. Pipette to mix the cells with MBs.
12. Add 4 mL electroporation buffer into the electroporation tube.
13. Microporate 10 μL of the cell suspension in an electroporation chamber at 1150 V with a 20 ms pulse width and 2 pulses total (*see Note 19*).
14. Gently transfer the microporated cells from the tip to a microcentrifuge tube prefilled with 1.5 mL of fresh cell culture medium (*see Note 18*).
15. Pellet the cells by centrifugation at $400 \times g$ for 5 min at 4 °C.
16. Aspirate the medium to avoid disturbing the cell pellet (*see Note 20*). Resuspend the pellet gently with 1.5 mL medium.
17. Repeat **steps 15** and **16** two more times.
18. After the last wash, resuspend the cells in 250 μL of cell culture medium.
19. Seed the cells into a well of an 8-well chambered cover glass coated with fibronectin (*see Note 21*).
20. Incubate the cells in a cell incubator (37 °C, 5% (v/v) CO_2 , and 90% relative humidity). Cells can be imaged after sufficient time is given to allow cells to attach and spread on the coverslip (approximately 8 h).

3.3 Validation of CRISPR/MB Signals by DNA FISH

It is important to validate the specificity of CRISPR/MB signal to test the labeling accuracy and to exclude nonspecific signals. One straightforward validation method is to use DNA FISH to label the same locus and determine if the resulting signal colocalizes with the CRISPR/MB signal. Note that because of the helicase activity of dCas9 to unwind the target DNA duplex, DNA FISH can be performed without the high-temperature heating employed in conventional DNA FISH protocols. The detailed protocol is shown below:

Day 1:

1. Pipette out the cell culture medium from the 8-well chambered cover glass and incubate each well with 350 μ L PBS prewarmed to 37 °C for 5 min.
2. Pipette out the PBS and add 250 μ L of 4% PFA pre-warmed to 37 °C per well. Incubate for 30 min at RT to fix the cells.
3. Pipette out the PFA and incubate each well of the cells in 350 μ L PBS at RT for 5 min.
4. Pipette out the PBS and permeabilize the cells in 250 μ L of 0.5% NP-40 at RT for 10 min.
5. Pipette out the NP-40 and incubate the cells in 350 μ L PBS at RT for 5 min.
6. Pipette out the PBS and incubate each well of the samples with 250 μ L of TAMRA-labeled FISH probes (diluted in DNA hybridization buffer to a final concentration of 100 nM).
7. Wrap the chambered cover glass with sealing film to minimize evaporation. Protect from light and incubate at 37 °C overnight (>16 h).

Day 2:

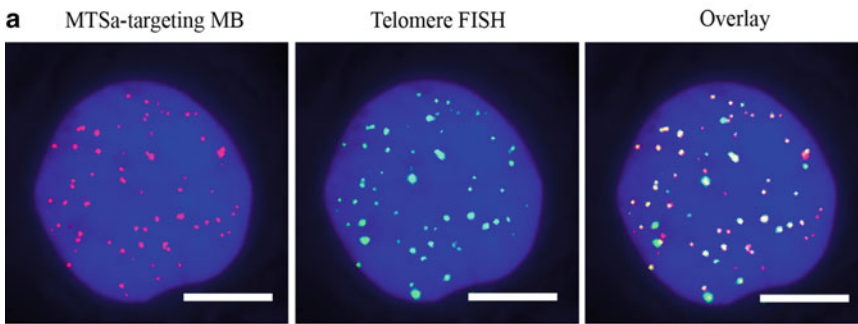
1. Gently pipette out unbound DNA FISH probes.
2. Wash cells in wash buffer followed by 2 \times SSC, 1 \times SSC, and 0.2 \times SSC to remove unhybridized probes. Do not let the samples dry between washes.
3. Incubate cells in PBS containing 100 ng/mL DAPI to stain the nucleus.
4. Use DAPI, TRITC, and Cy5 filter sets to image the nuclear, FISH, and MB signals, respectively. For FISH and MB signals, 3D image stacks should be obtained at an increment of 0.25 μ m in the z-direction. Representative maximum intensity projection images of the FISH and MB signals are shown in Fig. 2a (*see Note 22*).

3.4 Validation of CRISPR/MB Signals by Immunofluorescence (IF)

In some cases, IF is also an effective method to validate the labeling accuracy of CRISPR/MB, as the locus of interest, such as the major satellite repeats within centromere, is bound by many endogenous DNA-binding proteins. Thus, when antibodies that can specifically bind to the cognate binding proteins of the locus are used, the resulting IF signal can be used to validate the accuracy of the CRISPR/MB signal. The detailed protocol for IF is shown below.

1. Gently pipette out the cell culture medium from the 8-well chambered cover glass and incubate each well with 350 μ L PBS pre-warmed to 37 °C for 5 min.

SL2-sgTelo-MTSa



SL2-sgSat-MTSb

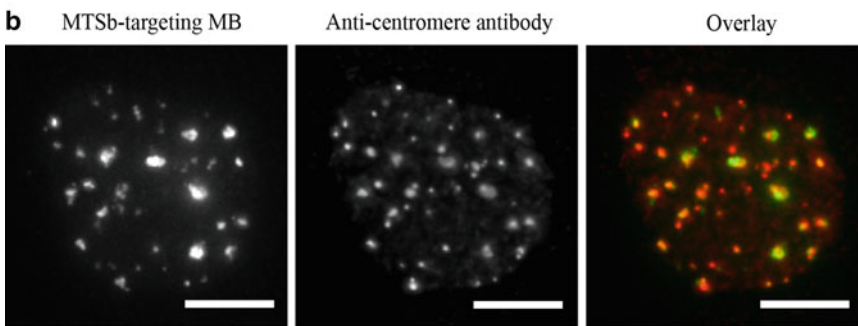


Fig. 2 Detection of telomeres or centromeres using CRISPR/MB and validation of labeling accuracy. **(a)** Labeling telomere loci by MBs and DNA FISH. Cells were first transfected with dCas9 and SL2-sgTelo-MTSa, followed by microporation of MTSa-targeting MBs (ATTO647N labeled). At 24 h post-microporation, cells were fixed and permeabilized and then processed by DNA FISH using telomere-targeting FISH probes (TAMRA labeled). Representative maximum intensity projection images of MTSa-targeting MBs and telomere-targeting FISH probes are shown. The nucleus is stained by DAPI. Scale bar = 10 μm . **(b)** HEK293 cell was transfected with dCas9 and SL2-sgSat-MTSb and microporated with MTSb-targeting MBs (ATTO488 labeled). Representative maximum intensity projection images of MTSb-targeting MBs and anti-centromere antibodies (Alexa647 labeled) are shown. Scale bar = 10 μm . This figure is created by modifying Fig. 2 and Fig. S5 of [27] with permission in accordance with the [Creative Commons Attribution Non-Commercial \(CC BY-NC 4.0\) License](#)

2. Pipette out the PBS and add 250 μL 4% PFA pre-warmed to 37 $^{\circ}\text{C}$ per well. Incubate at RT for 30 min to fix the cells.
3. Wash the cells with PBS briefly, and then permeabilize cells with 0.5% TritonX-100 for 30 min.
4. Wash the cells with 0.05% TritonX-100 for 5 min, followed by incubation for 60 min in blocking buffer.
5. Stain the cells with human anti-centromere antibodies (final concentration = 4.2 $\mu\text{g}/\text{mL}$) in blocking buffer for 60 min.
6. Wash cells thrice with 0.05% TritonX-100 for 5 min, and then stain cells with Alexa647-labeled anti-human secondary antibodies (final concentration = 1 $\mu\text{g}/\text{mL}$) in blocking buffer for 60 min.

7. Wash the labeled cells thrice with 0.05% TritonX-100 for 5 min.
8. Incubate cells in PBS, and then use FITC and Cy5 filter sets to image MB and IF signals, respectively. Representative fluorescence images of centromeres are shown in Fig. 2b (*see Note 23*).

3.5 Dual-Color Single-Particle Tracking Analysis

Dynamic properties of genomic loci can be determined by single-particle tracking analysis as described below (*see Notes 14 and 24*).

1. Open time-lapse images acquired at 100 ms per frame for 600 frames in Fiji.
2. Set image interval properties. Select Image > Properties, set *Channels (c)* to 1, *Slices (z)* to 1, *Frames (t)* to 600, *Unit of length* to “ μm ,” *Pixel width* and *Pixel height* to 0.16, *Voxel depth* to 0, *Frame interval* to 104 ms (*see Note 25*), and *Origin* to 0,0. Select *Global*.
3. Click Plugins > Tracking > TrackMate, check the parameters input in **step 2**, and click next.
4. Select *LoG detector* and click next.
5. Pre-filter the spots. Set *Estimated blob diameter* to 0.5 μm , and set appropriate *Threshold* to see most light spots. Select *Do sub-pixel localization*. Click next.
6. Review the settings for the pre-filtering process in **step 5**, and click next.
7. Improve spot selection by adjusting the initial threshold on the *Quality* feature and click next.
8. Select *HyperStack Displayer* so that the spots can be manually edited and click next.
9. Apply more filters, such as *Quality*, *Minimal Intensity*, and *Maximal intensity*, as needed. Click next.
10. Select *Simple LAP tracker*. Click next.
11. Set parameters for *Simple LAP tracker*. Set *Linking max distance* to 0.5 μm and *Gap-closing max frame gap* to 4 μm . For telomeres, *Gap-closing max distance* is set to 1 μm , and for centromeres, *Gap-closing max distance* is set to 0.7 μm (*see Note 26*). Click next.
12. Review the previous settings and click next.
13. Filter tracks by adjusting the threshold on the *Number of spots in track* feature. Click next.
14. Select *Display spots* and set *Spot display radius ratio* to 1. Select *Display tracks* and set *Limit frame depth* to 10. Click *Analysis* to obtain track statistics.

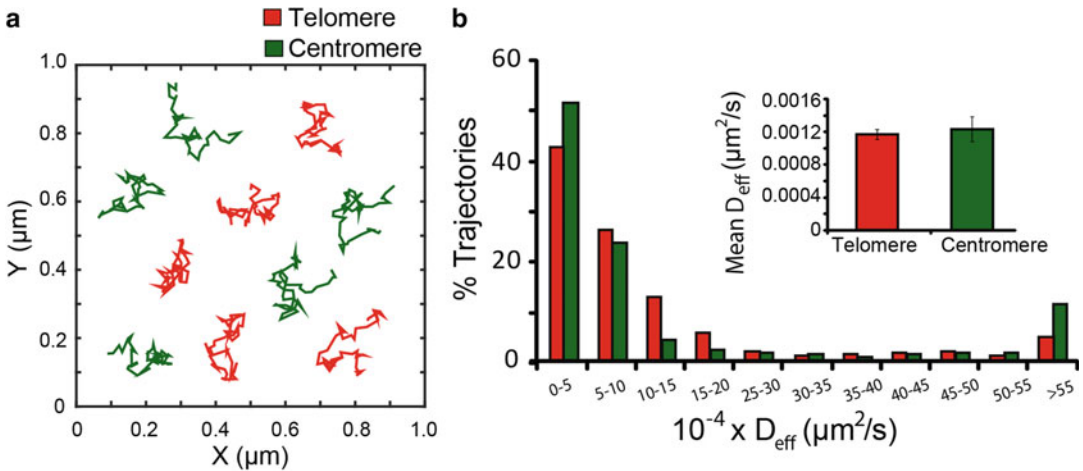


Fig. 3 Dual-color dynamic detection using CRISPR/MB. For dual-color labeling of telomere and centromere loci, HEK293 cells were transfected with dCas9, SL2-sgTelo-MTSa, and SL2-sgSat-MTSb, co-microperated with MTSa-targeting MBs (ATTO647N labeled) and MTSb-targeting MBs (ATTO488 labeled), and then imaged at 24 h post-microperation. **(a)** Representative full-track movements of single-telomere loci and single-centromere loci in living cells are shown. **(b)** The distribution of diffusion coefficients of telomeres ($n = 670$ tracks) and centromeres ($n = 243$ tracks) from at least 18 cells. Inset shows the mean \pm S.E. diffusion coefficients. This figure is created by modifying Fig. 4 of [27] with permission in accordance with the [Creative Commons Attribution Non-Commercial \(CC BY-NC 4.0\) License](#)

15. Save *Spots in Track Statistics* in the “.txt” format for further MSD analysis. Import the assigned tracks into @msdalyzer written in MATLAB (*see* **Note 27**). Results for MSD analysis of telomeres and centromeres are shown in Fig. 3.

4 Notes

1. We previously designed three different sgRNA-MTS scaffolds by inserting the MTS in the tetraloop, the stem-loop 2 (SL2-sgRNA-MTS), and the 3'-tail regions, and found that SL2-sgRNA-MTS is the most effective design. As a result, we used SL2-sgTelo-MTSa and SL2-sgSat-MTSb to label telomeres and centromeres, respectively.
2. To label a different locus, change the spacer sequence.
3. Q5[®] Hot Start High-Fidelity 2X Master Mix was used for PCR. Other commercially available PCR master mixes may be used.
4. CloneSmarter[®] seamless assembly cloning kit was used for Gibson assembly. An example protocol for preparing a Gibson assembly reaction mixture can be found at <http://miller-lab.net/MillerLab/protocols/molecular-biology-and-cloning/gibson-assembly/>.

5. Our previous studies have shown that MBs with such modifications are highly resistant to nuclease degradation and biocompatible in living cells [32]. Other MBs with similar features can potentially be used.
6. MTS-targeting MBs used in our experiments are not complementary to endogenous RNA targets in mammalian cells, and therefore the MB fluorescence should be significantly quenched unless hybridized to their MTS. MBs with other sequences not complementary to endogenous RNA targets in mammalian cells can potentially be used.
7. MBs with other dye-quencher pairs can also be used.
8. We have only tested this technique in mammalian cell lines, but we suspect that it would be applicable in other types of cells such as insect or plant cells.
9. Microporation was performed using equipment and buffers included in the Thermo Fisher Neon transfection system. Other electroporation methods can potentially be used for MB delivery.
10. Antibiotic-free medium was used to maximize cell survival during and after microporation.
11. Telomere-targeting FISH probes labeled with other dyes that are optically distinct from MTSa-targeting MBs can potentially be used.
12. We used anti-centromere antibodies derived from the serum of human patients with calcinosis, Raynaud's phenomenon, esophageal dysmotility, sclerodactyly, and telangiectasia (CREST) syndrome and Alexa647-labeled anti-human secondary antibodies for IF. Other anti-centromere antibodies and secondary antibodies labeled with other dyes that are optically distinct from MTSb-targeting MBs can potentially be used.
13. We used DV2-cube (ET525/50 m, 585dcxr, ET655lp, Photometrics) for simultaneous dual-color imaging of telomeres and centromeres.
14. Other software can potentially be used.
15. HEK293 cells attach and spread more rapidly on fibronectin-coated glass surfaces.
16. FuGENE[®] 6 was used for transfection in our experiments. Other transfection reagents can potentially be used.
17. Gentle pipetting minimizes cell damage.
18. When low-retention microcentrifuge tubes are used, cell pellets may not form.
19. Microporation parameters are cell line dependent.

20. Leave a small volume of medium ($\sim 50 \mu\text{L}$) in the microcentrifuge tube after every wash, as this minimizes the incidence of aspirating out the loose cell pellet formed by the small number of cells.
21. Wash the cover glass with enough PBS to remove unbound fibronectin. This step improves cell attachment as unbound fibronectin in solution can saturate the binding sites on the cells.
22. Detailed methods for identifying telomere loci and analyzing colocalization between FISH and MB signals in three dimensions can be found in [27].
23. Colocalization is not perfect because of the non-consensus nature of the α -satellite sequence within centromeres [16, 22].
24. Parameters used in this experiment are determined based on our dataset and experience. The operators should determine the optimal parameters and filter settings for their own experiments.
25. Although frame interval in cellSens Dimension for time-lapse acquisition was theoretically set to 100 ms, the real frame interval was ~ 104 ms due to the downtime between acquisitions.
26. *Linking max distance* defines the maximal displacement between two particles in adjacent frames that are considered to belong to the same track. *Gap-closing max frame gap* determines the maximal frame interval allowed between particle observations that may be considered as the same particle. *Gap-closing max distance* decides the maximal displacement allowed between particle observations with the gap-closing frame interval that may be considered to belong to the same track. For different datasets, these parameters could be altered accordingly.
27. For calculating the mean square displacement (MSD), tracks containing at least 15 time lags ($\Delta\tau$) were selected. The 2-dimensional diffusion coefficient (D_{eff}) was calculated by linear regression of the first 25% of total time lags of the MSD vs. $\Delta\tau$ dataset with minimum fitting threshold of $R^2 = 0.8$.

Acknowledgments

This work was supported by grants from the National Key R&D Program of China (2016YFA0501603), the National Natural Science Foundation of China (Nos. 31771583 and 81371613), the Beijing Natural Science Foundation (7162114), and China's 1000 Young Talent Award program.

References

- Misteli T (2013) The cell biology of genomes: bringing the double helix to life. *Cell* 152 (6):1209–1212. <https://doi.org/10.1016/j.cell.2013.02.048>
- Misteli T (2007) Beyond the sequence: cellular organization of genome function. *Cell* 128 (4):787–800. <https://doi.org/10.1016/j.cell.2007.01.028>
- Chen B, Guan J, Huang B (2016) Imaging specific genomic DNA in living cells. *Annu Rev Biophys* 45:1–23. <https://doi.org/10.1146/annurev-biophys-062215-010830>
- Li T, Meng YQ, Yao RY, Han H, Wu L, Zhou YN, Li ZQ, Zhang YF, Fu LG (2019) The associations between left-hand digit ratio (2D:4D) and puberty characteristics among Chinese girls. *Early Hum Dev* 130:22–26. <https://doi.org/10.1016/j.earlhumdev.2019.01.007>
- Horvath P, Barrangou R (2010) CRISPR/Cas, the immune system of bacteria and archaea. *Science* 327(5962):167–170. <https://doi.org/10.1126/science.1179555>
- Jinek M, Chylinski K, Fonfara I, Hauer M, Doudna JA, Charpentier E (2012) A programmable dual-RNA-guided DNA endonuclease in adaptive bacterial immunity. *Science* 337 (6096):816–821. <https://doi.org/10.1126/science.1225829>
- Anders C, Niewoehner O, Duerst A, Jinek M (2014) Structural basis of PAM-dependent target DNA recognition by the Cas9 endonuclease. *Nature* 513(7519):569–573. <https://doi.org/10.1038/nature13579>
- Jiang F, Zhou K, Ma L, Gressel S, Doudna JA (2015) A Cas9-guide RNA complex preorganized for target DNA recognition. *Science* 348 (6242):1477–1481. <https://doi.org/10.1126/science.aab1452>
- Sternberg SH, Redding S, Jinek M, Greene EC, Doudna JA (2014) DNA interrogation by the CRISPR RNA-guided endonuclease Cas9. *Nature* 507(7490):62–67. <https://doi.org/10.1038/nature13011>
- Cong L, Ran FA, Cox D, Lin S, Barretto R, Habib N, Hsu PD, Wu X, Jiang W, Marraffini LA, Zhang F (2013) Multiplex genome engineering using CRISPR/Cas systems. *Science* 339(6121):819–823. <https://doi.org/10.1126/science.1231143>
- Mali P, Yang L, Esvelt KM, Aach J, Guell M, DiCarlo JE, Norville JE, Church GM (2013) RNA-guided human genome engineering via Cas9. *Science* 339(6121):823–826. <https://doi.org/10.1126/science.1232033>
- Jinek M, East A, Cheng A, Lin S, Ma E, Doudna J (2013) RNA-programmed genome editing in human cells. *eLife* 2:e00471. <https://doi.org/10.7554/eLife.00471>
- Chen B, Gilbert LA, Cimini BA, Schnitzbauer J, Zhang W, Li GW, Park J, Blackburn EH, Weissman JS, Qi LS, Huang B (2013) Dynamic imaging of genomic loci in living human cells by an optimized CRISPR/Cas system. *Cell* 155(7):1479–1491. <https://doi.org/10.1016/j.cell.2013.12.001>
- Shao S, Chang L, Sun Y, Hou Y, Fan X, Sun Y (2017) Multiplexed sgRNA expression allows versatile single nonrepetitive DNA labeling and endogenous gene regulation. *ACS Synth Biol*. <https://doi.org/10.1021/acssynbio.7b00268>
- Ye H, Rong Z, Lin Y (2017) Live cell imaging of genomic loci using dCas9-SunTag system and a bright fluorescent protein. *Protein Cell* 8(11):853–855. <https://doi.org/10.1007/s13238-017-0460-0>
- Shao S, Zhang W, Hu H, Xue B, Qin J, Sun C, Sun Y, Wei W, Sun Y (2016) Long-term dual-color tracking of genomic loci by modified sgRNAs of the CRISPR/Cas9 system. *Nucleic Acids Res* 44(9):e86. <https://doi.org/10.1093/nar/gkw066>
- Fu Y, Rocha PP, Luo VM, Raviram R, Deng Y, Mazzoni EO, Skok JA (2016) CRISPR-dCas9 and sgRNA scaffolds enable dual-colour live imaging of satellite sequences and repeat-enriched individual loci. *Nat Commun* 7:11707. <https://doi.org/10.1038/ncomms11707>
- Qin P, Parlak M, Kuscü C, Bandaria J, Mir M, Szlachta K, Singh R, Darzacq X, Yildiz A, Adli M (2017) Live cell imaging of low- and non-repetitive chromosome loci using CRISPR-Cas9. *Nat Commun* 8:14725. <https://doi.org/10.1038/ncomms14725>
- Wang S, Su JH, Zhang F, Zhuang X (2016) An RNA-aptamer-based two-color CRISPR labeling system. *Sci Rep* 6:26857. <https://doi.org/10.1038/srep26857>
- Ma H, Tu LC, Naseri A, Huisman M, Zhang S, Grunwald D, Pederson T (2016) Multiplexed labeling of genomic loci with dCas9 and engineered sgRNAs using CRISPRainbow. *Nat Biotechnol* 34(5):528–530. <https://doi.org/10.1038/nbt.3526>
- Gibcus JH, Samejima K, Goloborodko A, Samejima I, Naumova N, Nuebler J, Kanemaki MT, Xie L, Paulson JR, Earnshaw WC, Mirny LA, Dekker J (2018) A pathway for mitotic

- chromosome formation. *Science* 359(6376). <https://doi.org/10.1126/science.aao6135>
22. Cheng AW, Jillette N, Lee P, Plaskon D, Fujiwara Y, Wang W, Taghbalout A, Wang H (2016) Casilio: a versatile CRISPR-Cas9-Pumilio hybrid for gene regulation and genomic labeling. *Cell Res* 26(2):254–257. <https://doi.org/10.1038/cr.2016.3>
 23. Ma H, Tu LC, Naseri A, Chung YC, Grunwald D, Zhang S, Pederson T (2018) CRISPR-Sirius: RNA scaffolds for signal amplification in genome imaging. *Nat Methods* 15(11):928–931. <https://doi.org/10.1038/s41592-018-0174-0>
 24. Ma H, Tu LC, Naseri A, Huisman M, Zhang S, Grunwald D, Pederson T (2016) CRISPR-Cas9 nuclear dynamics and target recognition in living cells. *J Cell Biol* 214(5):529–537. <https://doi.org/10.1083/jcb.201604115>
 25. Deng W, Shi X, Tjian R, Lionnet T, Singer RH (2015) CASFISH: CRISPR/Cas9-mediated in situ labeling of genomic loci in fixed cells. *Proc Natl Acad Sci U S A* 112(38):11870–11875. <https://doi.org/10.1073/pnas.1515692112>
 26. Knight SC, Xie L, Deng W, Guglielmi B, Witkowsky LB, Bosanac L, Zhang ET, El Beheiry M, Masson JB, Dahan M, Liu Z, Doudna JA, Tjian R (2015) Dynamics of CRISPR-Cas9 genome interrogation in living cells. *Science* 350(6262):823–826. <https://doi.org/10.1126/science.aac6572>
 27. Wu X, Mao S, Yang Y, Rushdi MN, Krueger CJ, Chen AK (2018) A CRISPR/molecular beacon hybrid system for live-cell genomic imaging. *Nucleic Acids Res* 46(13):e80. <https://doi.org/10.1093/nar/gky304>
 28. Ma Y, Wang M, Li W, Zhang Z, Zhang X, Wu G, Tan T, Cui Z, Zhang XE (2017) Live visualization of HIV-1 proviral DNA using a dual-color-labeled CRISPR system. *Anal Chem* 89(23):12896–12901. <https://doi.org/10.1021/acs.analchem.7b03584>
 29. Tyagi S, Kramer FR (1996) Molecular beacons: probes that fluoresce upon hybridization. *Nat Biotechnol* 14(3):303–308. <https://doi.org/10.1038/nbt0396-303>
 30. Gibson DG, Young L, Chuang RY, Venter JC, Hutchison CA 3rd, Smith HO (2009) Enzymatic assembly of DNA molecules up to several hundred kilobases. *Nat Methods* 6(5):343–345. <https://doi.org/10.1038/nmeth.1318>
 31. Schindelin J, Arganda-Carreras I, Frise E, Kaynig V, Longair M, Pietzsch T, Preibisch S, Rueden C, Saalfeld S, Schmid B, Tinevez JY, White DJ, Hartenstein V, Eliceiri K, Tomancak P, Cardona A (2012) Fiji: an open-source platform for biological-image analysis. *Nat Methods* 9(7):676–682. <https://doi.org/10.1038/nmeth.2019>
 32. Zhao D, Yang Y, Qu N, Chen M, Ma Z, Krueger CJ, Behlke MA, Chen AK (2016) Single-molecule detection and tracking of RNA transcripts in living cells using phosphorothioate-optimized 2'-O-methyl RNA molecular beacons. *Biomaterials* 100:172–183. <https://doi.org/10.1016/j.biomaterials.2016.05.022>



Using RNA Tags for Multicolor Live Imaging of Chromatin Loci and Transcription in *Drosophila* Embryos

Hongtao Chen and Thomas Gregor

Abstract

Elucidating the biological implications of higher order chromatin architectures in animal development requires simultaneous, quantitative measurements of chromatin dynamics and transcriptional activity in living specimen. Here we describe a multicolor labeling and live imaging approach in embryos of the fruit fly *Drosophila melanogaster*. The method allows simultaneous measurement of movements of specific loci and their transcriptional activity for developmental genes, enabling new approaches to probe the interaction between 3D chromatin architecture and regulation of gene expression in development.

Key words Quantitative live imaging, *Drosophila* embryos, Transcription, 3D genome architecture

1 Introduction

There is growing evidence for a regulatory role of the 3D architecture of chromatin for the control of gene expression during development and disease processes [1–3]. Ligation or thin sectioning-based genomic approaches provide snapshots of the global DNA connectivity map [4, 5]. However, the dynamics of the 3D chromatin architecture at the single-cell level has been difficult to assess due to fixed and pooled samples applied in such genomic assays. Here we present a multicolor labeling and live imaging method to visualize the movement of specific DNA loci in fly embryos. In particular, we combine molecular systems based on nascent RNA visualization and systems based on direct tagging of DNA loci to simultaneously measure the transcriptional activity of key developmental genes and their cis-regulatory elements using fluorescence microscopy. This method allows measurement and analysis of 3D chromatin dynamics and gene activity in real time and with single live-cell resolution.

Using CRISPR-Cas9 technology, endogenous genes are edited with RNA stem-loop cassettes, which were pioneered in single-celled organisms to study RNA transcription, splicing, and

transport [6–8]. Two orthogonal systems (MS2 and PP7) have been adopted for *Drosophila* [9–11]. Nascent mRNAs transcribed from the tagged loci carry stem-loops at their 5' ends, preferably intronic regions. These stem-loops are recognized by corresponding genetically encoded coupling or coat proteins fused to various fluorescent proteins, enabling visualization of the physical locations and transcriptional activity of the tagged loci. Furthermore, we introduced a DNA labeling approach based on the bacteria DNA partitioning system (parABS). Here, a *parS* sequence from *Burkholderia* was incorporated into the designated loci [12–14] and maternally supplied ParB proteins then bound to the *parS* sequence and aggregated to form diffraction-limited spots.

In this protocol, we provide details regarding the construction of CRISPR-edited flies, embryo preparation and mounting, choice of fluorescent protein combinations for multicolor live imaging, and optimized conditions of point-scanning confocal microscopy for acquisition of high-quality 3D time-lapse images for localization analysis. In particular, we discuss the relevant controls required to assess the experimental errors associated with the measured distance between the tagged loci.

2 Materials

2.1 Fly Lines

1. Maternal Cas9 lines [15, 16] (*see Note 1*).
2. Maternal phiC31 integrase lines [17] (*see Note 2*).
3. Maternal lines that contain three fluorescent protein fusions for three-color live imaging [18] (*see Note 3*).

2.2 Labeling Endogenous Loci

1. Plasmids for CRISPR-based *Drosophila* genome editing [15] (*see Note 4*).
2. Plasmids for recombination-mediated cassette exchange (RMCE) [19, 20].
3. Plasmids for stem-loop series [7] (*see Note 5*).
4. Plasmids for *parS*-based genome labeling [12, 18] (*see Note 6*).

2.3 Genome Editing and Recombination

1. Embryo collection cages.
2. Agar plates: 1% Agar in 20% Welch's concord grape juice.
3. Mesh wells for embryo collection.
4. Halocarbon 200.
5. 50% Commercial bleach: 4.1% Sodium hypochlorite solution.
6. Double-sided tapes (Scotch, permanent).
7. Cover glass (22 × 50 mm).

8. Drying chamber (15 × 10 × 5 cm) filled with Drierite desiccant (3 cm in depth).
9. Femtotip II microinjection needles (Eppendorf).
10. FemtoJet pump (Eppendorf).
11. Microinjection station.
12. Humidity chamber.
13. *Drosophila* food vials.
14. Fluorescence stereoscope for phenotyping.

2.4 Embryo Live Imaging

1. Embryo collection cages.
2. Agar plates: 1% Agar in 20% Welch's concord grape juice.
3. Ultrathin air-permeable membrane (Lumox film 25 μm, Sarstedt Inc.).
4. 3D printed membrane holders [21].
5. Dissecting needles.
6. Heptane glue (*see Note 7*).
7. Halocarbon 27.
8. Cover glass (18 × 18 mm, No. 1.5).
9. Confocal microscope with multiple laser lines and high-sensitivity photon detectors.
10. Three-color-coated TetraSpec beads (200 nm).
11. Autofluorescent plastic slide (Chroma) for flat-field adjustment.

3 Methods

We provide detailed protocols for generating fly lines that carry multiple-edited genomic loci. Crossing males from these lines with the three-color females will produce embryos for multicolor live imaging. We advocate strict controls during sample preparations and live imaging procedures in order to obtain high-quality and reproducible image data for quantitative analysis.

3.1 Editing of Endogenous Genes to Contain MS2, PP7, and parS Tags

Cas9-mediated homologous recombination is used to integrate RNA stem-loop sequences or parS sites at the target gene loci. To enhance the flexibility of the *in vivo* design, an intermediate step using recombination-mediated cassette exchange (RMCE) is adopted (Fig. 1a).

3.1.1 Cas9-Mediated Knock-In

1. Select a guide RNA (gRNA) target site that contains a protospacer adjacent motif (PAM, 5'-NGG-3') [15]. The PAM site should be as close to the targeted locus as possible. Two gRNA

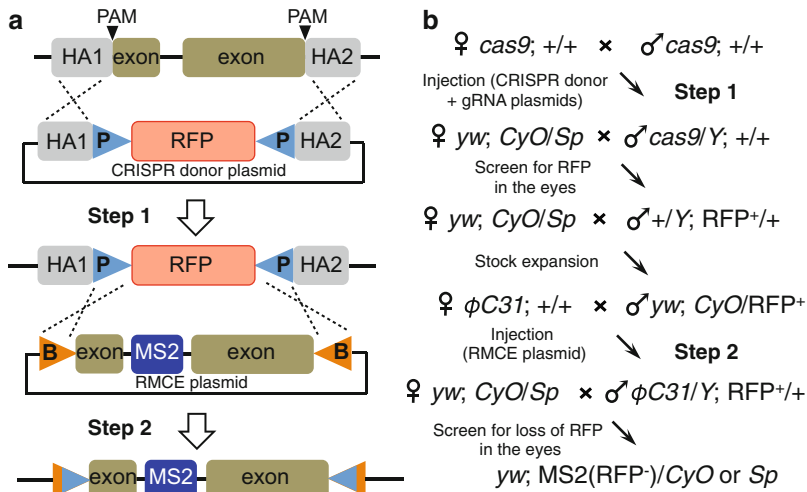


Fig. 1 Genomic integration of live imaging tags through CRISPR-Cas9-based genome editing and attB/attP cassette exchange. **(a)** A two-step approach to insert MS2 stem-loops in the intron of a target gene. In the first step, the intron and the adjacent exons are replaced by an eye-expressing RFP marker flanked by two attP sites (P) through CRISPR-mediated homologous recombination. PAM, protospacer adjacent motif. HA, homologous arm. In the second step, the deleted genomic sequence with an MS2 tag in the intron is inserted between two attB (B) sites and introduced back to the genome through attB/attP recombinations. The same method also applies to other imaging tags (PP7 or parS). **(b)** Crossing scheme to generate transgenic flies through the two-step integration approach. A target gene on the second chromosome is shown as an example. Appropriate balancers should be used for target genes on the other chromosomes (see **Note 12**)

target sites can be used to delete up to 20 kb genomic region if genomic modifications, such as deletions and point mutations, are desired in the following experiments. Depending on the locus of interest, the deleted region may include coding sequences and/or cis-regulatory elements.

2. Sequence the gRNA recognition sites from the target genome to avoid point mutations.
3. Generate plasmids that express the gRNAs [22] (see **Note 8**).
4. Clone the flanking homologous regions into the donor plasmid, in which a phenotypic selection marker flanked with two attP sites is located between the two homologous arms (see **Note 9**). The attP sites are designed for introducing stem-loops or parS tags through RMCE.
5. Set up embryo collection cages with germline-supplied Cas9 females and males carrying the target genome. Embryos collected from these cages are used for fly transformation.
6. Follow Subheading 3.2 to generate transgenic flies with the targeted deletion and integrated attP sites by co-injecting the gRNA-expressing plasmid (or two plasmids if two gRNA target sites are selected) and the homologous donor plasmid to embryo germline.

3.1.2 *Integration of MS2 Stem-Loops, PP7 Stem-Loops, or parS Tags Through RMCE*

1. Construct the RMCE plasmid that contains the designated stem-loops or parS sequence flanked by two attB sites (*see Note 10*). If a deletion is generated from the CRISPR step, the deleted genomic region should also be included in the RMCE plasmid.
2. Set up embryo collection cages with germline-supplied phiC31 females and males that carry the Cas9-mediated attP knock-in. Embryos collected from these cages are used for fly transformation. Follow Subheading 3.2 to generate transgenic flies with the integrated imaging tags. Negative selection, i.e., loss of the marker introduced with the Cas9-mediated knock-in, is used to identify transformants.

3.2 *Generation of Transgenic Fly Lines*

Transgenic fly lines are generated through germline injections. In-home injections are recommended to facilitate fly maintenance and speed up experiments. Different loci are generated separately and genetically combined in cis or trans to create embryos that carry multiple-edited loci.

3.2.1 *Embryo Collection and Mounting*

1. Collect ~300 virgin females from the maternal Cas9 or integrase lines and put them together in an embryo collection bottle with ~100 males that carry the targeted genomic loci. Multiple collection bottles may be set up to increase embryo yield.
2. 0–1-h-old embryos are collected on agar plates. 100–200 embryos are enough for a 1-h injection session.
3. To dissolve chorion, add 50% bleach onto the plates for 1 min. Swirl gently every 20 s. Pour the de-chorionated embryos into a plastic mesh well. Rinse with tap water for 1 min.
4. Transfer embryos onto a 60 × 30 × 10 mm 1% agar block and align them perpendicular to the edge of the block. The anterior tips of the embryos should face to the edge. Leave a space of 2 mm between the embryo tips and the edge of the agar block. The adjacent embryos should be separated by ~1 mm. An experienced injector is able to align 40 embryos in about 6 min.
5. Cover the long side of a piece of 50 mm cover glass with double-sided tape. Adhere the aligned embryos to the tape on the cover glass. The embryos' posterior tips should point to the edge of the coverslip after transfer.
6. Dry the embryos in the desiccant chamber. Drying time varies between 0 and 5 min depending on seasons and weather conditions (*see Note 11*).
7. Take out the coverslip from the desiccant chamber and cover the embryos with Halocarbon 200.
8. Repeat **steps 4–7** for 20 min or until all embryos are mounted.

3.2.2 *Germline Injection*

1. Load 4 μL of DNA solution to the Femtotip II needle and mount the needle to the microinjection station.
2. Load the embryo slide on the microinjection station.
3. Adjust the position of the needle to make sure that the embryos and the tip of the needle are on the same focal plane.
4. Gently push the needle into the germplasm. The embryo does not leak if appropriate drying time is applied.
5. Adjust the compensation pressure on the FemtoJet to avoid absorption of germplasm into the needle. For a new needle, 50 hPa is desirable. Compensation pressure needs to be adjusted during injection when the needle is worn or partially clogged.
6. Adjust the injection pressure to five times as high as the compensation pressure and inject.
7. After all the embryos on the cover glass are injected, move the cover glass into a humidity chamber saturated with water vapor. Larvae are expected to hatch after 48 h at 18 °C or after 24 h at 25 °C.
8. Pick the larvae using a dissecting needle and transfer them into regular *Drosophila* food vials (20–30 larvae per vial). Avoid halocarbon during the transfer.
9. When the adults hatch, cross them with appropriate balancer lines (*see Note 12*). In the next generation, screen for the gain or loss of selection markers (Fig. 2b, also *see Note 13*). PCR genotyping is optional to confirm the edited region.
10. Two edited loci can be recombined in cis following standard *Drosophila* genetics protocols. Screening for recombinants should be performed 3 days after hatching if eye markers are used.

3.3 *Embryo Preparation for Live Imaging*

1. Set up crosses to get triple-heterozygous females that supply all three fluorescent proteins (MCP-3xtagBFP2, PCP-3xmKate2, and ParB-eGFP).
2. Collect ~100 three-color virgin females and put them in an embryo-collecting cup with ~50 males that carry the edited loci (Fig. 2a).
3. Set up a sample holder with a piece of air-permeable membrane as described in [9]. Add 50 μL of heptane glue on at the center of the membrane. The glue should be completely dried when the embryos are mounted.
4. Collect embryos at desired age on agar plates.
5. Cut a piece of double-sided tape (2 cm long) and push it against the surface of the agar plates to adhere embryos on it.

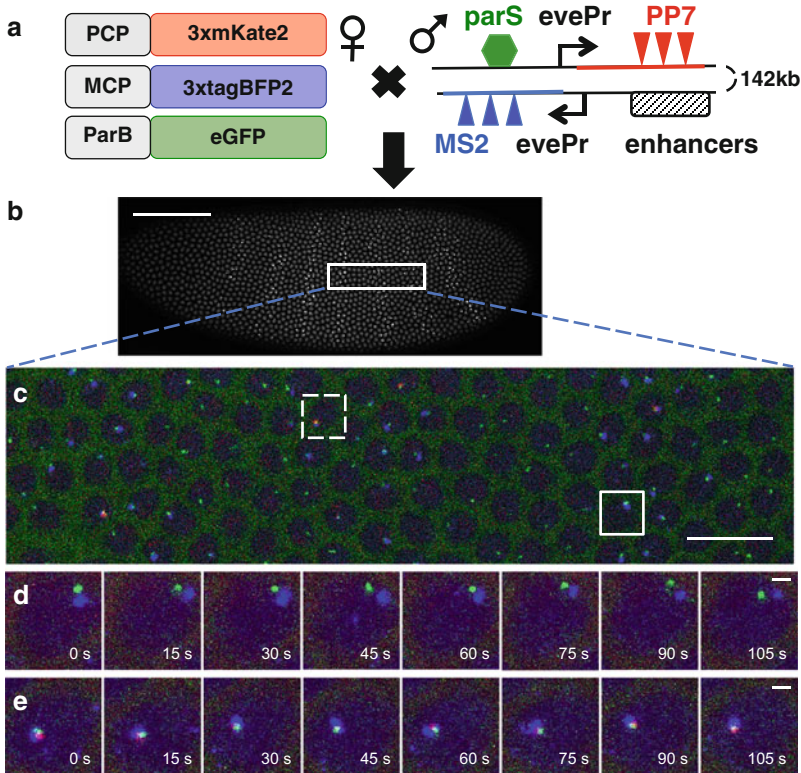


Fig. 2 Three-color live imaging of interactions between tagged genomic loci in *Drosophila* embryos. **(a)** Male flies carrying genomic loci labeled with MS2, PP7, and parS tags are crossed with females containing three fluorescent protein fusions that recognize the specific tags. In this example, we designed a synthetic system to visualize the long-range interaction between the *even-skipped* (*eve*) enhancers and a transgene reporter located 142 kb upstream to the *eve* locus. The endogenous *eve* gene is labeled with MS2 stem-loops, while the reporter transgene is labeled with PP7 stem-loops and parS tag. Physical locations and transcriptional activity of the tagged *eve* and reporter loci are measured in the embryos generated from this genetic cross. **(b)** Snapshot of a representative embryo from three-color live imaging; blue channel for the MS2 signal is shown; anterior is to the left. **(c)** Overlay image of the three channels of the region marked by the white box in **(b)**. Note that the blue spots (MS2) mark the locations of the *eve* locus (via tagged nascent RNA), green spots (parS) mark the locations of the reporter transgene, and red signal (PP7) indicates transcription activity of the reporter transgene. **(d)** A time series of eight snapshots following the nucleus marked with the solid white box in **(c)**. Note that the blue and the green signals are physically separated and the red signal is not present during the time course. **(e)** A time series of eight snapshots following the nucleus marked within the dashed white box as in **(c)**. Note the presence of red signals and the overlap of the blue and the green spots. All images are z (apical-basal axis) projections from 25 optical sections covering 8 μm . Scale bars: 100 μm in **(b)**, 10 μm in **(c)**, and 1 μm in **(d)** and **(e)**

6. Flip the double-sided tape. Use a dissecting needle to gently push each embryo from the direction perpendicular to its anterior-posterior axis, so that chorion sticks to the tape and breaks to expose the inside of the embryo. Prevent the embryo vitelline from touching the tape.

7. Mount the de-chorionated embryos on the air-permeable membrane with the designated dorsal-ventral orientation. The orientation should be adjusted before the embryos touch the glue (*see Note 14*). Finish embryo mounting in 8 min at 40% humidity and 25 °C. 20–30 embryos are expected to be mounted.
8. Add 50 μL of halocarbon 27 on the embryos and cover them with an 18×18 mm cover glass (No. 1.5). Avoid any shearing. The embryos should keep their dorsal-ventral orientation.

3.4 *Imaging of Embryos*

Here we provide protocols and microscope setups for the Leica SP5 point-scanning confocal system. The protocols are also suitable for other multicolor confocal microscopes (e.g., Zeiss, Nikon). Image examples are shown in Fig. 2. Three laser lines are used: a diode laser for 405 nm, an argon laser for 488 nm, and a HeNe for 591 nm. The powers are set at 0.4 μW , 1.1 μW , and 0.5 μW , respectively. Light intensities at the sample are estimated to be 13, 36, and 17 $\mu\text{W}/\text{cm}^2$, respectively.

1. Start imaging when the embryo develops to the desired stage. Find the embryos with bright-field illumination using a $20\times$ objective and save their XY locations.
2. Acquire images through a high-magnification ($63\times$), high-NA (1.44) oil-immersion objective. Use HyD photon counters to provide high sensitivity and a broad dynamic range. Set voxel size to $107 \times 107 \times 330$ nm. For cellular blastoderm, image a z-stack of 8 μm that covers the entire nuclei at the embryo periphery.
3. Scan at 700 Hz and accumulate three scans per line. Two sequential scans are used, alternating with each line, 405 nm and 591 nm scan simultaneously, followed by the 488 nm scan.
4. Once the acquisition is done, take a full embryo image at the midsagittal plane using a $20\times$ objective in order to register anterior-posterior positions.
5. Take a flat-field image using a Chroma autofluorescent plastic slide. Reduce power to avoid saturation. The flat-field image is used to control uneven illumination in the image field of view.

3.5 *Correction of Errors Associated with Fluorescent Spot Distance Measurements*

1. Measure three-color TetraSpec beads at different laser powers to obtain images with intensities matching the dynamic range of the acquired MS2-, PP7-, or parS-system-tagged spots.
2. Measure a control fly line in which blue, green, and red spots are physically co-localized. We use a reporter line with alternating MS2 and PP7 stem-loops. Cross males from this line with females carrying NLS-MCP-3xtagBFP2, MCP-eGFP, and PCP-mCherry (or PCP-mKate2). Image the embryos with the same microscope settings.

3. Localization errors are estimated from the distributions of the distance between the co-localized spots measured from fluorescent beads and live embryo control constructs. The variance of distance distribution from these controls can be subtracted from the mean squared distances between two spots obtained from a time series of measurement (e.g., Fig. 2d, e).

3.6 Image Analysis

Custom MATLAB code is available upon request. The code includes nuclear registration, spot segmentation and tracking, chromatic aberration correction, and MSD analysis. Detailed descriptions can be found in [18].

4 Notes

1. In these lines, Cas9 is materially expressed from a nos-Cas9 or vas-Cas9 source integrated at designated genomic locations. See genome editing resource at Bloomington Drosophila Stock Center (BDSC) for more information (https://bdsc.indiana.edu/stocks/genome_editing/crispr_cas9.html). In this protocol, we engineered the second chromosome as an example and used BDSC #51324, in which a vas-Cas9 transgene is inserted at the third chromosome and marked with a body color marker (*yellow, y*).
2. We used BDSC #34770 as the maternal phiC31 integrase source. These female flies provide integrase activity in their germlines, which induces attB/attP recombination to incorporate transgenes. For more information about the selection of integrase lines, see <https://bdsc.indiana.edu/stocks/phiC31/index.html>.
3. eGFP is fused to the N-terminus of the Burkholderia parB protein. Due to the slow turnover of ParB proteins at the parS site, the highly photostable eGFP fusion ensures long-time visualization of the parS-tagged loci. MCP is fused with a 3xtagBFP2. A nuclear localization signal (NLS) is added to the fusion, which leads to strong nuclear enrichment of the fusion protein. This increased nuclear background helps to overcome the relatively low photostability of blue fluorescent proteins and allows continuous detection of transcription spots across the blastoderm stage. PCP is fused with 3xmKate2 to provide good spectral separation from the green channel. An NLS is added to increase nuclear concentration of the fusion protein. NLS-PCP-3xmKate2 is enriched in the cytoplasm until 10 min before gastrulation. Three transgenic lines (nos-NLS-MCP-3xtagBFP2, nos-NLS-PCP-3xmKate2, and vas-ParB-eGFP) were generated separately through germline injections. A homozygously combined stock (PCP-3xmKate2; vas-ParB-eGFP) is maintained and available upon request.

4. See flyCRISPR (<http://flycrispr.molbio.wisc.edu/>) and Addgene (<http://www.addgene.org/crispr/oconnor-giles/>) for details about CRISPR designs. We used Addgene 51434 for generating CRISPR donor plasmid for homology-directed repair and Addgene 45946 for generating plasmids expressing guide RNAs.
5. The stems and/or the linkers in the step loop series may contain binding sites for tissue or temporal specific transcription factors; thus tagging the gene with stem-loop sequences may influence its expression pattern. A quantitative comparison between the expression pattern of the edited locus and the endogenous gene is recommended. In the case where undesired ectopic expression occurs, stem or linker sequences should be modified.
6. *parS* sequence from *Burkholderia cenocepacia* (J2315, chr3:3440-3821, GB: AM747722) is used for genome labeling. The method is adapted from reference [12]. See Addgene (https://www.addgene.org/Kerstin_Bystricky/) for more information about Bystricky group plasmids.
7. To create heptane glue, cut ~100 cm of permanent Scotch double-sided tape and put it into a 20 mL scintillation vial. Add 15 mL of heptane. Rock the vial on a horizontal shaker (100 rpm) for 24 h. Transfer the heptane into a 15 mL Corning tube and centrifuge at $1000 \times g$ for 10 min. Take the supernatant and store at 4 °C.
8. It is recommended to test the cutting efficiency of the two target gRNA plasmids before homologous donor injection.
9. Homologous arms from the target genome should be sequenced and used for constructing the integration donor plasmid. Length of homologous arms can range from 0.5 to 1.5 kb.
10. Presence of more than 12 repeats of MS2 or PP7 stem-loops in the 5'UTR of the tested genes (hb, Kr, kni, eve, and run) caused gene inactivation as seen by the lack of phenotypic rescue. In order to create viable tagged gene constructs able to rescue a null mutant, it is recommended that the stem-loops are integrated in the intron or in the 3'UTR.
11. A drying test before formal injections is recommended. An empirical indication of appropriate drying time is that about 20% embryos leak when the needle shoves into the germplasm.
12. Balancer lines contain chromosomes with multiple inversions, which prevent viable meiotic recombinations. This is particularly important for tracking and maintaining transgenes that lack visible markers. See BDSC information about balancers (<https://bdsc.indiana.edu/stocks/balancers/index.html>).

13. We recommend fluorescent eye markers (e.g., RFP or GFP). These are most clearly identified in a *white* (*w*) mutant background. If a *w* + background is used, adult flies should be screened 3 days after emergence for fluorescence. Ommatidia near the equator are the most conspicuous spots of fluorescent signals.
14. Adjust dorsal-ventral orientation using the dissecting needle. Gently rotate the embryos on the needle tip with the help of the broken chorion.

References

1. Furlong EEM, Levine M (2018) Developmental enhancers and chromosome topology. *Science* 361(6409):1341–1345. <https://doi.org/10.1126/science.aau0320>
2. Dekker J, Belmont AS, Guttman M, Leshyk VO, Lis JT, Lomvardas S, Mirny LA, O’Shea CC, Park PJ, Ren B, Politz JCR, Shendure J, Zhong S, Network DN (2017) The 4D nucleome project. *Nature* 549(7671):219–226. <https://doi.org/10.1038/nature23884>
3. Vermunt MW, Zhang D, Blobel GA (2019) The interdependence of gene-regulatory elements and the 3D genome. *J Cell Biol* 218(1):12–26. <https://doi.org/10.1083/jcb.201809040>
4. Beagrie RA, Scialdone A, Schueler M, Kraemer DC, Chotalia M, Xie SQ, Barbieri M, de Santiago I, Lavitas LM, Branco MR, Fraser J, Dostie J, Game L, Dillon N, Edwards PA, Nicodemi M, Pombo A (2017) Complex multi-enhancer contacts captured by genome architecture mapping. *Nature* 543(7646):519–524. <https://doi.org/10.1038/nature21411>
5. Gibcus JH, Samejima K, Goloborodko A, Samejima I, Naumova N, Nuebler J, Kanemaki MT, Xie L, Paulson JR, Earnshaw WC, Mirny LA, Dekker J (2018) A pathway for mitotic chromosome formation. *Science* 359(6376):eaaa06135. <https://doi.org/10.1126/science.aao6135>
6. Larson DR, Zenklusen D, Wu B, Chao JA, Singer RH (2011) Real-time observation of transcription initiation and elongation on an endogenous yeast gene. *Science* 332(6028):475–478. <https://doi.org/10.1126/science.1202142>
7. Hocine S, Raymond P, Zenklusen D, Chao JA, Singer RH (2013) Single-molecule analysis of gene expression using two-color RNA labeling in live yeast. *Nat Methods* 10(2):119–121. <https://doi.org/10.1038/nmeth.2305>
8. Golding I, Paulsson J, Zawilski SM, Cox EC (2005) Real-time kinetics of gene activity in individual bacteria. *Cell* 123(6):1025–1036. <https://doi.org/10.1016/j.cell.2005.09.031>
9. Garcia HG, Tikhonov M, Lin A, Gregor T (2013) Quantitative imaging of transcription in living *Drosophila* embryos links polymerase activity to patterning. *Curr Biol* 23(21):2140–2145. <https://doi.org/10.1016/j.cub.2013.08.054>
10. Fukaya T, Lim B, Levine M (2016) Enhancer control of transcriptional bursting. *Cell* 166(2):358–368. <https://doi.org/10.1016/j.cell.2016.05.025>
11. Lucas T, Ferraro T, Roelens B, De Las Heras Chanes J, Walczak AM, Coppey M, Dostatni N (2013) Live imaging of bicoid-dependent transcription in *Drosophila* embryos. *Curr Biol* 23(21):2135–2139. <https://doi.org/10.1016/j.cub.2013.08.053>
12. Saad H, Gallardo F, Dalvai M, Tanguy-le-Gac N, Lane D, Bystricky K (2014) DNA dynamics during early double-strand break processing revealed by non-intrusive imaging of living cells. *PLoS Genet* 10(3):e1004187. <https://doi.org/10.1371/journal.pgen.1004187>
13. Mariame B, Kappler-Gratias S, Kappler M, Balor S, Gallardo F, Bystricky K (2018) Real-time visualization and quantification of human cytomegalovirus replication in living cells using the ANCHOR DNA labeling technology. *J Virol* 92(18):e00571–e00518. <https://doi.org/10.1128/JVI.00571-18>
14. Dubarry N, Pasta F, Lane D (2006) ParABS systems of the four replicons of *Burkholderia cenocepacia*: new chromosome centromeres confer partition specificity. *J Bacteriol* 188(4):1489–1496. <https://doi.org/10.1128/JB.188.4.1489-1496.2006>
15. Gratz SJ, Harrison MM, Wildonger J, O’Connor-Giles KM (2015) Precise genome editing of *Drosophila* with CRISPR RNA-guided

- Cas9. *Methods Mol Biol* 1311:335–348. https://doi.org/10.1007/978-1-4939-2687-9_22
16. Kondo S, Ueda R (2013) Highly improved gene targeting by germline-specific Cas9 expression in *Drosophila*. *Genetics* 195(3):715–721. <https://doi.org/10.1534/genetics.113.156737>
 17. Bischof J, Maeda RK, Hediger M, Karch F, Basler K (2007) An optimized transgenesis system for *Drosophila* using germ-line-specific phiC31 integrases. *Proc Natl Acad Sci U S A* 104(9):3312–3317. <https://doi.org/10.1073/pnas.0611511104>
 18. Chen H, Levo M, Barinov L, Fujioka M, Jaynes JB, Gregor T (2018) Dynamic interplay between enhancer-promoter topology and gene activity. *Nat Genet* 50(9):1296–1303. <https://doi.org/10.1038/s41588-018-0175-z>
 19. Chen H, Xu Z, Mei C, Yu D, Small S (2012) A system of repressor gradients spatially organizes the boundaries of Bicoid-dependent target genes. *Cell* 149(3):618–629. <https://doi.org/10.1016/j.cell.2012.03.018>
 20. Bateman JR, Lee AM, Wu CT (2006) Site-specific transformation of *Drosophila* via phiC31 integrase-mediated cassette exchange. *Genetics* 173(2):769–777. <https://doi.org/10.1534/genetics.106.056945>
 21. Garcia HG, Gregor T (2018) Live imaging of mRNA synthesis in *Drosophila*. *Methods Mol Biol* 1649:349–357. https://doi.org/10.1007/978-1-4939-7213-5_23
 22. Gratz SJ, Cummings AM, Nguyen JN, Hamm DC, Donohue LK, Harrison MM, Wildonger J, O'Connor-Giles KM (2013) Genome engineering of *Drosophila* with the CRISPR RNA-guided Cas9 nuclease. *Genetics* 194(4):1029–1035. <https://doi.org/10.1534/genetics.113.152710>

Part VI

Specific Techniques for the Analysis of RNA Functions



Integrated Genome-Scale Analysis and Northern Blot Detection of Retrotransposon siRNAs Across Plant Species

Marcel Böhrrer, Bart Rymen, Christophe Himber, Aude Gerbaud, David Pflieger, Debbie Laudencia-Chingcuanco, Amy Cartwright, John Vogel, Richard Sibout, and Todd Blevins

Abstract

Cells have sophisticated RNA-directed mechanisms to regulate genes, destroy viruses, or silence transposable elements (TEs). In terrestrial plants, a specialized non-coding RNA machinery involving RNA polymerase IV (Pol IV) and small interfering RNAs (siRNAs) targets DNA methylation and silencing to TEs. Here, we present a bioinformatics protocol for annotating and quantifying siRNAs that derive from long terminal repeat (LTR) retrotransposons. The approach was validated using small RNA northern blot analyses, comparing the species *Arabidopsis thaliana* and *Brachypodium distachyon*. To assist hybridization probe design, we configured a genome browser to show small RNA-seq mappings in distinct colors and shades according to their nucleotide lengths and abundances, respectively. Samples from wild-type and *pol IV* mutant plants, cross-species negative controls, and a conserved microRNA control validated the detected siRNA signals, confirming their origin from specific TEs and their Pol IV-dependent biogenesis. Moreover, an optimized labeling method yielded probes that could detect low-abundance siRNAs from *B. distachyon* TEs. The integration of de novo TE annotation, small RNA-seq profiling, and northern blotting, as outlined here, will facilitate the comparative genomic analysis of RNA silencing in crop plants and non-model species.

Key words siRNAs, Northern blotting, RNA polymerase IV (Pol IV), Long terminal repeat (LTR) retrotransposon, *Arabidopsis thaliana*, *Brachypodium distachyon*

1 Introduction

RNA interference is a form of sequence-specific gene silencing in eukaryotes: double-stranded RNAs (dsRNAs), arising in cells or of exogenous origin, are diced into small interfering RNAs (siRNAs), which guide the cleavage of complementary RNA targets leading to transcript degradation [1, 2]. Key evidence for RNA interference was documented in plants in the early 1990s, culminating with the northern blot detection of siRNAs from transgenes and viruses undergoing silencing [2]. Around the beginning of the

millennium, multiple small RNA pathways were discovered in plants that have related biochemical machineries but distinct endogenous triggers and biological functions [3–12].

microRNA (miRNA) and *trans*-acting siRNA (tasiRNA) pathways are critical for plant development, affecting developmental timing, organ identity, and other key traits [13–15]. miRNA biogenesis initiates when RNA polymerase II (Pol II) transcribes *MIRNA* genes into primary miRNA transcripts (pri-miRNAs), which fold into stem-loop hairpin RNAs (Fig. 1a, left). In terrestrial plants these primary miRNAs and subsequent pre-miRNAs are processed by Dicer-like 1 (DCL1) to produce ~21 nt miRNAs. Different miRNAs can then guide Argonaute 1 (AGO1) to either target mRNAs for translational inhibition or guide cleavage of mRNAs [16–18]. A separate pathway produces tasiRNAs from Pol II-transcribed *TAS* genes (Fig. 1a, right). *TAS* transcripts are targeted by miRNA-guided binding/cleavage events (not shown) that trigger the production of dsRNA by RNA-dependent RNA polymerase 6 (RDR6). Dicer-like 4 (DCL4) processes these dsRNAs into 21 nt siRNAs, which can target AGO1 to complementary mRNAs and thereby regulate development [7, 19, 20].

Transposable elements (TEs) constitute a large percentage of many plant genomes, sometimes exceeding 80% in a given crop species, such as maize [21]. In terrestrial plants, a class of ~24 nt siRNAs silences TEs via RNA-directed DNA methylation [22]. This process initiates with the recruitment of RNA polymerase IV (Pol IV) to a locus (Fig. 1b). Pol IV is an enzyme related to Pol II but with distinct protein subunits, domains, and motifs specialized for its function in TE silencing [6, 23–26]. Pol IV transcribes chromosomal TEs and DNA repeats, channeling short non-coding RNAs to RNA-dependent RNA polymerase 2 (RDR2) [27, 28]. RDR2 then produces a second RNA strand, releasing ~30 bp dsRNAs that are processed by Dicer-like 3 (DCL3) [28–30]. Resulting 24 nt siRNAs guide AGO4-clade proteins to sites of RNA polymerase V transcription, leading to DNA methylation by Domains Rearranged Methyltransferase 2 [31]. Pol IV-dependent DNA methylation is accompanied by repressive histone modifications that silence TEs and protect genome integrity [23, 32–34].

TEs can be activated in response to environmental stresses [35, 36]. For example, the *Arabidopsis thaliana* LTR retrotransposon *ONSEN* is activated under acute heat stress conditions [33, 37, 38]. After many plant generations exposed to selective pressure, retrotransposition events may sometimes enable an adaptive stress response. However, they more frequently cause deleterious loss-of-function alleles or ectopic expression of genes. Detecting and annotating TEs is therefore an important, recurring task in functional and comparative genomics [21, 39, 40]. Because the majority of siRNA clusters overlap with TEs in plant genomes, small RNA sequencing (small RNA-seq) can assist in the TE annotation

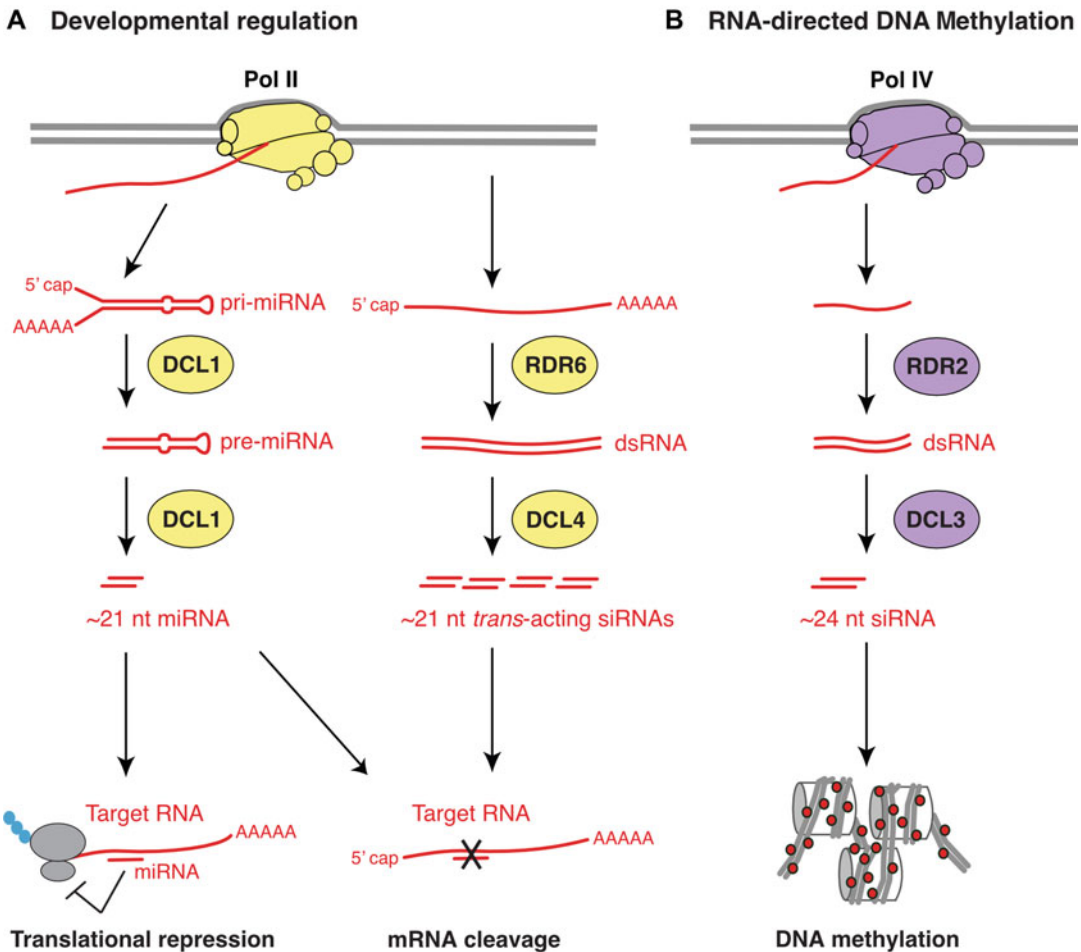


Fig. 1 Distinct small RNA classes guide developmental gene silencing and genome surveillance in plants. **(a)** Plant small RNAs play an essential role in developmental gene regulation by silencing specific messenger RNAs (mRNA). microRNAs (miRNAs) derive from RNA polymerase II (Pol II) transcripts called primary miRNAs (pri-miRNAs), which fold into a stem-loop hairpin structure. Dicer-like 1 (DCL1) ribonuclease processes pri-miRNAs, via a precursor miRNA (pre-miRNA) intermediate, into 21 nt miRNAs. Following 2'-O-methylation and Argonaute protein loading (not depicted), miRNAs can target mRNAs for cleavage or cause translational repression of such mRNA targets. *Trans*-acting siRNAs (ta-siRNAs) also derive from Pol II transcripts, but these initial precursors are converted to double-stranded RNA (dsRNA) by RNA-dependent RNA polymerase 6 (RDR6). DCL4 processes these long dsRNAs into ta-siRNAs that can cleave or inhibit translation of complementary mRNAs. **(b)** RNA-directed DNA methylation targets transposable elements (TEs) for silencing in plants. To facilitate this “genome surveillance,” RNA polymerase IV (Pol IV) is physically coupled to RNA-dependent RNA polymerase 2 (RDR2). As Pol IV transcribes a target locus, its non-coding RNA products are channeled directly to RDR2 for dsRNA synthesis. Dicer-like 3 (DCL3) then processes these ~30 bp dsRNAs into 24 nt siRNAs. The mature siRNAs then guide Argonaute effectors (not shown) to silence TEs via de novo DNA methylation and repressive chromatin modifications

process [41], and reveal small RNA-dependent mechanisms by which TEs regulate genes *in cis* and *in trans* [42–44]. Conversely, the full analysis of small RNA-seq data involves annotating and

curating genes, TEs, inverted repeats, and other complex features of the genome [45].

Routine application of deep small RNA-seq began around 2006, when 454 and Illumina sequencing became widely available, more affordable, and increasingly performant [46]. An advantage of small RNA-seq is that prior knowledge of miRNA/siRNA source loci, biogenesis pathways, and downstream effector systems is not obligatory to investigate RNA silencing in an organism [45]. However, small RNA northern blotting remains a key method in this field, because (1) validation of small RNA-seq is recommended to control for biases in library preparation, (2) blotting is less expensive than small RNA-seq when a large panel of genotypes or conditions are being screened, (3) blotting is significantly faster, and (4) advanced bioinformatics skills are not needed to interpret northern blot results.

The northern blot procedure (Fig. 2) begins with an electrophoretic migration of low-molecular-weight RNA or total RNA in

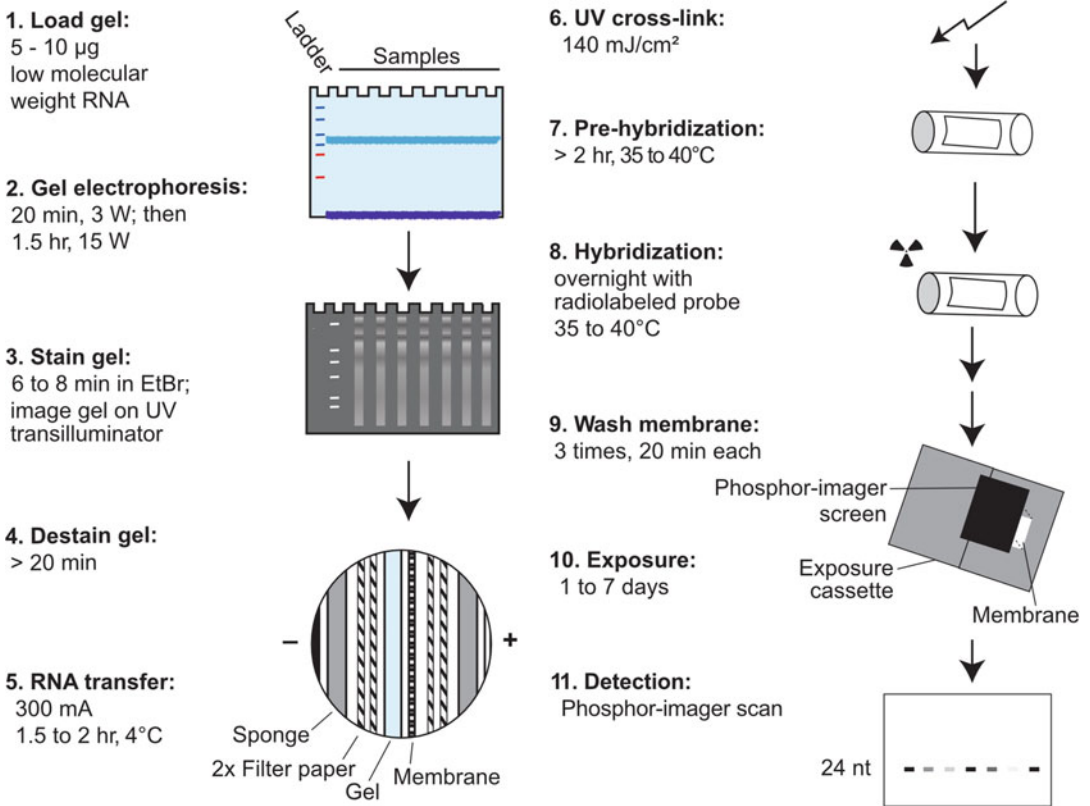


Fig. 2 Schematic overview of the northern blot procedure. Multiple steps are required for each small RNA northern blot experiment: electrophoretic migration of RNAs on a 16% polyacrylamide gel, followed by ethidium bromide (EtBr) staining to check for RNA equal loading and quality (steps 1–4); transfer of the RNAs to a nylon membrane and cross-linking (steps 5 and 6); and hybridization with radioactive probes, washing, and then signal detection by phosphor-imaging (steps 7–11)

a polyacrylamide gel. These size-separated small RNAs are then transferred to a nylon membrane. Cross-linking is performed to fix the RNA to the membrane, allowing successive hybridizations and detections using radiolabeled probes. One difficulty with this technique is its relatively low sensitivity compared to small RNA-seq. Even using sensitive phosphor-imaging systems, hybridization probes must be carefully designed and the hybridization procedure optimized to detect plant siRNAs, because these molecules can accumulate at orders of magnitude lower levels than miRNAs [47].

Here, we present an integrated protocol to study small RNA pathways and TE silencing in organisms that lack comprehensive, consolidated TE annotations, such as the model grass *Brachypodium distachyon*. We combined publicly available small RNA-seq data and standard bioinformatics tools to de novo annotate the *B. distachyon* genome (with both TEs and siRNA clusters), and then performed northern blot validation of siRNA source loci overlapping TEs. To this end, we developed a software pipeline that identifies long terminal repeats (LTRs), combines these regions with published TE annotations, and cross-compares all annotations to the mapped positions of siRNAs (Fig. 3). Validation was performed using an optimized northern blot hybridization procedure, with the goal of detecting Pol IV-dependent 24 nt siRNAs in both *B. distachyon* (monocot) and *A. thaliana* (eudicot) plant species.

2 Materials

2.1 Plant Materials

1. *Arabidopsis thaliana* wild-type (WT, ecotype Col-0) and *pol IV* null mutant (At *nripd1-3*) [6] plants grown with a day/night cycle of 16 h/8 h at 21 °C/18 °C.
2. *Brachypodium distachyon* WT (inbred line Bd21-3) and a *pol IV* point mutant (Bd *nripd1-1*) in the Bd21-3 background grown with a day/night cycle of 20 h/4 h at 25 °C.
3. RNA extractions from inflorescences of *A. thaliana* or from young leaves of *B. distachyon*. Plant materials harvested, flash frozen in liquid nitrogen, and stored at –80 °C.

2.2 Bioinformatics Analyses

1. *Brachypodium distachyon* Bd21v3.0 reference genome assembly (FASTA format) obtained from Phytozome (GCF_000005505.3_Brachypodium_distachyon_v3.0) [48, 49].
2. Publicly available small RNA-seq data from *B. distachyon* used for the analyses (GEO: GSM1266842, BDI09 sample from leaves) [50].

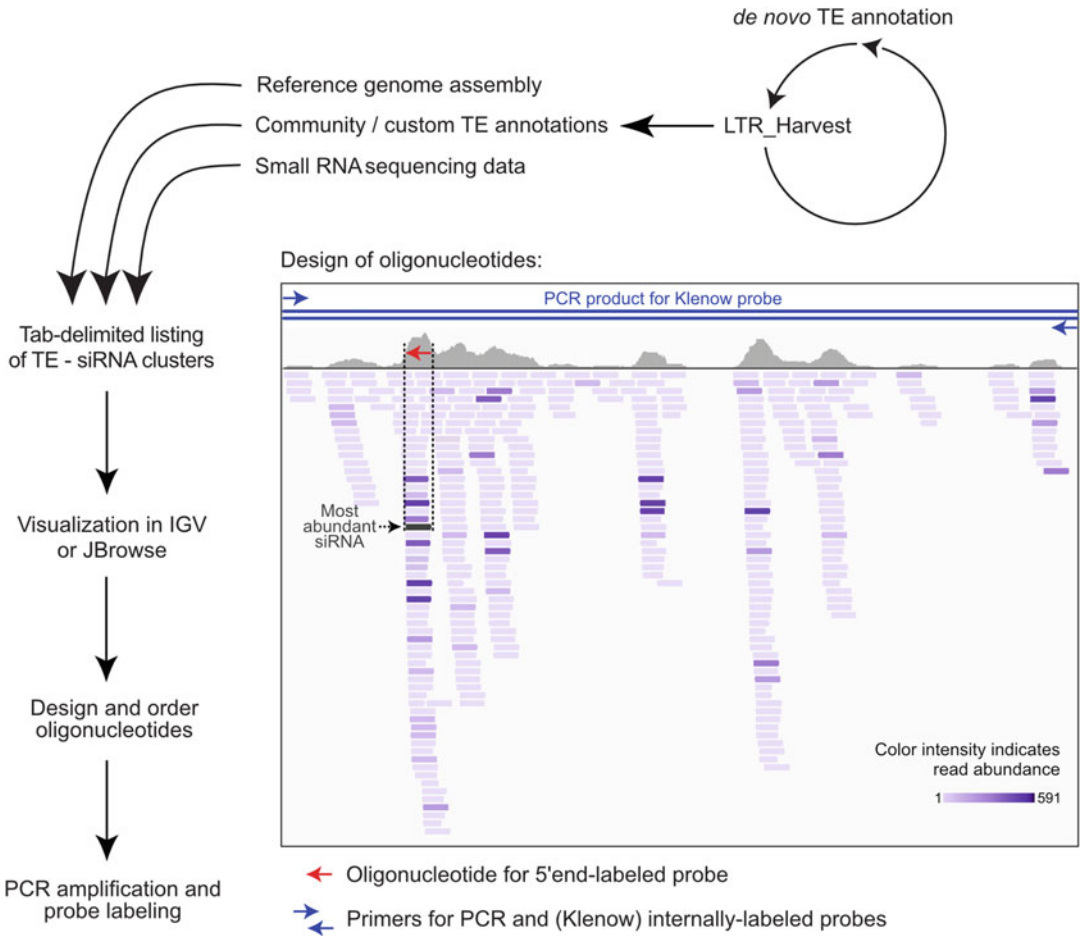


Fig. 3 Flowchart for the bioinformatics analysis and probe design. Bioinformatics data are key for the design of hybridization probes: this includes a reference genome assembly, transposable element (TE) annotations, and small RNA sequencing (small RNA-seq) data. TEs can also be identified using de novo annotation tools, such as LTR Harvest [51]. TEs that coincide with mapped positions of abundant small RNA-seq reads are the best candidates for siRNA detection by northern blot. Visualization of small RNA-seq data in genome browsers, such as Integrative Genomics Viewer (IGV) or JBrowse, can help explore siRNA clusters (screenshot). For the 5'-end-labeling protocol (Subheading 3.7), an extremely abundant siRNA is chosen, and then a reverse complement, synthetic DNA oligonucleotide is ordered as the probe (red arrow). For the Klenow labeling protocol (Subheading 3.6) a larger region of the siRNA cluster is chosen, such as a retrotransposon long terminal repeat, in order to integrate signals from multiple siRNAs. The entire region is amplified by PCR (blue arrows), and then this fragment is purified for input to the labeling reaction

3. Bioinformatics tools used for TE annotation and small RNA-seq data analyses: LTR_Harvest (GenomeTools version $\geq 1.5.9$) [51], SRA Toolkit version $\geq 2.9.2$ (<https://www.ncbi.nlm.nih.gov/sra/docs/toolkitsoft/>), Cutadapt version ≥ 1.18 [52], FastQC version $\geq 0.11.8$ (<http://www.bioinformatics>).

babraham.ac.uk/projects/fastqc/), ShortStack version $\geq 3.8.5$ [53, 54], Bowtie version $\geq 1.2.2$ [55] and SAMtools version ≥ 1.9 [56], JBrowse [57]/Integrative Genomics Viewer (version $\geq 2.7.0$) [58, 59], and Geneious Prime v2019.0 (<https://www.geneious.com/>).

2.3 RNA Extraction, Size Fractionation, and Northern Blotting

1. Autoclaved, pre-cooled ceramic mortars and pestles, and a metal spatula.
2. Liquid nitrogen.
3. 13 mL Round-bottomed, capped polypropylene tubes.
4. Beckman centrifuge, rotor JA17 or JA-25.5, and fitted rubber adapters.
5. TRIzol (Invitrogen, CA, USA): Store at 4 °C (*see Note 1*).
6. Serological 10 mL pipettes (single-use) and an electric pipette controller.
7. Cold chloroform: Store at -20 °C (*see Note 1*).
8. Cold isopropanol: Store at -20 °C.
9. Absolute ethanol: Store at RT.
10. 75% Ethanol (in Milli-Q water): Store at -20 °C.
11. Diethyl pyrocarbonate (DEPC)-treated water: DEPC inactivates RNases in aqueous solution. Prepare a 0.1% DEPC solution—e.g., 1 mL of DEPC diluted in 1 L Milli-Q water. Leave this solution at room temperature (RT) for 4 h and then autoclave (>15 min) to remove the DEPC. Store at RT (*see Note 1*).
12. RNase-free 1.5 mL Eppendorf tubes (also referred to as microfuge tubes).
13. NanoDrop-2000 Spectrophotometer (Thermo Fisher Scientific, MA, USA).
14. RNeasy Midi Kit (QIAGEN) or RNeasy Mini Kit, containing the RLT and RPE buffers.
15. β -Mercaptoethanol: Store at RT (*see Note 1*).
16. RNase-free 30 mL Corex glass centrifuge tubes.
17. A medium-sized polyacrylamide gel electrophoresis (PAGE) system (*see Note 2*).
18. 5 \times TBE stock solution: 54 g Tris base, 27.5 g boric acid, 20 mL 0.5 M ethylenediaminetetraacetic acid (EDTA, pH 8.0) filled up with Milli-Q water to 1 L. Store at RT.
19. 50 mL Falcon tubes.
20. Acrylamide/bis-acrylamide (19:1): Store at 4 °C (*see Note 1*).

21. *N,N,N',N'*-tetramethylethylenediamine (TEMED): Store at 4 °C.
22. 10% Ammonium persulfate (APS) in Milli-Q water: Aliquots can be stored at –20 °C for several months.
23. 10 mL Syringes with a 0.8 × 40 mm needle.
24. DNA oligonucleotides used for PCR amplification prior to Klenow probe synthesis, or for individual 5'-end-labeled probes (sequences of the used DNA oligonucleotides listed in Subheading 2.4).
25. RNA size standards for PAGE: Mix synthetic RNA oligonucleotides of 15 nt (2.5 µL), 21 nt (1.5 µL), 24 nt (1 µL), 30 nt (0.5 µL), and 40 nt (0.5 µL) length (100 µM stocks; sequences listed in Subheading 2.5). These RNA oligos should not be homologous to the genome of interest. Add 2 µl low-range ssRNA ladder (e.g., New England Biolabs, MA, USA) and bring this mixture to the same total volume as the RNA sample aliquots.
26. DynaMarker Prestain Marker “small RNA Plus” (BioDynamics Laboratory Inc., Tokyo, Japan) used to follow small RNA migration during gel electrophoresis.
27. SpeedVac Concentrator Savant (Thermo Fisher Scientific).
28. RNA-loading buffer: 95% Formamide, 0.025% bromophenol blue, 0.025% xylene cyanol FF, 5 mM EDTA, 0.025% SDS, pH 8.5.
29. High-current power supply for gel migration and transfer, such as PowerPac HC (Bio-Rad, CA, USA).
30. Ethidium bromide (EtBr, 10 mg/mL) solution: Store at 4 °C and protected from light.
31. Digital gel documentation system with UV transillumination.
32. Positively charged nylon membrane (Hybond-N+).
33. Whatman paper.
34. A rolling device (e.g., a plastic serological pipette).
35. A magnetic stirrer.
36. Trans-Blot Electrophoretic Transfer Cell (Bio-Rad) for RNA electroblotting.
37. UV crosslinker to fix RNA to nylon membrane.
38. 2× Saline sodium citrate (SSC): 0.3 M NaCl, 30 mM sodium citrate, pH 7.0.
39. PerfectHyb Plus Hybridization Buffer (Sigma-Aldrich).
40. Hybridization equipment: Glass hybridization tubes, an oven for the hybridizations, etc.

41. Random hexamer primers (100 μ M stock).
42. Klenow fragment enzyme.
43. dATP/dGTP/dTTP mix (1 mM each, without dCTP) prepared using a set of individual dNTP solutions.
44. [α^{32} P]-dCTP with a specific activity of 6000 Ci/mmol and radioactive concentration of 10 mCi/mL (*see Note 3*).
45. T4 polynucleotide kinase (PNK).
46. [γ^{32} P]-ATP with a specific activity of 6000 Ci/mmol and radioactive concentration of 10 mCi/mL (*see Note 3*).
47. Illustra MicroSpin G-25 columns (GE Healthcare) for probe purification.
48. Wash buffer: 2 \times SSC + 0.5% sodium dodecyl sulfate (SDS).
49. Stripping buffer: 0.1% SDS.
50. Microwave.
51. Phosphor-imager (e.g., Typhoon FLA-9500; GE Healthcare).

2.4 DNA Oligo-nucleotides for Hybridization Probes

Organism	Name	Sequence	Size (nt)	Hybridization/Wash temp.
<i>DNA primers used to make Klenow probes</i>				
<i>B. distachyon</i>	Bd_LTR_F01	GATGGACCTAACACATT ACGAGAG	24	PCR using F01 and R01, then Klenow labeling: 35/37 °C, or 42/45 °C
<i>B. distachyon</i>	Bd_LTR_R01	GTTCTTCAAATATTGTC TGTTGGAG	25	
<i>DNA oligos used as 5'-end-labeled probes</i>				
<i>B. distachyon</i>	Bd_LTR	AGTGGCTCTGCCGCCCG GAAGCTT	24	35/37 °C
<i>A. thaliana</i>	LTR_META1	GCCCATCATCTAAGCCCA TCATCT	24	40/40 °C
<i>A. thaliana</i>	SIMPLEHAT2	TGGGTTACCCATTTTGAC ACCCCTA	25	35/37 °C
<i>A. thaliana</i>	AtREP2	GCGGGACGGGTTTGGC AGGACGTTACTTAAT	31	35/37 °C
<i>B. distachyon</i> or <i>A. thaliana</i> (Universal probe)	miR160	TGGCATAACAGGGAGCCA GGCA	21	35/37 °C

2.5 RNA Oligonucleotides Used as Size Standards

Name	Sequence
GFP-15 nt-RNA	GUAAACGGCCACAAG
GFP-21 nt-RNA	GUAAACGGCCACAAGUUCAGC
GFP-24 nt-RNA	GUAAACGGCCACAAGUUCAGCGUG
GFP-30 nt-RNA	GUAAACGGCCACAAGUUCAGCGUGUCCGGC
GFP-40 nt-RNA	GUAAACGGCCACAAGUUCAGCGUG UCCGGCGAGGGCGAGG

3 Methods

3.1 Bioinformatics: De Novo TE Annotation and Small RNA Data Analysis

Brachypodium distachyon is a grass species used as a model for barley or wheat (Poaceae family), allowing multigenerational experiments to be performed in standard plant growth chambers [60]. However, TEs have not been fully annotated in *B. distachyon*, particularly with respect to TE silencing by the Pol IV-dependent siRNA pathway. Long terminal repeat retrotransposons (LTR TEs) are derepressed in DNA methylation-deficient backgrounds and *pol IV* mutants of *Arabidopsis thaliana*, or in heat-stress conditions [33, 34, 61–63]. Using the de novo TE annotation tool LTR_Harvest [51], and publicly available small RNA-seq data [50], it is possible to identify LTR TEs that are targeted by Pol IV-based genome surveillance in *B. distachyon*.

1. Download the *Brachypodium distachyon* reference genome in FASTA format.
2. To find LTR retrotransposons in the *B. distachyon* genome, run LTR_Harvest with the following LTR length range: min. 75 bp and max. 2000 bp. LTR_Harvest outputs the complete sequence of each candidate TE and genome coordinates for both its LTRs. Additionally, it detects 5–6 bp target-site duplications generated when an LTR TE integrates into a genomic locus. The output from LTR_Harvest allows to focus on the subset of genomic loci that are putative LTR TEs (Fig. 3).
3. To find siRNA-producing regions in the de novo-annotated TEs, search public databases (e.g., <https://www.ncbi.nlm.nih.gov/geo/>) or use in-house small RNA-seq data.
4. Download small RNA-seq data, here *B. distachyon* Bd21-3 leaf tissue (GEO: GSM1266842, BDI09) [50]. If necessary, extract FASTQ read files from SRA archive files using fasterq-dump (SRA Toolkit).
5. Perform quality control by running FastQC on the FASTQ read files. Evaluate sequence quality (>Q25 throughout the read) and check for the presence of adapter sequences.

6. If standard Illumina RA3 adapters are detected on the 3'-end of the FASTQ reads, then trim away these adapter sequences using Cutadapt (options: -a TGGGAATTCTCGGG --trim-n --minimum-length 15 --maximum-length 40 -q 30 --discard-untrimmed).
7. Evaluate the trimmed FASTQ reads by re-running FastQC on the Cutadapt output files.
8. Map the trimmed small RNA-seq reads to the reference genome (here: *B. distachyon* Bd21 v3.0) and tally small RNAs within annotated TEs using ShortStack (options: --nohp --dicermin 20 --dicermax 25). ShortStack will invoke the Bowtie read aligner and call SAMtools (*see Note 4*).
9. Classify the annotated LTR TEs in a tab-delimited file, sorted with TEs showing the highest levels of 24 nt siRNAs first, allowing the identification of putative Pol IV targets within the *B. distachyon* genome (TE-siRNA clusters).
10. Verify selected TE-siRNA clusters by loading sorted and indexed BAM files from **step 8** into either JBrowse [57] or Integrative Genomics Viewer [58] and viewing siRNA clusters along the *B. distachyon* chromosomes, focusing on LTR TE loci with the most abundant 24 nt siRNAs. Both de novo TE (**step 2**) and community TE/gene annotations can be integrated to support this analysis.
11. Curate promising candidates by hand, using Geneious Prime to annotate the LTRs, target-site duplications, tRNA primer-binding sites, polypurine tracks, and ORFs that could indicate whether individual LTR TEs are potentially functional. Functional TEs typically have intact ORFs and perfectly identical or nearly identical LTRs.
12. Finally, select LTR TEs with abundantly mapped 24 nt siRNAs for validation by small RNA northern blot. Very copious individual siRNA sequences can be used to design complementary DNA oligo probes for radioactive 5'-end-labeling. Otherwise, TE subfeatures displaying many distinct siRNA mappings, such as ~600 bp spanning an LTR, can be used to design PCR amplicons for Klenow probe labeling (Fig. 3).

3.2 Extraction of Total RNA from Plant Tissue

Wear a lab coat and gloves for all the following procedures. The pipettes, tips, and tubes should all be kept isolated and clean before RNA extraction. In addition, filter tips are recommended to avoid RNase contamination and degradation of the final RNA samples.

1. Grind plant tissue samples to a fine powder in liquid nitrogen using a pre-cooled mortar and pestle (*see Note 5*).
2. Transfer about 400 μ L of this powder from each sample to a 13 mL round-bottomed tube (kept in liquid nitrogen) (*see Note 6*).

3. Add 8 mL of TRIzol to each tube (ensure that the liquid nitrogen has evaporated from the powder before adding the reagent).
4. Vortex tubes until the powder melts and is homogeneously suspended in TRIzol. When extracting many samples in parallel, the homogenized samples can be left on ice.
5. Add 1.6 mL chloroform, vortex for ~40 s, and then leave tubes on ice for 3 min.
6. Centrifuge the samples for 15 min at $8500 \times g$ and 4°C .
7. Transfer the aqueous phase to a clean 13 mL round-bottomed tube.
8. Add 7 mL of cold isopropanol to each tube and mix by inverting the tube ten times.
9. Let the total RNA precipitate at -20°C for at least 2 h (*see Note 7*).
10. Centrifuge the samples for 30 min at $9200 \times g$ and 4°C , and then discard the supernatant.
11. Add 10 mL cold 75% ethanol, centrifuge for 15 min at $4500 \times g$ and 4°C , and then carefully discard the supernatant.
12. Repeat ethanol wash (**step 11**) to further purify the RNA.
13. Air-dry the RNA pellets, tubes upside down, for about 20 min at RT.
14. Resuspend the RNA pellets in 120 μL DEPC-treated Milli-Q water, preheated to 65°C (*see Note 8*).
15. Quantify the total RNA using a Nanodrop spectrophotometer (absorbance at 260 nm).
16. Store the samples at -20°C for up to 1 month, or for longer periods at -80°C .

3.3 Size Fractionation of Total RNA

Northern blot detection of 24 nt siRNAs can be difficult, especially if the input total RNA is isolated from tissues like *B. distachyon* leaves, which contain low levels of siRNAs compared to RNA samples isolated from *A. thaliana* inflorescences. RNA size fractionation enriches for low-molecular-weight (LMW) RNAs and thereby enhances siRNA detection (*see Note 9*). RNeasy Midi columns are used here to separate LMW RNAs from high-molecular-weight (HMW) RNAs, following the “RNA cleanup” protocol [64, 65]. HMW RNAs bind to the silica membrane of the columns, whereas <200 nt LMW RNAs pass through and can be recovered in flow-through and wash aliquots.

1. Transfer up to 1 mg of total RNA in a volume of 500 μL DEPC-treated water to a 13 mL round-bottomed tube.
2. Add 2 mL of RLT buffer complemented with β -mercaptoethanol (10 $\mu\text{L}/\text{mL}$ RLT) to each sample; if RNeasy Mini columns are used here, then adjust all volumes accordingly.

3. Add 1.4 mL 100% ethanol and immediately transfer each sample to an RNeasy Midi column.
4. Centrifuge the samples for 5 min at $4500 \times g$ and RT.
5. Transfer the flow-through to a RNase-free 50 mL Corex tube kept on ice.
6. Add 2.5 mL RPE buffer onto each column for the first wash of the column.
7. Centrifuge the samples for 5 min at $4500 \times g$ and RT.
8. Transfer the flow-through of the first wash to the previously used Corex tube.
9. Add 2.5 mL RPE buffer onto the column for the second wash of the column.
10. Centrifuge the samples for 5 min at $4500 \times g$ and RT.
11. Transfer the flow-through of this second wash to the Corex tube. The LMW RNA is now in the flow-through/wash aliquots that were combined in the Corex tube (for HMW RNA recovery, *see Note 10*).
12. Add 10 mL cold isopropanol to each LMW RNA sample.
13. Close the Corex tubes with parafilm and invert seven times.
14. Leave the samples overnight at -20°C for the small RNAs to precipitate.
15. The next day: Centrifuge the samples for 45 min at $24,000 \times g$ and 4°C .
16. Discard the supernatant carefully with a pipette.
17. Add 10 mL cold 75% ethanol to each sample for washing.
18. Centrifuge the samples for 15 min at $24,000 \times g$ and 4°C .
19. Discard the supernatant (*see Note 11*), air-dry the RNA pellets at RT for about 20 min, and then heat the tubes to 65°C for 5 min.
20. Resuspend the dried RNA pellets in 30 μL DEPC-treated water, preheated to 65°C .
21. Quantify the LMW RNA using the Nanodrop device. Samples can be stored at -20°C .

3.4 Northern Blot Procedure

A schematic overview of the northern blot procedure is depicted in Fig. 2.

1. Transfer up to 10 μg LMW RNA from each sample to a clean 1.5 mL microfuge tube, adjusting all samples to the same total volume using DEPC-treated water (*see Note 12*).
2. Prepare a size standard using synthetic RNA oligonucleotides and the low-range ssRNA ladder. Bring this mix to the same

total volume as the RNA sample aliquots, and then treat it like the other samples for all remaining steps.

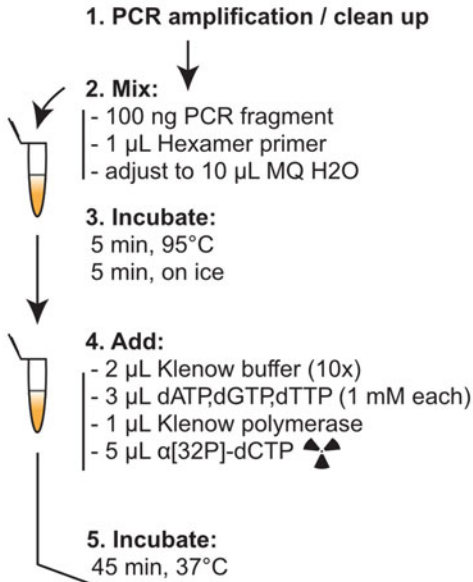
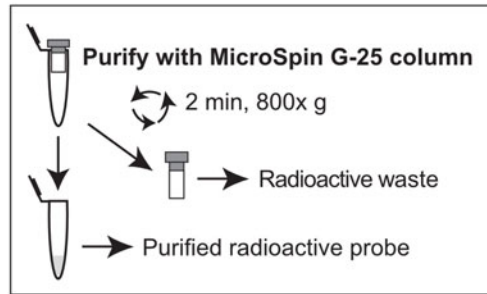
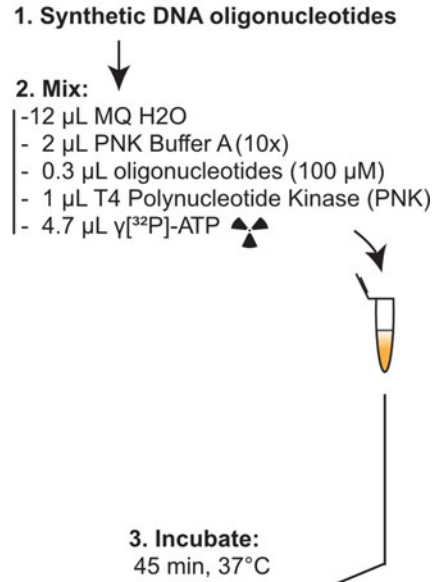
3. Freeze the samples at -20°C (overnight).
4. Dry the frozen samples completely by sublimation in a Speed-Vac concentrator (45 min for a 20–30 μL sample volume at RT).
5. Resuspend the samples in 12 μL RNA-loading buffer (*see Note 13*).
6. Heat the samples to 95°C for 3 min, and then keep them on ice.
7. After this RNA heat denaturation, add DynaMarker Prestain “small RNA Plus” marker (5.5 μL) into the RNA oligo size standard mix.
8. Set up the vertical gel apparatus for casting. Make sure that all the components are clean.
9. Prepare a 16% polyacrylamide gel mixture in a 50 mL Falcon tube, containing 11.1 g urea, 6.0 mL $5\times$ TBE, and 12.0 mL acrylamide/bis-acrylamide (19:1). Fill with Milli-Q water up to 30 mL and mix to dissolve all the components.
10. Rapidly add 30 μL TEMED and 300 μL 10% APS to the mixture just before casting. Immediately cap and invert the Falcon tube to mix. Then, without hesitation, steadily transfer this solution between the glass plates of the gel apparatus using a 10 mL pipette.
11. Add the comb while avoiding any air bubbles before the gel starts to polymerize.
12. Let the gel sit for about 20–30 min for complete polymerization. Leftover gel mixture in the Falcon tube can be observed as a reference for the polymerization reaction.
13. Place the gel in the vertical gel apparatus (reconfigured for running) and add $1\times$ TBE to both buffer reservoirs. Remove the comb carefully to avoid deformation of the wells. Pre-run the gel for 20 min (15 (W)).
14. Before RNA loading, use a syringe to wash out all wells thoroughly, removing excess urea, and remove any air bubbles that have accumulated under the gel.
15. Load the denatured RNA samples onto the polyacrylamide gel. Avoid loading samples into the first and the last wells of the gel.
16. Perform PAGE at 3 W for 15–20 min, until the RNA samples have entered the gel. Then, increase to 15 W for the rest of the electrophoresis, which lasts about 1.5 h.
17. The pre-stained size marker allows one to follow the RNA migration visually. The electrophoresis is usually stopped

when the bromophenol blue band (dark blue) flows into the lower buffer reservoir.

18. Carefully remove the gel from the vertical gel system and place it in 400 mL 1× TBE, using one of the glass plates to support the gel during this procedure (*see Note 14*).
19. Stain the gel for 8 min by adding 20 μL ethidium bromide solution to the 1× TBE bath. The gel is gently agitated in this ethidium bromide bath during staining.
20. Image the gel with UV transillumination in the gel doc system. This photo should not be oversaturated to enable using it as an RNA quality and loading control (*see Note 15*).
21. Move the gel into fresh 1× TBE for 20 min in order to destain before electroblotting.
22. Prepare the RNA transfer assembly. All layers should be equilibrated in 1× TBE buffer prior to assembly (*see Fig. 2*, RNA transfer). The layers of this “sandwich” are as follows: negative-facing surface (black plastic), sponge, two sheets of Whatman paper (slightly larger than gel), gel, Hybond-N+ nylon membrane (marked to indicate RNA sample orientation), two sheets of Whatman paper, sponge, and positive-facing surface (clear plastic). Avoid air bubbles between the different sandwich layers by rolling a serological pipette over each layer.
23. Slide the transfer assembly into a slot in the trans-blot electrophoretic transfer cell, verifying that the gel/membrane components are fully immersed. Use a magnetic stirrer to keep the 1× TBE buffer circulating. Apply 300 mA for transfer at 4 °C for 1.5–2 h.
24. After the transfer, use a UV crosslinker to fix the RNA to the membrane at 140 mJ/cm².
25. Dry the membrane between filter paper, or directly proceed to hybridization.

3.5 Hybridization with Radioactive Probes

1. Transfer the membrane into a hybridization tube with sufficient 2× SSC to wet the membrane. Remove all air bubbles between the membrane and the inner glass surface to avoid unequal hybridization (*see Note 16*).
2. Pre-hybridize the membrane for at least 2 h in 20 mL PerfectHyb Plus hybridization buffer at 35 °C or 40 °C depending on the probe (*see Note 17*).
3. Depending on the probe design chosen after the bioinformatic analysis in Fig. 3, this procedure bifurcates into two alternative options (Fig. 4a, b).

A Internally labeled probe (Klenow)**B 5'-end-labeled oligo probe (PNK)**

Denature before use:

- 3 min, 95°C
- 5 min, on ice

Ready for use

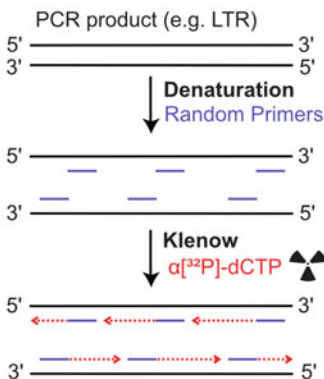
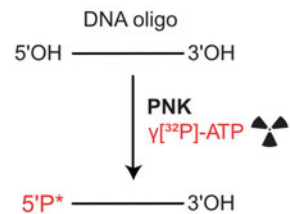
Products from Klenow:**Products from PNK:**

Fig. 4 Alternative radiolabeling methods for hybridization probes. **(a)** Klenow probe labeling permits very sensitive detection of multiple sequences from an siRNA cluster. The genomic target is amplified by standard PCR and then gel-purified prior to radiolabeling. Klenow polymerase produces internally labeled DNA probes representing both strands of the cold PCR fragment. **(b)** End-labeling using polynucleotide kinase (PNK) generates oligonucleotide probes radiolabeled only at their 5'-extremity. Each probe is complementary to a particular small RNA sequence, making them both sequence and strand-specific but less sensitive than Klenow probes. Radiolabeling is indicated in red

3.6 Internally Labeled Klenow Probe (Fig. 4a)

In order to generate more sensitive probes, we recommend using the Klenow labeling procedure. Such probes detect multiple siRNAs that arise in clusters—e.g., from the long terminal repeats of a retrotransposon (Fig. 3). Prior to probe radiolabeling, design PCR primers that flank a genomic region of interest. Amplify this region using Taq polymerase and purify the PCR fragment from an agarose gel. 100 ng of pure PCR fragment will be used for each Klenow probe preparation.

1. In a 1.5 mL safe-lock tube, prepare:

PCR fragment	100 ng
Random hexamer primer (100 μ M)	1 μ L
Milli-Q water	Fill to 9 μ L

2. Heat the mixture to 95 °C for 5 min.
3. Transfer the tube immediately to ice for at least 5 min.
4. Add the following components to the same tube (*see Note 3*):

10 \times Klenow buffer	2 μ L
dATP/dGTP/dTTP mix (1 mM each)	3 μ L
Klenow fragment enzyme	1 μ L
[α^{32} P]-dCTP (~50 μ Ci)	5 μ L

5. The labeling reaction is performed for 45 min at 37 °C.
6. The radiolabeled probe is then purified on an Illustra Micro-Spin G-25 column:

Prepare the column by vortexing, followed by centrifugation at $800 \times g$ for 1 min. Transfer the column to a clean 1.5 mL tube and load the sample. Centrifuge for 2 min at $800 \times g$. Radiolabeled DNA fragments are in the flow-through.
7. Denature this probe by heating to 95 °C for 3 min and then transfer it to ice for 5 min.
8. Pipette the probe into the tube with the pre-hybridized membrane (from Subheading 3.5). Do not touch the membrane with the pipette, or let the concentrated probe land directly on the membrane surface.
9. Hybridize overnight. Conditions are specified in Subheading 2.4.

3.7 5'-End-Labeled DNA Oligonucleotide Probe (Fig. 4b)

1. In a 1.5 mL safe-lock tube, prepare (*see Note 3*):

Milli-Q water	12 μ L
10 \times PNK buffer A	2 μ L
DNA oligonucleotide probe (100 μ M)	0.3 μ L
T4 polynucleotide kinase (PNK)	1 μ L
[γ ³² P]-ATP (~50 μ Ci)	4.7 μ L

2. Perform the labeling reaction for 45 min at 37 °C.
3. Purify the radiolabeled probe using an Illustra MicroSpin G-25 column:

Prepare the column by vortexing, followed by centrifugation at 800 $\times g$ for 1 min. Transfer the column to a clean 1.5 mL tube and load the sample. Centrifuge for 2 min at 800 $\times g$. Radiolabeled DNA oligos are in the flow-through.
4. Pipette this probe into the tube with the pre-hybridized membrane (from Subheading 3.5). Do not touch the membrane with the pipette, or let the concentrated probe land directly on the membrane surface.
5. Hybridize overnight. Conditions are specified in Subheading 2.4.

3.8 Membrane Washing and Exposure (Fig. 5)

1. Preheat the wash buffer (2 \times SSC, 0.5% SDS) to the optimal temperature, which is determined empirically. We recommend 37–40 °C, depending on the probe.
2. The membrane is washed three times for 20 min with 20 mL wash buffer.
3. Expose the washed blot in a thin plastic bag to a phosphor-imager screen in a cassette. siRNA detection requires between 1 and 7 days of exposure.
4. Scan the screen in a phosphor-imager.
5. Erase the signal on the screen before the next hybridization by exposure to intense white light for 20–30 min.

3.9 Stripping and Re-hybridization of the Blot

A large number of distinct small RNAs can be detected by successively hybridizing a membrane with different probes. It is essential that the membrane is stripped between hybridizations to avoid carryover signal from previous probes. Stripping is often less efficient after probes that detect highly abundant miRNAs, so one may need to wait for the signal to decay before the next hybridization after miRNA detection. Best practice is to start with probes yielding less intense signals (probes for TE-derived siRNAs) and to finish with probes that yield stronger signals (probes for miRNAs).

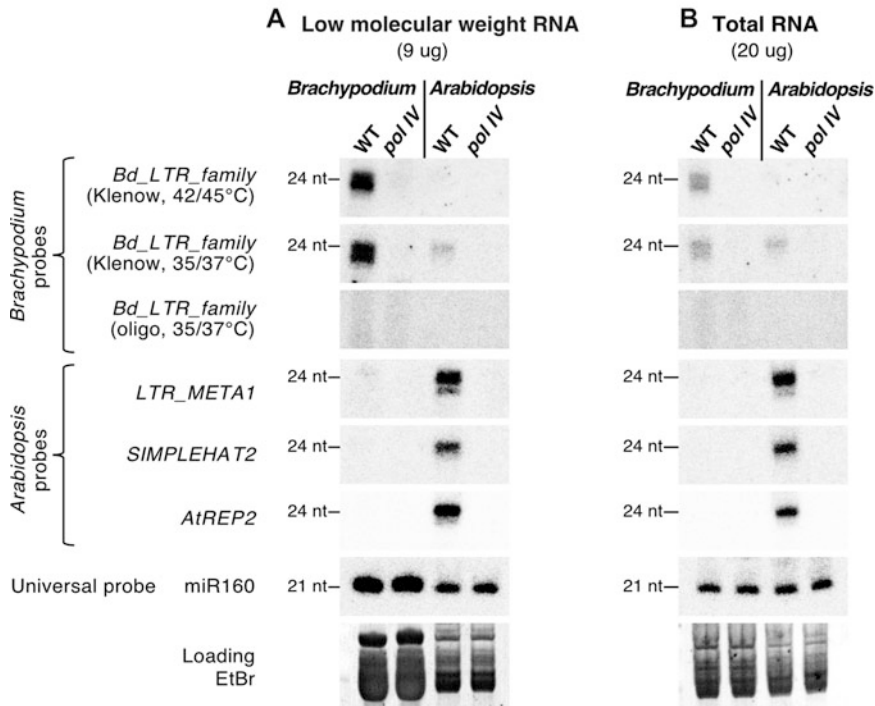


Fig. 5 Northern blot results for detection of *Brachypodium distachyon* and *Arabidopsis thaliana* small RNAs from (a) low-molecular-weight RNA, or (b) total RNA samples. 24 nt siRNAs derived from transposable elements show Pol IV-dependent accumulation in both plant species: they are detected in wild-type (WT) but absent in *pol IV* mutant plants (probes: *Bd_LTR_family* for *Brachypodium*; *LTR_META1*, *SIMPLEHAT2* and *AtREP2* for *Arabidopsis*). A universal probe detects 21 nt miR160 in WT and *pol IV* mutant plants. This evolutionarily conserved miRNA is easily detected in both species, whereas 24 nt siRNAs are less abundant in *Brachypodium* than the equivalent siRNA class in *Arabidopsis*. Weak hybridization signals observed in *Arabidopsis* samples using the *Brachypodium* long terminal repeat (LTR) probe illustrate the lower specificity of Klenow probes (Klenow, 35/37 °C). Higher hybridization/wash temperatures prevent non-specific signals, allowing accurate northern blot results to be obtained for *Brachypodium* siRNAs (Klenow, 42/45 °C). Both RNA size fractionation and Klenow probes (a, top two panels) are key for this successful detection of low-abundance siRNAs in *Brachypodium*. Ethidium bromide (EtBr) gel staining serves as an RNA-loading control

1. Prepare 0.1% SDS solution for the stripping.
2. Bring the stripping solution to boil using a microwave.
3. Put the membrane in a plastic box with the RNA surface upwards. Pour the hot stripping solution (85–95 °C) directly onto the membrane until the membrane floats in the solution.
4. Wait for 20 min.
5. Repeat steps 1–4.
6. Rinse the membrane in 2× SSC buffer to remove the SDS. Proceed to pre-hybridization in PerfectHyb Plus buffer, or store the membrane in a plastic sleeve at RT until needed.

4 Notes

1. Several hazardous chemicals are used for RNA extraction and northern blotting:
 - (a) Phenol present in TRIzol is toxic and corrosive, and should be handled under a fume hood.
 - (b) Chloroform is toxic and a suspected carcinogen.
 - (c) DEPC is a suspected carcinogen and should be handled under a fume hood. After autoclaving, the diluted aqueous solution is safe for benchtop experiments.
 - (d) β -Mercaptoethanol is toxic, and should be handled under a fume hood.
 - (e) Acrylamide monomer is a neurotoxin and a potential carcinogen.

Read the material safety data sheet of each chemical for further information.

2. The Dual Adjustable Slab Gel Kit (DASG-250-02, CBS Scientific—Fisher Scientific, NH, USA) is recommended for use with this protocol. It includes everything needed for gel casting and polyacrylamide gel electrophoresis (PAGE), including glass plates (16.5 cm \times 17 cm), spacers, and combs (0.75 mm with 20 wells).
3. Caution: Radiation protection measures must be taken while handling [$\alpha^{32}\text{P}$]-dCTP or [$\gamma^{32}\text{P}$]-ATP, and all derived materials.
4. Alternatively, one can directly map the trimmed reads to the reference genome using Bowtie (options: -v 1 -k 50 --best --strata --no-unal), and then perform SAM-BAM format conversion, mapped read sorting, and tallying using SAMtools.
5. Thorough grinding is essential for optimal RNA extraction. Automated grinders (e.g., Silamat S6; Ivoclar Vivadent, Liechtenstein) are available for higher throughput applications. Make sure that the samples never thaw during the grinding process.
6. This protocol can be adapted to smaller amounts of input material. In this case, freeze *A. thaliana* inflorescences (or other plant tissue) in 1.5 mL safe-lock microfuge tubes with 4–6 glass beads. Grind the samples for 8 s using a Silamat device, and then transfer the tube back to liquid nitrogen to avoid thawing. Repeat the grinding step a second time to obtain a fine powder. All volumes during the RNA extraction can thus be reduced tenfold. Centrifugation steps are performed at 15,000 $\times g$, and the RNA is resuspended in 50 μL DEPC-treated Milli-Q water.

7. RNA precipitation can also be performed overnight or over several days. Longer precipitation times will help maximize the yield of total RNA.
8. Somewhat larger volumes of DEPC-treated water can be used to assure that the RNA pellet is completely resuspended. However, do not dilute the total RNA excessively if a size fractionation step is to be performed.
9. The size fractionation step can be skipped for total RNA samples rich in small RNAs, such as total RNA extracted from *A. thaliana* inflorescences. In such cases, 15–30 μg total RNA can be directly used for PAGE and northern blotting.
10. To recover the high-molecular-weight (HMW) RNAs, which are bound to the RNeasy Midi column during size fractionation:
 - (a) Centrifuge the samples for 3 min at $4500 \times g$ and RT to completely dry the column.
 - (b) Transfer the column to a clean 15 mL tube. Add 250 μL of DEPC-treated Milli-Q water (65°C) onto the column for elution and incubate for 1 min.
 - (c) Centrifuge the samples for 3 min at $4500 \times g$ and RT.
 - (d) Put this eluted sample volume back onto the column for a second elution.
 - (e) Centrifuge the samples for 3 min at $4500 \times g$ and RT.
 - (f) Quantify the RNA using a Nanodrop device and store at -20°C (or at -80°C for a longer period of time).

If size fractionation was performed using RNeasy Mini columns, adjust the tube size, elution volume, and centrifugation speed accordingly.

11. Caution: The pellet is not very stable and can easily be lost at this stage.
12. Alternatively, 15–30 μg total RNA can be transferred to 1.5 mL microfuge tubes.
13. Samples can be stored frozen in RNA-loading buffer for several days at -20°C . These samples must then be reheated to thaw and denature the RNA (95°C for 3 min, then kept on ice) prior to polyacrylamide gel loading.
14. Caution: The gel should not be allowed to dry out.
15. Caution: Do not leave the gel on the UV transilluminator for an extended period.
16. Caution: Only touch the membrane on its edges, being careful not to scratch its surface.

17. Higher hybridization and wash temperatures may be required when using Klenow probes because of their lower specificity (Fig. 5). Caution: Ensure that all buffer components are fully dissolved by preheating the solution to 35 °C.

Acknowledgments

M.B., A.G., and D.P. developed the bioinformatics pipeline for TE annotation, genome browser display, and northern blot probe design. M.B., B.R., and C.H. performed the molecular genetic and benchtop experiments. R.S., D. L.-C., A.C., and J.V. provided *B. distachyon* mutant germplasm identified using high-throughput sequencing and bioinformatics; work at the US DOE Joint Genome Institute is supported by the Office of Science of the US Department of Energy under Contract no. DE-AC02-05CH1123 and by user agreement FP00004794 between JGI and the USDA Agricultural Research Service. M.B., B.R., and T.B. assembled the figures and wrote the manuscript. The authors thank Hugues Renault for advice on culturing *B. distachyon* and for providing wild-type seed (Bd21-3). This study relied upon the dedicated support of the IBMP gardeners, bioinformatics platform, and sequencing facility staff. The Blevins Group is supported by the LabEx consortium ANR-10-LABX-0036_NETRINA (“Investissements d’Avenir”) and by the French Agence Nationale de la Recherche (ANR) Grant ANR-17-CE20-0004-01.

References

1. Fire A, Xu S, Montgomery MK et al (1998) Potent and specific genetic interference by double-stranded RNA in *Caenorhabditis elegans*. *Nature* 391:806–811. <https://doi.org/10.1038/35888>
2. Hamilton AJ, Baulcombe DC (1999) A species of small antisense RNA in posttranscriptional gene silencing in plants. *Science* (80-) 286:950–952. <https://doi.org/10.1126/science.286.5441.950>
3. Mette MF, Aufsatz W, van der Winden J et al (2000) Transcriptional silencing and promoter methylation triggered by double-stranded RNA. *EMBO J* 19:5194–5201. <https://doi.org/10.1093/emboj/19.19.5194>
4. Hamilton A, Voinnet O, Chappell L, Baulcombe D (2002) Two classes of short interfering RNA in RNA silencing. *EMBO J* 21:4671–4679. <https://doi.org/10.1093/emboj/cdf464>
5. Xie Z, Johansen LK, Gustafson AM et al (2004) Genetic and functional diversification of small RNA pathways in plants. *PLoS Biol* 2:E104. <https://doi.org/10.1371/journal.pbio.0020104>
6. Onodera Y, Haag JR, Ream T et al (2005) Plant nuclear RNA polymerase IV mediates siRNA and DNA methylation-dependent heterochromatin formation. *Cell* 120:613–622. <https://doi.org/10.1016/j.cell.2005.02.007>
7. Vazquez F, Vaucheret H, Rajagopalan R et al (2004) Endogenous trans-acting siRNAs regulate the accumulation of Arabidopsis mRNAs. *Mol Cell* 16:69–79. <https://doi.org/10.1016/j.molcel.2004.09.028>
8. Zilberman D, Cao X, Johansen LK et al (2004) Role of Arabidopsis ARGONAUTE4 in RNA-directed DNA methylation triggered by inverted repeats. *Curr Biol* 14:1214–1220. <https://doi.org/10.1016/j.cub.2004.06.055>
9. Reinhart BJ, Weinstein EG, Rhoades MW et al (2002) MicroRNAs in plants. *Genes Dev* 16:1616–1626. <https://doi.org/10.1101/gad.1004402>

10. Llave C, Xie Z, Kasschau KD, Carrington JC (2002) Cleavage of Scarecrow-like mRNA targets directed by a class of Arabidopsis miRNA. *Science* 297:2053–2056. <https://doi.org/10.1126/science.1076311>
11. Fagard M, Boutet S, Morel JB et al (2000) AGO1, QDE-2, and RDE-1 are related proteins required for post-transcriptional gene silencing in plants, quelling in fungi, and RNA interference in animals. *Proc Natl Acad Sci U S A* 97:11650–11654. <https://doi.org/10.1073/pnas.200217597>
12. Park W, Li J, Song R et al (2002) CARPEL FACTORY, a Dicer homolog, and HEN1, a novel protein, act in microRNA metabolism in Arabidopsis thaliana. *Curr Biol* 12:1484–1495. [https://doi.org/10.1016/s0960-9822\(02\)01017-5](https://doi.org/10.1016/s0960-9822(02)01017-5)
13. Palatnik JF, Allen E, Wu X et al (2003) Control of leaf morphogenesis by microRNAs. *Nature* 425:257–263. <https://doi.org/10.1038/nature01958>
14. Aukerman MJ, Sakai H (2003) Regulation of flowering time and floral organ identity by a MicroRNA and its APETALA2-like target genes. *Plant Cell* 15:2730–2741. <https://doi.org/10.1105/tpc.016238>
15. Peragine A, Yoshikawa M, Wu G et al (2004) SGS3 and SGS2/SDE1/RDR6 are required for juvenile development and the production of trans-acting siRNAs in Arabidopsis. *Genes Dev* 18:2368–2379. <https://doi.org/10.1101/gad.1231804>
16. Vaucheret H, Vazquez F, Crete P, Bartel DP (2004) The action of ARGONAUTE1 in the miRNA pathway and its regulation by the miRNA pathway are crucial for plant development. *Genes Dev* 18:1187–1197. <https://doi.org/10.1101/gad.1201404>
17. Baumberger N, Baulcombe DC (2005) Arabidopsis ARGONAUTE1 is an RNA Slicer that selectively recruits microRNAs and short interfering RNAs. *Proc Natl Acad Sci U S A* 102:11928–11933. <https://doi.org/10.1073/pnas.0505461102>
18. Chen X (2004) A microRNA as a translational repressor of APETALA2 in Arabidopsis flower development. *Science* 303:2022–2025. <https://doi.org/10.1126/science.1088060>
19. Allen E, Xie Z, Gustafson AM, Carrington JC (2005) microRNA-directed phasing during trans-acting siRNA biogenesis in plants. *Cell* 121:207–221. <https://doi.org/10.1016/j.cell.2005.04.004>
20. Fahlgren N, Montgomery TA, Howell MD et al (2006) Regulation of AUXIN RESPONSE FACTOR3 by TAS3 ta-siRNA affects developmental timing and patterning in Arabidopsis. *Curr Biol* 16:939–944. <https://doi.org/10.1016/j.cub.2006.03.065>
21. Bennetzen JL, Park M (2018) Distinguishing friends, foes, and freeloaders in giant genomes. *Curr Opin Genet Dev* 49:49–55. <https://doi.org/10.1016/j.gde.2018.02.013>
22. Matzke MA, Mosher RA (2014) RNA-directed DNA methylation: an epigenetic pathway of increasing complexity. *Nat Rev Genet* 15:394–408. <https://doi.org/10.1038/nrg3683>
23. Ferrafiat L, Pflieger D, Singh J et al (2019) The NRPD1 N-terminus contains a Pol IV-specific motif that is critical for genome surveillance in Arabidopsis. *Nucleic Acids Res*. <https://doi.org/10.1093/nar/gkz618>
24. Law JA, Du J, Hale CJ et al (2013) Polymerase IV occupancy at RNA-directed DNA methylation sites requires SHH1. *Nature* 498:385–389. <https://doi.org/10.1038/nature12178>
25. Wendte JM, Haag JR, Pontes OM et al (2019) The Pol IV largest subunit CTD quantitatively affects siRNA levels guiding RNA-directed DNA methylation. *Nucleic Acids Res*. <https://doi.org/10.1093/nar/gkz615>
26. Ream TS, Haag JR, Wierzbicki AT et al (2009) Subunit compositions of the RNA-silencing enzymes Pol IV and Pol V reveal their origins as specialized forms of RNA polymerase II. *Mol Cell* 33:192–203. <https://doi.org/10.1016/j.molcel.2008.12.015>
27. Haag JR, Ream TS, Marasco M et al (2012) In vitro transcription activities of Pol IV, Pol V, and RDR2 reveal coupling of Pol IV and RDR2 for dsRNA synthesis in plant RNA silencing. *Mol Cell* 48:811–818. <https://doi.org/10.1016/J.MOLCEL.2012.09.027>
28. Singh J, Mishra V, Wang F et al (2019) Reaction mechanisms of Pol IV, RDR2, and DCL3 drive RNA channeling in the siRNA-directed DNA methylation pathway. *Mol Cell* 75:576–589.e5. <https://doi.org/10.1016/j.molcel.2019.07.008>
29. Zhai J, Bischof S, Wang H et al (2015) A one precursor one siRNA model for Pol IV-dependent siRNA biogenesis. *Cell* 163:445–455. <https://doi.org/10.1016/j.cell.2015.09.032>
30. Blevins T, Podicheti R, Mishra V et al (2015) Identification of Pol IV and RDR2-dependent precursors of 24 nt siRNAs guiding de novo DNA methylation in Arabidopsis. *elife* 4. <https://doi.org/10.7554/eLife.09591>
31. Wierzbicki AT, Ream TS, Haag JR, Pikaard CS (2009) RNA polymerase V transcription guides

- ARGONAUTE4 to chromatin. *Nat Genet* 41:630–634. <https://doi.org/10.1038/ng.365>
32. Blevins T, Pontvianne F, Cocklin R et al (2014) A two-step process for epigenetic inheritance in Arabidopsis. *Mol Cell* 54:30–42. <https://doi.org/10.1016/j.molcel.2014.02.019>
 33. Ito H, Gaubert H, Bucher E et al (2011) An siRNA pathway prevents transgenerational retrotransposition in plants subjected to stress. *Nature* 472:115–119. <https://doi.org/10.1038/nature09861>
 34. Mirouze M, Reinders J, Bucher E et al (2009) Selective epigenetic control of retrotransposition in Arabidopsis. *Nature* 461:427–430. <https://doi.org/10.1038/nature08328>
 35. Lanciano S, Mirouze M (2018) Transposable elements: all mobile, all different, some stress responsive, some adaptive? *Curr Opin Genet Dev* 49:106–114. <https://doi.org/10.1016/j.gde.2018.04.002>
 36. Grandbastien M-A (2015) LTR retrotransposons, handy hitchhikers of plant regulation and stress response. *Biochim Biophys Acta* 1849:403–416. <https://doi.org/10.1016/j.bbagr.2014.07.017>
 37. Cavrak VV, Lettner N, Jamge S et al (2014) How a retrotransposon exploits the plant's heat stress response for its activation. *PLoS Genet* 10:e1004115. <https://doi.org/10.1371/journal.pgen.1004115>
 38. Pietzenek B, Markus C, Gaubert H et al (2016) Recurrent evolution of heat-responsiveness in Brassicaceae COPIA elements. *Genome Biol* 17:209. <https://doi.org/10.1186/s13059-016-1072-3>
 39. Platt RN 2nd, Blanco-Berdugo L, Ray DA (2016) Accurate transposable element annotation is vital when analyzing new genome assemblies. *Genome Biol Evol* 8:403–410
 40. Underwood CJ, Henderson IR, Martienssen RA (2017) Genetic and epigenetic variation of transposable elements in Arabidopsis. *Curr Opin Plant Biol* 36:135–141. <https://doi.org/10.1016/j.pbi.2017.03.002>
 41. El Baidouri M, Do KK, Abernathy B et al (2015) A new approach for annotation of transposable elements using small RNA mapping. *Nucleic Acids Res* e84:43. <https://doi.org/10.1093/nar/gkv257>
 42. Ahmed I, Sarazin A, Bowler C et al (2011) Genome-wide evidence for local DNA methylation spreading from small RNA-targeted sequences in Arabidopsis. *Nucleic Acids Res* 39:6919–6931. <https://doi.org/10.1093/nar/gkr324>
 43. Forestan C, Farinati S, Aiese Cigliano R et al (2017) Maize RNA PolIV affects the expression of genes with nearby TE insertions and has a genome-wide repressive impact on transcription. *BMC Plant Biol* 17:161. <https://doi.org/10.1186/s12870-017-1108-1>
 44. Slotkin RK, Martienssen R (2007) Transposable elements and the epigenetic regulation of the genome. *Nat Rev Genet* 8:272–285. <https://doi.org/10.1038/nrg2072>
 45. Axtell MJ (2013) Classification and comparison of small RNAs from plants. *Annu Rev Plant Biol* 64:137–159. <https://doi.org/10.1146/annurev-arplant-050312-120043>
 46. Meyers BC, Souret FF, Lu C, Green PJ (2006) Sweating the small stuff: microRNA discovery in plants. *Curr Opin Biotechnol* 17:139–146. <https://doi.org/10.1016/j.copbio.2006.01.008>
 47. Lutzmayer S, Enugutti B, Nodine MD (2017) Novel small RNA spike-in oligonucleotides enable absolute normalization of small RNA-Seq data. *Sci Rep* 7:5913. <https://doi.org/10.1038/s41598-017-06174-3>
 48. Goodstein DM, Shu S, Howson R et al (2012) Phytozome: a comparative platform for green plant genomics. *Nucleic Acids Res* 40:D1178–D1186. <https://doi.org/10.1093/nar/gkr944>
 49. International Brachypodium Initiative (2010) Genome sequencing and analysis of the model grass *Brachypodium distachyon*. *Nature* 463:763–768. <https://doi.org/10.1038/nature08747>
 50. Jeong D-H, Schmidt SA, Rymarquis LA et al (2013) Parallel analysis of RNA ends enhances global investigation of microRNAs and target RNAs of *Brachypodium distachyon*. *Genome Biol* 14:R145. <https://doi.org/10.1186/gb-2013-14-12-r145>
 51. Gremme G, Steinbiss S, Kurtz S (2013) GenomeTools: a comprehensive software library for efficient processing of structured genome annotations. *IEEE/ACM Trans Comput Biol Bioinform* 10:645–656. <https://doi.org/10.1109/TCBB.2013.68>
 52. Martin M (2011) Cutadapt removes adapter sequences from high-throughput sequencing reads. *EMBnet J* 17:10. <https://doi.org/10.14806/ej.17.1.200>
 53. Johnson NR, Yeoh JM, Coruh C, Axtell MJ (2016) Improved placement of multi-mapping small RNAs. *G3 (Bethesda)* 6:2103–2111. <https://doi.org/10.1534/G3.116.030452>
 54. Axtell MJ (2013) ShortStack: comprehensive annotation and quantification of small RNA

- genes. *RNA* 19:740–751. <https://doi.org/10.1261/rna.035279.112>
55. Langmead B, Trapnell C, Pop M, Salzberg SL (2009) Ultrafast and memory-efficient alignment of short DNA sequences to the human genome. *Genome Biol* 10:R25. <https://doi.org/10.1186/gb-2009-10-3-r25>
56. Li H, Handsaker B, Wysoker A et al (2009) The Sequence Alignment/Map format and SAMtools. *Bioinformatics* 25:2078–2079. <https://doi.org/10.1093/bioinformatics/btp352>
57. Buels R, Yao E, Diesh CM et al (2016) JBrowse: a dynamic web platform for genome visualization and analysis. *Genome Biol* 17:66. <https://doi.org/10.1186/s13059-016-0924-1>
58. Thorvaldsdottir H, Robinson JT, Mesirov JP (2013) Integrative Genomics Viewer (IGV): high-performance genomics data visualization and exploration. *Brief Bioinform* 14:178–192. <https://doi.org/10.1093/bib/bbs017>
59. Robinson JT, Thorvaldsdóttir H, Winckler W et al (2011) Integrative genomics viewer. *Nat Biotechnol* 29:24–26. <https://doi.org/10.1038/nbt.1754>
60. Brkljacic J, Grotewold E, Scholl R et al (2011) Brachypodium as a model for the grasses: today and the future. *Plant Physiol* 157:3–13. <https://doi.org/10.1104/pp.111.179531>
61. Hirochika H, Okamoto H, Kakutani T (2000) Silencing of retrotransposons in Arabidopsis and reactivation by the ddm1 mutation. *Plant Cell* 12:357–369. <https://doi.org/10.1105/tpc.12.3.357>
62. Tsukahara S, Kobayashi A, Kawabe A et al (2009) Bursts of retrotransposition reproduced in Arabidopsis. *Nature* 461:423–426. <https://doi.org/10.1038/nature08351>
63. Thieme M, Lanciano S, Balzergue S et al (2017) Inhibition of RNA polymerase II allows controlled mobilisation of retrotransposons for plant breeding. *Genome Biol* 18:134. <https://doi.org/10.1186/s13059-017-1265-4>
64. Akbergenov R, Si-Ammour A, Blevins T et al (2006) Molecular characterization of geminivirus-derived small RNAs in different plant species. *Nucleic Acids Res* 34:462–471. <https://doi.org/10.1093/nar/gkj447>
65. Blevins T (2017) Northern blotting techniques for small RNAs. *Methods Mol Biol* 1456:141–162. https://doi.org/10.1007/978-1-4899-7708-3_12



Transfection of Small Noncoding RNAs into *Arabidopsis thaliana* Protoplasts

Stéphanie Lalande, Marjorie Chery, Elodie Ubrig, Guillaume Hummel, Julie Kubina, Angèle Geldreich, and Laurence Drouard

Abstract

Polyethylene glycol transfection of plant protoplasts represents an efficient method to incorporate foreign DNA and study transient gene expression. Here, we describe an optimized protocol to deliver small noncoding RNAs into *Arabidopsis thaliana* protoplasts. An example of application is provided by demonstrating the incorporation of a 20 nt long small noncoding RNA deriving from the 5' extremity of an *A. thaliana* cytosolic alanine tRNA into freshly isolated protoplasts.

Key words Transfection, Small noncoding RNAs, tRNA-derived fragments, Protoplasts, Northern blot

1 Introduction

Among the various classes of small noncoding RNAs (sncRNAs), tRNA-derived fragments (tRFs) are now recognized as important regulators of numerous biological processes [1–4]. In plants, tRFs represent a large and dynamic repertoire of small RNA fragments [5] but their molecular functions are still poorly understood [2]. Among the different ways to decipher the molecular processes in which tRFs are involved, the use of in vivo approaches is rather limited. Indeed, the production of specific tRFs in transgenic plants remains difficult to achieve. Facing this bottleneck, cell transfection represents an interesting option. This technique, mainly developed in the animal field to study the biology of miRNAs or siRNAs, is based on the use of lipofectamine, a reagent that facilitates efficient delivery of small RNA molecules into cells (see for instance [6, 7]). In plants, to deliver nucleic acids, researchers have chosen to work with plant protoplasts (i.e., cells without their cell wall). Nevertheless, chemicals such as lipofectamine appeared toxic and inefficient [8] and thus are rarely utilized. Rather, three other types of

methods have been developed to transfect macromolecules: electroporation (e.g., [9]), microinjection (e.g., [10]), and polyethylene glycol (PEG)-mediated transfection (e.g., [11], the latter method being the most widely used). Such protocols are often employed to deliver DNA into protoplasts for transient gene expression studies, but the incorporation of RNAs into plant protoplasts has also been developed. For instance, viral RNAs, siRNAs, and tRNAs were electroporated into protoplasts [12, 13] and a PEG method allowed viral RNA to be delivered [14]. Here, we have adapted and optimized an efficient DNA transfection method described in details by Yoo et al. [11] to incorporate sncRNAs into *Arabidopsis thaliana* protoplasts. As an example of application, we describe here the transfection of an *A. thaliana* 20 nt long tRF alanine (tRF Ala20) [5] into protoplasts isolated either from an *A. thaliana* cell culture or from young seedlings. To validate the PEG transfection protocol, incorporation of tRF Ala20 was verified by northern blot analysis of the small RNA population extracted from RNase-treated transfected protoplasts. Therefore, we propose this efficient RNA transfection method as a new tool to study the biology of sncRNAs. For example, tagged (e.g., fluorophores, biotin) sncRNAs could be applied for in vivo live imaging or interactome studies.

2 Materials

2.1 Plant Material

1. Culture of individualized cells obtained from the Landsberg *A. thaliana* ecotype.
2. *A. thaliana* Columbia (Col-0) ecotype seeds.

2.2 Nucleic Acids

1. 100 μM Synthetic oligoribonucleotide of interest dissolved in diethyl pyrocarbonate (DEPC)-treated water at a 100 μM concentration.
2. Any plasmid of small size (i.e., 3–4 kb).
3. 100 μM Oligodeoxynucleotide with a sequence complementary to the sequence of the small RNA of interest.

2.3 Solutions

All solutions should be prepared with RNase-free materials and reagents, and with RNase-free, sterile, and ultrapure water. Solutions are autoclaved for 15 min at 120 °C (except otherwise stated). Procedures for preparing classical solutions can be found in Sambrook and Russell [15].

1. Cell culture medium: 4.41 g/L MS256, 30 g/L sucrose, 5.4 μM α -naphthaleneacetic acid (NAA), 0.23 μM kinetin, pH 5.6. Weigh 4.41 g of MS256 and 30 g of sucrose. Transfer to a glass beaker. Add about 500 mL of water. Mix well and adjust pH to 5.6 with 1 N KOH. Add 100 μL of 10 mg/mL

NAA and 50 μL of 1 mg/mL kinetin. Transfer to a cylinder and adjust volume to 1 L with water. Autoclave and store at room temperature.

2. Seed sterilization solution: 0.1% (v/v) Tween-20, 70% (v/v) ethanol. Under a sterile hood, filter solution with a 0.20 μm filter in a sterile bottle. Store at room temperature.
3. Seedling culture medium: 2.21 g/L MS222, 0.5 g/L 2-(*N*-morpholino)ethanesulfonic acid (MES), 10 g/L sucrose, 0.68% agar, pH 5.7. Weigh 2.21 g of MS222, 0.5 g of MES monohydrate, and 10 g of sucrose. Transfer to a glass beaker. Add about 500 mL of water. Mix well and adjust pH to 5.7 with 1 N KOH. Transfer to a cylinder and adjust volume to 1 L with water. Transfer to a bottle and add 6.8 g of agar. Autoclave and store at room temperature.
4. 2 M KCl: Store at room temperature.
5. 1 M MgCl_2 : Store at room temperature.
6. 1 M CaCl_2 : Store at room temperature.
7. 5 M NaCl: Store at room temperature.
8. 0.5 M Mannitol, pH 5.7: Weigh 227.75 g of D-mannitol and 1.75 g of MES monohydrate. Transfer to a glass beaker. Add about 1.5 L of water. Mix and adjust pH to 5.7 with 10 N KOH. Transfer to a cylinder and adjust volume to 2.5 L with water. Autoclave and store at 4 °C.
9. 0.5 M MES, pH 5.7: Weigh 53.3 g of MES monohydrate and transfer to a glass beaker. Add about 400 mL of water. Mix and adjust pH to 5.7 with 10 N KOH. Transfer to a glass cylinder and adjust volume to 500 mL with water. Autoclave and store at room temperature.
10. MM buffer: 0.5 M Mannitol, 4 mM MES, pH 5.7. Pipette 8 mL of 0.5 M MES, pH 5.7, and transfer to a 1 L glass cylinder. Add 0.5 M mannitol, pH 5.7, to a final volume of 1 L and mix well. Autoclave and store at 4 °C.
11. MMG buffer: 0.5 M Mannitol, 4 mM MES, 15 mM MgCl_2 , pH 5.7. Pipette 7.5 mL of 1 M MgCl_2 and transfer to a 1 L glass cylinder. Add MM buffer to a final volume of 500 mL and mix well. Autoclave and store at 4 °C.
12. WI buffer: 0.5 M Mannitol, 4 mM MES, 20 mM KCl, pH 5.7. Pipette 5 mL of 2 M KCl and transfer to a 1 L glass cylinder. Add MM buffer to a final volume of 500 mL and mix well. Autoclave and store at 4 °C.
13. W5 buffer: 2 mM MES, 154 mM NaCl, 125 mM CaCl_2 , 5 mM KCl, pH 5.7. Mix in a glass cylinder 62.5 mL of 1 M CaCl_2 , 15.4 mL of 5 M NaCl, 2 mL of 0.5 M MES pH 5.7, and 1.25 mL of 2 M KCl. Add water to a final volume of 500 mL and mix well. Autoclave and store at 4 °C.

14. TriReagent™ (Sigma-Aldrich) or TRIzol™ Reagent (Ambion): Store at 4 °C.
15. Chloroform: Store at room temperature.
16. Isopropanol: Store at room temperature.
17. 100% Ethanol: Store at room temperature.
18. “Cold” ethanol: 50 mL 100% Ethanol cooled to –20 °C .
19. 95% Ethanol: Mix 47.5 mL of 100% ethanol with 2.5 mL of water. Mix well and store at –20 °C.
20. Diethyl pyrocarbonate (DEPC)-treated water: DEPC is toxic; prepare the solution under a chemical hood. In a bottle, add 0.001% volume of DEPC to 100 mL water. DEPC has limited solubility in water as evidenced by the appearance of globules; thus mix well until globules disappear. Incubate for 16 h, and autoclave. Make aliquots of 2–10 mL, and store at –20 °C.
21. 1 M Tris–HCl, pH 7.5: Weigh 12.11 g of Tris and transfer to a glass beaker. Add about 70 mL of water, mix, and adjust pH to 7.5 with 1 N HCl (*see Note 1*). Transfer to a glass cylinder and adjust volume to 100 mL with water. Autoclave and store at room temperature.
22. 5 M LiCl solution: 5 M LiCl, 50 mM Tris–HCl, pH 7.5. Weigh 21.2 g of LiCl and transfer to a glass beaker. Add 5 mL of 1 M Tris–HCl, pH 7.5, and water to a volume of 90 mL. Mix thoroughly until LiCl is completely dissolved. Transfer to a glass cylinder and adjust volume to 100 mL with water. Autoclave and store at room temperature.
23. 1 M Sodium acetate, pH 4.5: Weigh 8.2 g of sodium acetate and transfer to a glass beaker. Add water to a volume of 70 mL and mix until sodium acetate is completely dissolved. Adjust pH to 4.5 with 99% pure acetic acid. Transfer to a glass cylinder and adjust volume with water to 100 mL. Autoclave and store at room temperature.
24. 0.5 M EDTA, pH 8.0: Weigh 29.2 g of ethylenediaminetetraacetic acid (EDTA) and transfer to a glass beaker. Add 150 mL of water. Mix well and add NaOH pellets until EDTA is completely dissolved (*see Note 2*). Adjust pH to 8.0 with 1 N NaOH. Transfer to a glass cylinder and adjust volume to 200 mL with water. Autoclave and store at room temperature.
25. 2× Loading buffer: 95% (v/v) Formamide, 20 mM EDTA, pH 8.0, 0.05% (w/v), bromophenol blue, 0.05% (w/v) xylene cyanol. Weigh 0.025 g of bromophenol blue and 0.025 g of xylene cyanol and transfer to a 50 mL tube. Add 2 mL of 0.5 M EDTA, pH 8.0, and 0.5 mL of water. Mix by vortexing and add 47.5 mL of formamide. Mix well and store at room temperature.

26. 10× TBE: 900 mM Tris, 20 mM EDTA, 900 mM boric acid. Weigh 109 g of Tris and 55.6 g of boric acid and transfer to a glass beaker. Add 40 mL of 0.5 M EDTA, pH 8.0, and water to a volume of about 900 mL, and mix. Transfer to a glass cylinder and adjust volume to 1 L with water. Autoclave and store at room temperature (*see Note 3*).
27. 1× TBE: 90 mM Tris, 2 mM EDTA, 90 mM boric acid. Mix 100 mL of 10× TBE with 900 mL of water in a glass cylinder. Mix well and store at room temperature.
28. 0.5× TBE: 45 mM Tris, 1 mM EDTA, 45 mM boric acid. Mix 50 mL of 10× TBE with 950 mL of water in a glass cylinder. Mix well and store at room temperature.
29. 15% Denaturing acrylamide gel: 15% Acrylamide/bis-acrylamide 19/1, 7 M urea, 1× TBE. Weigh 84 g of urea and transfer to a glass beaker. Add 75 mL of 40% acrylamide/bis-acrylamide (19:1) and 20 mL of 10× TBE. Add water to a volume of 190 mL and mix thoroughly until the urea is completely dissolved. Transfer to a cylinder and adjust volume to 200 mL with water. Mix well and store at room temperature in a bottle wrapped in aluminum foil to avoid light exposure.
30. 10% (w/v) Ammonium persulfate (APS): Store at 4 °C.
31. *N,N,N,N'*-tetramethylethylenediamine (TEMED): Store at 4 °C.
32. 1% Ethidium bromide: Store at 4 °C.
33. G-50 resin: Pour about 1 mL of Sephadex G-50 resin powder in a 14 mL round-bottom tube. Add about 10 mL of water and mix well. Autoclave and store at 4 °C.
34. PerfectHyb™ Plus hybridization buffer (Sigma-Aldrich).
35. 20× Saline sodium citrate (SSC): 3 M NaCl, 300 mM trisodium citrate, pH 7.0. Weigh 175.3 g of NaCl and 88.2 g of sodium citrate dihydrate and transfer to a glass beaker. Add about 500 mL of water, and mix. Adjust pH to 7.0 with 99% pure acetic acid. Transfer to a glass cylinder and adjust volume to 1 L with water. Autoclave and store at room temperature.
36. 2× SSC: 0.3 M NaCl, 30 mM trisodium citrate, pH 7.0. Mix 50 mL of 20× SSC with 450 mL of water in a glass cylinder. Mix well and store at room temperature.
37. 10% (w/v) Sodium dodecyl sulfate (SDS) (*see Note 4*): Autoclave and store at room temperature.
38. 2× SSC, 0.1% SDS: Transfer 50 mL of 20× SSC into a 500 mL cylinder. Add 400 mL of water and then 5 mL of 10% SDS. Adjust volume to 500 mL by gently adding water to avoid foaming. Mix and store at room temperature (*see Note 5*).

2.4 Enzymes and Other Reagents

1. Cellulase R10 (Yakult Pharmaceutical Industry Co., Ltd).
2. Macerozyme R10 (Yakult Pharmaceutical Industry Co., Ltd).
3. 10% Acetylated BSA.
4. PEG-4000.
5. RNase A/T1 mix: 2 mg/mL RNase A, 5000 units/mL RNase T1.
6. 20 mg/mL Glycogen.
7. 10 units/ μ L Polynucleotide kinase.
8. 10 \times Polynucleotide kinase buffer.
9. 10 μ Ci/ μ L (2500 Ci/mmol) Radiolabeled [γ ³²P]-adenosine triphosphate (ATP).

2.5 Equipment and Miscellaneous Material

1. Erlenmeyer of 250 mL.
2. Water bath.
3. Centrifuge allowing deceleration without brake, with rotors compatible for 2 mL, 14 mL, and 50 mL tubes.
4. 2 mL Round-bottom tubes.
5. 14 mL Round-bottom tubes.
6. 50 mL Tubes.
7. Wide-mouth pipettes (tips of at least a 2 mm diameter).
8. Micropipette tips cut at their extremity to enlarge the opening (2 mm diameter).
9. Incubator.
10. Petri dishes (100 mm diameter; 20 mm height).
11. Square Petri dish (120 mm \times 120 mm).
12. Scalpel blade.
13. 12-Well plate (3.65 cm²/well) for cell culture.
14. Micropore gas-permeable tape.
15. Orbital shaker.
16. Tube rotator.
17. Vacuum chamber.
18. Miracloth.
19. Inverted bright-field microscope.
20. Fuchs-Rosenthal cell.
21. Mini PROTEAN™ TetraHandcast System (Biorad).
22. Mini PROTEAN™ TetraCell System (Biorad).
23. 15-Well comb.
24. Power supply Power Pac basic (Biorad).
25. UV transilluminator.

26. Trans-Blot™ Plus cell (Biorad).
27. Hybond™ N+ nylon membrane.
28. Whatman 3 MM paper.
29. UV stratalinker.
30. 1 mL Syringe.
31. Sephadex G-50.
32. Fiberglass.
33. Hybridization tubes.
34. Hybridization oven.
35. Phosphorimager (with plate) or X-ray developing unit (and X-ray film).

3 Methods

The workflow includes the isolation of protoplasts from either cell cultures or seedlings of *A. thaliana*, transfection of tRFs, extraction of total sncRNA from transfected protoplasts, and a northern blot experiment to confirm the uptake of tRFs into the cells.

Protoplasts must be manipulated very carefully to avoid lysis. Always use wide-mouth pipettes with a large hole. Tips for micro-pipettes must be cut at their extremity to expand the opening (*see Note 6*). Never vortex the protoplasts and always centrifuge them without brake (*see Note 7*). When removing the supernatant after a centrifugation, always let a minimal volume of culture medium to cover protoplasts with liquid and avoid excessive changes of osmotic pressure. Do not directly pour the solution into the tube with protoplasts but rather always allow the solution to flow along the tube wall (*see Note 8*).

3.1 *A. thaliana* Cell Culture

3.1.1 Cell Culture Maintenance

1. Under a sterile hood, pour 100 mL of cell culture medium into a 250 mL Erlenmeyer.
2. Gently stir to homogenize the distribution of cells in a 7-day-old *A. thaliana* cell culture. Delicately transfer 4 mL of the culture into the new medium using a pipette.
3. Incubate for 7 days at 24 °C under constant light on an orbital shaker at 130 rpm.
4. Repeat **steps 1–3** weekly to maintain the cell culture.

3.1.2 Cell Culture for Protoplast Isolation

1. To 100 mL of cell culture medium, add 4 mL of a 7-day-old *A. thaliana* cell culture as described above.
2. Incubate for 10–11 days at 24 °C under constant light condition on an orbital shaker at 130 rpm.

3.2 A. thaliana**Seedlings**

All steps requiring opening of a tube need to be performed under a sterile hood.

**3.2.1 Arabidopsis Seed
Sterilization**

1. Prepare around 50 μL of *A. thaliana* Col-0 seeds in a 1.5 mL microtube (*see Note 9*).
2. Add 1 mL of seed sterilization solution. Mix to resuspend the seeds.
3. Gently mix for 15 min on a tube rotator.
4. Centrifuge at $3000 \times g$ for 10 s to pellet the seeds.
5. Carefully remove the supernatant.
6. Add 1 mL of 100% ethanol and mix to resuspend the seeds.
7. Gently mix on a tube rotator for 2 min.
8. Centrifuge at $3000 \times g$ for 10 s to pellet the seeds.
9. Remove as much supernatant as possible.
10. Repeat **steps 6–9** one more time.
11. Gently hit the tube with a finger to spread seeds, open the tube, and allow the seeds to dry for 1 h.

**3.2.2 Growing
Arabidopsis Seedlings**

1. Heat seedling growth medium in a microwave to melt it. Under a sterile hood, pour 50 mL of the medium into a square Petri dish (120 mm \times 120 mm) and let the dish open until the medium is solidified.
2. Scatter the sterilized seeds onto the solidified medium.
3. Seal the dish with micropore gas-permeable tape.
4. Allow the seeds to vernalize by keeping the dish at 4 °C for 2–5 days.
5. Let seedlings grow for 7 days under long day conditions (8-h dark at 17 °C, 16-h light at 21 °C).

**3.3 Isolation
of Protoplasts**

Digestion buffer must be prepared just before use. The following protocol is given for 50 mL digestion buffer.

**3.3.1 Preparation
of Digestion Buffer**

1. Preheat a water bath to 55 °C.
2. Weigh 0.75 g of cellulase and 0.2 g of macerozyme and transfer to a 50 mL tube.
3. Add 40 mL of 0.5 M mannitol, pH 5.7, 2.5 mL of 0.4 M MES, and 500 μL of 2 M KCl. Vortex and heat at 55 °C until enzymes are completely dissolved.
4. Add 500 μL of 1 M CaCl_2 and 500 μL of acetylated BSA. Adjust volume to 50 mL with water and gently mix.

**3.3.2 Removal of Cell
Walls from Cultured Cells**

25 mL of digestion buffer per 10 mL of cell culture is required.

1. Transfer 10 mL of a 10–11-day-old cell culture (Fig. 1a) into a 50 mL tube using a pipette.
2. Centrifuge the cells for 1 min at $100 \times g$ without brake. Remove most of the supernatant (keep a small volume of medium on the top) by pipetting and gently tapping the tubes to resuspend cells.
3. Wash cells by adding 30 mL of 0.5 M mannitol, pH 5.7. Centrifuge for 1 min at $100 \times g$ without brake. As above, discard supernatant and tap the tubes to resuspend cells.
4. Add 25 mL of digestion buffer and pour the mixture into a Petri dish. Cover with aluminum foil and incubate for 4 h at 26°C at 50 rpm (orbital shaker).

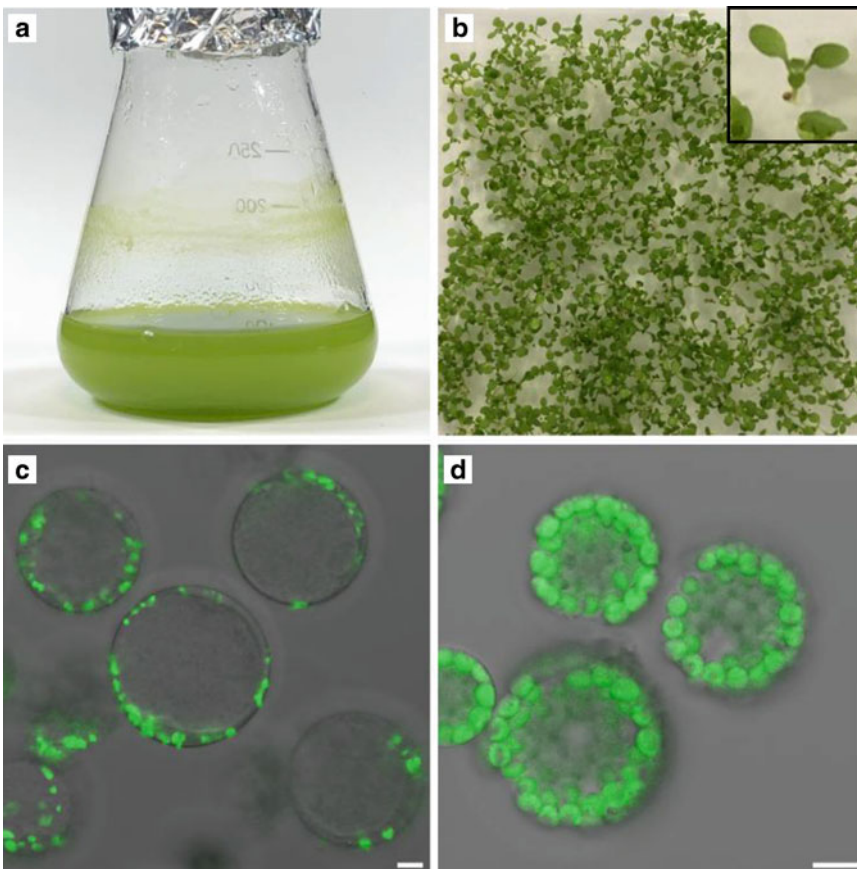


Fig. 1 Protoplast preparation from *A. thaliana* cell culture and seedlings. (a) 11-Day-old cell culture of *A. thaliana* ecotype Landsberg. (b) 7-Day-old seedlings of the *A. thaliana* Col-0 ecotype. Enlargement of a seedling is shown in the top-right edge. (c) Visualization by confocal microscopy of isolated protoplasts prepared from cell culture. (d) Visualization by confocal microscopy of isolated protoplasts from seedlings. Chlorophyll autofluorescence (green) reveals chloroplasts and their integrity (Zeiss LSM780 confocal microscope, 633 nm laser). Scale bars: 10 μm

3.3.3 Removal of Cell Walls from Seedlings

25 mL of digestion buffer per 200 mg of young seedling leaves is required.

1. Place 2 mL of digestion buffer into a Petri dish.
2. From a 7-day-old culture of seedlings (Fig. 1b), cut seedlings with scissors to remove the roots. Weigh 200 mg of the remaining young leaves and transfer them to the Petri dish.
3. Carefully lacerate leaves with a scalpel blade and cover them with 23 mL of digestion buffer. Lacerated leaves must never be in contact with air and must not dry.
4. Incubate in a vacuum chamber at 0.01 bar until bubbles appear. Wait for 1 min to allow buffer infiltration into tissues, and slowly break vacuum.
5. Cover Petri dish with aluminum foil, and incubate at 26 °C overnight at 50 rpm (orbital shaker).

3.3.4 Purification of Protoplasts

1. After cell wall digestion (using cells from either cell culture or seedlings), place a funnel with a single layer of Miracloth on an Erlenmeyer. Wet the Miracloth with 10 mL of MM buffer.
2. Add 10 mL of MM buffer to the protoplast digestion mixture (*see Note 8*). Break cell aggregates by pipetting 2–3 mL of the mixture with a 10 mL pipette and by creating bubbles by pipetting air. Pour the cell culture back into Petri dish, and repeat this operation several times, to allow the release of the majority of protoplasts. Disappearance of aggregates can be followed by observing a drop with an inverted microscope.
3. Filter protoplasts through the Miracloth layer and transfer 10 mL aliquots of the filtrate into 14 mL round-bottom tubes. This step removes the undigested cell walls and tissues.
4. Centrifuge for 3 min at $100 \times g$ without brake. Remove supernatant and resuspend the protoplasts by gentle swirling.
5. Add 5 mL of W5 buffer per tube. Gather the content of two tubes into one. Centrifuge for 1 min at $100 \times g$ without brake.
6. Remove supernatant and softly resuspend protoplasts.
7. Repeat **steps 5 and 6** until all protoplasts are gathered into two tubes.
8. Gently resuspend protoplasts by inversion of the tubes and add 10 mL of MMG buffer per tube. Centrifuge for 1 min at $100 \times g$ without brake. Remove supernatant and softly resuspend protoplasts.
9. Add 2 mL of MMG, gather tubes, and incubate for at least 15 min on ice.
10. Add 10 mL of MMG. Centrifuge for 1 min at $100 \times g$. Remove supernatant and softly resuspend protoplasts in 1 or 2 mL of MMG.

3.3.5 Determination of Protoplast Concentration

1. Clean a Fuchs-Rosenthal cell with 70% ethanol and fix the cover glass with water.
2. Put a drop of protoplast suspension between the slide and the cover glass.
3. Count the number of protoplasts under an inverted microscope, and determine the concentration (*see Note 10*). Protoplasts prepared either from cell culture or from seedlings are shown in Fig. 1.

3.4 Protoplast Transfection

1. Prepare transfection buffer (*see Note 11*). Weigh 3 g of PEG-4000 and transfer to a 50 mL tube. Add 1.5 mL of water, 4 mL of 0.5 M mannitol, pH 5.7, and 1 mL of 1 M CaCl₂. Vortex until PEG-4000 is completely dissolved.
2. Prepare 2 mL round-bottom microtubes each with at least 200,000 protoplasts at a final concentration of two million protoplasts/mL of MMG.
3. Add 1 μ L of 100 μ M small RNA and 15 μ g of plasmid carrier DNA to each tube.
4. Gently mix by slowly inverting the tubes. Do not pipette.
5. Add 1 volume of transfection buffer and homogenize the protoplast suspension by inverting the tubes 2–3 times. Do not pipette.
6. Incubate for 15–30 min at room temperature.

3.5 Washing of Transfected Protoplasts

1. Add 2 volumes of W5 and homogenize the protoplast suspension by gently inverting the tubes.
2. Centrifuge for 1 min at $100 \times g$ without brake. Remove supernatant and gently resuspend protoplasts.
3. Repeat **steps 1** and **2** three times.
4. Add 2 volumes of WI and homogenize the protoplast suspension by gently inverting the tubes.
5. Transfer the suspension to a 12-well plate and close with micropore tape. Wrap the plate in aluminum foil and incubate at 25 °C for the time required for preparing your experiment (e.g., 20 min is sufficient for northern blot analysis) (*see Note 12*).

3.6 RNase Treatment

RNase treatment allows demonstrating that the small RNA is not just bound to the surface of protoplasts but incorporated into *A. thaliana* protoplasts.

1. Delicately pour 100 μ L of the transfected protoplasts into a 2 mL round-bottom tube. Add 1 μ L of the RNase A/T1 mix. Incubate for 10 min at room temperature.

2. Add 1 mL of WI buffer. Centrifuge for 1 min at $100 \times g$ without brake. Remove supernatant by pipetting and gently resuspend the protoplasts.
3. Repeat **step 2**. After the last centrifugation, add 100 μL of WI to the protoplast pellet.

3.7 Small RNA Extraction

Due to the toxicity of TriReagent™, **steps 1–5** must be performed under a chemical hood.

1. Add 300 μL of TriReagent™ to the protoplast pellet. Vortex for 10 min.
2. Centrifuge for 10 min at $12,000 \times g$, at 4°C . Transfer aqueous phase to a new tube.
3. Add 120 μL of chloroform and vortex for 10 min.
4. Centrifuge for 15 min at $12,000 \times g$, at 4°C . Transfer aqueous phase to a new tube.
5. Add 240 μL of isopropanol. Delicately homogenize the solution by inverting the tube. Incubate for 5 min at room temperature, and then for 10 min at 4°C .
6. Centrifuge for 15 min at $12000 \times g$, at 4°C . Remove supernatant.
7. Wash pellet by adding 175 μL of 95% ethanol.
8. Centrifuge for 15 min at $12,000 \times g$, at 4°C . Carefully remove supernatant and let the pellet dry at room temperature for 10 min to ensure that no ethanol remains in the tube.
9. Resuspend the pellet in 200 μL of water. Add 133 μL of LiCl solution. Incubate for 16 h at 4°C (*see Note 13*).
10. Centrifuge for 30 min at $16,000 \times g$, at 4°C . Transfer supernatant to a new tube.
11. Add 30 μL of 1 M sodium acetate, pH 4.5, 0.5 μL of glycogen, and 2.5 volumes of cold ethanol. Precipitate the nucleic acids for at least 1 h at -20°C (*see Note 14*).
12. Centrifuge for 30 min at $16,000 \times g$, at 4°C . Remove supernatant, let the pellet dry, and then dissolve the nucleic acids in 5 μL of DEPC-treated water.

3.8 RNA Fractionation by Polyacrylamide Gel Electrophoresis

1. Assemble plates in the casting frame and fix the frame on the casting stand.
2. Mix 7 mL of 15% acrylamide, 49 μL of APS, and 2.45 μL of TEMED. Quickly pour the solution into the space between the plates. Insert the 15-well comb and wait until the polymerization of the gel is completed.
3. To the samples (5 μL) add 5 μL of $2\times$ loading buffer.

4. Load samples onto the gel. Run the electrophoresis at 150 V in $1\times$ TBE until the bromophenol blue band reaches the bottom of the gel.
5. Prepare a container with water and add ethidium bromide to a final concentration of $0.5\ \mu\text{g}/\text{L}$.
6. Separate the gel plates with a spatula. Carefully take off the gel and transfer it to the ethidium bromide solution. Incubate for 5–10 min at room temperature with gentle agitation. Image the RNA profile with a UV transilluminator.

3.9 Electrophoretic Blotting Procedure

1. Cut four Whatman sheets to the size of the plates, and a Hybond N+ membrane square to a size slightly larger than the gel.
2. Soak a sponge from the electroblot apparatus with $0.5\times$ TBE and place it in the opened electroblotting cassette. Wet two sheets of Whatman paper with $0.5\times$ TBE and place them onto the sponge. Soak the Hybond N+ membrane with $0.5\times$ TBE and place it onto the top of the Whatman sheets. Rinse the gel in $0.5\times$ TBE and transfer the gel onto the nylon membrane. Remove any bubbles (*see Note 15*). Soak two more sheets of Whatman paper and place them on top of the membrane. Wet the second sponge with $0.5\times$ TBE and place it on top. Clamp the cassette closed and place the assembled system into the chamber. Pay attention to the cassette orientation in the chamber to allow transfer of RNAs from the gel onto the membrane. Fill the chamber with $0.5\times$ TBE.
3. Carry out the transfer of the RNAs from the gel to the membrane at 300 mA for 80 min at $4\ ^\circ\text{C}$.
4. Place two sheets of Whatman paper in a container and soak them with $2\times$ SSC. Discard excessive buffer. Disassemble the electroblotting system, remove the nylon membrane, and place it onto the sheets of Whatman paper with the surface carrying the RNA facing up. Incubate for 10 min at room temperature. Place the container into a Stratalinker to cross-link the RNA to the membrane by applying two UV exposures of $120,000\ \mu\text{J}/\text{cm}^2$.

3.10 Labeling of the Oligodeoxynucleotide Probe

All steps requiring manipulation of radioactivity must be carried out in an appropriate room. The safety rules of your institution must be strictly followed.

1. Preheat a water bath at $37\ ^\circ\text{C}$.
2. Mix $4.5\ \mu\text{L}$ of water, $1\ \mu\text{L}$ of $100\ \mu\text{M}$ oligodeoxynucleotide complementary to the small RNA of interest, $1\ \mu\text{L}$ of $10\times$ T4 polynucleotide kinase (PNK) buffer, $1\ \mu\text{L}$ of PNK, and $2.5\ \mu\text{L}$ of $[\gamma^{32}\text{P}]\text{-ATP}$. Incubate for 30 min at $37\ ^\circ\text{C}$.

3. Remove unincorporated [$\gamma^{32}\text{P}$]-ATP with a Sephadex G-50 spin column. To prepare a G-50 column, add 2 mm of fiber-glass into the bottom of a 1 mL syringe. Place the syringe into a 14 mL tube. Load swelling watered G-50 resin into the syringe and allow the water to drop out (but do not let the resin dry). Add resin until the syringe is filled. Centrifuge for 45 s at $2000 \times g$. Place the syringe in a new 14 mL tube.
4. Add 50 μL of water to the PNK reaction mixture and load it onto the top of the G-50 column. Centrifuge for 45 s at $2000 \times g$ to elute the radioactive probe. Discard the syringe in the radioactive waste disposal container.

3.11 Northern Hybridization

1. Wet the membrane with PerfectHyb™ Plus solution and place it into a cylindrical glass hybridization tube. Make sure that the membrane is well attached to the tube wall.
2. Add 4 mL of PerfectHyb™ Plus hybridization solution into the tube.
3. Add 940 μL of PerfectHyb™ Plus to the radiolabeled probe, and transfer it into the hybridization tube.
4. Place the tube into the hybridization oven, and incubate with gentle rotation overnight at 42 °C.
5. Discard the probe into the radioactive waste disposal container or keep it at -20 °C if you wish to reuse the probe another time (the half-time of ^{32}P is 14 days).
6. Pour 10 mL of $2\times$ SSC into the tube and wash the membrane for 10 min at 42 °C with gentle rotation.
7. Discard the $2\times$ SSC buffer into the waste container dedicated to radioactivity. Repeat **step 6**.
8. Discard $2\times$ SSC as above. Add 10 mL of $2\times$ SSC and 0.1% SDS into the tube and wash the membrane for 30 min at 42 °C with gentle rotation.
9. Discard the washing solution. Place the membrane on a sheet of Whatman paper to remove excess liquid. Then place the membrane between two sheets of plastic wrap.
10. Expose the radioactive signal of membrane to a phosphorimager screen or to X-ray film. Image the screen using a phosphor-imager or develop the X-ray film (*see Note 16*).
11. As an illustration, the autoradiography of a northern blot showing the successful transfection of sncRNA into *A. thaliana* protoplasts is presented Fig. 2. In this example, an oligoribonucleotide (5'-ACCATCTGAGCTACATCCCC-3') corresponding to a previously identified tRF Ala of 20 nt (tRF Ala20) derived from the 5' extremity of an *A. thaliana* cytosolic alanine tRNA [5] has been incorporated by the protoplasts. The oligoribonucleotide transfection was further

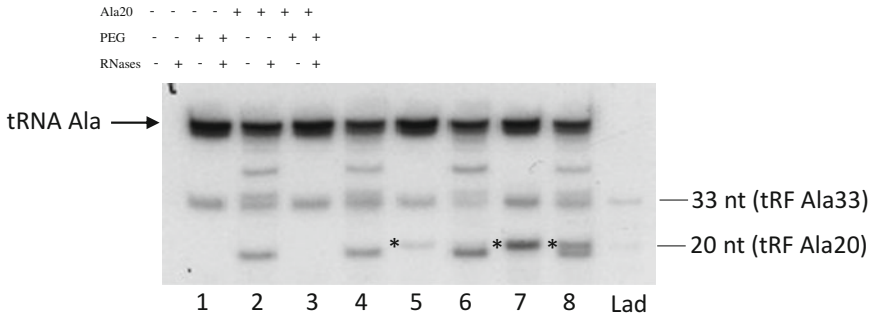


Fig. 2 Analysis by northern blot of the transfection of tRF Ala20 into *A. thaliana* protoplasts. Autoradiography of the northern blot experiment performed with RNA samples extracted from *A. thaliana* protoplasts transfected with an oligoribonucleotide (tRF Ala20) corresponding to the cytosolic *A. thaliana* tRNA alanine (UGC) of 20 nt in size. The same oligoribonucleotide was used as a ladder (Lad), together with an oligoribonucleotide corresponding to tRF Ala33 (33 nt of the 5' extremity of tRNA^{Ala} (UGC)). Protoplasts prepared from an *A. thaliana* cell culture were transfected in the absence (–) or in the presence (+) of tRF Ala20 as well as in the absence (–) or in the presence (+) of PEG. Transfected protoplasts were treated (+) or not treated (–) with a mix of RNase A and RNase T1 (RNases). Extracted RNAs were probed with a ³²P-radiolabeled oligodeoxynucleotide probe complementary to the 5' extremity of tRNA^{Ala} (UGC), (5'-GGGGATGTAGCTCAGATGGT-3'). In all samples, signals corresponding to the endogenous alanine tRNA and the endogenous tRF Ala33 are seen. RNA samples from protoplasts treated with RNases exhibit additional bands, which is likely due to protoplast lysis and accessibility of alanine tRNA to nucleases (lanes 2, 4, 6, and 8). Lane 5 with RNA samples of protoplasts treated for transfection in the absence of PEG shows a band corresponding to tRF Ala20. This signal is not present upon treatment of the protoplasts with RNases (lane 6). By contrast, this signal is higher when protoplasts were treated for transfection in the presence of PEG (lane 7) and this signal is still present when such protoplasts were post-treated with RNases (lane 8), thus demonstrating the successful transfection and internalization of tRF Ala20 into *A. thaliana* protoplasts

analyzed by a northern blot experiment as described above. Control experiments were performed. In the absence of the Ala20 oligoribonucleotide (control with water), or in the absence of PEG, no signal corresponding to the tRF was observed. After RNase treatment, a signal corresponding to the tRF Ala20 was still visible in the transfected protoplasts, thus demonstrating successful incorporation into protoplasts. This oligoribonucleotide transfection method could be widely used to identify the interactome of a biotinylated tRF or the subcellular localization of a fluorescently tagged tRF.

4 Notes

1. The addition of HCl increases the temperature of the solution and distorts pH measurement. Always wait for temperature cooling before measuring pH.

2. EDTA can only be dissolved at a basic pH. Add NaOH pellets and wait for a few minutes. Then add additional pellets one by one until the EDTA powder is dissolved.
3. Boric acid precipitates after long storage (around 1 month). Thus, preparing a large volume of $10\times$ TBE is not advised.
4. Heating is required to dissolve SDS.
5. SDS can precipitate if the room temperature decreases below $20\text{ }^{\circ}\text{C}$. Heat the solution to dissolve SDS before use, if needed.
6. Pipetting with normal tips exposes protoplasts to an excessive osmotic pressure change and can smash them. Better use pipettes with wide-mouth tips, and cut micropipette tips with scissors to enlarge the opening hole. Avoid pipetting and rather pour protoplast solutions to the new containers if possible.
7. Applying braking combined with centrifuge force can smash the cells.
8. Add the buffer slowly along the wall of the tube or the Petri dish to avoid excess of pressure and mechanical force, which could smash the protoplasts.
9. Quality of the seeds is important. Better to use freshly harvested seeds (less than 1 year old). If you use old seeds, sterilization is less efficient. In the case of old seeds or mutant seeds, we have used 80% ethanol and 4% TweenTM 20 (rather than 70% ethanol, 0.1% TweenTM 20) as sterilization solution. Please note that times must be respected to avoid damage to the seeds.
10. Intact protoplasts are perfectly round and well isolated (*see* Fig. 1). Their size can vary, but both large and small ones can be counted if they are not damaged. The number of protoplasts prepared from 10 mL of cell culture is usually around 2×10^6 whereas 200 mg of seedlings will give about 1×10^6 protoplasts.
11. The transfection buffer must be freshly prepared on the day of transfection.
12. Protoplasts can be kept in the 12-well plate for a maximum of 30 h. The longer the protoplasts are kept in the plate, the more of them will die.
13. LiCl causes the precipitation of large RNAs (i.e., >200 nt in size). After centrifugation, the supernatant contains tRNAs and small noncoding RNAs (including tRFs).
14. One hour is usually sufficient for precipitation if ethanol kept at $-20\text{ }^{\circ}\text{C}$ is used. Otherwise, precipitation can also be performed overnight.
15. To avoid bubbles, the membrane should be wet before placing the gel on it. Bubbles can be chased by smoothly pressing a pipette on the gel.

16. To increase signal with X-ray exposure, use a reflective screen placed on the film and incubate the cassette at -80°C . Under these conditions, a strong signal can be obtained after 6 h of exposure. At room temperature, an exposure time of 24–48 h is recommended.

References

1. Shen Y, Yu X, Zhu L, Li T, Yan Z, Guo J (2018) Transfer RNA-derived fragments and tRNA halves: biogenesis, biological functions and their roles in diseases. *J Mol Med* 96:1167–1176
2. Megel C, Morelle G, Lalande S, Duchêne A-M, Small I, Maréchal-Drouard L (2015) Surveillance and cleavage of eukaryotic tRNAs. *Int J Mol Sci* 16:1873–1893
3. Schimmel P (2018) RNA processing and modifications: the emerging complexity of the tRNA world: mammalian tRNAs beyond protein synthesis. *Nat Rev Mol Cell Biol* 19:45–58
4. Cristodero M, Polacek N (2017) The multifaceted regulatory potential of tRNA-derived fragments. *Noncoding RNA Investig* 1:7
5. Cognat V, Morelle G, Megel C, Lalande S, Molinier J, Vincent T, Small I, Duchêne A-M, Maréchal-Drouard L (2017) The nuclear and organellar tRNA-derived RNA fragment population in *Arabidopsis thaliana* is highly dynamic. *Nucleic Acids Res* 45:3460–3472
6. Haas G, Cetin S, Messmer M, Chane-Woon-Ming B, Terenzi O, Chicher J, Kuhn L, Hammann P, Pfeffer S (2016) Identification of factors involved in target RNA-directed microRNA degradation. *Nucleic Acids Res* 44:2873–2887
7. Han Z, Ge X, Tan J, Chen F, Gao H, Lei P, Zhang J (2015) Establishment of lipofection protocol for efficient miR-21 transfection into cortical neurons in vitro. *DNA Cell Biol* 34:703–709
8. Spörlein B, Koop H-U (1991) Lipofectin: direct gene transfer to higher plants using cationic liposomes. *Theor Appl Genet* 83:1–5
9. Miao Y, Jiang L (2007) Transient expression of fluorescent fusion proteins in protoplasts of suspension cultured cells. *Nat Protoc* 2:2348–2353
10. Masani MYA, Noll GA, Parveez GKA, Sambanthamurthi R, Prüfer D (2014) Efficient transformation of oil palm protoplasts by PEG-mediated transfection and DNA microinjection. *PLoS One* 9:e96831
11. Yoo S-D, Cho Y-H, Sheen J (2007) Arabidopsis mesophyll protoplasts: a versatile cell system for transient gene expression analysis. *Nat Protoc* 2:1565–1572
12. Qi Y, Zhong X, Itaya A, Ding B (2004) Dissecting RNA silencing in protoplasts uncovers novel effects of viral suppressors on the silencing pathway at the cellular level. *Nucleic Acids Res* 32:e179
13. Wintz H, Dietrich A (1996) Electroporation of small RNAs into plant protoplasts: mitochondrial uptake of transfer RNAs. *Biochem Biophys Res Commun* 223:204–210
14. McCormack JC, Simon AE (2006) Callus cultures of Arabidopsis. *Curr Protoc Microbiol* 00:16D.1.1–16D.1.9
15. Sambrook J, Russell DW (2001) In: Harbor CS (ed) *Molecular cloning: a laboratory manual*. Cold Spring Harbor Laboratory Press, Cold Spring Harbor, NY



In Vivo Reporter System for miRNA-Mediated RNA Silencing

Károly Fátyol

Abstract

Argonaute proteins play a central role in the evolutionarily conserved mechanisms of RNA silencing. Programmed by a variety of small RNAs, including miRNAs, they recognize their target nucleic acids and modulate gene expression by various means. Argonaute proteins are large complex molecules. Therefore, to better understand the mechanisms they use to regulate gene expression, it is necessary to identify regions of them bearing functional importance (protein-protein interaction surfaces, acceptor sites of posttranslational modifications, etc.). Identification of these regions can be performed using a variety of mutant screens. Here we describe a transient reporter assay system, which is suitable to carry out rapid functional assessment of mutant Argonaute molecules before proceeding to their more detailed biochemical characterization.

Key words Argonaute, miRNA, In vivo reporter system, RNA silencing, Translational repression, Slicing

1 Introduction

The basic mechanisms of miRNA-mediated posttranscriptional gene regulation—including the production, processing, and execution stages—are highly conserved from animals to plants [1–4]. Primary miRNAs are usually produced as polII transcripts. RNase III-like enzymes (called DCLs in plants) process these transcripts, resulting in the release of mature miRNA/miRNA* duplexes. These duplexes are subsequently loaded into Argonaute proteins (AGOs), producing miRISCs (RNA-induced silencing complexes). Using the simple rules of Watson-Crick base pairing, the miRNA-programmed miRISCs recognize their substrate RNAs and regulate their expression by two major mechanisms: transcript cleavage (slicing) and translational repression. Earlier it was assumed that the degree of complementarity between the miRNA and its target determines which of the above mechanisms is used. Since in plants the miRNA/target complementarity is nearly perfect, plant miRISCs were presumed to employ slicing as their main mode of action. Newer data however have contested this assumption. It was

demonstrated that translational repression is frequently used by plant miRISCs even on mRNAs, which under different conditions could be a subject of slicing. These findings imply that it is not the degree of miRNA/target complementarity, but rather the biochemical properties of miRISCs (posttranslational modifications of AGOs, interacting protein partners) and perhaps other still poorly understood factors (e.g., dynamic properties of the target RNA) that determine the mechanism of repression employed [5].

Recently, we have reported the cloning of *Nicotiana benthamiana* Argonaute proteins [6]. To characterize these molecules, we have developed an in vivo transient reporter system. Our system is based on the *Agrobacterium*-mediated transient expression assay developed earlier to analyze miRNA-dependent gene silencing [7–9]. The three components of the system are the following: (1) sensor transcript, (2) miRNA expression cassette, and (3) AGO expression cassette (Fig. 1a). These elements are incorporated into binary plasmid vectors to allow their efficient co-delivery into tobacco leaves by agroinfiltration. The sensor plasmid encodes a GFP-*Renilla* luciferase fusion protein under the control of a constitutively active CaMV 35S promoter. miRNA target sites are inserted into various positions of the sensor mRNA (3'UTR or ORF). The second component of the reporter system encodes a miRNA. This plasmid also constitutively produces GFP protein, which is used as an internal control to normalize for the varying efficiencies of agroinfiltration. The AGO protein under study is expressed from the third binary plasmid. The effector complexes— assembled from the co-expressed AGO proteins and miRNAs—interact with the sensor mRNAs via the miRNA target sites. Monitoring the expression of the sensor mRNA allows the assessment of gene silencing.

Using the above system, detailed characterization of *N. benthamiana* AGO2 has been performed [6]. We have shown that AGO2 can directly repress translation via various miRNA target site constellations (ORF, 3'UTR). In addition, we have observed that AGO2 is able to inhibit its target RNAs via both slicing-dependent and -independent fashion. Several functionally important amino acid residues of AGO2 have also been identified that affect its small RNA loading, cleavage activity, translational repression potential, and antiviral activity.

In this chapter we provide a detailed description of our in vivo reporter system. The use of this system allows the rapid initial assessment of the activities of both wild-type and mutant forms of AGO proteins. Based on the results, further biochemical studies (cleavage assays, binding assays, etc.) can be initiated to better understand the mechanisms these molecules employ to regulate gene expression.

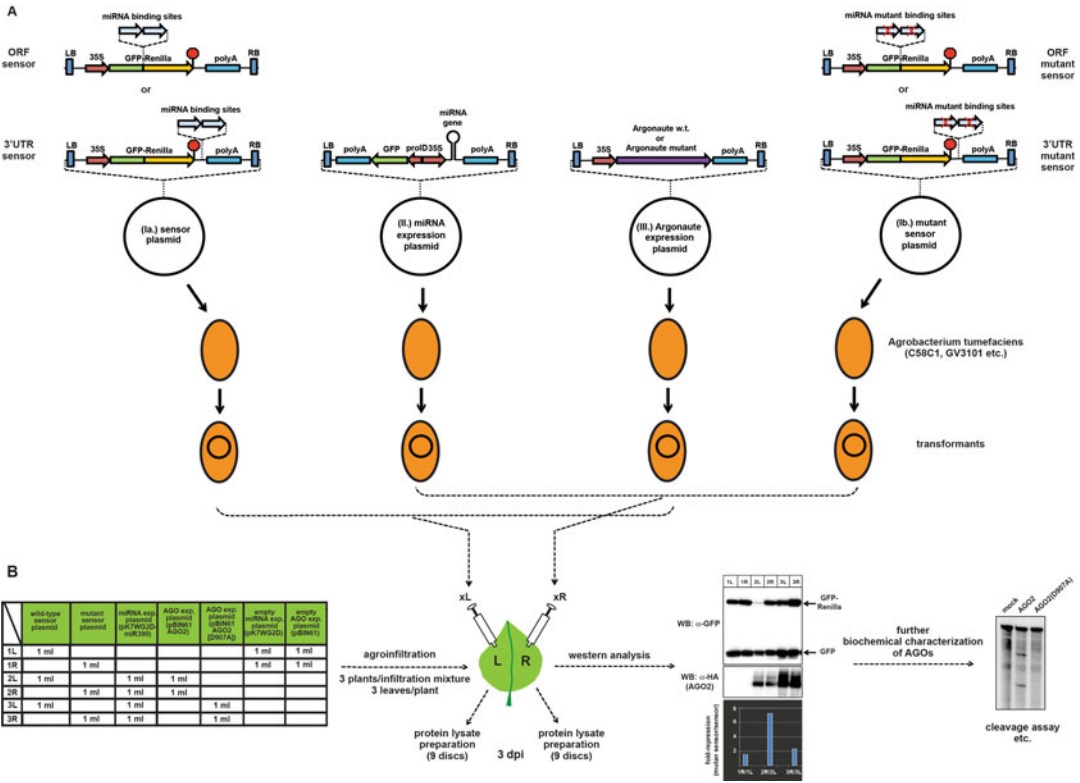


Fig. 1 In vivo reporter system for miRNA-mediated gene silencing. **(a)** Schematic structures of components of the transient gene silencing assay. The sensor/mutant sensor, miRNA expression cassette, and Argonaute expression cassette are incorporated into binary plasmid vectors to allow their efficient co-delivery into *N. benthamiana* leaves by agroinfiltration. **(b)** Setup and result of a typical gene silencing assay. Infiltration mixtures are assembled from diluted *Agrobacterium* suspensions ($OD_{600} = 1$) according to the table. For each assay three plants are used and three leaves per plant are infiltrated. Into the left side of the leaf the wild-type sensor-containing mixture (xL) is infiltrated, while into the right side of the same leaf the mutant sensor-containing mixture (xR) is introduced. Samples are collected at 3 days post-infiltration (dpi) and processed for protein lysate preparation. Sensor activities are analyzed by quantitative Western blotting. The sensor/mutant sensor-encoded GFP-*Renilla* luciferase fusion protein signals are normalized for the GFP signals. Gene silencing is plotted as the ratio of the amounts of GFP-*Renilla* fusion protein produced by the mutant and the wild-type sensors. Due to the complexity of the system rigorous statistical analysis of the data is cumbersome and sometimes could even be misleading. Repetitions of the experiments (at least three times) with a sufficiently high number of biological replicates (at least three) will improve the statistical evaluation. Conclusions should only be drawn from experiments that are highly reproducible

2 Materials

Solutions should be prepared in autoclaved deionized water unless otherwise indicated. Kits, enzymes, reagents, and chemicals can be purchased from various suppliers and should be of molecular biology or analytical grade.

**2.1 Vector
Construction,
Site-Directed
Mutagenesis**

1. Oligonucleotides.
2. DNeasy Plant Mini Kit.
3. pGEM-T easy vector system.
4. Restriction and modifying enzymes.
5. T4 DNA ligase.
6. 10× T4 DNA ligase buffer: 400 mM Tris-HCl pH 7.8, 100 mM MgCl₂, 100 mM DTT, 5 mM ATP.
7. Tango buffer: 33 mM Tris-acetate pH 7.9, 10 mM magnesium acetate, 66 mM potassium acetate, 0.1 mg/mL BSA.
8. Agarose.
9. DNA molecular weight markers.
10. 6× DNA-loading dye: 10 mM Tris-HCl pH 7.6, 0.03% bromophenol blue, 0.03% xylene cyanol FF, 60% glycerol, 60 mM EDTA.
11. TBE buffer: 89 mM Tris, 89 mM boric acid, 2 mM EDTA.
12. Luria-Bertani (LB) medium: 10 g/L Tryptone, 5 g/L yeast extract, 10 g/L NaCl.
13. LB agar plates: LB supplemented with 1.5% [w/v] agar and appropriate antibiotics (100 µg/mL ampicillin, 100 µg/mL spectinomycin, or 50 µg/mL kanamycin).
14. Plasmid purification kit.
15. DNA fragment isolation kit.
16. Taq polymerase.
17. Phusion polymerase.
18. 100 mM dATP/dGTP/dCTP/dTTP: Prepare a 10 mM dNTP mix from the 100 mM deoxynucleotide triphosphate stocks.
19. LR Clonase II Plus enzyme.
20. Gateway entry vectors: pENTR11, pENTR2B, pENTR4.
21. Binary expression vectors: pBIN61, pK7WG2D, pK7WGF2 (*see Note 1*).
22. psiCHECK reporter plasmid.
23. *E. coli* strains TOP10 and DB3.1 (*see Note 2*).
24. Gel electrophoresis apparatus.
25. Power supply.
26. Heatable water bath.
27. Shaking incubator set to 37 °C and 180–200 rpm.
28. Non-shaking incubator set to 37 °C.
29. Microcentrifuge.
30. Thermocycler.
31. Nanodrop microvolume spectrophotometer.

2.2 Agroinfiltration

2.2.1 *Agrobacterium* Transformation/Growth

1. *A. tumefaciens* strains: C58C1 or GV3101.
2. 20 mM CaCl₂.
3. YEB medium: 5 g/L Tryptone, 1 g/L yeast extract, 5 g/L nutrient broth, 5 g/L sucrose 0.49 g/L MgSO₄·7H₂O.
4. YEB-RT agar plates: YEB supplemented with 1.5% (w/v) agar, 20 µg/mL rifampicin, and 5 µg/mL tetracycline.
5. YEB-RTK agar plates: YEB supplemented with 1.5% (w/v) agar, 20 µg/mL rifampicin, 5 µg/mL tetracycline, and 50 µg/mL kanamycin.
6. YEB-RTS agar plates: YEB supplemented with 1.5% (w/v) agar, 20 µg/mL rifampicin, 5 µg/mL tetracycline, and 100 µg/mL spectinomycin.
7. Liquid N₂.
8. Heatable water bath.
9. Shaking incubator set to 28 °C and 180–200 rpm.
10. Non-shaking incubator set to 28 °C.
11. Centrifuge

2.2.2 Agroinfiltration

1. YEB medium: 5 g/L Tryptone, 1 g/L yeast extract, 5 g/L nutrient broth, 5 g/L sucrose, 0.49 g/L MgSO₄·7H₂O.
2. Acetosyringone stock solution: 1 M Acetosyringone dissolved in DMSO.
3. 1 M 2-(N-morpholino)ethanesulfonic acid (MES-K) (pH 5.7).
4. 1 M MgCl₂.
5. Infiltration medium: 10 mM MgCl₂, 250 µM acetosyringone (prepare freshly each time from stock solutions).
6. 1-mL Hypodermic syringe.

2.3 Western Blotting

2.3.1 Protein Lysate Preparation

1. Liquid N₂.
2. 100 mM Phenylmethylsulfonyl fluoride (PMSF) dissolved in isopropanol.
3. Complete protease inhibitor cocktail.
4. 200 mM Activated Na₃VO₄ (*see Note 3*).
5. 1 M Dithiothreitol (DTT).
6. Lysis buffer: 10 mM Tris-HCl pH 7.6, 1 mM EDTA pH 8.0, 150 mM NaCl, 10% (v/v) glycerol, 0.5% (v/v) Nonidet P-40, 5 mM NaF, 1 mM DTT, 0.5 mM Na₃VO₄, 1 mM PMSF, complete protease inhibitor cocktail (the last four components are added to the lysis buffer just before use).
7. Porcelain mortar and pestle.
8. Refrigerable microcentrifuge.

2.3.2 *Sodium Dodecyl Sulfate-Polyacrylamide Gel Electrophoresis (SDS-PAGE)*

1. Resolving gel buffer: 1.5 M Tris-HCl pH 8.8, 0.4% (w/v) SDS.
2. Stacking gel buffer: 0.5 M Tris-HCl pH 6.8, 0.4% (w/v) SDS.
3. Resolving gel solution (8% acrylamide; 15 mL): 4 mL 30% acrylamide/bis-acrylamide solution, 3.75 mL resolving gel buffer, 7.25 mL water, 50 μ L 10% ammonium persulfate (APS, prepared fresh), 10 μ L *N,N,N,N'*-tetramethyl-ethylene-diamine (TEMED).
4. Stacking gel solution (5 mL): 650 μ L 30% acrylamide/bis-acrylamide solution, 1.25 mL stacking gel buffer, 3.05 mL water, 25 μ L 10% APS, 5 μ L TEMED.
5. SDS-PAGE running buffer: 0.025 M Tris, 0.192 M glycine, 0.1% (w/v) SDS.
6. 6 \times SDS sample buffer: 0.35 M Tris-HCl pH 6.8, 30% (v/v) glycerol, 10% (w/v) SDS, 6 M DTT, 0.012% (w/v) bromophenol blue.
7. Pre-stained protein molecular weight marker.
8. Gel-casting apparatus.
9. Electrophoresis chamber.
10. Power supply

2.3.3 *Electro-Transfer*

1. Towbin buffer: 0.025 M Tris, 0.192 M glycine, 20% (v/v) methanol.
2. Electro-blotting apparatus.
3. Power supply.
4. Nitrocellulose membrane, 0.45 μ m pore size.

2.3.4 *Immunological Detection*

1. Ponceau staining solution: 0.1% (w/v) Ponceau S, 5% (v/v) acetic acid.
2. Tris-buffered saline (TBS): 50 mM Tris-HCl pH 7.6, 150 mM NaCl.
3. TBS-T: TBS supplemented with 0.1% (v/v) TWEEN 20.
4. Blocking solution: TBS-T supplemented with 5% (w/v) nonfat dry milk powder.
5. Polyclonal anti-GFP antibody.
6. Horseradish peroxidase (HRP)-conjugated rat monoclonal anti-HA (3F10) antibody.
7. HRP-conjugated secondary antibody (goat anti-rabbit IgG, etc.).
8. Clarity Western ECL Substrate.
9. Orbital shaker.
10. Luminescence gel imaging equipment, including software.

3 Methods

Use kits according to manufacturers' instructions unless otherwise indicated.

3.1 Generation of Mutant AGO Expression Constructs

Recently, we have provided a detailed report of the cloning of the *N. benthamiana* AGO proteins [6]. Here we only describe the generation of expression constructs producing various mutant forms of these molecules. The full-length cDNAs of AGOs are initially assembled in pGEM-T easy plasmid vector. Due to their simplicity and relatively small size these pGEM-AGO plasmids can be used as templates for site-directed mutagenic PCR reactions. The core biochemical properties of AGO proteins are evolutionarily conserved. Thus, multiple sequence alignments (Clustal) of AGOs from evolutionarily distant organisms can help to predict regions of potential functional importance. Appropriately designed forward and reverse mutagenic primers are used to introduce the desired mutations into the AGO proteins by the Quickchange method [10] (see Note 4). The presence of the intended mutation has to be confirmed by sequencing of the mutagenized pGEM-AGO plasmid clones. Finally, the altered AGO ORFs are swapped into plant binary expression vectors, which allows their functional testing in the in vivo reporter system.

3.1.1 Site-Directed Mutagenesis of *N. benthamiana* AGO cDNAs

1. Set up a 50 μ L PCR mixture by mixing 10 ng of pGEM-AGO plasmid, 10 μ L of 5 \times Phusion buffer, 1 μ L of 10 μ M mutagenic forward primer, 1 μ L of 10 μ M mutagenic reverse primer, 1 μ L of 10 mM dNTP mix, appropriate amount of water, and finally 0.5 μ L of Phusion polymerase.
2. Place the tube into the thermocycler and apply the following temperature cycling conditions: 98 $^{\circ}$ C for 2 min (initial denaturation); 18 cycles of 98 $^{\circ}$ C for 10 s (denaturation), 54–64 $^{\circ}$ C for 20 s (annealing) (see Note 5), and 72 $^{\circ}$ C for 15 s/kb of plasmid to be amplified (extension); and 72 $^{\circ}$ C for 5 min (polishing).
3. Add 2 μ L (20 U) of DpnI restriction enzyme to the completed PCR reaction. Incubate at 37 $^{\circ}$ C for 2 h to eliminate original, methylated plasmid template.
4. Transform chemically competent TOP10 *E. coli* cells with 10 μ L of the digested PCR reaction (see Note 6). Spread bacteria onto an LB agar plate containing 100 μ g/mL of ampicillin. Incubate the plates overnight at 37 $^{\circ}$ C.
5. Purify plasmids from 4 to 6 colonies and verify the presence of the desired mutation in the AGO cDNA by sequencing (see Note 7).

3.1.2 Insertion of Mutagenized AGO into Binary Expression Vector

1. Digest 2 µg of the mutagenized pGEM-AGO plasmid with appropriate restriction enzymes (*see Note 8*).
2. Resolve the digested plasmid on a 1.2% agarose gel and purify the AGO ORF-containing restriction fragment using a DNA fragment purification kit.
3. Mix the isolated AGO ORF-containing restriction fragment with pBIN61 plasmid linearized with the appropriate restriction enzymes in a 3:1 molar ratio. Set up a 10 µL ligation reaction by adding 1 µL of 10× T4 DNA ligase buffer, appropriate amount of water, and 1 µL (5 U) of T4 DNA ligase to the above mixture. Incubate the reaction at room temperature for 2–4 h.
4. Competent TOP10 *E. coli* cells are transformed with the ligation mixture. Spread bacteria onto LB agar plates containing 50 µg/mL kanamycin and incubate plates overnight at 37 °C.
5. Screen the appearing colonies by colony PCR (*see Note 9*).
6. Purify plasmids from colonies which carry the AGO ORF. Verify the structure of plasmids by restriction digestion.

3.2 Generation of miRNA Expression Constructs

The draft genome sequence of *N. benthamiana* is available from several sources [11–13]. Based on these data, forward and reverse primers can be designed to isolate conserved miRNA genes of *N. benthamiana*. In order to ensure efficient processing of the cloned miRNA, in addition to the region encoding the miRNA hairpin, sufficiently long flanking regions should also be included in the amplified DNA fragment (at least 200–300 nt in both 5' and 3' directions).

3.2.1 Isolation and Cloning of miRNA Genes of *N. benthamiana*

1. Isolate plant genomic DNA from young *N. benthamiana* leaves using DNeasy Plant Mini Kit.
2. Quantify genomic DNA by nanodrop spectrophotometry.
3. Set up a 50 µL PCR mixture by mixing 100 ng of genomic DNA, 10 µL of 5× Phusion buffer, 1 µL of 10 µM forward primer, 1 µL of 10 µM reverse primer, 1 µL of 10 mM dNTP mix, appropriate amount of water, and finally 0.5 µL of Phusion polymerase. Place tube into a thermocycler and apply the following temperature cycling conditions: 98 °C for 2 min (initial denaturation); 35 cycles of 98 °C for 10 s (denaturation), $T_m + 3$ °C of the lower T_m primer for 20 s (annealing), and 72 °C for 30 s/kb of fragment to be amplified (extension); and 72 °C for 5 min (polishing).
4. Test an aliquot (1/10th) of the PCR mixture on a 1.2% agarose TBE gel. Use the rest of the sample to purify the amplified product by a PCR purification kit.

5. Digest PCR fragment with restriction enzymes (primers are designed to contain recognition sites for appropriate restriction enzymes, which here can subsequently be used to clone the PCR product). Gel purify digested PCR fragment after electrophoresis in a 1.2% TBE agarose gel.
6. Digest 1 μg of pENTR11 plasmid with appropriate restriction enzymes. Gel purify the digested plasmid.
7. Set up a 10 μL ligation reaction by mixing 100 ng of digested pENTR11 plasmid, 3 \times molar excess of the digested PCR product, 1 μL of 10 \times T4 DNA ligase buffer, appropriate amount of water, and 1 μL (5 U) of T4 DNA ligase. Incubate the reaction at room temperature for 2–4 h.
8. Chemically competent TOP10 *E. coli* cells are transformed with the ligation reaction. Spread bacteria onto an LB agar plate containing 50 $\mu\text{g}/\text{mL}$ of kanamycin. Incubate the plates overnight at 37 $^{\circ}\text{C}$.
9. Screen the appearing colonies by colony PCR.
10. Purify plasmids from colonies carrying inserts of the expected size and verify identity of the fragments by sequencing.

3.2.2 Transfer of miRNA Genes into a Gateway-Compatible Binary Expression Vector

1. Set up LR recombination reaction by mixing 1 μL (50 ng) of entry plasmid (pENTR11 containing the cloned miRNA gene) with 1 μL (50 ng) of plant binary destination vector (e.g., pK7WG2D). Finally, add 0.5 μL of LR clonase. Incubate the reaction at room temperature for 1–12 h.
2. Chemically competent TOP10 *E. coli* cells are transformed with the recombination reaction. Spread bacteria onto an LB agar plate containing 100 $\mu\text{g}/\text{mL}$ of spectinomycin. Incubate the plates overnight at 37 $^{\circ}\text{C}$.
3. Screen the appearing colonies by colony PCR.
4. Purify plasmids from colonies and verify correct structure of the plasmid by restriction digestion.

3.3 Generation of Sensor Constructs

A crucial component of the reporter system is the sensor plasmid. AGOs can repress gene expression via miRNA-binding sites located either in the 3'UTR or the ORF, with a considerably stronger effect on the latter. Although the underlying mechanisms are still not completely elucidated, this may be related to the divergent repression mechanisms acting on the topologically different target sites: inhibition of translation initiation on 3'UTR sites versus steric hindrance on ORF sites. In animals, miRNA-binding sites are generally present in the 3'UTR, while in plants the ORF location is predominant. Our comparative assessment revealed that miRNA-binding sites in the ORF behaved more like binary switches, while in the 3'UTR they bestowed graded response to the sensor.

Regardless, one has to keep in mind that testing of both target site constellations may become necessary to find the arrangement which fits best to one's purpose.

We have designed a GFP-*Renilla* luciferase fusion gene platform to test the effectiveness of miRNA-binding sites in the two different constellations [6]. The use of the fusion protein provides several advantages: (1) GFP serves as a tag to detect and quantify the expression levels of the fusion protein by sensitive GFP antibodies in Western blotting; (2) it allows parallel visual monitoring and quantitative assessment of silencing (by observing GFP fluorescence and measuring enzymatic activity of the *Renilla* luciferase) (*see Note 10*); (3) to generate ORF sensors, the linker region connecting the two functional domains of the fusion protein can be used as a suitable position to insert miRNA-target sites without disrupting the activities of either GFP or *Renilla* luciferase.

To properly assess gene silencing, the activity measured on a wild-type sensor construct has to be compared to the activity observed on a corresponding mutant sensor (Fig. 1a). The two sensors differ from each other only by three point mutations. These mutations are introduced into the miRNA-binding site at positions 10, 11 (flanking the AGO cleavage site), and 16 (the 3' supplementary region).

3.3.1 Generation of miRNA Target Site Entry Vectors

1. Generate the pENTR11-*Renilla* luciferase vector by inserting the 982 bp long NcoI-NotI fragment of psiCHECK—bearing the *Renilla* luciferase ORF—into pENTR11 by conventional asymmetric sticky-end ligation.
2. Anneal tandem wild-type or mutant miRNA-binding site containing complementary oligonucleotides to produce double-stranded DNA with the miRNA-binding sites as follows: (1) mix 1 nmole of each of the complementary oligonucleotides in 100 μ L of 1 \times Tango buffer; (2) heat the mixture to 100 $^{\circ}$ C for 5 min, then turn off the heating block, and allow it to cool down slowly to room temperature (usually overnight).
3. Digest 1 μ g of the pENTR11-*Renilla* luciferase plasmid (*see above*) with either XhoI-XbaI (to yield 3'UTR entry vector) or BstBI (to yield ORF entry vector) (Fig. 2). Gel purify the digested plasmid.
4. Mix 100 ng of digested pENTR11-*Renilla* luciferase plasmid with 0.1 pmole of the annealed miRNA-binding site-containing oligonucleotides. Set up a 10 μ L ligation reaction by adding 1 μ L of 10 \times T4 DNA ligase buffer, appropriate amount of water, and 1 μ L (5 U) of T4 DNA ligase to the above mixture. Incubate the reaction at room temperature for 2–4 h.
5. Chemically competent TOP10 *E. coli* is transformed by the ligation reaction as above.

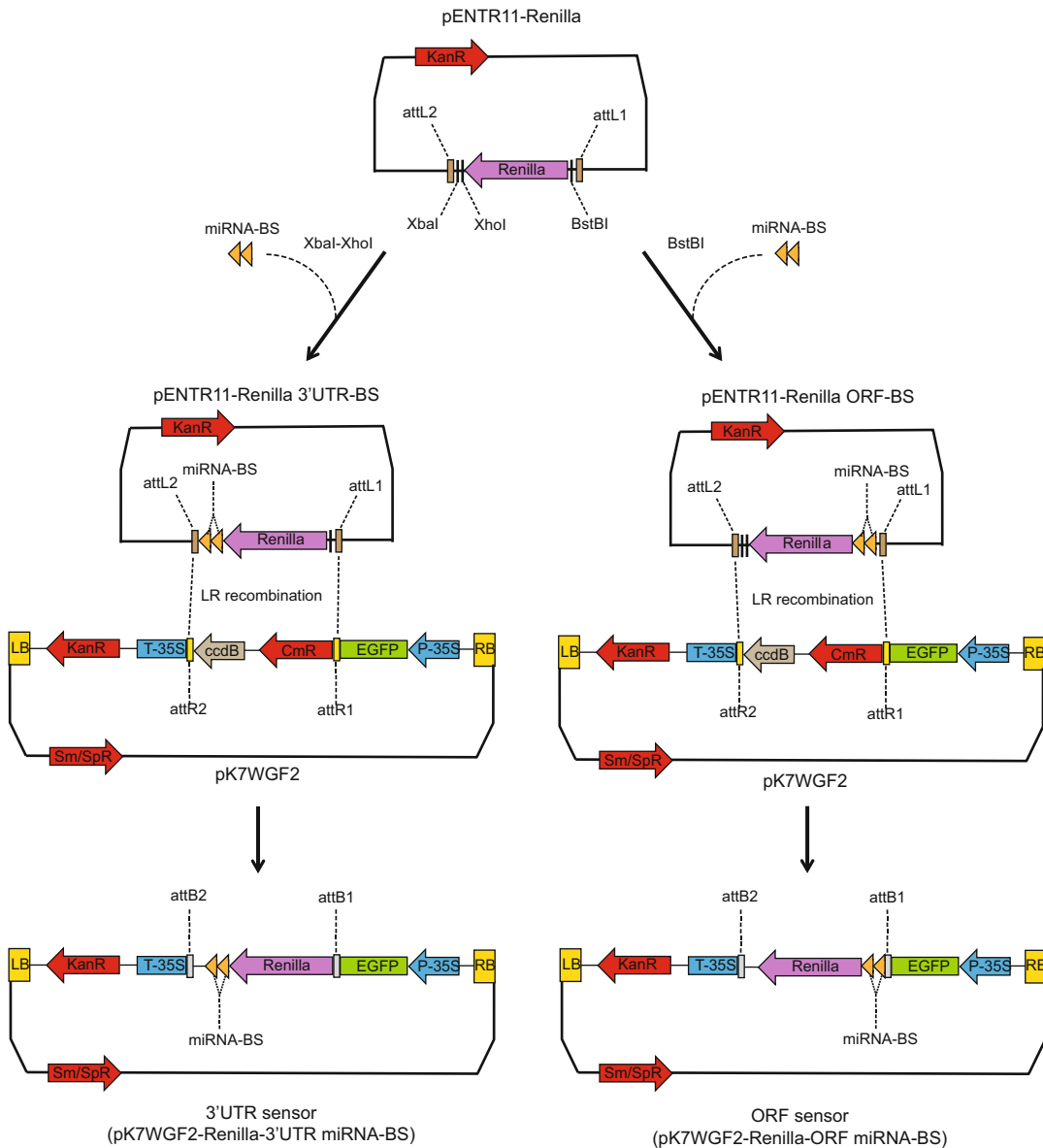


Fig. 2 Construction of the binary sensor/mutant sensor plasmids. Double-stranded DNA oligonucleotides containing tandem miRNA-binding sites are inserted either at the 5' or the 3' end of a *Renilla* luciferase (cloned into a pENTR11 plasmid vector). In the subsequent LR recombination step the *Renilla* luciferase-coding region along with the miRNA-binding sites is transferred into the pK7WGF2 binary plasmid. LR recombination ensures the precise in-frame fusion between the GFP and *Renilla* luciferase-coding regions

- Identify colonies carrying plasmids containing the miRNA-binding site oligonucleotide by colony PCR.
- Confirm correct insertion of the miRNA-binding site oligonucleotide by sequencing (*see Note 11*).

3.3.2 Generation of Binary 3'UTR or ORF Sensors

1. Set up LR recombination reactions from the 3'UTR or ORF entry vectors (see Subheading 3.3.1) and the Gateway-compatible pK7WGF2 binary vector as follows: mix 1 μ L (50 ng) of entry plasmid (pENTR11-*Renilla* 3'UTR-BS or pENTR11-*Renilla* ORF-BS, Fig. 2) with 1 μ L (50 ng) of pK7WGF2. Add 0.5 μ L of LR clonase. Incubate the reaction at room temperature for 1–12 h.
2. Chemically competent TOP10 *E. coli* cells are transformed with the recombination reaction. Spread bacteria onto an LB agar plate containing 100 μ g/mL of spectinomycin. Incubate the plates overnight at 37 °C.
3. Screen the appearing colonies by colony PCR. Correct recombination leads to in-frame fusions between the *Renilla* luciferase and GFP-coding regions. In the resulting plasmids the miRNA-binding sites are located either in the 3'UTR of the *Renilla* luciferase-GFP (pK7WGF2-*Renilla*-3'UTR miRNA-BS) or in the linker region connecting the GFP and *Renilla* luciferase domains of the fusion gene (pK7WGF2-*Renilla*-ORF miRNA-BS) (Fig. 2).

3.4 Agroinfiltration

To ensure efficient co-delivery of components of the reporter system into plants, agroinfiltration is used. First, the constructed binary vectors are separately transformed into cells of a suitable *A. tumefaciens* strain (e.g., C58C1). Next, the transformed bacterium strains are introduced into *N. benthamiana* leaves in various combinations by syringe infiltration.

3.4.1 Agrobacterium Transformation/Growth

1. Streak C58C1 *A. tumefaciens* strain from a frozen glycerol stock onto a YEB-RT plate. Incubate the plate for 3–5 days at 28 °C.
2. Inoculate a single colony of C58C1 into 5 mL of YEB medium containing 20 μ g/mL of rifampicin and 5 μ g/mL of tetracycline. Shake the culture vigorously (200–250 rpm) overnight at 28 °C.
3. Add 2 mL of the overnight culture to 50 mL of YEB medium (without antibiotics) in a 250 mL flask. Shake the culture vigorously (250 rpm) at 28 °C until it grows to OD₆₀₀ of 0.5–1.0 (this generally takes 4–6 h).
4. Chill the culture on ice for 10 min.
5. Centrifuge the cell suspension at 3000 $\times g$ for 10 min at 4 °C.
6. Discard supernatant and resuspend the bacterium pellet in 1 mL of ice-cold 20 mM CaCl₂ (see Note 12).
7. Add 1–2 μ g of binary plasmid DNA to 100 μ L of bacterium suspension.
8. Freeze mixture in liquid N₂.

9. Thaw the bacteria at 37 °C for 5 min.
10. Add 1 mL of YEB medium to the bacteria and incubate the mixture at 28 °C for 2–4 h. This period allows the bacteria to express the antibiotic resistance genes.
11. Centrifuge bacterium suspension in a microcentrifuge for 1 min at maximum speed.
12. Remove majority of supernatant leaving ~100 µL of YEB medium on the bacterium pellet.
13. Resuspend bacteria and spread suspension onto a YEB plate containing appropriate antibiotics (*see Note 13*).
14. Incubate the plate for 3–5 days at 28 °C.

3.4.2 Preparation of *Agrobacterium* for Infiltration

1. Inoculate a single colony of each C58C1 strain of the reporter system into 5 mL of YEB medium containing appropriate antibiotics (AGO expression strain, 50 µg/mL kanamycin; miRNA expression strain, 100 µg/mL spectinomycin; wild-type sensor/mutant sensor strains, 100 µg/mL spectinomycin). Empty expression vector (pK7WG2D and pBIN61) containing bacterium strains should be grown as well, as negative controls. In addition to the antibiotics, supplement the growth media with MES and acetosyringone to the final concentrations of 10 mM and 20 µM, respectively.
2. Shake the cultures (250 rpm) at 28 °C overnight to reach saturation.
3. Centrifuge cultures at $3000 \times g$ for 10 min at 25 °C.
4. Decant supernatants and resuspend bacterium pellets in 1 mL of freshly prepared infiltration medium. Incubate suspensions at room temperature for at least 3 h.
5. Measure optical density of bacterium suspensions. Prepare $OD_{600} = 1$ dilutions from suspensions using infiltration medium.
6. Prepare infiltration mixtures from the strains of the reporter system (AGO expression strain, miRNA expression strain, sensor/mutant sensor strains). The mixing ratios of the strains have to be optimized for each AGO/miRNA/sensor combination. In addition, mixtures containing the appropriate empty vector strains, instead of the AGO or miRNA expression strains, should also be prepared as negative controls. In our hands, mixing the three strains at 1:1:1 ratio works well for most of the time. Setup of a typical experiment is given in Fig. 1b.

3.4.3 Agroinfiltration

1. *N. benthamiana* plants are grown at 25 °C under long-day conditions (16-h light, 8-h dark). Four–five-week-old plants are most suitable for infiltration. The day before the experiment, irrigate plants well in order to ensure that their stomata are fully open at the time of the infiltration.

2. Fill a 1 mL hypodermic syringe with the infiltration mixture. Infiltrate leaves from the abaxial side. For each infiltration mixture use three plants. Infiltrate three leaves per plant. Into the left side of the leaf infiltrate the wild-type sensor-containing mixture, while into the right side of the same leaf introduce the mutant sensor-containing mixture (Fig. 1b). Choose leaves that are fully expanded and avoid the wrinkled ones, which are highly resistant to infiltration.
3. Grow the infiltrated plants at 25 °C under long-day conditions for 72 h before analyzing protein expression.

3.5 Analysis of Protein Expression

As a measure of gene silencing, expression of the wild-type sensor/mutant sensor-encoded GFP-*Renilla* luciferase fusion protein is analyzed by quantitative Western blotting. Western blot analysis of proteins is composed of three consecutive steps. First the proteins are separated according to their apparent molecular masses using SDS-PAGE. Next, the gel is electro-transferred to nitrocellulose or PVDF membranes. Generally, nitrocellulose membranes give lower background than PVDF membranes; however the latter is more durable. Therefore, if multiple rounds of stripping/immunological detection are planned, PVDF membranes should be used instead of nitrocellulose. The final step is the immunological detection of the protein to be studied. Since Western blot analysis is a routine technique in most molecular biology laboratories, no detailed protocols for SDS-PAGE and electro-transfer of gels are provided here. Instead, the reader is referred to a number of excellent laboratory manuals [14, 15]. Only the protein lysate preparation and immunological detection/quantitation of signals are described here in more details.

3.5.1 Preparation of Protein Lysates from Infiltrated Leaves

1. Punch 1 cm diameter disks from both sides of infiltrated leaves. Pool disks from the same side of leaves infiltrated with the same suspensions (total of nine disks).
2. Collect the disks into a porcelain mortar. Freeze disks by pouring a small volume of liquid N₂ into the mortar and quickly grind them into a fine powder using a porcelain pestle.
3. Add 1800 µL of ice-cold lysis buffer to the mortar and continue homogenization for 30 s.
4. Pour lysate into a 2 mL tube. Keep tubes on ice until all samples are collected.
5. Centrifuge lysates at 20,000 × *g* for 20 min at 4 °C.
6. Transfer supernatants into clean tubes.
7. Store samples at -70 °C until further analysis.

3.5.2 SDS-PAGE and Electro-Transfer of Gel

1. Prepare resolving gel solution for 8% SDS-PAGE.
2. Cast gels using an appropriate gel-casting apparatus.
3. Prepare stacking gel solution.
4. Cast stacking gel on top of the 8% resolving gel. Use appropriate comb depending on the number of samples to be analyzed.
5. Prepare samples by mixing 30 μ L of cleared protein lysate (from Subheading 3.5.1) with 6 μ L of 6 \times SDS sample buffer.
6. Heat samples at 95 $^{\circ}$ C for 5 min.
7. Place gels into an electrophoresis chamber. Fill the appropriate amount of SDS-PAGE running buffer into the chamber. Load samples immediately onto the gel. Load pre-stained protein marker along the samples as well.
8. Run gel at 100 V constant voltage until bromophenol blue reaches the bottom of the gel.
9. Blot the gel onto nitrocellulose membrane using an appropriate electro-blotting apparatus. Transfer is performed in Towbin buffer at 300 mA constant power in the cold room (at \sim 4 $^{\circ}$ C) for 2 h.
10. Stain nitrocellulose membrane with Ponceau S solution to check protein transfer efficiency. If transfer is satisfactory proceed with immunological detection. If inefficient transfer is detected (usually missing bands in the high-molecular-weight range) repeat gel running and blot gel for a longer period of time (up to 3–4 h).

3.5.3 Immunological Detection, Quantitation

1. Block membrane in blocking solution with gentle agitation on an orbital shaker for 1 h at room temperature.
2. To detect GFP and GFP-*Renilla* luciferase fusion protein, incubate membrane in diluted polyclonal anti-GFP antibody (1:2000 dilution in blocking solution) with constant agitation for 1 h at room temperature.
3. Wash membrane in TBS-T, three times for 10 min with agitation.
4. Incubate membrane with HRP-conjugated anti-rabbit IgG (1:10,000 dilution in blocking solution) with constant agitation for 1 h at room temperature.
5. Wash membrane in TBS-T, three times for 10 min with agitation.
6. Develop membrane using Clarity Western ECL substrate according to manufacturers' instructions.
7. Use luminescence gel imaging equipment to image membrane. The sensor-encoded GFP-*Renilla* luciferase fusion protein can be detected on the membrane at \sim 66 kDa while the miRNA

expression vector (or the pK7WG2D empty vector)-encoded GFP runs at ~33 kDa (*see* Fig. 1b). Take multiple pictures of the membrane with various exposure times. Be sure to have images where signal intensities are not at saturating levels. Use these images for accurate quantitation of the protein bands.

8. Use your imaging software (e.g., Image Lab) for identification and accurate quantitation of protein bands. Identification of bands can be done automatically or manually. Manual labeling of the bands is necessary if they are too faint for automatic detection. Image Lab generates an analysis table, which contains absolute values of band intensities (with background subtracted). The analysis table can be exported to Excel for further statistical analysis. The GFP signal serves as an infiltration control and is used to normalize the GFP-*Renilla* luciferase fusion protein signal. The efficiency of gene silencing can be defined as the ratio of the normalized fusion protein levels:

$$\text{Gene silencing} = \frac{\text{GFP} - \text{Renilla protein}_{(\text{mutant sensor})}}{\text{GFP} - \text{Renilla protein}_{(\text{wild-type sensor})}}$$

9. After exposure, rinse membrane twice with TBS-T and proceed with the detection of AGO protein expression. Repeated blocking of the membrane is not necessary.
10. Incubate membrane in diluted HRP-conjugated rat monoclonal 3F10 anti-HA antibody (1:2000 dilution in blocking solution) with constant agitation for 1 h at room temperature (*see* **Note 14**).
11. Wash membrane in TBS-T three times for 10 min with agitation.
12. Develop membrane using Clarity Western ECL Substrate as described above.

4 Notes

1. The Gateway-compatible pK7WG2D and pK7WGF2 binary destination vectors along with a number of similar plasmids can be obtained from the University of Gent, VIB, Plant Systems Biology (<https://gateway.psb.ugent.be>).
2. For general cloning and sub-cloning purposes TOP10, DH5 α , or similar *E. coli* strains can be used. For propagating plasmid components of the Gateway system (entry vectors, destination vectors) the DB3.1 *E. coli* strain must be used. This strain tolerates the presence of the *ccdB* gene (a component of the destination cassette), which is highly toxic to regular *E. coli* strains.

3. Na_3VO_4 should be activated for maximal inhibition of protein phosphotyrosyl-phosphatases as follows:
 - (a) Prepare a 200 mM solution of Na_3VO_4 .
 - (b) Adjust the pH to 10 using either 1 N NaOH or 1 N HCl. At pH 10 the solution will be yellow.
 - (c) Boil the solution until it turns colorless.
 - (d) Cool to room temperature.
 - (e) Readjust the pH to 10 and repeat **steps 3c** and **3d** until the solution remains colorless and the pH stabilizes at 10.
 - (f) Store the activated Na_3VO_4 in aliquots at -20°C .
4. The pGEM-AGO plasmids are mutagenized by the Quick-change method wherein a pair of complementary mutagenic primers are used to amplify the entire plasmid in a PCR reaction using a high-fidelity DNA polymerase such as Pfu polymerase or Phusion. Mutagenic primers contain the desired mutation and are complementary to the template DNA around the mutation site (approximately 15 nt up- and downstream of the mutation). If possible choose triplets, which creates a new or eliminates an existing restriction site; thereby the mutant plasmid can be identified by restriction digestion. An important step of the method is the elimination of the original non-mutagenized template. This is performed by DpnI restriction digestion. DpnI preferentially degrades the methylated template plasmid molecules (produced by the bacterial host), while leaves the unmethylated plasmid molecules (produced during the mutagenic PCR) intact. With this simple procedure significant enrichment of the mutagenized plasmids can be achieved.
5. The annealing temperature used in PCR mutagenesis does not correspond exactly to the calculated T_m values of the mutagenic primers. Annealing temperature between 64 and 54 $^\circ\text{C}$ should be used. Start at higher temperatures. If the number of growing *E. coli* colonies after mutagenesis is low (indicating that the procedure of PCR mutagenesis was not successful) decrease the annealing temperature gradually.
6. Good-quality chemically competent *E. coli* can be prepared following the Inoue protocol [16]. High-efficiency competent *E. coli* cells are also available from a number of commercial sources.
7. Mutagenesis has to be confirmed by sequencing. The pGEM-T easy vector contains SP6 and T7 primer sites flanking the poly-linker. These primers can be used for sequencing. The entire AGO insert has to be sequenced to confirm that only the desired mutation is introduced into the ORF. Alternatively, a shorter DNA segment around the introduced mutation can be

sequenced. In this case, only the sequenced fragment, bearing the desired mutation, is swapped into the binary expression vector using appropriate restriction enzymes.

8. The polylinker region of pGEM-T easy plasmid vector contains recognition sites for a relatively large number of rare-cutting restriction enzymes. Various combinations of these enzymes can be used to isolate the intact AGO ORFs from the vector. If not sufficient, additional recognition sites can also be added to the vector using appropriate oligonucleotides.
9. Colony PCR can be used to screen for bacterial colonies carrying plasmids with the desired insert. The protocol is carried out as follows:
 - (a) Touch isolated bacterial colonies with a pipet tip and transfer the attached cells into 20 μL of water (in a PCR tube).
 - (b) Lyse bacteria by heating the suspension to 95 $^{\circ}\text{C}$ for 5 min in a thermocycler.
 - (c) Transfer 0.5 μL of the bacterial lysate into a PCR tube containing 12 μL of PCR mix. The PCR mix is assembled as follows: 0.25 μL of 10 μM forward primer, 0.25 μL of 10 μM reverse primer, 0.25 μL of 10 mM dNTP mix, 0.75 μL of 25 mM MgCl_2 , 1.25 μL of 10 \times Taq buffer, 9 μL of water, and 0.25 μL of Taq polymerase. By up-scaling the above volumes, a PCR master mix can be prepared to screen the desired number of colonies. At least one of the applied primers should be specific for the plasmid vector. This helps to eliminate the amplification of background products, which derive from the unused insert. Additionally, this allows to determine the orientation of the inserted DNA fragment within the vector.
 - (d) Use the following temperature cycling program: 94 $^{\circ}\text{C}$ for 2 min (initial denaturation); 40 cycles of 94 $^{\circ}\text{C}$ for 30 s (denaturation), T_m $^{\circ}\text{C}$ of the lower T_m primer for 30 s (annealing), and 72 $^{\circ}\text{C}$ for 30 s/kb of the fragment to be amplified (extension); and 72 $^{\circ}\text{C}$ for 7 min (polishing).
 - (e) Check PCR reactions on a TBE agarose gel (adjust gel density by changing agarose concentration according to the size of the expected DNA fragment).
10. Using the specific substrate of *Renilla* luciferase (coelenterazine), we have demonstrated the functionality of the sensor plasmid-encoded GFP-*Renilla* fusion protein. We also found that the protein's enzymatic activity correlated perfectly with the signal intensity measured in quantitative Western blots using anti-GFP antibody. In addition, we demonstrated that the protein is suitable for dual-luciferase assays (combined with firefly luciferase normalization control, unpublished result).

11. When generating ORF sensors carefully check that no in-frame STOP codons are introduced into the linker region between GFP and *Renilla* luciferase.
12. At this point the competent bacteria can be aliquoted into 1.5 mL tubes (100 μ L/tube) and snap-frozen in liquid N₂. The frozen aliquots can be stored at -70° C and used for a few months.
13. Either YEB-RTK or YEB-RTS plates are used. Rifampicin and tetracycline select for the strain-specific markers of C58C1. Kanamycin selection allows for the selection of the pBIN61-based (here: AGO) vectors. Spectinomycin is used to select for the pK7WG2D- or pK7WGF2-derived plasmids (miRNA expression vectors, sensors).
14. Expression of the AGO proteins can be detected by either HA or FLAG antibodies. However, in our hands the 3F10 anti-HA antibody proved to be more sensitive than the M2 FLAG antibody. For detection of AGO proteins stripping of the membrane is not necessary. All *N. benthamiana* AGOs are >100 kDa in their size; thus, none of the bands recognized by the GFP antibody (GFP at ~33 kDa, GFP-*Renilla* luciferase at ~66 kDa) interferes with their detection.

Acknowledgments

This work was supported by the National Research, Development and Innovation Office, Hungary (K124705).

References

1. Voinnet O (2009) Origin, biogenesis, and activity of plant microRNAs. *Cell* 136:669–687
2. Martinez de Alba AE, Elvira-Matelot E, Vaucheret H (2013) Gene silencing in plants: a diversity of pathways. *Biochim Biophys Acta* 1829:1300–1308
3. Bologna NG, Voinnet O (2014) The diversity, biogenesis, and activities of endogenous silencing small RNAs in *Arabidopsis*. *Annu Rev Plant Biol* 65:473–503
4. Yu Y, Jia T, Chen X (2017) The ‘how’ and ‘where’ of plant microRNAs. *New Phytol* 216:1002–1017
5. Merchante C, Stepanova AN, Alonso JM (2017) Translation regulation in plants: an interesting past, an exciting present and a promising future. *Plant J* 90:628–653
6. Fátýol K, Ludman M, Burgyán J (2016) Functional dissection of a plant Argonaute. *Nucleic Acids Res* 44:1384–1397
7. Llave C, Xie Z, Kasschau KD, Carrington JC (2002) Cleavage of Scarecrow-like mRNA targets directed by a class of *Arabidopsis* miRNA. *Science* 297:2053–2056
8. Franco-Zorrilla JM, Valli A, Todesco M, Mateos I, Puga MI, Rubio-Somoza I, Leyva A, Weigel D, Garcia JA, Paz-Ares J (2007) Target mimicry provides a new mechanism for regulation of microRNA activity. *Nat Genet* 39:1033–1037
9. Allen E, Xie Z, Gustafson AM, Carrington JC (2005) microRNA-directed phasing during trans-acting siRNA biogenesis in plants. *Cell* 121:207–221
10. Braman J, Papworth C, Greener A (1996) Site-directed mutagenesis using double-stranded plasmid DNA templates. *Methods Mol Biol* 57:31–44
11. Bombarely A, Rosli HG, Vrebalov J, Moffett P, Mueller LA, Martin GB (2012) A draft genome sequence of *Nicotiana benthamiana*

- to enhance molecular plant-microbe biology research. *Mol Plant-Microbe Interact* 25:1523–1530
12. Nakasugi K, Crowhurst RN, Bally J, Wood CC, Hellens RP, Waterhouse PM (2013) De novo transcriptome sequence assembly and analysis of RNA silencing genes of *Nicotiana benthamiana*. *PLoS One* 8:e59534
 13. Nakasugi K, Crowhurst R, Bally J, Waterhouse P (2014) Combining transcriptome assemblies from multiple de novo assemblers in the allo-tetraploid plant *Nicotiana benthamiana*. *PLoS One* 9:e91776
 14. Maniatis T, Fritsch EF, Sambrook J (1982) *Molecular cloning: a laboratory manual*. Cold Spring Harbor Laboratory Press, Cold Spring Harbor, NY
 15. Ausubel FM, Brent R, Kingston RE, Moore DD, Seidman JG, Smith JA, Struhl K (eds) (2003) *Current protocol in molecular biology*. Wiley, Hoboken, NJ
 16. Inoue H, Nojima H, Okayama H (1990) High efficiency transformation of *Escherichia coli* with plasmids. *Gene* 96:23–28



TRAP-SEQ of Eukaryotic Translatomes Applied to the Detection of Polysome-Associated Long Noncoding RNAs

Soledad Traubenik, Flavio Blanco, María Eugenia Zanetti, and Mauricio A. Reynoso

Abstract

Translating ribosome affinity purification (TRAP) technology allows the isolation of polysomal complexes and the RNAs associated with at least one 80S ribosome. TRAP consists of the stabilization and affinity purification of polysomes containing a tagged version of a ribosomal protein. Quantitative assessment of the TRAP RNA is achieved by direct sequencing (TRAP-SEQ), which provides accurate quantitation of ribosome-associated RNAs, including long noncoding RNAs (lncRNAs). Here we present an updated procedure for TRAP-SEQ, as well as a primary analysis guide for identification of ribosome-associated lncRNAs. This methodology enables the study of dynamic association of lncRNAs by assessing rapid changes in their transcript levels in polysomes at organ or cell-type level, during development, or in response to endogenous or exogenous stimuli.

Key words Long noncoding RNAs (lncRNAs), Ribosome immunopurification, Polysomes, Cell-type-specific gene expression, RNA-seq

1 Introduction

Noncoding RNAs (ncRNAs) constitute a highly diverse class of RNA molecules that are not translatable into proteins, including both housekeeping (e.g., ribosomal, transfer, small nuclear, and small nucleolar RNAs) and regulatory RNAs. The category of regulatory ncRNAs can be further classified into small (sncRNAs) and long noncoding RNAs (lncRNAs). sncRNAs are molecules of less than 50 nucleotides (nts) such as microRNAs (miRNAs), small interference RNAs (siRNAs), and piwi-associated RNAs (piRNAs), which control gene expression at the transcriptional and posttranscriptional level by guiding DNA methylases to certain genomic *loci*, endonucleases to specific transcripts, or inhibiting translation of complementary mRNAs [1, 2]. On the other hand, lncRNAs are

transcripts longer than 200 nt with limited or no coding potential, which have gained major attention due to their function in developmental processes, diseases, and responses to environmental cues in both mammals and plants [3]. lncRNAs are highly heterogeneous in length and sequence and have been classified or grouped into four categories according to their genomic position (i.e., the genome location from where they are transcribed) relative to protein-coding genes: (1) long intergenic ncRNAs (lincRNAs) or stand-alone lncRNAs, which are transcribed from independent transcriptional units located in genomic regions that do not overlap with any protein-coding gene; (2) intronic lncRNAs, which are transcribed from introns of protein-coding genes; (3) natural antisense transcripts (NATs), which are transcribed from the opposite strand of a protein-coding gene and overlap with at least one exon; and (4) promoter- or enhancer-associated lncRNAs, which are transcribed from the vicinity of the transcriptional start site or from remote regulatory regions of a protein-coding gene, respectively (Fig. 1) [4–28].

lncRNAs have been implicated in the control of almost every step of gene expression, including RNA-dependent DNA methylation and chromatin remodeling, splicing and alternative splicing, nucleocytoplasmic trafficking, kidnapping of proteins or RNA

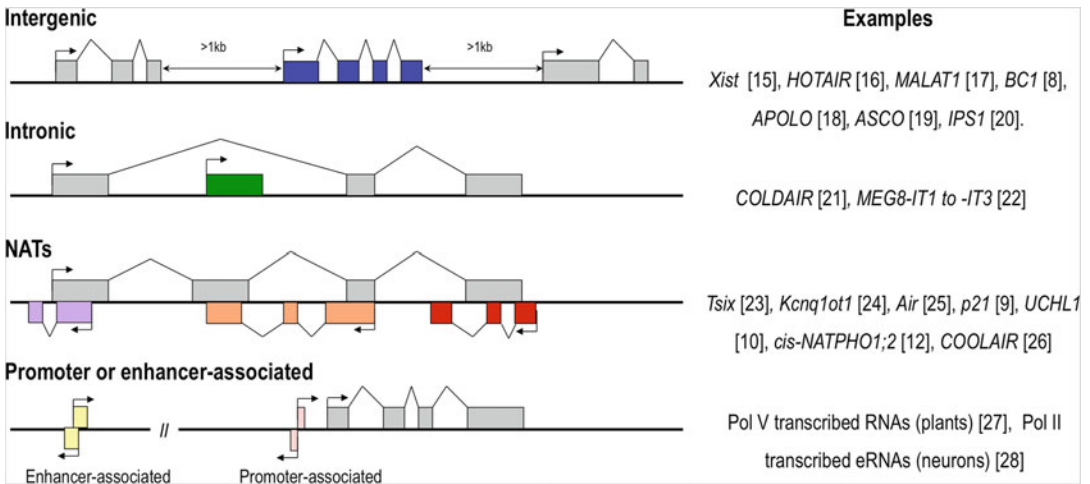


Fig. 1 Classification of long noncoding RNAs (lncRNAs) according to their genomic context. Intergenic lncRNAs (blue boxes) are independent transcriptional units located more than 1 kb apart from protein-coding genes (gray boxes). Intronic lncRNAs (green box) are transcribed from an intron of a protein-coding gene (gray boxes). Natural antisense transcripts (NATs) are transcribed in the opposite direction of a protein-coding gene. The overlap between the sense and the antisense transcripts might be extensive (orange boxes) or partial, i.e., near the 5'-end or the 3'-end of the NAT (violet or red boxes, respectively). Promoter (pink boxes)- or enhancer (yellow boxes)-associated lncRNAs are transcribed from regions located near or distant to the transcriptional start site of a protein-coding gene in both sense and antisense directions. Examples of each category and their references are presented. eRNAs: enhancer RNAs; PolV: RNA polymerase V; Pol II: RNA polymerase II

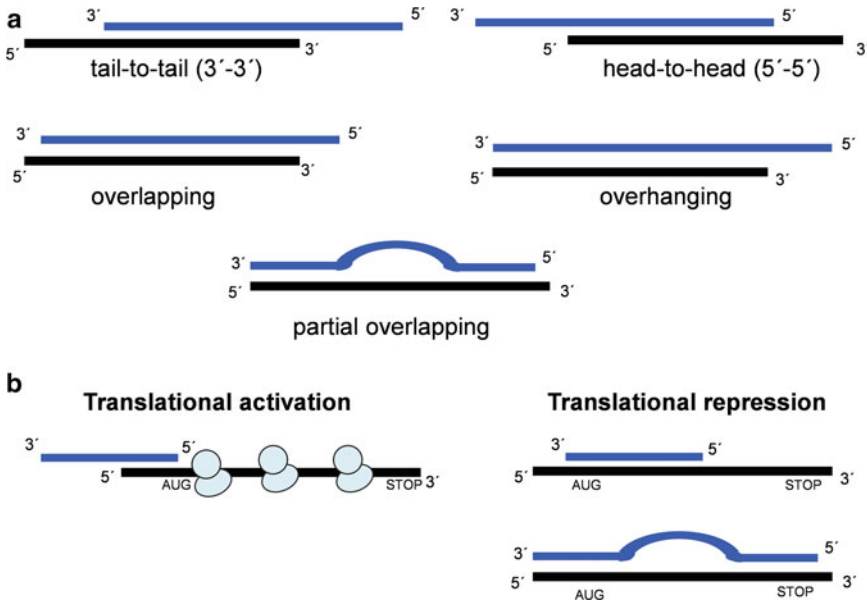


Fig. 2 NAT association to sense RNA and their action on translational regulation. **(a)** NATs are indicated in blue and sense RNAs are shown in black. cisNATs can associate to sense RNAs produced from the same locus generating partial (3'-3' or 5'-5') or extended overlaps. Trans-NATs can hybridize RNAs transcribed in a different locus by partial complementation. **(b)** Translational activation or repression produced by NAT association to mRNAs

molecules, mRNA stability, and mRNA translation. Translational regulation exerted by the action of lncRNAs can be positive or negative (Fig. 2). Several mammalian lncRNAs have been implicated in the regulation of protein translation. For example, the *BCI* RNA plays a role in several types of cancer, as well as in cell migration and proliferation [5, 6]. This lncRNA interacts and sequesters polyA-binding proteins (PABP), preventing translation of other polyadenylated mRNAs in human and mouse cell-free lysates [7]. In addition, it has been shown that *BCI* interacts with the eukaryotic translation initiation factor 4A (eIF4A), inhibiting the formation of the 48S complex in a rat brain lysate [8]. Thus, *BCI* RNA globally represses translation. Other lncRNAs implicated in the regulation of translation act on specific mRNAs. One of them, designated as p21, is a lincRNA that associates with the translational apparatus suppressing the translation of *JUNB* and *CTNNB1* mRNAs [9]. Another lncRNA acting on specific mRNAs is a neuron-specific NAT lncRNA transcribed in the opposite strand of the ubiquitin carboxy-terminal hydrolase L1 (*Uchl1*)-coding gene, which has been involved in Parkinson's and Alzheimer's diseases. This NAT lncRNA, which exhibits base pair complementarity with its target sense mRNA, is translocated from the nucleus to the cytoplasm under rapamycin treatment and recruited to active polysomes, where it specifically promotes the translation of

UCHL1 [10]. More recently, Tran et al. [11] reported a NAT-lncRNA, named AS-RBM15 (antisense RNA of RNA-binding protein 15 involved in megakaryocyte differentiation), which enhances the translation of the RBM15 in a cap-dependent manner during megakaryocyte differentiation and is also involved in a chromosome translocation in acute megakaryocyte leukemia.

The role of lncRNAs in translation has also been elucidated in the plant kingdom. A *cis*-NAT lncRNA (i.e., a NAT that acts on the transcript originated from the opposite strand) enhances the translation of its cognate sense mRNA, the *PHOSPHATE 1;2*, contributing to maintain phosphate homeostasis in rice during phosphate deficiency [12]. Another three *cis*-NAT lncRNAs associated with ribosomes (ribo-*cis*-NATs) have been found in Arabidopsis, which also showed a positive correlation with translation of their sense transcripts in plants subjected to phosphate limitation [13]. The sense mRNAs displaying NAT regulation encode *ATP-BINDING CASSETTE SUBFAMILY G* transporters (*ABCG2* and *ABCG20*) and a *POLLEN-SPECIFIC RECEPTOR-LIKE KINASE 7* (*PRK7*) family member. More recently, Deforges et al. [14] used RNA-seq and translome (i.e., the population of transcripts associated with actively translating ribosomes) data obtained in Arabidopsis to identify ribo-*cis*-NAT RNAs whose levels are correlated (positively or negatively) with their sense transcripts across several experimental conditions. Fourteen *cis*-NAT RNAs were identified, and some were validated using transgenic plants and protoplasts, showing that translome datasets can be used to systematically identify *cis*-NAT RNAs that regulate translation.

Association of lncRNAs with the translational machinery has been revealed by different experimental approaches that include differential ultracentrifugation through sucrose density gradients, ribosome footprinting (Ribo-seq), translating ribosome affinity purification (TRAP), or a combination of these approaches [29–35]. In this chapter, we focus on the protocol of TRAP combined with direct RNA sequencing (RNA-seq) and ulterior bioinformatics analysis used to detect lncRNAs associated with actively translating ribosomes. The TRAP methodology is based on the expression of a cytosolic ribosomal protein fused to an epitope (FLAG, c-myc, or HA) or a fluorescent protein (e.g., GFP, RFP, YFP) in the tissues or specific cells of interest [36, 37]. The fusion protein is incorporated into ribosomes and polysomes, allowing the isolation of these ribonucleoprotein (RNPs) complexes by immunopurification using specific antibodies coupled to magnetic or agarose beads (Fig. 3a). The TRAP approach has the advantage of excluding RNPs other than ribosomes and polysomes, which due to similar sedimentation coefficient are usually co-purified when differential ultracentrifugation is used. TRAP RNA is purified using standard RNA purification procedures and can subsequently be

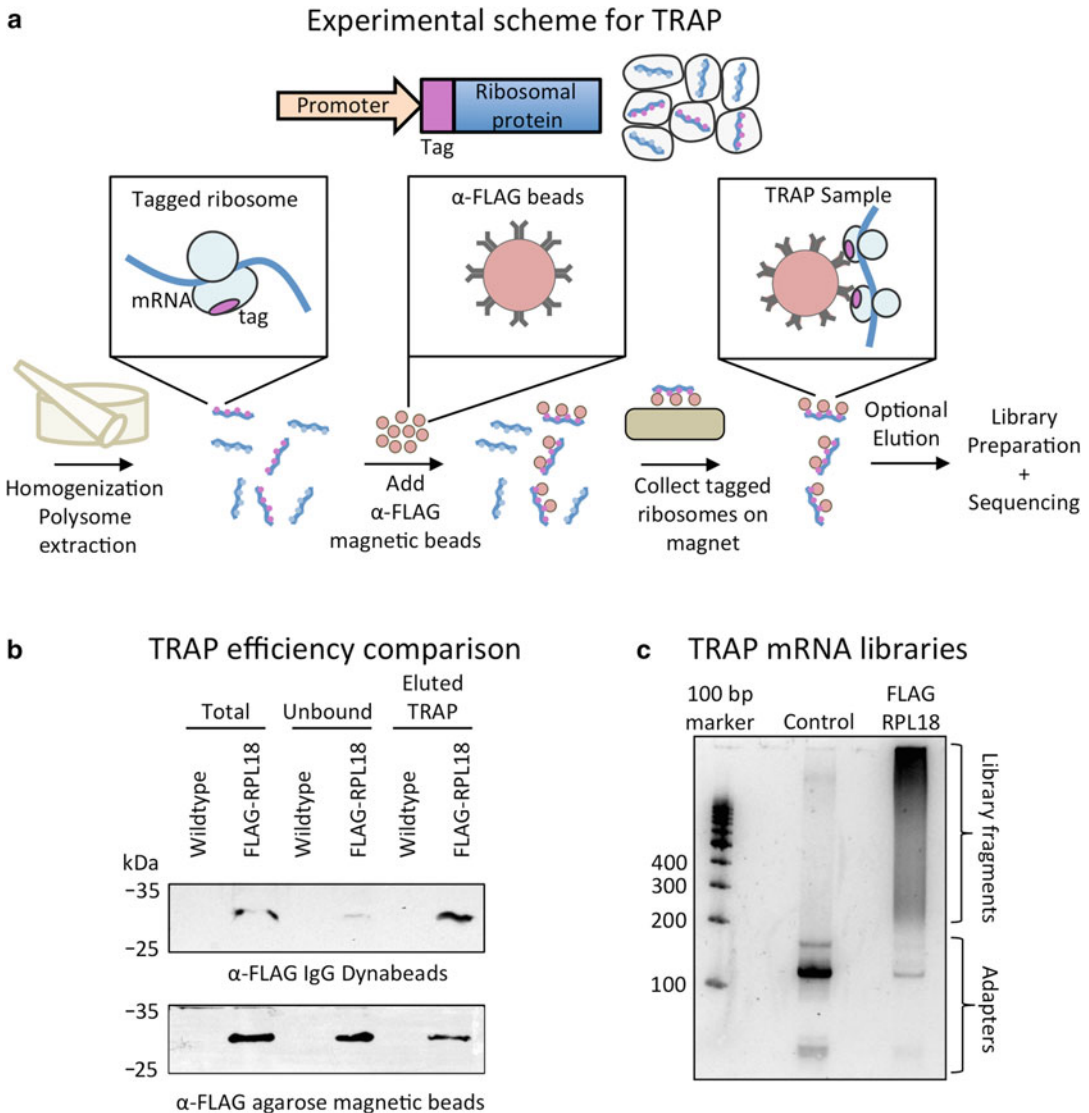


Fig. 3 Experimental scheme and yield evaluation for translating ribosome affinity purification (TRAP). **(a)** TRAP takes advantage of cells expressing an epitope-tagged ribosomal protein (FLAG-tagged RPL18 in plants). After homogenization, polysomes are stabilized in polysome extraction buffer. mRNAs and lncRNAs associated with ribosomes are captured to anti-FLAG (α -FLAG) magnetic beads. The beads are collected using a magnet and washed extensively before RNA extraction for directional RNA-sequencing library preparation. Optionally, ribosomal complexes can be eluted by competition with an excess of 3XFLAG peptide. **(b)** Western blot of rice extracts obtained from seedlings that express *p35S:FLAG-RPL18* or wild-type control in different steps of TRAP, using α -FLAG-coupled IgG Dynabeads or α -FLAG agarose magnetic beads for polysome purification. The blot was developed with α -FLAG antibodies. α -FLAG coupled to IgG Dynabeads yields more FLAG-RPL18 compared to α -FLAG in agarose beads. **(c)** mRNA libraries obtained after TRAP from rice roots expressing *p35S:FLAG-RPL18* or an INTACT construct as a control [47]. A final amplification step of 17 cycles was used to test the presence of mRNA not specifically bound to α -FLAG IgG Dynabeads. Obtained products, without final cleanup, were separated in an 8% (w/v) acrylamide gel and stained with SYBR Gold. Library fragments and adapters are indicated

analyzed by any method used to study RNA expression, including quantitative PCR (qPCR), microarray, or RNA sequencing. The TRAP methodology has been successfully applied to study the translomes of whole organs or specific cell types in mouse, *Drosophila*, zebrafish, *Xenopus*, Arabidopsis, rice, tomato, and *Medicago truncatula*, among others (Table 1) [29–45].

Table 1
Examples of TRAP studies in pluricellular organisms

Organism	Ribosomal protein	Tag used	Beads	Tissue or cell types	References
Mouse	RPL10	GFP	Anti-GFP magnetic beads	Central nervous system-specific cell types	[32, 33]
Mouse	RPL22	HA	Anti-HA magnetic beads	Brain and testis-specific cell types	[34]
<i>Drosophila</i>	RPL10A	GFP	Anti-GFP Protein A Sepharose beads	Neurons	[35]
<i>Drosophila</i>	RPL3	FLAG	Anti-FLAG magnetic beads	Neuromuscular junction	[36]
Zebrafish	RPL10	GFP	Anti-GFP magnetic beads	All tissues/melanocyte specific	[37]
<i>Xenopus</i>	RPL10A	GFP	Anti-GFP magnetic beads	Retinal ganglion cell (RGC) axons and rods	[38]
<i>Arabidopsis</i>	RPL18	FLAG	Anti-FLAG agarose beads	Whole seedling, shoot- and root-specific cell types, floral meristem cell types, pollen tubes and microspore, shoot apical meristem cell types	[29–31, 39–41]
<i>Medicago truncatula</i>	RPL18	FLAG	Anti-FLAG agarose beads	Whole roots	[42]
Tomato	RPL18	FLAG	Anti-FLAG agarose beads	Root-specific cell types	[43]
Rice	RPL18	FLAG	Anti-FLAG magnetic beads	Callus, panicle, and shoots	[44]
Soybean	RPL18	FLAG	Anti-FLAG agarose beads	Whole roots	[45]

A disadvantage of the previously described TRAP protocol [46] is the large amount of starting material of transgenic animal or plant tissue required to obtain acceptable yields of RNA material. The former procedure made use of antibodies coupled to agarose beads and an elution step; for example, for a FLAG-tagged ribosomal protein, TRAP assays are performed with anti-FLAG-agarose beads and elution is achieved by competition with an excess of 3X FLAG peptide (Fig. 3b). Then, RNA is purified from the eluted fraction to obtain the TRAP RNA. Here, we describe an optimized procedure that makes use of magnetic beads and eliminates the elution step, which significantly increases RNA yield as compared to the previously reported TRAP procedure. We also provide details of library construction and bioinformatics analysis of the RNA-seq data followed to identify ribosome-associated lncRNAs (Fig. 3c) [47].

2 Materials

2.1 Biological Material, Reagents, and Kits

1. Biological material: Fresh tissue expressing a tagged ribosomal protein (e.g., *CaMV35S:FLAG-RPL18 Medicago truncatula* roots). The amount of tissue depends on the number of cells expressing the fusion protein.
2. Dynabeads™ Protein G for immunoprecipitation (Invitrogen).
3. Monoclonal anti-FLAG antibody (*see Note 1*).
4. TRIzol Reagent (Invitrogen).
5. Miracloth.
6. Glycogen (molecular biology grade).
7. TruSeq® Stranded mRNA Library Prep (Illumina, cat. # 20020610) or YourSeq Dual (FT + 3'-DGE) RNAseq Library Kits (Amaryllis Nucleics, <https://amaryllisnucleics.com/kits/dual-rnaseq-library-kit>) or a homemade version as described [48].
8. Agencourt AMPure XP Beads (Beckman Coulter).
9. Agilent RNA 6000 Pico kit.
10. Agilent DNA 1000 kit.

2.2 Stock Buffers and Solutions

The following solutions need to be autoclaved and can be stored at room temperature for a month. Unless otherwise indicated, the solvent for solutions is molecular biology-grade water.

1. 2 M Tris-HCl, pH 9.0. Adjust the pH using concentrated HCl (*see Note 2*).
2. 2 M KCl.
3. 0.5 M Ethylene glycol-bis (2-aminoethylether)-*N,N,N',N'*-tetraacetic acid (EGTA), pH 8.0. Adjust the pH using NaOH pellets (*see Note 3*).

4. 1 M MgCl₂.
5. 20% (v/v) Detergent mix: Dissolve 4 g Brij[®] L23 Polyoxyethylene (23) lauryl ether (Brij 35) by heating to about 60 °C in 4 mL of TritonX-100, 4 mL of Igepal CA-630, and 4 mL of Tween-20 (polyoxyethylene (20) sorbitan monolaurate), and fill up with molecular biology-grade water to 20 mL (*see Note 4*).
6. 20% (v/v) Polyoxyethylene (10) tridecyl ether (PTE) in molecular biology-grade water: Shake the stock solution before pipetting PTE. Protect from light.
7. 10% (v/v) Tween-20 in molecular biology-grade water.
8. 5 M NaCl.
9. 40% (v/v) Poly(ethylene glycol) 8000 (PEG8000) in molecular biology-grade water.

The following solutions are not autoclaved and are stored in aliquots at −20 °C.

10. 0.5 M Dithiothreitol (DTT) (*see Note 2*).
11. 100 mM Phenylmethylsulfonyl fluoride (PMSF): Dissolve 87 mg of PMSF in 3.5 mL of isopropanol. Fill up with isopropanol to 5 mL (*see Note 2*).
12. 50 mg/mL Cycloheximide: Dissolve 50 mg of cycloheximide in 1 mL of 96% (v/v) ethanol (*see Note 2*). Freshly prepared in each occasion.
13. 50 mg/mL Chloramphenicol: Dissolve 50 mg of chloramphenicol in 1 mL of 96% (v/v) ethanol (*see Note 2*).

2.3 Buffers for TRAP

The following buffers are prepared fresh on the day of use from stock solutions (described in the previous Subheading 2.2) and kept on ice for the duration of the procedure.

1. Polysome extraction buffer (PEB): 200 mM Tris-HCl, 200 mM KCl, 25 mM EGTA, 35 mM MgCl₂, 1% (v/v) detergent mix, 1% (v/v) PTE, 1 mM DTT, 1 mM PMSF, 50 µg/µL cycloheximide, and 50 µg/µL chloramphenicol. Keep the buffer on ice for 10 min before adding DTT, PMSF, cycloheximide, and chloramphenicol (*see Note 4*).
2. Bead wash and binding buffer (BWBB): 200 mM Tris-HCl, 200 mM KCl, 25 mM EGTA, 35 mM MgCl₂, 0.02% (v/v) Tween-20.
3. Wash buffer (WB): 200 mM Tris-HCl, 200 mM KCl, 25 mM EGTA, 35 mM MgCl₂, 1 mM DTT, 1 mM PMSF, 50 µg/µL cycloheximide, and 50 µg/µL chloramphenicol. Keep the buffer on ice for 10 min before adding DTT, PMSF, cycloheximide, and chloramphenicol.

2.4 Equipment

1. Mortar and pestle.
2. Teflon pestle and glass tube homogenizer.
3. Standard glass centrifuge tubes, 50 mL.
4. Standard microfuge tubes, 1.5 mL.
5. Standard thin-wall PCR tubes, 0.2 mL.
6. Low-retention microfuge tubes, 1.5 mL.
7. Standard lab centrifuges for microfuge tubes and conical tubes.
8. Neodymium magnet separation racks for 1.5 mL, 15 mL, and 50 mL (*see Note 5*).
9. Standard lab centrifuge for 50 mL tubes.
10. Standard thermocycler.
11. Back-and-forth shaker.
12. NanoDrop microvolume spectrophotometer.
13. Agilent 2100 BioAnalyzer.
14. RNA-SEQ data analysis: 64-bit computer with at least 1 Tb hard disk space and 16 Gb of memory.

3 Methods

All steps in this protocol are carried out with solutions and materials free of nucleases at 4 °C. Commercial RNase/DNase-free pipette tips and microcentrifuge tubes can be used without autoclaving. Glassware, mortars, and pestles should be cleaned extensively and must be sterilized by autoclaving. Miracloth must be autoclaved as well. The protocol describes the procedure for plant tissue expressing a FLAG-tagged version of RPL18. For other organisms *see Table 1*.

3.1 Tissue Collection and Polysome Extraction

1. Harvest tissue from transgenic plants expressing FLAG-RPL18 and flash-freeze in liquid nitrogen. Grind to a fine powder maintaining the tissue frozen at all times (*see Note 6*).
2. Add approximately one volume of frozen packed pulverized tissue to at least two volumes of PEB and mix with a glass bar (*see Note 7*).
3. Let the mixture stand on ice while thawing.
4. Transfer the mixture to a glass homogenizer and make ten strokes to homogenize the mixture.
5. Incubate the mixture on ice for 10 min.
6. Transfer the mixture to a 50 mL or a 15 mL centrifuge tube and centrifuge at $16,000 \times g$ for 15 min at 4 °C.

7. Filter the supernatant of $16,000 \times g$ (SN-16) through Miracloth and transfer to 50 mL or a 15 mL plastic conical tube. It is recommended to centrifuge the samples again in the same manner to ensure removal of any insoluble material. Keep the SN-16 on ice before binding of polysomes.
8. Save a small aliquot (200–400 μL) of each (SN-16) to isolate total RNA. Optionally save other aliquots for western blot analysis (*see* **Note 8**). Keep the rest on ice for affinity purification of polysomes.

Steps 2–8 take approximately 3 h for four 5 mL of tissue sample. A larger amount of tissue requires more time at the homogenization step.

3.2 Preparation of the α -FLAG-Coupled Beads

These steps can be done prior to the preparation of tissue extracts described above and will take approximately 1 h and 20 min.

1. Resuspend Protein G Dynabeads by gently shaking the stock container from side to side by hand. Transfer 50 μL of the beads per sample (up to 8 samples per batch) to a new 1.5 mL microfuge tube.
2. Separate the beads by placing to a magnet rack for 3 min.
3. Discard the supernatant by pipetting.
4. Wash beads by adding 400 μL of BWBB and pipet to mix until complete homogenization is achieved. Repeat **steps 2** and **3** to discard wash.
5. Add the original volume of BWBB per sample (i.e., 200 μL for 4 samples) and prepare 50 μL aliquots in new 1.5 mL microfuge tubes.
6. Place 5 μL (1 $\mu\text{g}/\mu\text{L}$) of ANTI-FLAG monoclonal antibody per sample into a new 15 mL conical tube. Dilute with 400 μL of BWBB per sample.
7. Remove BWBB of the aliquots prepared in **step 5** by repeating **steps 2** and **3**. Pay attention to avoid bead drying.
8. Add 400 μL of diluted antibody to each aliquot of washed beads.
9. Incubate with gentle back-and-forth rocking for 1 h at room temperature.
10. Separate the beads and discard the supernatant by pipetting carefully.
11. Wash the beads as described in **step 4**. These are now the α -FLAG-coupled beads.
12. Add 400 μL of BWBB per sample and precool the beads on ice until the SN-16 is ready.

3.3 Affinity Purification of Polysomes

The following steps take approximately 4 h.

1. Separate the α -FLAG-coupled beads (saved at Subheading 3.2, step 12) by placing them to a magnet rack for 3 min.
2. Discard the supernatant by pipetting.
3. Use each SN-16 sample (saved at Subheading 3.1, step 7) to resuspend the beads in one 1.5 mL microfuge tube and transfer the resuspension to the conical tube containing the rest of the corresponding SN-16.
4. Incubate for 2 h at 4 °C with gentle back-and-forth rocking or gyration to bind the FLAG-tagged ribosomes to the affinity beads (*see Note 8*).
5. Put the tubes in a magnetic rack for 5 min in a 4 °C cold room.
6. Transfer the supernatant to a new 15 mL plastic conical tube. This fraction is the supernatant of the affinity purification or unbound fraction.
7. Add 6 mL of ice-cold WB to the beads, and mix by gentle back-and-forth rocking of the tube. Separate on magnet for 5 min at 4 °C and discard supernatant.
8. Repeat 6 mL wash twice as in step 7.
9. Add 1 mL of ice-cold WB and transfer to a new 1.5 mL microfuge tube at 4 °C. Add 200 μ L of WB to the original tube to complete the transfer of the remaining beads.
10. Separate the beads on a small magnetic rack for 3 min. Discard the supernatant and add 1 mL of ice-cold WB.
11. Repeat 1 mL wash twice as in step 10 and discard the supernatant.
12. Proceed immediately to RNA extraction (*see Note 9*).

3.4 RNA Extraction and Estimation of RNA Yield

This section takes about 1–2 h. Use a fume hood to work with TRIzol, chloroform, and isopropanol. After use, TRIzol and chloroform should be discarded as hazardous waste following local regulations. Optionally, if working with only polyadenylated RNAs, it is possible to extract those RNAs directly from beads without the need of a TRIzol extraction (this option is specially recommended when working with promoters expressed in a low number of cells). For an example see <http://plant-plasticity.github.io/resources/RNA-prep-magnetic-beads-share.pdf>.

1. Process in parallel TRIzol RNA extractions from the TRAP sample, consisting of washed magnetic beads from Subheading 3.3, step 12, and the SN-16 aliquot put aside in Subheading 3.1, step 8.

2. Add 800 μL of TRIzol to each sample, vortex for 30 s, and incubate at room temperature for 5 min to allow the dissociation of ribonucleoprotein complexes.
3. Add 200 μL of chloroform, shake the tube vigorously by hand for 15 s, and incubate at room temperature for 3 min.
4. Centrifuge at $12,000 \times g$ for 15 min at 4°C .
5. Transfer the clear upper phase to a new 1.5 mL microfuge tube.
6. Repeat the chloroform extraction **steps 3–5** to remove residual TRIzol traces that can inhibit downstream enzymatic reactions.
7. To precipitate RNA, add 500 μL of isopropanol, invert the tube gently by hand to mix, and incubate at room temperature for 10 min or at -20°C overnight. For samples with low yields of affinity-purified polysomes (less than 100 ng), add 1 μL of 20 $\mu\text{g}/\mu\text{L}$ glycogen along with the isopropanol, to aid in the precipitation.
8. Centrifuge at $12,000 \times g$ for 15 min at 4°C . The RNA pellet is visible after centrifugation. Discard the supernatant as hazardous waste following local regulations.
9. Wash pellet with 1 mL of 70% (v/v) ethanol. Centrifuge at $7,500 \times g$ for 5 min at 4°C .
10. Discard supernatant and let the pellet air-dry at room temperature for 20 min.
11. Resuspend the pellet in 50 μL of molecular biology-grade water by incubating the sample at 60°C for 10 min to allow the complete resuspension of the RNA pellet. Store at -80°C until use.
12. Use 1 μL of each sample to estimate the yield and concentration of RNA with a NanoDrop spectrophotometer according to the manufacturer's instructions (*see Note 10*).
13. Evaluate the quality of the sample using an Agilent 2100 Bioanalyzer with RNA 6000 Nano or Pico Assay reagent kits (*see Note 11*).

3.5 Preparation and Sequencing of RNAseq Illumina Compatible Libraries

1. Use an RNA-seq kit of choice and follow the manufacturer's protocol or the homemade version available at your lab (*see Note 12*).
2. For DNA purification steps use AMPure XP Beads. The range of DNA fragments to purify can be manipulated by changing the concentration of PEG in the buffer (Fig. 4; *see Note 13*).
3. For indexing of the libraries choose a manufacturer-recommended combination of adapters to allow multiplex sequencing. The procedures can take 1–2 days.

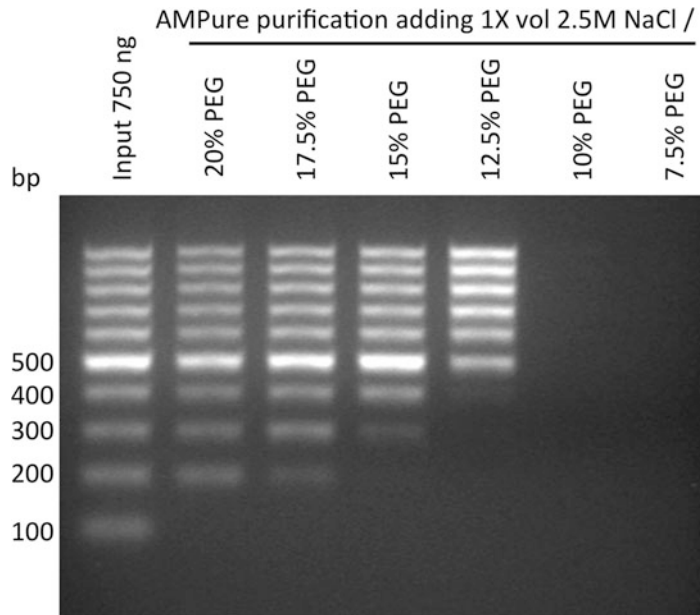


Fig. 4 Optimization of DNA fragment purification with AMPure XP beads. 100 bp DNA ladder was purified by adding 1× volume of beads diluted in buffers with different concentrations of PEG. After binding and two 80% (v/v) EtOH washes, the eluted DNA was separated in each lane. DNA fragments of intermediate range can be obtained by a standard purification of unbound fractions

4. Assess the quality of the libraries using Agilent 2100 Bioanalyzer with DNA 1000 Assay reagent kits (*see Note 14*). This step takes about 1 h.
5. Quantify the libraries according to the Kapa Library Quantification Kit (Complete kit, Kapa Biosystems). Normalize each library to 10 nM and pool libraries using equal volumes of each library. Alternatively, quantify by qPCR using DNA standards and primers for IlluminaP5 “AATGATACGGCGAC-CACCGA” and IlluminaP7 “CAAGCAGAAGACGGCA-TACGA”. This step takes approximately 3 h.
6. Sequence the libraries on an Illumina NextSeq500 or a HiSeq3000/4000 sequencing platform (see a comparison of different Illumina sequencing systems at <https://www.illumina.com/systems/sequencing-platforms.html>). The run time ranges from 12 h to 3.5 days and depends on the sequencing system, the read length, and the choice of single versus paired-end sequencing (*see Note 15*).

3.6 Data Analysis

In this section, we present a pipeline for computational analysis of RNA-seq data consisting of a quality check followed by read alignment, transcript assembling, and quantification and evaluation of coding potential for new transcripts. In this analysis we use the

FastQC software [49] to check the quality of the reads. Illumina sequences are aligned to the reference genome using a splice-aware aligner such as *TopHat* [50] or *HISAT2* [51]. Transcript assembly is performed using *Cufflinks* and differentially expressed genes and transcripts are identified using *Cuffdiff* [52]. Transcript variants aligned to the genome are visualized using the Integrative Genomic Viewer [53]. Open reading frames of lncRNAs are predicted using the NCBI Open Reading Frame Finder. Coding potential analysis is performed using two different alignment-free methods: Coding Potential Calculator 2 [54] and Coding Potential Assessment Tool [55]. Finally, the annotation for lncRNAs according to the genomic context is discussed [56].

1. Connect to Galaxy (<https://usegalaxy.org/>) using your username and password. Enter to the section Get Data on the tools panel and select Upload File from your computer. Upload the sequence of your genome of reference in FASTA format and the file with annotation information in GFF3 format. The files can be accessed by direct uploading from your computer using the option Choose File or by downloading from the web, using the option Paste/Fetch Data. Once appointed the files, click on the bottom Start. Loaded files appear on the History panel.
2. Upload sequence reads in FASTQ format selecting the tool Upload file from your computer. Select them and confirm uploading by clicking the bottom Start.
3. Check the quality of sequence data using the *FastQC Read Quality* reports tool located on the tools panel, Genomic File Manipulation section, folder FASTQ Quality Control. Select the FASTQ files as input for the analysis. Click the Execute bottom. The tool produces an output file that contains basic statistics, per base sequence quality score and per base sequence content, GC content, N content, sequence length distribution, sequence duplication levels, and overrepresented sequences.
4. Filter reads based on the quality scores using the *Filter by quality* tool located on the tools panel, Genomic File Manipulation section, folder FASTA/FASTQ. Quality score distribution is calculated for each read (cutoff value of quality score of 30 is recommended). The *FASTQ Trimmer* tool can be used to trim low-quality ends of reads.
5. Map reads to your reference genome using *TopHat* or *HISAT2* tool located on the tools panel, Genomic Analysis section, folder RNA-seq. Select the FASTQ file or two FASTQ files depending on if the library was sequenced by single end or paired end, and the FASTA file containing the genome sequence previously uploaded. If your reads are from a stranded library, choose the appropriate setting under Specify strand information. A set of parameters can be modified by

selecting Advanced Options. Execute the alignments by clicking the Execute bottom. A list of read alignments (BAM files) and tracks of junctions (BED files) are produced as output files.

6. Assemble and measure the relative transcript abundance using the *Cufflinks* tool located on the tools panel, Genomic Analysis section, folder RNA-seq. Use the BAM output file of *TopHat* as Input file. Use the reference annotation file in GFF3 format as a guide of the assembly process. If your reads are from a stranded library, choose the appropriate setting under Specify strand information. The output includes all expressed reference transcripts and any novel transcripts and splice isoforms that are assembled based on *TopHat* read alignments. *Cufflinks* produces three outputs: a GTF file containing the assembled transcripts and two files containing the estimated level of expression for each transcript and gene, respectively.
7. Merge assemblies using *Cuffmerge* tool located on the tools panel, Genomic Analysis section, folder RNA-seq. Use the GTF output files of *Cufflinks* and the GFF3 reference genome annotation file. *Cuffmerge* merges annotation files to include novel genes or alternative splicing isoforms that were not included in the reference genome annotation and produces a GTF output file that contains an assembly that merges together the input assemblies.
8. Find significant changes in transcript expression, splicing, and promoter usage between two conditions using the *Cuffdiff* tool located on the tools panel, Genomic Analysis section, folder RNA-seq. Use the GTF file containing the merged assemblies produced by *Cuffmerge* and the BAM output files of *TopHat* for the samples. *Cuffdiff* produces output files such as transcript and gene FPKM expression tracking, transcript and gene differential FPKM, and differential splicing and promoter use tests.
9. Visualize the read alignment at the genome level using the Integrative Genomics Viewer (IGV). This software can be downloaded from the website <https://software.broadinstitute.org/software/igv/download>. IGV allows the visualization of *TopHat* outputs, such as read alignment data (BAM files) and track intron/exon junction data (BED files) as well as a wide variety of data types.
 - (a) If the genome is not included in the software database, create a genome file using the menu Genomes, Create genome file.
 - (b) Upload the genome using the menu Genomes, Load genome from file, or use the menu Load genome from URL if it is available online.

- (c) Load the alignment files using the menu File, Load from file or Load from URL depending on the case.
 - (d) Upload annotation files to show novel transcript isoforms or alternative spliced transcripts.
10. To identify long noncoding RNAs, use the GTF file containing the merged assemblies produced by *Cuffmerge*. Filter-out well-annotated genes in a spreadsheet editor and keep those that have not been annotated as protein-coding genes in your reference genome. Include also those that have been annotated as hypothetical proteins. Keep transcripts longer than 200 nt.
11. Predict lncRNA open reading frames (ORFs) using NCBI Open Reading Frame Finder (www.ncbi.nlm.nih.gov/orffinder/). NCBI ORF Finder searches for open reading frames in the DNA sequence supplied by the user and returns the range of each ORF, along with its protein translation. Enter query sequence in FASTA format and choose searching parameters. Click Submit bottom. For sequences longer than 50 kb, a stand-alone version is available for Linux x64. Keep only those transcripts that do not contain ORFs longer than 100 amino acids.
12. Perform the coding potential analysis of transcripts using two different alignment-free methods:
 - (a) The support vector machine-based classifier, Coding Potential Calculator 2 (CPC2) (<http://cpc2.cbi.pku.edu.cn>). Enter query sequence in FASTA, BED, or GTF format. When using a FASTA file as input, the reference genome is not required. Select Genome assembly version if your input file is in BED or GTF format. Click “Check the reverse strand too”, and press bottom Run. The CPC2 server uses RNA transcript sequences as input, and outputs protein-coding probability of the transcripts using four intrinsic features: Fickett score derived from the weighted nucleotide frequency of the inputted full-length transcript, and the rest of the three features, ORF length, ORF integrity, and isoelectric point, which are calculated based on the longest putative ORF identified *in silico*. For lncRNAs, coding probability must be between 0 and 1 and the resulting label must indicate “noncoding.”
 - (b) The Coding Potential Assessment Tool (CPAT) (<http://lilab.research.bcm.edu/cpat/>): Enter a query sequence in FASTA or BED format. When using a FASTA file as input, the reference genome is not required. Select Species assembly if your input file is in BED format. Click Submit button. CPAT uses RNA transcript sequences as input, and outputs its coding probability by using logistic

regression model based on four sequence-based features: ORF size, ORF coverage, Fickett Score, and Hexamer usage bias. A cutoff of coding potential (CP) score < -0.5 can be used to distinguish coding RNAs from noncoding RNAs.

13. Putative lncRNAs that passed the filters on **steps 11** and **12** can be annotated to the reference genome using PAVIS webtools in the website <https://manticore.niehs.nih.gov/pavis2/annotate>. Species of interest and length of upstream and downstream regions should be selected. A strand-specific BED file containing chromosomal locations for the lncRNAs is the input required for the analysis. The output classifies each lncRNA region according to its genomic context in upstream, 5'UTR, exon, intron, 3'UTR, downstream, and intergenic, similar to the classifications shown in Fig. 1. Alternatively, a pipeline known as PLAR (Pipeline for lncRNA annotation from RNA-seq data; http://www.weizmann.ac.il/Biological_Regulation/IgorUlitsky/PLAR) can be used to annotate lncRNAs [56]. Comparison to known databases of lncRNAs and a final manual inspection in a genome browser (i.e., IGV) is recommended to check location and strand specificity for new lncRNAs.

4 Notes

1. Good results have been obtained using the monoclonal ANTI-FLAG® M2 antibody produced in mouse (Sigma-Aldrich, www.sigmaaldrich.com, cat. # F1804).
2. Use a mask for lung protection while weighing the following reagents: Tris base, EGTA, Brij-35, DTT, PMSF, cycloheximide, and chloramphenicol.
3. Take EGTA to the desired pH with NaOH pellets instead of solutions or highly concentrated solutions. Diluted NaOH solutions can absorb carbon dioxide from the air over time, which lowers the pH, producing the precipitation of EGTA.
4. Pipette detergents with a 1000 μ L tip enlarged by cutting 0.5 cm from the end. It takes time for the detergents to go into solution. Add heparin and RNase inhibitor to PEB if working with tissue with high RNase content such as mature maize leaves. When working with seeds or mature leaves improve the disruption of ribosome-cytoskeleton association by including 1% (w/v) sodium deoxycholate DOC, prepared from a 20% (w/v) stock solution, in the PEB. Use freshly prepared solutions including cycloheximide and DTT.

5. Commercial magnetic racks can be replaced by placing two strong neodymium bars on opposite sides of two plastic racks. For pictures see <https://bio-protocol.org/e2458>.
6. Use finely grinded tissue to maximize polysome yield. Tissue collected may be whole plant, a specific organ, or a dissected region (i.e., root tips). A homogenous pulverization is accomplished with a porcelain mortar and pestle. This step takes approximately 30 min for four samples. The tissue can be kept at -80°C until use. Alternatively, it is possible to pulverize tissue with a frozen bead beater (TissueLyser II, QIAGEN), when using small amounts of tissue ($\sim 100\text{--}200\ \mu\text{L}$). Transgenic tissue from mice and zebrafish embryos is obtained fresh and immediately homogenized in cold polysome-stabilizing buffer [32–34, 37]. *Drosophila* larva dissections can be flash-frozen in dry ice before polysome extraction [35, 36]. Keeping everything at 4°C throughout the procedure is essential to maintain the polysome integrity.
7. The amount of tissue depends on the quantity of cells expressing the tagged ribosomal protein (i.e., FLAG-RPL18). In the case of strong plant promoters, such as *CaMV35S*, 1 mL of packed pulverized tissue is enough to get RNA for library preparation. For larger amount of tissue increase the volume of PEB buffer to five volumes to facilitate the homogenization.
8. It is recommended to test the efficiency of the procedure by Western blot with an anti-FLAG antibody conjugated to horseradish peroxidase or an antibody against the epitope tag used for the ribosomal protein. A band of the expected molecular weight (e.g., 25 kDa for FLAG-RPL18) should be visualized in the samples from clarified cellular extract and the eluted material (or the beads after affinity purification, but not in those corresponding to the unbound fraction as shown in Fig. 3b). A low amount of tagged ribosomal protein in the affinity-purified sample may indicate inefficient binding to the beads or low efficiency of elution. Possible solutions include increasing binding time and elution time, as well as using a fresh stock of beads and 3X FLAG peptide. It can also be useful to increase the amount of both of them if FLAG-RPL18 is detected in the unbound fraction.
9. The polysome composition obtained by TRAP can be evaluated by fractionation in sucrose density gradients. Stable polysome complexes can be eluted by competition incubating for 30 min at 4°C , with back-and-forth shaking, in wash buffer supplemented with purified peptide (i.e., $\sim 300\ \text{ng/mL}$ 3X FLAG peptide). The eluate should be used immediately for polysome fractionation in sucrose density gradients. This

procedure requires considerably more affinity-purified complexes than the amount needed for the RNA-SEQ library construction [31].

10. TRAP yield from tissues expressing FLAG-RPL18 protein in nearly all cell types is about 500 ng of RNA per mL of ground tissue. TRAP RNA yield ranges between 10 and 150 ng per mL of tissue when the FLAG-RPL18 protein is expressed in a limited number of cells (e.g.: root atrichoblast, cortical cells of the root meristematic zone, root vasculature); therefore, a significantly higher amount of tissue should be processed in order to obtain ~500 ng of RNA [46].
11. The quality of the RNA starting material is crucial for the success of RNA-SEQ library preparation. The RNA integrity number (RIN) provides robust and reliable prediction of RNA integrity. The RIN is calculated by a method that automatically selects features from signal measurements recorded with an Agilent 2100 Bioanalyzer and constructs regression models based on a Bayesian learning technique. RIN values range from 10 (intact RNA) to 1 (totally degraded RNA). In order to proceed with RNA-SEQ library preparation, RIN should be 8 or higher and the ratio of the 25S signal to the 18S signal should be about 1.8.
12. Take into consideration that for low initial RNA amount it is recommended to dilute adapters (e.g., starting with 400 ng of total RNA, we used a 1:8 dilution of adapters in TE buffer with good results) to avoid an excess of adapters that can lead to the formation of contaminating adapter dimers or oligomers (*see* Fig. 3c).
13. Commercial beads can be collected and diluted to 3× the original volume in 20% PEG/2.5 M NaCl without affecting the purification.
14. TRAP RNA-SEQ libraries of sufficient quality for Illumina RNA-SEQ should produce a signal distribution between 200 and 500 bp with a maximum at approximately 260 bp, such as those illustrated in Fig. 3c. Prior to running DNA samples in the Bioanalyzer, they can be evaluated in an ethidium bromide-stained 1.5% (w/v) agarose gel when working with abundant RNA, or an acrylamide gel stained with SYBR Gold. A distribution of DNA fragments between 200 and 500 bp with no adapter dimers should be observed (Fig. 3c).
15. The HiSeq3000/4000 system can yield approximately 300–400 million single-end reads (101 bp length) allowing the sequencing of up to 32 multiplexed libraries in a single lane.

Acknowledgments

We thank Julia Bailey-Serres, Kaisa Kajala, and others that have contributed to improving the TRAP-SEQ technology. We also thank Claudio Rivero for discussion and advice on RNA-SEQ analysis. This work has been financially supported by grants from ANPCyT, Argentina, funded to M.E.Z. (PICT 2016-0582, PICT 2017-0581), F.A.B. (PICT 2016-0333), and M.A.R. (PICT 2017-2272). M.E.Z., F.A.B., and M.A.R. are members of CONICET. S.T. is a fellow of the same institution and has been awarded a Fulbright Scholarship.

References

- Farazi TA, Juranek SA, Tuschl T (2008) The growing catalog of small RNAs and their association with distinct Argonaute/Piwi family members. *Development* 135:1201–1214
- Axtell MJ (2013) Classification and comparison of small RNAs from plants. *Annu Rev Plant Biol* 64:137–159
- Kung JT, Colognori D, Lee JT (2013) Long noncoding RNAs: past, present, and future. *Genetics* 193:651–669
- Ariel F, Romero-Barrios N, Jegu T, Benhamed M, Crespi M (2015) Battles and hijacks: noncoding transcription in plants. *Trends Plant Sci* 20:362–371
- Booy EP, McRae EK, Koul A, Lin F, McKenna SA (2017) The long non-coding RNA BC200 (BCYRN1) is critical for cancer cell survival and proliferation. *Mol Cancer* 16:109
- Shin H, Lee J, Kim Y, Jang S, Lee Y, Kim S, Lee Y (2017) Knockdown of BC200 RNA expression reduces cell migration and invasion by destabilizing mRNA for calcium-binding protein S100A11. *RNA Biol* 14:1418–1443
- Kondrashov AV, Kieffmann M, Ebnet K, Khanam T, Muddashetty RS, Brosius J (2005) Inhibitory effect of naked neural BC1 RNA or BC200 RNA on eukaryotic in vitro translation systems is reversed by poly(A)-binding protein (PABP). *J Mol Biol* 353:88–103
- Wang H, Iacoangeli A, Popp S, Muslimov IA, Imataka H, Sonenberg N, Lomakin IB, Tiedge H (2002) Dendritic BC1 RNA: functional role in regulation of translation initiation. *J Neurosci* 22:10232–10241
- Yoon JH, Abdelmohsen K, Srikantan S, Yang X, Martindale JL, De S, Huarte M, Zhan M, Becker KG, Gorospe M (2012) LincRNA-p21 suppresses target mRNA translation. *Mol Cell* 47:648–655
- Carrieri C, Cimatti L, Biagioli M, Beugnet A, Zucchelli S, Fedele S, Pesce E, Ferrer I, Collavin L, Santoro C, Forrest AR, Carninci P, Biffo S, Stupka E, Gustincich S (2012) Long non-coding antisense RNA controls Uchl1 translation through an embedded SINEB2 repeat. *Nature* 491:454–457
- Tran NT, Su H, Khodadadi-Jamayran A, Lin S, Zhang L, Zhou D, Pawlik KM, Townes TM, Chen Y, Mulloy JC, Zhao X (2016) The AS-RBM15 lincRNA enhances RBM15 protein translation during megakaryocyte differentiation. *EMBO Rep* 17:887–900
- Jabnourne M, Secco D, Lecampion C, Robaglia C, Shu Q, Poirier Y (2013) A rice cis-natural antisense RNA acts as a translational enhancer for its cognate mRNA and contributes to phosphate homeostasis and plant fitness. *Plant Cell* 25:4166–4182
- Bazin J, Baerenfaller K, Gosai SJ, Gregory BD, Crespi M, Bailey-Serres J (2017) Global analysis of ribosome-associated noncoding RNAs unveils new modes of translational regulation. *Proc Natl Acad Sci U S A* 114: E10018–E10027
- Deforges J, Reis RS, Jacquet P, Sheppard S, Gadekar VP, Hart-Smith G, Tanzer A, Hofacker IL, Iseli C, Xenarios I, Poirier Y (2019) Control of cognate sense mRNA translation by cis-natural antisense RNAs. *Plant Physiol* 180:305–322
- Brown CJ, Hendrich BD, Rupert JL, Lafrenière RG, Xing Y, Lawrence JP, Willard HF (1992) The human XIST gene: analysis of a 17 kb inactive X-specific RNA that contains conserved repeats and is highly localized within the nucleus. *Cell* 71:527–542
- Rinn JL, Kertesz M, Wang JK, Squazzo SL, Xu X, Bruggmann SA, Goodnough LH, Helms JA, Farnham PJ, Segal E, Chang HY (2007) Functional demarcation of active and silent chromatin domains in human HOX loci by noncoding RNAs. *Cell* 129:1311–1323

17. Liu P, Yang H, Zhang J, Peng X, Lu Z, Tong W, Chen J (2017) The lncRNA MALAT1 acts as a competing endogenous RNA to regulate KRAS expression by sponging miR-217 in pancreatic ductal adenocarcinoma. *Sci Rep* 7:5186
18. Ariel F, Jegu T, Latrasse D, Romero-Barrios N, Christ A, Benhame M, Crespi M (2014) Non-coding transcription by alternative RNA polymerases dynamically regulates an auxin-driven chromatin loop. *Mol Cell* 55:343–504
19. Bardouin F, Ariel F, Simpson CG, Romero-Barrios N, Laporte P, Balzergue S, Brown JW, Crespi M (2014) Long noncoding RNA modulates alternative splicing regulators in Arabidopsis. *Dev Cell* 30:166–176
20. Franco-Zorrilla JM, Valli A, Todesco M, Mateos I, Puga MI, Rubio-Somoza I, Leyva A, Weigel D, García JA, Paz-Ares J (2007) Target mimicry provides a new mechanism for regulation of microRNA activity. *Nat Genet* 39:1033–1037
21. Heo JB, Sung S (2011) Vernalization-mediated epigenetic silencing by a long intronic noncoding RNA. *Science* 331:76–79
22. Yang W, Li D, Wang G, Zhang C, Zhang M, Zhang W, Li S (2017) Three intronic lncRNAs with monoallelic expression derived from the MEG8 gene in cattle. *Anim Genet* 48:272–277
23. Lee JT, Lu N (1999) Targeted mutagenesis of Tsix leads to nonrandom X inactivation. *Cell* 99:47–57
24. Mohammad F, Mondal T, Guseva N, Pandey GK, Kanduri C (2010) Kcnq1ot1 noncoding RNA mediates transcriptional gene silencing by interacting with Dnmt1. *Development* 137:2493–2499
25. Lyle R, Watanabe D, te Vruchte D, Lerchner W, Smrzka OW, Wutz A, Schageman J, Hahner L, Davies C, Barlow DP (2000) The imprinted antisense RNA at the Igf2r locus overlaps but does not imprint Mas1. *Nat Genet* 25:19–21
26. Csorba T, Questa JI, Sun Q, Dean C (2014) Antisense COOLAIR mediates the coordinated switching of chromatin states at FLC during vernalization. *Proc Natl Acad Sci U S A* 111:16160–16165
27. Wierzbicki AT, Haag JR, Pikaard CS (2008) Noncoding transcription by RNA polymerase Pol IVb/Pol V mediates transcriptional silencing of overlapping and adjacent genes. *Cell* 135:635–648
28. Kambiz M, Zare H, Dell’Orso S, Grontved L, Gutierrez-Cruz G, Derfoul A, Hager GL, Sartorelli V (2013) eRNAs Promote Transcription by Establishing Chromatin Accessibility at Defined Genomic. *Mol Cell* 51:606–617
29. Juntawong P, Girke T, Bazin J, Bailey-Serres J (2014) Translational dynamics revealed by genome-wide profiling of ribosome footprints in Arabidopsis. *Proc Natl Acad Sci U S A* 111: E203–E212
30. Jiao Y, Meyerowitz EM (2010) Cell-type specific analysis of translating RNAs in developing flowers reveals new levels of control. *Mol Syst Biol* 6:419
31. Zanetti ME, Chang IF, Gong F, Galbraith DW, Bailey-Serres J (2005) Immunopurification of polyribosomal complexes of Arabidopsis for global analysis of gene expression. *Plant Physiol* 138:624–635
32. Doyle JP, Dougherty JD, Heiman M, Schmidt EF, Stevens TR, Ma G, Bupp S, Shrestha P, Shah RD, Doughty ML, Gong S, Greengard P, Heintz N (2008) Application of a translational profiling approach for the comparative analysis of CNS cell types. *Cell* 135:749–762
33. Heiman M, Schaefer A, Gong S, Peterson JD, Day M, Ramsey KE, Suárez-Fariñas M, Schwarz C, Stephan DA, Surmeier DJ, Greengard P, Heintz N (2008) A translational profiling approach for the molecular characterization of CNS cell types. *Cell* 135:738–748
34. Sanz E, Yang L, Su T, Morris DR, McKnight GS, Amieux PS (2009) Cell type-specific isolation of ribosome-associated mRNA from complex tissues. *Proc Natl Acad Sci U S A* 106:13939–13944
35. Thomas A, Lee PJ, Dalton JE, Nomie KJ, Stoica L, Costa-Mattioli M, Chang P, Nuzhdin S, Arbeitman MN, Dierick HA (2012) A versatile method for cell-specific profiling of translated mRNAs in Drosophila. *PLoS One* 7:e40276
36. Chen X, Dickman D (2017) Development of a tissue-specific ribosome profiling approach in Drosophila enables genome-wide evaluation of translational adaptations. *PLoS Genet* 13: e1007117
37. Tryon RC, Pisat N, Johnson SL, Dougherty JD (2013) Development of translating ribosome affinity purification for zebrafish. *Genesis* 51:187–192
38. Watson FL, Mills EA, Wang X, Guo C, Chen DF, Marsh-Armstrong N (2012) Cell type-specific translational profiling in the *Xenopus laevis* retina. *Dev Dyn* 241:1960–1972
39. Muströph A, Zanetti ME, Jang CJ, Holtan HE, Repetti PP, Galbraith DW, Girke T, Bailey-Serres J (2009) Profiling translatoemes of discrete cell populations resolves altered cellular priorities during hypoxia in Arabidopsis. *Proc Natl Acad Sci U S A* 106:18843–18848

40. Lin SY, Chen PW, Chuang MH, Juntawong P, Bailey-Serres J, Jauh GY (2014) Profiling of translomes of in vivo-grown pollen tubes reveals genes with roles in micropylar guidance during pollination in Arabidopsis. *Plant Cell* 26:602–618
41. Tian C, Wang Y, Yu H, He J, Wang J, Shi B, Du Q, Provart NJ, Meyerowitz EM, Jiao Y (2019) A gene expression map of shoot domains reveals regulatory mechanisms. *Nat Commun* 10:141
42. Reynoso MA, Blanco FA, Bailey-Serres J, Crespi M, Zanetti ME (2013) Selective recruitment of mRNAs and miRNAs to polyribosomes in response to rhizobia infection in *Medicago truncatula*. *Plant J* 73:289–301
43. Ron M, Kajala K, Pauluzzi G, Wang D, Reynoso MA, Zumstein K, Garcha J, Winte S, Masson H, Inagaki S, Federici F, Sinha N, Deal RB, Bailey-Serres J, Brady SM (2014) Hairy root transformation using *Agrobacterium rhizogenes* as a tool for exploring cell type-specific gene expression and function using tomato as a model. *Plant Physiol* 166:455–469
44. Zhao D, Hamilton JP, Hardigan M, Yin D, He T, Vaillancourt B, Reynoso M, Pauluzzi G, Funkhouser S, Cui Y, Bailey-Serres J, Jiang J, Buell CR, Jiang N (2017) Analysis of ribosome-associated mRNAs in rice reveals the importance of transcript size and GC content in translation. *G3 (Bethesda)* 7:203–219
45. Castro-Guerrero NA, Cui Y, Mendoza-Cozatl DG (2016) Purification of translating ribosomes and associated mRNAs from soybean (*Glycine max*). *Curr Protoc Plant Biol* 1:185–196
46. Reynoso MA, Juntawong P, Lancia M, Blanco FA, Bailey-Serres J, Zanetti ME (2015) Translating ribosome affinity purification (TRAP) followed by RNA sequencing technology (TRAP-SEQ) for quantitative assessment of plant translomes. *Methods Mol Biol* 1284:185–207
47. Reynoso MA, Pauluzzi GC, Kajala K, Cabanlit S, Velasco J, Bazin J, Deal R, Sinha NR, Brady SM, Bailey-Serres J (2018) Nuclear transcriptomes at high resolution using retooled INTACT. *Plant Physiol* 176:270–281
48. Townsley BT, Covington MF, Ichihashi Y, Zumstein K, Sinha NR (2015) BrAD-seq: breath adapter directional sequencing: a streamlined, ultra-simple and fast library preparation protocol for strand specific mRNA library construction. *Front Plant Sci* 6:366
49. Blankenberg D, Gordon A, Von Kuster G, Coraor N, Taylor J, Nekrutenko A (2010) Manipulation of FASTQ data with Galaxy. *Bioinformatics* 26:1783–1785
50. Trapnell C, Pachter L, Salzberg SL (2009) TopHat: discovering splice junctions with RNA-Seq. *Bioinformatics* 25:1105–1111
51. Kim D, Langmead B, Salzberg SL (2015) HISAT: a fast spliced aligner with low memory requirements. *Nat Methods* 12:357
52. Trapnell C, Williams BA, Pertea G, Mortazavi A, Kwan G, van Baren MJ, Salzberg SL, Wold BJ, Pachter L (2010) Transcript assembly and quantification by RNA-Seq reveals unannotated transcripts and isoform switching during cell differentiation. *Nat Biotechnol* 28:511
53. Thorvaldsdottir H, Robinson JT, Mesirov JP (2013) Integrative genomics viewer (IGV): high-performance genomics data visualization and exploration. *Brief Bioinform* 14:178–192
54. Kang YJ, Yang DC, Kong L, Hou M, Meng YQ, Li W, Gao G (2017) CPC2: a fast and accurate coding potential calculator based on sequence intrinsic features. *Nucleic Acids Res* 45:W12–W16
55. Wang L, Park HJ, Dasari S, Wang S, Kocher JP, Li W (2013) CPAT: coding-potential assessment tool using an alignment-free logistic regression model. *Nucleic Acids Res* 41:e74
56. Hezroni H, Koppstein D, Schwartz MG, Avrutin A, Bartel DP, Ulitsky I (2015) Principles of long noncoding RNA evolution derived from direct comparison of transcriptomes in 17 species. *Cell Rep* 11:1110–1122



Posttranscriptional Suzuki-Miyaura Cross-Coupling Yields Labeled RNA for Conformational Analysis and Imaging

Manisha B. Walunj and Seergazhi G. Srivatsan

Abstract

Chemical labeling of RNA by using chemoselective reactions that work under biologically benign conditions is increasingly becoming valuable in the *in vitro* and *in vivo* analysis of RNA. Here, we describe a modular RNA labeling method based on a posttranscriptional Suzuki-Miyaura coupling reaction, which works under mild conditions and enables the direct installation of various biophysical reporters and tags. This two-part procedure involves the incorporation of a halogen-modified UTP analog (5-iodouridine-5'-triphosphate) by a transcription reaction. Subsequent posttranscriptional coupling with boronic acid/ester substrates in the presence of a palladium catalyst provides access to RNA labeled with (a) fluorogenic environment-sensitive nucleosides for probing nucleic acid structure and recognition, (b) fluorescent probes for microscopy, and (3) affinity tags for pull-down and immunoassays. It is expected that this method could also become useful for imaging nascent RNA transcripts in cells if the nucleotide analog can be metabolically incorporated and coupled with reporters by metal-assisted cross-coupling reactions.

Key words Nucleotide analog, Suzuki-Miyaura reaction, Bio-orthogonal reaction, Posttranscriptional chemical modification, RNA labeling, RNA imaging, Environment-sensitive probe

1 Introduction

Several chemoselective transformations that can be carried out under biologically benign conditions serve as valuable tools to label and study biomacromolecular structure and function in both cell-free and cellular environments [1–4]. Some of the prominent examples of chemical labeling approaches, which have been categorized as bio-orthogonal reactions, include azide-alkyne cycloaddition [5], Staudinger ligation [6], and inverse electron demand Diels-Alder reactions [7]. While these reactions have been conveniently implemented in labeling proteins, sugars, and DNA, their use in labeling RNA has not been very straightforward due to inherent low stability of RNA [8]. In this regard, we and other groups have designed posttranscriptional and chemo-enzymatic labeling approaches employing above-said bio-orthogonal

reactions to functionalize [9–13] and image RNA in cells [14–19]. Nevertheless, new chemoselective reactions that can be tuned to work in aqueous and under milder conditions are constantly needed to expand the repertoire of functionalized RNA. In this context, palladium (Pd)-catalyzed C-C bond formation, which is a powerful reaction in synthetic organic chemistry, is proving useful as a chemoselective transformation for post synthetic labeling of biomolecules [20–23].

Like other methods, Pd-mediated cross-coupling reactions were first established on DNA and protein [20, 21]. Bromo- or iodo-modified DNA oligonucleotides (ONs) and proteins, prepared by chemical or enzymatic methods, are reacted with a cognate reactive handle tagged with a reporter in the presence of a water-soluble Pd-ligand catalytic system. The Manderville and Jäschke groups developed aqueous-phase Suzuki-Miyaura coupling reaction to functionalize DNA by reacting halogen-modified DNA ONs with boronic acid/ester substrates in the presence of Pd(OAc)₂ and a water-soluble triphenylphosphane-3,3',3'-trisulfonate ligand [24, 25]. However, this catalyst-ligand combination requires elevated temperature (>70 °C), basic pH buffer conditions, and long reaction times to produce coupled ON products. Understandably, RNA will not survive these high temperature and basic pH buffer conditions. Meanwhile, Davis and Lin group formulated a Pd-ligand catalytic system to execute Suzuki and Sonogashira reactions, respectively, on proteins under very mild conditions [26, 27]. The catalytic system was made of Pd(OAc)₂ and 2-aminopyrimidine-4,6-diol (ADHP) or dimethylamino-substituted ADHP (DMADHP), which enabled the direct incorporation of functional labels onto DNA ONs at room temperature and at a pH (8.5) slightly higher than physiological pH [28]. Encouraged by this report, we established a milder and efficient Suzuki-based labeling method to generate RNA functionalized with different biophysical reporters [29]. In this strategy, 5-iodouridine-5'-triphosphate (IUTP **1**) was incorporated into RNA transcripts by in vitro transcription reaction catalyzed by T7 RNA polymerase. Iodo-labeled transcripts were then posttranscriptionally reacted with various cognate reactive partners (boronic acid/ester substrates) labeled with a desired biophysical reporter or tag in the presence of Pd(OAc)₂ and ADHP or DMADHP complex. The reaction proceeds under benign conditions (37 °C and pH 8.5) and produces coupled RNA products in moderate to good yields. Taken together, this method is modular, and provides access to RNA labeled with (a) fluorogenic environment-sensitive nucleoside for probing nucleic acid structure and recognition, (b) fluorescent probes for microscopy, and (c) affinity tags for pull-down and immunoassays (Fig. 1). Further, metabolic labeling

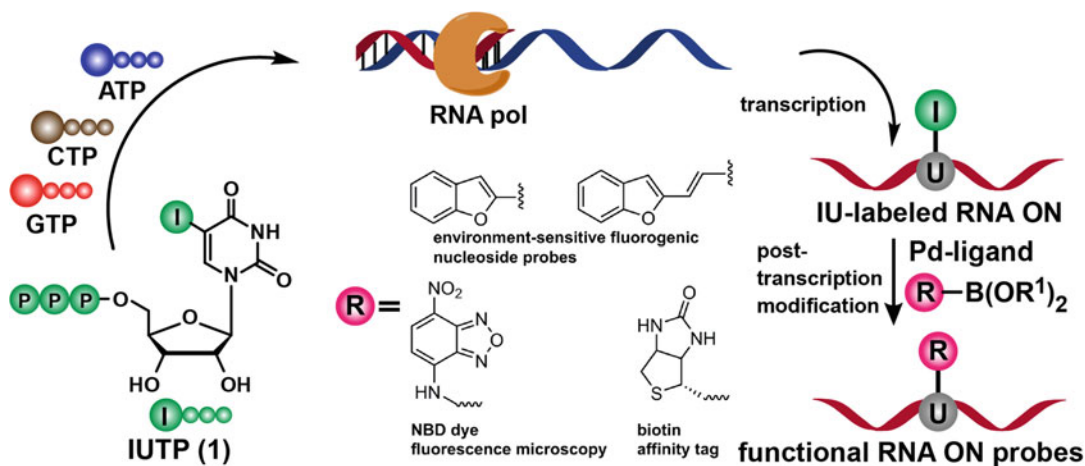


Fig. 1 Schematic diagram illustrating the incorporation of IUTP **1** into RNA transcripts by in vitro transcription followed by posttranscriptional functionalization using a Suzuki-Miyaura cross-coupling reaction to generate RNA labeled with different probes. This figure has been reproduced by permission of Nucleic Acids Research: Oxford Journals [29]

of nascent RNA with IU/IUTP followed by Pd-mediated coupling chemistry could be potentially used to image as well as profile cellular RNA. This notion is supported by the recent development of a Pd nanoparticle-based catalytic system, which enables the Suzuki reaction in the cellular environment [30].

Here, we describe a detailed stepwise protocol to incorporate 5-iodouridine-5'-triphosphate into RNA transcripts during in vitro transcription using T7 RNA polymerase. Following this section, the preparation of water-soluble Pd-ligand catalysts, the setting up of posttranscriptional Suzuki reactions and the purification of coupled RNA products are illustrated in detail. Although we have performed coupling reactions with several substrates, emphasis is laid on preparing RNA labeled with fluorogenic environment-sensitive nucleoside probes (**4** and **7**), a fluorescent probe (**9**) suitable for imaging, and an affinity tag (**10**) suitable for pull-down and immunoassays (Fig. 2).

2 Materials

Prepare all reagents, substrates, and buffer stocks in autoclaved water unless indicated otherwise. Store enzymes, DNA ONs, NTPs, and reagents in a deep freezer (-20 or -40 °C).

2.1 In Vitro Transcription

1. $5\times$ Transcription buffer: 200 mM Tris-HCl (pH 7.9), 30 mM $MgCl_2$, 50 mM DTT, 50 mM NaCl, and 10 mM spermidine. This buffer is usually supplied along with T7 RNA polymerase.

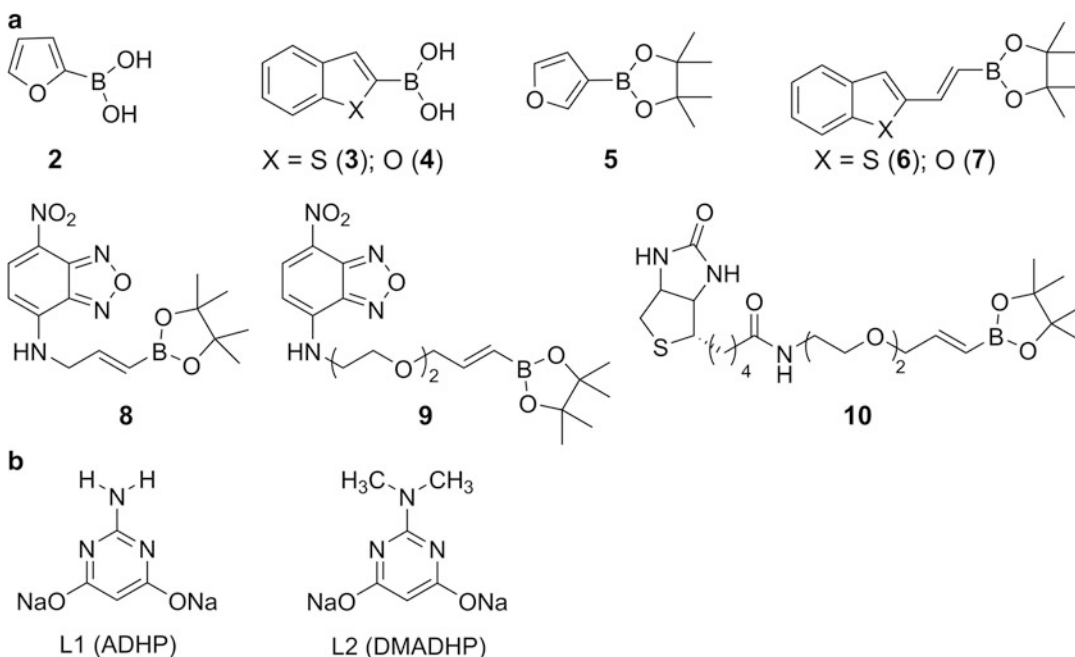


Fig. 2 (a) Chemical structure of boronic acid/ester substrates used in the posttranscriptional Suzuki-Miyaura coupling reactions. (b) Ligand L1 and L2

- Annealing buffer: 10 mM Tris-HCl, 1 mM EDTA, 100 mM NaCl, pH 7.8. Weigh 12.11 mg of Tris base and 58.44 mg of NaCl in a 15 mL centrifuge tube. Add 8–9 mL of water and 20 μL of 0.5 M EDTA. Adjust the pH to 7.8 by adding 1 M HCl. Make the final volume to 10 mL using autoclaved water and check the pH again.
- 20 U/ μL T7 RNA polymerase stock (*see Note 1*).
- NTPs minus UTP mix: 20 mM Stock solution in autoclaved water. Mix 20 μL of 100 mM stock solutions of guanosine triphosphate (GTP), cytidine triphosphate (CTP), and adenosine triphosphate (ATP) in a 1.5 mL microcentrifuge tube. Make it to 100 μL by adding 40 μL autoclaved water. Vortex, centrifuge, and store the NTP-UTP mix at -40°C .
- 20 mM 5-Iodouridine-5'-triphosphate (IUTP **1**, $\epsilon_{260} = 3100 \text{ M}^{-1} \text{ cm}^{-1}$, can be purchased from a supplier): Prepare this stock solution in autoclaved water. Store the stock solution at -40°C .
- 200 mM MgCl_2 : Weigh 40.66 mg of MgCl_2 in a 1.5 mL microcentrifuge tube. Dissolve the solid in 1 mL of autoclaved water. Store the solution at -40°C .
- 40 U/ μL RiboLock (*see Note 1*).

8. 1 M Dithiothreitol (DTT): Weigh 7.71 mg in 0.5 mL microcentrifuge tube and dissolve in 50 μ L of autoclaved water (*see Note 2*).
9. 5 μ M Promoter-template DNA duplex: Transfer 5 μ L of promoter DNA ON **11** (100 μ M) and template DNA ON **12** (100 μ M) into a 1.5 mL microcentrifuge tube containing 90 μ L of the annealing buffer. Vortex the solution and centrifuge for 10 s. Anneal the ON mix by placing the centrifuge tube on the heating block at 90 °C for 3 min. Remove the heating block from the dry-block heater and allow it to cool to room temperature (RT). Place the annealed promoter-template DNA duplex (final conc. 5 μ M) in an ice bath for 30 min. Store the promoter-template duplex at -40 °C.

2.2 PAGE Equipment

1. Gel electrophoresis equipment.
2. Glass plates (45 cm \times 20 cm, 4.8 mm thick).
3. Power supply.
4. 1.5 mm Spacer.
5. 1.5 mm Comb.
6. Plastic wrap (UV transparent).
7. Sterile scalpel.
8. Sterile glass rod.
9. Poly-Prep columns (Bio-Rad Laboratories).
10. Sep-Pak C18 cartridges (Waters Corporation).
11. UV lamp.
12. Rotary mixture.

2.3 PAGE Purification of IU-Labeled RNA Transcript

1. 10 \times TBE resolving buffer: 0.89 M Tris, 0.89 M boric acid, and 20 mM EDTA. Dissolve 108 g Tris base and 55 g boric acid in 800 mL autoclaved water. To this solution add 40 mL of 0.5 M EDTA (pH 8.0). Adjust the volume to 1 L with autoclaved water. Filter the buffer through 0.45 μ m filter paper. Store the buffer at RT.
2. Denaturing acrylamide/bis-acrylamide solution (19:1): Weigh 190 g of acrylamide and 10 g of bis-acrylamide in 1 L reagent bottle. Add autoclaved water to a volume of 300 mL. Further add 420 g of urea followed by addition of 100 mL 10 \times TBE buffer. Stir the mixture vigorously using a magnetic stir bar. Make up the volume to 1000 mL with autoclaved water and filter using 0.45 μ m filter paper. Store this solution at 4 °C protected from light (*see Note 3*).
3. 10% (wt/vol) Ammonium persulfate (APS): Weigh 1 g of APS in 15 mL centrifuge tube and make the volume up to 10 mL by adding autoclaved water (*see Note 4*).

4. *N,N,N',N'*-tetramethylethylenediamine (TEMED).
5. Denaturing loading buffer: 7 M Urea, 10 mM Tris-HCl, 100 mM EDTA, pH 8.0. Dissolve 4.2 g urea and 15.76 mg Tris-HCl in 5 mL of autoclaved water. Add 2 mL of 0.5 M EDTA (pH 8.0). Adjust the volume to 10 mL. Store the buffer at room temperature.
6. 0.3 M Sodium acetate solution: Prepare 20 mL of 0.3 M sodium acetate solution in autoclaved water.

**2.4 Posttrans-
criptional
Suzuki-Miyaura
Coupling Reactions**

1. 100 mM Stock solution of boronic acids/esters: Prepare 50 μ L solution of each substrate by dissolving respective amount of boronic acid/ester substrates in BioUltra-grade DMSO (*see Note 5*). Vortex the solution, spin, and store at $-40\text{ }^{\circ}\text{C}$ (*see Note 5*).
2. Pd-ligand catalyst (*see Note 6*): Add ADHP (65 mg, 0.5 mmol, 2 equiv.) or DMADHP (78 mg, 0.5 mmol, 2 equiv.) to a 5 mL volumetric flask containing 3 mL of autoclaved water. Add 100 μ L of 10 mM NaOH (4 mole equivalents) to above solution. Stir the solution for 5 min at RT until all solids dissolve completely. Add 56 mg of Pd(OAc)₂ (0.25 mmol, 1 mol equivalent) to the flask. Stir the mixture at $65\text{ }^{\circ}\text{C}$ for 60 min. Allow the solution to attain RT. Remove the stir bar and adjust the volume to 5 mL with autoclaved water to make a 50 mM stock solution of the Pd-ligand catalyst. Store the catalyst at $-40\text{ }^{\circ}\text{C}$. For cross-coupling reactions use 10 mM solution of the catalyst diluted using autoclaved water. Store 10 mM stock solution at $-40\text{ }^{\circ}\text{C}$ (*see Note 6*).
3. 250 mM Tris-HCl reaction buffer (5 \times), pH 8.5: Weigh 303 mg of Tris base in 15 mL centrifuge tube. Dissolve Tris base in 8 mL of autoclaved water. Adjust the pH of the solution to 8.5 by adding 1 M HCl. Adjust the volume to 10 mL by adding autoclaved water and filter the buffer using 0.22 μ m syringe filter. Store the buffer at room temperature.

**2.5 HPLC Purification
of Cross-Coupled RNA
Products**

1. 1 M Triethylammonium acetate buffer (TEAA), pH 7.0: Take 139.4 mL of HPLC-grade triethylamine in 1 L reagent bottle. Add 700 mL of autoclaved water and stir the mixture on an ice bath. Add dropwise 57.2 mL HPLC-grade acetic acid with stirring. Adjust the pH of the solution to 7.0 and make the total volume to 1 L by adding autoclaved water. Check the pH again and store the buffer at $4\text{ }^{\circ}\text{C}$. From this stock make 1 L of 50 mM solution of TEAA in autoclaved water. Filter the buffer through 0.22 μ m filter paper prior to HPLC purification.
2. Phenomenex-Luna C18 column (250 \times 4.6 mm, 5 μ m) or an equivalent column.

- Use spin filters (0.45 μm) to filter the samples before injecting on to the HPLC column.
- Mobile phase A: 50 mM TEAA buffer, pH 7.0.
- Mobile phase B: Acetonitrile. Filter the HPLC-grade acetonitrile through 0.22 μm filter paper.

3 Methods

3.1 Incorporation of IUTP into RNA Transcript by In Vitro Transcription Reaction (Fig. 3)

- Thaw transcription buffer, reagents, and enzymes necessary for transcription reaction on an ice bath.
- Spin, vortex, and spin the buffer and reagents, and keep them on ice bath (*see Note 1*).
- Perform large-scale transcription reaction in 250 μL reaction volume. Pipette 72.50 μL autoclaved water and 50 μL transcription buffer (5 \times) into a 1.5 mL microcentrifuge tube.
- Add 25 μL of 20 mM NTPs-UTP mix, 25 μL of 20 mM IUTP, 17.5 μL of 200 mM MgCl_2 , 2.5 μL of 1 M DTT, and 15 μL of 5 μM promoter-template DNA duplex.

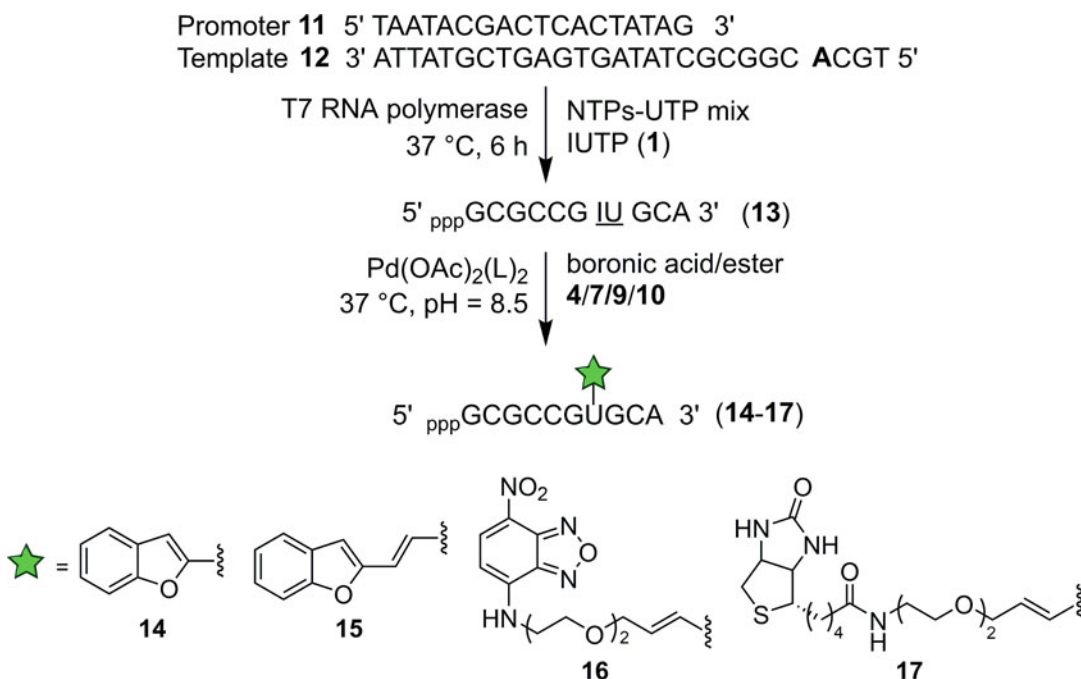


Fig. 3 Incorporation of IUTP **1** by in vitro transcription reaction using T7 RNA polymerase, template DNA ON **12**, and T7 promoter **11**. The sequence of IU-modified RNA transcript **13** is shown, which upon posttranscriptional Suzuki coupling with boronic acid/ester substrates **4**, **7**, **9**, and **10** gives coupled RNA ON products **14**, **15**, **16**, and **17**, respectively. Part of this figure has been reproduced by permission of Nucleic Acids Research: Oxford Journals [29]

5. Mix the above reaction mixture well with pipette and add 2.5 μL of 40 U/ μL RiboLock.
6. Initiate the transcription reaction by adding 40 μL T7 RNA polymerase (20 U/ μL). Mix the reaction mixture by pipetting up and down few times.
7. Incubate the reaction mixture at 37 °C for 6 h (*see Note 7*).

3.2 Preparative-Scale PAGE Purification of IU-Labeled RNA Transcript

1. Mix 150 mL of 20% denaturing acrylamide/bis-acrylamide solution with 1.4 mL of 10% aqueous APS in a 250 mL Erlenmeyer flask and add 70 μL of TEMED.
2. Pour the solution between the glass plates and insert a comb (1.5 mm thick with 4 wells). Polymerize for ~1 h.
3. Rinse the wells thoroughly with Millipore or autoclaved water to remove unpolymerized acrylamide and place it on the electrophoresis apparatus.
4. Fill the upper and lower chambers with 1 \times TBE buffer; pre-run the gel for at least 60 min at 25 W.
5. In the meantime, reduce the reaction volume (*see Subheading 3.1*) to nearly 1/3 in a speed vac (e.g., Labconco). Add 50 μL denaturing loading buffer (*see Note 8*).
6. After pre-run, turn off the power supply and wash the wells again thoroughly with 1 \times TBE buffer.
7. Load the samples on the preparative 20% denaturing polyacrylamide gel using pipette.
8. Run the gel at constant 25 W for ~6 h.
9. Turn off the power supply and carefully separate the gel from the plates. Cover the gel using plastic wrap.
10. Mark the band corresponding to the full-length transcript by UV shadowing (254 nm). This is usually a slower migrating intense band. Cut this band using a sterile scalpel.
11. Carefully transfer the gel pieces to a Poly-Prep column (BioRad) and crush the gel with a sterile glass rod into fine pieces.
12. Add 3 mL of 0.3 M aqueous sodium acetate solution and cap the Poly-Prep column.
13. Place the Poly-Prep column on a rotary mixer and allow the contents to mix well for ~12 h at RT.
14. Centrifuge the Poly-Prep column for 10–15 min and collect the solution in a 15 mL centrifuge tube.
15. Meanwhile condition the reversed-phase Sep-Pak column (Waters) by washing with 5 mL of acetonitrile and 15 mL of autoclaved water. The Sep-Pak column can be easily connected to a plastic syringe, which can be used for washing and loading the sample.

16. Load the filtrate from **step 14** onto the conditioned reversed-phase Sep-Pak column.
17. Wash the column with 12 mL of autoclaved water and then elute the transcript with 4 mL of 40% (v/v) acetonitrile in autoclaved water. Collect ~1 mL fractions in 1.5 mL microcentrifuge tubes.
18. Record the absorbance of the fractions at 260 nm to confirm the presence of the transcript.
19. Evaporate the fractions containing the transcript to dryness. Dissolve the residue in a known volume of autoclaved water and determine the concentration using the molar extinction coefficient at 260 nm ($\epsilon_{260} = 84,300/\text{M}/\text{cm}$) [29].
20. Confirm the purity and identity of IU-labeled RNA transcript by HPLC and mass analysis. For details refer supporting information of reported literature [29].

3.3 Posttranscriptional Suzuki-Miyaura Cross-Coupling (Fig. 3)

1. Pipette 10 μL of $5\times$ Tris-HCl buffer and 7.5 μL DMSO into a 0.5 mL microcentrifuge tube. Add IU-labeled RNA **ON 13** (9.1 μL of 550 μM stock, 5 nmol, 1 mol equivalent).
2. To the above reaction mixture add boronic acid/ester (2.5 μL of 100 mM stock in DMSO, 50 equiv.). Add 19.9 μL of autoclaved water.
3. Initiate the reaction by adding $\text{Pd}(\text{OAc})_2(\text{L1})_2$ or $\text{Pd}(\text{OAc})_2(\text{L2})_2$ catalyst (1 μL of 10 mM stock, 2 equiv.). The final reaction volume is 50 μL . The final concentration of RNA **13**, boronic acid/ester substrate, catalyst, and DMSO% is 100 μM , 5 mM, 200 μM , and 20%, respectively (*see Note 9*).
4. Incubate the reaction mixture at 37 °C for 6 h (*see Note 10*).
5. Quench the reaction by freezing the sample at -40 °C.

3.4 HPLC Purification of Functionalized RNA Products

1. Filter the reaction mixture and wash the spin filter with 40 μL of autoclaved water (*see Note 11*).
2. Analyze the filtrate by RP-HPLC (*see Note 12*).
Separate the cross-coupled product from the reaction mixture using following mobile phases and gradient: mobile phase A: 50 mM TEAA buffer (pH 7.0); mobile phase B: acetonitrile. Flow rate of 1 mL/min gradient: 0–30% B (100–70% A) in 35 min, 30–100% B (70–0% A) in 10 min, 100% B for 5 min, and 100% A for 5 min (*see Note 13*).
3. Monitor the HPLC run at 260 nm and at the respective wavelength of each fluorophore (*see Note 14*).
4. Collect the fraction corresponding to the coupled RNA product (*see Note 14*) and lyophilize the buffer. Add water to the residue and lyophilize again. This step removes the volatile TEAA buffer efficiently.

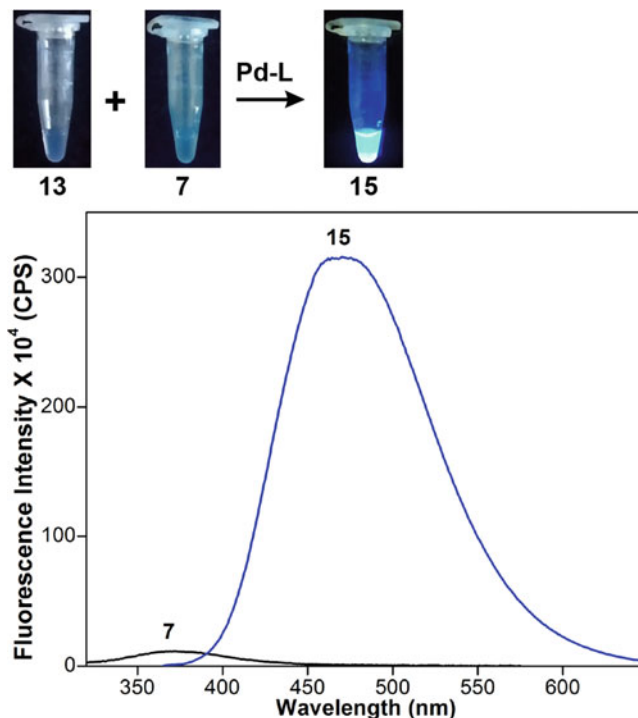


Fig. 4 Top: Image showing the fluorogenic Suzuki coupling of IU-labeled transcript **13** with boronic ester **7** and the reaction product **15**. The samples were irradiated using 365 nm light source. Bottom: Emission spectrum of boronic ester **7** and coupled RNA product **15**. CPS = counts per second. Part of this figure has been reproduced by permission of Nucleic Acids Research: Oxford Journals [29]

5. Dissolve the residue in a known volume of autoclaved water and quantify the coupled RNA product by measuring the absorbance. Refer reported literature for the molar extinction coefficient of each cross-coupled product [29] (*see Note 15*).
6. Confirm the identity of coupled RNA products by mass spectroscopy (*see Note 16*). If the product is fluorescent, then analyze its emission properties. For example, *see* Figs. 4 and 5 for the fluorescence profile of coupled RNA products, which are labeled with a fluorogenic dye, environment-sensitive fluorescent nucleoside probe [31, 32], and fluorescence microscopy-compatible NBD dye [33].

4 Notes

1. Thaw T7 RNA polymerase and RiboLock on an ice bath. Centrifuge the enzymes for few seconds (3–4 s). Do not vortex the enzyme solutions as they may denature.

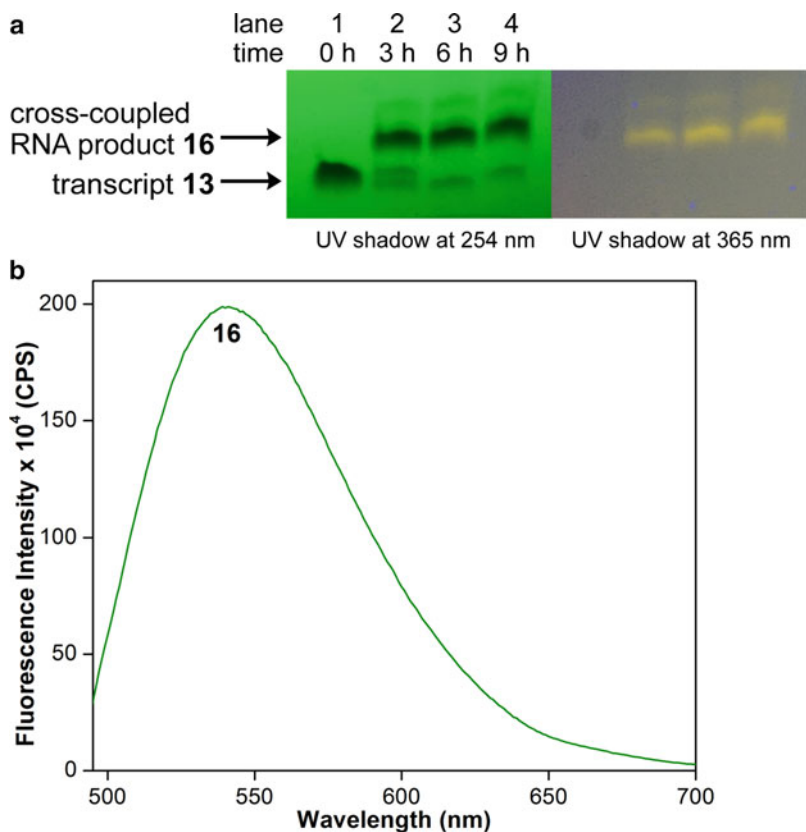


Fig. 5 (a) Suzuki reaction on IU-labeled RNA ON **13** using 2 equiv. of Pd catalyst and 50 equiv. of NBD boronic ester **9**. The reaction mixture was resolved by PAGE under denaturing conditions and UV shadowed. UV shadow of the gel at 254 nm (left) and at 365 nm (right) shows the formation of dye-labeled RNA product **16**. **(b)** Emission spectrum of the NBD-modified RNA product **16**. The sample was excited at 480 nm with an excitation and emission slit width of 8 nm and 10 nm, respectively. Part of this figure has been reproduced by permission of Nucleic Acids Research: Oxford Journals [29]

2. Make aliquots of 20 μ L of 1 M DTT solution and store at -20 or -40 $^{\circ}$ C. Do not use DTT that is freeze-thawed more than two times.
3. Acrylamide is highly toxic. Always wear protective gloves while handling acrylamide. The acrylamide solution can be stored at 4 $^{\circ}$ C for a month; however, it hydrolyzes to acrylic acid and ammonia if kept for longer period of time.
4. Use freshly prepared APS for efficient polymerization. If APS solution is old, the efficiency of polymerization will dramatically reduce. Store APS solution at 4 $^{\circ}$ C.
5. Boronic acid substrate **4** can be purchased from a supplier, and substrates **7**, **9**, and **10** can be prepared as has been reported [29]. Avoid prolonged exposure to light, in particular fluorescent NBD boronic ester **9**. Store the stock solutions in aluminum-wrapped centrifuge tube or in amber-colored plastic/glass vials.

6. ADHP (L1) can be purchased from a supplier. DMADHP (L2) can be synthesized as described [34]. The catalyst is stable when stored at -20 or -40 °C. Precipitation was observed when stored at RT for more than a month. We preferred to use freshly prepared 10 mM solution from 50 mM stock solution stored at -40 °C.
7. We have observed deiodination of the IU-labeled transcripts if the transcription reaction is performed for longer time. 6 h of incubation time gave 10–12 nmol of the IU-labeled transcript without detectable deiodination of the RNA transcript. So we recommended shorter reaction time (e.g., 6 h) and wrapping the microcentrifuge tube with aluminum foil.
8. We preferred not to add bromophenol blue (BPB) in the loading buffer so as to avoid any adventitious contamination of BPB in the transcript. To track the electrophoresis, we loaded an extra lane with BPB in the same denaturing buffer.
9. After optimization, we found that this concentration and ratio of IU-labeled RNA **13**, boronic acid/ester substrate, and catalytic system gave the best results.
10. Depending on the boronic acid/ester substrate the reaction time and yield could differ.
11. Filter the reaction mixture before injecting into the HPLC column. Otherwise fine particles of Pd formed in the reaction could affect the performance of the HPLC column.
12. We preferred HPLC purification of Suzuki-coupled RNA products as opposed to gel electrophoretic purification because it was observed that Pd chelated to the RNA was not easily removable by PAGE. However, with TEAA buffer system we were able to successfully isolate the pure coupled products by HPLC.
13. In our experiments, using the substrates listed in Fig. 2, we used the conditions given in Subheading 3.4. These conditions provide good separation between the coupled RNA product, IU-labeled RNA substrate, deiodinated RNA, and boronic acid/ester substrates. However, the HPLC purification method could vary depending on the substrate and product, and hence the readers are recommended to optimize the purification conditions.
14. Apart from monitoring the run at 260 nm (λ_{\max} of RNA), it would be useful to monitor HPLC chromatogram at the characteristic absorption wavelength of the probe attached to boronic acid/ester. A peak corresponding to the retention time that absorbs at 260 nm and also at the characteristic wavelength of the probe indicates that the fraction corresponds to the coupled RNA product.

15. Coupling of boronic esters **6** and **7** with RNA transcript **13** using catalyst Pd(OAc)₂(L1)₂ gave two regioisomers (major *trans* and minor *cis*) of the RNA product [29]. When Pd(OAc)₂(L2)₂ was used a single isomer (*trans*) was formed. However, the overall yield of the coupled RNA product was better when the reaction was performed using Pd(OAc)₂(L1)₂. Therefore, depending on the boronic acid/ester substrate, we recommend the users of this protocol to optimize the conditions in terms of reaction time and type of catalyst that can be used.
16. Mass of oligonucleotides can be measured using Applied Biosystems 4800 Plus MALDI TOF/TOF analyzer.

Acknowledgments

This work was supported by Wellcome Trust-DBT India Alliance (IA/S/16/1/502360) grant to S.G.S. M.B.W. thanks CSIR, India, for a graduate research fellowship. The authors wish to thank Arun Tanpure for discussion and help with work that has led to the optimization of this protocol.

References

1. Prescher JA, Bertozzi CR (2005) Chemistry in living systems. *Nat Chem Biol* 1:13–21
2. Weisbrod SH, Marx A (2011) Novel strategies for the site-specific covalent labelling of nucleic acids. *Chem Commun* 47:7018
3. Spicer CD, Davis BG (2014) Selective chemical protein modification. *Nat Commun* 5:4740
4. Holstein JM, Rentmeister A (2016) Current covalent modification methods for detecting RNA in fixed and living cells. *Methods* 98:18–25
5. McKay CS, Finn MG (2014) Click chemistry in complex mixtures: bioorthogonal bioconjugation. *Chem Biol* 21:1075–1101
6. van Berkel SS, van Eldijk MB, van Hest JCM (2011) Staudinger ligation as a method for bioconjugation. *Angew Chem Int Ed* 50:8806–8827
7. Wu H, Devaraj NK (2016) Inverse electron-demand Diels-Alder bioorthogonal reactions. *Top Curr Chem* 374:3
8. George JT, Srivatsan SG (2017) Posttranscriptional chemical labeling of RNA by using bioorthogonal chemistry. *Methods* 120:28–38
9. El-Sagheer AH, Brown T (2010) New strategy for the synthesis of chemically modified RNA constructs exemplified by hairpin and hammerhead ribozymes. *Proc Natl Acad Sci U S A* 107:15329–15334
10. Rao H, Tanpure AA, Sawant AA, Srivatsan SG (2012) Enzymatic incorporation of an azide-modified UTP analog into oligoribonucleotides for post-transcriptional chemical functionalization. *Nat Protoc* 7:1097–1112
11. Samanta A, Krause A, Jäschke A (2014) A modified dinucleotide for site-specific RNA-labelling by transcription priming and click chemistry. *Chem Commun* 50:1313–1316
12. Someya T, Ando A, Kimoto M, Hirao I (2015) Site-specific labeling of RNA by combining genetic alphabet expansion transcription and copper-free click chemistry. *Nucleic Acids Res* 43:6665–6676
13. Holstein JM, Stummer D, Rentmeister A (2016) Enzymatic modification of 5'-capped RNA and subsequent labeling by click chemistry. *Methods Mol Biol* 428:45–60
14. Jao CY, Salic A (2008) Exploring RNA transcription and turnover in vivo by using click chemistry. *Proc Natl Acad Sci U S A* 105:15779–15784
15. Grammel M, Hang H, Conrad NK (2012) Chemical reporters for monitoring RNA synthesis and poly (A) tail dynamics. *Chembiochem* 13:1112–1115

16. Sawant AA, Tanpure AA, Mukherjee PP, Athavale S, Kelkar A, Galande S, Srivatsan SG (2016) A versatile toolbox for posttranscriptional chemical labeling and imaging of RNA. *Nucleic Acids Res* 44:e16
17. Nguyen K, Fazio M, Kubota M, Nainar S, Feng C, Li X, Atwood SX, Bredy TW, Spitale RC (2017) Cell-selective bioorthogonal metabolic labeling of RNA. *J Am Chem Soc* 139:2148–2151
18. Sawant AA, Galande S, Srivatsan SG (2018) Imaging newly transcribed RNA in cells by using a clickable azide-modified UTP analog. *Methods Mol Biol* 1649:359–371
19. Zhang Y, Kleiner RE (2019) A metabolic engineering approach to incorporate modified pyrimidine nucleosides into cellular RNA. *J Am Chem Soc* 141:3347–3351. <https://doi.org/10.1021/jacs.8b11449>
20. Defrancq E, Messaoudi S (2017) Palladium-mediated labeling of nucleic acids. *Chembiochem* 18:426–443
21. Jbara M, Maity SK, Brik A (2017) Palladium in the chemical synthesis and modification of proteins. *Angew Chem Int Ed* 56:10644–10655
22. George JT, Srivatsan SG (2017) Vinyluridine as a versatile chemoselective handle for the post-transcriptional chemical functionalization of RNA. *Bioconjug Chem* 28:1529–1536
23. Walunj MB, Sabale PM, Srivatsan SG (2018) Advances in the application of Pd-mediated transformations in nucleotides and oligonucleotides: palladium-catalyzed modification of nucleosides, nucleotides and oligonucleotides. Elsevier, Amsterdam, pp 269–293
24. Omumi A, Beach DG, Baker M, Gabryelski W, Manderville RA (2011) Postsynthetic guanine arylation of DNA by Suzuki–Miyaura cross-coupling. *J Am Chem Soc* 133:42–50
25. Cahová H, Jäschke A (2013) Nucleoside-based diarylethene photoswitches and their facile incorporation into photoswitchable DNA. *Angew Chem Int Ed* 52:3186–3190
26. Chalker JM, Wood CSC, Davis BG (2009) A convenient catalyst for aqueous and protein Suzuki–Miyaura cross-coupling. *J Am Chem Soc* 131:16346–16347
27. Li N, Lim RKV, Edwardraja S, Lin Q (2011) Copper-free Sonogashira cross-coupling for functionalization of alkyne-encoded proteins in aqueous medium and in bacterial cells. *J Am Chem Soc* 133:15316–15319
28. Lercher L, McGouran JF, Kessler BM, Schofield CJ, Davis BG (2013) DNA modification under mild conditions by Suzuki–Miyaura cross-coupling for the generation of functional probes. *Angew Chem Int Ed* 52:10553–10558
29. Walunj MB, Tanpure AA, Srivatsan SG (2018) Posttranscriptional labeling by using Suzuki–Miyaura cross-coupling generates functional RNA probes. *Nucleic Acid Res* 46:e65
30. Yusop RM, Unciti-Broceta A, Johansson EMV, Sánchez-Martín RM, Bradley M (2012) Palladium-mediated intracellular chemistry. *Nat Chem* 3:239–243
31. Pawar MG, Srivatsan SG (2011) Synthesis, photophysical characterization, and enzymatic incorporation of a microenvironment-sensitive fluorescent uridine analog. *Org Lett* 13:1114–1117
32. Tanpure AA, Srivatsan SG (2011) A microenvironment-sensitive fluorescent pyrimidine ribonucleoside analogue: synthesis, enzymatic incorporation, and fluorescence detection of a DNA abasic site. *Chem Eur J* 17:12820–12827
33. Yamaguchi T, Asanuma M, Nakanishi S, Saito Y, Okazaki M, Dodo K, Sodeoka M (2014) Turn-ON fluorescent affinity labeling using a small bifunctional *O*-nitrobenzoxadiazole unit. *Chem Sci* 5:1021–1029
34. Boon WR (1952) 6-Dichloro-2-dimethylamino pyrimidine. *J Chem Soc* 1532

INDEX

A

Adipic acid dihydrazide agarose beads 242, 244, 248
 Affinity purification of polysomes 460, 461
Agrobacterium 108, 113, 148, 159,
 170, 176, 347, 349, 350, 433, 435, 442, 443
 Agroinfiltration 108, 114, 117,
 347, 351, 432, 433, 435, 442–444
 Alexa 488 60, 61, 64
 Alexa 594 26
 Alexa 647 61–62, 65
 Alkaline phosphatase (Fast Red) 4, 9,
 13, 14, 16, 19, 20
 Alkaline phosphatase (NBT/BCIP) 5, 13,
 14, 16, 19, 20
 APEX2 284, 285, 289, 293, 300, 302–304
 Arabidopsis 14, 115, 147,
 182, 242, 255, 260, 308, 405, 420, 454, 456
 Arabidopsis seed sterilization 420
Arabidopsis thaliana 3, 7, 256,
 257, 388, 391, 396, 405, 413–429
Arabidopsis thaliana cell culture 414, 419,
 421, 427

B

Binary expression vectors 434, 437–439, 448
 Bioanalyzer analysis 206, 209
Botrytis cinerea 216, 218, 222, 223, 228, 230
Brachypodium distachyon 391, 396, 405
 Broccoli (aptamer) 73–95, 106, 107, 197

C

Caenorhabditis elegans 24, 216
 CDNA synthesis 199, 212, 229, 231
 Cell sorting 195–213
 CHARGE technology 88, 91
 Chemical labeling of RNA 473
 Clustered regularly interspaced short palindromic repeats
 (CRISPR) 47, 137, 158,
 331–340, 343–355, 357–370, 376, 381, 382
 Corn (aptamer) 84, 87
 CRISPR/Cas9 system 331
 CRISPR/dCas9 method 353
 CRISPR/MB 358, 359, 364–366, 368

CRISPR prediction tools 335

D

Deep sequencing 199, 205, 206, 209
 Degassing of leaf samples 351
 DFHO 76, 84, 86, 87
 3,5-Difluoro-4-hydroxybenzylidene imidazolinone
 (DFHBI) 76, 78, 84, 86, 89, 92, 93
 Digitonin extraction 38, 40, 41, 45, 46, 48
 Digoxigenin 4, 23
 Double-stranded RNA 227, 307–327, 389
Drosophila 332, 333, 373–383, 456, 468
 DsRNA pull-down 309

E

Electrophoretic blotting 425
 Endonuclease Csy4 158
 Endoplasmic reticulum 35, 104
 Environmental RNAi 228
 Enzymatic signal amplification 5

F

FASTmiR technology 90
 Fiji software 30, 272
 FISH 23, 37, 38, 40,
 42–44, 47, 51–67, 74, 197, 212, 343, 346–348,
 352–354, 361, 364–366, 369, 370
 FISH-quant 30, 61, 62, 64,
 65, 131, 132, 134, 135, 207
 α -FLAG-coupled beads 460, 461
 Flock House virus 308
 Flow cytometry 201–205
 Fluorescein-labeled double-stranded
 RNAs 216–221
 Fluorescence activated cell sorter (FACS) 76, 80,
 81, 139, 203
 Fluorescent spot distance measurements 379
 Fluorescent sRNAs 217, 218, 221–223
 Fluorogens 73–95
 Förster resonance energy transfer (FRET) 78,
 79, 93, 94
 Fungal mycelium 223, 224, 229
 Fungus culture 228

G

- Gateway 108, 109, 111, 113,
115, 159, 166, 167, 434, 446
- Gene-linked RNA aptamer particle (GRAP)
display 81
- Genome editing 137, 331–340,
374–376, 381
- Germline injections 376, 378, 381
- Green fluorescent protein (GFP) 74, 81,
88, 90, 109, 111, 113–117, 124, 126, 128, 136,
146, 153, 158, 165, 170, 171, 183, 184, 187,
196, 203, 257, 271, 272, 274, 280, 293, 308,
309, 312, 315, 318, 320, 323–326, 344–348,
351–353, 383, 432, 433, 440–442, 445, 446,
449, 454, 456
- Guide RNAs 331–340, 343–355, 375, 382

H

- HEK-293T cells 132, 135
- HeLa cells 196, 271, 273
- Horseshoe peroxidase (HRP) 5, 286,
292, 310, 312, 316, 326, 436, 468
- HPLC purification 478, 481, 482, 484
- Human breast carcinoma (MCF7) cells 198
- Human osteosarcoma cells (U2OS) 37–39,
44, 196
- Hybridization with radioactive probes 390, 400

I

- ImageJ 30
- Immunofluorescence (IF) 46–48, 51–67, 288–290, 293,
302, 362, 365, 366
- Individual nucleotide resolution and
immunoprecipitation (iCLIP) 256, 257
- In situ hybridization (ISH) 3–20, 23–32, 36, 51, 73, 122,
138, 196, 343, 361
- Integrative Genomics Viewer (IGV) 392, 465, 467
- In vitro compartmentalization (μ IVC) 76
- In vitro transcription 9, 18, 80, 82, 91, 92,
185–187, 190, 192, 223, 233, 474–477, 479, 480
- Isolation of protoplasts 419–423

K

- Kinesin 269, 271

L

- Labeled dsRNAs 215–224, 230,
231, 233–235, 237
- Lentivirus 131, 135, 139
- Light-up aptamers 74, 80, 81, 83, 88, 92–95
- Long non-coding RNAs (lncRNAs) 196,
451–455, 457, 464, 466, 467

M

- Magnetic sorting 196, 198, 199, 205
- Malachite green 74, 75, 84, 106
- Mammalian cells 24, 35–48, 52,
84, 94, 123, 124, 127–132, 135, 137, 140,
195–213, 285, 369
- Mango (aptamers) 82–85, 94
- Mass spectrometry 241–252, 284,
285, 302, 308, 309, 318, 322, 323
- Microporation 358, 361, 363, 366, 369
- Microprojectile bombardment 168
- Microscopy 4, 7, 13–16, 20, 32,
45, 46, 60, 66, 88, 104, 106, 109, 114, 115, 122,
132, 136, 137, 146, 151–154, 207, 236, 281,
283, 286, 290, 302, 303, 308, 313, 320, 323,
325, 346, 347, 351, 353, 354, 358, 373, 374,
421, 474
- miRNA expression 432, 433,
438–439, 443, 445, 449
- Mobile mRNAs 145–154
- Molecular beacons 74, 91, 357–370
- Molecular motors 104, 269–281
- Motif enrichment analysis 245
- Mouse embryonic fibroblasts 196, 197
- MS2 103–118, 121–140,
145–154, 158, 196, 197, 199, 212, 270, 271,
374–376, 379, 382
- Myosins 106, 269, 271

N

- Neurospora crassa* 158
- Nicotiana benthamiana* 105, 108,
109, 113, 114, 146, 148, 151, 152, 158, 168,
170, 346, 432
- Non-coding RNAs (ncRNAs) 388, 389, 451
- Northern blots 3, 52, 122, 308,
310, 311, 315, 318, 319, 387–408, 414, 419,
423, 426, 427
- North-western blot 308, 314, 315, 318
- Nuclear-localization sequence (NLS) 107,
114–117, 126, 146, 166, 167, 175, 176, 347, 381

O

- On beads protein trypsinization 294

P

- PANDAN technology 91
- Paraffin embedding 27
- Plant viruses 105, 307
- Polyethylene glycol (PEG) 78, 259,
414, 427, 458, 462, 463, 469
- Polysome extraction 455, 458, 459, 468

Potato virus X (PVX)..... 158, 159, 163,
 167, 168, 170, 171, 176, 182–188, 191
 PP7.....93, 123, 270, 374–376, 379, 382
 Protein-RNA crosslinking 245, 284
 Protoplast transfection 423
 Proximity biotinylation 288, 290,
 292, 300, 304
Proximity-CLIP..... 283–305
Pseudomonas aeruginosa 158

Q

Quantitative RT-PCR..... 185

R

Radioactive labeling of RNA 259, 263
 Recombination-mediated cassette exchange
 (RMCE)..... 374–376
 Renilla luciferase 271, 440–442,
 448, 449
 Ribosomes 35, 36, 38, 46,
 47, 454, 455, 457, 461, 467
 RNA affinity purifications 241–252
 RNA-binding proteins (RBPs)..... 103, 104,
 106, 241–252, 255, 269, 278, 284, 285
 RNA extractions 185, 190, 191,
 199, 203, 229, 231, 293, 391–395, 397, 406,
 455, 461, 462
 RNA fractionation by polyacrylamide gel
 electrophoresis 424
 RNA immunoprecipitation..... 255–266
 RNA interference 216, 227, 387
 RNA isolation..... 190, 256,
 260, 264, 309, 314
 RNA labeling 7, 9, 117, 150,
 216, 220, 233
 RNA mobility 182, 183, 187, 270, 271
 RNA particles 274–277
 RNase decontamination 9
 RNAseq.....285, 457, 462, 463
 RNA silencing 182, 390, 431–449
 RNA uptake..... 215–224
 RNA virus 105, 309
 RNP footprints 294–299

S

Saccharomyces cerevisiae..... 107
 SDS PAGE..... 264, 266, 311,
 312, 321, 436, 444, 445
 Seeding cells 273
 Seed sterilization 415, 420
 Short oligonucleotide probes 24

Signal recognition particle (SRP).....35, 36
 Single-molecule FISH (smFISH)..... 24, 29–32,
 36–43, 45–48, 51–67, 122, 124, 125, 127, 128,
 132, 133, 135, 138, 196, 197, 207, 208, 211
 Single-molecule RNA mobility assay 269–281
 Site directed mutagenesis 434, 437
 Size fractionation of total RNA..... 398–399
 Small RNA cDNA libraries..... 293–299
 Small RNA data analysis 396–397
 Small RNA extraction 424
 Spectral unmixing24, 26
 Spinach (aptamer) 82, 84, 86, 89, 92
 Split aptamers 91
 Spray-induced gene silencing (SIGS) 216, 228
 SP6 RNA polymerase.....7, 18
 Stellaris mRNA probes.....41, 47
 Streptavidin affinity purification 286, 295
 Suzuki-Miyaura cross-coupling 473–485
 Systematic Evolution of Ligands by EXponential
 enrichment (SELEX) 76, 80, 81, 83

T

Tagging RNA with agarose beads..... 246, 248
 Tethering assays..... 270, 271
 4-Thiouridine (4SU)-labeled RNA.....285
 Tissue fixation 11
 Tissue permeabilization 12
 Tobacco mosaic virus (TMV)..... 105–107,
 111, 115, 117
 Tobacco rattle virus (TRV)..... 308, 318, 323
 Transcription activator-like effector nucleases
 (TALENs) 335
 Translating ribosome affinity purification
 (TRAP) 257, 454–458,
 461, 468, 469
 Translatomes 451–470
 Transport granule 269
 TRAP RNA is achieved by direct sequencing
 (TRAP-SEQ) 451–470
 T7 RNA polymerase 7, 9, 89, 92, 186, 187,
 216, 220, 234, 474–476, 479, 480, 482
 Tyramide signal amplification (TSA) system 5

U

Urea-PAGE 288, 294, 296, 298, 302, 304
 UV cross-linker 257, 260, 286, 310, 394, 401

V

Verticillium longisporum..... 228, 230, 236
 Virus replication complexes..... 307, 320
 Volocity 26, 30, 31

W

Western blots250, 289,
291–293, 302, 304, 308, 311, 312, 314, 318,
320, 322, 326, 444, 448, 455, 460, 468

Y

Yeast cells56, 57, 66, 126, 128, 129, 133

Z

Zinc-finger nucleases (ZFNs)335